Friedrich-Schiller-
Universität
Jena

Physikalisch-Astronomische Fakultät

Astrophysikalisches Institut und
Universitäts-Sternwarte


# The multiplicity of intermediate and high-mass B-type stars in the near infrared

# Die Multiplizität mittelschwerer und massereicher B-Sterne im Nahen Infrarot

—Dissertation—

zur Erlangung des Akademischen Grades

Doctor Rerum Naturalium (Dr. rer. nat.)

vorgelegt dem Rat der Physikalisch-Astronomischen Fakultät
der Friedrich-Schiller-Universität Jena

von Dipl.-Phys. Christian Adam
geboren am 09. Februar 1980 in Aschersleben

Gutachter:

1. Gutachter: Prof. Dr. Ralph Neuhäuser
Friedrich-Schiller-Universität Jena
Astrophysikalisches Institut und Universitäts-Sternwarte

2. Gutachter: Prof. Dr. Ernst Paunzen
Faculty of Sciences Masaryk University
Department of Theoretical Physics and Astrophysics

3. Gutachter: Prof. Dr. Pavel Kroupa
Rheinische Friedrich-Wilhelms-Universität Bonn
Argelander-Institut für Astronomie

Tag der Disputation: 29. 06. 2017

*"A work as this is never finished, one must simply declare it finished when one has within limits of time and circumstances, done what is possible."*

*"So eine Arbeit wird eigentlich nie fertig, man muß sie für fertig erklären, wenn man nach Zeit und Umständen das Möglichste getan hat."*

Johann Wolfgang von Goethe,
16. März 1787

# Abstract

In this thesis a volume-limited sample ($D \leq 1\,\mathrm{kpc}$) of 316 B-type stars was investigated regarding their multiplicity status and the distribution of fundamental parameter such as their separation or mass-ratio distributions to improve our understanding of the formation processes of stellar and multiple systems.

For this purpose public archival data of B-type stars in combination with own observations were analysed, obtained by diffraction-limited near-infrared imaging with NAOS-CONICA at the Very Large Telescope located at the Paranal observation site in Chile. For each of the selected target stars the presence of visual companions was investigated and their physical association confirmed or rejected either by analysing their common proper motion or based on a statistical assessment. Given the measured flux-ratio, relative to the primary, for each identified companion, the spectral type, distance and age of the primary, as well as the combined brightness from the 2MASS point source catalogue, the mass of the companion and consequently the mass-ratio $q$ between companion and primary was determined.

The projected separation range covered by this sample extends from 20 to about 7000 au. Among the 316 B-type stars a total of 194 sources were resolved in the vicinity of 148 primary stars, including 9 new confirmed detections, 19 previously known but first-time confirmed detections and 38 new resolved candidate companions, respectively. Additional, a white dwarf was found within the sample, the central star of a planetary nebula NGC 246, misleadingly classified as B-type main sequence star. Alongside one previously known companion located about 3.8″ south-east of the white dwarf central star, one new companion was resolved located about 1″ ($\approx 500\,\mathrm{au}$) north-east of the primary. Combining the results from multi-epoch observations the physical association of both companions could be confirmed by common proper motion, making this system the first confirmed hierarchical triple system in the centre of a planetary nebula. Using the obtained separation measurements in combination with available literature data the physical association of 86 stellar companions to their primaries could be confirmed, whereas the results of the common proper motion analysis of 75 visual companions remain inconclusive. Additionally, 33 potential candidate companions have been identified as background objects.

Similar to the solar-type binary distribution the measured separation distribution forms a log-normal distribution, but with a peak shifted towards a significantly wider separation of $214^{+38}_{-24}\,\mathrm{au}$. The estimated mass ratio distribution follows a power-law $f(q) \propto q^{\Gamma}$, with $\Gamma \approx -0.50$. Furthermore, there is evidence for a dependency of the mass ratio distribution on the binary separation, which tends towards smaller mass ratios for wider binaries. The measured companion star fraction of the sample, uncorrected for biases, is $51.3^{+2.8}_{-2.8}$ per cent and the assessment of higher-order multiples within the sample, combined with literature data yields a lower limit on the frequency of single, binary, triple and higher-order multiple B-type star systems of $38.6^{+2.8}_{-2.7}$, $38.0^{+2.8}_{-2.6}$, $15.2^{+2.2}_{-1.8}$ and $\approx 8$ per cent, respectively.

# Zusammenfassung

Diese Dissertation befasst sich mit der Untersuchung einer räumlich begrenzten Stichprobe ($D \leq 1\,\mathrm{kpc}$) von 316 B Sternen bezüglich ihrer Multiplizität sowie der Verteilung grundlegender Parameter wie zum Beispiel deren Abstands- und Massen-Verteilung, mit dem Ziel unser Verständnis über die zugrunde liegenden Entstehungsprozesse stellarer und multipler Systeme zu erweitern.

Hierfür wurden frei verfügbare Archivdaten mit eigenen Beobachtungen kombiniert und analysiert. Die hoch-auflösenden Nah-Infrarot Daten wurden dabei mit Hilfe des NAOS-CONICA Instruments gewonnen, welches am Very Large Telescope montiert ist und sich am Paranal in Chile befindet. Jedes der gewählten Beobachtungsobjekte wurde auf das Vorhandensein von möglichen Begleitern hin untersucht und deren mögliche physikalische Verbindung zum Primärstern bestätigt bzw. widerlegt mittels einer Analyse der gemeinsamen Eigenbewegung oder aufgrund statistischer Überlegungen. Mit Hilfe des gemessenen Fluss-Verhältnisses zwischen Primärstern und jedem identifizierten Begleiter, dem Spektraltyp, Abstand und Alter der Primärkomponente sowie der kombinierten Helligkeit aus dem 2MASS Katalog wurde anschließend die Masse der Begleiter und in letzter Konsequenz das Massenverhältnis $q$ zwischen Mutterstern und Begleiter bestimmt.

Der Bereich, der durch diese Stichprobe abgedeckten projizierten Abstände, erstreckt sich zwischen 20 und 7000 AE. Unter den 316 B Sternen wurden insgesamt 194 Quellen in der näheren Umgebung von 148 Primärsternen entdeckt, einschließlich 9 neuer bestätigter Begleiter, 19 bereits bekannter Begleiter, die hier zum ersten Mal bestätigt werden konnten, und 38 neu entdeckter Begleiterkandidaten. Zusätzlich wurde in der Stichprobe ein Weißer Zwerg, der Zentralstern des planetarischen Nebels NGC 246, identifiziert, welcher fälschlicherweise in der Stichprobe als B Stern gelistet wurde. Neben einem bereits bekannten Begleiter, der sich etwa 3.8 Bogensekunden süd-östlich des Zentralsterns befindet, konnte ein weiterer neuer Begleiter aufgelöst werden, welcher sich nord-östlich vom Primärstern in einem Abstand von etwa 1 Bogensekunde ($\approx 500$ AE) befindet. Durch Kombination verschiedener Beobachtungen und mit Hilfe der Eigenbewegung des Sterns konnte festgestellt werden, dass es sich um einen physikalischen Begleiter handelt, was dieses System zum ersten bestätigten hierarchischen Dreifachsystem im Zentrum eines planetarischen Nebels macht. Durch die Kombination der gemessenen Abstände mit verfügbaren Literaturdaten konnte die gravitative Verbindung von 86 stellaren Begleitern zu ihren Muttersternen nachgewiesen werden, wohingegen für 75 Begleiterkandidaten keine aussagekräftigen Ergebnisse aus der Eigenbewegungsanalyse gewonnen werden konnten. Des Weiteren wurden 33 potenzielle Begleiter Kandidaten als Hintergrundobjekte identifiziert.

Die beobachtete Abstandsverteilung kann, ähnlich zu der bei sonnenähnlichen Sternen gemessenen, durch eine log-normal Verteilung beschrieben werden, welche allerdings mit einem Höchstwert der Verteilung von $214^{+38}_{-24}$ AE signifikant zu weiteren Abständen hin verschoben ist. Die hier bestimmte Verteilung der Massenverhältnisse genügt einer power-law Funk-

tion $f(q) \propto q^{\Gamma}$, wobei $\Gamma \approx -0.50$ ist. Es wurden weiterhin deutliche Hinweise für eine Abhängigkeit des Massenverhältnisses vom Abstand der Komponenten gefunden, mit der Tendenz massenärmere Begleiter bei größeren Abständen zu finden. Die gemessene, unkorrigierte und allgemeine Begleiterhäufigkeit beträgt $51.3^{+2.8}_{-2.8}$ %, während eine Abschätzung höherrangiger Mehrfachsysteme kombiniert mit Literaturwerten eine untere Grenze für die Häufigkeit von Einzel-, Doppel-, Dreifach-, und höherrangigen Systemen von $38.6^{+2.8}_{-2.7}$ %, $38.0^{+2.8}_{-2.6}$ %, $15.2^{+2.2}_{-1.8}$ % bzw. $\approx 8$ % ergab.

# Acknowledgements

The creation of this dissertation would not have been possible without the direct, moral and of course financial support of many people, which I would like to express my sincere appreciation for their cooperation.

First of all I would especially like to thank my doctoral advisor Prof. Dr. Ralph Neuhäuser for mentoring this PhD thesis. I highly appreciate his continued support and his imperturbable trust in the success of this work.

I also want to thank Dr. Markus Mugrauer for his guidance throughout the creation of this thesis. We had many fruitful discussions and I learned a great deal from him, especially during our shared observations at the University Observatory Jena in Großschwabhausen or our joint lunches.

I am especially indebted to Dr. Tobias Schmidt and Dr. Christian Ginski for their generous helpfulness whenever I came across a problem during the past years. I also had many wide range, fruitful but also critical discussions with Dr. Thomas Eisenbeiß, Dr. Martin Seeliger or Dr. Janós Schmidt for which I am very grateful, and which in turn, I believe, helped me to become a better scientist. Furthermore, I want to especially thank Dr. Tristan Roell for introducing me to the Python programming language which became the primary tool for all research conducted in this thesis.

In addition to the scientific staff, my colleagues and friends at the AIU I would like to thank Jürgen Weiprecht for the computer support and Monika Müller for all the administrative problems she solved for me. I also want to thank all my other friends for their moral support, the motivation and help they always provided to me.

But most of all, I am deeply indebted to my family, who supported me throughout my entire life. Without my beloved mother Karin Adam, my father Johann Adam, my grandmother and their support no matter what, I would not be the person I am at this point.

# Contents

# List of Figures

# List of Tables

# List of Units

This thesis employs units of measurement which are commonly used in astronomy, but not part of the SI unit system. In the following, these units are defined and their conversion to SI units is given.

**1 au** (Astronomical Unit) is the mean distance between the Earth and the Sun.
$1\,\mathrm{au} = 1.495\,978\,707 \times 10^{11}\,\mathrm{m}$

**1 pc** (Parsec) is the distance from the Sun to an astronomical object which has a parallax angle of one arcsecond.
$1\,\mathrm{pc} \approx 2.062\,648 \times 10^{5}\,\mathrm{au} \approx 3.085\,678 \times 10^{16}\,\mathrm{m}$

**1 arcsec** (Arc Second) is a unit of angular measurement equal to the 1 296 000th part of a circle. 1 arcsec is also written as $1''$.
$1\,\mathrm{arcsec} = \frac{1}{3600}^{\circ} = \frac{\pi}{648\,000}\,\mathrm{rad}$

**1 mas** (Milliarcsecond) is the 1000th part of an arc second.
$1\,\mathrm{mas} = 10^{-3}\,\mathrm{arcsec} = \frac{\pi}{648\,000\,000}\,\mathrm{rad}$

**1 $\mathrm{M}_\odot$** (Solar rest mass) is the current rest mass of the Sun.
$1\,\mathrm{M}_\odot = 1.9884 \times 10^{30}\,\mathrm{kg}$
$1\,\mathrm{M}_\odot \approx 1047\,\mathrm{M}_{\mathrm{Jup}}$

**1 $\mathrm{R}_\odot$** (Solar radius) is the equatorial radius of the Sun.
$1\,\mathrm{R}_\odot = 6.96 \times 10^{8}\,\mathrm{m}$
$1\,\mathrm{R}_\odot \approx 10\,\mathrm{R}_{\mathrm{Jup}} \approx 109\,\mathrm{R}_{\mathrm{Earth}}$

**1 $\mathrm{L}_\odot$** (Solar luminosity) is the total energy irradiated by the Sun.
$1\,\mathrm{L}_\odot = 3.828 \times 10^{26}\,\mathrm{J\,s^{-1}}$

**1 $\mathrm{M}_{\mathrm{Jup}}$** (Jovian rest mass) is the rest mass of Jupiter.
$1\,\mathrm{M}_{\mathrm{Jup}} = 1.8996 \times 10^{27}\,\mathrm{kg}$
$1\,\mathrm{M}_{\mathrm{Jup}} \approx 9.55 \times 10^{-4}\,\mathrm{M}_\odot$

**1 $\mathrm{R}_{\mathrm{Jup}}$** (Jupiter radius) is the equatorial radius of Jupiter.
$1\,\mathrm{R}_{\mathrm{Jup}} = 7.1492 \times 10^{9}\,\mathrm{m}$
$1\,\mathrm{R}_{\mathrm{Jup}} \approx 11\,\mathrm{R}_{\mathrm{Earth}}$

**1 $\mathrm{R}_{\mathrm{Earth}}$** (Earth radius) is the equatorial radius of the Earth.
$1\,\mathrm{R}_{\mathrm{Earth}} = 6.378 \times 10^{6}\,\mathrm{m}$

# 1 Introduction

The physical association of many stars in binary and multiple systems was already recognized as early as in the 17$^{th}$ century. Since then, the technique of astronomical instrumentation and the theoretical understanding of the processes occurring during the formation and evolution of stellar systems has made huge progress. However, there are still unresolved questions needed to be answered to complete our picture of star formation and stellar evolution of different stellar populations and in different environments. For instance, whether low-mass stars and high-mass stars are formed by different processes, or whether star formation is characterized by a universal multiplicity distribution, similar to the observed apparently universal Initial Mass Function (IMF), in the present day Universe, is still under debate.

Another important fact revealed by observations during the past decades, in particular observations of star-forming regions, is that almost all stars (70–90 %) do form in cluster (e.g., Lada and Lada 2003), and that the number of multiple systems within these clusters is remarkably high. Thus, the understanding of star formation also requires to understand the formation of multiple systems, from binaries to cluster, by means of both observation and theory.

From the theoretical standpoint, the goal of a complete theory of star formation is the understanding of the origin of all statistical properties of stellar cluster, stellar systems themselves, proto-planetary discs and planetary systems, and how these depend on environment and initial conditions. Along with the more general properties such as the stellar IMF, star formation rate and efficiency there are many more statistical properties that require understanding. These are, for instance, the structure of stellar clusters and stellar velocity dispersions, the properties of multiple stellar systems, jets, proto-planetary discs, and the rotation rates and magnetic fields of stars (Bate 2009). In particular, the properties of binary, triple or higher-order multiple systems such as their multiplicity fractions (MF), their companion star fractions (CSF), i.e. the average number of companions per target star, which can exceed 100 %, their distribution of mass-ratios, separations and eccentricities have a huge impact on star formation theories, since these properties and their dependence on the primary mass, age and environment should contain the imprint of the physical processes that play a role throughout the lifetime of stellar populations (Kuiper 1935) and therefore can serve as an important posteriori test for star formation theories. However, in order to be able to compare the results of different theoretical binary formation scenarios (e.g., Bonnell 1994, Stamatellos et al. 2011) or large numerical simulations (e.g., Bate 2009; 2012) empirically, it is necessary to survey binary properties of a large sample of stars and on a large-scale parameter space, utilizing different companion detection techniques, to cover all possible binary orbits and mass ratios.

From an observational point of view, there are various surveys that have been conducted during the past decades to investigate the frequencies and multiplicity properties of different stellar populations. Thereby two types of surveys are common, those limited by magnitude

and those limited by a selected volume in space. However, magnitude limited surveys are affected by an inevitable Malmquist-like bias (Malmquist 1922) and can also be affected by selection biases such as preferences for less extinct and/or more massive, i.e. brighter, targets (Duchêne and Kraus 2013), and therefore the community has shifted their attention towards volume limited surveys, preferably.

The general trend of an increasing multiplicity fraction as function of the primary mass, as it can be seen in both empirical and simulated data, is illustrated in Figure 1. The plot shows a comparison of the multiplicity fraction as a function of the primary mass for different populations between hydrodynamical simulations of more than 1250 stars and brown dwarfs by Bate (2009) and empirical data, plotted as open black squares from surveys of Close et al. (2003), Basri and Reiners (2006), Fischer and Marcy (1992), Duquennoy and Mayor (1991), Preibisch et al. (1999) and Mason et al. (1998), from left to right. Among

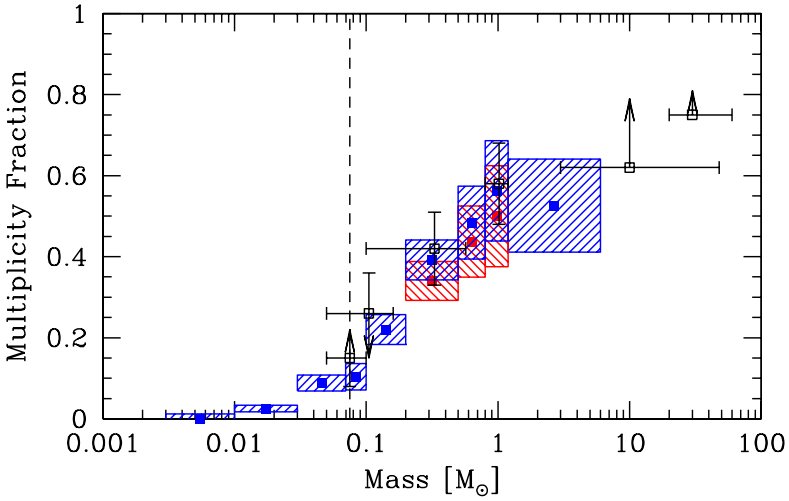


**Figure 1.** Multiplicity fraction as a function of the primary mass, reprinted from Bate (2009). The results from the hydrodynamical simulation of more than 1250 stars and brown dwarfs and their statistical uncertainties are shown as blue filled squares surrounded by shaded regions. The open black squares with error bars and/or upper/lower limits represent the observed multiplicity fractions from the surveys of Close et al. (2003), Basri and Reiners (2006), Fischer and Marcy (1992), Duquennoy and Mayor (1991), Preibisch et al. (1999) and Mason et al. (1998), from left to right. The red filled squares and associated shaded regions give the multiplicity fractions excluding brown dwarf companions ($M < 0.075\,\mathrm{M}_\odot$) to allow better comparison with the surveys of Duquennoy and Mayor (1991) and Fischer and Marcy (1992).

nearby solar-type F to G main sequence stars the first, modern survey of a volume limited sample was conducted by Duquennoy and Mayor (1991) and later revisited by Raghavan et al. (2010), yielding a multiplicity fraction of at least 50 %. For low-mass stars the investigation of M-type stars by Delfosse et al. (2004) currently represents one of the most accurate surveys, with an estimated multiplicity fraction of about 25 %. Very low-mass stars (VLM) and substellar objects also have been subject to various surveys (e.g., Burgasser et al. 2007, Reid et al. 2008). The fact that these types of objects are typically

very faint, fast rotating and the presence of broad molecular bands in their spectra, makes them difficult targets for both high-resolution imaging and spectroscopy. From a Bayesian analysis of various input surveys Allen (2007) estimated the multiplicity fraction of VLM field objects to be about 22 %. Towards higher-mass stars the VAST survey of A-type stars by De Rosa et al. (2014) and the investigations of the Scorpius-Centaurus (Sco-Cen) OB association by e.g., Kouwenhoven et al. (2005; 2007) or Shatsky and Tokovinin (2002) currently represent the most robust estimates on the multiplicity frequencies and properties for intermediate ranges of stellar masses up to $\approx 5\,M_{\odot}$. The estimated frequency of visual companion, thereby, ranges from about 37 % for the Sco-Cen OB association (Kouwenhoven et al. 2005) to about 44 % for A-type stars estimated by De Rosa et al. (2014). Interestingly, the orbital period distribution of A-type stars appears to be bimodal, contrary to lower-mass field binaries, with a peak among spectroscopic binaries around $P \sim 10\,d$ (e.g., Carquillat and Prieur 2007) and one for visual binaries around 390 au (De Rosa et al. 2014). Although high-mass galactic OB stars have been subject to numerous surveys and intensive studies during the last decades (e.g., Zinnecker and Yorke 2007; and references therein), their large distances from the Sun, large rotational velocity and the extremely high brightness contrast requirements conspire to draw an incomplete picture (Sana and Evans 2011). As a result, the range of estimated frequencies is remarkably high. For instance, the spectroscopic survey of galactic OB stars by Chini et al. (2012) yields a frequency of about 52 %, whereas Sana et al. (2012) found a bias- and completeness-corrected frequency of spectroscopic companions of about 70 %. Imaging surveys for visual companions, on the other hand, such as "all-sky" surveys (e.g., Mason et al. 2009, Turner et al. 2008) or surveys of single cluster/associations (e.g., Peter et al. 2012, Preibisch et al. 1999) yield an even broader range of frequencies and a consensus has emerged that the frequency of visual companions over two decades of projected separations is about 45 %. The best-estimate multiplicity and companion star fraction numbers, reviewed and summarized by Duchêne and Kraus (2013), are shown in Figure 2. Although incompleteness still precludes a proper functional analysis, the known dependence of multiplicity frequency as a function of the primary mass, i.e. a steep, monotonic function, is well reproduced.

Regarding their impact on the galactic chemical evolution and the physics of the interstellar medium (ISM), in particular the stars with final masses greater than about $8\,M_{\odot}$, i.e. main-sequence stars of spectral types O and B0 to B3, although low in number compared to lower-mass stars, are extremely important as they evolve to become Type II supernovae producing and ejecting a significant amount of the heavy-element material and UV radiation in the Galaxy. O and B type stars are typically very young compared to other stars with spectral type F or G, for instance, and hence most of them are found in or close to their birth environment. The heavy elements, which act as cooling agents in the interstellar gas, along with dynamical effects as a result of the UV radiation, strong stellar winds and supernova remnants are thought, in some cases, to induce the formation of a new generation of stars, while on the other hand the resulting ionization and heating can erode

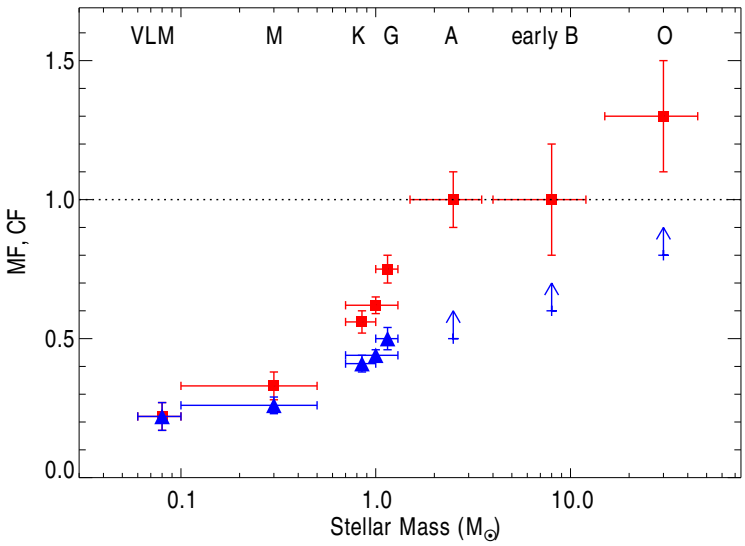


**Figure 2.** Multiplicity fraction (blue triangles) and companion star fraction (red sqaures) as function of primary mass, reprinted from Duchêne and Kraus (2013). Shown are the best-estimate numbers collected from various surveys (see text). The incompleteness of the data towards higher-mass objects is accounted by showing only the lower limits of the total multiplicity fraction found for the different populations.

nearby molecular cloud material, and hence suppress star formation. Thus, distinguishing empirically between the frequencies of binary and multiple systems in field, "runaway", or cluster/association member stars would also be very valuable in terms of understanding the dynamical interactions of these stars with their surrounding neighbourhood during their formation and evolution.

Despite the numerous surveys available for B-type stars (e.g., Hubrig et al. 2001, Oudmaijer and Parr 2010, Roberts et al. 2007, Schöller et al. 2010), most of them typically include less than 100 stars complicating a robust statistical analysis, and are largely tailored to a certain sub-sample of B-type stars showing specific features, such as Be stars or B-type stars that show high X-ray fluxes, although this is not expected. Especially the latter example can induce severe selection biases as this peculiarity might be caused by multiplicity. Additionally, most of the available surveys of B-type stars rely on unconfirmed visual companion and hence the presence of unrelated background stars in the sample might biased their results. In fact, there is no large comprehensive survey of B-type stars with sample sizes comparable to the surveys of Raghavan et al. (2010), with 454 investigated solar-type stars out to 25 pc, or the one by De Rosa et al. (2014), consisting of 435 investigated A-type stars out to 75 pc, taking into account the results of searches for spectroscopic, interferometric, visual and astrometric confirmed companions.

Therefore, this thesis was constructed to explore the frequencies and binary properties such as the multiplicity fraction, companion star fraction, mass-ratio and separation distribution, respectively, of a volume-limited sample of B-type stars located within a distance $D \leq 1$ kpc around the Sun. The examined sample consists of public available data obtained by diffraction-limited, near-infrared imaging with NAOS-CONICA (NaCo) at the

10 m class Very Large Telescope (VLT), located at the Paranal desert in Chile. Alongside the search for previously unknown or unpublished companions in the VLT/NaCo archive data, additional observations (2nd epoch imaging) have been obtained during this study using NaCo in order to confirm or reject the identified companion candidates employing a common proper motion analysis. As one goal of this thesis also is to fully characterize the multiplicity status of all the investigated B-type stars, the results of this survey are finally combined with the outcome of various observation techniques, as each of them is tailored to a certain type of companion.

While spectroscopy is limited to companion at small separations, i.e. periods of less then about 3000 days, and higher mass companions ($q = M_{\mathrm{sec}}/M_{\mathrm{prim}} > 0.1$), interferometry is capable of detection of companions at larger separations up to a few hundred milli-arcseconds. However, this method is limited by the reachable contrast sensitivity, e.g., for bright B-type stars low-mass companions of spectral type G or later are hardly detectable. A powerful technique that can help to fill in the gap in coverage, between high-angular resolution and contrast sensitivity at the same time, are observations obtained using adaptive optics (AO). In combination with large telescopes, such as the VLT, AO imaging is well suited to cover a large separation range from about 0.1 arcsec to several arcsec, i.e. depending on the distance of the star, about 10 up to several thousands of astronomical units, hence orbital periods of a few years up to centuries. Along with its high-angular resolution, down to the diffraction limit of the telescope, AO systems also provide an increased contrast sensitivity, as they are operated in near-infrared wavelength ranges. Whereas stellar objects of solar mass, or higher, are well detectable in both wavelength ranges, optical and infrared, due to their large total luminosity, the situation is different for lower-mass stellar or even sub-stellar objects. According to Wien's displacement law ($\lambda_{\mathrm{max}} \approx 2898\,\mu\mathrm{mK}/T_{\mathrm{eff}}$), the radiation maximum of these objects is shifted towards infrared wavelengths with decreasing surface temperature. Hence, low-mass objects are much easier to detect in the infrared part of the spectrum rather than in the optical wavelength range. The dependence of the absolute brightness as function of the stellar mass in the optical $V$ band ($\lambda \approx 0.55\,\mu\mathrm{m}$) and the near-infrared $K$ band ($\lambda \approx 2.19\,\mu\mathrm{m}$) is exemplary illustrated in Figure 3. The graph was compiled from evolutionary tracks by Bressan et al. (2012) for an age of 100 Myr. The plot demonstrates that the brightness, in particular those of low-mass objects, increases by several orders of magnitude in the $K$ band compared to the $V$ band ($\approx 8$ mag at $0.1\,\mathrm{M}_{\odot}$ and 100 Myr), but it also shows that the brightness difference between a low-mass stellar or sub-stellar object and a more massive primary, such as a B-type star, is much lower in the near-infrared compared to the optical wavelength range, and thus significantly simplifies the detection of lower mass companions and consequently also systems with "extreme" mass-ratios ($q \ll 0.1$).

The structure of this thesis is as follows. In chapter 2 a brief overview on stellar formation and evolutionary processes as well as a summary of the currently discussed processes involved in the formation of binaries and higher-order multiple systems, such as fission, tidal

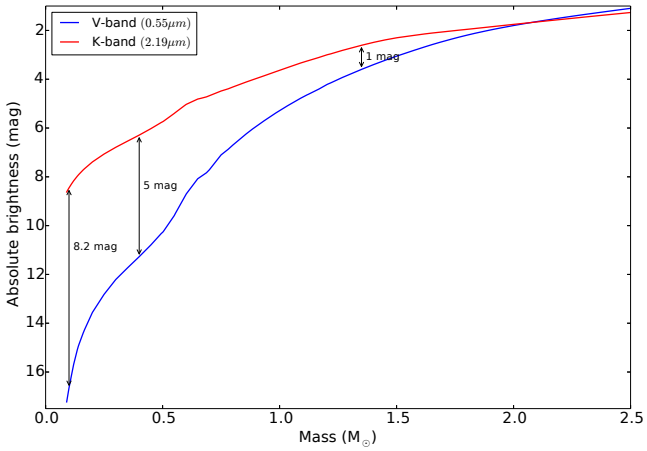


**Figure 3.** Absolute brightness as function of stellar mass for optical ($V = 0.55\,\mu m$; blue solid line) and near-infrared ($K = 2.19\,\mu m$; red solid line) wavelengths compiled from evolutionary tracks by Bressan et al. (2012) for an age of 100 Myr. The magnitude difference between the wavelengths increases towards lower masses e.g., 8.2 mag for $M = 0.1\,M_{\odot}$. While stellar objects are well detectable in both wavelengths, very low-mass stellar or substellar objects can only be detected in the infrared wavelength range.

capture or fragmentation, is given. In chapter 3, the general properties of the selected volume limited sample of B-type stars and data acquisition are characterized, followed by a detailed description of their reduction and astrometric calibration in chapter 4. Therein a special point is made to the calibration of those sample data without known astrometric calibration and an alternative approach for the estimation of the pixel scale and the detector orientation is introduced. The data analysis is presented in chapter 5, including object identification, astrometric and photometric analysis of companion candidates found, estimation of physical parameter of both, primary and companion, as well as the analysis of the multiplicity status of each object, either by common proper motion or on a statistical base. The limitations on the observed sample and a completeness estimation of this survey are described in chapter 6. The results are then given and discussed in chapter 7 and conclusively summarized in chapter 8.

# 2 Theoretical and physical background

Stellar evolution is subject to a vast number of books, publications and reviews (e.g., Bodenheimer 2011, McKee and Ostriker 2007, Shu et al. 1987, Zinnecker and Yorke 2007), and therefore this chapter is intended to give only a general, summarized overview on the current state of research on star formation and evolution, focused, in particular on the processes before the star reaches the main-sequence.
Star formation and evolution involves several time scales which have an important bearing such as the nuclear, free-fall or thermal time scale, also known as Kelvin-Helmholtz time scale and their disparity is one of the reasons why stellar evolution and structure is quantitatively predictable in large parts. The most important time scales involved in stellar evolution and star formation are therefore firstly introduced and briefly characterized in subsection 2.1.1. In subsection 2.1.2, a compendious description of the three major phases of early stellar evolution – star formation involving molecular clouds or cloud fragments, the protostellar collapse and the pre-main-sequence contraction – is given. As the primary focus of this thesis is the multiplicity of stars, the suggested formation mechanisms of binary and multiple systems, such as fragmentation, fission or tidal capture, are highlighted in section 2.2.

## 2.1 On the formation and evolution of stars

### 2.1.1 Time-scales

Star formation includes a vast range of length and times scales. For instance, the size of molecular clouds, the birthplace of stars, is typically measured in parsec, while the size of the end products, the stars, is measured in solar radii typically, which are several order of magnitude smaller. A notable length scale, in this regard, is the so-called "Jeans length", i.e. the critical radius of a cloud where thermal energy is counteracted by gravitational energy.
However, in particular the time scales have an important bearing as each of them is representative for the different phases of stellar evolution. The range of the time scales involved thereby is quite impressive, varying from seconds up to several Gyr for the main sequence lifetime of stars, i.e. the time-scale on which a star converts its hydrogen to helium by nuclear fusion. The time scales described below can be ordered in the following way:

$$t_{\mathrm{N}} \gg t_{\mathrm{KH}} \gg t_{\mathrm{ff}},$$

where $t_{\mathrm{N}}$ is the nuclear time scale, $t_{\mathrm{KH}}$ is the Kelvin-Helmholtz time scale and $t_{\mathrm{ff}}$ is the free-fall time scale, respectively.

*Nuclear time scale*

The nuclear time scale $t_{\mathrm{N}}$, sometimes also called development time, describes how long a star can sustain the conversion of hydrogen into helium by nuclear fusion in its core. It can be readily estimated from the total amount energy available from fusion ($E_{\mathrm{N}}$) divided by the amount of energy radiated away in a certain period of time by the star, i.e. its luminosity $L$, and hence

$$t_{\mathrm{N}} = \frac{E_{\mathrm{N}}}{L}.$$

The amount of energy released from fusion $E_{\mathrm{N}}$ is given by $E_{\mathrm{N}} = f\epsilon Mc^2$, where $f$ is the fraction of mass that is converted by fusion, $\epsilon$ is the efficiency of the matter-energy conversion, $M$ is the total mass of the star and $c$ is the speed of light. For the sun, about 10 % of its total mass are available for fusion and the matter-energy conversion efficiency is 7 % and thus

$$t_{\mathrm{N}} = \frac{f\epsilon Mc^2}{L} = \frac{0.007Mc^2}{L} \approx 1 \times 10^{10}\,\mathrm{years},$$

or in terms of solar units

$$t_{\mathrm{N}} \approx 1 \times 10^{10}\,\mathrm{years} \left(\frac{M}{M_\odot}\right) \cdot \left(\frac{L}{L_\odot}\right)^{-1}.$$

In combination with the mass-luminosity relation for main-sequence stars $L \approx M^4$ for $M < 10\,\mathrm{M}_\odot$ the so-called main-sequence lifetime $t_{\mathrm{MS}}$ can be estimated by

$$t_{\mathrm{MS}} \propto \frac{1}{M^3}. \tag{2.1}$$

As a consequence of the strong dependency on the stellar mass, a massive star with $M = 10\,\mathrm{M}_\odot$ has a main-sequence lifetime of only 10 Myr, whereas a low-mass star with $M = 0.1\,\mathrm{M}_\odot$ remains on the main-sequence for 10 trillion years, i.e. much longer than the current age of the universe with about 13.7 Gyr.

*Kelvin-Helmholtz time scale*

The Kelvin-Helmholtz time scale $t_{\mathrm{KH}}$, also known as potential or thermal time scale, refers to the contraction phase of a protostellar object, i.e. an object with star-like properties, when the object has heated up to a point where gas pressure can support it in equilibrium against gravity, but nuclear fusion as source of energy is not yet available. At this point in time, the only source of energy of a star that can be radiated away in a certain amount of time is its gravitational or thermal energy. A slow contraction phase, in near hydrostatic equilibrium, begins and the corresponding time scale on which the star can meet its luminosity on

expense of the gravitational energy $E_G = GM^2(1/R)$ is in the order of

$$t_{KH} \simeq \left|\frac{E_G}{L}\right| \simeq G \cdot \frac{M^2}{RL},$$

where $G$ is the gravitational constant[1], $M$ is the mass, $R$ is the radius and $L$ is the luminosity of the star. For $M = 1\,M_\odot$, the contraction time to the point where nuclear reactions are established is about $3 \times 10^7$ yr. In terms of solar units the Kelvin-Helmholtz time for any other star can then be simply estimated by

$$t_{KH} \simeq 3 \times 10^7\,\text{yr} \cdot \left(\frac{M}{M_\odot}\right)^2 \cdot \left(\frac{R}{R_\odot}\right)^{-1} \cdot \left(\frac{L}{L_\odot}\right)^{-1}. \tag{2.2}$$

*"free-fall" time scale*

The free-fall time scale $t_{ff}$ belongs to the dynamical time scales, and is directly related to the stability of stars or molecular cloud cores that have become unstable to collapse under gravity. In general, the dynamical time scale refers to a characteristic time for a particular change to take place, for instance, small mechanical disturbances such as flares, convection or even from in-falling comets. The free-fall time can be estimated in different ways, however all give the same result within a factor of about two and therefore a rather simple approach is given here, ignoring all dimensionless factors of order unity.
Assuming a spherical object of radius $R$ and mass $M$, the gravitational acceleration on the surface of the sphere pulling the particle towards the centre is given by

$$g_s = \frac{GM}{R^2} \approx \frac{GR^3\rho}{R^2} = GR\rho,$$

where $G$ is the gravitational constant and $\rho$ is the density with $\rho \approx M/R^3$. If it is furthermore assumed that the particle starts initially at rest and the acceleration is constant, it will reach the centre according to

$$R \approx g_s \cdot t^2.$$

Replacing $g_s$ and solving for $t$ gives the desired estimate for the free-fall time

$$t_{ff} \approx \sqrt{\frac{1}{G\rho}}. \tag{2.3}$$

For the Sun, $t_{ff}$ is in the order of half an hour and hence, the free-fall time in terms of solar units, can be approximately calculated by

$$t_{ff} \approx 30\,\text{min} \left(\frac{R}{R_\odot}\right)^{3/2} \cdot \left(\frac{M}{M_\odot}\right)^{-1/2}. \tag{2.4}$$

[1]Constant of gravitation, $G = 6.674\,28 \times 10^{-11}\,\text{m}^3\,\text{kg}^{-2}\,\text{s}^{-1}$

Given the typical density of a molecular cloud core of about 100 $H_2$ molecules per $cm^3$, the core would collapse under gravity within the free-fall time in the order of a few times $10^5$ years.

### 2.1.2 The early phases of stellar evolution

Based on the numerous observation astronomers have made it is commonly accepted that stars are formed by gravitational collapse of diffuse interstellar gas clouds or parts of them. The requirement that must be satisfied before a cloud or a fragment of a cloud can collapse and form a star is the so-called "Jeans instability", first derived by Sir James Jeans (Jeans 1928). A simple approach for an estimation of the instability requirement on a region in an interstellar cloud, including all physical relevant effects, is that the absolute value of the gravitational energy $E_{\mathrm{grav}}$ must exceed the sum of the thermal $E_{\mathrm{th}}$, rotational $E_{\mathrm{rot}}$, turbulent $E_{\mathrm{turb}}$ and magnetic energies $E_{\mathrm{mag}}$, and thus

$$|E_{\mathrm{grav}}| > E_{\mathrm{th}} + E_{\mathrm{rot}} + E_{\mathrm{turb}} + E_{\mathrm{mag}}. \tag{2.5}$$

Assuming an isothermal gas of uniform-density and considering only gravitational and thermal effects, as Sir Jeans did, the requirement for a spherical configuration of gas to be gravitational bound is given by

$$\left| -\frac{3}{5} \cdot \frac{GM^2}{R} \right| > \frac{3}{2} \cdot \frac{\Re TM}{\mu}, \tag{2.6}$$

where 3/5 refers to a uniform mass and consequently uniform-density distribution, $\Re$ is the gas constant[2], and $\mu$ is the molecular weight of the gas in atomic mass units. The equation above leads to the so-called "Jeans length":

$$R_{\mathrm{J}} = \frac{5}{2} \cdot \frac{GM\mu}{\Re T} > R_{\mathrm{cloud}}, \tag{2.7}$$

and hence, for a cloud of a given mass and temperature, the radius $R_{\mathrm{cloud}}$ must be smaller than $R_{\mathrm{J}}$ to be unstable to gravitational collapse. An alternative estimate for the Jeans length can be obtained by eliminating the mass in Equation 2.7 in favour of density and radius:

$$R_{\mathrm{J}} \approx \left( \frac{\Re T}{\mu} \right)^{1/2} \cdot \frac{1}{\sqrt{G\rho}} \approx c_S t_{\mathrm{ff}} < R_{\mathrm{cloud}}, \tag{2.8}$$

where $c_S$ is the isothermal speed of sound and $t_{\mathrm{ff}}$ is the free-fall time, described above.
The commonly used "Jeans mass", i.e. the minimum mass that a cloud of given mass ($M_{\mathrm{cloud}} = M(\rho, T)$) must have to be unstable to gravitational collapse, can be estimated eliminating $R$ in favour of the density $\rho$ from Equation 2.6, assuming again a spherical

[2] Ideal gas constant, $\Re = 8.314\,459\,8(48)\ \mathrm{J\,mol^{-1}\,K^{-1}}$

configuration, and is given by

$$M_{\mathrm{J}} = \left(\frac{5}{2} \cdot \frac{\Re T}{\mu G}\right)^{3/2} \cdot \left(\frac{4}{3}\pi\rho\right)^{-1/2} < M_{\mathrm{cloud}}. \tag{2.9}$$

Given typical values of $T$ and $\rho$ for gas, dust or molecular clouds, the minimum mass for such a cloud to be unstable to gravitational collapse varies between a few hundred up to thousands of solar masses. The fact that there are also stars with masses down to less than $1\,\mathrm{M}_{\odot}$ can be explained by the breakup of the cloud into smaller pieces, i.e. fragmentation of the cloud, whose details are briefly described in section 2.2 in connection with the formation of binary and multiple systems. Considering only gravitational and thermal energies of course only gives a very simplified picture of the collapse of a molecular cloud and for a complete physical description the effects of rotation, turbulence and magnetic fields need to be taken into account.

There are at least three different scenarios, that are currently discussed to play a role in star formation theory, and by which the cloud core is bought to the onset of star formation. The first is magnetically controlled star formation. The criterion for the collapse in the presence of a magnetic field is often expressed as a critical mass-to-flux ratio:

$$\left(\frac{M}{\phi}\right)_{\mathrm{crit}} = \frac{0.17}{\sqrt{G}}, \tag{2.10}$$

where the constant depends on the details of the geometry. If pre-stellar cores are magnetically sub-critical, i.e. the ratio of the actual value $M/\phi$ to the critical value is less than one or, in other words, they have less mass than the magnetic Jeans mass, they can contract in quasi-equilibrium, and bring the densest central regions to the point of collapse through the process of ambipolar diffusion. The related time scale $t_{AD}$ can be estimated by

$$t_{AD} \approx 4 \times 10^6\,\mathrm{yr} \left(\frac{n_{\mathrm{H2}}}{10^4\,\mathrm{cm}^{-3}}\right)^{3/2} \left(\frac{B}{30\,\mu\mathrm{G}}\right)^{-2} \left(\frac{R}{0.1\,\mathrm{pc}}\right)^{2}, \tag{2.11}$$

where $n_{\mathrm{H2}}$ is the density of neutral molecular hydrogen, $B$ is the magnetic field and $R$ is the radius of the cloud core. Given typical values the required time scale to produce cloud cores in this picture is relatively long, about 10 free-fall times, but it can be shortened if turbulence is present and there are local strong compressions of material. The main problem here is that most, but not all, cores have been observed to be supercritical, in which case ambipolar diffusion will still occur but will not control the star formation rate.

A second possible scenario is turbulence controlled star formation, meaning that in supersonically turbulent regions, shocks of various strengths can compress randomly located regions to high enough density for long enough times so they become Jeans unstable and begin to collapse. On more global scales, on the other hand, the turbulence is the primary mechanism that supports most molecular cloud regions against gravitational collapse. The time scale for star formation in the turbulence picture is in the order of 1 Myr, which can

explain numerous observations. Despite this advantage, there are some problems in regard of this scenario such as the requirement of very special properties of the turbulence to obtain reasonable efficiencies of star formation, or that turbulences decays on the time scale of one crossing time, which requires a mechanism that can continuously regenerate it. A third possible scenario by which the cloud core is bought to the onset of star formation is the induced ("triggered") star formation. In this scenario an intrinsically stable to collapse interstellar cloud can be compressed by some external agent, resulting in a reduction of their Jeans mass to a point where they are forced into collapse. Such external "triggers" can be galaxy-galaxy mergers as well as the galactic spiral arms on large scales, and smaller scale processes induced by supernova shock waves, expanding HII region, by cloud-cloud collisions, or the sweeping up of dense shells and clumps of gas by massive-star winds. The time scale for triggered star formation is given by the shock crossing time and can be as short as $10^5$ yr. Although there is some evidence that induced star formation has occurred, it is still thought, however, that only a small fraction of the observed star formation rate can be accounted by induced processes.

The second phase of early stellar evolution, the protostellar phase, starts when the mass of the core of a molecular cloud exceeds the thermal Jeans mass, and other physical processes such as magnetic forces, turbulences and rotational effects have become dynamically unimportant. The protostellar collapse can be basically divided into three phases, an isothermal collapse, an adiabatic collapse and an accretion phase, which are described here in the spherical case. The physical description of protostellar collapse, thereby, is based on some initial conditions for a spherical protostar in a molecular cloud core, such as an isothermal core at $T \approx 10\,\mathrm{K}$, a mass of about 1 to a few solar masses, a radius of 0.05–0.1 pc, and the form of the density distribution, which could be uniform, a power-law with $\rho \propto r^{-n}$ or a Bonnor-Ebert sphere (Bonnor 1956, Ebert 1955) with a flat density distribution in the centre, but approaching $\rho \propto r^{-2}$ in the outer regions.

At the beginning of the isothermal phase, when the opacity $\kappa$ from dust grains is below $1\,\mathrm{cm^2\,g^{-1}}$, the density $\rho$ is about $10^{-19}\,\mathrm{g\,cm^{-3}}$ and the size $R$ is about $10^{17}$ cm, the optical depth $\tau \approx \kappa\rho R$ is much less than 1, and thus the energy released by contraction is radiated away almost freely and the temperature remains approximately isothermal a 10 K over several orders of magnitude increase in density. The time scale for the isothermal phase is given by the the free-fall time, which falls in the range $1\text{–}2 \times 10^5$ yr assuming the standard initial conditions from above. The approximate in-fall rate of material during this phase is given by $\dot{M} \approx M_{\mathrm{core}}/t_{\mathrm{ff}}$, or $\dot{M} \approx \text{const.} \times c_S^3/G$, where $c_S$ is the speed of sound and $G$ is the gravitational constant. For the isothermal sphere ($T_{init} = 10\,\mathrm{K}$) the in-fall rate $\dot{M}$ is roughly constant in time at a typical value of $2 \times 10^{-6}\,\mathrm{M_\odot/yr}$ (e.g., Larson 1969, Shu 1977).

Spherical collapse, with the temperature fixed in time and space, is governed by the equation of motion of mass elements, mass conservation and the isothermal equation of state. These equations are sufficient to specify the solution for $\rho$, $r$, and $P$ as function of $(m, t)$,

whereat the solution is subject to the inner boundary condition $m = 0$ at $r = 0$ and the outer boundary condition that either the pressure is constant in time or that the radius is fixed with zero velocity at the outer surface.

One possible solution was obtained numerically by Larson (1969), starting from near the Jeans limit for an isothermal sphere of $1\,M_\odot$ and initially uniform density, and therefore uniform free-fall time. Even in this case the inner region increase their pressure relative to the surface value, which is constrained by the outer boundary condition. Thus, a pressure gradient is set up and the rarefaction wave generated at the boundary of the region that has this gradient propagates inwards at the speed of sound relative to the velocity of the in-falling material. In the limit of long times the result is a very centrally condensed configuration with $\rho \propto r^{-2}$ outside a central plateau indicating that the collapse evolves towards a steady state, with a constant mass accretion rate of material, at any radius, into the density peak. Once the gradient in pressure and density is established, the collapse is no longer a true free-fall, and the evolution becomes far shorter in the central regions than in the outer regions.

Another possible solution was obtained by Shu (1977), assuming a singular isothermal sphere with a power-law density distribution profile $\rho \propto r^{-2}$. In this scenario the dynamical time is shortest at the centre, and thus the collapse begins there and the rarefaction wave spreads outwards rather than inwards at the speed of sound. This situation is known as "inside-out collapse". The accretion rate in this scenario is approximately constant with time and similar to the value obtained by Larson (1969) as long as the $r^{-2}$ profile is maintained. Please note that at later phases of the collapse, on scales smaller than $10^{14}$ cm, this profile changes.

Once the optical depth in the central regions exceeds unity, which corresponds to a density of about $10^{-13}\,\mathrm{g\,cm^{-3}}$, the isothermal approximation no longer holds, because the energy released by the compression of the gas can no longer be radiated freely by the dust. The heating of the gas, thus results in a temperature gradient, and it rapidly becomes optically thick, because opacity increases with temperature. After a short period of readjustment due to excitation of the rotational degrees of freedom in the $H_2$ molecules, the collapse approaches an adiabat. During this phase the photo diffusion time scale is longer than the free-fall time ($t_{\mathrm{diff}} > t_{\mathrm{ff}}$), and hence the radiation released from the material is not able to escape but is carried along with the in-falling material. The radiative diffusion time scale (Shu 1991), representing the time for photons to diffuse by random walk over a distance $\Delta r$ in a medium with Rosseland mean opacity $\kappa_R$, is given by

$$t_{\mathrm{diff}} \approx \frac{3\kappa_R \rho (\Delta r)^2}{c}, \tag{2.12}$$

where $c$ is the speed of light. As heating progresses, the forces produced by the pressure gradient exceeds that of gravity, the collapse slows down and a small amount of mass in the centre approaches hydrostatic equilibrium, called the *first core*. It has a mass of $\approx 5 \times 10^{-2}\,M_\odot$, and a radius of about 5 au. Outside the core a shock wave forms at its

outer edge as the in-fall velocities become supersonic with respect to the slowly compressing core material. However, before the core has had the chance to accumulate much mass, it further contracts to a density of about $10^{-8}\,\mathrm{g\,cm^{-3}}$ and $T = 1600\,\mathrm{K}$, where $H_2$ begins to dissociate. The energy per molecule $H_2$ needed in this process is 4.48 eV, while the thermal energy of a $H_2$ molecule is only 0.78 eV. Hence most of the gravitational contraction energy can be absorbed through the dissociation of a small fraction of the total molecular hydrogen. As a consequence, the temperature rise becomes more moderate, and the pressure gradient can no longer balance gravity, leading to a second collapse in the centre of the first core. The collapse continues over several orders magnitude in density, until most of the $H_2$ is dissociated in the very centre. Due to the rapidly increasing pressure at the centre, the material in this second collapse regains equilibrium after the dissociation has completed, a second *stellar* core forms. The density at this time has increased to about $10^{-2}\,\mathrm{g\,cm^{-3}}$ and the temperature reaches about 20 000 K. The initial mass of the second core is only about $10^{-3}\,\mathrm{M_\odot}$, and most of the mass of the *protostar* is still in the outer isothermal regions, at densities of $10^{-18}$–$10^{-19}\,\mathrm{g\,cm^{-3}}$. The second (stellar) core again develops a shock front at its edge, with a radius of only a few $R_\odot$, by which it gradually builds up to become a star. This third phase of protostellar evolution, the accretion phase, involves the collapse of the remaining protostellar material onto the second (stellar) core. During this phase the total energy irradiated from the protostar can be written as

$$L = L_{\mathrm{int}} + L_{\mathrm{acc}}, \tag{2.13}$$

where $L_{\mathrm{int}}$ is the energy released from the interior of the gravitational collapsing core, and $L_{\mathrm{acc}}$ is the accretion luminosity generated by the in-fall kinetic energy of the material falling into the accretion shock at the outer edge of the stellar core. Assuming that all the in-fall kinetic energy per unit mass into the core is converted to radiation in the shock, $L_{\mathrm{acc}}$ can be estimated by

$$L_{\mathrm{acc}} \approx \frac{GM_{\mathrm{core}}}{R_{\mathrm{core}}} \cdot \dot{M} \tag{2.14}$$

For a low-mass star with a core of $0.5\,\mathrm{M_\odot}$ at $3\,\mathrm{R_\odot}$ and $L_{\mathrm{int}} = 1\,\mathrm{L_\odot}$, typical of the main accretion phase, the thermal contraction time of the core is about 3 Myr, while the accretion time scale $t_{\mathrm{acc}} = M_{\mathrm{core}}/\dot{M}$, for such a core, is about $2 \times 10^5\,\mathrm{yr}$. Thus, in this case, the accretion time is much smaller than the contraction time of the core and because the core is compressed adiabatically, only little radiation escapes from the interior. The result is that $L$ is almost completely supplied by $L_{\mathrm{acc}}$. If this inequality is reversed, which is the case for higher-mass stars, the star evolves through the Hertzsprung-Russell diagram while accreting and $L \approx L_{\mathrm{int}}$. The energy released at the shock front then propagates outward on the diffusion time scale which now becomes much shorter then the accretion time. Thereby it first passes an optically thin region just ahead the shock. Farther out, the radiation is

absorbed, re-radiated and thermalized in the optically thick dusty in-falling region. The outer edge of this region, where the dust optical depth is unity, known as dust photosphere, represents the "visible" surface for a distant observer. For a given frequency $\nu$ the dust photosphere occurs at an inward integrated optical depth $\tau_\nu = \int \kappa_\nu \rho dz = 2/3$, where $z$ is the distance inward from the edge of the protostar. Typical temperatures for this region range from 100 to 300 K, hence the observable radiation lies in the infrared wavelength range. Calculations for the main accretion phase show that the radius of the shock front remains nearly constant at 2–3 $R_\odot$. The radius of the dust destruction front, the region where the temperature is high enough to evaporate dust (roughly 1500–2000 K) also remains nearly constant at about 1 au but dependent on the accretion rate. The "mean" photosphere, however, averaged over frequency, is located at about 10 au for typical parameter, because its radial position is strongly dependent on frequency.

When accretion has come to an end and a large fraction of the gas is fully ionized, the pre-main-sequence (PMS) phase begins, and the star starts a slow contraction towards the main-sequence, in near hydrostatic equilibrium. The characteristic time scale for this phase is the *Kelvin-Helmholtz* time $t_{KH}$, whose length is in the order of a few $10^7$ yr for a solar mass star. At this point the mass accretion rate $\dot{M}$ for low-mass stars drops to very low values (typically $\dot{M} \lesssim 10^{-7}\,M_\odot/yr$), and the stellar mass remains practically fixed. The stellar luminosity, i.e. the energy released during this phase, is dominated by the gravitational energy ensured in the contraction while the energy generated from the accretion of material becomes negligible. At this point in their evolution the protostars become optical visible in the Hertzsprung-Russell diagram (HRD) on a well defined line, the "birth-line" (e.g., Stahler and Palla 2005).

Theoretical calculations of the pre-main-sequence evolution show that a star of a given mass first passes through a convective phase while evolving towards the main-sequence, known as Hayashi track (Hayashi 1961). It is defined as the locus in the HRD where a star of given mass and radius is fully convective, depending on its mass, composition and the opacity in the radiative surface layer. The region to the right of the Hayashi track is "forbidden" for stars of given mass in hydrostatic equilibrium, at any phase of evolution, including the red giant phase. However, objects which are not in hydrostatic equilibrium, such as variable stars or contracting protostars, can exist in this forbidden region.

During the convective phase, energy transport in the interior is very efficient, and the rate of energy loss is controlled by the thin radiative layer at the stellar surface, the photosphere. The opacity in the relatively cool photosphere is a strongly increasing function of the temperature, mainly due to $H^+$ and molecules. The increase in the radiative opacity forces the radiating surface farther away from the inner boundary, causing the effective temperature to remain almost unchanged. As the surface area decreases, the luminosity drops and $T_{eff}$ stays nearly constant between 2000–4000 K. Upon further contraction of the star, the interior temperature increase and in most of the star the opacity decreases as a function of $T$. Once the adiabatic gradient $\bigtriangledown_{ad}$ starts to exceed the radiative gradient $\bigtriangledown_{rad}$, the

star becomes stable against convection, gradually forming a radiative region starting at the centre. When this region includes about 75 % of the total mass, the rate of energy release no longer is controlled by the photosphere, but rather by the opacity of the entire radiative region. The evolutionary path towards the main-sequence, during this radiative phase, is known as Henyey track (Henyey et al. 1955), along which the temperature increases rapidly while the increase in luminosity is relatively moderate as the star contracts.

The pre-main-sequence evolution times of a star, as already mentioned, starting at the birth line, depends on its mass. For instance, the total pre-main-sequence time for a star of $1\,M_\odot$ is about $4 \times 10^7$ yr. During this time, the star spends about $10^7$ yr on the Hayashi track. For the next $2 \times 10^7$ yr, the star is primarily radiative, evolving along the Henyey track. The final $10^7$ yr of the contraction represents the transition to the main-sequence. During this phase the contraction slows down as the primary energy source switches to nuclear reactions starting at the centre and the luminosity declines slightly. In case of masses below $1\,M_\odot$ the convective phase begins to dominate the evolution towards the main-sequence and stars of $0.3\,M_\odot$ and less remain fully convective all the way to the main-sequence, which, for instance, takes a star of $0.1\,M_\odot$ about $10^9$ yr.

For higher-mass stars the situation is different. They actually can reach the main-sequence before the accretion phase has ended, and hence the mass at which the star arrives at the main-sequence depends on the accretion rate. The time scale for a high-mass star to reach its final mass is therefore best estimated from the accretion time, which, for instance, is $5 \times 10^5$ yr for a final mass of $5\,M_\odot$ accreting at $10^{-5}\,M_\odot/\mathrm{yr}$.

An observational classification of early stellar evolution, from the earliest phase to its end on the Zero-Age-Main-Sequence (ZAMS) was introduced by Charles J. Lada in 1987 (Lada 1987, Lada and Kylafis 1999). His original classification of young stellar objects (YSO's) contains three classes, overlapping the protostellar collapse phase and the pre-main-sequence contraction, and is based on the spectral energy distribution (SED) longward of 2 µm. Later, this classification was complemented with a Class 0 (Andre et al. 1993), which appear to correspond to protostars at an even earlier evolutionary phase than that represented by Class I objects. One criteria for Class 0 is that the mass of the envelope is greater than the mass in the central hydrostatic region. Their SED is comparable to a black-body with temperatures of 15–30 K and a peaks near 100 µm. Class I objects, on the other hand, have less mass in their envelope than in the central regions. These objects, also known as "embedded" IR-sources or candidate protostars, have SED which are broader than that of a single black body and peak at far-infrared or submillimeter wavelengths. For Class II sources the SED is broader than that of a single black body with a significant continuum excess emission in the UV and IR. The shape of the infrared portion of Class II SED's suggests that the infrared excess arises in an optically thick circumstellar disk. This class of objects is observable in the optical and they are often called T Tauri stars (TTS) in case of low-mass stars ($M < 1.5\,M_\odot$), or *Herbig-Ae/Be* stars (see e.g., Herbig 1960) in case of intermediate mass stars with spectral type mid-B to late A ($1.5\,M_\odot < M < 8\,M_\odot$),

respectively. Class III objects, finally, have a spectrum close to that of a black body of single temperature and show little or no evidence for excess IR radiation or dust. These class of objects are supposed to be either young main-sequence (MS) stars or weak line T Tauri stars (WTTS; Herbig and Bell 1988), without indications of an optically thick disk.
Above the idealized case of the spherical symmetric collapsing protostar was described. It is clear, however, that this rather simple model is not consistent with the observations of most protostars, and hence additional effects must be included. In particular the effects of rotation is crucial and needs to be considered as there is a requirement of significant transfer of angular momentum out from the material that eventually ends up in the star. There are various physical processes operating at different phases of stellar evolution that can contribute to the solution of the angular momentum problem such as magnetic braking in the molecular cloud phase, the formation of disks and binaries or multiple systems during protostellar collapse and stellar winds, gravitational or magneto-rotational instability after the disk has formed.
Disc evolution may be divided into a formation stage, a viscous stage and a disk dispersal (clearing) stage. In the first stage, which lasts about 2–5 $\times$ $10^5$ yr, the disk structure is build up from the in-fall of material from the protostellar cloud and observationally this stage may be identified with Class 0 and Class I sources. Also, the initial mass of the disk may be relatively high, so that it already becomes gravitationally unstable right after formation and can undergo a rapid process of mass accretion onto the central star. In the second stage, known as viscous stage, the angular momentum in the disk is redistributed due to internally generated torques, for example, those arising from turbulent viscosity in the presence of a magnetic field. The disk then evolves, with both accretion of matter onto the star and the spreading of the outer regions of the disk, while the disk is still accreting gas from molecular cloud core. The lifetime of this stage is approximately $10^6$-$10^7$ yr and usually identified with Class II objects, which exhibit a photo-spheric spectrum along with infrared excess due to the dust emission in the disk. During the final clearing stage the disk either is blown away by the action of irradiation from the central star or external sources, blown away by a stellar wind, accreted onto the star, accumulated into protoplanets, or disrupted by external encounters. For a more detailed description of disk evolution and the processes by which the disk can disappear see for instance Bodenheimer (2011).

### 2.1.3 Formation of high-mass stars

The evolutionary processes described above refer to the early evolution of stars with masses around 1 $M_\odot$, and although there is no sharp distinction between the formation of massive stars, with masses above 8 $M_\odot$, and low-mass stars, there are significant differences between the two cases. First, for massive stars $t_{KH}$ is less than the accretion time of the envelope ($t_{acc} \propto M/\dot{M}$), and thus the core can reach the main-sequence while accretion from the surrounding envelope is still ongoing. Second, the protostellar evolution time is not much different between high-mass and low-mass stars, and thus the mass accretion

rate $\dot{M}$ of high-mass stars must be significantly greater than that of low-mass stars, and third, when the massive stellar core approaches the main-sequence, radiative acceleration in the in-falling envelope, arising from radiation interacting with the dust, becomes more important than gravity, while in low-mass star formation gravity always dominates in the in-falling envelope.

There are basically two models which are under ongoing debate regarding the formation mechanisms of massive stars, namely the monolithic collapse (core accretion) and the competitive accretion (Bonnell et al. 1997; 2001). Here only a summarized overview is given, and for a more detailed review of massive star formation see e.g., Bodenheimer (2011), Tan et al. (2014), Zinnecker and Yorke (2007).

In the monolithic collapse picture, supersonic turbulences in molecular clouds, in a region that is overall stable to gravitational collapse, produces occasional high-density fluctuations which can form molecular cloud cores of $\sim 0.1\,\mathrm{pc}$ size and then collapse as single, perhaps as binary, massive star. Thus, in this model, fragmentation occurs first, then collapse, and there is only little interaction between cores once they have formed. This picture has several consequences, which turn out to be in good agreement with observations. First, the initial mass function (IMF) is essentially already determined by the process of fragmentation of the cloud clump to form cores, and hence the observed core mass function should be very similar to the observed IMF (e.g., Beuther and Schilke 2004, Motte et al. 1998). Second, the fact that the cores in this model are non-interacting suggests that the star formation efficiency in a given clump should be relatively low, i.e. only a small fraction of the clump actually evolves to cores that are gravitationally unstable (Zuckerman and Evans 1974). And third, in young systems, the spatial and velocity distribution of young stars and cloud cores should be similar (Krumholz and Bonnell 2009).

The competitive accretion model otherwise is based on the premise that massive star formation is controlled by the overall collapse of a much larger region, containing initially gas with several thousand solar masses. Thus, in this picture, the overall collapse occurs first, then the fragmentation into a cluster of stars, containing high-mass and low-mass members, takes place. Individual fragments do form at low mass and compete for the remaining gas, and also there can be dynamical interactions between the various cloud fragments. This model also implies the formation of a massive star in the centre, since as the cloud collapses and develops a gravitational potential well, a significant amount of gas can be funnelled towards the centre, and in fact it is observed that massive stars are found to be preferentially located near the centre of cluster. However, it is not clear whether they have formed there or if they have settled to the centre after formation as a result of dynamical interactions with other surrounding stars.

The major advantages of the competitive accretion model are, first, that it considers the massive star formation problem in the context of cluster formation. Second, it is able to predict an initial mass function also consistent with observations, if the physical effects of radiative feedback and magnetic fields, both of which tend to suppress fragmentation, are

taken into account. And third, it can be used to explain the observed properties of binary and multiple systems. Whether this process or the monolithic model dominates is yet to be worked out, but the structure of the observed molecular clouds could account for both possibilities.

## 2.2 The formation of binary and multiple systems

Observational studies of stars and their properties obtained in the last years indicate that the majority of stars are formed in binary or multiple systems and also that they form very early in the history of a star. The challenge from the theoretical point of view is to explain observational facts such as the non-negligible occurrence of multiple systems, the present day overall binary frequency and its variation with primary mass and the distributions of period, eccentricity and mass ratio among the individual binary. In addition to that, observations show that most of the stars are formed in clusters and the complicated interactions between stars and between stars and gas, respectively, require massive numerical simulations (e.g., Bate 2009) to account for the details of binary properties deduced from observations. However, the range of input parameter is wide and the results often depend sensitively on them. Thus, the theory is not yet at a point where it can fully explain the observed variety of binary properties. Furthermore there remain significant physical effects to be explored, such as feedback on the cloud from outflows and radiation from the stars that have been formed (Krumholz et al. 2005). Also the role of magnetic fields in regulating the protostellar collapse and fragmentation phase must be explored in more detail. In particular the formation of close binaries with periods of only a few days and separations of only a small fraction of au is still a major issue.
The main binary formation mechanism which are currently under study and summarized in the following are fragmentation occurring either in a collapsing cloud or as a result of disk instability, capture and fission.

*Fragmentation and disk instabilities*

Fragmentation which basically refers to the breakup of a rotating protostar during the hydrodynamical collapse phase, was originally proposed by Hoyle (1953). He simply argued that an isothermal collapsing cloud, originally unstable on a large scale, can become dynamically unstable on progressively smaller scales because the density increases during collapse, i.e as the density increases and the temperature remains nearly constant, the thermal Jeans mass decreases. However as pointed out by Low and Lynden-Bell (1976) there is a lower limit to fragmentation due to the fact that once the centre of the cloud becomes optically thick, the temperature, and consequently the Jeans mass, starts to increase. Various theoretical calculations show that, depending on the dust opacity, the lower limit to the mass of a fragment is at about 7 to 10 Jupiter masses.

Fragmentation can occur in various forms such as during the collapse of an isolated, rotating, low-mass core, producing a binary or a small multiple system with separations ranging from 100–1000 au, or as fragmentation of a higher-mass core, leading to the formation of a small cluster and a much wider range of binary properties.
The results of such numerical calculation indicate that fragmentation during a rotating collapse is most likely the dominant mechanism in the formation of binary and multiple systems. A variation of the fragmentation process is triggered fragmentation by cloud-cloud collisions (Pringle 1989) with the angular momentum of the orbit arising from the initial condition of an off-centre collision. A numerical calculation of such a collision was done for instance by Kitsionas and Whitworth (2007) in which the outcome was a single star with a circumstellar disk. However, only a slight change in the initial condition, an increase in the relative velocity of the two clouds from $1\,\mathrm{km\,s^{-1}}$ to $2\,\mathrm{km\,s^{-1}}$, already results in the formation of two protostars of nearly same mass with circumstellar disks, which later capture each other into a binary with a circumbinary disk (Kitsionas et al. 2008).
Finally, disks that form around young stars itself can become gravitational unstable and possibly fragment, under the right conditions (Adams et al. 1989) and can produce stellar mass secondaries or possibly giant planets if the disk is massive and cool enough and if the Toomre $Q$ parameter (Toomre 1964) is $\approx 1$. This parameter is as indicator of gravitational instability and it is given by

$$Q = \frac{\kappa c_S}{\pi G \Sigma}, \tag{2.15}$$

where $\Sigma$ is the surface density and $\kappa$ is the so-called epicyclic frequency, which reduces to $\kappa = \Omega$ for Keplerian rotation. If $Q$ is less than one, the material is locally unstable to an axisymmetric gravitational perturbation resulting in a dense ring-like configuration. An other basic requirement, however, for a disk to fragment is that the cooling time has to be comparable or shorter than the orbital time (Gammie 2001), because otherwise in fact the disk will heat up as result of the instability and remain stable to fragmentation.

*Capture*

The capture process, in general, requires some mechanism of energy dissipation. This process was first suggested in 1867 by Stoney (see Aitken 1935), although Laplace (see Tassoul 1978) already proposed in 1796 that binaries may form from separate stellar nuclei during star formation and that this nuclei then somehow came into orbit. However, the physics behind this picture never was fully explained and therefore it might be only assumed that the nuclei are combined by capture.
Capture of two independently formed star into orbit in principle is possible through mechanisms such as, first, three-body capture, i.e. a third body is present to take away excess energy, producing wide separations, or second, if the encounter of the stars is close enough so that energy is taken away by tidal dissipation. This two-body tidal capture produces

very close separations. A third mechanism due to which two independently formed stars can come into orbit is the presence of a dissipative medium such as residual gas, ambient in a newly forming cluster or in form of a circumstellar disk. This process produces separations comparable to the disk outer radius. Considering only the processes of three-body capture and two-body tidal capture, the expected capture rates in the galactic disk or in even young dense cluster have been shown to be far too slow to explain the observed binary frequency (Boss 1988). Although the presence of residual gas could change the picture, capture occurs only in a limited range of circumstances (Clarke and Pringle 1991), because stellar encounters with disks could also result in truncating or ejecting the disk.
Given typical distances in the galactic disk capture is unlikely under normal circumstances and therefore its role must be investigated through detailed numerical simulations of cluster formation where fragmentation could produce protostars with typical separations that are close enough for captures to occur. Although N-body simulations of interacting point masses indeed can result in capture, the results of such simulations have shown that they are extremely sensitive to changes in the initial conditions and that a wide variety of orbital parameter and eccentricities is possible. In addition to that, the gas plays a very important role in actual cluster formation, so the capture process must be simulated by full three-dimensional hydrodynamic calculations as, for instance, done by Bate et al. (2002). However, the description of the results of such simulations in regard of the capture process is complicated, because other processes are active as well.

*Fission*

The third process, fission, is quite distinct from fragmentation, as it occurs in configurations which are assumed to be already in hydrostatic equilibrium, while fragmentation refers to the breakup of a rotating protostar during the hydrodynamical collapse phase. Historically, fission is attributed to Kelvin and Tait in 1883 (Tassoul 1978) and was strongly advocated by Jeans (Jeans 1928).
Assuming conservation of angular momentum a star tends to spin up, as it accumulates gas during the protostar collapse, or as it contracts towards the main sequence after disk accretion has been completed, i.e. the ratio $\beta$ of the rotational energy to the absolute value of the gravitational energy increases. When $\beta$ obtains a critical value, the star becomes unstable to non-axialsymmetric perturbations and it is hypothetically possible that then a breakup into orbiting sub-condensations occurs which would produce close binaries, because only a small amount of angular momentum can be stored in a star.
The process of fission, however, has some major problems as pointed out by Tassoul (1978), for instance. First, the observed rotation rate of T Tauri stars is very slowly, and thus they have far too little angular momentum to reach a point of secular or dynamical instability. Second, the required binary mass ratio of $\sim 1:10$ by angular momentum considerations is in disagreement with observations. If the result of fission were a system with comparable

masses, and if conservation of angular momentum is assumed, the stars would overlap in space. Third, even if the critical $\beta$ for dynamical instability were reached, numerical calculations in fact show that an initially axisymmetric object deforms into a triaxial configuration. However, fission does not occur due to the transfer of angular momentum out from the core by spiral waves, so that $\beta$ is reduced below the critical value.

# 3 Data Sample and Acquisition

For the investigation of the frequency of multiple B-type stars, the distribution of their separations and mass ratios, and the search for unknown companions, this thesis utilizes data obtained in a dedicated observation program at the Very Large Telescope at the European Southern Observatory (ESO) in Chile, as well as publicly available archive data. In section 3.1 the used instrument and its characteristics are briefly described. The details of the selected target sample are characterized in section 3.2. The properties of the data taken from the public archive and the new observations are discussed in section 3.3.

## 3.1 NAOS-CONICA at the ESO Very Large Telescope

This thesis is focused on data obtained with the **N**asmyth **A**daptive **O**ptics **S**ystem (NAOS) and the **CO**udé **N**ear **I**nfrared **C**amera (CONICA). NAOS-CONICA, or short NaCo, is currently mounted at the Nasmyth A focus of the Unit Telescope 1 (UT1) "Antu". From 2001 through 2013 it was installed at the Nasmyth B focus of UT4 "Yepun", one of the four 8.2 m telescopes of the ESO/VLT located at Cerro Paranal, near Antofagasta in the Chilean Atacama desert. The instrument is briefly described below. Detailed information on NaCo and its on-sky performance can be found in Girard et al. (2010), Lenzen et al. (2003), or Rousset et al. (2003).

The adaptive optics (AO) system NAOS is equipped with two wavefront sensors of the Shack-Hartmann type[3], one operating in the visible (0.45–1 µm) and one in the near-infrared (0.8–2.5 µm) wavelength range. The measured wavefront distortions, due to the effects of atmospheric turbulence, are used to calculate real-time corrections of the wavefront which are then applied via a tip-tilt mirror and a deformable mirror, containing 185 actuators. NAOS also contains 5 dichroic filters which split the incoming light from the telescope between one of the NAOS wavefront sensors and the CONICA detector. One of the main characteristics for the achieved image quality is the Strehl ratio. It basically corresponds to the percentage of light contained in the diffraction-limited core of a source relative to its total flux. For good seeing conditions ($\lesssim 0.8$ arcsec) and a sufficiently bright ($V \leq 10$ mag), nearby point-like reference source (up to 55 arcsec) the Strehl ratio can be as high as 50 % in the K band (Girard et al. 2010).

The adaptive optic NAOS is operated together with the infrared imager and spectrograph CONICA and was equipped with an InSb Aladdin 3 array[4] of 1024×1026 pixels during May 2004 and September 2013. The detector is sensitive to wavelengths from 0.8 µm to 5.5 µm and capable of imaging, spectroscopy, polarimetry and Sparse Aperture Masking

[3] A Shack-Hartmann wavefront sensor is an array of lenses (lens-lets) focused on a CCD array, which allows measurement of the focal position on the sensor for each lens. From this the local tilt of the wavefront can be determined and used for corrections.

[4] Since the recommissioning in December 2014 on UT1, the CONICA detector has been replaced with an Aladdin 2 array from the ISAAC instrument.

observations. The optical path of the instrument includes several wheels which can be selected depending on the used observation mode. Among others there are wheels containing polarizers, grisms, the different filter, e.g., *JHK*s broad band, or narrow band (NB) and intermediate band (IB) filter, respectively, and the various camera objectives. Each camera has a corresponding field mask with a characteristic plate scale, field of view (FoV), and selectable filters summarized in Table 1. NaCo also offers different readout and detector

**Table 1.** Characteristics of the used cameras of CONICA.

| Camera | Pixel Scale (mas/pixel) | FoV (arcsec$^2$) | Filter | Spectral Range (μm) |
|---|---|---|---|---|
| S13 | 13.221±0.017 | 14×14 | *JHK*s, *NB*, *IB* | 1–2.5 |
| S27 | 27.053±0.019 | 28×28 | *JHK*s, *NB*, *IB* | 1–2.5 |
| SDI+ | 17.250±0.060 | 8×8 | *H* | 1.6 |

**Notes.** Scale and relative errors for S13 and S27 were measured by B. Sicardy using Pluto's motion against field stars, using an accurate Pluto ephemeris. The 1-sigma errors were obtained by $\chi^2$ tests, with stellar trails.

modes. The readout mode defines the read-out sequence, e.g., *Double_RdRstRd*, i.e. that the array is first read than reset and read again. The detector mode refers to the array bias voltage; the well depth and the number of hot pixel are directly related to it. The readout mode is chosen depending on the background. For observations in the IR, the sky background becomes high and variable compared to observations in the optical. The sky background below ∼2.2 μm is dominated by OH emission that originates at an altitude of ∼80 km, whereas at longer wavelengths the thermal background of the atmosphere and the telescope dominates. The standard practice which is mostly used for *JHK*s observations with the S13 or S27 camera, is the jitter or, more precisely, the dither technique. This imaging technique basically consists of taking several images with small offsets in the telescope position between each exposure. These offsets are typically in the order of a few arc-seconds. The sky background is then estimated from the combination of all observations.

Alongside the observation modes using the dither technique, NaCo offers more exclusive imaging modes such as Simultaneous Differential Imaging (SDI, Marois et al. 2000, Racine et al. 1999). SDI exploits the fact that extra-solar giant planets have strong CH4 (methane) absorption beyond 1.62 μm in the near-infrared (NIR) *H* band atmospheric window. By obtaining 4 simultaneous images through 3 slightly different filters sampling both inside and outside the CH4 feature, the limiting Speckle-noise floor can be significantly suppressed allowing the detection of very faint planetary-mass companions at close separations to the primary star.

## 3.2 The Data Sample

The investigated sample of B-type stars was constructed from a volume limited set of stars selected from the *Hipparcos* catalogue (ESA 1997, van Leeuwen 2007) and on declinations

that can be observed at the ESO/VLT in Chile. The first, temporary sample of stars with spectral type B was limited to objects within 1000 pc, corresponding to a *Hipparcos* parallax of $\pi \geq 1$ mas, and declinations below +45 degree. In particular, no selection on binarity or brightness was applied.

This resulting list of 7386 possible target stars was then matched with publicly available "IMAGING" data from the ESO-VLT NaCo archive, yielding data-sets for 316 B-type stars, with at least one observation, obtained with S13, S27 or SDI in *J*, *H*, *K*s band, or with *NB* or *IB* filter, respectively. The spectral type of the B-type sample stars was matched with the available spectral classifications by Skiff (2014) and updated with the most recent value, if notwithstanding from the spectral type given in the *Hipparcos* catalogue (ESA 1997, van Leeuwen 2007).

In addition to the spectral type, parallax and proper motion, the optical *B* and *V* magnitudes from Kharchenko (2001) and near-infrared *JHK* magnitudes from the 2MASS All-sky Catalog of Point Sources (Cutri et al. 2003) were collected for each target and listed in Table 2. The full list for all sample stars can be found in Table A1, attached to the appendix.

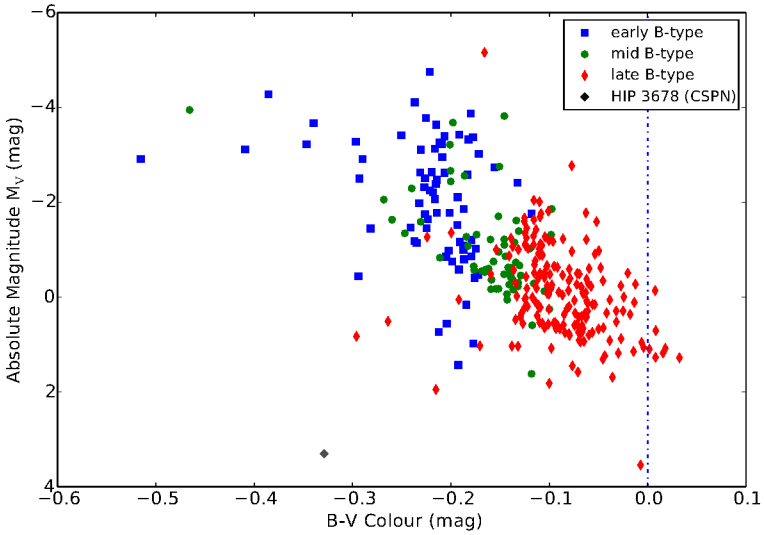


**Figure 4.** The colour–magnitude diagram of the volume limited sample of B-type stars observed with NaCo at the ESO/VLT in Chile. The investigated sample stars are shown coloured and shaped by their reported spectral class. The intersection between B and A-type main sequence stars according to Kenyon and Hartmann (1995) is indicated by the blue dashed line. Correction for interstellar extinction was applied using the estimated *V* band extinction values $A_V$ according to the procedure by Schmidt et al. (2014).

Figure 4 shows the positions of the target stars in the colour-magnitude diagram (CMD). The $(B - V)$ colours listed in Table 2 were taken from the *Hipparcos* catalogue and the absolute *V* band magnitudes were calculated from the given apparent *V* band magnitudes and distances for each target. The plotted magnitude and colour values for each star of the sample were corrected for interstellar extinction in the *V* band $A_V$.

**Table 2.** B-type star target sample information. The full overview is presented in Table A1.

| HIP | Spectral[a] type | Plx (mas) | $\mu_\alpha \cos\delta$ (mas/yr) | $\mu_\delta$ (mas/yr) | $B$ (mag) | $V$ (mag) | $J$ (mag) | $H$ (mag) | $Ks$ (mag) | Age (Myr) | ≈Mass ($M_\odot$) | 2MASS sources[c] (arcmin$^{-2}$) |
|---|---|---|---|---|---|---|---|---|---|---|---|---|
| 145 | B6V | 7.18±0.3 | 19.1±0.29 | -9.67±0.16 | 5.005±0.002 | 5.12±0.002 | 5.399±0.019 | 5.453±0.043 | 5.438±0.019 | 80±9 | 4.0 | 0.115 |
| 377 | B8IV/V | 5.7±0.24 | 29.78±0.23 | -12.85±0.19 | 5.486±0.002 | 5.584±0.003 | 5.775±0.018 | 5.835±0.032 | 5.822±0.026 | 152±9 | 3.4 | 0.196 |
| 1191 | B9V | 9.63±0.39 | 23.65±0.43 | -7.8±0.2 | 5.695±0.004 | 5.756±0.003 | 5.929±0.026 | 5.972±0.037 | 5.94±0.017 | 182±75 | 2.5 | 0.104 |
| 1830 | B9 IV | 5.79±0.47 | 22.04±0.48 | 3±0.42 | 6.491±0.004 | 6.553±0.004 | 6.635±0.019 | 6.645±0.02 | 6.656±0.017 | 146±25 | 2.7 | 0.103 |
| 2548 | B9.5V | 12.35±0.55 | 31.9±0.8 | 4.1±0.8 | 5.686±0.003 | 5.693±0.002 | 5.677±0.037 | 5.681±0.039 | 5.637±0.019 | 1139±93 | 2.0 | 0.117 |
| 3678 | B0 (PG1159)[b] | 2.12±3.01 | -18.1±1.9 | -9.8±1.9 | 11.47±0.01 | 11.769±0.01 | 12.612±0.057 | 12.795±0.029 | 12.869±0.029 | 200±10 | 0.8 | 0.102 |
| 3741 | B9Va | 9.51±0.77 | 24.5±0.8 | -11.2±0.8 | 5.514±0.002 | 5.559±0.004 | 5.647±0.026 | 5.686±0.026 | 5.644±0.02 | 210±58 | 2.5 | 0.097 |
| 5778 | B8IV HgMn metallic lines | 7.17±0.44 | -29.8±0.8 | -24.3±0.8 | 5.876±0.003 | 5.958±0.004 | 6.065±0.024 | 6.21±0.028 | 6.212±0.016 | 84±26 | 3.2 | 0.149 |
| 10602 | B6V | 21.22±0.12 | 92.5±0.9 | -24±0.9 | 3.453±0.002 | 3.546±0.002 | 4.026±0.298 | 3.95±0.261 | 4.126±0.268 | 58±12 | 4.0 | 0.119 |
| 13951 | B8 V | 9±0.43 | -5.62±0.5 | -22.11±0.51 | 5.493±0.008 | 5.543±0.004 | 5.688±0.032 | 5.686±0.024 | 5.664±0.02 | 87±26 | 3.2 | 0.120 |
| 14131 | B9V | 6.34±0.2 | 26.2±0.7 | 14.6±0.7 | 5.38±0.002 | 5.5±0.003 | 5.761±0.026 | 5.863±0.027 | 5.837±0.026 | 282±8 | 3.1 | 0.197 |
| 15627 | B5III | 6.41±0.73 | 25.7±1.1 | -25.2±1.1 | 5.225±0.008 | 5.306±0.004 | 5.388±0.028 | 5.439±0.017 | 5.436±0.02 | 44±8 | 4.4 | 0.210 |
| 16511 | B9IV | 9.31±0.38 | 31.38±0.39 | -48.67±0.31 | 5.69±0.003 | 5.75±0.003 | 5.809±0.02 | 5.894±0.028 | 5.881±0.017 | 126±37 | 2.7 | 0.172 |
| 16803 | B9Vp lambda Boo | 6.7±0.51 | 28.5±0.7 | -10.3±0.7 | 5.123±0.004 | 5.236±0.004 | 5.459±0.018 | 5.563±0.048 | 5.526±0.024 | 297±22 | 3.1 | 0.128 |
| 17563 | B3V | 6.11±0.29 | 21.3±0.9 | -13.8±1 | 5.236±0.003 | 5.335±0.003 | 5.541±0.048 | 5.625±0.05 | 5.592±0.02 | 13±10 | 5.9 | 0.169 |
| 17921 | B9IVpHgMnSi sn | 8.86±0.42 | 23.73±0.4 | -44.68±0.34 | 6.06±0.004 | 6.067±0.004 | 5.967±0.018 | 6.051±0.061 | 5.975±0.02 | 113±39 | 2.6 | 0.289 |
| 18213 | B6/7 V | 9.42±0.22 | 32.12±0.17 | -0.92±0.22 | 4.969±0.002 | 5.092±0.002 | 5.39±0.024 | 5.446±0.037 | 5.454±0.017 | 36±12 | 3.7 | 0.130 |
| 18788 | B5V | 7.88±0.27 | 27.84±0.32 | -14.32±0.31 | 5.138±0.003 | 5.269±0.003 | 5.57±0.024 | 5.647±0.028 | 5.662±0.02 | 29±10 | 4.0 | 0.164 |
| 19720 | B8Vn | 7.56±0.81 | 22.49±0.92 | -23.94±0.76 | 6.272±0.004 | 6.243±0.007 | 6.046±0.02 | 6.041±0.041 | 6.028±0.019 | 83±24 | 3.2 | 0.219 |
| 19860 | B3IV | 7.16±0.34 | 19.73±0.31 | -22.04±0.27 | 4.217±0.004 | 4.28±0.003 | 4.684±0.252 | 4.413±0.035 | 4.433±0.034 | 54±10 | 6.0 | 0.218 |
| : | : | : | : | : | : | : | : | : | : | : | : | : |

**Notes.** The age estimates and associated errors are rounded to nearest integer value. The mass estimates are given without error as a matter of clarity.

[a] Most recent spectral type as given in the Catalogue of Stellar Classifications (Skiff 2014)

[b] HIP 3678 is a white dwarf and the central star of the planetary nebula NGC 246, a hierarchical triple found in this study.
The actual suggested spectral type of HIP 3678 A is PG1159 (Lamontagne et al. 2000).

[c] Total number of 2MASS point sources within a $2^\circ \times 2^\circ$ box surrounding each sample star scaled to one square arc minute.

The applied values of $A_V$ for each target were taken from the procedure created by Schmidt et al. (2014), which was used to calculate the stellar parameter, i.e. mass and age of the primary stars. A detailed description of the procedural method can be found in section 5.4. The vast majority of the stars included in this sample have $(B-V)$ colours consistent with the expected colour range of B-type stars (e.g., Kenyon and Hartmann (1995), $(B-V) < 0.0$ mag).

Generally, the obtained extinction values $A_V$ vary depending on distance, position on sky, or due to the presence of a circumstellar disk between zero mag and up to $\approx 4.5$ mag in the $V$ band. However, the interstellar extinction is wavelength dependent with decreasing values towards longer wavelengths. In particular, for the near-infrared (NIR) data studied in this thesis, the interstellar extinction reduces to only about 10 % of its value in the visible wavelength. The median extinction of the target sample is about 0.1 mag in the $V$ band, and hence, the interstellar extinction in the NIR is roughly 0.01 mag. This is negligible compared to the large distance uncertainties for instance. However, the interstellar extinction was considered in all calculations.

HIP 3678 (black diamond in Figure 4), the central star of the planetary nebula (CSPN) NGC 246, was found within the compiled sample marked as B0-type star. The analysis of this object revealed HIP 3678 to be a hot white dwarf multiple system with one known visual and a previously unknown companion first identified and confirmed by common proper motion, hereafter donated with CPM, during this study. A more detailed description of this object is given in section 7.1.

The distributions of spectral types and luminosity classes for the total sample of B-type stars, except of the CSPN HIP 3678, are shown as a histogram in Figure 5. The sample includes stars with spectral types from O9.5–B9, but most stars are mid to late B-type stars[5] with spectral types from B5 to B9. This might be a selection effect due to the brightness and distance and hence the observability of such objects.

A histogram of the distances to the sample objects is shown in Figure 6 (left panel). The shading of the histogram indicates the precision of the parallax measurements $(\sigma_\pi/\pi)$ from which the distances and, consequently, the absolute magnitudes of the primaries and any found companion were determined. Out of the total sample of 316 target stars, 107 objects have high-quality uncertainties ($\sigma_\pi/\pi \lesssim 0.05$, green histogram), 179 have moderate quality uncertainties ($0.05 \lesssim \sigma_\pi/\pi \lesssim 0.32$, blue histogram) and 30 objects show poor quality uncertainties ($\sigma_\pi/\pi \gtrsim 0.32$, red histogram). The majority of the stars were observed at distances smaller than approximately 300 pc which is most likely an effect of the target selection by the different observer, due to the increased sensitivity for binary companions at small separations for stars at closer distances. In general the distance of the targets ranged from $\sim$38 pc up to $\sim$980 pc with a median distance of about 162 pc.

[5] Historically, hot, luminous stars were thought to be at an earlier stage in their evolution than late-type stars, such as those that are cooler than the Sun. However, it is known today that their high temperature is an outcome of their high mass. In general, the term "early" is used today to describe any star that is at the hotter end of its spectral class, e.g., a B2 star is said to be earlier than a B5 star.

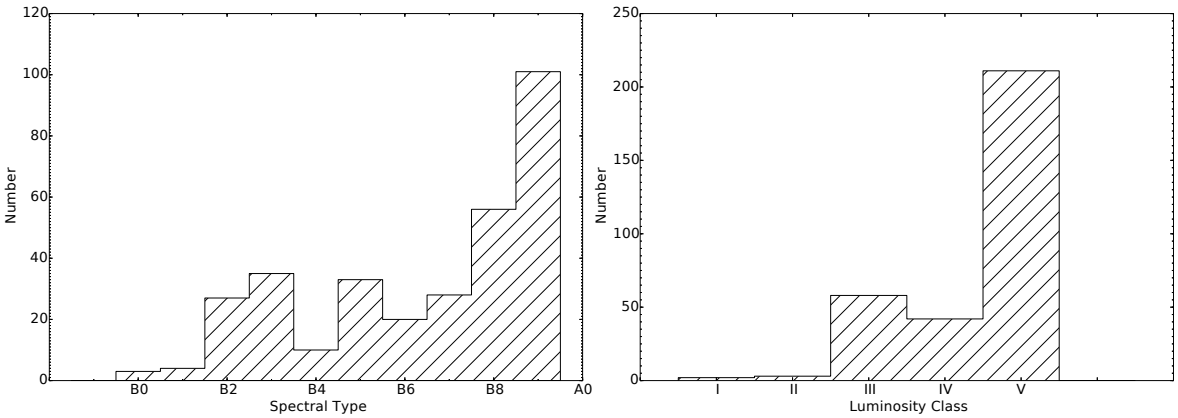


**Figure 5.** The distribution of spectral types (left) and luminosity classes (right) for all stars of the sample as reported in the *Hipparcos* catalogue.

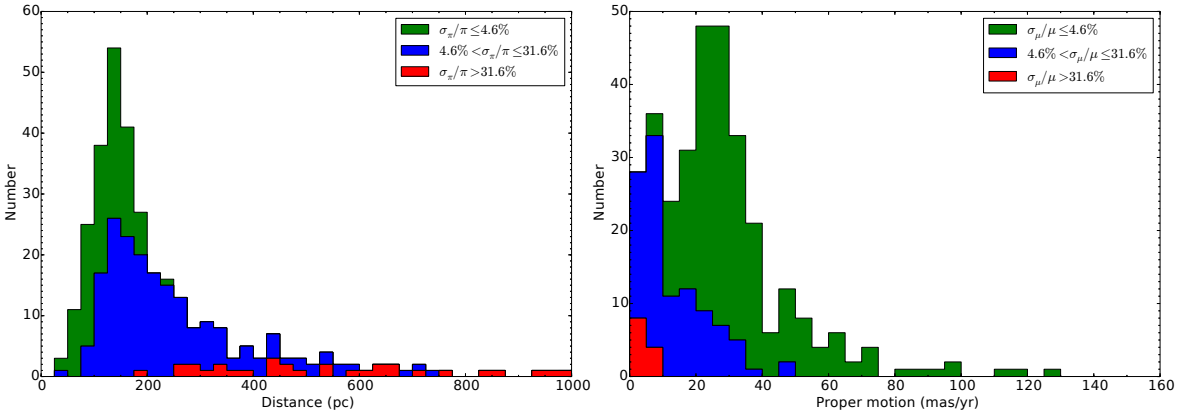


**Figure 6.** The distribution of distances (left) and apparent proper motions (right) for the 316 stars of the sample selected from the *Hipparcos* catalogue. The shading of the histogram indicates whether the relative errors of the measurements are below 4.6 % (green histogram), between 4.6 % and 31.6 % (blue histogram), or larger than 31.6 % (red histogram).

The same shading was applied to the distribution of the total apparent proper motion of the sample stars, calculated from $\mu_\alpha \cos\delta$ and $\mu_\delta$ and shown in Figure 6 (right-panel). Whereas the parallax is used to estimate the physical properties of the primary or a companion, the proper motion together with the time difference between two or more observations is needed to estimate whether a found companion candidate is physically bound to the primary or not. For 209 stars, high quality uncertainties (green histogram) of the proper motion measurements are available, 95 objects have moderate uncertainties (blue histogram) and only 12 stars from the sample have poor quality uncertainties (red histogram).

Due to the age dependence of the mass-magnitude relation, an estimation of the age is needed, in order to convert the measured magnitude difference between a B-type star primary and a resolved companion into a mass ratio for the system. The mass and age estimation for each primary target star was done using a photometry based procedure developed by Schmidt et al. (2014), described in section 5.4, with the resulting age and mass distribution of the sample shown in Figure 7. The obtained ages and masses for the primary stars are also summarized in Table 2, and Table A1, respectively. The ages

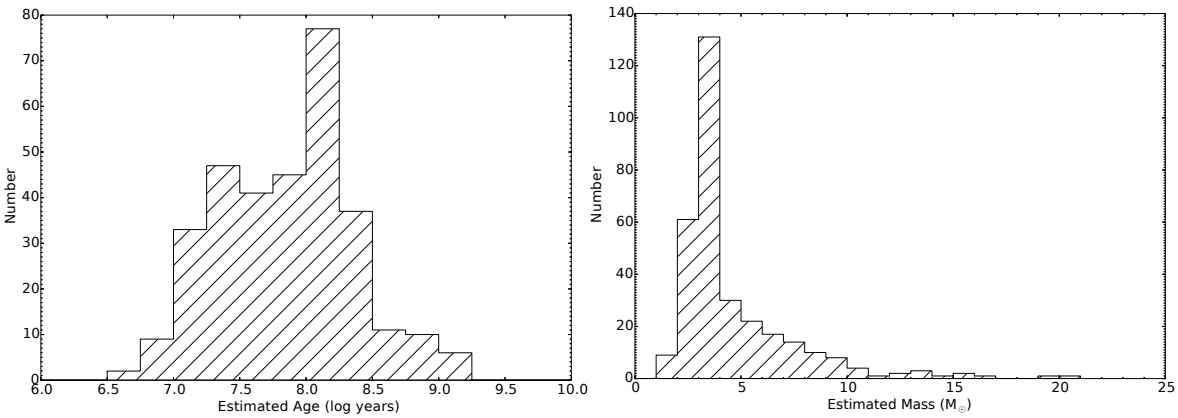


**Figure 7.** The distribution of ages (left) and masses (right) for all target star of the sample as estimated from spectral type, distance, and *BVJHK* photometry using models by Bertelli et al. (1994), Claret (2004) and Schaller et al. (1992).

estimated for the sample stars with this method range from about 3 Myr to a few Gyr, while the calculated masses of the primary stars vary between $\approx 1.8\,M_\odot$ and $\approx 20\,M_\odot$, at which 302 (90 %) of the primary stars have intermediate masses of less than $10\,M_\odot$.

## 3.3 Data Acquisition

The data obtained from the ESO VLT/NaCo archive and described below split in general into two distinct samples. On the one hand there are 133 stars with at least two epochs of observation available. These objects plus 32 stars with only one epoch, but additional data-points available from literature, are suitable for CPM analysis if one or more companion candidates can be found in each epoch. On the other hand there are 152 stars with only one epoch found in the VLT/NaCo archive. For these stars the CPM analysis can not be applied, and therefore the assessment of physical association of any companion candidate is based on a statistical estimate using 2MASS source counts. The details of this method are described in section 5.2.

Figure 8 shows the spatial distribution of the sample stars on the sky superimposed on the surface density of 2MASS point sources brighter than 14 mag in the *Ks* band. The path of the Galaxy is apparently visible showing an increase in the surface density towards the Galactic Centre ($R.A. = 266\overset{\circ}{.}416$, $Dec = 29\overset{\circ}{.}007$, Petrov et al. 2011) of $N(Ks < 14) \gtrsim 10^{-2}$ 2MASS point sources per square arc second.

### 3.3.1 Archive Data

The science data taken from the ESO VLT/NaCo archive have been observed in 221 different nights between January 2003 and February 2013. The ESO programmes in which the data were obtained, alongside the corresponding principal investigator (PI) and the number of objects observed within the programme are listed in Table 3. The programmes with new observations are marked in boldface. In total the investigated sample consists of 668 data sets and was obtained in 62 different programmes by 33 PI, including the new observations

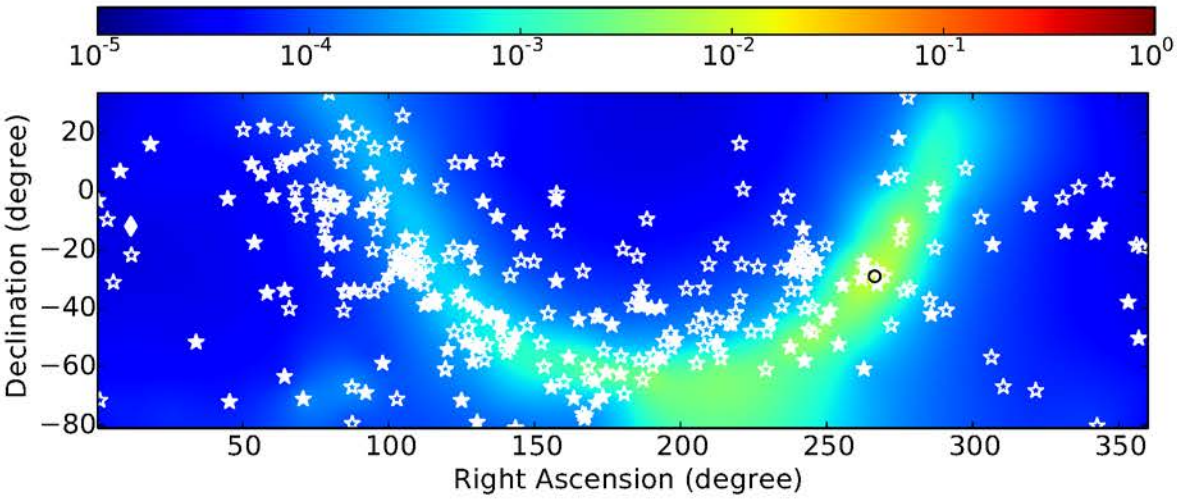


**Figure 8.** Distribution of the sample target stars throughout the celestial sphere (filled and open stars). The CPM objects are shown as filled stars, and objects for which the physical assessment is based on statistics are shown as open stars. Also shown is the surface density of 2MASS point sources with a magnitude of $Ks < 14$ mag, within an area of 1 square arc second surrounding each sample star, illustrated by the coloured surface. The path of the Galaxy through the sky is apparent, with the Galactic Centre (black circle) showing an increase in the surface density. The position of the CSPN HIP 3678 is marked by the white diamond.

briefly described in the section below. Additionally, for each data-set the corresponding calibration images, i.e., darks, sky- or lamp-flats, were obtained from the archive for the data reduction (see section 4.1). In cases where these calibration data were not available for the particular night, darks or flats which were taken in other nights, before or after the observation night, were used. The resolution limit $\lambda/D$ of the used filter in the data sample ranged from 0.026 arcsec for $NB\_1.04$ band images to 0.056 arcsec for $IB\_2.24$ band images. The measured full width at half maximum (FWHM) of the image core typically was in the order of ∼0.09 arcsec, depending on the used filter, the weather conditions in that particular night and consequently the quality of the AO correction. Given the median distance of the stars of ∼162 pc, the resolution limit corresponds to projected separations of about 15 au. Furthermore, the 668 data sets are composed of 394 sets taken with the S13 camera, 229 sets observed with the S27 camera and 45 SDI data sets. Adopting the field of view of the S27 camera with 28×28arcsec$^2$, binary systems at least as wide as ∼2200 au are detectable. Due to the dither method used for the S13 and S27 observations and the chosen jitter offset, therein the effective field of view for individual targets can be increased, making also binary systems at larger projected separations detectable. The total exposure time given is made up from the product of a single detector integration time (DIT) in seconds and the number of integrations (NDIT) used to compose a single image, multiplied by the number of exposures (NExp) taken for an object. Details on the used filter, total exposure time, camera and measured FWHM of the individual targets are given in Table 4 and Table A2, respectively, alongside the obtained calibration results and the used method described in section 4.2.

**Table 3.** Sources of ESO/VLT NaCo archive data

| Programme ID | PI | Observed stars | Programme ID | PI | Observed stars |
|---|---|---|---|---|---|
| 072.C-0624(B) | MOUILLET | 2 | 083.C-0459(A) | SCHREIBER | 1 |
| 073.C-0178(A) | FELDT | 1 | 084.C-0364(A) | VOGT | 1 |
| 073.C-0379(A) | ZINNECKER | 1 | 086.C-0600(B) | VOGT | 1 |
| 073.D-0534(A) | KOUWENHOVEN | 11 | 086.C-0638(A) | VOGT | 1 |
| 074.C-0628(A) | NEUHÄUSER | 1 | 086.C-0762(D) | DAEMGEN | 1 |
| 074.D-0180(A) | IVANOV | 61 | 087.D-0150(B) | KERVELLA | 1 |
| 074.D-0315(A) | POLLACCO | 1 | 087.D-0197(A) | SCHOELLER | 6 |
| 074.D-0374(A) | HUBRIG | 39 | **087.D-0261(A)** | **ADAM** | **15** |
| 075.C-0475(A) | OUDMAIJER | 75 | 087.D-0426(C) | MARTAYAN | 2 |
| 075.C-0521(B) | CHAUVIN | 1 | 088.D-0145(A) | DOMICIANO DE SOUZA | 1 |
| 075.C-0668(A) | DOUCET | 1 | 089.C-0494(A) | KURTEV | 1 |
| 075.D-0660(A) | DE LAVERNY | 1 | 089.C-0494(B) | KURTEV | 7 |
| 076.C-0170(A) | HUBRIG | 13 | 089.C-0494(C) | KURTEV | 4 |
| 076.C-0579(A) | BRANDEKER | 3 | **089.D-0366(A)** | **ADAM** | **19** |
| 076.C-0708(A) | THOMAS | 2 | 089.D-0800(A) | DOMICIANO DE SOUZA | 1 |
| 076.D-0108(A) | IVANOV | 47 | 090.C-0448(A) | VOGT | 2 |
| 077.D-0147(A) | IVANOV | 7 | 090.D-0038(A) | SCHOELLER | 8 |
| 077.D-0606(A) | LEAO | 1 | 090.D-0755(A) | DOMICIANO DE SOUZA | 1 |
| 078.C-0535(A) | VOGT | 2 | 184.C-0567(F) | BEUZIT | 1 |
| 078.D-0639(A) | BOUY | 11 | 272.D-5068(A) | IVANOV | 12 |
| 079.D-0537(A) | HUBRIG | 1 | 279.D-5064(A) | KERVELLA | 1 |
| 079.D-0546(A) | WERNER | 1 | 382.D-0065(A) | KERVELLA | 1 |
| 080.C-0424(A) | VOGT | 2 | 383.C-0657(A) | DREIZLER | 1 |
| 080.D-0348(A) | IVANOV | 46 | 384.D-0504(A) | KERVELLA | 1 |
| 080.D-0532(A) | BOUY | 24 | 386.D-0706(E) | DOMICIANO DE SOUZA | 1 |
| 081.C-0519(A) | PATIENCE | 3 | 482.L-0802(A) | FORVEILLE | 1 |
| 081.C-0653(A) | LAGRANGE | 3 | 485.L-0725(A) | FORVEILLE | 1 |
| 082.C-0489(A) | VOGT | 1 | 60.A-9026(A) | NACO TEAM | 6 |
| 082.D-0172(A) | KERVELLA | 1 | 60.A-9800(J) | OBSERVATORY, P | 6 |
| 083.C-0151(A) | LAGRANGE | 2 | 70.C-0701(A) | ZINNECKER | 1 |
| 083.C-0151(B) | LAGRANGE | 1 | 71.C-0507(A) | MOUILLET | 1 |

**Note.** Own observations obtained with NaCo are marked in boldface.

### 3.3.2 Own Observations

In order to increase the available sample size for the CPM analysis, two successful proposals for additional observations at the ESO/VLT of stars with companion candidates and only one prior data point, have been written during this thesis. The observations were carried out in visitor mode on 8th and 9th May 2011 under programme ID 087.D-0261(A) and on 18th and 19th September 2012 under programme ID 089.D-0366(A), with a total of 34 stars observed.

For objects with bright companion candidates, the same instrumental set-up, i.e., same filters, cameras, and exposure times, as in the first epoch were used to reach at least the achieved sensitivity as in the first observation. For fainter companion candidates, longer exposure times were chosen, without saturating the primary, for an increased sensitivity to the faint companion candidates and to increase the signal to noise ratio for any detection. In addition to the science exposures, darks, and flats, images of the wide binary system HIP 73357 or the globular cluster 47 Tuc were taken in every night, which were used for the astrometric calibration of the data. For a detailed description and discussion of this topic see section 4.2.

**Table 4.** Observation log and astrometric calibration results of the investigated target sample

| HIP | MJD (days) | Observation date | Programme ID | PI | Exposure time (s) | Filter | Camera | FWHM (mas) | Pixel scale (mas/pixel) | Orientation (degree) | Method[a] |
|---|---|---|---|---|---|---|---|---|---|---|---|
| 145 | 53349.04 | 2004-12-10 | 074.D-0180(A) | IVANOV | 2.5×10×21 | *IB*2.18 | S27 | 74.1 | 27.110±0.021 | -0.020±0.046 | A |
| | 53690.07 | 2005-11-16 | 076.C-0170(A) | HUBRIG | 1.8×40×10 | *K*s | S13 | 76.6 | 13.266±0.023 | -0.013±0.097 | A |
| 377 | 53698.02 | 2005-11-24 | 076.D-0108(A) | IVANOV | 0.3454×149×9 | *K*s | S27 | 82.0 | 27.144±0.032 | -0.009±0.060 | A |
| 1191 | 53698.05 | 2005-11-24 | 076.D-0108(A) | IVANOV | 0.3454×149×9 | *K*s | S27 | 74.8 | 27.161±0.040 | 0.042±0.088 | A |
| 1830 | 53284.15 | 2004-10-06 | 074.D-0374(A) | HUBRIG | 10.0×5×20 | *K*s | S13 | 70.1 | 13.261±0.014 | -0.000±0.057 | A |
| 2548 | 53710.05 | 2005-12-06 | 076.D-0108(A) | IVANOV | 1.0×50×9 | *K*s | S27 | 80.8 | 27.174±0.042 | -0.029±0.092 | A |
| | 54359.25 | 2007-09-16 | 080.D-0348(A) | IVANOV | 1.0×51×9 | *K*s | S27 | 85.7 | 27.160±0.055 | 0.017±0.115 | A |
| 3678 | 53331.08 | 2004-11-22 | 074.D-0315(A) | POLLACCO | 3.6×20×5 | *H* | S13 | 71.2 | 13.254±0.069 | -0.03±0.29 | A |
| | 53331.09 | 2004-11-22 | 074.D-0315(A) | POLLACCO | 6.1×20×5 | *K*s | S13 | 75.7 | 13.269±0.066 | -0.003±0.295 | A |
| | 54265.40 | 2007-06-14 | 079.D-0546(A) | WERNER | 40.0×5×15 | *K*s | S27 | 97.1 | 27.136±0.063 | -0.050±0.132 | A |
| 3741 | 53710.07 | 2005-12-06 | 076.D-0108(A) | IVANOV | 1.0×50×9 | *K*s | S27 | 79.5 | 27.127±0.038 | -0.038±0.081 | A |
| 5778 | 53285.21 | 2004-10-07 | 074.D-0374(A) | HUBRIG | 6.0×9×20 | *K*s | S13 | 72.4 | 13.263±0.020 | 0.007±0.084 | A |
| 10602 | 53710.10 | 2005-12-06 | 076.C-0170(A) | HUBRIG | 0.65×200×10 | *K*s | S13 | 83.2 | 13.276±0.019 | -0.049±0.076 | A |
| | 53712.09 | 2005-12-08 | 076.C-0170(A) | HUBRIG | 0.65×200×10 | *K*s | S13 | 70.1 | 13.264±0.019 | -0.030±0.079 | A |
| 13951 | 53358.10 | 2004-12-19 | 074.D-0180(A) | IVANOV | 0.3454×149×9 | *K*s | S27 | 84.5 | 27.092±0.040 | -0.023±0.086 | A |
| | 54370.30 | 2007-09-27 | 080.D-0348(A) | IVANOV | 2.0×26×9 | *K*s | S27 | 89.3 | 27.140±0.045 | -0.006±0.097 | A |
| 14131 | 53284.28 | 2004-10-06 | 074.D-0374(A) | HUBRIG | 3.8×4×64 | *K*s | S13 | 78.0 | 13.257±0.003 | 0.002±0.012 | A |
| | 54357.39 | 2007-09-14 | 080.D-0348(A) | IVANOV | 1.0×51×13 | *K*s | S27 | 96.0 | 27.144±0.012 | 0.013±0.026 | A |
| 15627 | 54024.21 | 2006-10-16 | 078.D-0639(A) | BOUY | 4.4×12×128 | *H* | SDI | 76.5 | 17.250±0.060 | 0.000±0.500 | U |
| 16511 | 53376.05 | 2005-01-06 | 074.D-0374(A) | HUBRIG | 3.8×13×20 | *K*s | S13 | 73.8 | 13.264±0.013 | -0.012±0.054 | A |
| | 53700.14 | 2005-11-26 | 076.C-0170(A) | HUBRIG | 1.0×60×10 | *K*s | S13 | 69.1 | 13.287±0.026 | -0.013±0.121 | A |
| | 55798.41 | 2011-08-25 | 087.D-0197(A) | SCHOELLER | 15.0×4×16 | *K*s | S13 | 85.8 | 13.268±0.015 | 0.045±0.065 | A |
| 16803 | 53379.10 | 2005-01-09 | 074.D-0180(A) | IVANOV | 10.0×5×12 | *IB*2.18 | S27 | 90.4 | 27.104±0.032 | -0.013±0.066 | A |
| : | : | : | : | : | : | : | : | : | : | : | : |

**Note.** The total exposure time is the product of DIT(s)×NDIT×NExp. The full list is presented in Table A2.

[a] Used method for astrometric calibration: A–Auto-calibration; B–Binary; C–Cluster; U–Uncalibrated

# 4 Data Reduction and Astrometric Calibration

In this section the procedures used for data reduction and the different methods for the astrometric calibration of the obtained VLT/NaCo archive data, and the observations made, are described in detail. The reduction methods for the objects observed with the S13, S27 camera or the SDI technique are characterized in section 4.1. In section 4.2 the processes for the astrometric calibration of the data using binaries and clusters are discussed. In addition the newly developed approach for the calibration of archival data obtained with NaCo is extensively described and discussed in detail.

## 4.1 Data Reduction

The imaging techniques provided by the ESO VLT/NaCo instrument require reduction through different procedures. For this purpose ESO offers several software packages which were utilized for reduction, alongside small programs written using the `PYTHON` programming language (Rossum 1995) to run and control the required processes. For the reduction of the calibration frames the ESO Recipe Execution Tool (EsoRex) was used. The science data observed with S13 or S27 were reduced using the `jitter` routine which is part of the ESO `ECLIPSE` software package (Devillard 2001). The reduction of images obtained in SDI mode follows the reduction procedure described by Biller et al. (2006).
The first step in creating the reduced science image for the analysis was the reduction of the calibration frames obtained for each science image, in the same night. Therefore, dark images with the same detector settings, i.e., same DIT, detector mode, detector window, readout mode and camera, as the science exposure were taken from the NaCo archive. Typically there are three darks from which the median master dark was constructed using the `esorex naco_img_dark` recipe. The reduced dark then contains information on the dark current of the detector array. The second important calibration frame is the flat field image from which the pixel-to-pixel variations of the detector were measured and corrected. The flats obtained from the archive for each science exposure have the same setup, i.e., filter, camera, detector readout mode, as the science image. They are typically taken as a series of lamp-on/lamp-off frames. For the reduction, the `esorex naco_img_lampflat` recipe was used. In the process of the reduction using the recipe, the median lamp-off image was subtracted from the median lamp-on frame and normalized to get the reduced flat field image.
The science images obtained with the S13 or S27 were processed using the `jitter` routine controlled by a `PYTHON` program written for this purpose. After registration of the single

images, the so called odd-even column effect[6] was removed from the images. Then the dark was subtracted from each image and the dark current corrected frame was divided by the flat image to correct the sensitivity differences between the single pixels. As mentioned, the sky background in the NIR is considerably high compared to optical wavelengths (due to the OH emission in the earth's atmosphere) and needs to be removed to be able to detect faint objects. This is achieved using the jitter technique where the telescope is slightly shifted between subsequent images and hence the star is at different positions on the detector. The used offsets are typically four to eight arc seconds.

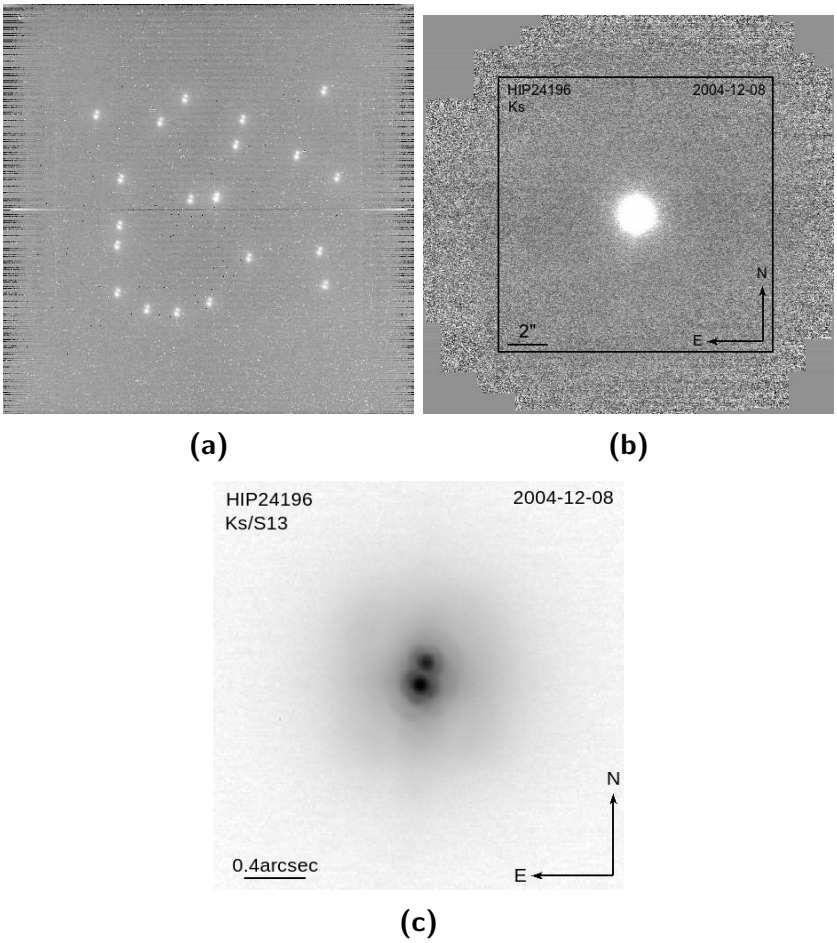


**Figure 9.** Example for the reduction of science images obtained with NaCo. Shown is the close binary system HIP 24196 observed on 8th December 2004 in *K*s band. In Figure (a) the combination of all raw images obtained for this object is shown, illustrating the effects of the jitter technique, the contamination of the image with the 50 Hz noise pattern and the cold and hot pixels from the detector. Figure (b) shows the final reduced image of HIP 24196 with slightly different cut-levels to illustrate the effects of reduction. The black box indicates the window size of a single frame (1024×1026 pixels). The effective FoV is increased compared to the single frames, making it possible to detect objects at greater distances, i.e., larger projected separations. The central region of the image with the binary companion located $\sim$ 0.15 arcsec North of the primary is shown highlighted in Figure (c).

[6]The odd-even column effect is a response property of the detector and depends on the array and the flux. It is characteristic for the pixel-to-pixel gain variations of IR arrays and varies between odd and even columns.

Figure 9a shows a combination of the 21 raw images for the close binary system HIP 24196 observed on 8th December 2004 in the $Ks$ band. Alongside the object at different jitter positions, the 50 Hz noise pattern causing regular stripes on the image, and the hot and cold pixel of the NaCo detector can be seen.

From the dark subtracted and flat field divided images, the `jitter` routine computes a median image, where the stars have been removed, and subtract that image from each frame. After removal of the 50 Hz noise pattern, the images were combined using the shift and add procedure implemented in the `jitter` routine. During this process the point spread function (PSF) of an objects is shifted typically relative to the first frame by cross-correlation, and then the images are added together to construct the final science image. In the final image the row median was then subtracted from each row to remove saturation effects. Figure 9b exemplary shows the fully reduced image of HIP 24196. The 50 Hz noise pattern was fully removed as well as almost all artefacts introduced by the detector. The window size of a single frame with typically $1024\times1026$ pixels is indicated by the black box. Also visible is the increased effective FoV due to the chosen jitter offset, which allows the detection of objects outside the FoV of a single image, i.e., at larger projected separations. In Figure 9c, the resolved close binary system HIP 24196 AB is shown for completeness.

The same procedure described above was applied to images observed in cube mode apart from the preparation of the single raw images for the reduction. In this observation mode every image taken with a specific DIT is saved separately in a cube file with $n$ planes corresponding to the selected NDIT plus one additional plane where the single DIT images are co-added. For the reduction of these data sets, the last plane of the cube which is similar to an image observed in normal mode with DIT$\times$NDIT integrations, was extracted with the `extract` routine and then reduced using the described procedure.

The data sets obtained using the SDI imaging technique required a slightly different method for reduction. The SDI data investigated in this thesis were usually observed in a sequence of $2\times20$ frames where 20 images have $0^\circ$ rotator angle and 20 images were taken with a $33^\circ$ rotator angle, to be able to distinguish between real sources and any residual speckles. This is done because instrumental and telescope "super speckles" (Racine et al. 1999) should not rotate with a change of the rotator angle; however, a real source should appear to rotate by the change in the rotator angle (Biller et al. 2006). Each sequence of 20 frames consists of 16 science images, and 4 sky frames which were used to create the master dark for sky background subtraction. A `PYTHON` program was written to control the reduction process using again the ESO `ECLIPSE` software package and in particular the `catcube`, `average`, `extract`, and `jitter` routines therein. The following procedure (except the flat reduction) was applied separately for each sequence.

For each data set, the flats with the corresponding instrument set-up were obtained from the archive and the master flat was created using the `naco_img_lampflat` recipe. This is possible due to the fact that the lamp-flat calibration frame also contains the four simultaneously observed sub-images like the science frames. The master darks for each sequence

were created from the sky images taken in each series by constructing a cube file containing the sky images using the `catcube` routine. The cubes were then linear averaged along its z-axis with the `average` routine. Next, the darks were subtracted from each science frame and the resulting corrected image was divided by the normalized flat to obtain a single reduced science image which contains the 4 frames simultaneously observed through 3 narrow band filters. Using the `extract` routine, a rectangular aperture around each filter frame was extracted and finally the single images for each filter were co-added using the `jitter` routine.

## 4.2 Astrometric Calibration

In order to convert the measured separation and position angle of identified companion candidates from pixel into on-sky units, an astrometric calibration is needed. A widely-used method to obtain the pixel scale and the detector orientation is using astrometric measurements obtained from either a binary system or a cluster, which were observed with same instrument settings and observing technique as the science targets. The details on this method are described in subsection 4.2.1. However, since there are no informations about calibration objects observed for most of the investigated sample stars in this thesis, a new method was developed to obtain pixel scale and detector orientation using the science data itself for calibration. This different approach is extensively described in subsection 4.2.2.

### 4.2.1 VLT/NaCo data calibration using binary/cluster

*Calibration with HIP 73357*

For astrometric calibration of the own VLT/NaCo observations taken in 2011 and 2012, the wide binary system HIP 73357 and the globular cluster 47 Tuc, respectively, were imaged in every observing night. Thereby, the same instrument settings, i.e. filter, camera, read-out and detector mode, and imaging technique as the science targets were used. Furthermore, the public archive was searched for additionally available data yielding 5 extra nights for HIP 73357 and 4 nights for 47 Tuc. In order to monitor possible short term variations in the pixel scale or the detector orientation, and to check for consistency of the overall calibration results, an astrometric calibration of all these data was done.
HIP 73357 is located at a distance of 102.25 pc (van Leeuwen 2007) from the Sun, and both components have spectral types of mid to early A (Houk 1982). Assuming a circular orbit with a radius of about 8.4 arcsec and a total system mass of $\sim 4\,M_{\odot}$, the orbital period would be approximately 12 600 yr or shorter if eccentric, respectively. For HIP 73357 precise astrometric measurements with *Hipparcos* taken in epoch 1991.25 are available, which are listed in Table 5. The time difference between the *Hipparcos* measurement and the science data epochs is about 20 years. In the case of an circular orbit which is seen edge-on, the separation of the components would change by 2.6 mas/yr or 53 mas in $\sim 20$ yr. This

equates to a change of 3.5 pixel for the NaCo S13 camera, which is significantly larger than detection accuracy reachable with available software. In the case of an circular orbit which is viewed pole-on, the position angle (PA) would change by $\sim$0.03 °/yr or 0.6 ° in $\sim$ 20 yr. This very simple estimate, and in particular the change in separation over several years, shows that the orbital motion of this calibration binary needs to be taken into account.

**Table 5.** *Hipparcos* reference measurement of the NaCo calibration binary

| Binary | Epoch | Separation (arcsec) | PA[a](deg) |
|---|---|---|---|
| HIP73357 | 1991.25 | 8.430±0.028 | 337.30±0.06 |

[a] Position angle (PA) is measured from North over East to South.

There are 29 astrometric data points taken over the past $\sim$ 170 yr available for HIP 73357 in the Washington Double Star Catalogue (WDS, Mason et al. 2001). These data points were used to fit the linear change in separation and position angle of the binary component yielding a linear decrease in separation of $0.0018 \pm 0.0010$ arcsec/yr and a decrease in position angle of $0.0368 \pm 0.0055$ °/yr. The corresponding diagrams for separation angle and position alongside the best fits and their one sigma confidence interval are shown in Figure 10. However, WDS does not provide uncertainties for any of the given astrometric data points and hence, the results have to be taken with reservations due to the quite large scatter of the measurements. Also, the observational data, of the position angle, available since 1970 show a lower decrease than the overall result of linear orbital motion fit, indicating that the assumption of a linear orbital motion might be inappropriate. Given the available amount of data points up to date, which cover only about 1.3 % of the entire orbit it is, however, not yet possible to detect significant curvature in the orbital motion.

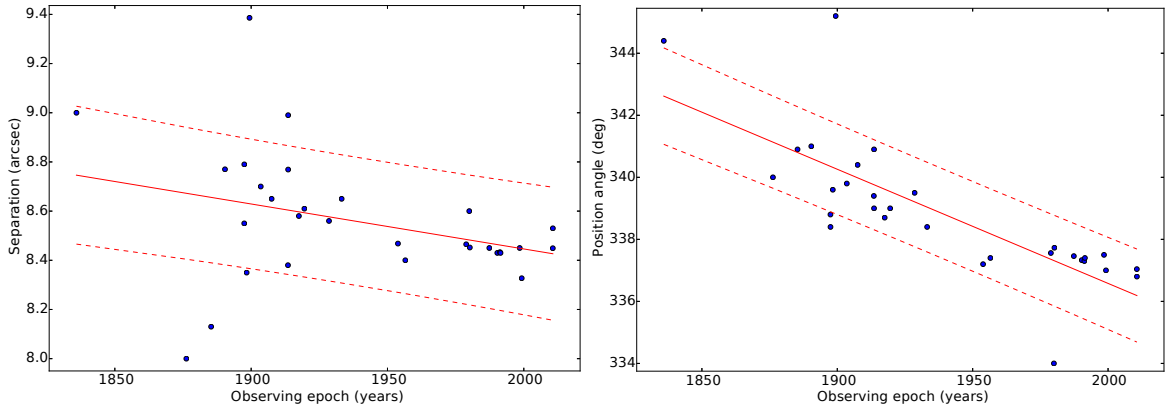


**Figure 10.** Astrometric data points for the calibration binary HIP 73357 obtained from the WDS catalogue. The solid red line shows the linear fit to the change of the separation (left) and the position angle (right) over time. The 68% ($1\sigma$) confidence interval of the fit is indicated by the dashed red lines.

To determine the pixel scale and the orientation, first the detector positions of the binary components were measured in each individual jitter position in the respective observing night, to account for geometric distortions of the detector. This was done employing the

IDL[7]/starfinder routine (Diolaiti et al. 2000), which uses a Point Spread Function (PSF) fitting algorithm to detect the sources in an image. For a more detailed description see section 5.1.The separation and position angle on the detector were then calculated for each individual jitter position and the results averaged. Using the calculated rate of change in separation and position angle, the ephemerides of the binary at the time of the science epoch were then extrapolated from the *Hipparcos* reference measurement. With this result and the measured separation and position angle on the detector in each observing night, pixel scale and detector orientation was calculated for each science epoch. The results for the pixel scale and the detector orientation are listed in Table 6. As can be seen from the data, pixel scale and orientation vary between the epoch, but are consistent within their uncertainties.

**Table 6.** Astrometric calibration results of HIP 73357 using linear orbit fit of WDS data

| Observation date | Epoch (year) | Pixel scale (mas/pixel) | Orientation (deg) |
|---|---|---|---|
| 2007-03-01 | 2007.163 | 13.202±0.044 | -0.216±0.183 |
| 2008-01-08 | 2008.020 | 13.208±0.045 | 0.085±0.185 |
| 2008-01-17 | 2008.045 | 13.210±0.045 | 0.120±0.185 |
| 2008-02-20 | 2008.138 | 13.208±0.045 | 0.074±0.185 |
| 2009-02-20 | 2009.138 | 13.200±0.046 | 0.136±0.188 |
| 2011-03-25 | 2011.229 | 13.189±0.048 | 0.309±0.195 |
| 2011-05-09 | 2011.352 | 13.190±0.048 | 0.048±0.271 |

*Calibration with the globular cluster 47 Tucanae*

The calibration of science data taken in September 2012 was done using the globular cluster 47 Tuc. The cluster, also known as NGC 104, is located near the Small Magellanic Cloud towards the constellation Tucana at a distance of about 4.7 kpc (Woodley et al. 2012) from the Sun. For this object precise astrometry data are available from the Hubble Space Telescope (HST). There are 4 additional nights with observational data available in the archive, two in December 2011 and 2012, respectively, at which this cluster was observed in the same night as target stars contained in the sample. In Figure 11, the HST/ASC image of 47 Tuc (left) and an image of the same cluster observed with NaCo in 2012 (right) is shown. Therein, the field of view of the NaCo S13 objective in the HST image is indicated by the white rectangle, and the stars employed to extract their position in the NaCo image are marked with circles.

First, an astrometric reference catalogue was created from the HST image. Therefore, the star positions were extracted using GAIA (**G**raphical **A**stronomy and **I**mage **A**nalysis Tool, Draper 2000) and the included SExtractor[8] (**S**oruce-**Extractor**, Bertin and Arnouts 1996)

[7] IDL (Interactive Data Language) is a commercial plotting, image processing, programming, and graphical user interface (GUI) development language distributed by the Research Systems Inc., Boulder CO.

[8] SExtractor is an image processing software which contains automated techniques that detects, de-blends, measures and classifies sources from astronomical images.

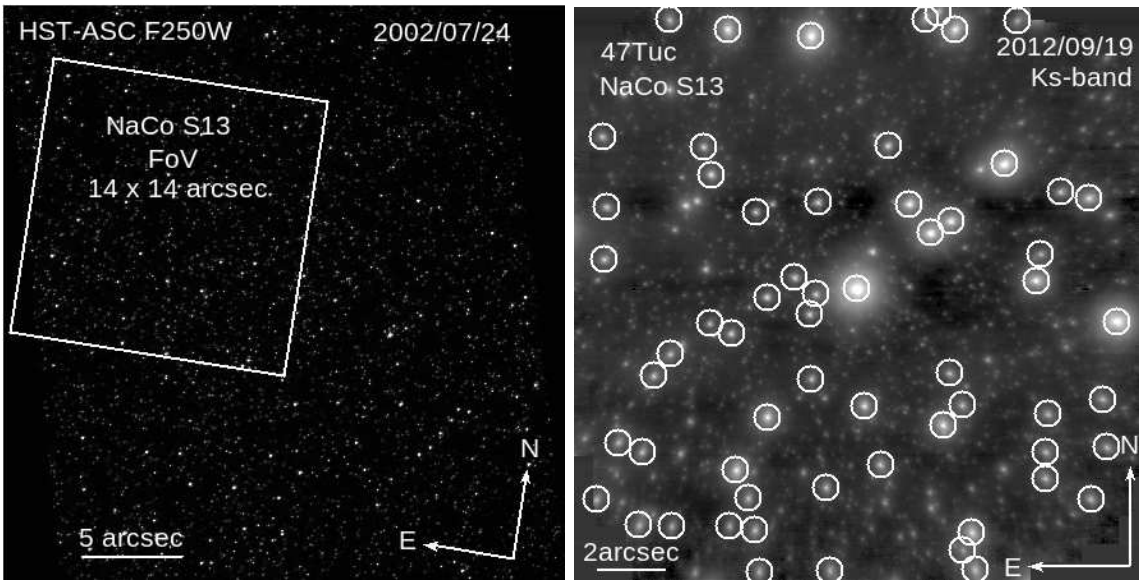


**Figure 11.** HST/ASC image of 47 Tuc (left) used as reference for astrometric calibration taken on 2002-07-24 with the F 250 W wide band filter in the ultra-violet, and exemplary VLT/NaCo *K*s band image (right) of the same cluster taken on 2012-09-19 with the S13 camera. The field of view of the NaCo S13 example image is indicated by the white rectangle (left image), and the stars used for calibration are marked with white circles (right image).

**Table 7.** Astrometric calibration results of the globular cluster 47 Tuc

| Observation date | Epoch (year) | Pixel scale (mas/pixel) | Orientation (deg) |
|---|---|---|---|
| 2010-12-24 | 2010.979 | 13.265±0.020 | 0.642±0.087 |
| 2010-12-25 | 2010.982 | 13.271±0.016 | 0.599±0.069 |
| 2012-09-19 | 2012.717 | 13.273±0.011 | 0.679±0.046 |
| 2012-12-04 | 2012.925 | 13.267±0.011 | 0.572±0.049 |
| 2012-12-05 | 2012.928 | 13.262±0.014 | 0.615±0.062 |

therein. The same was done for all NaCo images of 47 Tuc. Then, the obtained NaCo catalogues were matched with the reference catalogue using a written `PYTHON` routine, and the pixel scales and detector orientations were computed from the found matches. Additionally, sigma clipping was applied to exclude those results with significantly different pixel scales and orientations, which are most likely caused by stars with high proper motion and hence, larger deviations between the measured positions in the HST and NaCo images, respectively. The results are summarized in Table 7.

The comparison of the results of both calibration methods shows differences in the estimated pixel scales, and in particular in the found detector orientations. As mentioned, one reason can be the inaccurate assumption of a linear model for the orbital motion.

The use of a cluster, in general, is more appropriate for calibration purposes, due to the amount of stars that can be used for the position matching and hence, higher precision of the estimated pixel scale and rotation of the detector. For that reason, 47 Tuc was used for a more precise calibration of the available HIP 73357 data, and thus more precise and

updated ephemerides of the binary.

There are 3 nights available in the NaCo archive where HIP 73357 and 47 Tuc were observed in the same night; two of them taken with the S13 objective and one with S27, respectively. These nights were used to correct the discrepancies in pixel scale and orientation of the detector. Therefore, the detector was first calibrated using the 47 Tuc and the afore described procedure. The computed results are listed in Table 8, column 2 and 3. With the obtained calibration for each of the three observing nights, separation and the position angle of HIP 73357 could be measured in the respective epoch yielding the ephemerides listed in Table 8, column 4 and 5. With the new computed ephemerides

**Table 8.** Recalculated ephemerides of the calibration binary HIP 73357

| | 47 Tuc | | HIP 73357 | |
|---|---|---|---|---|
| Observation date | Pixel scale (mas/pixel) | Orientation (deg) | Separation (arcsec) | PA[a] (deg) |
| 2009-08-07/08 | 13.290±0.014 | 0.384±0.059 | 8.454±0.010 | 336.94±0.06 |
| 2010-08-18/19 | 27.070±0.012 | 0.523±0.027 | 8.445±0.006 | 337.05±0.03 |
| 2011-06-02/03 | 13.278±0.014 | 0.513±0.061 | 8.451±0.009 | 336.87±0.06 |

[a] Position angle (PA) is measured from N over E to S.

and the *Hipparcos* reference measurement of epoch 1991.25, the linear orbit motion of HIP 73357 was then re-estimated. For HIP 73357 the result is an increase in separation of $0.0011 \pm 0.0003$ arcsec/yr and a decrease of the position angle of $0.018 \pm 0.005\,^{\circ}$/yr. The pixel scales and detector orientations for the available science epochs were re-calculated using these values. The final results for pixel scale and detector orientation, applied to the respective science data in this thesis, are listed in Table 9. In Figure 12, the pixel scale

**Table 9.** Final astrometric calibration results

| Observation date | Epoch (year) | Calibrator name | Pixel scale (mas/pixel) | Orientation (deg) |
|---|---|---|---|---|
| 2007-03-01 | 2007.163 | HIP 73357 | 13.268±0.045 | 0.040±0.101 |
| 2008-01-08 | 2008.020 | HIP 73357 | 13.278±0.045 | 0.356±0.105 |
| 2008-01-17 | 2008.045 | HIP 73357 | 13.280±0.045 | 0.391±0.105 |
| 2008-02-20 | 2008.138 | HIP 73357 | 13.279±0.045 | 0.347±0.105 |
| 2009-02-20 | 2009.138 | HIP 73357 | 13.275±0.045 | 0.428±0.109 |
| 2010-12-24 | 2010.979 | 47 Tuc | 13.265±0.020 | 0.642±0.087 |
| 2010-12-25 | 2010.982 | 47 Tuc | 13.271±0.016 | 0.599±0.069 |
| 2011-03-25 | 2011.229 | HIP 73357 | 13.274±0.045 | 0.639±0.118 |
| 2011-05-09 | 2011.352 | HIP 73357 | 13.275±0.045 | 0.604±0.119 |
| 2012-09-19 | 2012.717 | 47 Tuc | 13.273±0.011 | 0.679±0.046 |
| 2012-12-04 | 2012.925 | 47 Tuc | 13.267±0.011 | 0.572±0.049 |
| 2012-12-05 | 2012.928 | 47 Tuc | 13.262±0.014 | 0.615±0.062 |

data of the two calibration methods alongside the re-calculated results for HIP 73357 are plotted. Although consistent within their uncertainties, the results of the linear orbital motion fit using the available WDS data points, shown as black dots, deviate significant from

the calibration result obtained using the globular cluster 47 Tuc shown as red squares. The re-calculated results for the calibration binary shown as black diamonds still vary slightly between the epochs. However, they now are consistent with the more precise calibration results determined from the globular cluster 47 Tuc.

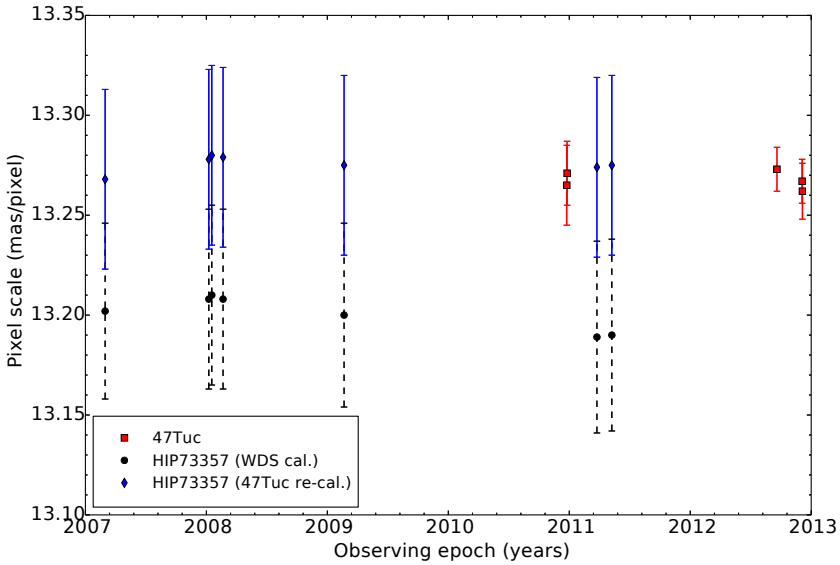


**Figure 12.** Summary plot of derived NaCo S13 pixel scales for the science epochs versus time. The pixel scales calculated from the linear orbit fit of the WDS data are shown as black dots. The red squares indicate the derived pixel scales using the 47 Tuc cluster, and the corrected results of HIP 73357 using new calculated ephemerides from 47 Tuc calibrated data are plotted as blue diamonds.

### 4.2.2 Automated calibration of VLT/NaCo data

The calibration of the science data using a binary or a globular cluster described in the previous section was only applicable for 45 target stars out of the total sample of 316 B-type stars, i.e. about 14 %. To obtain an adequate calibration for the remaining target stars a method, named "auto-calibration", was developed which uses the information contained in the science images for determination of the pixel scale and the detector orientation. The method is not entirely new. A first limited usage was performed in Schmidt et al. (2008) and Neuhäuser et al. (2010). In this section, a detailed description of the approach to this method is given.

The basic idea of the auto-calibration is to reconstruct the pixel scale and the rotation angle of the detector from the science images itself using the non-shifted and non-added reduced science images. The investigated NIR NaCo data were obtained using the already mentioned dither technique, i.e. the telescope was slightly moved between consecutive images to get a better constrain on the background emission in the near-infrared. This also means that a shift of the telescope can be seen as a shift of the star on the detector. The movement in both coordinate systems is connected by an affine transformation which contains two parameter, in the simplest case, the pixel scale and a possible misalignment of the detector. The problem was solved using a maximum log-likelihood estimation of

the parameter, i.e. pixel scale and detector orientation, and a Markov Chain Monte Carlo (MCMC) simulation for marginalization and uncertainty estimation. For the calculation the following information are needed:

(1) the position of objects on the detector $x_i$,$y_i$ in pixel units in each frame,
(2) the RA and Dec. coordinates of the telescope pointing, stored in the FITS[9]-header keywords *CRVAL1* and *CRVAL2* and
(3) the reference point of the world coordinate system (WCS) on the detector in pixel coordinates $x_{c,i}$,$y_{c,i}$, stored in the FITS-header keywords *CRPIX1* and *CRPIX2*.

A `PYTHON` routine was written to solve this problem. For object detection, `SExtractor` was used to get the position of the objects on the detector. In addition, the pointing coordinates of the telescope were obtained from each image. From the resulting set of pixel positions $\{x_i, y_i\}_k$ ($k = 1 \dots N$, where $N$ is the total number of frames) the shift of an object on the detector, between each frame, was calculated via

$$\Delta x \overset{i \neq j}{=} x_i - x_{c,i} - (x_j - x_{c,j}), \qquad \Delta y \overset{i \neq j}{=} y_i - y_{c,i} - (y_j - y_{c,j}).$$

For a particular set of observations of one object the reference coordinates of the WCS are the same, so that $x_{c,i} \equiv x_{c,j}$ and $y_{c,i} \equiv x_{c,j}$. Therefore, the equation above can be re-written as:

$$\Delta x \overset{i \neq j}{=} x_i - x_j, \qquad \Delta y \overset{i \neq j}{=} y_i - y_j.$$

The result is a new set of variables $\{\Delta x, \Delta y\}_{m=1}^{n}$ in which the number of sets $n$ is given by

$$n = \frac{N(N-1)}{2}.$$

Hence, an observation containing of $N = 9$ number of frames, i.e. different telescope offsets, would result in $n = 36$ different pairs of values, assuming that at least one object, namely the brightest, was detected in each frame. The set of coordinate values $\{\Delta\text{RA}, \Delta\text{Dec.}\}_{m=1}^{n}$, which gives the shift of the telescope pointing, was calculated by

$$\Delta\text{RA} \overset{i \neq j}{=} (\text{RA}_i - \text{RA}_j) \cdot \cos(\overline{\text{Dec.}})$$

and

$$\Delta\text{Dec.} \overset{i \neq j}{=} \text{Dec.}_j - \text{Dec.}_i,$$

where $\overline{\text{Dec.}}$ is the average of $\text{Dec.}_i$ and $\text{Dec.}_j$, and $\cos(\overline{\text{Dec.}})$ is the cosine correction between the three dimensional world coordinate system (WCS) and the two dimensional image coordinate system. The described method is based on relative offsets, therefore the tracking

[9] FITS (**F**lexible **I**mage **T**ransport **S**ystem) is the standard data format used in astronomy and endorsed by NASA and the International Astronomical Union (IAU) Pence et al. (2010)

error of the telescope, 0.1 arcsec[10] was used as uncertainty for the shift in right ascension and declination. The shifts measured in both coordinate systems are connected via

$$\begin{bmatrix} \Delta\mathrm{RA} \\ \Delta\mathrm{Dec.} \end{bmatrix} = \mathbf{A} \cdot \begin{bmatrix} \Delta x \\ \Delta y \end{bmatrix}, \tag{4.1}$$

where $A$ is the transformation matrix which is given by

$$\mathbf{A} = \begin{bmatrix} s \cdot \cos(\alpha) & -s \cdot \sin(\alpha) \\ s \cdot \sin(\alpha) & s \cdot \cos(\alpha) \end{bmatrix}.$$

Therein, $s$ is the pixel scale, which is assumed to be uniform in x and y direction, and $\alpha$ is the rotation angle of the detector. The expanded transformation model between the image and the world coordinate system is then given by

$$\Delta\mathrm{RA}_i = s \cdot (\cos(\alpha) \cdot \Delta x_i - \sin(\alpha) \cdot \Delta y_i) \tag{4.2}$$

$$\Delta\mathrm{Dec.}_i = s \cdot (\sin(\alpha) \cdot \Delta x_i + \cos(\alpha) \cdot \Delta y_i) \tag{4.3}$$

The best fitting parameter $s$ and $\alpha$ for pixel scale and detector orientation determination were derived using a maximum log-likelihood estimation. Assuming that the parameter are normal distributed, the likelihood functions for Equation 4.2 and Equation 4.3 are given by

$$\prod_{i=1}^{n} p(\Delta\mathrm{RA}_i | \Delta x_i, \Delta y_i, \Delta\mathrm{RA}_{err,i}; s, \alpha) = \prod_{i=1}^{n} \frac{1}{\sqrt{2\pi}\Delta\mathrm{RA}_{err,i}} e^{-\frac{(\Delta\mathrm{RA}_i - (s\cdot(\cos(\alpha)\cdot\Delta x_i - \sin(\alpha)\cdot\Delta y_i)))^2}{\Delta\mathrm{RA}_{err,i}}} \tag{4.4}$$

$$\prod_{i=1}^{n} p(\Delta\mathrm{Dec.}_i | \Delta x_i, \Delta y_i, \Delta\mathrm{Dec.}_{err,i}; s, \alpha) = \prod_{i=1}^{n} \frac{1}{\sqrt{2\pi}\Delta\mathrm{Dec.}_{err,i}} e^{-\frac{(\Delta\mathrm{Dec.}_i - (s\cdot(\sin(\alpha)\cdot\Delta x_i + \cos(\alpha)\cdot\Delta y_i)))^2}{\Delta\mathrm{Dec.}_{err,i}}} \tag{4.5}$$

However, it is much more convenient to work with the log-likelihood, which is calculated for Equation 4.2 as follows:

$$\begin{aligned} \log \mathcal{L}_{\Delta\mathrm{RA}}(s, \alpha) &= \log \prod_{i=1}^{n} p(\Delta\mathrm{RA}_i | \Delta x_i, \Delta y_i, \Delta\mathrm{RA}_{err,i}; s, \alpha) \\ &= \sum_{i=1}^{n} \log p(\Delta\mathrm{RA}_i | \Delta x_i, \Delta y_i, \Delta\mathrm{RA}_{err,i}; s, \alpha), \end{aligned} \tag{4.6}$$

[10] RMS of tracking error for all VLT/UTs according to ESO.

and similar for Equation 4.3 by

$$\begin{aligned}\log \mathcal{L}_{\Delta\text{Dec.}}(s, \alpha) &= \log \prod_{i=1}^{n} p(\Delta\text{Dec.}_i | \Delta x_i, \Delta y_i, \Delta\text{Dec.}_{err,i}; s, \alpha) \\ &= \sum_{i=1}^{n} \log p(\Delta\text{Dec.}_i | \Delta x_i, \Delta y_i, \Delta\text{Dec.}_{err,i}; s, \alpha) \end{aligned} \tag{4.7}$$

The final log-likelihood function is the sum of the log-likelihood functions Equation 4.6 and Equation 4.7 and is given by

$$\log \mathcal{L} = \log \mathcal{L}_{\Delta\text{RA}} + \log \mathcal{L}_{\Delta\text{Dec.}}. \tag{4.8}$$

The optimum of the log-likelihood function given in Equation 4.8 was derived using `scipy.optimize` (Jones et al. 2001), and most specifically the `minimize` function therein. In order to maximize the log-likelihood the negative log-likelihood was minimized.
The uncertainties on the estimated parameter were calculated using a Markov Chain Monte Carlo (MCMC) approach. The posterior probability function, i.e. the distribution of parameters that is consistent with the dataset, needed for the MCMC is given, up to a constant, by

$$p(s, \alpha | \Delta x, \Delta y, \Delta\text{RA}, \Delta\text{Dec.}, \Delta\text{RA}_{err}, \Delta\text{Dec.}_{err}) \propto p(s, \alpha) p(\Delta\text{RA}, \Delta\text{Dec.} | \Delta x, \Delta y; s, \alpha) \tag{4.9}$$

where $p(\Delta\text{RA}, \Delta\text{Dec.}|\Delta x, \Delta y; s, \alpha)$ is the likelihood function discussed above and $p(s, \alpha)$ is the "prior" function, which encodes any previous knowledge of the parameter, such as the physically acceptable range. In this thesis uniform, so-called "uninformative", priors for $s$ and $\alpha$ were used, depending for example on the given objective. Below, the prior function for the S13 objective $p(s)_{\text{S13}}$ is given exemplary.

$$p(s)_{\text{S13}} = \begin{cases} 1, & \text{if } 12 \leq s \leq 14 \\ 0, & \text{otherwise} \end{cases}$$

The full log-probability distribution function was sampled using `emcee` Foreman-Mackey et al. (2013), starting with 20 walker, initialized in a tiny Gaussian ball around the obtained maximum likelihood result. The MCMC run was then started for each walker with 2500 steps.
The results for both parameter and for each walker as a function of the number of steps in the chain is shown in Figure 13. Plotted are the traces of each walker for the pixel scale and the detector orientation, obtained for HIP 73357 and taken on 2011-09-05 in the $K$s band. In addition, the so-called "burn-in" limit applied to all data is shown as black vertical dashed line. The steps of the MCMC run below this limit, which was chosen as 5 % of the total step size, are excluded from the further analysis. The results of the MCMC

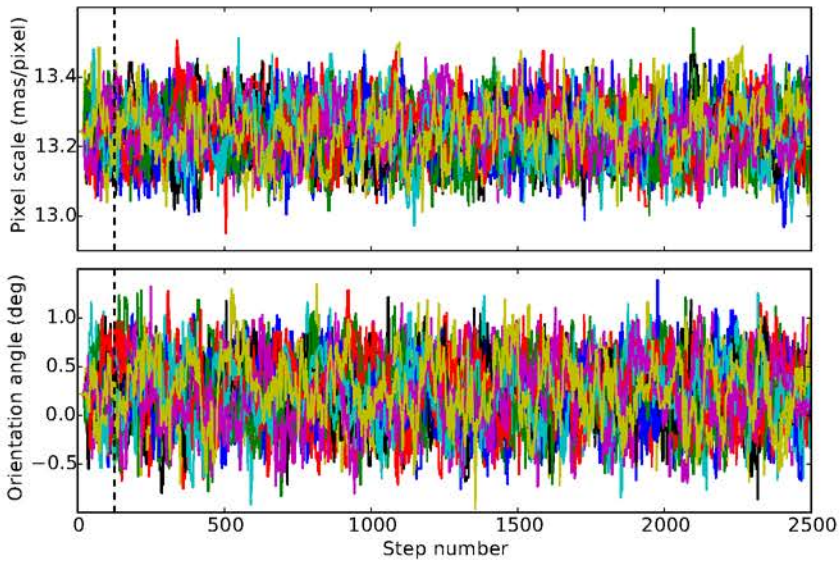


**Figure 13.** Plot of the positions of each walker as a function of the number of steps in the Markov chain for each parameter. The "burn-in" limit of 5% of the total step size is indicated by the vertical dashed line.

run for each investigated data-set are illustrated in a so-called "corner plot". As example, the corner plot for HIP 73357 is shown in Figure 14. The plot shows the one and two dimensional projections of the posterior probability distributions of the parameter. Thereby, the marginalized distribution for each parameter independently is shown in the histograms along the diagonal and the marginalized two dimensional distribution, i.e. the covariances between the parameter, in the other panel. Also shown as blue vertical line is the mean, obtained by fitting a Gaussian to the cumulative density function of the posterior probability distribution of each parameter. As final pixel scale and detector orientation, the results of

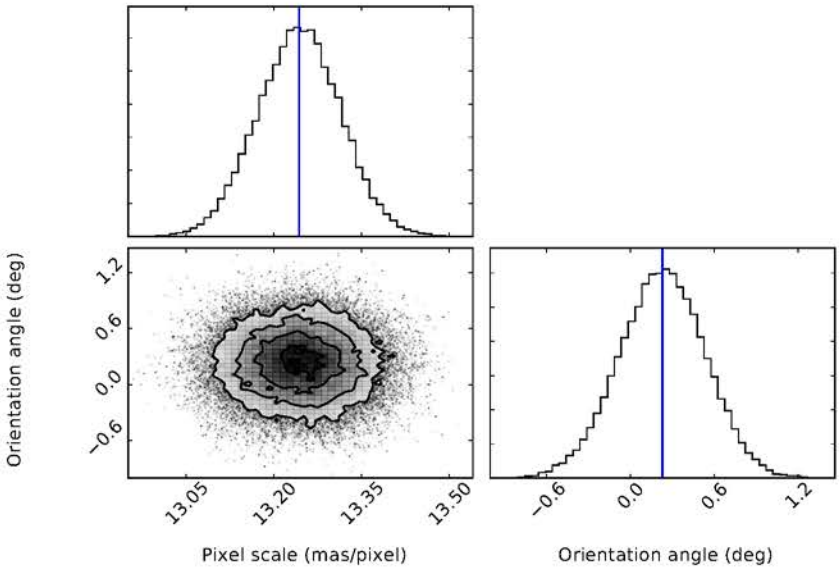


**Figure 14.** Corner plot of the MCMC results showing the one and two dimensional projections of the posterior probability distributions of the found parameter. Shown are the marginalized distribution for each parameter independently in the histograms along the diagonal and the marginalized two dimensional distribution in the other panel. The mean value of the distribution of each parameter is shown as blue vertical line.

the Gaussian fitting, i.e. mean and standard deviation, were applied to the data in this thesis. The consistency of the results of the auto-calibration method was tested against the available data of HIP 73357, which have been calibrated with the globular cluster 47 Tuc. The results of this test are listed in Table 10. As can be seen from the data, the results

**Table 10.** Comparison of astrometric calibration results and auto-calibration method

| | | | astrom. cal. | | auto-cal. | |
|---|---|---|---|---|---|---|
| Observation date | Epoch (year) | Calibrator name | Pixel scale (mas/pixel) | Orientation (deg) | Pixel scale (mas/pixel) | Orientation (deg) |
| 2007-03-01 | 2007.163 | HIP 73357 | 13.268±0.045 | 0.040±0.101 | 13.230±0.112 | -0.018±0.458 |
| 2008-01-08 | 2008.020 | HIP 73357 | 13.278±0.045 | 0.356±0.105 | 13.246±0.078 | 0.163±0.326 |
| 2008-01-17 | 2008.045 | HIP 73357 | 13.280±0.045 | 0.391±0.105 | 13.279±0.050 | 0.130±0.208 |
| 2008-02-20 | 2008.138 | HIP 73357 | 13.279±0.045 | 0.347±0.105 | 13.260±0.028 | 0.052±0.121 |
| 2009-02-20 | 2009.138 | HIP 73357 | 13.275±0.045 | 0.428±0.109 | 13.272±0.066 | -0.100±0.283 |
| 2011-03-25 | 2011.229 | HIP 73357 | 13.274±0.045 | 0.639±0.118 | 13.275±0.093 | -0.079±0.393 |
| 2011-05-09 | 2011.352 | HIP 73357 | 13.275±0.045 | 0.604±0.119 | 13.242±0.072 | 0.218±0.307 |

for the pixel scale are well consistent with the results obtained by the common calibration methods. However, the comparison of the results for the detector orientation shows some discrepancies in the obtained data. These discrepancies might be due to shifts in the detected positions of the objects caused by variations in the quality of the AO-correction during the observation, and/or due to field distortions, which also cause a shift of the detected position. However, the data vary no more than $\sim 1\sigma$ and therefore, the method is deemed to be plausible and applicable for the calibration of science data without available astrometric calibrator.

# 5 Data Analysis

This section provides detailed information on the procedures applied for the analysis of the data. Starting from a visual inspection of the reduced images, the positions of the primary and any found companion candidate were measured and converted to a separation and position angle, described in section 5.1. In section 5.2, the calculation of the evolution of the separation and the position angle between the companion candidate and the host star over several observation epochs is specified and the the probability that the found candidate is an unrelated non-moving background object was investigated either by analysing the common proper motion, which is indicative for a physical association, or on a statistical base, depending on the available data. Using the flux-ratio between the primary and the companion candidate, distance to the Earth and the estimated system age, apparent and absolute magnitudes as well as the mass of the companion candidate were calculated, or estimated from evolutionary models, respectively (section 5.3 and section 5.4). For the different processes in the systematic analysis of each sample star `PYTHON` scripts were written to control and monitor the procedures contained in the software packages and programs utilized for this study.

## 5.1 Candidate identification and detection

The candidate identification and the determination of the positions was done using the `IDL/starfinder` routine (Diolaiti et al. 2000) after a first visual inspection of the reduced images. As mentioned, `IDL/starfinder` uses a PSF fitting algorithm applied simultaneous to all sources in the image which is particularly advantageous for close objects since the PSF's of the stars interfere with each other. This overlap would cause an underestimation of the separation and, therefore, has to be taken into account. As mentioned, the observations with NaCo were obtained using the jitter technique, where the telescope is shifted slightly between single exposures. Due to the geometric distortions of the detector the positions of the objects in the different quadrants vary slightly in each image, and thus the separation and the position angle also change between the single exposures of one observation. The effect of the field distortions was taken into account as error in the determination of the angular separation and the position angle by averaging the computed results for the single images.

Using the final reduced image, a reference PSF was constructed with `IDL/psf_extract` which was then used to fit the object positions with `IDL/starfinder` in the single images. In order to avoid false detections or missed objects a reference catalogue of the found stars was constructed and compared with the detection results. Then the relative distances to

the primary star for each identified companion candidate was calculated by

$$\begin{aligned} \Delta x_i &= x_i - x_0 \\ \Delta y_i &= y_i - y_0 \end{aligned} \tag{5.1}$$

where $x_0$, $y_0$ are the detector coordinates of the primary and $x_i$, $y_i$ the coordinates of any found companion candidate within the image. Given the relative distances, the separation $\rho$ in pixel units was calculated by

$$\rho_i = \sqrt{\Delta x_i^2 + \Delta y_i^2} \tag{5.2}$$

and the position angle which is measured counterclockwise from North over East was computed by

$$\phi_i = \arctan\left[\frac{\Delta y_i}{\Delta x_i}\right] + \kappa. \tag{5.3}$$

Since the arctan is defined relative to the x–axis, an angle $\kappa$ was added to correct the calculated angle placing the estimated angle in the right quadrant, starting from the y–axis (North). The result is a set of separations and position angles $\{\rho_i, \phi_i\}_k$, with $i = 1 \ldots N_{\mathrm{cc}}$ and $k = 1 \ldots N$, where $N_{\mathrm{cc}}$ is the number of identified companion candidates and $N$ is the total number of images available in a data set. The obtained averaged separations $\mu_\rho$ and position angles $\mu_\phi$ for each found object were then converted into an angular separation $\Theta$ and the true position angle PA by applying the calibration results, i.e. the pixel scale $PS$ and the detector orientation $\theta$, either from the HIP 73357 binary, the 47 Tuc cluster, or the "auto-calibration" result for the corresponding data set, through

$$\Theta = \mu_\rho \cdot PS \qquad \Delta\Theta = \sqrt{(\sigma_\rho \cdot PS)^2 + (\mu_\rho \cdot \Delta PS)^2} \tag{5.4}$$

$$\mathrm{PA} = \mu_\phi + \theta \qquad \Delta\mathrm{PA} = \sqrt{\sigma_\phi^2 + \Delta\theta^2} \quad . \tag{5.5}$$

For comparison of the results and the statistical analysis of the period distribution the angular separation $\Theta$ was then converted into a projected distance $a_{\mathrm{proj}}$ from the primary star, given in au, by

$$a_{\mathrm{proj}} = \frac{\Theta}{\pi} \qquad \Delta a_{\mathrm{proj}} = \sqrt{\left(\frac{\Delta\Theta}{\pi}\right)^2 + \left(\frac{\Theta \cdot \sigma_\pi}{\pi^2}\right)^2}, \tag{5.6}$$

where $\pi$ is the parallax in arc seconds, given in the *Hipparcos* catalogue and listed in Table A1. As the majority of the orbital parameters for each resolved system are not known, the projected separations within this study are given, without applying a correction factor to estimate the true semi-major axis (Couteau 1960, Kuiper 1935).

However, in a few cases of very faint companion candidates which were only visible in the reduced and co-added images and not or only marginal visible in the single exposures, the

described procedure did not succeed. In these cases the ESO-MIDAS (**M**unich **I**mage **D**ata **S**ystem, Warmels 1992) image processing software was used to measure the position of the objects in the final reduced image by fitting a two-dimensional Gaussian to the companion candidate positions with the `center/gauss` routine implemented therein.
In addition to the visual inspection of all images and the detection using `starfinder` or ESO-MIDAS the PSF of the primary was subtracted to check for the presents of objects in the halo of the primary PSF. Therefore, the image was rotated by 360° in 2° steps of angular increment. For each step the difference between the rotated and the original image was computed and then all difference–images were averaged. The result is a PSF subtracted image where the radial symmetric parts of the primary stars PSF have been eliminated. The result of the PSF subtraction is shown on the right side in Figure 15, exemplary for HIP 20804. Since the PSF of the primary also contains non-radial symmetric contingents, the star is not fully removed in the PSF subtracted image.

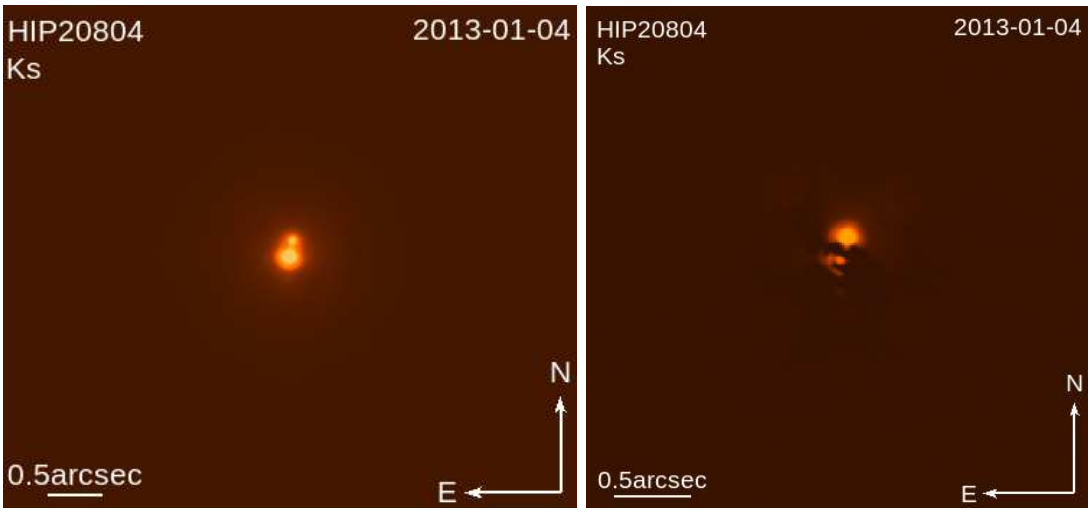


**Figure 15.** Example images for the illustration of the PSF subtraction applied to the primary star. Shown is the final reduced VLT/NaCo image of the binary system HIP 20804 before (left) and after the PSF was subtracted (right). The star was observed on 2013-01-04 with the S13 camera in the *K*s band.

## 5.2 Common Proper Motion analysis

The separation and the position angle obtained for each target star in the sample combined with literature values and the estimated masses for the primary and the companion candidate(s) were used to investigate the common proper motion of the found candidate(s) with respect to the primary star.
Therefore, a background hypothesis test was applied. Assuming that the found companion candidate is a non-moving background object the theoretical change in the position, and consequently in separation and position angle, of the primary with respect to the fixed companion candidate was calculated, relative to the first/last observation epoch. If a star possesses a real companion both objects orbit their common centre of mass while orbiting

the centre of the Milky Way galaxy. For average *seeing* conditions and an assumed distance from the Sun of about 160 pc with a measured separation of 0.8 arcsec, the projected separation of a companion would be 128 au. Assuming a total system mass of 4 solar masses and using Kepler's third law the orbital motion of such an companion would be roughly 1 au/yr. The angular velocity would then correspond to a value of about 0.006 arcsec/yr. Given the median proper motion of the sample with about 0.03 arcsec/yr the orbital motion contributes roughly 20 % to the proper motion. Although the values for distance, system mass and proper motion vary for each sample star, this estimation shows that the orbital motion needs to be taken into account in the search for companions, especially for less distant target stars with companion candidates at small separations.

## Estimation of the background motion

The theoretical change in right ascension $\Delta\alpha_{\mathrm{bg}}$ and declination $\Delta\delta_{\mathrm{bg}}$, and consequently in separation and position angle, seen from Earth is a superposition of the proper motion of the star and the parallactic motion of the star due to Earth's orbit around the Sun and was calculated by

$$\begin{aligned} \Delta\alpha_{\mathrm{bg}} &= \Delta\alpha_{\mathrm{pm}} + \Delta\alpha_{\pi} & \sigma(\Delta\alpha_{\mathrm{bg}}) &= \sqrt{\sigma(\Delta\alpha_{\mathrm{pm}})^2 + \sigma(\Delta\alpha_{\pi})^2} \\ \Delta\delta_{\mathrm{bg}} &= \Delta\delta_{\mathrm{pm}} + \Delta\delta_{\pi} & \sigma(\Delta\delta_{\mathrm{bg}}) &= \sqrt{\sigma(\Delta\delta_{\mathrm{pm}})^2 + \sigma(\Delta\delta_{\pi})^2} \end{aligned} \quad . \qquad (5.7)$$

As a first approximation the change of the position $\Delta\alpha_{\mathrm{pm}}$ and $\Delta\delta_{\mathrm{pm}}$ of the primary with respect to a fixed background source due to its proper motion is given by

$$\begin{aligned} \Delta\alpha_{\mathrm{pm}} &= (t - t_0) \cdot \mu_{\alpha} & \sigma(\Delta\alpha_{\mathrm{pm}}) &= \Delta t \cdot \sigma(\mu_{\alpha}) \\ \Delta\delta_{\mathrm{pm}} &= (t - t_0) \cdot \mu_{\delta} & \sigma(\Delta\delta_{\mathrm{pm}}) &= \Delta t \cdot \sigma(\mu_{\delta}) \end{aligned} \qquad (5.8)$$

where $(t - t_0 = \Delta t)$ is the time difference relative to the reference observation and $\mu_{\alpha}$ and $\mu_{\delta}$ are the proper motions obtained from the *Hipparcos* catalogue and listed in Table 2 and Table A1. The second quantity which contributes to the background motion is the change of the position $\Delta\alpha_{\pi}$ and $\Delta\delta_{\pi}$ of the primary with respect to a fixed background source due to its parallactic motion while the Earth revolves the Sun. For the calculation of this motion it is necessary to calculate the position of the Earth on its orbit for the observation date. The formula's used were taken from the Astronomical Almanac 2007 (Nautical Almanac Office 2007).
As a start the observation dates were converted into Julian dates (*JD*) and from this the number of days *n* from the equinox J2000.0 was calculated by

$$n = JD - 2451545.0.$$

The mean longitude of the Sun $L$, corrected for aberration, and the mean anomaly $g$ are given by

$$L = 280.460^\circ + 0.9856474^\circ \cdot n$$
$$g = 357.528^\circ + 0.9856003^\circ \cdot n.$$

Putting $L$ and $g$ in the range of 0° and 360° by adding multiples of 360°, the ecliptic longitude $\lambda_\odot$ and latitude $\beta_\odot$ of the Sun can be expressed as:

$$\lambda_\odot = L + 1.915^\circ \sin g + 0.020^\circ \sin 2g$$
$$\beta_\odot = 0^\circ$$

Given the obliquity of the ecpliptic $\epsilon$ and the distance of the Sun from Earth $R_{\odot\oplus}$, in au, by

$$\epsilon = 23.439^\circ - 0.0000004^\circ \cdot n$$
$$R_{\odot\oplus} = 1.00014 - 0.01671 \cos g - 0.00014 \cos 2g$$

the equatorial rectangular coordinates of the Earth, in au, for a certain Julian date are given by

$$X = -R_{\odot\oplus} \cos \lambda_\odot, \qquad Y = -R_{\odot\oplus} \cos \epsilon \sin \lambda_\odot, \qquad Z = -R_{\odot\oplus} \sin \epsilon \sin \lambda_\odot.$$

Using the calculated coordinates of the Earth, the annual parallax $\pi$ in the sexagesimal system and the geocentric equatorial coordinates of the star $\alpha_0 = \alpha_{\mathrm{J2000}}$ and $\delta_0 = \delta_{\mathrm{J2000}}$, the change in right ascension and declination was estimated via

$$\Delta\alpha_\pi = \alpha - \alpha_0 = \frac{\pi}{15 \cos \delta_0}(X \sin \alpha_0 - Y \cos \alpha_0) \tag{5.9}$$
$$\Delta\delta_\pi = \delta - \delta_0 = \pi(X \cos \alpha_0 \sin \delta_0 + Y \sin \alpha_0 \sin \delta_0 - Z \cos \delta_0). \tag{5.10}$$

## Estimation of the maximum expected orbital motion

There are several methods for the estimation of the maximum expected orbital motion. However, in principle they base on the assumption that the greatest change in separation or position angle would be visible for a circular orbit. Considering the alignment of an imaged system as seen by an observer from Earth the change in separation of a companion orbiting his host star would be maximised for an edge-on orbit, whereas, for a pole-on orbit no change would be visible at all. The same applies for the change of the position angle, except that the change would be maximised for a pole-on view on the orbit.
The measured separation between a companion candidate an its host star does not necessarily corresponds to the semi-major axis of the system. To take this into account in this study the maximum possible orbital motion was estimated solving a maximum value prob-

lem determining the semi-major axis which maximises the velocity of a circular orbit seen from the edge. Assuming a circular orbit the projected velocity $v_{\mathrm{proj}}$ is given as function of the true orbital speed $v_{\mathrm{circ}}$ and the angle $\alpha$ under which the projection is seen by

$$v_{\mathrm{proj}} = \cos(90^\circ - \alpha) \cdot v_{\mathrm{circ}}.$$

The angle $\alpha$ also corresponds to the angle between projected and true semi-major axis and can be expressed as:

$$\alpha = \arccos\left(\frac{a_{\mathrm{proj}}}{a_{\mathrm{true}}}\right).$$

This means for an angle of $\alpha = 0^\circ$ the orbit would be seen pole-on, i.e. the separation seen by an observer would be similar to the true semi-major axis of the system, but no orbital motion would be visible. On the other hand, for $\alpha = 90^\circ$ both objects would fulfil a transit, and the orbital speed would correspond to the relative velocity of the objects. The orbital speed itself can be estimated using Kepler's third law, via

$$v_{\mathrm{circ}} = \frac{2\pi a_{\mathrm{true}}}{T} \qquad \text{with} \qquad T \propto \sqrt{\frac{a_{\mathrm{true}}^3}{(M_1 + M_2)}},$$

and hence the projected velocity can be calculated by

$$\begin{aligned} v_{\mathrm{proj}} &= \cos\left(90^\circ - \arccos\left(\frac{a_{\mathrm{proj}}}{a_{\mathrm{true}}}\right)\right) \cdot v_{\mathrm{circ}} \\ &= \left[\underbrace{\cos 90^\circ}_{=0} \cdot \underbrace{\cos\left(\arccos\left(\frac{a_{\mathrm{proj}}}{a_{\mathrm{true}}}\right)\right)}_{=\frac{a_{\mathrm{proj}}}{a_{\mathrm{true}}}} + \underbrace{\sin 90^\circ}_{=1} \cdot \sin\left(\arccos\left(\frac{a_{\mathrm{proj}}}{a_{\mathrm{true}}}\right)\right)\right] \cdot \frac{2\pi a_{\mathrm{true}}}{\sqrt{\frac{a_{\mathrm{true}}^3}{(M_1+M_2)}}} \\ v_{\mathrm{proj}} &= \sin\left(\arccos\left(\frac{a_{\mathrm{proj}}}{a_{\mathrm{true}}}\right)\right) \cdot \frac{2\pi a_{\mathrm{true}}}{\sqrt{\frac{a_{\mathrm{true}}^3}{(M_1+M_2)}}} \end{aligned} \tag{5.11}$$

Equation 5.11 was solved numerically resulting in an estimated "true" semi-major $a_{\mathrm{true}}$ at which the projected velocity $v_{\mathrm{proj}}$ is at maximum. From this values the change in separation $\Delta\Theta_{\mathrm{orb}}$ and position angle $\Delta\mathrm{PA}_{\mathrm{orb}}$ relative to a reference epoch can be calculated, via

$$\Delta\Theta_{\mathrm{orb}} = \frac{v_{\mathrm{proj}}}{d[\mathrm{pc}]} \cdot \Delta t,$$
$$\Delta\mathrm{PA}_{\mathrm{orb}} = \frac{360^\circ}{\sqrt{\frac{a_{\mathrm{true}}^3}{M_{\mathrm{sys}}}}} \cdot \Delta t.$$

Therein, $d$[pc] is the distance of the system given in parsec and $\Delta t$ is the time difference of a measurement relative to the reference epoch. At this point the reader should be reminded that these estimations were made assuming a circular orbit. Therefore, the obtained results

have to be taken with reservations, due to the fact that the vast majority of the investigated systems, if not all, will have most likely orbital eccentricities greater than zero.

## Companionship

In order to be able to decide whether a found companion candidate is a unrelated background object or a physically associated companion, bound by gravity, two approaches were used. The first is a $\chi^2$ probability test following the description by Ehrenreich et al. (2010), and the second is an estimation of the deviation of the measured and expected values with respect to a reference observation (e.g., Vogt et al. 2012).
The probability of observing a value of $\chi^2$ that is larger than that obtained form the measurements and literature values for a sample of $N$ observations with $\nu = 2N-2$ degrees of freedom ($df$) is the integral of the probability density of a $\chi^2$ distribution (Bevington and Robinson 2003), and is calculated via

$$P_\chi(\chi^2;\nu) = \frac{1}{2^{\nu/2}\Gamma(\nu/2)} \int_{\chi^2}^{+\infty} (x^2)^{(\nu-2)/2} e^{-(x^2)/2} d(x)^2, \tag{5.12}$$

where the $\Gamma(n)$ function is equivalent to the factorial function n! extended to non-integral arguments, and $(x^2)$ represents the possible values of $\chi^2$ within the integral sum.
The shift in the position, i.e. in right ascension $\alpha$ and declination $\delta$, of a companion candidate between two epochs $i$ and $j$, obtained either from measurements in this work or from literature, is given by

$$\Delta\alpha_{i\to j} = \Theta_j \sin \mathrm{PA}_j - \Theta_i \sin \mathrm{PA}_i \tag{5.13}$$

$$\Delta\delta_{i\to j} = \Theta_j \cos \mathrm{PA}_j - \Theta_i \cos \mathrm{PA}_i, \tag{5.14}$$

where $\Theta$ is the separation and PA is the position angle, measured from north to east. These measured shifts were first compared to the theoretical apparent motion of an object on the sky assuming that the companion candidate is a non-moving background source. The $\chi^2_{\mathrm{bg}}$ value, for observations performed at $N$ epochs and with $2N-2$ degrees of freedom, is given by

$$\chi^2_{\mathrm{bg}} = \sum_{n=1}^{N} \left[ \frac{(\Delta\alpha_{1\to i} - \Delta\alpha^\star_{1\to i})^2}{\sigma^2_{\Delta\alpha_{1\to i}} + \sigma^2_{\Delta\alpha^\star_{1\to i}}} + \frac{(\Delta\delta_{1\to i} - \Delta\delta^\star_{1\to i})^2}{\sigma^2_{\Delta\delta_{1\to i}} + \sigma^2_{\Delta\delta^\star_{1\to i}}} \right]. \tag{5.15}$$

Therein $\Delta\alpha^\star_{1\to i}$ and $\Delta\delta^\star_{1\to i}$ are the theoretical shifts in $\alpha$ and $\delta$ in the position of the host star between epoch 1 and $i$, taking into account the primaries proper motion and the parallactic motion. The $\chi^2_{\mathrm{bg}}$ value obtained from Equation 5.15 was injected in Equation 5.12 and the probability $P_{\chi,\mathrm{bg}}$ calculated using the `PYTHON scipy.stats.chi2` function. For $P_{\chi,\mathrm{bg}} < 0.01\,\%$ the object is considered to be background object, labelled as (B)ackground in the last column in Table A6. However, due to systematic offsets in the position measurements

such as variations in the stellar proper motions, discrepancies between the real values and those from the literature, or the fact that background objects possess a non-negligible proper motion on the sky, it is possible that $P_{\chi,\mathrm{bg}} < 0.01\,\%$ for some objects that are evidently not co-moving with the primary star.

Therefore, additionally the probability $P_{\chi,\mathrm{cmv}}$, that a companion candidate is co-moving with the primary star, was defined, using a $\chi^2$ test similar to Equation 5.15 and calculated via

$$\chi^2_{\mathrm{cmv}} = \sum_{n=1}^{N} \left[ \left( \frac{\Delta\alpha_{1\to i}}{\sigma_{\Delta\alpha_{1\to i}}} \right)^2 + \left( \frac{\Delta\delta_{1\to i}}{\sigma^2_{\Delta\delta_{1\to i}}} \right)^2 \right]. \tag{5.16}$$

The result again was injected into Equation 5.12. For $P_{\chi,\mathrm{cmv}} > 0.01\,\%$ the object is considered to be co-moving companion, labelled as (C)o-moving in the last column in Table A6. However, the value of $P_{\chi,\mathrm{cmv}}$ is only a hint of a physical association as it does not take into account a possible orbital motion of a true co-moving companion. Thus, an object with very small values of $P_{\chi,\mathrm{bg}}$ and $P_{\chi,\mathrm{cmv}}$ ($< 0.01\,\%$) is not necessarily a background object, due to possible orbital motion.

The second approach, applied in this thesis, uses the deviation between the measured and expected values for separation and position angle to support or disprove the made conclusions on the object status from the first method. The significance, i.e. the deviation in terms of sigma, of a measurement taken at epoch *i* not being a fixed background object ($\sigma_{\Theta,\mathrm{bg},i}$ and $\sigma_{\mathrm{PA,bg},i}$) was calculated from the measured deviation in the separation and position angle of the components between epoch *i* and the corresponding expected values of epoch *i* with respect to the reference epoch with index 0, via

$$\sigma_{\Theta,\mathrm{bg},i} = \frac{|\Theta_i - \Theta_{\mathrm{bg},i}(\Theta_0)|}{\sqrt{\delta^2_{\Theta,i} + \delta^2_{\Theta,\mathrm{bg},i}(\delta_{\Theta_0})}} \quad \text{and} \quad \sigma_{\mathrm{PA,bg},i} = \frac{|\mathrm{PA}_i - \mathrm{PA}_{\mathrm{bg},i}(\mathrm{PA}_0)|}{\sqrt{\delta^2_{\mathrm{PA},i} + \delta^2_{\mathrm{PA,bg},i}(\delta_{\mathrm{PA}_0})}}. \tag{5.17}$$

Therein, for instance $\Theta_{\mathrm{bg},i}(\Theta_0)$ would be the expected separation in case the identified companion candidate is a non-moving background object. The associated uncertainty in that value $\delta_{\Theta,\mathrm{bg},i}(\delta_{\Theta_0})$, essentially represents the background cone at epoch *i* relative to the reference epoch 0 taking into account the proper motion and the measurement uncertainty at the reference epoch. If the combined significance ($\sigma_{\Theta,\mathrm{bg},i} + \sigma_{\mathrm{PA,bg},i}$) is greater than $3\,\sigma$, the hypothesis of a non-moving background object is rejected and the companion candidate can be considered co-moving.

The significance of a measurement at epoch *i* representing possible orbital motion, on the other hand, was estimated similarly to the significance not being a background object for each epoch as a measure of the differences in separation and position angle from the

reference epoch with index 0, and is given by

$$\sigma_{\Theta,\mathrm{orb},i} = \frac{|\Theta_i - \Theta_0|}{\sqrt{\delta^2_{\Theta,i} + \delta^2_{\Theta_0}}} \qquad \text{and} \qquad \sigma_{\mathrm{PA},\mathrm{orb},i} = \frac{|\mathrm{PA}_i - \mathrm{PA}_0|}{\sqrt{\delta^2_{\mathrm{PA},i} + \delta^2_{\mathrm{PA}_0}}}. \tag{5.18}$$

No significant changes over time ($\sigma_{\Theta,\mathrm{orb},i} + \sigma_{\mathrm{PA},\mathrm{orb},i} < 3\,\sigma$) are a strong hint for a co-moving object, while monotonically increasing deviations over time, in combination with significant variations from a non-moving background source, support the status of a physical companion showing possible orbital motion. Please note that orbital motion in this context has to be taken with reservation, due to the orbital periods that are possible ranging from a few hundred up to several thousands of years. This is very long compared to the typical observation intervals of maybe five, ten or in some cases one-hundred years.
The results of the astrometric search for companions as well as the calculated significances and results of the $\chi^2$ probability tests, are listed exemplary in Table 11. The full list of all results obtained from the sample target stars with more than one observation or objects with an archival data set and previously published data points is given in Table A3. Please note that only literature data points with explicitly given uncertainties were used to avoid biases introduced by under-/overestimation of the measurement uncertainties.

**Table 11.** Astrometric results for visual binaries and multiples identified in this study.

| HIP | MJD (days) | Ref. | Sep (arcsec) $\Theta \pm \delta_\Theta$ | $\mathrm{Sep}_{\mathrm{bg}}$ (arcsec) $\Theta_{\mathrm{bg}} \pm \delta_{\Theta,\mathrm{bg}}$ | Sign.[a] not Backg. $\sigma_{\Theta,\mathrm{bg}}$ | Sign. orb. motion $\sigma_{\Theta,\mathrm{orb.}}$ | PA[b] (deg) $\mathrm{PA} \pm \delta_{\mathrm{PA}}$ | $\mathrm{PA}_{\mathrm{bg}}$ (deg) $\mathrm{PA}_{\mathrm{bg}} \pm \delta_{\mathrm{PA,\,bg}}$ | Sign.[a] not Backg. $\sigma_{\mathrm{PA,bg}}$ | Sign. orb. motion $\sigma_{\mathrm{PA,orb.}}$ | $P_{\chi,\mathrm{bg}}$ (%) | $P_{\chi,\mathrm{cmv}}$ (%) |
|---|---|---|---|---|---|---|---|---|---|---|---|---|
| | | | | | Binaries | | | | | | | |
| 2548 | 51065.000 | Mason et al. (2001) | 0.274±0.001 | 0.489±0.005 | 45.5 | 51.3 | 284.4±0.1 | 335.9±0.6 | 86.5 | 88.8 | 0.00 | 0.00 |
| | 51466.000 | Horch et al. (2000) | 0.29±0.01 | 0.445±0.004 | 14.4 | 6.8 | 278.1±0.1 | 333.4±0.6 | 93.3 | 53.8 | | |
| | 51477.000 | Mason et al. (2001) | 0.270±0.001 | 0.444±0.004 | 41.3 | 47.4 | 283.1±0.1 | 333.4±0.6 | 84.8 | 81.5 | | |
| | 52872.000 | Horch et al. (2008) | 0.283±0.001 | 0.310±0.002 | 11.0 | 60.1 | 279.4±0.1 | 316.5±0.5 | 67.7 | 61.0 | | |
| | 53297.000 | Mason et al. (2006) | 0.30±0.05 | 0.273±0.002 | 0.5 | 1.6 | 281.4±0.1 | 309.3±0.5 | 54.4 | 72.1 | | |
| | 53710.049 | (1) | 0.2710±0.0009 | 0.245±0.001 | 17.3 | 52.6 | 278.0±0.2 | 299.9±0.4 | 45.5 | 38.9 | | |
| | 54359.246 | (1) | 0.241±0.001 | 0.2247±0.0004 | 14.8 | 18.7 | 275.6±0.2 | 280.6±0.3 | 15.4 | 31.2 | | |
| | 54746.000 | Tokovinin et al. (2010) | 0.2217±0.0002 | c | c | c | 268.4±0.1 | c | c | c | | |
| 15627 | 48475.000 | Fabricius et al. (2002) | 0.990±0.007 | 1.04±0.01 | 3.2 | 13.2 | 228.2±0.6 | 192.4±0.9 | 32.8 | 12.3 | 0.00 | 0.00 |
| | 54024.221 | (1) | 0.874±0.005 | c | c | c | 218.4±0.5 | c | c | c | | |
| : | : | : | : | : | : | : | : | : | : | : | : | : |
| | | | | | Higher-order multiple systems | | | | | | | |
| 24925AB | 48348.000 | ESA (1997) | 0.53±0.01 | d | d | d | 196.0±0.5 | d | d | d | 0.00 | 0.00 |
| | 53379.159 | (1) | 0.5102±0.0008 | 0.48±0.02 | 1.3 | 1.5 | 199.66±0.08 | 189.8±2.0 | 5.6 | 7.2 | | |
| | 56189.342 | (1) | 0.5084±0.0008 | 0.45±0.03 | 1.7 | 1.7 | 200.39±0.06 | 185.4±3.0 | 5.8 | 8.7 | | |
| | 56296.120 | (1) | 0.5086±0.0006 | 0.45±0.03 | 1.7 | 1.7 | 199.49±0.06 | 185.4±3.0 | 5.4 | 6.9 | | |
| 24925AC | 53379.159 | (1) | 4.570±0.006 | d | d | d | 284.94±0.08 | d | d | d | 0.00 | 0.00 |
| | 56189.342 | (1) | 4.579±0.004 | 4.56±0.01 | 1.7 | 1.2 | 284.79±0.05 | 285.5±0.1 | 5.7 | 1.6 | | |
| | 56296.120 | (1) | 4.586±0.005 | 4.56±0.01 | 2.3 | 2.0 | 283.93±0.06 | 285.5±0.1 | 12.3 | 10.4 | | |
| 26237AB | 53469.976 | (1) | 0.151±0.001 | 0.21±0.02 | 3.8 | 1.6 | 330.1±0.6 | 345.1±2.0 | 8.3 | 62.1 | 0.01 | 0.00 |
| | 56189.387 | (1) | 0.1586±0.0006 | 0.168±0.007 | 1.3 | 0.1 | 358.2±0.1 | 361.0±0.5 | 5.9 | 56.9 | | |
| | 56970.000 | Tokovinin et al. (2015) | 0.159±0.005 | c | c | c | 366.2±0.1 | c | c | c | | |
| : | : | : | : | : | : | : | : | : | : | : | : | : |

**Notes.** The full list is presented in Table A3.
[a] Assuming the fainter component is a non-moving background star.
[b] Position angle (PA) is measured from N over E to S.
[c] Significances are given relative to the last epoch.
[d] Significances are given relative to the first epoch.
**References.** (1) This work; otherwise given in table

The computed data for each object listed in Table 11 and Table A3 are additionally illustrated in so-called common proper motion diagrams (CPMD). These plots also help to interpret the results correctly. In Figure 16 the outcome for the common proper motion analysis of HIP 20042 is visualized as example. Shown are the separation (left panel) and position angle (right panel) versus observing epoch for the data obtained in course of this

work as well as additional data points from literature, if available. The background hypothesis, i.e. the expected change in separation or position angle that a non-moving background object would have due to the primary stars proper motion on the sky, is represented by the area enclosed by the wobbled red dashed lines. This wobble is induced by the parallactic motion due to the Earth's revolution around the Sun. The dotted lines represent the area for the maximum possible orbital motion assuming a circular orbit seen edge-on in case of the separation and pole-on for the position angle. HIP 20042 is a spectroscopic binary of

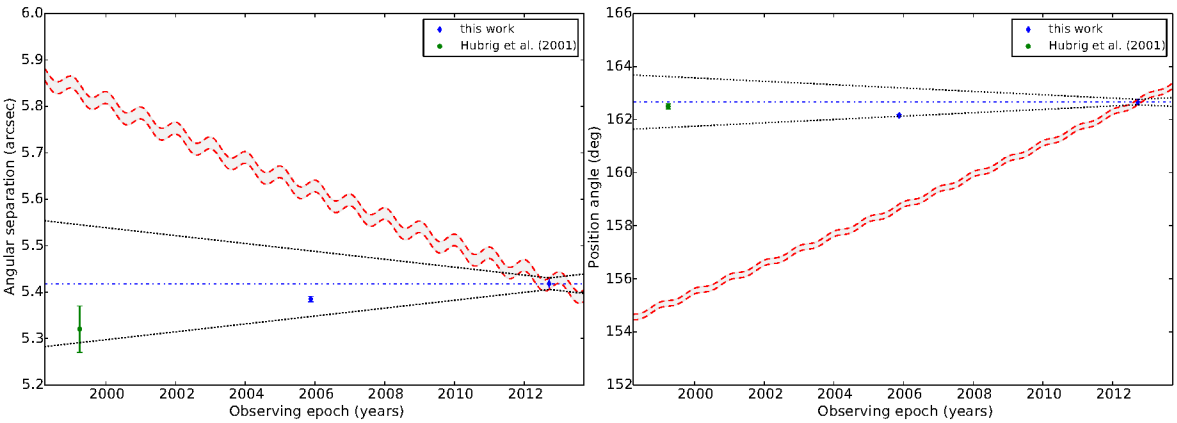


**Figure 16.** Common proper motion diagrams for HIP 20042 as example for a co-moving object. Shown are the separation (a) and position angle (b) over time. The expected change in separation and position angle for a non-moving background object, due to the proper motion of the primary and the annual parallax of the Earth (wobble), is indicated by the red dashed lines. The maximum expected orbital motion for a circular edge-on orbit (a), or a circular pole-on orbit (b), respectively, is shown as black dotted line. The origin of the data points is indicated by colour and shape.

spectral type B9 V. The observed companion candidate was first identified in 1999 (Hubrig et al. 2001). The background hypothesis for this object can be rejected at a $10\,\sigma$ level for the separation and at a $65\,\sigma$ level for the position angle. The probability $P_{\chi,\mathrm{bg}}$ that this companion candidate is a background object is 0.00 %, and the probability $P_{\chi,\mathrm{cmv}}$ for a co-moving companion is 0.68 %. Hence, it is most likely that the found object is gravitationally bound to the primary star. In this case the computed data and the illustration of these data fit the conclusion of a co-moving companion.

However, this is not necessarily the case. For some objects neither the calculated probabilities, the estimated deviations nor the CPM-digram allow a final conclusion on the companionship. In these cases the companion status of the object is set to (U)ndefined in Table A6 and additional observations for these object are required to derive final conclusions on their companionship.

The CPM diagrams for each target star with one or more detected companion candidate and the corresponding probabilities are illustrated in the appendix in section A.2.

## Estimation of the chance projection

The common proper motion analysis can not be applied for sample systems with only one observation or where the time difference between the observations is not large enough to measure significant changes in the separation or the position angle. For those systems a statistical approach was applied to estimate the probability of any found companion candidate being a chance superposition (see e.g., Brandner et al. 2000, Correia et al. 2006).
To dispose this method it is necessary to determine the local surface density of background/-foreground sources in a field surrounding each primary. Given the apparent magnitude of the companion candidate(s) in $J$, $H$, or $K$s calculated from the flux-ratio between primary and companion candidate(s), the number of sources as least as bright as the companion candidate(s) was determined from the 2MASS point source catalogue within a $2^\circ \times 2^\circ$ box surrounding each primary. The result is an average surface density of objects brighter than this limiting magnitude, herein after referred to as $\Sigma(m < m_{\mathrm{comp}})$. The total number of 2MASS point sources surrounding each sample star scaled to one square arc minutes is given as last column in Table 2 and Table A1.
The probability $\Pr(\Sigma, \Theta)$ of at least one unrelated source being located within a certain angular separation $\Theta$ from a particular primary star was derived employing the laws of probability, particularly using the binomial distribution $B(k|N, p)$ as ansatz.
Assuming that the random variable $X$ follows the binomial distribution with parameter $N$ and $p$, the probability of finding exactly $k$ unrelated sources among a sample of $N$ random uniform distributed stars, which are as least as bright as the companion candidate, is given by the probability mass function (pmf), and can be expressed as:

$$f(k; N, p) = \Pr(X = k) = \frac{N!}{k!(N-k)!} p^k (1-p)^{N-k} \tag{5.19}$$

The probability of success $p$ to find one unrelated source around any random selected object only depends on the ratio between investigated area $\pi\Theta^2$ and total area $A$ and is given by the geometric probability

$$p = \frac{\pi\Theta^2}{A}. \tag{5.20}$$

The FoV of the S 27 objective of the NaCo imager is about $27'' \times 27''$ for instance, i.e. $\Theta_{max}$ is $\approx$ 14 arcsec and the area therefore $\sim$ 616 arcsec$^2$. Thus, with the selected area $A$ of $2^\circ \times 2^\circ \cong 51.8 \times 10^6$ arcsec$^2$ the probability of finding one unrelated object in the vicinity of any primary source, within a sample of $N$ uniform distributed sources, is about 0.001 %. This estimation is an upper limit, i.e. in practice, $p$ is even lower for almost all investigated objects in this thesis. Hence, it can be assumed that the probability of success $p$ is much less than one ($p \ll 1$). The number of stars $N$, as least as bright as the investigated companion candidate, typically contained in an area $A$ around any target primary is much larger than the number of observed sources $k$ within an NaCo image, i.e. it is assumed

that $k << N(m < m_{\text{comp}})$.
Using these assumptions, the following two approximations can be made to Equation 5.19:

1) for $p << 1$

$$(1-p)^{N-k} \approx e^{-Np}, \text{and}$$

2) for $k << N(m < m_{\text{comp}})$

$$\frac{N!}{(N-k)!} \approx N^k.$$

The result is the Poisson distribution, also known as law of rare events, which is given by

$$f(k; N, p) = \frac{(Np)^k}{k!} \cdot e^{-Np}. \tag{5.21}$$

Replacing $p$ in Equation 5.21 by Equation 5.20 gives the probability of finding exactly $k$ objects among $N$ sources:

$$f(k; N, \Theta, A) = \left(\frac{\pi\Theta^2 N}{A}\right)^k \frac{1}{k!} \cdot e^{-N\frac{\pi\Theta^2}{A}} \qquad \text{with } \Sigma = \frac{N}{A}$$
$$f(k; \Sigma, \Theta) = \frac{(\pi\Sigma\Theta^2)^k}{k!} \cdot e^{-\pi\Sigma\Theta^2} \tag{5.22}$$

The probability of finding at least one unrelated source ($k = 1$), namely the identified companion candidate, in a certain distance of the primary $\Theta$ is equal to the probability of finding at most zero objects ($k = 0$). Hence,

$$\Pr(X \geq 1) = 1 - \Pr(X < 1) = 1 - \underbrace{(\pi\Sigma\Theta^2)^0}_{=1} \cdot e^{-\pi\Sigma\Theta^2}$$
$$\Rightarrow \qquad \Pr(\Sigma, \Theta) = 1 - e^{-\pi\Sigma\Theta^2}. \tag{5.23}$$

The probability $\Pr(\Sigma, \Theta)$ of finding an unrelated source in the vicinity of a primary source, calculated for each sample star with a found companion candidate, is listed in the second last column in Table A6. The objects whose probability $\Pr(\Sigma, \Theta)$ of being a chance projection is less than 5 % are considered to be likely co-moving companions, while in those cases where $\Pr(\Sigma, \Theta) > 5\,\%$ the source is likely background containment, respectively. However, further observations are required to prove or reject their physical association to the primary.

## 5.3 Photometry

The photometry, i.e the magnitude difference, the apparent and absolute magnitudes of the primary star and any found companion candidate, was calculated using the measured flux

ratios between the host star and the companion candidates, the combined near-infrared *JHK*s magnitudes obtained from the 2MASS point source catalogue (Cutri et al. 2003) and the distance of the system. A `PYTHON` program was written using `IDL-DAOPHOT`[11] procedures to quantify the flux ratios and calculate the individual magnitudes for each epoch in the observed bands.

For target systems with companion candidates at small separations simultaneous PSF-fitting of all sources was applied using `IDL/nstar`. At larger separations aperture photometry was employed using `IDL/aper` to obtain the flux ratios. This differentiation was made to take advantage of the capabilities of both measurement processes.

The basic principle of PSF-fitting is that every point source in an image, at least in theory, has the same intrinsic profile shape, i.e. they differ only in their brightness and amplitude. This means that a standard star profile can be established, which then can be scaled up or down in amplitude to fit any individual source. PSF-fitting, in general, is more immune to crowding than aperture photometry. The best-scale factor is determined by using the pixels in the core of the stars profile, which contain most of the signal. It is not necessary to use the wings, because all sources have the same profile. Therefore, the profiles of nearby sources such as a close binary can overlap partially and it is still possible to obtain accurate PSF scaling factors. However, in reality the images of point sources are convolved with the telescope optics and blurring by the Earth's atmosphere.

The latter one can be removed almost completely using AO systems. However, the quality of such systems, in turn, depend on parameter such as seeing, the Fried parameter $r_0$, the atmospheric time constant $\tau_0$ and the isoplanatic angle.

To illustrate the deformation of the stellar profiles an image of the dense globular cluster 47 Tuc taken on September 2012 is shown in Figure 17. The deformation of the stars with increasing distance to the central star of this image is clearly visible. The reference star for the AO correction is marked with a white circle.

In aperture photometry on the other hand, the sources are enclosed by a circle of radius $r$ and all the flux contained in that circle is added. The contribution of the background in the same area is subtracted afterwards yielding an "absolute" measurement of the source's brightness, in Analogue Digital Units (ADU). This value can be converted directly to the number of photoelectrons $N(e^-)$ captured by the CCD when multiplied by the CCD gain factor. The advantage of aperture photometry is that it does not depend on the shape of the stellar profile, since all arriving photoelectrons of a source within the aperture are counted. However, if the light from a source is contaminated by a secondary source for instance, the measured flux would be overestimated and consequently would produce wrong results. The stars were selected from the `IDL/starfinder` detection results, and the positions were used as input for either aperture or PSF photometry after selecting the appropriate procedure.

The magnitude differences of the detected objects in each epoch, relative to the primary

[11] Astronomy User's Library, a collection of astronomy-related procedures written in the IDL programming language (Landsman 1995), and adopted from IRAF-DAOPHOT packages (Stetson 1987).

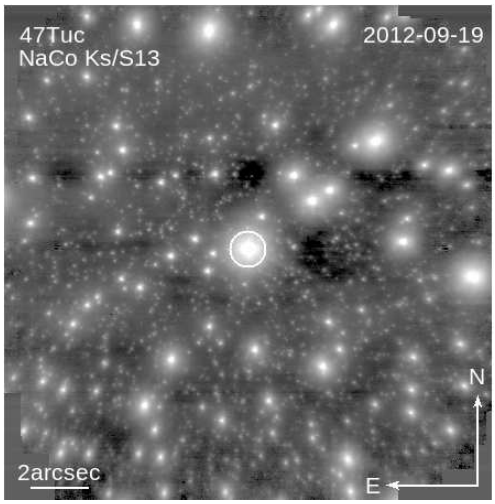


**Figure 17.** Image of 47 Tuc observed with the NaCo S13 objective in the *K*s band on September 2012. The image illustrates the effect of deformation of the stellar profiles by AO correction with increasing distance to the reference star, marked with a white circle.

star, were then computed, via

$$\Delta m_i = -2.5 \cdot \log_{10}\left(\frac{F_i}{F_{\text{prim}}}\right)$$
$$\delta(\Delta m_i) = \frac{2.5}{\log(10)} \cdot \left(\frac{F_i}{F_{\text{prim}}}\right)^{-1} \cdot \Delta\left(\frac{F_i}{F_{\text{prim}}}\right), \tag{5.24}$$

where $F_i$ is the measured flux of source $i$, and $F_{\text{prim}}$ is the measured flux of the primary star. Owing to the lack of photometric calibrators or photometric conditions in the vast majority of the investigated nights, the apparent magnitude of each individual object was calculated by assuming the combined brightness of the objects, measured by 2MASS in one epoch. The combined brightness $m_{X,\text{2MASS}}$ was divided into individual magnitudes $m_{X,i}$ according to the measured flux ratio in each filter band $X$, via

$$m_{X,i} = m_{X,\text{2MASS}} - 2.5 \cdot \log_{10}\left(\frac{F_{X,i}}{F_{X,0} + F_{X,1} + \cdots + F_{X,N}}\right), \tag{5.25}$$

where $F_{X,i}$ is the flux of the investigated source $i$ and $F_{X,0} + F_{X,1} + \cdots + F_{X,N}$ is the total flux of all sources contributing to the combined brightness, obtained from 2MASS. However, it should be pointed out that by using the combined brightness from the 2MASS catalogue a possible variability of the objects is not taken into account, and hence has to be taken with reservations.

The absolute magnitude $M_{X,i}$ of the object $i$ in the image, including the correction for interstellar extinction, is given by

$$M_{X,i} = m_{X,i} - A_X + 5 - 5 \cdot \log_{10} D[\text{pc}] \tag{5.26}$$
$$\Delta M_{X,i} = \Delta m_{X,i} + \Delta A_X + \frac{5 \cdot \Delta D}{D \cdot \log(10)}, \tag{5.27}$$

where $m_{X,i}$ is the calculated apparent magnitude of the investigated source $i$, $A_X$ is the estimated interstellar extinction in the used filter band $X$ ($X$ = *JHK*s) and $D$ is the distance of the system, given in parsec. $A_X$ was calculated from the constant extinction ratios $A_X/A_V$ published by Savage and Mathis (1979), Rieke and Lebofsky (1985) and Cardelli et al. (1989), and listed in Table 12. The visual extinction $A_V$ was obtained from the procedures used for the determination of physical parameter (see section 5.4). The listed extinction ratio values in Table 12 vary slightly, therefore, the average constant extinction ratio $C_X$, at near-infrared wavelengths, was utilized to calculate the interstellar extinction $A_X$ in this study. For observations taken in intermediate band (IB) or narrow band (NB) filter, e.g., *IB*2.18 or *NB*2.12, the interstellar extinction was calculated applying the nearest corresponding *JHK*s filter coefficient according to their central wavelength. The obtained

**Table 12.** Extinction ratios at near-infrared wavelengths

| | $A_X/A_V$ for $R_V = 3.1$ | | | |
|---|---|---|---|---|
| Filter ($X$) | (1) | (2) | (3) | $C_X$ |
| $J$ | 0.282 | 0.281 | 0.282 | 0.282±0.001 |
| $H$ | 0.190 | - | 0.175 | 0.182±0.011 |
| $K$ | 0.114 | 0.123 | 0.112 | 0.114±0.006 |

**Notes.** $R_V$ is the ratio of the visual extinction $A_V$ and the colour excess $E_{B-V}$. $C_X$ is the constant average extinction ratio in filter band $X$ applied in this study.
**References.** (1) Cardelli et al. (1989). (2) Savage and Mathis (1979). (3) Rieke and Lebofsky (1985).

magnitude differences as well as the calculated apparent an absolute magnitudes are listed exemplary in Table 13 and the full list of all investigated objects is given in Table A4.

## 5.4 Determination of physical parameter

This section deals with the determination of the fundamental parameter of the primary and the found companions. In subsection 5.4.1, the procedure to estimate the primary mass and the system age is described, and in subsection 5.4.2 the estimation of the physical parameter of any found companion is explained.

### 5.4.1 Primary mass and age

The method presented in this section is based on the work by Dr. Janos Schmidt, which is also published in Schmidt et al. (2014). The procedure therein was adopted for this work to get an estimate of the primary mass and age using the most recent version of the `MATLAB` program (MATLAB 2010) developed and kindly provided by Dr. Schmidt.
With the observational parameter for each investigated object, i.e. *BVJHK*s photometry,

**Table 13.** Measured brightness differences, apparent and absolute magnitudes for the visual companions identified in this study.

| Object | Distance (pc) | Observation date | Band | $\Delta m$[a] (mag) | $m_{\mathrm{system}}$ (mag) | $m_{\mathrm{prim}}$ (mag) | $m_{\mathrm{comp}}$ (mag) | $M_{\mathrm{prim}}$ (mag) | $M_{\mathrm{comp}}$ (mag) |
|---|---|---|---|---|---|---|---|---|---|
| | | | | Binaries | | | | | |
| 2548 | $81.0^{+3.8}_{-3.5}$ | 2005-12-06 | $K$s | 1.1620±0.0044 | 5.637±0.019 | 5.96±0.02 | 7.119±0.022 | $1.415^{+0.103}_{-0.095}$ | $2.577^{+0.104}_{-0.095}$ |
| | | 2007-09-16 | $K$s | 1.1400±0.0054 | 5.637±0.019 | 5.96±0.02 | 7.103±0.023 | $1.421^{+0.103}_{-0.095}$ | $2.561^{+0.104}_{-0.095}$ |
| 15627 | $156.0^{+20.1}_{-16.0}$ | 2006-10-16 | $H$ | 2.166±0.049 | 5.439±0.017 | 5.578±0.025 | 7.743±0.075 | $-0.44^{+0.28}_{-0.22}$ | $1.73^{+0.29}_{-0.23}$ |
| 16511 | $107.4^{+4.6}_{-4.2}$ | 2005-01-06 | $K$s | 2.547±0.025 | 5.881±0.017 | 5.980±0.019 | 8.53±0.04 | $0.824^{+0.094}_{-0.087}$ | $3.371^{+0.101}_{-0.094}$ |
| | | 2005-11-26 | $K$s | 2.710±0.025 | 5.881±0.017 | 5.967±0.019 | 8.68±0.04 | $0.811^{+0.094}_{-0.087}$ | $3.521^{+0.101}_{-0.094}$ |
| | | 2011-08-25 | $K$s | 2.353±0.029 | 5.881±0.017 | 6.00±0.02 | 8.351±0.043 | $0.843^{+0.095}_{-0.087}$ | $3.195^{+0.102}_{-0.095}$ |
| 16803 | $149.3^{+12.3}_{-10.6}$ | 2005-01-09 | $K$s | 0.884±0.012 | 5.526±0.024 | 5.924±0.028 | 6.808±0.032 | $0.07^{+0.18}_{-0.16}$ | $0.96^{+0.18}_{-0.16}$ |
| | | 2007-09-20 | $K$s | 0.812±0.026 | 5.526±0.024 | 5.947±0.032 | 6.759±0.042 | $0.09^{+0.18}_{-0.16}$ | $0.91^{+0.18}_{-0.16}$ |
| | | 2007-09-30 | $K$s | 0.798±0.013 | 5.526±0.024 | 5.951±0.028 | 6.749±0.033 | $0.10^{+0.18}_{-0.16}$ | $0.90^{+0.18}_{-0.16}$ |
| 17563 | $163.7^{+8.2}_{-7.4}$ | 2005-01-10 | $K$s | 5.88±0.13 | 5.592±0.02 | 5.597±0.021 | 11.48±0.16 | $-0.5^{+0.1}_{-0.1}$ | $5.38^{+0.19}_{-0.18}$ |
| : | : | : | : | : | : | : | : | : | : |
| | | | | Higher-order multiple systems | | | | | |
| 24925AB | $281.7^{+158.8}_{-74.7}$ | 2005-01-09 | $K$s | 2.27637±0.00077 | 6.433±0.019 | 6.62±0.02 | 8.899±0.021 | $-0.65^{+1.22}_{-0.58}$ | $1.62^{+1.22}_{-0.58}$ |
| | | 2012-09-19 | $K$s | 2.2885±0.0043 | 6.433±0.019 | 6.618±0.021 | 8.906±0.024 | $-0.66^{+1.22}_{-0.58}$ | $1.63^{+1.22}_{-0.58}$ |
| | | 2013-01-04 | $K$s | 2.258±0.001 | 6.433±0.019 | 6.62±0.02 | 8.878±0.021 | $-0.66^{+1.22}_{-0.58}$ | $1.60^{+1.22}_{-0.58}$ |
| 24925AC | | 2005-01-09 | $K$s | 2.920±0.015 | 6.433±0.019 | 6.62±0.02 | 9.542±0.034 | $-0.65^{+1.22}_{-0.58}$ | $2.27^{+1.22}_{-0.58}$ |
| | | 2012-09-19 | $K$s | 2.988±0.022 | 6.433±0.019 | 6.618±0.021 | 9.605±0.041 | $-0.66^{+1.22}_{-0.58}$ | $2.33^{+1.23}_{-0.58}$ |
| | | 2013-01-04 | $K$s | 3.001±0.012 | 6.433±0.019 | 6.62±0.02 | 9.62±0.03 | $-0.66^{+1.22}_{-0.58}$ | $2.35^{+1.22}_{-0.58}$ |
| 26237AB | $271.0^{+130.6}_{-66.5}$ | 2005-04-09 | $K$s | 0.9890±0.0089 | 5.056±0.017 | 5.536±0.025 | 6.525±0.029 | $-1.67^{+1.05}_{-0.53}$ | $-0.68^{+1.05}_{-0.53}$ |
| | | 2012-09-19 | $K$s | 1.0510±0.0058 | 5.056±0.017 | 5.516±0.018 | 6.567±0.021 | $-1.69^{+1.05}_{-0.53}$ | $-0.63^{+1.05}_{-0.53}$ |
| 26237AC | | 2005-04-09 | $K$s | 2.036±0.054 | 5.056±0.017 | 5.536±0.025 | 7.572±0.068 | $-1.67^{+1.05}_{-0.53}$ | $0.37^{+1.05}_{-0.54}$ |
| | | 2012-09-19 | $K$s | 2.07312±0.00018 | 5.056±0.017 | 5.516±0.018 | 7.589±0.019 | $-1.69^{+1.05}_{-0.53}$ | $0.39^{+1.05}_{-0.53}$ |
| : | : | : | : | : | : | : | : | : | : |

**Notes.** The given companion identification AB, AC, etc. for visual higher-order multiples indicates the sequences of detection by increasing magnitude difference. The full list is presented in Table A4.

[a] Measured magnitude difference in the given band.

parallax, spectral type and luminosity class, the effective temperature $T_{\rm eff}$, the interstellar extinction in the $V$ band $A_{\rm V}$ and the bolometric luminosity $L_{\rm bol}$ were derived, and then the mass and age were estimated comparing the results with theoretical models. The most important steps of the procedure are described in the following.

The given spectral type from literature was employed to calculate the effective temperature using data from Lang (1992)[12] and Kenyon and Hartmann (1995) for main sequence stars. The temperature was then linear interpolated between neighbouring grid-points for a decimal spectral type. To get an estimate on the error of the temperature an uncertainty of the spectral type of $\pm 1$ subclass was assumed. This rather conservative assumption was made to take into account that the source of the given spectral type is mostly unknown, i.e. it is not clear whether the given spectral type was determined by photometric or spectroscopic analysis.

The interstellar reddening in the $V$ band $A_{\rm V}$ due to interstellar extinction was compiled from the measured colours $(X-V)_{\rm m}$ and the model colours $(X-V)_0$ by Bessell et al. (1998), via

$$A_{\rm V} = \frac{(X-V)_{\rm m} - (X-V)_0}{\frac{A_{\rm X}}{A_{\rm V}} - 1}. \tag{5.28}$$

The constant ratios $\frac{A_{\rm X}}{A_{\rm V}}$ applied for the different available bands $X$ ($X = BVJHK$) are listed in Table 12. However, the model data by Bessell et al. (1998) depend on $\log g$ and the temperature, hence on the spectral classification. The investigated sample does not contain objects with negative parallax values. Therefore, no correction of the parallaxes according to Smith and Eichhorn (1996) was applied. The bolometric luminosity was then derived by

$$L_{\rm bol} = 10^{0.4\cdot(5\log d - 5 + 4.74 - BC_V - m_V + A_V)}, \tag{5.29}$$

where $d$ is the distance in pc, $BC_V$ the bolometric correction in the $V$ band, $m_V$ the apparent $V$ band magnitude, and $A_V$ the corresponding interstellar extinction. The $BC_V$ obtained from Bessell et al. (1998) was calibrated to the bolometric magnitude of the Sun $M_{\rm bol,\odot} = 4.74$ mag and is consistent with the apparent magnitude of the Sun $V_\odot = -26.76$ mag given in their paper. This test is suggested by Torres (2010), because the zero point of $BC_V$ is arbitrary, while the bolometric magnitude of the Sun $M_{\rm bol,\odot}$ cannot be chosen arbitrary.

Mass and age were estimated by comparing the calculated bolometric luminosities and effective temperatures with theoretical models for solar metallicity by Schaller et al. (1992), Bertelli et al. (1994) and Claret (2004). The metallicity is only well known for few stars and affect the mass estimation only by a few percent. The differences in mass between the models with the same metallicity are comparable to this (Hohle et al. 2010). The results were averaged from the error-weighted closest grip points per model.

The results of the parameter estimation for the 315 primary stars (blue dots), without the post-RGB star HIP 3678, contained in this sample are shown in the left-hand panel of

[12] Originally from Schmidt-Kaler (1982)

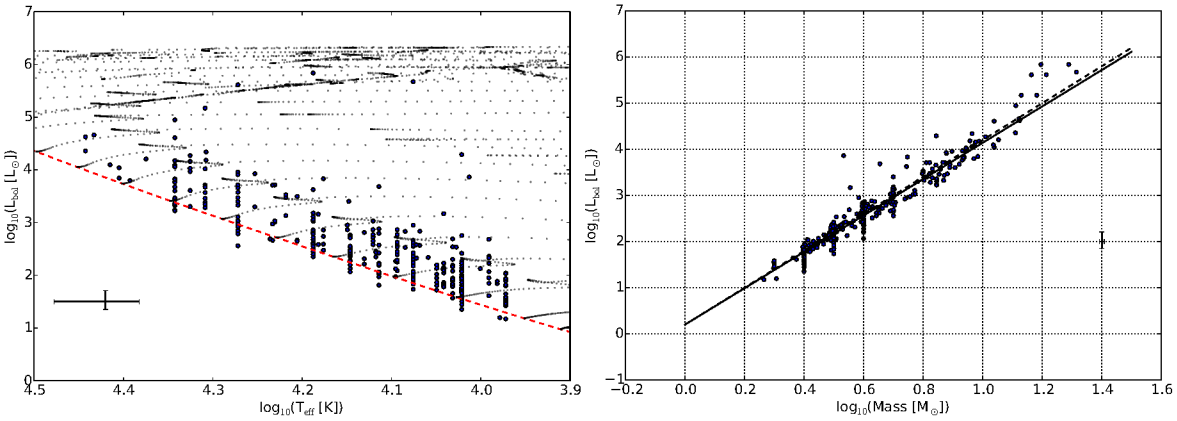


**Figure 18.** *Left:* Hertzsprung-Russell diagram of the B-type sample stars investigated in this study. Shown are the modelled luminosities vs effective temperature for 316 primary stars (blue dots). The CSPN HIP 3678 is excluded in this plot. The evolutionary model data by (Claret 2004) are indicated as black dots and the zero age main sequence (ZAMS) is plotted as red dashed line. The average error of the estimated luminosities and effective temperatures is represented by the black cross on the left side. *Right:* Plot of the derived mass luminosity relation $L \propto M^{\beta}$ for main sequence stars with $M \leq 10\,\mathrm{M}_{\odot}$, yielding $\beta = 3.94 \pm 0.07$ (solid line). Also shown for comparison is the published value by Hilditch (2001) with $\beta = 4.0$ (dashed line). The average error of the estimated luminosities and masses is represented by the black cross.

Figure 18. The plot shows the Hertzsprung-Russell diagram of the luminosity as function of the temperature. Also indicated are the zero age main sequence (ZAMS, red dashed line) and the theoretical mass tracks (black dots) according to Claret (2004). The average uncertainty is indicated by the black cross.

To check consistency of the obtained masses for the primary sample stars, the empirical mass luminosity relation $L \propto M^{\beta}$ was determined from the main sequence stars contained in the sample. Out of the sample of 315 stars, 212 are assumed to be main sequence stars. Within this sub-sample 199 stars have an estimated mass $M \leq 10\,\mathrm{M}_{\odot}$. The mass luminosity relation for these stars yields $\beta = 3.94 \pm 0.07$ and is shown in the right-hand panel of Figure 18 as solid line. The result is consistent with the value from Hilditch (2001) with $\beta = 4.0$, for main sequence stars with less than $10\,\mathrm{M}_{\odot}$, also shown as dashed line.

### 5.4.2 Companion mass

The fundamental parameter, i.e. temperature, luminosity and mass, of any found companion were determined using the derived absolute magnitude in the *JHK*s bands from the photometry (see section 5.3) and the estimated age of the primary assuming that the primary age corresponds to the system age, i.e. all components have formed at the same time. The evolutionary models by Baraffe et al. (1998; 2002), Girardi et al. (2000), Siess et al. (2000), Bertelli et al. (2009) and Bressan et al. (2012), as well as empirical mass-luminosity relations by Delfosse et al. (2000) were employed to determine the parameter of any companion. For all models solar metallicity was assumed, i.e. from the available model

data those tables were selected where the metallicity $Z$ is about 0.02 and the fraction of helium $Y$ is roughly 0.26. The main characteristics of the used models are summarised in Table 14. The evolutionary models slightly differ in their assumed metallicity. This also effects the obtained masses. However, the variation between these models is very low, and therefore the variation of the results is also expected to be at a negligible level of percentage. The mass range covered by the evolutionary tracks varies from 0.02 $M_\odot$ to more than 20 $M_\odot$, and the available isochrones range from a few thousand year up to several Gyr. For each model a three-dimensional grid was constructed with the input parameter age

**Table 14.** Parameter ranges covered by the utilised evolutionary models.

| Model | Y | Z | Mass $M_\odot$ | Age $\log_{10}([yr])$ |
|---|---|---|---|---|
| Baraffe et al. (1998; 2002) | 0.275 | -[a] | 0.02–1.4 | 6.0–9.9 |
| Siess et al. (2000) | 0.279 | 0.02 | 0.1–7.0 | ∼3.0–10.4 |
| Girardi et al. (2000) | 0.273 | 0.019 | 0.1–7.0 | 7.8–10.25 |
| Bertelli et al. (2009) | 0.26 | 0.017 | 0.15–20.0 | 8.95–10.15 |
| Bressan et al. (2012) | 0.275 | 0.0152 | 0.1–350 | 6.0–10.1 |

[a] Baraffe et al. (1998) only gives the total metal abundance [M/H]=0.

and magnitude in the x-y plane and the resulting physical parameter in z direction. Points between the model grid points were estimated by linear interpolation. Given the input parameter, magnitude and age, and their associated uncertainties (3×3 values in total), the mass and the other parameter were determined as median and standard deviation of this set of 9 result data points. Finally, the results of the different models were averaged to obtain mass, luminosity and effective temperature of any found companion. The uncertainty of the results was determined from the average error of each model.

In order to analyse the binary properties of the sample statistically, the mass ratio $q$ for each system and each model was calculated from the estimated mass of the primary and the companion. The mass ratio as a function of the primary is given by

$$q = \frac{M_S}{M_P},$$

where $M_S$ donates the mass of the companion and $M_P$ the mass of the primary. The obtained mass ratios from each model were also averaged. The physical parameter derived for each sample stars and their identified companion(s) as well as the calculated average masses and mass ratios are summarised in Table 15 and Table A5.

**Table 15.** Estimated masses for the visual companions resolved in this study. The full list is presented in Table A5.

| Object | log(*Age*[*yr*]) | Observation date | Band | $M_{X,\mathrm{comp}}$ (mag) | $M_{\mathrm{prim}}$ ($M_\odot$) | $M_{\mathrm{comp}}$ (1) ($M_\odot$) | (2) ($M_\odot$) | (3) ($M_\odot$) | (4) ($M_\odot$) | (5) ($M_\odot$) | (6) ($M_\odot$) | $M_{\mathrm{comp}}$ ($M_\odot$) | $q$ |
|---|---|---|---|---|---|---|---|---|---|---|---|---|---|
| | | | | | | Binaries | | | | | | | |
| 2548 | $9.06^{+0.03}_{-0.04}$ | 2005-12-06 | *Ks* | $2.577^{+0.104}_{-0.095}$ | 2.00±0.01 | | 1.26±0.02 | 1.24±0.03 | 1.28±0.03 | 1.28±0.03 | 1.29±0.03 | 1.27±0.03 | 0.64±0.01 |
| | | 2007-09-16 | *Ks* | $2.561^{+0.104}_{-0.095}$ | | | 1.27±0.03 | 1.24±0.03 | 1.28±0.03 | 1.28±0.03 | 1.30±0.03 | 1.28±0.03 | 0.64±0.01 |
| 15627 | $7.64^{+0.08}_{-0.09}$ | 2006-10-16 | *H* | $1.73^{+0.29}_{-0.23}$ | 4.4±0.1 | | | | 2.1±0.3 | 2.0±0.2 | 2.1±0.2 | 2.1±0.2 | 0.46±0.06 |
| 16511 | $8.1^{+0.1}_{-0.2}$ | 2005-01-06 | *Ks* | $3.371^{+0.101}_{-0.094}$ | 2.65±0.07 | | 1.06±0.02 | 1.03±0.02 | 1.07±0.02 | 1.06±0.02 | 1.07±0.03 | 1.06±0.02 | 0.40±0.01 |
| | | 2005-11-26 | *Ks* | $3.521^{+0.101}_{-0.094}$ | | | 1.02±0.02 | 0.99±0.02 | 1.03±0.02 | 1.02±0.02 | 1.03±0.02 | 1.02±0.02 | 0.38±0.01 |
| | | 2011-08-25 | *Ks* | $3.195^{+0.102}_{-0.095}$ | | | 1.12±0.02 | 1.08±0.02 | 1.12±0.03 | 1.11±0.03 | 1.13±0.03 | 1.11±0.03 | 0.42±0.01 |
| 16803 | $8.47^{+0.03}_{-0.03}$ | 2005-01-09 | *Ks* | $0.96^{+0.18}_{-0.16}$ | 3.13±0.04 | | 2.34±0.09 | | 2.5±0.1 | 2.5±0.1 | 2.5±0.1 | 2.4±0.1 | 0.78±0.03 |
| | | 2007-09-20 | *Ks* | $0.91^{+0.18}_{-0.16}$ | | | 2.4±0.1 | | 2.5±0.1 | 2.5±0.1 | 2.5±0.1 | 2.5±0.1 | 0.79±0.03 |
| | | 2007-09-30 | *Ks* | $0.90^{+0.18}_{-0.16}$ | | | 2.38±0.09 | | 2.5±0.1 | 2.5±0.1 | 2.5±0.1 | 2.5±0.1 | 0.79±0.03 |
| 17563 | $7.1^{+0.3}_{-0.7}$ | 2005-01-10 | *Ks* | $5.38^{+0.19}_{-0.18}$ | 5.9±0.3 | 0.58±0.03 | | 0.2±0.1 | 0.2±0.1 | 0.56±0.03 | 0.3±0.1 | 0.39±0.09 | 0.07±0.02 |
| 20020 | $8.26^{+0.03}_{-0.04}$ | 2004-12-08 | *Ks* | $2.04^{+0.12}_{-0.11}$ | 2.79±0.06 | | 1.61±0.07 | | 1.69±0.07 | 1.65±0.08 | 1.67±0.08 | 1.66±0.08 | 0.59±0.03 |
| | | 2007-09-20 | *Ks* | $2.06^{+0.13}_{-0.12}$ | | | 1.58±0.08 | | 1.68±0.07 | 1.64±0.08 | 1.66±0.08 | 1.64±0.08 | 0.59±0.03 |
| | | 2007-09-30 | *Ks* | $2.0^{+0.1}_{-0.1}$ | | | 1.61±0.07 | | 1.69±0.07 | 1.65±0.08 | 1.67±0.07 | 1.66±0.07 | 0.59±0.03 |
| 20042 | $7.4^{+0.2}_{-0.3}$ | 2005-11-16 | *Ks* | $6.48^{+0.32}_{-0.32}$ | 3.9807±0.0005 | 0.37±0.04 | | 0.17±0.05 | 0.15±0.05 | 0.35±0.05 | 0.19±0.05 | 0.25±0.05 | 0.06±0.01 |
| | | 2012-09-19 | *Ks* | $7.24^{+0.35}_{-0.35}$ | | 0.26±0.04 | | 0.10±0.03 | 0.10±0.01 | 0.24±0.03 | 0.13±0.03 | 0.17±0.03 | 0.042±0.007 |
| : | : | : | : | : | : | : | : | : | : | : | : | : | : |
| | | | | | | Higher-order multiple systems | | | | | | | |
| 24925AB | $8.12^{+0.04}_{-0.05}$ | 2005-01-09 | *Ks* | $1.62^{+1.22}_{-0.58}$ | 3.8±0.1 | | 2.0±0.7 | | 2.1±0.8 | 2.3±0.7 | 2.3±0.7 | 2.2±0.7 | 0.6±0.2 |
| | | 2012-09-19 | *Ks* | $1.63^{+1.22}_{-0.58}$ | | | 2.0±0.7 | | 2.1±0.8 | 2.3±0.7 | 2.3±0.7 | 2.2±0.7 | 0.6±0.2 |
| | | 2013-01-04 | *Ks* | $1.60^{+1.22}_{-0.58}$ | | | 2.0±0.7 | | 2.1±0.8 | 2.3±0.7 | 2.3±0.7 | 2.2±0.7 | 0.6±0.2 |
| 24925AC | | 2005-01-09 | *Ks* | $2.27^{+1.22}_{-0.58}$ | | | 1.5±0.6 | 1.1874±0.0008 | 1.6±0.7 | 1.8±0.6 | 1.8±0.6 | 1.6±0.5 | 0.4±0.1 |
| | | 2012-09-19 | *Ks* | $2.33^{+1.23}_{-0.58}$ | | | 1.4±0.6 | 1.1654±0.0005 | 1.5±0.6 | 1.7±0.6 | 1.8±0.6 | 1.5±0.5 | 0.4±0.1 |
| | | 2013-01-04 | *Ks* | $2.35^{+1.22}_{-0.58}$ | | | 1.4±0.6 | 1.1601±0.0005 | 1.5±0.6 | 1.7±0.6 | 1.7±0.6 | 1.5±0.5 | 0.4±0.1 |
| 26237AB | $6.98^{+0.05}_{-0.06}$ | 2005-04-09 | *Ks* | $-0.68^{+1.05}_{-0.53}$ | 10.9±0.4 | | | | 7.0±0.7 | 7.3±2.0 | 7.3±2.0 | 7.2±2.0 | 0.7±0.2 |
| | | 2012-09-19 | *Ks* | $-0.63^{+1.05}_{-0.53}$ | | | | | 6.9±0.7 | 7.2±2.0 | 7.2±2.0 | 7.1±2.0 | 0.6±0.2 |
| 26237AC | | 2005-04-09 | *Ks* | $0.37^{+1.05}_{-0.54}$ | | | | | 4.4±2.0 | 4.6±1.0 | 4.6±1.0 | 4.5±2.0 | 0.4±0.1 |
| | | 2012-09-19 | *Ks* | $0.39^{+1.05}_{-0.53}$ | | | | | 4.3±2.0 | 4.6±1.0 | 4.6±1.0 | 4.5±2.0 | 0.4±0.1 |
| 39331AB | $7.34^{+0.04}_{-0.05}$ | 2007-01-20 | *Ks* | $7.25^{+1.36}_{-0.61}$ | 9.2±0.5 | 0.3±0.1 | | 0.13±0.08 | | 0.3±0.1 | 0.19±0.08 | 0.2±0.1 | 0.02±0.01 |
| 39331AC | | 2007-01-20 | *Ks* | $7.49^{+1.37}_{-0.61}$ | | 0.3±0.1 | | 0.11±0.07 | | 0.3±0.1 | | 0.2±0.1 | 0.02±0.01 |
| 42504AB | $7.2^{+0.2}_{-0.4}$ | 2006-01-07 | *Ks* | $2.6^{+0.1}_{-0.1}$ | 5.0±1.0 | | | 1.23±0.04 | 1.30±0.06 | 1.31±0.04 | 1.30±0.06 | 1.28±0.05 | 0.26±0.01 |
| 42504AC | | 2006-01-07 | *Ks* | $4.75^{+0.12}_{-0.11}$ | | 0.71±0.02 | | 0.5±0.1 | 0.5±0.1 | 0.69±0.02 | 0.5±0.1 | 0.6±0.1 | 0.11±0.02 |
| : | : | : | : | : | : | : | : | : | : | : | : | : | : |

**Note.** $M_{\mathrm{comp}}$ is the average mass obtained from available models. $q$ is the mass ratio as function of the primary mass; $q = M_{\mathrm{comp}}/M_{\mathrm{P}}$.
**References.** (1) Delfosse et al. (2000); empirical mass-luminosity relation for $M \lesssim 1.0\,M_\odot$. (2) Girardi et al. (2000). (3) Baraffe et al. (2002). (4) Siess et al. (2000). (5) Bertelli et al. (2009). (6) Bressan et al. (2012)

# 6 Detection limits and completeness

In order to minimize the bias in the characterisation of the multiplicity status of all target objects, and consequently in the resulting distribution of the companion properties, the quantitative detection limits were estimated in the course of the analysis of each target star. These limits depend on a variety of parameter such as the atmospheric conditions, i.e. seeing and coherence time, in the observing night, the total exposure time, but also on the angular separation and magnitude difference from the bright primary star. The achieved contrast level for each target star were used to create a completeness map of the survey in order to be able to estimate reasonable limits for the statistical analysis.

*Detection limits*

To measure the detection limits as a function of the angular separation, a one-dimensional sensitivity curve was created using the following procedure. First, for each pixel $i$ on the detector the distance $r_i$ to the previously determined position of the central star was calculated, and the corresponding measured flux $F_j$ stored. Then, $n$ annuli of equal width $w$ were selected depending on the central wavelength $\lambda$ of the used filter by

$$w = 0.61 \cdot \frac{\lambda}{D},$$

the half diffraction limit available in the observation. $D$ is the size of the mirror at the VLT, with $D = 8.2\,\mathrm{m}$. For a typical observation investigated in this study, taken in the $K$s band ($\lambda = 2.18\,\mu\mathrm{m}$) with the S13 objective, the width of an annulus $w$ is $\approx 2.5\,\mathrm{Px}$.
The flux values $F_j$ from all $r_j \in (R_i, R_{i+1}]$, with $i = 0, 1, \ldots n-1$, were than sorted, the upper and lower 10 % excluded and those values rejected which deviate by more than $3\sigma$[13] from the median in order to remove the contribution of the stars contained in the annulus from the calculation. The standard deviation of the remaining values $\sigma(R)$ was than used as estimate of the background noise. The resulting $3\,\sigma$ contrast level as a function of the angular separation is then estimated to be

$$\Sigma(R) = 2.5 \cdot \log\left[\frac{F_{\mathrm{peak}}}{3\sigma(R)}\right] \ \mathrm{mag}. \tag{6.1}$$

The procedure described above was also applied to the PSF-subtracted image. However, the differences between the two resulting curves is only marginal. The main reason for this is that the main source of the noise is the photon-noise which is superimposed with the measured signal. The removal of the signal by subtraction of the PSF does not significantly change the measured residual noise, and thus the computed sensitivity remains almost equal.

[13] The choice of the $3\,\sigma$ noise level was confirmed by inserting and retrieving simulated companions at this contrast level by Haase (2009).

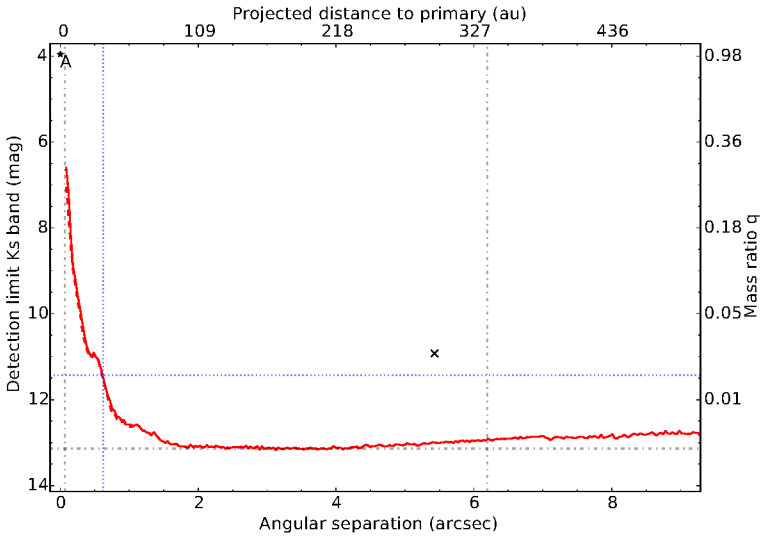


**Figure 19.** Detection limit example plot for HIP 20042 observed in September 2012. Shown is the achieved apparent magnitude (left y-axis) in the observed band as function of angular (bottom x-axis) and projected separation (top x-axis), in au. The position of the primary (A) is marked with an asterisk and the position of the found companion as cross. The measured $3\,\sigma$ sensitivity curve is shown as red line. Objects below this line cannot be detected. The measured sensitivity curve from the PSF-subtracted image is also shown as red dashed line. The detectable mass ratios $q$ (right y-axis) obtained from evolutionary models by Baraffe et al. (1998; 2002), Bressan et al. (2012) are indicated, as well as the brown dwarf limit ($75\,M_{Jup}$) at the given age of $\approx 27$ Myr, shown as blue dotted line, if available. In addition, the diffraction limit (left vertical dash-dotted line) of the telescope in the observed band, and the closest image border to the central star (right vertical dash-dotted line) are given.

The detection limit curve estimated for each investigated object is illustrated in a dynamic range plot. As an example, the deepest available sensitivity curve for HIP 20042 AB is shown in Figure 19. The image was taken with the NaCo S 13 objective in the $Ks$ band on September 2012. The location of the primary (A) is marked with asterisk and the position of the companion by a cross. The plot shows the reachable apparent magnitude as function of the angular separation in the observed filter band (red line). Objects below this line cannot be detected. As can be seen the detection limit increases towards larger distance from the primary with a maximum between about 2 and 4 arc second which corresponds to an apparent magnitude of $\approx 13$ mag (grey dash-dotted line). The decrease in sensitivity beyond 4 arcsec can be explained with jitter-technique used to obtain the image. Since the telescope has been moved slightly between each image, the position of the primary varies on the detector with respect to the image boundaries (see Figure 9a). During reduction, the images are aligned to the central star. Therefore, the number of overlapping images decreases towards the outer regions of the reduced image (e.g., Figure 9b). This variation causes an increase of the background noise, and hence a decrease of the achieved contrast. The top x-axis of the plot shows the projected separation, in au, calculated from the distance of the primary star and the angular separation and the right y-axis shows the sensitivity curve converted into the mass ratio $q$ using distance, age and mass of the primary star and evolutionary models (Baraffe et al. 1998; 2002, Bressan et al. 2012). If available, also the

brown dwarf limit ($M \lesssim 75\,M_{Jup}$) is indicated by the blue dotted lines. In case of HIP 20042, located at a distance of about 55 pc from Earth and with an estimated age of $\approx$ 27 Myr, sub-stellar objects could have been detected at separations larger than $\approx$ 0.6 arcsec or $\approx$ 33 au, respectively. The diffraction limit in the observed band and the closest image boundary are plotted for completeness by the vertical dash-dotted lines.

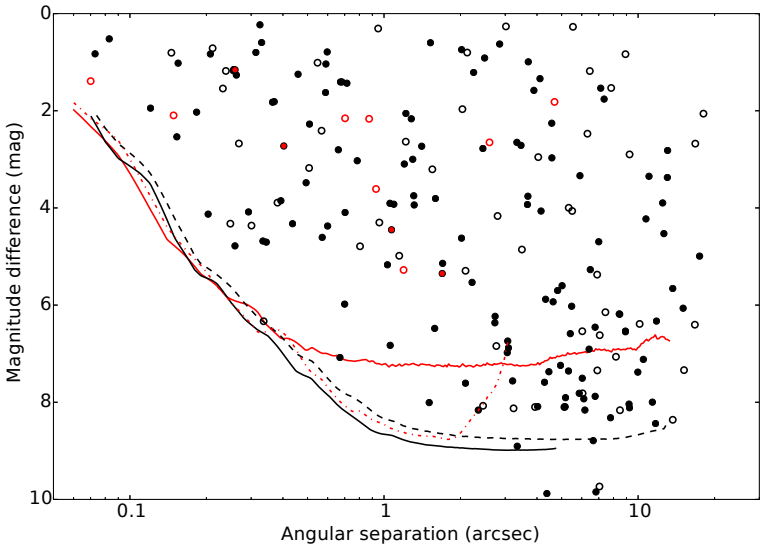


**Figure 20.** Plot of the average sensitivity, i.e. the achieved magnitude difference as function of the angular separation of all NaCo observations investigated in this study, including stars without detection of candidate companions in the FoV of the NaCo image. Companion candidates with more than one NaCo observation are plotted as filled circles, those with only one NaCo observation are indicated by open circles. The used filter band is illustrated by the colour of the observed objects and the average sensitivity curves ($H$-red; $Ks$-black), respectively, while the used objectives (S13-solid; S27-dashed; SDI-dotted) are represented by the shape of the lines. Duplicate observations of the same companion have not been removed in this picture.

The average sensitivity curve for each used NaCo objective and filter band is shown in Figure 20. Companion candidates with more than one VLT/NaCo observation within this study are shown as filled circles, while companion candidates with only one available observation are plotted as open circles. The used NaCo objectives are indicated by the shape of the lines, whereas the colour of the lines and the circles represent the filter band in which the images were taken. Note that duplicate observations of the same companion have not been removed in the picture.

The detection limits in the different bands and observed with SDI, S13 or S27 are comparable for separations smaller than about 0.3″ and typical average contrasts achieved are 5 mag, 7.5 mag and 8 mag at 0.2″, 0.5″ and >0.8″ from the primary star, respectively. The best average contrast of $\Delta m \approx 9$ mag, however, was achieved in the $Ks$ band images obtained with the NaCo S13 and S27 objective for separations $\rho \gtrsim 2$ arcsec. Towards larger angular distances the survey is limited by the field of view of the S27 objective, and thus objects with $\rho \gtrsim 15''$ cannot be measured. At closer separations this survey is limited by the PSF wings of the corresponding primary star which hinder the detection of even relatively

bright, very close objects, for instance.
The majority of the investigated observations ($> 98\,\%$) were, however, obtained in the $Ks$ band with the S13 and S27 objective, and because the achieved dynamic range is best with these objectives, only these data were considered to estimate the completeness.

*Completeness*

The overall completeness map of the sample, in per cent, is illustrated in Figure 21 and was computed using the one-dimensional sensitivity curve constructed for each sample star mentioned and shown above. For each grid point in the plane of the observable quantities ($\rho, \Delta m$), and in the plane of the computed physical quantities ($a_{\mathrm{proj}}, q$), respectively, the fraction of sample stars was determined to which the observations would have been sensitive to a companion at that mass and separation (De Rosa et al. 2014; and priv. comm.).

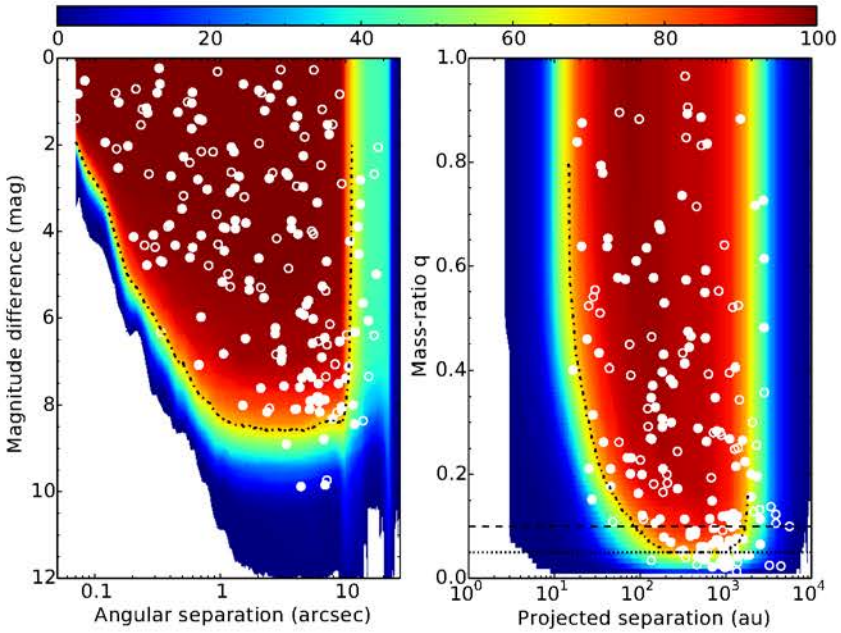


**Figure 21.** Achieved completeness, in per cent, within the investigated adaptive optics sample ($N = 316$, $\rho \lesssim 15$ arcsec, $a_{\mathrm{proj}} \lesssim 5000$ au). In the left-hand panel the completeness is expressed in terms of magnitude difference and angular separation, and in the right-hand panel in terms of mass ratio and projected separation. The CPM companions with more than one NaCo observation are plotted as filled circles, companion candidates with only one NaCo observation are indicated by open circles, while the 68 % completeness level is indicated by the dash-dotted line in both panels. To guide the eye the mass ratios $q = 0.05$ and $q = 0.1$ are plotted as dotted and dashed lines, respectively. The regions which are not sampled by the observations are shown in white for clarity.

The left-hand panel shows the achieved sensitivity in terms of the observed quantities, the angular separation $\rho$ and the magnitude difference $\Delta m$, while in the right-hand panel the completeness is plotted in terms of the computed distance dependent projected separation $a_{\mathrm{proj}}$ and the model dependent mass ratio $q$. Also shown are the CPM companions and the companion candidates with only one observation, indicated by filled or open circles,

respectively.

The completeness distribution appears smoother in terms of the angular separation $\rho$ and the magnitude difference $\Delta m$ compared to the right-hand panel due to the relatively small uncertainties in the astrometric and photometric measurements. In this plane a completeness of more than 90 % was achieved at a K band magnitude difference of about 7 mag for separations between 1 to 9 arcsec. Beyond this separation the completeness drops rapidly due to the FoV of the S 13 objective and its superimposition with the FoV of the S 27 objective. The completeness in the plane of the deduced parameter, on the other hand, appears less smooth due to the uncertainties in a variety of parameter such as distance to the star, spectral type or magnitude of the primary, respectively, which were employed for the calculations. The uncertainties are reflected in the calculated ages, and consequently in the derived masses, as well as in the projected separations. This leads to the reduced completeness observed in the sample.

Also visible is the mentioned deficiency of low mass-ratio companions ($q \lesssim 0.1$) at close separations smaller than about 100 au, due to the PSF wings of the corresponding primary star, while numerous possible companions are observed with $q < 0.1$ at projected distances between about 100 and 2000 au.

As pointed out in section 5.2, the probability of finding a background source in the vicinity of a target star is a function of the distance to the star and the brightness of the candidate companion, and in particular distant, very faint companion candidates therefore show an increased probability of being a background source. While this is no problem for those targets with more than one observation, where background sources are identified through the CPM analysis, it is well possible that the sample of remaining companion candidates, with an inconclusive companion status, includes a few background sources. However, given the low number of objects with only one observation the number of background sources is expected to be negligible.

The following limits were specified for the statistical analysis as reasonable compromise between the minimum number of background objects included by mistake in the sample, the number of missed possible companions due to incompleteness, but also to ensure a fair, quantitative comparison of the results with other surveys, respectively.

(1) A main sample containing the companions confirmed by the CPM analysis, which is not affected by background objects. To minimise the detection bias in $q$ at small separations the mass ratio was limited to $q \geq 0.05$.

(2) A combined sample including the confirmed companions as well as the remaining candidate companions with $q \geq 0.1$ to minimise the number of possible background sources.

(3) A second sub-sample, constructed for completeness, including the confirmed companions as well as the remaining candidate companions with $q \geq 0.05$, which marginally increases the chance of included background sources.

(4) All sample were also restricted to detections at separations between 20 and 2000 au, following the completeness limit of 68 % (dashed line), because at smaller and larger distances the detection bias in $q$ becomes too important.

From the inspection of the completeness, achieved in this thesis, it is evident that a future extension of this work requires a combination of different observation techniques to minimise observational and target selection biases, inherited in the analysed archive data. While larger separations can be mapped using wide-field adaptive optic observations and may include also historical photographic plate observations, next-generation extreme AO systems, such as VLT/SPHERE, and advanced imaging and analysis techniques, are required to map the regions between about 10 to 100 au and mass ratios $q < 0.1$. Below the resolution limit of current AO systems, only radial velocity measurements provide a sufficient sensitivity to low-mass companions with $q = 0.1$ compared to interferometric observation techniques which are currently limited by their dynamic range.

# 7 Results and Discussion

## 7.1 Identified companions

### General results

In this thesis, a total of 317 stars were investigated, containing 316 B-type stars and the central star of the planetary nebula NGC 246 (HIP 3678 A), which was found by chance in the selected volume-limited sample.
In the vicinity of 148 B-type stars, about 47 % of the whole analysed sample, in total 194 sources were resolved. The physical association of 86 objects, in the vicinity of 79 primary stars, could be confirmed using the common proper motion analysis technique, and hence these sources are considered to be co-moving companions, hereafter. The status of 75 companion candidate sources, detected in the proximity of 55 primary stars, remains uncertain. This is mainly due to inconclusive results obtained in the common proper motion analysis which can be introduced by, for instance, only two available observational data-sets that are insufficiently separated in time, discrepancies in separation or position angle due to different calibration methods, used in observations by other authors, different instrumentation, or an underestimation in the assumed maximum possible orbital motion which was estimated for a circular orbit not taking into account the likely eccentricity of the orbit, for instance.
Because a second-epoch observation was not available for 34 of the 75 inconclusive sources their companion status is based on the statistical assessment being a chance projection, described in section 5.2. 25 of these sources, satisfying the probability criterion of less than 5 %, are considered to be likely physical associated companion candidates whereas 9 sources are presumable background. However, all these 75 objects are subject to further investigation and will be observed at least one more time in the near future to be able to derive robust conclusions on their companion status. Furthermore 33 sources, detected in the surrounding area of 21 B-type primaries, were identified as background and are therefore not included in the analysis.
A study of the available literature for each sample star ended up with 106 already known objects found among the 194 detected sources, while 25 objects, resolved in the vicinity of 23 stars, were identified as known sources for which the companion status, either co-moving, inconclusive/undefined or background objects, respectively, could be confirmed for the first time within this thesis. In addition to that no published data were found for 63 objects in the direct surrounding of 45 sample stars. A more detailed overview on these new companions and companion candidates is presented in the adjacent section.
The observed and computed properties for systems with physical or visual companions are summarized in extracts in Table 16. The full result table for all sample stars is presented in Table A6. For those objects identified as background, the derived properties such as the mass or the mass ratio were left blank to avoid confusion.

In addition to these properties auxiliary infos such as the assigned WDS component designation and the evaluated companion status are given. These data as well as information about other known, physically associated companions, such as spectroscopic, interferometric companions or objects outside the field of view of NaCo are of particular interest for a robust estimation of the multiplicity- and companion star fraction.
The known additional companions identified via *VizieR* and the catalogues therein, for instance through the Ninth Catalogue of Spectroscopic Binary Orbits (SB9; Pourbaix et al. 2004) or the Washington Double Star Catalogue (WDS; Mason et al. 2001), are listed in Table A7. The table shows the observed sample star, the separation data of any known companion and the corresponding reference, where the data have been taken from. The separation data listed are either recorded as period, in days, for e.g., spectroscopic companions or as apparent angular distance, in arc-second, for instance, for wide visual systems, outside the field of view of the VLT/NaCo instrument.
The companion status codes presented in Table 16 and Table A6 are as follows:

C – for co-moving (physical) companion;
B – for definite background object (optical companion);
U – for undefined analysis results, i.e. a final assessment of the companion status was not possible based on the available and analysed data.
n – for newly resolved sources, presented for the first time in this thesis.

**Table 16.** Result table of visual binaries and multiple systems detected within the investigated VLT/NaCo data sample (excerpt)

| HIP | CC# | WDS desig. | MJD (days) | Θ (arcsec) | PA[a] (deg) | Band | $\Delta m$ (mag) | $a_{\mathrm{proj.}}$ (au) | log(*Age*[*yr*]) | $M_1$ ($M_\odot$) | $M_{\mathrm{comp}}$ ($M_\odot$) | $q$ | Chance proj. prob. (%) | Comp. status[b] |
|---|---|---|---|---|---|---|---|---|---|---|---|---|---|---|
| Visual binaries and multiples with only one observation and without additional data points from literature | | | | | | | | | | | | | | |
| 17563 | 1 | – | 53380.085 | 4.325±0.007 | 277.2±0.1 | *Ks* | 5.88±0.13 | $707.8^{+35.3}_{-32.1}$ | $7.1^{+0.3}_{-0.7}$ | 5.9±0.3 | 0.39±0.09 | 0.07±0.02 | $4.43 \times 10^{-2}$ | nU |
| 18213 | 1 | – | 53266.307 | 0.259±0.004 | 239.0±0.9 | *Ks* | 4.78±0.12 | $27.5^{+0.8}_{-0.7}$ | $7.6^{+0.1}_{-0.2}$ | 3.7±0.1 | 0.56±0.06 | 0.15±0.02 | $4.27 \times 10^{-5}$ | nU |
| 25657 | 1 | – | 54097.209 | 1.070±0.006 | 74.1±0.5 | *H* | 4.4793±0.0091 | $184.5^{+24.9}_{-19.6}$ | $7.9^{+0.1}_{-0.1}$ | 2.5117±0.0002 | 0.52±0.04 | 0.21±0.02 | $1.35 \times 10^{-2}$ | nU |
| 26549 | 4 | – | 53289.404 | 17.44±0.05 | 116.2±0.2 | *Ks* | 6.7±0.1 | $5737.9^{+8704.5}_{-4279.5}$ | $7.02^{+0.02}_{-0.03}$ | 13.3±0.5 | 1.2±1.0 | 0.09±0.09 | $2.66 \times 10^{0}$ | nU |
| 26549 | 5 | – | 53289.404 | 3.35±0.01 | 17.0±0.2 | *Ks* | 7.32±0.14 | $1102.1^{+1671.9}_{-822.0}$ | $7.02^{+0.02}_{-0.03}$ | 13.3±0.5 | 0.9±0.9 | 0.07±0.07 | $1.52 \times 10^{-1}$ | nU |
| 26549 | 6 | – | 53289.404 | 17.20±0.04 | 116.4±0.2 | *Ks* | 7.59±0.16 | $5657.0^{+8581.8}_{-4219.1}$ | $7.02^{+0.02}_{-0.03}$ | 13.3±0.5 | 0.7±0.7 | 0.06±0.06 | $4.70 \times 10^{0}$ | nU |
| 27810 | 1 | – | 53454.001 | 1.037±0.007 | 198.2±0.4 | *Ks* | 5.1701±0.0031 | $106.4^{+2.5}_{-2.4}$ | $7.5^{+0.1}_{-0.2}$ | 3.9807±0.0004 | 0.48±0.05 | 0.12±0.01 | $1.70 \times 10^{-3}$ | U |
| 32823 | 1 | – | 54458.281 | 1.194±0.007 | 250.9±0.5 | *H* | 5.277±0.021 | $918.5^{+28932.7}_{-452.1}$ | $7.4^{+0.2}_{-0.3}$ | 3.981±0.001 | 0.4±2.0 | 0.1±0.4 | $1.73 \times 10^{-1}$ | nU |
| 34041 | 1 | – | 54497.142 | 0.149±0.006 | 134.3±0.7 | *H* | 2.095±0.064 | $75.4^{+20.1}_{-13.4}$ | $7.40^{+0.06}_{-0.07}$ | 6.77±0.09 | 3.0±0.6 | 0.45±0.08 | $6.09 \times 10^{-5}$ | nU |
| : | : | : | : | : | : | : | : | : | : | : | : | : | : | : |
| Visual binaries and multiples with more than one observation, including data points from literature | | | | | | | | | | | | | | |
| 2548 | 1 | – | 53710.049 | 0.2710±0.0009 | 278.0±0.2 | *Ks* | 1.1620±0.0044 | $21.9^{+1.0}_{-0.9}$ | $9.06^{+0.03}_{-0.04}$ | 2.00±0.01 | 1.27±0.03 | 0.64±0.01 | $3.12 \times 10^{-6}$ | C |
| | | | 54359.246 | 0.241±0.001 | 275.6±0.2 | *Ks* | 1.1400±0.0054 | $19.5^{+0.9}_{-0.8}$ | | 2.00±0.01 | 1.28±0.03 | 0.64±0.01 | $2.46 \times 10^{-6}$ | C |
| 15627 | 1 | * | 54024.221 | 0.874±0.005 | 218.4±0.5 | *H* | 2.166±0.049 | $136.3^{+17.5}_{-14.0}$ | $7.64^{+0.08}_{-0.09}$ | 4.4±0.1 | 2.1±0.2 | 0.46±0.06 | $1.11 \times 10^{-4}$ | U |
| 16511 | 1 | – | 53376.049 | 0.128±0.003 | 110.1±1.0 | *Ks* | 2.547±0.025 | $13.7^{+0.6}_{-0.6}$ | $8.1^{+0.1}_{-0.2}$ | 2.65±0.07 | 1.06±0.02 | 0.40±0.01 | $3.77 \times 10^{-6}$ | C |
| | | | 53700.139 | 0.143±0.002 | 112.6±0.3 | *Ks* | 2.710±0.025 | $15.3^{+0.7}_{-0.6}$ | | 2.65±0.07 | 1.02±0.02 | 0.38±0.01 | $4.96 \times 10^{-6}$ | C |
| | | | 55798.407 | 0.189±0.004 | 107.8±0.7 | *Ks* | 2.353±0.029 | $20.3^{+1.0}_{-0.9}$ | | 2.65±0.07 | 1.11±0.03 | 0.42±0.01 | $7.79 \times 10^{-6}$ | C |
| 16803 | 1 | – | 53379.102 | 0.195±0.001 | 84.0±0.2 | *Ks* | 0.884±0.012 | $29.0^{+2.4}_{-2.1}$ | $8.47^{+0.03}_{-0.03}$ | 3.13±0.04 | 2.4±0.1 | 0.78±0.03 | $9.22 \times 10^{-7}$ | C |
| | | | 54363.350 | 0.229±0.005 | 80.9±1.0 | *Ks* | 0.812±0.026 | $34.2^{+2.9}_{-2.6}$ | | 3.13±0.04 | 2.5±0.1 | 0.79±0.03 | $1.27 \times 10^{-6}$ | C |
| | | | 54373.246 | 0.198±0.001 | 78.4±0.3 | *Ks* | 0.798±0.013 | $29.6^{+2.4}_{-2.1}$ | | 3.13±0.04 | 2.5±0.1 | 0.79±0.03 | $9.50 \times 10^{-7}$ | C |
| 20020 | 1 | – | 53347.154 | 4.102±0.005 | 2.56±0.06 | *Ks* | 1.331±0.028 | $579.4^{+28.3}_{-25.8}$ | $8.26^{+0.03}_{-0.04}$ | 2.79±0.06 | 1.66±0.08 | 0.59±0.03 | $2.65 \times 10^{-3}$ | C |
| | | | 54363.374 | 4.115±0.007 | 1.94±0.08 | *Ks* | 1.355±0.034 | $581.2^{+28.4}_{-25.9}$ | | 2.79±0.06 | 1.64±0.08 | 0.59±0.03 | $2.67 \times 10^{-3}$ | C |
| | | | 54373.288 | 4.113±0.004 | 1.94±0.03 | *Ks* | 1.3306±0.0095 | $581.0^{+28.4}_{-25.9}$ | | 2.79±0.06 | 1.66±0.07 | 0.59±0.03 | $2.67 \times 10^{-3}$ | C |
| 20042 | 1 | AB | 53690.201 | 5.389±0.005 | 162.16±0.06 | *Ks* | 6.208±0.067 | $294.0^{+2.4}_{-2.4}$ | $7.4^{+0.2}_{-0.3}$ | 3.9807±0.0005 | 0.25±0.05 | 0.06±0.01 | $2.01 \times 10^{-2}$ | C |
| | | | 56189.188 | 5.431±0.009 | 162.51±0.05 | *Ks* | 7.0±0.1 | $296.3^{+2.5}_{-2.5}$ | | 3.9807±0.0005 | 0.17±0.03 | 0.042±0.007 | $4.11 \times 10^{-2}$ | C |
| 20554 | 1 | * | 53266.307 | 6.319±0.005 | 42.0±0.1 | *Ks* | 2.472±0.025 | $1388.8^{+175.3}_{-140.0}$ | $7.8^{+0.1}_{-0.1}$ | 3.979±0.001 | 1.00±0.07 | 0.25±0.02 | $3.44 \times 10^{-2}$ | C |
| 20804 | 1 | – | 53409.032 | 0.112±0.003 | 385.1±0.9 | *Ks* | 1.284±0.021 | $20.1^{+3.1}_{-2.4}$ | $8.18^{+0.05}_{-0.05}$ | 3.8±0.2 | 2.8±0.2 | 0.72±0.07 | $1.67 \times 10^{-6}$ | U |
| | | | 56189.333 | 0.127±0.005 | 351.0±0.4 | *Ks* | 1.349±0.021 | $22.9^{+3.6}_{-2.8}$ | | 3.8±0.2 | 2.7±0.2 | 0.71±0.07 | $2.25 \times 10^{-6}$ | U |
| | | | 56296.083 | 0.142±0.003 | 348.6±0.5 | *Ks* | 1.359±0.015 | $25.5^{+3.9}_{-3.0}$ | | 3.8±0.2 | 2.7±0.2 | 0.71±0.07 | $2.81 \times 10^{-6}$ | U |
| 23794 | 1 | AB | 53286.342 | 1.600±0.005 | 308.3±0.2 | *Ks* | 3.8271±0.0011 | $151.5^{+5.1}_{-4.7}$ | $8.73^{+0.02}_{-0.02}$ | 2.497±0.009 | 0.82±0.02 | 0.327±0.007 | $1.54 \times 10^{-3}$ | C |
| | | | 56296.100 | 1.588±0.002 | 309.50±0.06 | *Ks* | 3.7869±0.0012 | $150.4^{+5.0}_{-4.7}$ | | 2.497±0.009 | 0.83±0.02 | 0.332±0.007 | $1.48 \times 10^{-3}$ | C |
| : | : | : | : | : | : | : | : | : | : | : | : | : | : | : |

**Notes.** Component designation as assigned in the WDS catalogue. –: No WDS entry; *: Companion is listed in WDS certainly without component designation. The full list of all detected sources is presented in Table A6.

[a] Position angle (PA) is measured from N over E to S.

[b] Companion status: (B)ackground; (C)o-moving; (U)ndefined; (n)ew detection

## New detections and notes on individual targets

Following are a more detailed explanation of the examined companion status and the publicity of the detected sources as well as the notes on individual systems which have been newly identified in course of this study. The breakdown of all 194 detected and investigated sources into co-moving, refuted or candidate companions, and their grading into already known, or new objects, respectively, is shown in Table 17.

**Table 17.** Overview on publicity and companion status of the detected sources

| | Physical companion | Companion candidates | Background sources | Total |
|---|---|---|---|---|
| known | 58 | 37 | 17 | 112 |
| known, new confirmed[a] | 19 | | | 19 |
| new unpublished | 9 | 38 | 16 | 63 |
| Total | 86 | 75 | 33 | 194 |

**Notes.** [a] The source was published as candidate before. Its companionship was first confirmed in this thesis.

In this study 33 detected sources have been classified as background according to the results of the common proper motion analysis. While for 13 of them published data were found in the literature, no data were found for 16 sources. One reason for this might be that these sources have already been identified as background object in the original analysis by the observer and therefore not have been published. Four sources in the vicinity of 3 primary stars, namely HIP 58326, HIP 60189 and HIP 85727, respectively, were found to have one additional observation in the literature. However, the common proper motion analysis of these sources clearly indicates that they are not physically connected to the observed B-type star.

Another minor point to be mentioned here is in regards to the data published in the WDS catalogue (Mason et al. 2001). Ten objects, identified as background sources, were found in the sample with an assigned WDS designation. However, no explicit note was found that they are non-physical. This may lead to a confusing interpretation of the multiplicity of some sample stars and needs to be checked with reasonable care.

The companion status of 75 detected objects in the direct surrounding of 55 B-type primaries still remain uncertain and hence, all these stars will be targets for future observations. The uncertainty of the companionship is partly based on the insufficient amount of available observations for a common proper motion analysis but also due to uncertainties introduced by the employed literature data or the results of the obtained measurements and the consecutive calculations and estimations, respectively, such as the possible maximum orbital motion evaluated for a circular orbit seen either pole-on or edge-on. Even though this is a reasonable assumption, eccentric and inclined orbits are much more likely and it is possible that the used true semi-major axis is underestimated. Other possibilities would be for instance systematic offsets between observations taken with diverse telescopes, in different

filters under varying ambient conditions or the assigned calibration which can cause shifts in the measured separation and/or position angle.

While 37 out of the 75 candidate companions are known and have been published before, a total of 38 sources was identified in the data without any publication. The reasons for that are not known, and thus a statement would be speculative. However, all of the 75 companion candidates require additional observations, either to confirm or reject their companionship, respectively.

A secondary goal of this thesis, the search for new, previously unknown co-moving companions in the analysed archive data, was achieved by the detection of 9 completely new physically companion and the first-time confirmation of 19 objects which are already known, but with only one reported data point in the literature from a total of 86 physical companions found.

The VLT/NaCo images of the $9+1$ new co-moving companions identified within this study are presented in Figure 22. The name of the primary star, observing epoch, used filter and utilised camera objective as well as a scale and a compass for orientation are illustrated within each image. The off-centred primary component of the HIP 3678 system is marked with A.

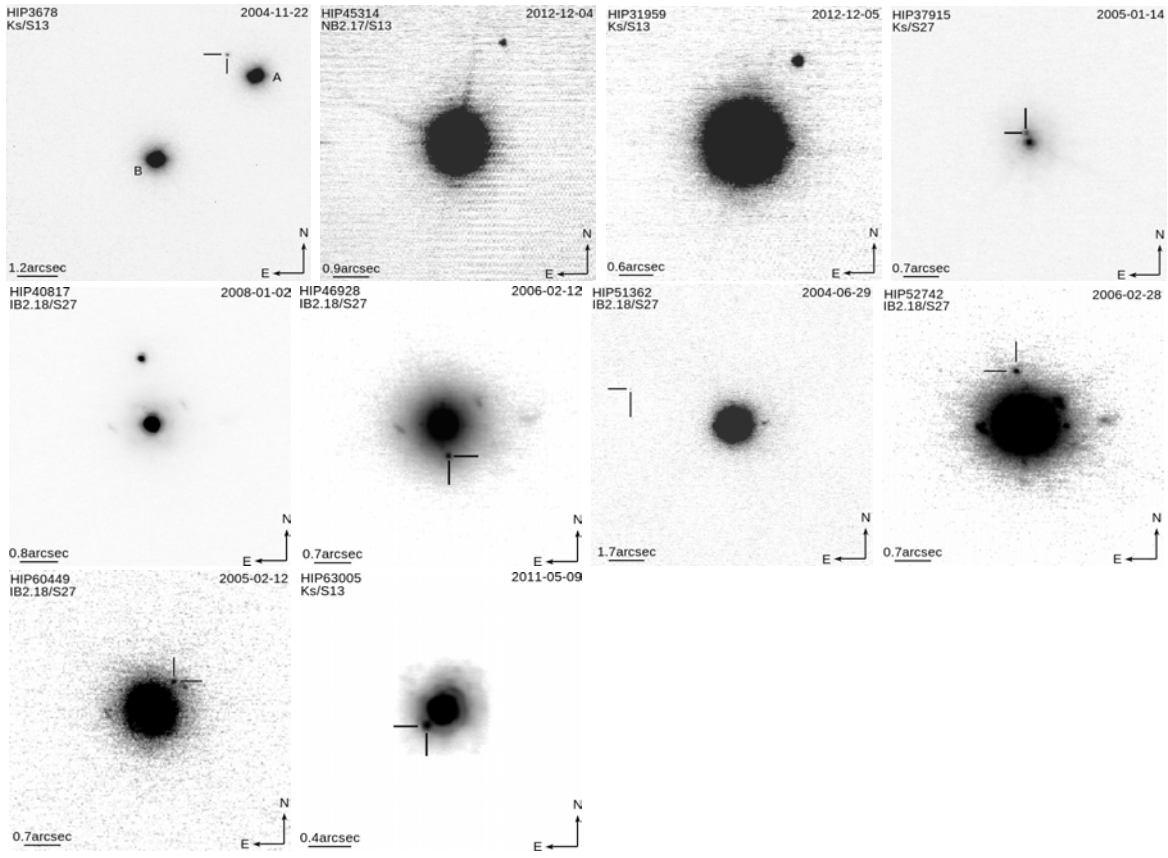


**Figure 22.** VLT/NaCo images of new binary and multiple systems, detected and presented for the first time in this thesis, including the new companion found in the vicinity of the CSPN HIP 3678 A (first upper-left image). For each of the shown companions the assumption of a physical association to its host-star is supported by the common proper motion analysis.

In the following a brief overview on the studied systems with new, previous unpublished and confirmed co-moving companions is given. The first two systems presented below have already been published during the preparation of this thesis and for more details reference is therefore made at this point to **Adam** and Mugrauer (2014) and **Adam** et al. (2013).

**HIP 3678 = NGC 246**: *Triple*, in *planetary nebula*. The object was found by chance in a early stage sample version due to an unclear spectral classification. However, the data analysis of this object revealed a new common proper motion companion to the known double star system HIP 3678 AB which makes this system the first confirmed hierarchical triple in the centre of a planetary nebula.

A pattern of reduced images of HIP 3678 composed from the analysed *HST* and NaCo data and a composite image from the Digitized all Sky Survey (DSS) is shown in Figure 23. NGC 246, also known as "Skull Nebula", is located in the Cetus constellation at

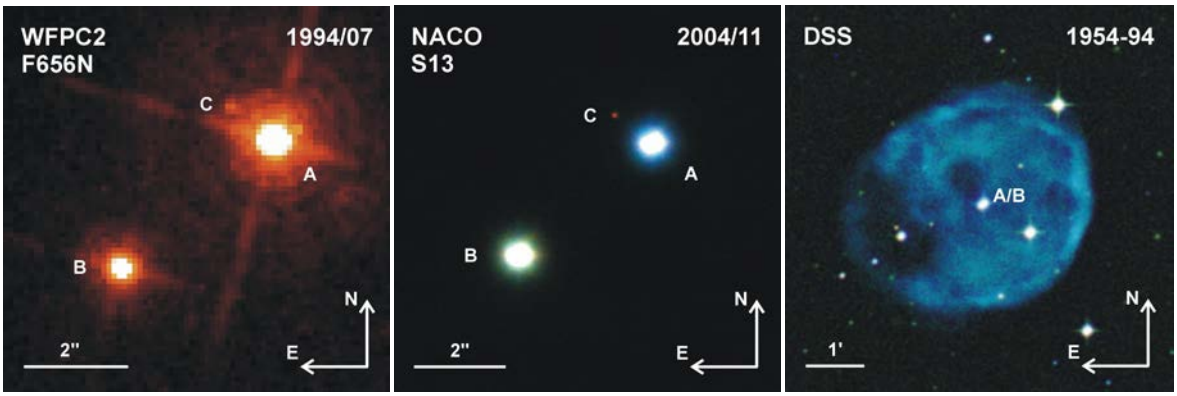


**Figure 23.** This pattern shows the fully reduced images of HIP 3678, taken with WFPC2 (left) in the visual in 1994, the *JHK*s band colour-composite image taken with NaCo in 2004 (middle), as well as the colour-composite DSS-image (blue channel: POSSI.O-DSS2.706 (0.41 µm) taken in 1954; green channel: SERC ER DSS2.S681 (0.64 µm) taken in 1989; red channel: SERC I DSS2.S681 0.807 µm taken in 1994) of the planetary nebula NGC 264 with the stellar system HIP 3678 in its centre. The slightly elliptical shape of the planetary nebula is clearly visible in the colour-composite DSS image with its semi-major axis aligned in the east to west direction, induced by the motion of the system through space. The western leading edge of the nebular shell is brighter due to its interaction with the interstellar medium. In the WFPC2 and NACO images the individual components of the HIP 3678 system in the centre of NGC 246 are marked with letters. Caption taken from **Adam** and Mugrauer (2014).

an approximate distance of 500 pc (**Adam** and Mugrauer 2014) from the Sun. The white dwarf central star of the planetary nebula, HIP 3678 A, is a very hot $O_{VI}$ sequence planetary nuclei (Smith and Aller 1969), or PG 1159-35(lg E) (Werner and Herwig 2006) star with an effective temperature of about 150 000 K, a mass of 0.84 $M_{\odot}$, and a surface gravity of log(g) $\sim$ 5.7 (cgs) (Koesterke et al. 1998). The mass of its progenitor star was probably about 4.3 $M_{\odot}$ and was estimated using the initial to final mass relationship of white dwarf from Catalán et al. (2008). This yields a main-sequence lifetime of the progenitor star of about 260 Myr, assuming a mass-luminosity relation of $L \propto M^{3.5}$, and was also adopted as system age due to the short dynamical age of the planetary nebula of only 6600 yr, derived by Ali et al. (2012).

The newly found companion is located about 1 arcsec, north-east of HIP 3678 A (PA ≈ 52 deg), at a projected separation of about 500 au, and shares a common proper motion with the white dwarf and its known co-moving companion HIP 3678 B which is located about 3.9 arcsec south-east of HIP 3678 A (PA ≈ 130 deg), at a projected separation of about 1950 au.
Within the given total epoch difference between the first and the latest observing epoch, 1972 and 2007, respectively, of about 35 yr, the background hypothesis that the astrometry of HIP 3678 B significantly deviates from the expected one for a non-moving background object, is rejected at a significance level of more than $8\,\sigma$. In contrast to HIP 3678 B, the newly found faint companion candidate is imaged only in three observing epochs, between 1994 and 2007, with a total epoch difference of about 13 yr. According to the common proper motion analysis, the background hypothesis for this candidate is rejected at a significance level of more than $8\,\sigma$.
The masses of both companion stars were computed employing the results of photometry, especially in *J* and *K* band, the derived corresponding absolute magnitude, assuming a system age of 260 Myr and the Bessell et al. (1998) evolutionary models. Both companion are low mass stars which exhibit masses of about 0.85 $M_\odot$ and 0.1 $M_\odot$, and hence, it is expected from the absolute magnitude-spectral-type relation (Reid et al. 2004) that HIP 3678 B is an early to mid-K dwarf, while HIP 3678 C is a M5 to M6 dwarf. For further details, however, reference is made at this point to **Adam** and Mugrauer (2014).

**HIP 45314 = HD 79694**: *Binary*. This second already published star from this thesis (**Adam** et al. 2013) is located in the Vela constellation, at a distance of about 161 pc. HIP 45314 A is also a probable member of the Platais 9 cluster (HIP 45189; Platais et al. 1998), based the analysis of the U, V, W heliocentric space motion of the star compared to the surrounding cluster.
The spectral type of the primary is B7–8 V, as computed from unpublished *IUE* UV spectra. The calculated age for this star ranges from ≈ 60 Myr and ≈ 220 Myr, depending on the adopted spectral type, and its mass is expected to be between 3 and 4 $M_\odot$.
The found, new companion is situated ≈ 2.7 arcsec north-west of HR 3672 A (PA ≈ 336 deg), which corresponds to a projected distance of about 441 au. The companionship was confirmed by common proper motion analysis of the two published observations, taken in 2004 and 2008 with 4 years of epoch difference. In the meantime a third own observation was obtained in 2012 and with a total of 8 years of epoch difference the background hypothesis is now rejected by more than $30\,\sigma$ in both separation and position angle. Given the measured and computed magnitudes, the assumed system age range and evolutionary models, HR 3672 B is a low-mass star of spectral type M with a mass of 0.15–0.5 $M_\odot$. However, the large uncertainties in the computed companion mass require additional observations, for instance by taking spectra of the system components, to minimize the uncertainties of the physical parameter.

**HIP 31959 = HD 48165**: *Binary*, candidate *Triple*. The primary star is an early-type

main sequence star with spectral type B3 V Houk (1982) and is located in the Canis Majoris constellation, at a distance of about 614 pc from the Earth.
The system is also probable member of the Collinder 121 OB association (de Zeeuw et al. 1999) and according to Bragança et al. (2012) HIP 31959 A is a spectroscopic binary. However, no measurements of this object were published and hence the star is considered here as candidate spectroscopic binary.
Given its spectral type, available photometric information from different bands and employing evolutionary models, the mass of the host star was estimated with about 6 $M_\odot$, and the age with $\approx$ 20 Myr, respectively.
The found companion is located $\approx$ 1.7 arcsec north-west of the primary (PA $\approx$ 327 deg) and was first observed with NaCo in 2008. During this thesis a second, own observation was taken in 2012 to be able to investigate whether the candidate companions shares common proper motion with the host star, or not. Despite the time difference of four years between the two observations, the background hypothesis can only be rejected by about 4 $\sigma$ due to the low proper motion of the host star. Hence, further observations, in particular spectra, are required to consolidate the results and confirm this system as a *triple*.
From the assumed system age, the calculated absolute magnitudes and evolutionary models the estimated mass of the new companion HIP 31959 B is $0.7 \pm 0.3\,M_\odot$ which corresponds to a low-mass, early or mid-K stellar object.

**HIP 37915 = HR 3022**: *Triple*. This B5 V star Houk (1982), also named V392 Pup, is located in the Puppis constellation at a distance of approximate 181 pc and a member of the NGC 2451 cluster.
In this thesis a mass of 4 $M_\odot$ and an age of about 31 Myr was estimated for HR 3022 A. But, according to the General Catalogue of Variable Stars (GCVS) by Samus et al. (2009), this star is a eclipsing binary which causes a periodic variation in the brightness of about 0.1 mag and hence, the estimated age and the computed masses have to be taken with reservation.
The newly detected candidate companion was first observed with NaCo in 2005 and a second time in 2007. However no published data were found in the literature on the new source, located 0.18 arcsec north-east of HR 3022 A (PA $\approx$ 5 deg). The background hypothesis for this object can be rejected at a very high significance level of more than 50 $\sigma$ from the available data with only two years between the observations.
The obtained mass for the co-moving companion, estimated from the derived absolute magnitude, the assumed system age of 31 Myr and employing evolutionary models, is 1.6 $M_\odot$.
However, whereas the physical association is strongly supported by common proper motion, future observations, are needed in particular to make more precise constrains on the companion mass, for instance by taking high-resolution spectra of HR 3022 A and B or obtain multi-wavelength photometry for both objects.

**HIP 40817 = HD 71046**: *Quadruple*, possible *Quintuple*. The primary is a B9 III/IV star (Houk and Cowley 1975), located in the Volans constellation, at a distance of $\approx$

133 pc. According to the Bright Star Catalogue (Hoffleit 1964), HIP 40817 is a double-lined spectroscopic binary (SB2). The star, however, was again investigated by Chini et al. (2012) but the authors did not report any signature of a spectroscopic companion around kap01 Vol and hence, its SB2-status remains unclear.
The mass estimated for the primary is about 3 $M_\odot$ and the calculated age of $\sim$ 267 Myr for star is comparable to the age of $\sim$ 276 Myr reported by Gontcharov (2012).
HIP 40817 A forms a common proper motion pair with HR 3302, also named kap02 Vol, and is located $\approx$ 64 arcsec north-east of the host star (PA $\approx$ 60 deg). HIP 40817 B alias HIP 40834 was also analysed in this thesis, but within the achieved sensitivity $K_{\mathrm{lim}} \approx 15$ mag no additional companion were detected within the FoV of $\approx$ 12 arcsec. A second companion is situated $\approx$ 100 arcsec north-east of the primary (PA $\approx$ 50 deg).
The new companion to the *triple* was detected $\approx$ 1.4 arcsec north-east of the primary (PA $\approx$ 9 deg), and was first observed with NaCo in 2005. A second and third observation were obtained in 2008 and with three years epoch difference the background hypothesis for this object is rejected by more than 30 $\sigma$ for both, separation and position angle. The companion is therefore considered as co-moving.
The mass of the new companion HIP 40817 D, employed from photometry, the system age of 267 Myr and evolutionary models, is $\approx$ 1.3 $M_\odot$.

**HIP 46928 = HD 83979**: *Binary*. The B5 V primary (Cucchiaro et al. 1976) is a variable star of $\beta$ Cephei type[14] with a reported period of about 1.08d and a variation amplitude of about 0.1 mag in the visible (Watson 2006). The object is situated about 176 pc away from Earth in the Chameleon constellation.
Given this spectral type and utilising evolutionary models the mass and age HIP 46928 were derived as 5 $M_\odot$ and 55 Myr, respectively.
There was no companion found in the literature for the primary, but a detection of X-ray emission is reported from the *ROSAT* All-Sky Survey (Berghoefer et al. 1996) with $\log(\mathrm{Lx/Lbol}) = -6.28$. The offset between X-Ray source and optical counterpart is given with 25.7 arcsec. The measured X-ray emission is unusual given the fact that B-type stars have no convection zone. A probable candidate as source of the X-rays is the new found co-moving companion, but further investigations are required.
HD 83979 was first observed with NaCo in 2006 and a second time in 2008. The identified close companion is located $\approx$ 0.6 arcsec south-east of the host star (PA $\approx$ 189 deg), and from analysis of the data, obtained with two year time difference, it is rejected with about 17 $\sigma$ that the found companion is a non-moving background source. The measured shifts in separation and position angle might be due to the orbital motion of HIP 46928 B, but more observations are required to verify this assumption.
The companion mass of about 1 $M_\odot$ was calculated using derived absolute magnitudes,

[14] $\beta$ Cephei type (BCEP, $\beta$ Cep, $\beta$ CMa) stars are variable, non-super-giant pulsating O8–B6 stars with light and radial-velocity variations caused by low-order pressure and gravity mode pulsations. Their periods are in the range of 0.1 to 0.6 days and light amplitudes vary from 0.01 to 0.03 mag in $V$.

assuming a system age of 55 Myr and employing evolutionary models. Given the assumed age and derived mass it is therefore well possible that the source of X-ray emission is the found companion.

**HIP 51362 = HD 90882**: *Binary*. This star of spectral type B9.5 V (Cowley et al. 1969) is located in the Sextans constellation, at a proximate distance of only 99 pc.
The mass estimates by Gullikson et al. (2016) and Allende Prieto and Lambert (1999) of 2.6 $M_\odot$ and 2.7 $M_\odot$, respectively, are conform with the calculated primary mass of 2.5 $M_\odot$, while the age of 181 Myr derived by Gullikson et al. (2016) differs significantly from the age of 560 Myr calculated in this thesis.
The new faint companion is located about $\approx$ 5.2 arcsec north-east of the primary (PA $\approx$ 70 deg). Two observations were analysed in this study, taken with NaCo in 2004 and 2006. From these data with two year epoch difference the background hypothesis is rejected by about 6 $\sigma$ in total.
Adopting both given ages of 181 Myr (Gullikson et al. 2016) and 560 Myr (this work), respectively, and using the computed absolute magnitude and evolutionary models, the mass of the companion is derived as 0.13 to 0.15 $M_\odot$. This makes HIP 51362 B the lowest mass, co-moving companion, identified in this study.

**HIP 52742 = HD 93563**: *Binary*. HIP 52742 is a Be star of spectral type is B8 III(e) shell Slettebak (1982) and located in the Vela constellation, at distance of 161 pc. Rizzuto et al. (2011) calculated a 61 per cent probability that HR 4221 is a member of the Sco OB2 moving group.
The star was also reported by Koen and Eyer (2002) as new candidate periodic variable, extracted from the epoch photometry of the *Hipparcos* catalogue, with a period of 20.93 h and an amplitude of only 0.003 mag in the visible.
Employing the given spectral type, available photometry and evolutionary models, HR 4221 exhibits a mass of 4 $M_\odot$ and an age of 149 Myr, respectively. This derived age, however, is lower compared to $\approx$ 250 Myr, as computed by Gontcharov (2012).
The new companion is located about 1.1 arcsec north of HIP 52742 A (PA $\approx$ 8 deg) and was first observed in 2006. In combination with a second observation, taken in 2008, the background hypothesis can be rejected by more than 20 $\sigma$.
The mass of the co-moving companion HIP 52742 B is $\approx$ 0.5 $M_\odot$, corresponding to a young, low-mass M-type stellar object.

**HIP 60449 = HD 107832**: *Binary*. The primary star is a B9 III giant star (Garrison and Gray 1994) and located in the Centaurus constellation, at a distance of about 136 pc. Utilising the given spectral type, available photometry and evolutionary models, a mass of about 3 $M_\odot$ and an age of $\approx$ 290 Myr, respectively, was derived for HIP 60449. The found age of $\approx$ 290 Myr is consistent with the age of 266 Myr, reported by Gontcharov (2012).
No additional companions were found in the literature orbiting this star.
The new companion is located about 0.7 arcsec north-west of HIP 60449 A (PA $\approx$ 320 deg), and the background hypothesis for this object is rejected by more than 13 $\sigma$ in both,

separation and position angle, respectively, based on the available NaCo observations taken with a time difference of three years in 2005 and 2008.
The derived mass of the new companion from photometry and evolutionary models is $\approx 0.5\,M_{\odot}$.

**HIP 635005 = HD 112091**: *Triple*. This Be star of spectral type B5 Vne (Levenhagen and Leister 2006) forms a common proper motion pair with HIP 63003, which is located about 36 arcsec south-west of HIP 63005 (PA $\approx$ 204 deg). The object is situated in the Lower Centaurus Crux (LCC) constellation at a distance of 136 pc and a probable member of the correspondent OB association de Zeeuw et al. (1999). Remarkable about this star is that it is a GCAS type variable according to Ruban et al. (2006) with a magnitude range of about 0.2 mag[15].
The age of HIP 63005, given in the literature, varies between 16 to 43 Myr. This is in well agreement with the age of about $30 \pm 12$ Myr derived in this thesis. The computed mass of HIP 63005, adopting the spectral type B5 Vne is $\approx 4\,M_{\odot}$.
Shatsky and Tokovinin (2002) reported two apparently optical candidate companions, found in observations taken with the VLT/ADONIS instrument in 2000, one about 5 arcsec north-west (PA $\approx$ 333 deg), and one $\approx$ 4.7 arcsec south-west (PA $\approx$ 241 deg), respectively. These very faint objects, both with $Ks > 16$ mag, were neither detected in the re-analysed NaCo data from 2005 nor in the own second-epoch observation of HIP 63005 taken in 2011 in *JHK*s as they are below the sensitivity limit of the taken data with $Ks \lesssim 14$ mag. However, another close companion was identified in the 2005 observation, located about 0.2 arcsec south-east (PA $\approx$ 134 deg) at a projected distance of only 27 au. The very close candidate companion was also identified in the 2011 observation, and with a time difference of about six years the background hypothesis can be rejected at a significance level of $6\,\sigma$.
Given the system age of 30 Myr, the derived absolute magnitude and evolutionary models, the mass of the companion is $\approx 0.84\,M_{\odot}$.
Assuming a total system mass of $\approx 5\,M_{\odot}$ and semi-major axis of $\approx$ 30 au the period is round about 74 yr, and hence with 6 yr of observation almost 10 % of the orbit are covered. Continuous observations in the near future therefore would allow to make better constrains on the true orbit and consequently on the mass of both components, and proof the existence of a X-ray source as reported by Malkov et al. (2015).

## 7.2 Separation and Mass ratio distribution

Following are the results of the statistical analysis of the derived, most immediate accessible quantities the projected separation $a_{\text{proj.}}$ and the mass ratio $q$. In order to put the results of this study in context, a comparison with previous observations from other multiplicity

[15] $\gamma$ Cassiopeia type stars (GCAS) are eruptive irregular variables. These are rapidly rotating O9-A0 III-Ve stars with mass outflow from their equatorial zones. The formation of equatorial rings or disks is accompanied by a temporary brightening (pole-on stars like $\omega$ CMa) or fading (equator-on stars like Pleione).

surveys and the prediction of theoretical models was carried out.

In addition to that, the orbital period $P$ distribution, estimated from the projected separation and assuming a circular orbit for each companion, was analysed. However, these results have to be taken with reservations, because robust estimates on the period are only possible if the orbit of a binary system is mapped sufficiently enough to derive needed orbital parameter, such as inclination, eccentricity or the true semi-major axis, for the calculation of the period. This is not the case for almost all found companions and would have required long-term observations over several years or even decades, which is, however, beyond the scope of this thesis.

The obtained sample of was limited to objects with separations between 16 au and 2000 au and divided into two sub-sample containing (1) the confirmed companions, and (2) the combination of co-moving and candidate companions, respectively. The latter sub-sample was limited to candidate companions with mass ratios $q \geq 0.1$. For completeness, the calculations were also repeated for this sub sample with $q \geq 0.05$, increasing marginally the observational bias of background sources falsely identified as candidate companions. The derived results, however, do not alter significantly.

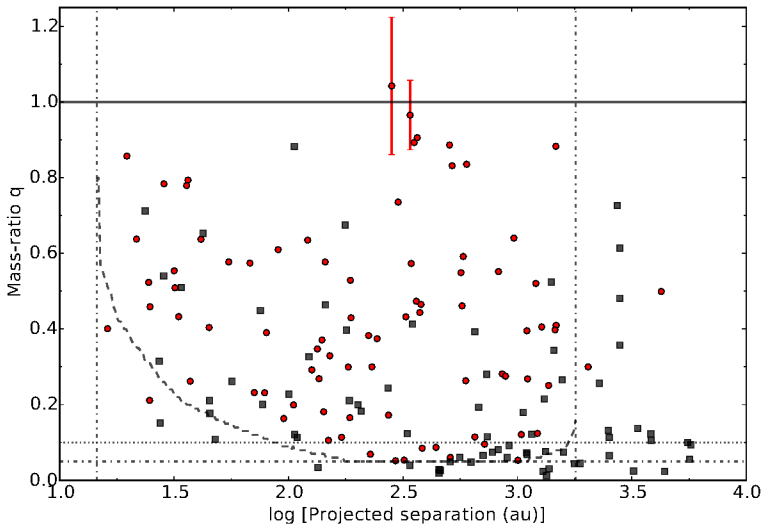


**Figure 24.** Mass ratio $q$ as function of the projected separation $\log[a_{\text{proj.}}(\text{au})]$. The 86 confirmed and 75 remaining companion star candidates are indicated by red dots and grey squares, respectively. The completeness level of 68 % and the selected analysis limits ($1.2 \leq \log(a_{\text{proj.}}) \lesssim 3.3$ ($\approx 16 - 2000$ au), $q \geq 0.05$) are shown as dashed and dash-dotted lines. The mass ratio $q = 0.1$ is plotted as dotted line.

The general relation of the derived quantities q and $\log(a_{\text{proj.}})$ is illustrated in Figure 24. Shown are the computed mass ratios as a function of the derived projected separation for each detected co-moving (red circles) or candidate companion (grey squares). Also indicated are the process of the 68 % completeness level from chapter 6, by the black dashed line and the lower and upper separation limit of $1.2 \leq \log(a_{\text{proj.}}) \lesssim 3.3$ ($\approx 16 - 2000$ au) by the vertical dash-dotted lines, respectively. In addition, the mass ratios $q = 0.05$ and $q = 0.1$ are shown to guide the eye. Three systems were identified with $q > 0.9$. Two of them, namely HIP 26602 ($q = 1.04 \pm 0.08$) and HIP 80473 ($q = 0.97 \pm 0.10$), are

shown in the image with the corresponding error-bar. Due to the uncertainties in the mass estimation it is not possible to concluded which star in these systems is more massive, and consequently, which is the primary. The smallest mass ratios were found for the physical companion of HIP 20042 ($q = 0.05 \pm 0.01$) and the candidate companion of HIP 76503 ($q = 0.013 \pm 0.001$). However, the probability that the candidate companion of HIP 76503 is a chance projection is about 10 %, and thus it is likely that this object is a background source.

### 7.2.1 Separation and period distribution

Similar to previous multiplicity surveys (e.g., De Rosa et al. 2014, Fischer and Marcy 1992, Raghavan et al. 2010), a log-normal function was utilised for the statistical description. To avoid additional biases introduced by a binning scheme, the fit was applied to the observed Empirical Cumulative Distribution Function (ECDF) instead of the Probability Density Function (PDF). The uncertainties of the fit parameter, i.e. the location and the width of the distribution, were derived using a bootstrap method which the advantage compared to *normal* assumptions, that the results generated are robust even if the underlying data are very far from normal. 5000 samples with replacement were drawn from the available data and then the best-fit parameter computed from each sample. Finally, the estimated determinants were rank-ordered to calculate the 16 and 84 percentile value for the 68 % confidence interval (CI), i.e. the 1 $\sigma$ uncertainties.

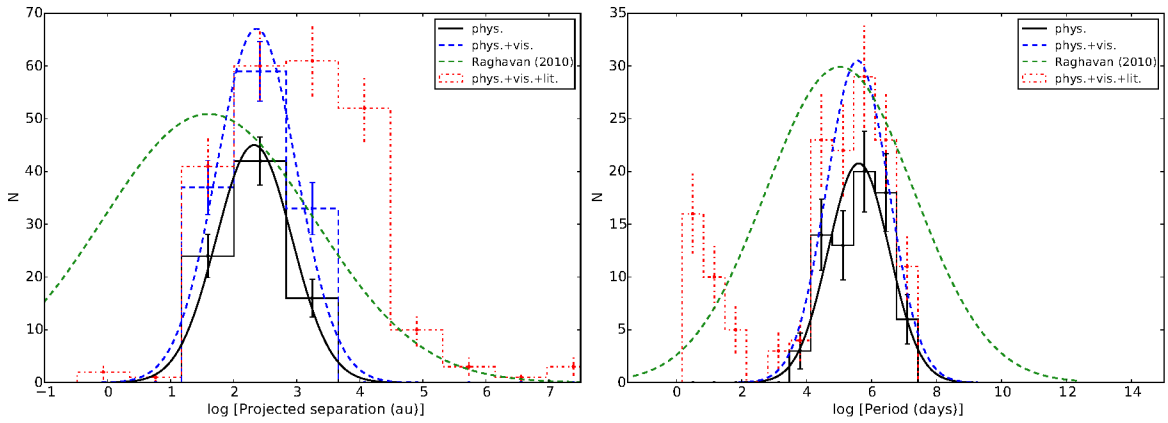


**Figure 25.** *Left:* Final separation distribution plot of confirmed physical companions (black, solid), the full investigated sample (blue, dashed), including physical and candidate companions, both with $q \geq 0.05$, respectively. Note that each triple contributes two separations, each quadruple contributes three separations, etc. *Right:* The corresponding period distribution and best fit estimates for the investigated sub-samples. The representation is the same as in the left panel. Also shown in both panels are the fit to the separation/period distribution (green, dashed), adopted from the survey by Raghavan et al. (2010), and to put the results in context, the presumable distribution of the separation and the period (red, dash-dotted), if multiplicity data from literature are included (see Table A7).

The resulting separation distributions for the analysed sub-samples and the fitted log-normal functions are shown Figure 25 in the left-hand panel, whereas the distributions of the as-

sessed periods and their corresponding best-fit estimate are illustrated in the right-hand panel. The peak of the separation distribution fit for the sub-sample of physical companions, is located at $\log a_{\text{proj.}} = 2.33 \pm 0.07$, corresponding to $a_{\text{proj.}} = 214^{+38}_{-24}$ au, and a width of $\sigma_{\log a_{\text{proj.}}} = 0.60 \pm 0.05$. A similar result, with the peak situated at $\log a_{\text{proj.}} = 2.36 \pm 0.06$ and a width of $\sigma_{\log a_{\text{proj.}}} = 0.64 \pm 0.04$, was obtained including the visual companions in the analysed sample. The peak of the period distribution estimated from both sub samples is roughly located at $\log \text{P} \approx 5.6$, which corresponds to an orbital period of about 1100 yr, and has a width of $\sigma_{\log a_{\text{proj.}}} \approx 1.0$. Also indicated, for comparison, is the fit result to the period distribution, with a peak at $\log \text{P} = 5.03$, about 300 yr, and a standard deviation of $\sigma_{\log \text{P}} = 2.28$, estimated by Raghavan et al. (2010) from their survey of multiplicity to solar-type primaries.

As can be seen, the location of the separation distribution is shifted towards wider separations in multiple systems with B-type primaries compared to the distribution of companions around solar-type stars. This tendency is consistent with the general observed trend of an increase in the location of the separation distribution peak as function of the primary mass from previous multiplicity surveys of A-type (De Rosa et al. 2014), M-type (Fischer and Marcy 1992) or brown dwarf (Burgasser et al. 2006) primaries, respectively, and illustrated in Figure 26. The measured width of the companion separation distribution is also significantly narrower compared to the one observed by Raghavan et al. (2010), and extrapolating the obtained distribution to the full range of companion separations covered by the survey of solar-type stars, suggests a complete lack of close-in ($\log a_{\text{proj.}} < 0$) and very wide companions ($\log a_{\text{proj.}} > 3.5$). This is of course fully inconsistent with the present known companion population to B-type stars. For the purpose of demonstration the known companions to the investigated sample stars from literature, which are listed in Table A7, were included in the distribution samples, according to their availability (red, dash-dotted histograms in Figure 25).

As can be also seen the presumable shape of the separation/period distribution suggests a more complex functional form then the uni-modal reported for the companion separation distribution to solar-type and lower mass stars and observed in the analysed data, respectively. The data suggest a combination of at least two different distributions, similar to the bimodal form observed for A-type stars. While the population of visual companions might be adequately described by log-normal representation, the results for companions with periods of less than 3000 days are indicative for a declining number of companions with increasing orbital period as it is also observed for high-mass binaries (e.g., Sana et al. 2013). However, since spectroscopic observations were not part of the sample, and because the limits on the available spectroscopic data were not quantified, reference has to be made at this point to Duchêne and Kraus (2013) for a further discussion on this topic.

As also shown in Figure 26, the measured peak location and the general observed trend are consistent with a predicted increased location of the distribution peak as function of the primary mass from hydrodynamical simulation of star cluster formation (Bate 2009; 2012),

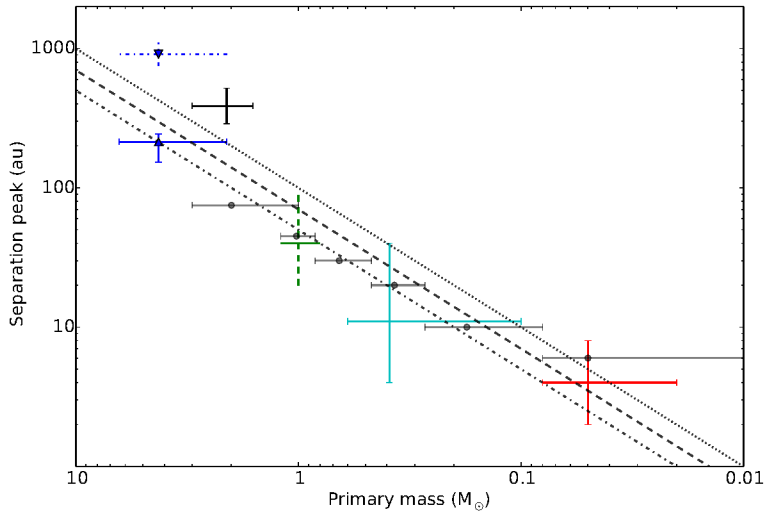


**Figure 26.** The location of the separation distribution peak as function of the primary mass for, from left to right; B-type (blue, this work), A-type (black, De Rosa et al. 2014), solar-type (green, Raghavan et al. 2010), M-type (light-blue, Fischer and Marcy 1992) and brown dwarf (red, Burgasser et al. 2006) primaries. Along the sample of co-moving companion (upward triangle, lower limit) the sample including all objects (downward triangle, dashed error-bars) is shown for comparison. Also plotted are the predictions from models of secondary fragmentation (black lines, Whitworth and Stamatellos 2006) and dynamical simulations (grey points, Sterzik and Durisen 2003). These predictions are conform with the general observed trend of an increase of the peak location with increasing primary mass.

Simulations of dynamical interactions within stellar clusters (Sterzik and Durisen 2003) or numerical calculations of companion formation through disc fragmentation (Whitworth and Stamatellos 2006). If, however, also the wide companions from literature are included and it is assumed that the distribution is adequately described by a log-normal function for $\log a_{\text{proj.}} > 0$, the peak of the distribution is significantly shifted towards larger separations, with the peak located at $a_{\text{proj.}} \approx 1000$ au compared to the current measured location of about 200 au and similar to the results for A-type stars ($a_{\text{proj.}} \approx 390$ au), reported by De Rosa et al. (2014). These quite distinct results have significant bearings from a theoretical point of view, as the perturbations induced by a companion at a certain separation may significantly affect formation processes in the interior of the system (Boss 1998, Kley and Nelson 2008, Nelson 2000), but also the long-term orbital evolution of any companion (e.g., Wu et al. 2007). However, due to the insufficient knowledge of the apparently complex shape of the companion separation, a conclusive statement on the impact on the theory of star or planet formation processes can not be made at this point.

### 7.2.2 Mass ratio distribution

The distribution of mass ratios was constructed from the derived masses for each primary-companion pair, identified in this study, according to the procedure described in section 5.4, and with the results listed in Table A5 and Table A6, respectively. The data presented, were mainly derived from the sample of confirmed companions, but in favour of a larger sample

size also candidate companions with $q \geq 0.1$ were included in the analysis for comparison, assuming they are indeed companions and that the bias introduced by falsely enclosed background objects in the data is negligible. In addition, all objects with known spectroscopic or unresolved companions, respectively, were excluded accounting that the flux of these close companions contribute to the measured primary brightness, and consequently, significantly affects the mass ratio results.

The derived masses of the analysed primaries generally range between 1.8 and 13 $M_\odot$, whereas the masses of the found confirmed companions vary between 0.1 and 9 $M_\odot$, covering a mass ratio range which extends from 0.05 to 0.91 . Not included in this mass ratio range are the two systems, which are consistent with $q \approx 1$ within their error-bars.

The average error in the mass due to uncertainties in the distance, colour, magnitude and applied spectral type for the primaries is about 0.1 $M_\odot$, whereas the average error in the mass of the companions is 0.3 $M_\odot$, as a result of the uncertainties in the estimated system age and the absolute companion magnitude. The average error on the mass ratios is about 0.1 mainly due to the uncertainties in the obtained companion masses.

Similar to previous surveys a power-law, $f(q) \propto q^{\Gamma}$, was utilised to characterize the distribution of mass ratios. The function again was fitted to the cumulative distribution of each sub-sample to avoid biases introduced by a binning scheme. Furthermore, previous multiplicity surveys also have repeatedly shown that the mass ratio distribution not only depends on the primary mass but also that the mass ratio distribution is a function of the binary separation with high-q systems preferable found at shorter periods compared to low-q systems found at wider separations. Thus, only a more detailed study of this dependency can give implications for the various formation scenarios of binary companion frequently discussed.

To test whether the obtained data contain statistically distinct populations depending on the separation a two-sided Kolmogorov–Smirnov (KS) test was performed, employing the sample of confirmed companions down to $q = 0.05$. The procedure utilised equates to the method presented by De Rosa et al. (2014) for A-type stars, to be able to compare the results fairly with different stellar populations. Following their description, the sample was divided into an inner and an outer mass ratio distribution, with the dividing separation marched from 16 to 2000 au in steps of $\log a_{\text{proj.}} = 0.05$. Then, at each dividing separation the statistical similarity of the two sample was calculated employing the two-sided KS test statistics.

The resulting overall mass ratio distributions are plotted in the left-hand panel of Figure 27 along with the best estimate power-law index obtained from the cumulative q-distribution fit to the confirmed companions, with $\Gamma = -0.39 \pm 0.14$ (blue, solid), and including candidate companions with mass ratios down to $q = 0.1$, with $\Gamma = -0.53 \pm 0.12$ (black, dashed). The results are comparable within the given uncertainties and indicate a rather flat distribution of mass ratios mildly increasing towards low-q systems. This is in agreement with previous observations of B-type stars, with power-law indices in the range between 0.3 and 0.5

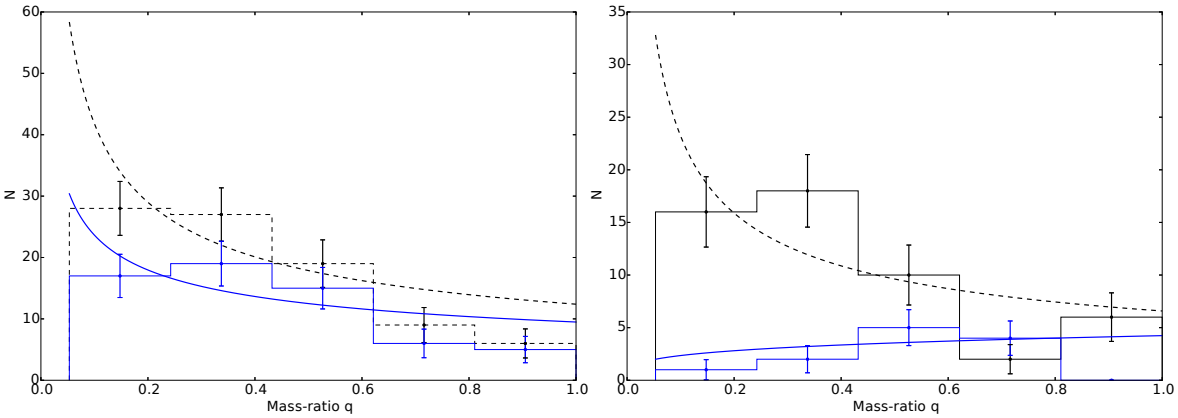


**Figure 27.** *Left:* The overall q-distributions estimated in the range between 16 to 2000 au and the results of the corresponding power-law fit to the cumulative distribution, for the confirmed companions (blue, solid) and including candidate companions (black, dashed), assuming they are physical, and with $q \geq 0.1$ to minimise the number of falsely included background objects. *Right:* The two statistical distinct q-distributions of companions with separations of 16–60 au (blue histogram) and 60–2000 au (black histogram). The inner distribution, with a power-law index of $\Gamma = 0.26^{+0.66}_{-0.55}$ (blue, solid), appears flat, while the outer distribution, found with $\Gamma = -0.55^{+0.15}_{-0.14}$ (black, dashed), is indicative for a greater abundance of low-mass companions at larger separations.

estimated for instance by Shatsky and Tokovinin (2002) or Rizzuto et al. (2013) in their survey of the Scorpius OB2 association. In a survey of the same region in the sky obtained by Kouwenhoven et al. (2007), which included visual as well as spectroscopic companions, a similar result with $\Gamma = -0.4$ was found. Please note, however, that this is not entirely surprising since the investigated sample contains also re-analysed NaCo observations from their survey which were found in the archive data.

The two statistical distinct sub-sample found in the investigated sample, an inner distribution ranging from 16 to 60 au and an outer distribution between 60 and 2000 au, are shown in Figure 27, in the right-hand panel as blue and black histogram, respectively. The null hypothesis that these two samples are drawn from the same distribution can be rejected at a 99 % level, with a minimum p-value of 0.53% found at $\log a_{\text{proj.}} = 1.78$ ($\sim 60$ au). Also shown are the results of the power-law fit to the cumulative distributions, with a power-law index of $\Gamma = 0.26^{+0.66}_{-0.55}$ for the inner distribution (blue, solid), and $\Gamma = -0.55^{+0.15}_{-0.14}$ for the outer distribution (black, dashed). The presented data are indicative for a greater abundance of low-q systems outside of about 60 au, whereas the data at smaller separations suggest a shallow increase of systems with higher mass ratios. This result, however, is only preliminary due to the very low number of close confirmed companions resolved by NaCo within the given sensitivity limits. It is therefore expected that the results will change extending the analysis to spectroscopic and close companions within 20 au and wide companions with separations greater than 2000 au.

To put the obtained results in context, a comparison with the estimated power-law indices from other stellar population was performed. The results are illustrated in Figure 28. Presented in the left-hand panel of Figure 28 are the estimated power-law indices as function

of the separation, as reported by De Rosa et al. (2014).

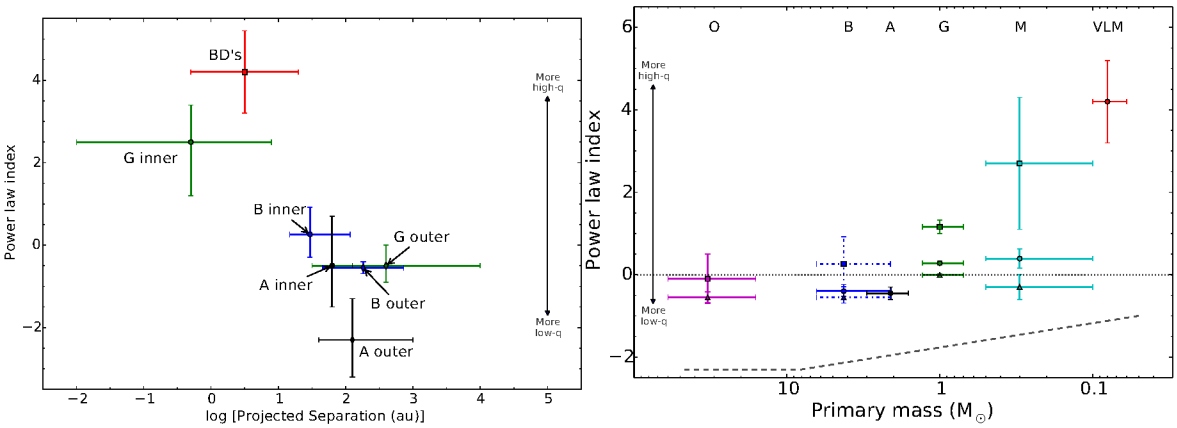


**Figure 28.** *Left:* Shown are the best power-law fit indices estimates for the inner an outer q-distribution found in this study (blue) and as reported by De Rosa et al. (2014), for A-type (black), for solar-type (green) and for brown dwarf (red) primaries, respectively. *Right:* Plotted are the power law indices estimated in this study (blue) and the best-estimate numbers reported by Duchêne and Kraus (2013; and references therein). In addition to the results derived for the overall population of multiple systems within a certain primary mass range (dots), the results of fits to the subsets of "tight" (square, $P \leq \overline{P}$) and "wide" (upward triangle, $P \geq \overline{P}$) binaries, respectively, are shown. The dashed curve represents the index that would be derived if the companions followed the single stars IMF of Chabrier (2003) and a simple power law would be fit to the resulting companion mass distribution over the mass ratio range $0.1 \leq q \leq 1$ (Duchêne and Kraus 2013).

The results for an inner and an outer distribution found in this work, constructed over a range from 16 to 2000 au are consistent with the measurements by De Rosa et al. (2014) obtained for A-type stars between 30 and 800 au and solar-type stars at a dividing separation of about 30 au, although, as stated, derived from a significant smaller range of separations compared to solar-type stars. Also plotted is the observed q-distribution for companions to brown dwarf primaries, considering all companions resolved with separations above 2 au by Burgasser et al. (2006).

A comparison of the power-law indices as function of the primary mass is shown in the right-hand panel of Figure 28. The observed almost flat overall distribution $\Gamma \approx -0.4$ estimated in this study is consistent with the overall q-distributions ($q \gtrsim 0.1$) of all primary masses $M \gtrsim 0.3$ with $|\Gamma| \lesssim 0.5$. Below $M \lesssim 0.3$ the distribution of mass ratios is clearly skewed towards high-q systems. Also visible from the plots is the described tendency of low-mass companions preferentially located at wider separations among A-type (De Rosa et al. 2014), solar-type (Raghavan et al. 2010) and M-type (Delfosse et al. 2004, Duchêne and Kraus 2013) primaries. If the derived mass ratio distributions for companions to B-type and the results obtained for other populations are compared to what is expected if the companions follow the single star IMF of field objects (e.g., Chabrier 2003), shown as dashed line, random paring from the IMF can be generally excluded over the entire range of primary masses.

Regarding the binary formation mechanism no specific conclusions are possible at this point,

although a fragmentation scenario is generally favoured in the investigated separation range between 20 and 2000 au, and beyond. In general, for instance, the initial fragmentation of a pre-stellar molecular cloud (e.g., Bonnell et al. 1991, Boss and Bodenheimer 1979) can produce multiple systems in the observed range of separations and mass ratios, but this model would also suggest that the mass ratio distribution of companions (see Figure 28) as well as the multiplicity fraction (see subsequent section 7.3) are almost independent of the primary mass, which is not seen in the data and in comparison with solar-type and A-type stars. On the other hand, however, it has to be taken into account that most stars are formed in clustered environments which may introduce a dependence on primary mass, with more massive primaries having q-distributions skewed towards less massive companions (e.g., Bonnell and Bastien 1992).

A second possible formation scenario, which can explain the observed distribution of mass ratios with low-mass companions preferentially found at wider separations, is the fragmentation of a large circumstellar disc (e.g., Bonnell 1994, Stamatellos et al. 2011), subsequent to the initial fragmentation of a cloud. In this scenario the conservation of angular momentum causes the in-fall of material from the surrounding cloud to form a protostellar disc Bonnell (1994), which than themselves can become gravitational unstable under the right conditions to produce a significant number of disc-born low-mass stars or even sub-stellar objects (Stamatellos et al. 2011). Although this scenario is presumable the more dominant formation process for higher-mass stars like O, B or early A-type stars (Kratter 2011), due to the larger reservoir of material in the more massive discs, and as it might explain the preferential equalisation of the mass ratios of those binaries formed at close separations (e.g., Bate and Bonnell 1997), the formation via disc fragmentation is not possible for the widest companions.

However, given the current uncertainties in the sample and the remaining lack of information about close ( $\lessapprox 20$ au) and wide companions ($\gtrapprox 2000$ au), which are not quantified in this thesis, it is very likely that the actual formation process of multiple systems among higher-mass stars is a combination of both theses scenarios.

## 7.3 Companion stars and multiplicity fractions

The fraction of stars within multiple systems are commonly expressed by three quantities, namely the multiplicity fraction (MF; e.g., Reipurth and Zinnecker 1993), the fraction of non-single stars, hereafter labelled as NSF, and the companion star fraction (CSF; e.g., Ghez et al. 1997, Goodwin et al. 2004), which are defined as

$$\mathrm{MF} = (B + T + Q + \cdots)/(S + B + T + Q + \cdots); \tag{7.1}$$

$$\mathrm{NSF} = (2B + 3T + 4Q + \cdots)/(S + 2B + 3T + 4Q + \cdots); \tag{7.2}$$

$$\mathrm{CSF} = (B + 2T + 3Q + \cdots)/(S + B + T + Q + \cdots), \tag{7.3}$$

where $S$, $B$, $T$ and $Q$ are the number of single, binary, triple and quadruple, respectively. Whereas MF describes the fraction of multiple systems found within a sample of stars, NSF refers to the number of non-single stars in the sample, since $1 - \mathrm{NSF}$ is the number of stars that are single. The CSF gives the average number of companion stars per primary star, which by number can exceed 100 %. The companion, multiplicity and non-single star fractions were estimated from the absolute numbers of identified physical and candidate companions found in the sample and their combination with known visual and spectroscopic companions from literature, utilising Equation 7.1, Equation 7.2 and Equation 7.3, respectively, and employing binomial statistics to calculate the frequencies and the statistical uncertainties. For more details on the calculation of these and the subsequent frequencies, respectively, reference is made at this point to Burgasser et al. (2003), for instance. The employed numbers and the calculated results are listed in Table 18.

**Table 18.** Result companion star and multiplicity fraction from this thesis

| Companion Type | N | S | B | T | Q | $> 4$ | CSF (*per cent*) | MF (*per cent*) | NSF (*per cent*) |
|---|---|---|---|---|---|---|---|---|---|
| phys.+vis. | 316 | 185 | 112 | 15 | 1 | 3 | $51.3^{+2.8}_{-2.8}$ | $41.5^{+2.8}_{-2.7}$ | $61.3^{+2.2}_{-2.3}$ |
| phys.+vis.+lit. | 316 | 123 | 120 | 46 | 15 | 12 | $99.7^{+0.1}_{-0.7}$ | $61.1^{+2.7}_{-2.8}$ | $80.5^{+1.5}_{-1.7}$ |

As can be seen from the frequencies listed in the table, on average every second investigated stars (CSF $\approx 51 \pm 3$ %) statistically exhibits a companion, and almost two third are non-single stars (NSF $\approx 61 \pm 2$ %). If also known companions to the primaries from literature are included, the frequencies change significant resulting in a non-single star fraction of almost three quarter (NSF $\approx 81 \pm 2$ %) among the investigated stars and on average one companion to each primary (CSF $\approx 100 \pm 1$ %). These discrepancies in the different samples are indicative for the lack of completeness in the current sample. The derived MF, NSF and CSF as well as the corresponding statistical uncertainties, additionally, can only be considered as lower limits, as the numbers will change with (1) the discovery of newly resolved companions, (2) by including and combining different observation techniques such as interferometric or spectroscopic observations, and/or (3) the confirmation/rejection of candidate companions as result of a common proper motion analysis in a future extension of this work.

For the calculation presented above no restrictions on the separation or the mass ratio range of the companions identified in this thesis where made. This, however, complicates a proper comparison between different populations of stars because the results of each survey are based on various selection and observation criteria which result in, for instance, different separation ranges covered by each survey, or varying lower limits on the companion mass and hence, the mass ratio ranges that can be explored.

In attempt to compensate for these differences in the sensitivity and to seek a fair comparison with other surveys, the approach and the data reported by De Rosa et al. (2014) from their VAST survey were used and complemented with estimates of the CSF made in

this thesis. Similar to the method used in the VAST survey, therefore, the CSF was simply calculated by counting the number of companions found between 30 and 800 au and with mass ratios of $q \geq 0.1$. Because each triple contributes two separations, each quadruple three separations, etc. to the separation distribution, these number equates to the dividend in Equation 7.3 and with the total number of sample stars the CSF can be readily determined using the given equation. While, as also pointed out by De Rosa et al. (2014), the uniform $q \geq 0.1$ limit reaches the bottom of the main sequence for the solar-type and lower mass samples, this limit does not include all stellar companions to A-type stars and in particular not all stellar companions to the investigated B-type stars. Thus, a second subsample was created for comparison, extending the mass ratio range to also include systems with $q \geq 0.05$. Please note, however, that the values estimated for $q \geq 0.05$ only represent lower limits to the CSF within 30 and 800 au, since the data are not uniformly sensitive to companions at these "extreme" mass ratios (De Rosa et al. 2014). The overall frequencies estimated in this thesis as well as those which were conducted over the restricted separation range ($1.5 \leq \log a_{\mathrm{proj}} < 2.9$) and mass ratios down to $q = 0.1$, and additionally down to $q = 0.05$, are illustrated in Figure 29 and summarised in Table 19, respectively.

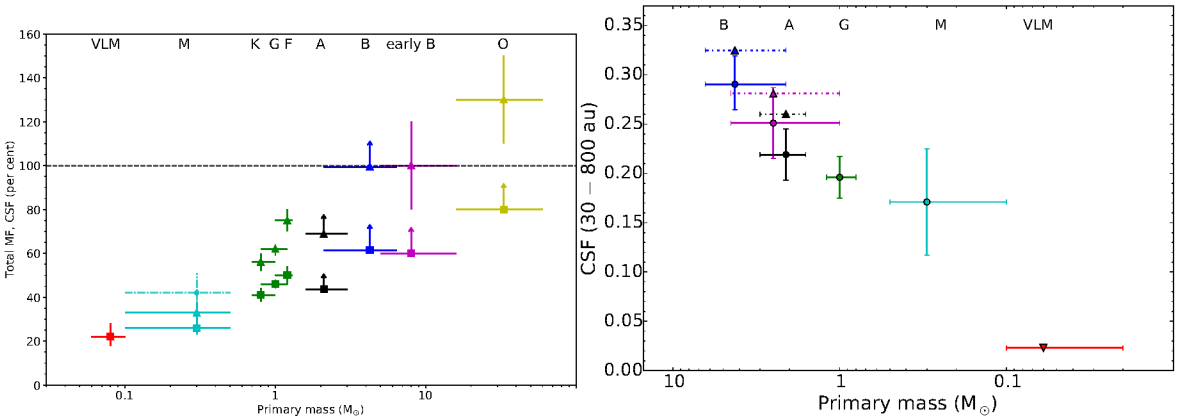


**Figure 29.** *Left:* Total MF (squares) and CSF (triangles) as function of primary mass for different populations. The estimated frequencies of A, early B and O type stars are given as lower limits because only companions down to $q \approx 0.1$ are included. *Right:* CSF measured within the separation range 30–800 au and $q \gtrsim 0.1$ as function of the primary mass for, from left to right, B-type stars (blue point, this work), Sco OB2 primaries (magenta point, Kouwenhoven et al. 2005), field A-type stars (black point, De Rosa et al. 2014), field solar-type stars (green point, Raghavan et al. 2010) and field M-type stars (light blue point, Fischer and Marcy 1992). Additionally, the upper limit for companions to brown-dwarf primaries within this separation range is illustrated (pink downward triangle). Also shown is the lower limit on the CSF(30–800 au) including also stellar companions with $0.05 \leq q \leq 0.1$ (upward triangles, dashed error bars). The results illustrated here are listed in Table 19.

Shown in the left-hand panel of Figure 29 are the total multiplicity and companion star fractions as function of the primary mass estimated from left to right, for very low-mass (VLM) field stars with $M_\star \lesssim 0.1\,\mathrm{M}_\odot$ (red, Allen et al. 2007); M-type stars with $M_\star = 0.1$–$0.5\,\mathrm{M}_\odot$ (light blue, Delfosse et al. 2004, Dieterich et al. 2012) and solar-type field stars with $M_\star = 0.7$–$1.3\,\mathrm{M}_\odot$ (green, Raghavan et al. 2010), respectively. Furthermore shown as

**Table 19.** Comparison of companion star and multiplicity fraction with various surveys.

| Spectral Type | Ref. | Separation range log *[au]* | Companion mass range | Type | Value (*per cent*) |
|---|---|---|---|---|---|
| B | (1) | $1.5 \leq \log a_{\rm proj} < 2.9$ | $q \geq 0.10$ | CSF | 29.0±2.7 |
| | | $1.5 \leq \log a_{\rm proj} < 2.9$ | $q \geq 0.05$ | CSF | $\geq 32.5$ |
| | | *all* | *all* | CSF | $\geq 99.7 \pm 0.5$ |
| | | *all* | *all* | MF | $\geq 61.1 \pm 2.8$ |
| BA (ScoCen) | (2) | $1.5 \leq \log a_{\rm proj} < 2.9$ | $q \geq 0.10$ | CSF | 25.1±3.6 |
| | | $1.5 \leq \log a_{\rm proj} < 2.9$ | $q \geq 0.05$ | CSF | $\geq 28.1$ |
| A | (3) | $1.5 \leq \log a_{\rm proj} < 2.9$ | $q \geq 0.10$ | CSF | 21.9±2.6 |
| | | $1.5 \leq \log a_{\rm proj} < 2.9$ | $q \geq 0.05$ | CSF | $\geq 26.0$ |
| | | *all* | $M_2 \geq 0.08\ M_\odot$ | CSF | 68.9±7.0 |
| | | *all* | $M_2 \geq 0.08\ M_\odot$ | MF | $\geq 43.6 \pm 5.3$ |
| FGK | (4) | $1.5 \leq \log a_{\rm proj} < 2.9$ | $q \geq 0.10$ | CSF | 19.6±2.1 |
| | | *all* | $M_2 \geq 0.08 M_\odot$ | CSF | 61.0±3.7 |
| | | *all* | $M_2 \geq 0.08 M_\odot$ | MF | 46.0±2.0 |
| M | (5) | $1.5 \leq \log a_{\rm proj} < 2.9$ | $M_2 \geq 0.08\ M_\odot$ | CSF | 17.1±5.4 |
| | (6,7) | *all* | $M_2 \geq 0.08 M_\odot$ | CSF | 33.0±5.0 |
| | (6) | *all* | $M_2 \geq 0.08 M_\odot$ | MF | 26.0±3.0 |
| | (5) | *all* | $M_2 \geq 0.08 M_\odot$ | MF | 42.0±9.0 |
| LT | (8) | $\log a_{\rm proj} \geq 1.6$ | $M_2 \geq 0.03 M_\odot$ | CSF | $\leq 2.3$ |
| | (8) | | | MF,CSF | $\approx 22 \pm 5.0$ |
| | (9) | *all* | $q \geq 0.20$ | MF | 12.5±3.0 |

**Note**. Table and values are reproduced from De Rosa et al. (2014) and Duchêne and Kraus (2013; and references therein), respectively, and completed with results from this study.
**References**: (1) This work; (2) Kouwenhoven et al. (2005); (3) De Rosa et al. (2014); (4) Raghavan et al. (2010); (5) Fischer and Marcy (1992); (6) Delfosse et al. (2004); (7) Dieterich et al. (2012); (8) Allen et al. (2007); (9) Reid et al. (2008)

lower limits are the frequencies for A-type primaries (black, De Rosa et al. 2014), B and early-B type stars (blue, this work, and e.g., magenta, Abt et al. 1990) as well as those for O-type stars (yellow, Duchêne and Kraus 2013; and references therein), accounting for the mentioned incompleteness to stellar and sub-stellar companions at the bottom of the main sequence. For completeness the frequently used multiplicity fraction estimated by Fischer and Marcy (1992) for M-type stars is indicated by dashed error-bars in the left-hand panel of Figure 29. In the solar-mass range, Raghavan et al. (2010) found that slightly less than the half of all solar type stars are actually single stars like our Sun. Taking advantage of their large sample of 454 solar-mass dwarfs within 25 pc of the Sun, Raghavan et al. (2010) also found that super-solar dwarfs (F-type stars) have a marginally higher multiplicity rate than sub-solar dwarfs (K-type stars), which is indicated by the additional data points located left and right of the binary fractions measured for solar-type primaries.

In general, however, the progress of the CSF and the MF, both increasing as function of the primary mass, are qualitatively similar, although the multiplicity fraction possesses a shallower slope due its intrinsic upper limit at 100 %.

The right-hand panel of Figure 29 illustrates the calculated companion star fractions as function of the primary mass obtained between 30 and 800 au for mass ratios down to $q = 0.1$ as represented by the solid points, as well as for mass ratios down to $q = 0.05$ indicated by the upward triangles with dashed error-bars. Shown from left to right are the results for, the investigated B-type primaries (blue, this work); the Sco OB2 survey of A and B-type stars (magenta, Kouwenhoven et al. 2005); A-type primaries investigated in the VAST survey (black, De Rosa et al. 2014); for solar-type stars (green, Raghavan et al. 2010) and for M-type stars (light blue, Fischer and Marcy 1992), respectively. Additionally plotted is the upper limit to the L-dwarf CSF beyond 40 au (red, Allen et al. 2007).
The general trend observed in the comparison of the different surveys and demonstrated in both plots, is consistent with the predicted increase of the total multiplicity with increasing primary mass, for instance, from hydrodynamical simulations by Bate (2009; 2012) or numerical N-body simulations of stellar cluster by Sterzik and Durisen (2003), respectively. However, the large statistical uncertainties and the lack of sensitivity to sub-stellar and very low-mass companions in the sample currently still prevent the derivation of a conclusive functional form for the companion star or the multiplicity fraction over the whole possible range of primary masses.

**A note on higher-order multiple systems**

Within the analysed sample of 316 stars the numbers of single, binary, triple and higher-order multiple systems, with more than four components, are 185, 112, 15, 1, 0, 2, 0 and 1, respectively. These numbers were conducted from the available sample of physical companions and the number of identified candidate companions, assuming they are real. Given those numbers the corresponding relative frequencies are $58.5^{+2.7}_{-2.8}$, $35.4^{+2.8}_{-2.6}$, $4.8^{+1.5}_{-0.9}$, $0.6^{+0.8}_{-0.2}$ and $0.3^{+0.7}_{-0.1}$. Expanding the sample to include all available multiplicity data for the investigated B-type stars from the WDS catalogue (Mason et al. 2001) and the SB9 catalogue (Pourbaix et al. 2004), respectively, listed in Table A7 and again assuming that the compiled literature companions are physical, the number of single, binary, triple and higher-order multiple systems changes to 123, 120, 46, 15,8 , 1, 1, 1, 1, and the computed corresponding relative frequencies are $38.9^{+2.8}_{-2.7}$, $38.0^{+2.8}_{-2.6}$, $14.6^{+2.2}_{-1.8}$, $4.8^{+1.5}_{-0.9}$, $2.5^{+1.2}_{-0.6}$, and $0.3^{+0.7}_{-0.1}$ for systems with five and more components, respectively. As can be seen in particular the number of triple systems is significantly increased, mainly due to the included unresolved spectroscopic and close companions, identified for instance via interferometry.
Compared to binaries, higher-order multiple systems, i.e. systems with three and more components, have more parameter (periods, mass ratios, etc.) and hence their statistics can bring additional insights on the formation mechanisms. However, given the low-number of higher-order multiples no meaningful statistical analysis is possible at this point and the following results are only informative.
In this study, 46 triple systems were identified, with 43 triples composed of close pair and distant companion and 3 triple systems consisting of a single primary and a wide binary system with small separations, i.e. in a tight orbit. Figure 30 compares the inner, short

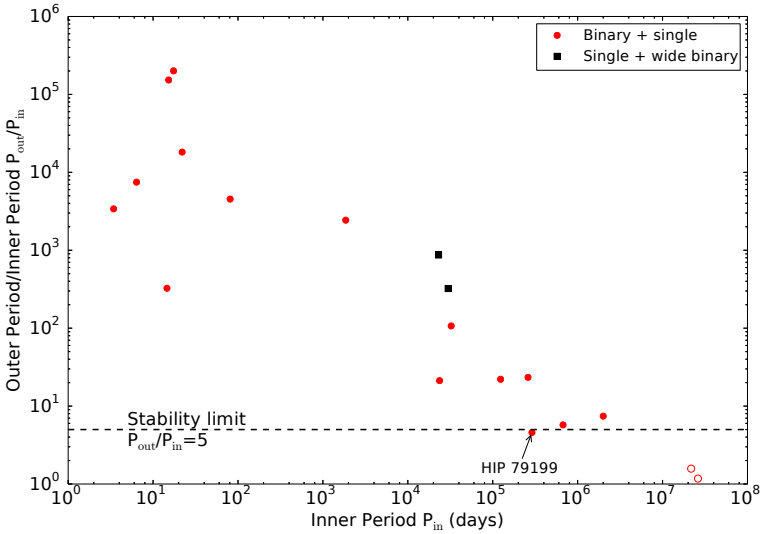


**Figure 30.** Illustrated is the ratio of the outer and inner period as a function of the inner period for hierarchical triple systems consisting of a binary and a wide tertiary component (red circles), and those consisting of a single star with a distant pair of lower-mass components in a tight orbit (black squares). Also shown is the stability limit of $P_{out}/P_{in} = 5$ (dashed line), with systems below this line being susceptible to dynamical processing (Eggleton 2006). The only confirmed hierarchical triple system found to be in a potentially unstable configuration within this study is indicated, as well as the two potential unstable candidate triple systems (open circles).

periods $P_{in}$ at levels *11* and *12* to the outer, long periods $P_{out}$ at level *1* (for a definition of levels see e.g., Reipurth et al. 2014) for the 19 triple systems, 17 level *11* triple and 2 level *12* triple, respectively, with sufficient information to estimate the orbital period by assuming that the projected separation equals the orbital semi-major axis. Also shown is the stability limit of $P_{out}/P_{in} = 5$, with systems below this line being susceptible to dynamical processing (Eggleton 2006).

The only triple system with both companion confirmed by CPM and found just beneath the stability limit is HIP 79199. However, due to the fact that the true semi-major axis is not known the ratio of periods is only a rough estimation and it is likely that the system is in a dynamically stable configuration. On the other hand, two systems were identified with a ratio of periods $< 2$, namely HIP 88012 and HIP 39331. Both systems were observed only once, and given the high probabilities of being chance projections, ranging from 16 to 37 percent, it is very likely that either one or both candidate companions in these systems are actually unrelated, i.e. not gravitationally bound, to the primary target.

Although most of the found higher-order systems are not yet confirmed, all these multiple systems might represent suitable candidates for future orbital motion monitoring work. With sufficient orbital coverage, model-independent mass estimates, the so-called dynamical masses, can be derived for each component within the system, which can be a very useful diagnostic tool to test evolutionary models, since multilevelled hierarchical systems, for instance, are potentially products of multiple fragmentation events during the star formation process.

# 8 Summary

This thesis explored the multiplicity of intermediate and high-mass B-type stars which appears to be a natural and rather frequent outcome of the star formation process. For this purpose, a volume-limited ($D \leq 1\,\mathrm{kpc}$) sample of 316 B-type stars was conducted and analysed, employing a combination of public available high-angular resolution archival data and own observations, obtained with the adaptive optics near-infrared imager NaCo which is mounted at the Very Large Telescope in Chile.

Each data-set was systematically reduced and calibrated according to availability of an astrometric calibrator such as a binary or a cluster, respectively, observed in the same night as the science target. This, however, was not the case for the majority of the observations and therefore a new approach was applied in this study, the "auto-calibration". This method uses the science data itself to estimate the pixel scale and detector orientation, without observed astrometric calibrator. As demonstrated in section 4.2, the results are consistent with calibrations obtained from a binary or a cluster. However, the small offsets observed between the calibration methods can alter the results and prevent a solid conclusion. Thus, care needs to be taken when comparing data points taken with different instruments or in differing observing epochs, and ideally observations should be executed with the same instrument set-up and the same astrometric calibrators in each observing epoch.

Given the separation and position angle of any object observed in the vicinity of the primary target either from multi-epoch observations or from the combination with evaluated literature data, a common proper motion analysis was performed, taking into account the possible orbital motion in a system, the proper motion of the primary star and the revolution of the Earth around the Sun.

Within the sample of 316 B-type stars a total of 194 sources was resolved in the vicinity of 148 stars. As a result of the common proper motion analysis, 33 of these objects were identified as unrelated background sources, while the physical association of 86 objects to their host-star could be confirmed by this technique. However, for the 75 remaining candidate companions no conclusive estimation on their companion status was possible, mainly due to uncertainties in the results introduced by, for instance, distance and proper motion estimates of the primary, respectively, the applied calibration, the time difference between consecutive observations or offsets in the data between the various instruments and sources employed for the analysis. In particular for those objects more observations are needed to derive a final companion status. Also, numerous previously unpublished companions and candidate companions were identified, including 9 new confirmed common proper motion pairs, 38 candidate companions and 19 previously known candidates confirmed for the first time here. A particular interesting finding, within this thesis, was the discovery of the first ever confirmed hierarchical triple in the centre of the planetary nebula HIP 3678, falsely classified as normal main sequence B-type star and found by chance in the sample.

The projected separations of the confirmed companions, in general, vary between about 16

and approximately 7000 au, with orbital periods ranging from about 30 up to several hundred thousands of years. Assuming a log-normal distribution, the peak of the separation distribution fit to the sub-sample of physical companions, is located at $\log a_{\text{proj.}} = 2.33 \pm 0.07$, corresponding to $a_{\text{proj.}} = 214^{+38}_{-24}$ au, and a width of $\sigma_{\log a_{\text{proj.}}} = 0.60 \pm 0.05$. This result is well consistent with the general trend of an increase in the location of the peak as a function of the primary mass (Figure 26), although the combination of the measured and available literature data strongly suggest a more complex shape of the separation distribution, and thus more in-depth investigations are required.

The derived masses of the analysed primaries range between 1.8 and 13 $M_\odot$, whereas the masses of the found confirmed companions vary between 0.1 and 9 $M_\odot$, covering a mass ratio range which extends from 0.05 to 0.91 . Similar to previous surveys a power-law, $f(q) \propto q^\Gamma$, was utilised to characterize the distribution of mass ratios. The best estimate power-law index obtained from the cumulative q-distribution fit to the confirmed companions is $\Gamma = -0.39 \pm 0.14$, consistent with previous smaller surveys of B-type stars. Also, similar to previous studies of solar-type and A-type stars, evidence was found for a dependency of the mass ratio as a function of separation with two statistically distinct distributions for confirmed companions with $q \geq 0.05$ (Figure 27). Based only on low numbers, the preliminary results, with low-q systems preferentially found at larger separations ($a_{\text{proj.}} > 60$ au), are indicative of a population of companions formed through either initial (Bonnell and Bastien 1992) or disc fragmentation (Kratter et al. 2010).

The measured companion star fraction (CSF) over a restricted separation range of 30–800 au and a uniform mass ratio range down to $q = 0.1$ is $29.0 \pm 2.7$ per cent (Figure 29). Compared with the CSF of $21.9 \pm 2.6$ per cent measured for A-type primaries (De Rosa et al. 2014), $19.6 \pm 2.1$ per cent for solar-type primaries (Raghavan et al. 2010), and $17.1 \pm 5.4$ per cent for M-dwarf primaries (Fischer and Marcy 1992) the observed trend is indicative for an increasing multiplicity as function of primary mass and also consistent with theoretical predictions of the frequency of binary systems determined from numerical simulations (Bate 2009; 2012, Sterzik and Durisen 2003).

Although the data presented and analysed in this thesis represent a competitive attempt to characterize the multiplicity of B-type stars, the statistical uncertainties and the lack of sensitivity to close ($a_{\text{proj.}} \leq 20$ au) and wide companions ($a_{\text{proj.}} \geq 2000$ au) in this study require a much larger sample size to draw a complete picture. In this regard especially probing the regions close to the primary star ($a_{\text{proj.}} \leq 100$ au) would be of great interest to fully constrain the shape of separation/period and mass-ratio distribution. An important extension of this thesis, therefore, would be to search for companions interior to the detection limits of the AO data presented here. Interferometric and spectroscopic monitoring of these targets will provide sensitivity to companions interior to $a_{\text{proj.}} \lesssim 10$ au, while next-generation high-contrast AO instruments such as VLT/SPHERE can be used to tightly constrain the population of low-mass stellar companions within a more restricted separation range of about 10–100 au, i.e. with orbital periods of only tens of years. Thus, already relatively small epoch differences would allow the determination of dynamical masses, a useful tool to test evolutionary models.

# References


Abt, H. A. Observed Orbital Eccentricities. *ApJ*, 629:507–511, August 2005. doi: 10.1086/431207.

Abt, H. A., Gomez, A. E., and Levy, S. G. The frequency and formation mechanism of B2-B5 main-sequence binaries. *ApJS*, 74:551–573, October 1990. doi: 10.1086/191508.

Adam, C. and Mugrauer, M. HIP 3678: a hierarchical triple stellar system in the centre of the planetary nebula NGC 246. *MNRAS*, 444:3459–3465, November 2014. doi: 10.1093/mnras/stu1677.

Adam, C., Neuhäuser, R., Mugrauer, M., Schmidt, J. G., and Schmidt, T. O. B. The low-mass companion of HIP 45314 (HR 3672). *MNRAS*, 433:402–411, July 2013. doi: 10.1093/mnras/stt733.

Adams, F. C., Ruden, S. P., and Shu, F. H. Eccentric gravitational instabilities in nearly Keplerian disks. *ApJ*, 347:959–976, December 1989. doi: 10.1086/168187.

Aikman, G. C. L. The spectroscopic binary characteristics of the mercury-manganese stars. *Publications of the Dominion Astrophysical Observatory Victoria*, 14:379–410, 1976.

Aitken, R. G. *The binary stars*. 1935.

Ali, A., Sabin, L., Snaid, S., and Basurah, H. M. Interacting planetary nebulae. I. Classification and orientation. *A&A*, 541:A98, May 2012. doi: 10.1051/0004-6361/201118389.

Allen, P. R. Star Formation via the Little Guy: A Bayesian Study of Ultracool Dwarf Imaging Surveys for Companions. *ApJ*, 668:492–506, October 2007. doi: 10.1086/521207.

Allen, P. R., Koerner, D. W., McElwain, M. W., Cruz, K. L., and Reid, I. N. A New Brown Dwarf Desert? A Scarcity of Wide Ultracool Binaries. *AJ*, 133:971–978, March 2007. doi: 10.1086/510346.

Allende Prieto, C. and Lambert, D. L. Fundamental parameters of nearby stars from the comparison with evolutionary calculations: masses, radii and effective temperatures. *A&A*, 352:555–562, December 1999.

Andersen, J. Spectroscopic observations of eclipsing binaries. I - Description of methods, and results for RS Chamaeleontis and chi-2 Hydrae. *A&A*, 44:445–458, November 1975.

Andre, P., Ward-Thompson, D., and Barsony, M. Submillimeter continuum observations of Rho Ophiuchi A - The candidate protostar VLA 1623 and prestellar clumps. *ApJ*, 406:122–141, March 1993. doi: 10.1086/172425.

Baraffe, I., Chabrier, G., Allard, F., and Hauschildt, P. H. Evolutionary models for solar metallicity low-mass stars: mass-magnitude relationships and color-magnitude diagrams. *A&A*, 337:403–412, September 1998.

Baraffe, I., Chabrier, G., Allard, F., and Hauschildt, P. H. Evolutionary models for low-mass stars and brown dwarfs: Uncertainties and limits at very young ages. *A&A*, 382:563–572, February 2002. doi: 10.1051/0004-6361:20011638.

Basri, G. and Reiners, A. A Survey for Spectroscopic Binaries among Very Low Mass Stars. *AJ*, 132:663–675, August 2006. doi: 10.1086/505198.

Bate, M. R. Stellar, brown dwarf and multiple star properties from hydrodynamical simulations of star cluster formation. *MNRAS*, 392:590–616, January 2009. doi: 10.1111/j.1365-2966.2008.14106.x.

Bate, M. R. Stellar, brown dwarf and multiple star properties from a radiation hydrodynamical simulation of star cluster formation. *MNRAS*, 419:3115–3146, February 2012. doi: 10.1111/j.1365-2966.2011.19955.x.

Bate, M. R. and Bonnell, I. A. Accretion during binary star formation - II. Gaseous accretion and disc formation. *MNRAS*, 285:33–48, February 1997. doi: 10.1093/mnras/285.1.33.

Bate, M. R., Bonnell, I. A., and Bromm, V. The formation of close binary systems by dynamical interactions and orbital decay. *MNRAS*, 336:705–713, November 2002. doi: 10.1046/j.1365-8711.2002.05775.x.

Berghoefer, T. W., Schmitt, J. H. M. M., and Cassinelli, J. P. The ROSAT all-sky survey catalogue of optically bright OB-type stars. *A&AS*, 118:481–494, September 1996.

Bertelli, G., Bressan, A., Chiosi, C., Fagotto, F., and Nasi, E. Theoretical isochrones from models with new radiative opacities. *A&AS*, 106:275–302, August 1994.

Bertelli, G., Nasi, E., Girardi, L., and Marigo, P. Scaled solar tracks and isochrones in a large region of the Z-Y plane. II. From 2.5 to 20 $M_{\odot}$ stars. *A&A*, 508:355–369, December 2009. doi: 10.1051/0004-6361/200912093.

Bertin, E. and Arnouts, S. SExtractor: Software for source extraction. *A&AS*, 117:393–404, June 1996.

Bessell, M. S., Castelli, F., and Plez, B. Model atmospheres broad-band colors, bolometric corrections and temperature calibrations for O - M stars. *A&A*, 333:231–250, May 1998.

Beuther, H. and Schilke, P. Fragmentation in MassiveStar Formation. *Science*, 303:1167–1169, February 2004. doi: 10.1126/science.1094014.

Bevington, P. R. and Robinson, K. D. *Data Reduction and Error Analysis for the Physical Sciences*. Boston: McGraw-Hill, 3rd ed. edition, 2003.

Biller, B. A., Close, L. M., Lenzen, R., Brandner, W., McCarthy, D., Nielsen, E., Kellner, S., and Hartung, M. Suppressing Speckle Noise for Simultaneous Differential Extrasolar Planet Imaging (SDI) at the VLT and MMT. In Aime, C. and Vakili, F., editors, *IAU Colloq. 200: Direct Imaging of Exoplanets: Science & Techniques*, pages 571–576, 2006. doi: 10.1017/S1743921306009975.

Bjorkman, K. S., Miroshnichenko, A. S., McDavid, D., and Pogrosheva, T. M. A Study of $\pi$ Aquarii during a Quasi-normal Star Phase: Refined Fundamental Parameters and Evidence for Binarity. *ApJ*, 573:812–824, July 2002. doi: 10.1086/340751.

Bodenheimer, P. H. *Principles of Star Formation*. 2011.

Bonnell, I. and Bastien, P. Fragmentation of elongated cylindrical clouds. V - Dependence of mass ratios on initial conditions. *ApJ*, 401:654–666, December 1992. doi: 10.1086/172093.

Bonnell, I., Martel, H., Bastien, P., Arcoragi, J.-P., and Benz, W. Fragmentation of elongated cylindrical clouds. III - Formation of binary and multiple systems. *ApJ*, 377: 553–558, August 1991. doi: 10.1086/170384.

Bonnell, I. A. A New Binary Formation Mechanism. *MNRAS*, 269, August 1994. doi: 10.1093/mnras/269.3.837.

Bonnell, I. A., Bate, M. R., Clarke, C. J., and Pringle, J. E. Accretion and the stellar mass spectrum in small clusters. *MNRAS*, 285:201–208, February 1997. doi: 10.1093/mnras/285.1.201.

Bonnell, I. A., Bate, M. R., Clarke, C. J., and Pringle, J. E. Competitive accretion in embedded stellar clusters. *MNRAS*, 323:785–794, May 2001. doi: 10.1046/j.1365-8711.2001.04270.x.

Bonnor, W. B. Boyle's Law and gravitational instability. *MNRAS*, 116:351, 1956. doi: 10.1093/mnras/116.3.351.

Boss, A. P. Binary stars - Formation by fragmentation. *Comments on Astrophysics*, 12: 169–190, 1988.

Boss, A. P. Giant Planet Formation Induced by a Binary Star Companion. In *AAS/Division for Planetary Sciences Meeting Abstracts #30*, volume 30 of *Bulletin of the American Astronomical Society*, page 1057, September 1998.

Boss, A. P. and Bodenheimer, P. Fragmentation in a rotating protostar - A comparison of two three-dimensional computer codes. *ApJ*, 234:289–295, November 1979. doi: 10.1086/157497.

Bragança, G. A., Daflon, S., Cunha, K., Bensby, T., Oey, M. S., and Walth, G. Projected Rotational Velocities and Stellar Characterization of 350 B Stars in the Nearby Galactic Disk. *AJ*, 144:130, November 2012. doi: 10.1088/0004-6256/144/5/130.

Brandner, W., Zinnecker, H., Alcalá, J. M., Allard, F., Covino, E., Frink, S., Köhler, R., Kunkel, M., Moneti, A., and Schweitzer, A. Timescales of Disk Evolution and Planet Formation: HST, Adaptive Optics, and ISO Observations of Weak-Line and Post-T Tauri Stars. *AJ*, 120:950–962, August 2000. doi: 10.1086/301483.

Bressan, A., Marigo, P., Girardi, L., Salasnich, B., Dal Cero, C., Rubele, S., and Nanni, A. PARSEC: stellar tracks and isochrones with the PAdova and TRieste Stellar Evolution Code. *MNRAS*, 427:127–145, November 2012. doi: 10.1111/j.1365-2966.2012.21948.x.

Burgasser, A. J., Kirkpatrick, J. D., Reid, I. N., Brown, M. E., Miskey, C. L., and Gizis, J. E. Binarity in Brown Dwarfs: T Dwarf Binaries Discovered with the Hubble Space Telescope Wide Field Planetary Camera 2. *ApJ*, 586:512–526, March 2003. doi: 10.1086/346263.

Burgasser, A. J., Kirkpatrick, J. D., Cruz, K. L., Reid, I. N., Leggett, S. K., Liebert, J., Burrows, A., and Brown, M. E. Hubble Space Telescope NICMOS Observations of T Dwarfs: Brown Dwarf Multiplicity and New Probes of the L/T Transition. *ApJS*, 166: 585–612, October 2006. doi: 10.1086/506327.

Burgasser, A. J., Reid, I. N., Siegler, N., Close, L., Allen, P., Lowrance, P., and Gizis, J. Not Alone: Tracing the Origins of Very-Low-Mass Stars and Brown Dwarfs Through Multiplicity Studies. *Protostars and Planets V*, pages 427–441, 2007.

Bystrov, N. F., Polojentsev, D. D., Potter, H. I., Yagudin, L. I., Zallez, R. F., and Zelaya, J. A. The final FOCAT-S star catalogue for southern hemisphere. *Bulletin d'Information du Centre de Donnees Stellaires*, 44:3, January 1994.

Cardelli, J. A., Clayton, G. C., and Mathis, J. S. The relationship between infrared, optical, and ultraviolet extinction. *ApJ*, 345:245–256, October 1989. doi: 10.1086/167900.

Carquillat, J.-M. and Prieur, J.-L. Contribution to the search for binaries among Am stars - VIII. New spectroscopic orbits of eight systems and statistical study of a sample of 91 Am stars. *MNRAS*, 380:1064–1078, September 2007. doi: 10.1111/j.1365-2966.2007.12143.x.

Catalán, S., Isern, J., García-Berro, E., and Ribas, I. The initial-final mass relationship of white dwarfs revisited: effect on the luminosity function and mass distribution. *MNRAS*, 387:1693–1706, July 2008. doi: 10.1111/j.1365-2966.2008.13356.x.

Catanzaro, G. and Leto, P. Orbital solutions for SB2 systems with a HgMn component. *A&A*, 416:661–668, March 2004. doi: 10.1051/0004-6361:20034445.

Chabrier, G. Galactic Stellar and Substellar Initial Mass Function. *PASP*, 115:763–795, July 2003. doi: 10.1086/376392.

Chini, R., Hoffmeister, V. H., Nasseri, A., Stahl, O., and Zinnecker, H. A spectroscopic survey on the multiplicity of high-mass stars. *MNRAS*, 424:1925–1929, August 2012. doi: 10.1111/j.1365-2966.2012.21317.x.

Claret, A. New grids of stellar models including tidal-evolution constants up to carbon burning. I. From 0.8 to 125 $M_{sun}$ at Z=0.02. *A&A*, 424:919–925, September 2004. doi: 10.1051/0004-6361:20040470.

Clarke, C. J. and Pringle, J. E. Star-disc interactions and binary star formation. *MNRAS*, 249:584–587, April 1991. doi: 10.1093/mnras/249.4.584.

Close, L. M., Siegler, N., Freed, M., and Biller, B. Detection of Nine M8.0-L0.5 Binaries: The Very Low Mass Binary Population and Its Implications for Brown Dwarf and Very Low Mass Star Formation. *ApJ*, 587:407–422, April 2003. doi: 10.1086/368177.

Correia, S., Zinnecker, H., Ratzka, T., and Sterzik, M. F. A VLT/NACO survey for triple and quadruple systems among visual pre-main sequence binaries. *A&A*, 459:909–926, December 2006. doi: 10.1051/0004-6361:20065545.

Couteau, P. Contribution à l'étude du dénombrement des étoiles doubles visuelles. *Journal des Observateurs*, 43:41, 1960.

Cowley, A., Cowley, C., Jaschek, M., and Jaschek, C. A study of the bright A stars. I. A catalogue of spectral classifications. *AJ*, 74:375–406, April 1969. doi: 10.1086/110819.

Cucchiaro, A., Jaschek, M., Jaschek, C., and Macau-Hercot, D. Spectral classification from the ultraviolet line features of S2/68 spectra. I. Early B-type stars. *A&AS*, 26:241, November 1976.

Curtis, H. D. Orbit of the spectroscopic binary kappa Velorum. *Lick Observatory Bulletin*, 4:155–156, 1907. doi: 10.5479/ADS/bib/1907LicOB.4.155C.

Cutri, R. M., Skrutskie, M. F., van Dyk, S., Beichman, C. A., Carpenter, J. M., Chester, T., Cambresy, L., Evans, T., Fowler, J., Gizis, J., Howard, E., Huchra, J., Jarrett, T., Kopan, E. L., Kirkpatrick, J. D., Light, R. M., Marsh, K. A., McCallon, H., Schneider, S., Stiening, R., Sykes, M., Weinberg, M., Wheaton, W. A., Wheelock, S., and Zacarias, N. 2MASS All-Sky Catalog of Point Sources (Cutri+ 2003). *VizieR Online Data Catalog*, 2246:0, March 2003.

De Cat, P., Aerts, C., De Ridder, J., Kolenberg, K., Meeus, G., and Decin, L. A study of bright southern slowly pulsating B stars. I. Determination of the orbital parameters and of the main frequency of the spectroscopic binaries. *A&A*, 355:1015–1030, March 2000.

De Rosa, R. J., Patience, J., Wilson, P. A., Schneider, A., Wiktorowicz, S. J., Vigan, A., Marois, C., Song, I., Macintosh, B., Graham, J. R., Doyon, R., Bessell, M. S., Thomas, S., and Lai, O. The VAST Survey - III. The multiplicity of A-type stars within 75 pc. *MNRAS*, 437:1216–1240, January 2014. doi: 10.1093/mnras/stt1932.

de Zeeuw, P. T., Hoogerwerf, R., de Bruijne, J. H. J., Brown, A. G. A., and Blaauw, A. A HIPPARCOS Census of the Nearby OB Associations. *AJ*, 117:354–399, January 1999. doi: 10.1086/300682.

Delfosse, X., Forveille, T., Ségransan, D., Beuzit, J.-L., Udry, S., Perrier, C., and Mayor, M. Accurate masses of very low mass stars. IV. Improved mass-luminosity relations. *A&A*, 364:217–224, December 2000.

Delfosse, X., Beuzit, J.-L., Marchal, L., Bonfils, X., Perrier, C., Ségransan, D., Udry, S., Mayor, M., and Forveille, T. M dwarfs binaries: Results from accurate radial velocities and high angular resolution observations. In Hilditch, R. W., Hensberge, H., and Pavlovski, K., editors, *Spectroscopically and Spatially Resolving the Components of the Close Binary Stars*, volume 318 of *Astronomical Society of the Pacific Conference Series*, pages 166–174, December 2004.

Devillard, N. ESO C Library for an Image Processing Software Environment (eclipse). In Harnden, F. R., Jr., Primini, F. A., and Payne, H. E., editors, *Astronomical Data Analysis Software and Systems X*, volume 238 of *Astronomical Society of the Pacific Conference Series*, page 525, 2001.

Dieterich, S. B., Henry, T. J., Golimowski, D. A., Krist, J. E., and Tanner, A. M. The Solar Neighborhood. XXVIII. The Multiplicity Fraction of Nearby Stars from 5 to 70 AU and the Brown Dwarf Desert around M Dwarfs. *AJ*, 144:64, August 2012. doi: 10.1088/0004-6256/144/2/64.

Diolaiti, E., Bendinelli, O., Bonaccini, D., Close, L. M., Currie, D. G., and Parmeggiani, G. StarFinder: an IDL GUI-based code to analyze crowded fields with isoplanatic correcting PSF fitting. In Wizinowich, P. L., editor, *Adaptive Optical Systems Technology*, volume 4007 of *Society of Photo-Optical Instrumentation Engineers (SPIE) Conference Series*, pages 879–888, July 2000.

Dommanget, J. and Nys, O. The visual double stars observed by the Hipparcos satellite. *A&A*, 363:991–994, November 2000.

Draper, P. W. GAIA: Recent Developments. In Manset, N., Veillet, C., and Crabtree, D., editors, *Astronomical Data Analysis Software and Systems IX*, volume 216 of *Astronomical Society of the Pacific Conference Series*, page 615, 2000.

Duchêne, G. and Kraus, A. Stellar Multiplicity. *ARA&A*, 51:269–310, August 2013. doi: 10.1146/annurev-astro-081710-102602.

Duquennoy, A. and Mayor, M. Multiplicity among solar-type stars in the solar neighbourhood. II - Distribution of the orbital elements in an unbiased sample. *A&A*, 248:485–524, August 1991.

Dworetsky, M. M. Orbit of the Double-Lined Binary Mercury Star Chi LUPI. *PASP*, 84: 254, April 1972a. doi: 10.1086/129280.

Dworetsky, M. M. The Orbit of 53 Tauri (B9p-Mn). *PASP*, 84:652, October 1972b. doi: 10.1086/129356.

Dworetsky, M. M. Orbit of the Spectroscopic Binary HR1883. *MNRAS*, 199:303, April 1982. doi: 10.1093/mnras/199.2.303.

Ebert, R. Über die Verdichtung von H I-Gebieten. Mit 5 Textabbildungen. *ZAp*, 37:217, 1955.

Eggleton, P. *Evolutionary Processes in Binary and Multiple Stars*. July 2006.

Ehrenreich, D., Lagrange, A.-M., Montagnier, G., Chauvin, G., Galland, F., Beuzit, J.-L., and Rameau, J. Deep infrared imaging of close companions to austral A- and F-type stars. *A&A*, 523:A73, November 2010. doi: 10.1051/0004-6361/201014763.

ESA, editor. *The HIPPARCOS and TYCHO catalogues. Astrometric and photometric star catalogues derived from the ESA HIPPARCOS Space Astrometry Mission*, volume 1200 of *ESA Special Publication*, 1997.

Fabricius, C., Høg, E., Makarov, V. V., Mason, B. D., Wycoff, G. L., and Urban, S. E. The Tycho double star catalogue. *A&A*, 384:180–189, March 2002. doi: 10.1051/0004-6361: 20011822.

Fischer, D. A. and Marcy, G. W. Multiplicity among M dwarfs. *ApJ*, 396:178–194, September 1992. doi: 10.1086/171708.

Foreman-Mackey, D., Hogg, D. W., Lang, D., and Goodman, J. emcee: The MCMC Hammer. *PASP*, 125:306–312, March 2013. doi: 10.1086/670067.

Gammie, C. F. Nonlinear Outcome of Gravitational Instability in Cooling, Gaseous Disks. *ApJ*, 553:174–183, May 2001. doi: 10.1086/320631.

Garrison, R. F. and Gray, R. O. The late B-type stars: Refined MK classification, confrontation with stromgren photometry, and the effects of rotation. *AJ*, 107:1556–1564, April 1994. doi: 10.1086/116967.

Ghez, A. M., McCarthy, D. W., Patience, J. L., and Beck, T. L. The Multiplicity of Pre-Main-Sequence Stars in Southern Star-forming Regions. *ApJ*, 481:378–385, May 1997. doi: 10.1086/304031.

Gies, D. R. and Bolton, C. T. The binary frequency and origin of the OB runaway stars. *ApJS*, 61:419–454, June 1986. doi: 10.1086/191118.

Girard, J. H. V., Kasper, M., Quanz, S. P., Kenworthy, M. A., Rengaswamy, S., Schödel, R., Gallenne, A., Gillessen, S., Huerta, N., Kervella, P., Kornweibel, N., Lenzen, R., Mérand, A., Montagnier, G., O'Neal, J., and Zins, G. Status and new operation modes of the versatile VLT/NaCo. In *Society of Photo-Optical Instrumentation Engineers (SPIE) Conference Series*, volume 7736 of *Society of Photo-Optical Instrumentation Engineers (SPIE) Conference Series*, page 2, July 2010. doi: 10.1117/12.856799.

Girardi, L., Bressan, A., Bertelli, G., and Chiosi, C. Evolutionary tracks and isochrones for low- and intermediate-mass stars: From 0.15 to 7 $M_{\odot}$, and from Z=0.0004 to 0.03. *A&AS*, 141:371–383, February 2000. doi: 10.1051/aas:2000126.

Gontcharov, G. A. Spatial distribution and kinematics of OB stars. *Astronomy Letters*, 38: 694–706, November 2012. doi: 10.1134/S1063773712110035.

Goodwin, S. P., Whitworth, A. P., and Ward-Thompson, D. Simulating star formation in molecular cores. II. The effects of different levels of turbulence. *A&A*, 423:169–182, August 2004. doi: 10.1051/0004-6361:20040285.

Gullikson, K., Kraus, A., and Dodson-Robinson, S. The Close Companion Mass-ratio Distribution of Intermediate-mass Stars. *AJ*, 152:40, August 2016. doi: 10.3847/0004-6256/152/2/40.

Haase, D. Detection of faint companions around young stars in speckle patterns of vlt/naco cube mode images. Student research project, Friedrich-Schiller-University, 2009.

Hartkopf, W. I., Mason, B. D., Finch, C. T., Zacharias, N., Wycoff, G. L., and Hsu, D. Double Stars in the USNO CCD Astrographic Catalog. *AJ*, 146:76, October 2013. doi: 10.1088/0004-6256/146/4/76.

Hayashi, C. Stellar evolution in early phases of gravitational contraction. *PASJ*, 13, 1961.

Henyey, L. G., Lelevier, R., and Levée, R. D. The Early Phases of Stellar Evolution. *PASP*, 67:154, June 1955. doi: 10.1086/126791.

Herbig, G. H. The Spectra of Be- and Ae-TYPE Stars Associated with Nebulosity. *ApJS*, 4:337, March 1960. doi: 10.1086/190050.

Herbig, G. H. and Bell, K. R. *Third Catalog of Emission-Line Stars of the Orion Population : 3 : 1988*. 1988.

Hilditch, R. W. *An Introduction to Close Binary Stars*. May 2001.

Hoffleit, D. *Catalogue of bright stars*. 1964.

Hohle, M. M., Neuhäuser, R., and Schutz, B. F. Masses and luminosities of O- and B-type stars and red supergiants. *Astronomische Nachrichten*, 331:349, April 2010. doi: 10.1002/asna.200911355.

Holdenried, E. R. and Rafferty, T. J. New methods of forming and aligning the instrumental frames of absolute transit circle catalogs. *A&AS*, 125, November 1997. doi: 10.1051/aas:1997246.

Houk, N. *Michigan Catalogue of Two-dimensional Spectral Types for the HD stars. Volume 3. Declinations 40°.0 to 26°.0.* 1982.

Houk, N. and Cowley, A. P. *University of Michigan Catalogue of two-dimensional spectral types for the HD stars. Volume I. Declinations 90°.0 to 53°.0.* 1975.

Hoyle, F. On the Fragmentation of Gas Clouds Into Galaxies and Stars. *ApJ*, 118:513, November 1953. doi: 10.1086/145780.

Hubrig, S., Le Mignant, D., North, P., and Krautter, J. Search for low-mass PMS companions around X-ray selected late B stars. *A&A*, 372:152–164, June 2001. doi: 10.1051/0004-6361:20010452.

Huélamo, N., Neuhäuser, R., Stelzer, B., Supper, R., and Zinnecker, H. X-ray emission from Lindroos binary systems. *A&A*, 359:227–241, July 2000.

Jasinta, D. M. D., Raharto, M., and Soegiartini, E. Photographic observations of visual double stars. *A&AS*, 114:487, December 1995.

Jeans, J. H. *Astronomy and cosmogony*. 1928.

Jones, E., Oliphant, T., Peterson, P., et al. SciPy: Open source scientific tools for Python, 2001. URL `http://www.scipy.org/`.

Kenyon, S. J. and Hartmann, L. Pre-Main-Sequence Evolution in the Taurus-Auriga Molecular Cloud. *ApJS*, 101:117, November 1995. doi: 10.1086/192235.

Kharchenko, N. V. All-sky compiled catalogue of 2.5 million stars. *Kinematika i Fizika Nebesnykh Tel*, 17:409–423, October 2001.

Kitsionas, S. and Whitworth, A. P. High-resolution simulations of clump-clump collisions using SPH with particle splitting. *MNRAS*, 378:507–524, June 2007. doi: 10.1111/j.1365-2966.2007.11707.x.

Kitsionas, S., Whitworth, A. P., and Klessen, R. S. SPH simulations of star/planet formation triggered by cloud-cloud collisions. In Sun, Y.-S., Ferraz-Mello, S., and Zhou, J.-L., editors, *Exoplanets: Detection, Formation and Dynamics*, volume 249 of *IAU Symposium*, pages 271–278, May 2008. doi: 10.1017/S1743921308016694.

Kley, W. and Nelson, R. P. Planet formation in binary stars: the case of $\gamma$ Cephei. *A&A*, 486:617–628, August 2008. doi: 10.1051/0004-6361:20079324.

Koen, C. and Eyer, L. New periodic variables from the Hipparcos epoch photometry. *MNRAS*, 331:45–59, March 2002. doi: 10.1046/j.1365-8711.2002.05150.x.

Koesterke, L., Dreizler, S., and Rauch, T. On the mass-loss of PG1159 stars. *A&A*, 330: 1041–1046, February 1998.

Kouwenhoven, M. B. N., Brown, A. G. A., Zinnecker, H., Kaper, L., and Portegies Zwart, S. F. The primordial binary population. I. A near-infrared adaptive optics search for close visual companions to A star members of Scorpius OB2. *A&A*, 430:137–154, January 2005. doi: 10.1051/0004-6361:20048124.

Kouwenhoven, M. B. N., Brown, A. G. A., Portegies Zwart, S. F., and Kaper, L. The primordial binary population. II.. Recovering the binary population for intermediate mass stars in Scorpius OB2. *A&A*, 474:77–104, October 2007. doi: 10.1051/0004-6361: 20077719.

Kratter, K. M. The Formation of Close Binaries. In Schmidtobreick, L., Schreiber, M. R., and Tappert, C., editors, *Evolution of Compact Binaries*, volume 447 of *Astronomical Society of the Pacific Conference Series*, page 47, September 2011.

Kratter, K. M., Matzner, C. D., Krumholz, M. R., and Klein, R. I. On the Role of Disks in the Formation of Stellar Systems: A Numerical Parameter Study of Rapid Accretion. *ApJ*, 708:1585–1597, January 2010. doi: 10.1088/0004-637X/708/2/1585.

Krumholz, M. R. and Bonnell, I. A. *Models for the formation of massive stars*, page 288. Cambridge University Press, January 2009.

Krumholz, M. R., McKee, C. F., and Klein, R. I. The formation of stars by gravitational collapse rather than competitive accretion. *Nature*, 438:332–334, November 2005. doi: 10.1038/nature04280.

Kuiper, G. P. Problems of Double-Star Astronomy. I. *PASP*, 47:15, February 1935. doi: 10.1086/124531.

Lada, C. J. Star formation - From OB associations to protostars. In Peimbert, M. and Jugaku, J., editors, *Star Forming Regions*, volume 115 of *IAU Symposium*, pages 1–17, 1987.

Lada, C. J. and Kylafis, N. D., editors. *The Origin of Stars and Planetary Systems*, volume 540 of *NATO Advanced Science Institutes (ASI) Series C*, 1999.

Lada, C. J. and Lada, E. A. Embedded Clusters in Molecular Clouds. *ARA&A*, 41:57–115, 2003. doi: 10.1146/annurev.astro.41.011802.094844.

Lamontagne, R., Demers, S., Wesemael, F., Fontaine, G., and Irwin, M. J. The Montreal-Cambridge-Tololo Survey of Southern Subluminous Blue Stars: The South Galactic Cap. *AJ*, 119:241–260, January 2000. doi: 10.1086/301181.

Landsman, W. B. The IDL Astronomy User's Library. In Shaw, R. A., Payne, H. E., and Hayes, J. J. E., editors, *Astronomical Data Analysis Software and Systems IV*, volume 77 of *Astronomical Society of the Pacific Conference Series*, page 437, 1995.

Lang, K. R. *Astrophysical Data I. Planets and Stars*. 1992.

Larson, R. B. Numerical calculations of the dynamics of collapsing proto-star. *MNRAS*, 145:271, 1969. doi: 10.1093/mnras/145.3.271.

Lenzen, R., Hartung, M., Brandner, W., Finger, G., Hubin, N. N., Lacombe, F., Lagrange, A.-M., Lehnert, M. D., Moorwood, A. F. M., and Mouillet, D. NAOS-CONICA first on sky results in a variety of observing modes. In Iye, M. and Moorwood, A. F. M., editors, *Instrument Design and Performance for Optical/Infrared Ground-based Telescopes*, volume 4841 of *Society of Photo-Optical Instrumentation Engineers (SPIE) Conference Series*, pages 944–952, March 2003. doi: 10.1117/12.460044.

Levato, H., Malaroda, S., Morrell, N., and Solivella, G. Stellar multiplicity in the Scorpius-Centaurus association. *ApJS*, 64:487–503, June 1987. doi: 10.1086/191204.

Levato, H., Garcia, B., Lousto, C., and Morrell, N. Radial velocities in the open cluster IC 2391. *Ap&SS*, 146:361–373, July 1988. doi: 10.1007/BF00637586.

Levenhagen, R. S. and Leister, N. V. Spectroscopic analysis of southern B and Be stars. *MNRAS*, 371:252–262, September 2006. doi: 10.1111/j.1365-2966.2006.10655.x.

Low, C. and Lynden-Bell, D. The minimum Jeans mass or when fragmentation must stop. *MNRAS*, 176:367–390, August 1976. doi: 10.1093/mnras/176.2.367.

Luyten, W. J. A Rediscussion of the Orbits of Seventy-Seven Spectroscopic Binaries. *ApJ*, 84:85, July 1936. doi: 10.1086/143751.

Maíz Apellániz, J. High-resolution imaging of Galactic massive stars with AstraLux. I. 138 fields with $\delta >$ - 25°. *A&A*, 518:A1, July 2010. doi: 10.1051/0004-6361/201014409.

Malkov, O. Y., Oblak, E., Snegireva, E. A., and Torra, J. A catalogue of eclipsing variables. *A&A*, 446:785–789, February 2006. doi: 10.1051/0004-6361:20053137.

Malkov, O. Y., Tamazian, V. S., Docobo, J. A., and Chulkov, D. A. Dynamical masses of a selected sample of orbital binaries. *A&A*, 546:A69, October 2012. doi: 10.1051/0004-6361/201219774.

Malkov, O. Y., Tessema, S. B., and Kniazev, A. Y. Binary star database: binaries discovered in non-optical bands. *Baltic Astronomy*, 24:395–402, 2015.

Malmquist, K. G. On some relations in stellar statistics. *Meddelanden fran Lunds Astronomiska Observatorium Serie I*, 100:1–52, March 1922.

Marois, C., Doyon, R., Racine, R., and Nadeau, D. Efficient Speckle Noise Attenuation in Faint Companion Imaging. *PASP*, 112:91–96, January 2000. doi: 10.1086/316492.

Mason, B. D., Gies, D. R., Hartkopf, W. I., Bagnuolo, W. G., Jr., ten Brummelaar, T., and McAlister, H. A. ICCD speckle observations of binary stars. XIX - an astrometric/spectroscopic survey of O stars. *AJ*, 115:821, February 1998. doi: 10.1086/300234.

Mason, B. D., Wycoff, G. L., Hartkopf, W. I., Douglass, G. G., and Worley, C. E. The 2001 US Naval Observatory Double Star CD-ROM. I. The Washington Double Star Catalog. *AJ*, 122:3466–3471, December 2001. doi: 10.1086/323920.

Mason, B. D., Hartkopf, W. I., Wycoff, G. L., and Wieder, G. Speckle Interferometry at the US Naval Observatory. XIII. *AJ*, 134:1671–1678, October 2007. doi: 10.1086/521555.

Mason, B. D., Hartkopf, W. I., Gies, D. R., Henry, T. J., and Helsel, J. W. The High Angular Resolution Multiplicity of Massive Stars. *AJ*, 137:3358–3377, February 2009. doi: 10.1088/0004-6256/137/2/3358.

Mason, B. D., Hartkopf, W. I., and Friedman, E. A. Speckle Interferometry at the U.S. Naval Observatory. XVIII. *AJ*, 143:124, May 2012. doi: 10.1088/0004-6256/143/5/124.

MATLAB. *version 7.10.0 (R2010a)*. The MathWorks Inc., Natick, Massachusetts, 2010.

McKee, C. F. and Ostriker, E. C. Theory of Star Formation. *ARA&A*, 45:565–687, September 2007. doi: 10.1146/annurev.astro.45.051806.110602.

Motte, F., Andre, P., and Neri, R. The initial conditions of star formation in the rho Ophiuchi main cloud: wide-field millimeter continuum mapping. *A&A*, 336:150–172, August 1998.

Nautical Almanac Office, H. N. A. O. R. A. L., United States Naval Observatory. *The Astronomical Almanac*. TSO (The Stationary Office), 2007.

Nelson, A. F. Planet Formation is Unlikely in Equal-Mass Binary Systems with A ˜ 50 AU. *ApJ*, 537:L65–L68, July 2000. doi: 10.1086/312752.

Neuhäuser, R., Schmidt, T. O. B., Hambaryan, V. V., and Vogt, N. Orbital motion of the young brown dwarf companion TWA 5 B. *A&A*, 516:A112, June 2010. doi: 10.1051/0004-6361/200913917.

Oudmaijer, R. D. and Parr, A. M. The binary fraction and mass ratio of Be and B stars: a comparative Very Large Telescope/NACO study. *MNRAS*, 405:2439–2446, July 2010. doi: 10.1111/j.1365-2966.2010.16609.x.

Pence, W. D., Chiappetti, L., Page, C. G., Shaw, R. A., and Stobie, E. Definition of the Flexible Image Transport System (FITS), version 3.0. *A&A*, 524:A42, December 2010. doi: 10.1051/0004-6361/201015362.

Peter, D., Feldt, M., Henning, T., and Hormuth, F. Massive binaries in the Cepheus OB2/3 region. Constraining the formation mechanism of massive stars. *A&A*, 538:A74, February 2012. doi: 10.1051/0004-6361/201015027.

Peters, G. J. Orbital motion and mass flow in the interacting binary Be star HR 2142. *PASP*, 95:311–318, May 1983. doi: 10.1086/131164.

Petrov, L., Kovalev, Y. Y., Fomalont, E. B., and Gordon, D. The Very Long Baseline Array Galactic Plane Survey—VGaPS. *AJ*, 142:35, August 2011. doi: 10.1088/0004-6256/142/2/35.

Platais, I., Kozhurina-Platais, V., and van Leeuwen, F. A Search for Star Clusters from the HIPPARCOS Data. *AJ*, 116:2423–2430, November 1998. doi: 10.1086/300606.

Pourbaix, D., Tokovinin, A. A., Batten, A. H., Fekel, F. C., Hartkopf, W. I., Levato, H., Morrell, N. I., Torres, G., and Udry, S. S$_{B<SUP>9</SUP>}$: The ninth catalogue of spectroscopic binary orbits. *A&A*, 424:727–732, September 2004. doi: 10.1051/0004-6361:20041213.

Preibisch, T., Balega, Y., Hofmann, K.-H., Weigelt, G., and Zinnecker, H. Multiplicity of the massive stars in the Orion Nebula cluster. *New A*, 4:531–542, December 1999. doi: 10.1016/S1384-1076(99)00042-1.

Pringle, J. E. On the formation of binary stars. *MNRAS*, 239:361–370, July 1989. doi: 10.1093/mnras/239.2.361.

Racine, R., Walker, G. A. H., Nadeau, D., Doyon, R., and Marois, C. Speckle Noise and the Detection of Faint Companions. *PASP*, 111:587–594, May 1999. doi: 10.1086/316367.

Raghavan, D., McAlister, H. A., Henry, T. J., Latham, D. W., Marcy, G. W., Mason, B. D., Gies, D. R., White, R. J., and ten Brummelaar, T. A. A Survey of Stellar Families: Multiplicity of Solar-type Stars. *ApJS*, 190:1–42, September 2010. doi: 10.1088/0067-0049/190/1/1.

Reid, I. N., Cruz, K. L., Allen, P., Mungall, F., Kilkenny, D., Liebert, J., Hawley, S. L., Fraser, O. J., Covey, K. R., Lowrance, P., Kirkpatrick, J. D., and Burgasser, A. J. Meeting the Cool Neighbors. VIII. A Preliminary 20 Parsec Census from the NLTT Catalogue. *AJ*, 128:463–483, July 2004. doi: 10.1086/421374.

Reid, I. N., Cruz, K. L., Burgasser, A. J., and Liu, M. C. L-Dwarf Binaries in the 20-Parsec Sample. *AJ*, 135:580–587, February 2008. doi: 10.1088/0004-6256/135/2/580.

Reipurth, B. and Zinnecker, H. Visual binaries among pre-main sequence stars. *A&A*, 278: 81–108, October 1993.

Reipurth, B., Clarke, C. J., Boss, A. P., Goodwin, S. P., Rodríguez, L. F., Stassun, K. G., Tokovinin, A., and Zinnecker, H. Multiplicity in Early Stellar Evolution. *Protostars and Planets VI*, pages 267–290, 2014. doi: 10.2458/azu_uapress_9780816531240-ch012.

Rieke, G. H. and Lebofsky, M. J. The interstellar extinction law from 1 to 13 microns. *ApJ*, 288:618–621, January 1985. doi: 10.1086/162827.

Rizzuto, A. C., Ireland, M. J., and Robertson, J. G. Multidimensional Bayesian membership analysis of the Sco OB2 moving group. *MNRAS*, 416:3108–3117, October 2011. doi: 10.1111/j.1365-2966.2011.19256.x.

Rizzuto, A. C., Ireland, M. J., Robertson, J. G., Kok, Y., Tuthill, P. G., Warrington, B. A., Haubois, X., Tango, W. J., Norris, B., ten Brummelaar, T., Kraus, A. L., Jacob, A., and Laliberte-Houdeville, C. Long-baseline interferometric multiplicity survey of the Sco-Cen OB association. *MNRAS*, 436:1694–1707, December 2013. doi: 10.1093/mnras/stt1690.

Roberts, L. C., Jr., Turner, N. H., and ten Brummelaar, T. A. Adaptive Optics Photometry and Astrometry of Binary Stars. II. A Multiplicity Survey of B Stars. *AJ*, 133:545–552, February 2007. doi: 10.1086/510335.

Rossum, G. Python reference manual. Technical report, Amsterdam, The Netherlands, The Netherlands, 1995.

Rousset, G., Lacombe, F., Puget, P., Hubin, N. N., Gendron, E., Fusco, T., Arsenault, R., Charton, J., Feautrier, P., Gigan, P., Kern, P. Y., Lagrange, A.-M., Madec, P.-Y., Mouillet, D., Rabaud, D., Rabou, P., Stadler, E., and Zins, G. NAOS, the first AO system of the VLT: on-sky performance. In Wizinowich, P. L. and Bonaccini, D., editors, *Adaptive Optical System Technologies II*, volume 4839 of *Society of Photo-Optical Instrumentation Engineers (SPIE) Conference Series*, pages 140–149, February 2003. doi: 10.1117/12.459332.

Ruban, E. V., Alekseeva, G. A., Arkharov, A. A., Hagen-Thorn, E. I., Galkin, V. D., Nikanorova, I. N., Novikov, V. V., Pakhomov, V. P., and Puzakova, T. Y. Spectrophotometric observations of variable stars. *Astronomy Letters*, 32:604–607, September 2006. doi: 10.1134/S1063773706090052.

Samus, N. N., Durlevich, O. V., and et al. VizieR Online Data Catalog: General Catalogue of Variable Stars (Samus+ 2007-2013). *VizieR Online Data Catalog*, 1, January 2009.

Sana, H. and Evans, C. J. The multiplicity of massive stars. In Neiner, C., Wade, G., Meynet, G., and Peters, G., editors, *Active OB Stars: Structure, Evolution, Mass Loss,*

*and Critical Limits*, volume 272 of *IAU Symposium*, pages 474–485, July 2011. doi: 10.1017/S1743921311011124.

Sana, H., de Mink, S. E., de Koter, A., Langer, N., Evans, C. J., Gieles, M., Gosset, E., Izzard, R. G., Le Bouquin, J.-B., and Schneider, F. R. N. Binary Interaction Dominates the Evolution of Massive Stars. *Science*, 337:444, July 2012. doi: 10.1126/science.1223344.

Sana, H., de Mink, S. E., de Koter, A., Langer, N., Evans, C. J., Gieles, M., Gosset, E., Izzard, R. G., Le Bouquin, J.-B., and Schneider, F. R. N. Multiplicity of massive O stars and evolutionary implications. In Pugliese, G., de Koter, A., and Wijburg, M., editors, *370 Years of Astronomy in Utrecht*, volume 470 of *Astronomical Society of the Pacific Conference Series*, page 141, January 2013.

Savage, B. D. and Mathis, J. S. Observed properties of interstellar dust. *ARA&A*, 17: 73–111, 1979. doi: 10.1146/annurev.aa.17.090179.000445.

Scarfe, C. D., Barlow, D. J., and Fekel, F. C. 64 Orionis: Three-Dimensional Orbit and Physical Parameters. *AJ*, 119:2415–2421, May 2000. doi: 10.1086/301366.

Schaller, G., Schaerer, D., Meynet, G., and Maeder, A. New grids of stellar models from 0.8 to 120 solar masses at Z = 0.020 and Z = 0.001. *A&AS*, 96:269–331, December 1992.

Schmidt, J. G., Hohle, M. M., and Neuhäuser, R. Determination of a temporally and spatially resolved supernova rate from OB stars within 5 kpc. *Astronomische Nachrichten*, 335:935–948, November 2014. doi: 10.1002/asna.201312070.

Schmidt, T., Neuhäuser, R., and Mugrauer, M. Finding orbital motion of sub-stellar companions - the case of TWA 5B. In Jin, W. J., Platais, I., and Perryman, M. A. C., editors, *IAU Symposium*, volume 248 of *IAU Symposium*, pages 126–127, July 2008. doi: 10.1017/S1743921308018851.

Schöller, M., Correia, S., Hubrig, S., and Ageorges, N. Multiplicity of late-type B stars with HgMn peculiarity. *A&A*, 522:A85, November 2010. doi: 10.1051/0004-6361/201014246.

Shatsky, N. The long-period companions of multiple stars tend to have moderate eccentricities. *A&A*, 380:238–244, December 2001. doi: 10.1051/0004-6361:20011401.

Shatsky, N. and Tokovinin, A. The mass ratio distribution of B-type visual binaries in the Sco OB2 association. *A&A*, 382:92–103, January 2002. doi: 10.1051/0004-6361:20011542.

Shaya, E. J. and Olling, R. P. Very Wide Binaries and Other Comoving Stellar Companions: A Bayesian Analysis of the Hipparcos Catalogue. *ApJS*, 192:2, January 2011. doi: 10.1088/0067-0049/192/1/2.

Shu, F. *Physics of Astrophysics: Volume I Radiation*. University Science Books, 1991.

Shu, F. H. Self-similar collapse of isothermal spheres and star formation. *ApJ*, 214:488–497, June 1977. doi: 10.1086/155274.

Shu, F. H., Adams, F. C., and Lizano, S. Star formation in molecular clouds - Observation and theory. *ARA&A*, 25:23–81, 1987. doi: 10.1146/annurev.aa.25.090187.000323.

Siess, L., Dufour, E., and Forestini, M. An internet server for pre-main sequence tracks of low- and intermediate-mass stars. *A&A*, 358:593–599, June 2000.

Sinachopoulos, D., Gavras, P., Dionatos, O., Ducourant, C., and Medupe, T. CCD astrometry and components instrumental magnitude difference of 432 Hipparcos wide visual double stars. *A&A*, 472:1055–1057, September 2007. doi: 10.1051/0004-6361:20066290.

Skiff, B. A. VizieR Online Data Catalog: Catalogue of Stellar Spectral Classifications (Skiff, 2009-2016). *VizieR Online Data Catalog*, 1, October 2014.

Slettebak, A. Spectral types and rotational velocities of the brighter Be stars and A-F type shell stars. *ApJS*, 50:55–83, September 1982. doi: 10.1086/190820.

Smith, H., Jr. and Eichhorn, H. On the estimation of distances from trigonometric parallaxes. *MNRAS*, 281:211–218, July 1996.

Smith, L. F. and Aller, L. H. On the Classification of Emission-Line Spectra of Planetary Nuclei. *ApJ*, 157:1245, September 1969. doi: 10.1086/150151.

Stahler, S. W. and Palla, F. *The Formation of Stars*. 2005.

Stamatellos, D., Maury, A., Whitworth, A., and André, P. The lower limits of disc fragmentation and the prospects for observing fragmenting discs. *MNRAS*, 413:1787–1796, May 2011. doi: 10.1111/j.1365-2966.2011.18254.x.

Sterzik, M. F. and Durisen, R. H. Imprints of dynamical interactions on brown dwarf pairing statistics and kinematics. *A&A*, 400:1031–1042, March 2003. doi: 10.1051/0004-6361:20030073.

Stetson, P. B. DAOPHOT - A computer program for crowded-field stellar photometry. *PASP*, 99:191–222, March 1987. doi: 10.1086/131977.

Stickland, D. J. and Lloyd, C. Spectroscopic binary orbits from ultraviolet radial velocities. Paper 31: Stars with few IUE observations. *The Observatory*, 121:1–54, February 2001.

Stickland, D. J. and Weatherby, J. Radial velocities of northern Mercury stars. *A&AS*, 57: 55–67, July 1984.

Stickland, D. J., Lloyd, C., Pike, C. D., and Aikman, G. C. L. The orbit of HR 3361. *The Observatory*, 104:74–76, April 1984.

Tan, J. C., Beltrán, M. T., Caselli, P., Fontani, F., Fuente, A., Krumholz, M. R., McKee, C. F., and Stolte, A. Massive Star Formation. *Protostars and Planets VI*, pages 149–172, 2014. doi: 10.2458/azu_uapress_9780816531240-ch007.

Tassoul, J.-L. *Theory of rotating stars*. 1978.

Thackeray, A. D. The double-lines spectroscopic binary epsilon Lupi (HD 136504). *MNRAS*, 149:75–80, 1970. doi: 10.1093/mnras/149.1.75.

Toomre, A. On the gravitational stability of a disk of stars. *ApJ*, 139:1217–1238, May 1964. doi: 10.1086/147861.

Torres, G. On the Use of Empirical Bolometric Corrections for Stars. *AJ*, 140:1158–1162, November 2010. doi: 10.1088/0004-6256/140/5/1158.

Turner, N. H., ten Brummelaar, T. A., Roberts, L. C., Mason, B. D., Hartkopf, W. I., and Gies, D. R. Adaptive Optics Photometry and Astrometry of Binary Stars. III. a Faint Companion Search of O-Star Systems. *AJ*, 136:554–565, August 2008. doi: 10.1088/0004-6256/136/2/554.

van Leeuwen, F. Validation of the new Hipparcos reduction. *A&A*, 474:653–664, November 2007. doi: 10.1051/0004-6361:20078357.

Vogt, N., Schmidt, T. O. B., Neuhäuser, R., Bedalov, A., Roell, T., Seifahrt, A., and Mugrauer, M. Astrometric confirmation of young low-mass binaries and multiple systems in the Chamaeleon star-forming regions. *A&A*, 546:A63, October 2012. doi: 10.1051/0004-6361/201118410.

Warmels, R. H. The ESO–MIDAS System. In Worrall, D. M., Biemesderfer, C., and Barnes, J., editors, *Astronomical Data Analysis Software and Systems I*, volume 25 of *Astronomical Society of the Pacific Conference Series*, page 115, 1992.

Watson, C. L. The International Variable Star Index (VSX). *Society for Astronomical Sciences Annual Symposium*, 25:47, May 2006.

Werner, K. and Herwig, F. The Elemental Abundances in Bare Planetary Nebula Central Stars and the Shell Burning in AGB Stars. *PASP*, 118:183–204, February 2006. doi: 10.1086/500443.

Whitworth, A. P. and Stamatellos, D. The minimum mass for star formation, and the origin of binary brown dwarfs. *A&A*, 458:817–829, November 2006. doi: 10.1051/0004-6361:20065806.

Woodley, K. A., Goldsbury, R., Kalirai, J. S., Richer, H. B., Tremblay, P.-E., Anderson, J., Bergeron, P., Dotter, A., Esteves, L., Fahlman, G. G., Hansen, B. M. S., Heyl, J., Hurley, J., Rich, R. M., Shara, M. M., and Stetson, P. B. The Spectral Energy Distributions of

White Dwarfs in 47 Tucanae: The Distance to the Cluster. *AJ*, 143:50, February 2012. doi: 10.1088/0004-6256/143/2/50.

Wu, Y., Murray, N. W., and Ramsahai, J. M. Hot Jupiters in Binary Star Systems. *ApJ*, 670:820–825, November 2007. doi: 10.1086/521996.

Wycoff, G. L., Mason, B. D., and Urban, S. E. Data Mining for Double Stars in Astrometric Catalogs. *AJ*, 132:50–60, July 2006. doi: 10.1086/504471.

Wyse, A. B. The Spectroscopic Orbit of the Eclipsing Binary AR Aurigae. *PASP*, 48:24, February 1936. doi: 10.1086/124650.

Zinnecker, H. and Yorke, H. W. Toward Understanding Massive Star Formation. *ARA&A*, 45:481–563, September 2007. doi: 10.1146/annurev.astro.44.051905.092549.

Zuckerman, B. and Evans, N. J., II. Models of massive molecular clouds. *ApJ*, 192: L149–L152, September 1974. doi: 10.1086/181613.

# A Appendix

## A.1 Tables

Following is a list of the tables containing the data observed, computed and utilised in this thesis:

**Table A1:** – General object information for each sample star. Presented are the name, spectral type, distance, apparent near-infrared magnitudes, the estimated age and mass of the investigated B-type primary star as well as expected number of 2MASS sources per square arc minute.

**Table A2:** – Observation log of the investigated ESO/VLT NaCo archive data. Listed are the *Hipparcos* ID, observation epoch, program id and principle investigator (PI) as well as the exposure time, filter, camera objective, and the measured FWHM of the PSF, in milliarcsecond. Also presented are the estimated pixel scale and detector orientation and the employed calibration method.

**Table A3:** – Astrometric results. Observed and theoretical change in separation and position angle for each resolved candidate companion with more than one available VLT/-NaCo observation and/or literature values. Also shown are the deviations from the background hypothesis and the results of the $\chi^2$ probability test to derive the companion status.

**Table A4**: – Photometric results. The table shows the measured magnitude difference, the used filter as well as the calculated apparent and absolute magnitudes of each primaries and any candidate source detected.

**Table A5**: – Companion mass estimation results. Presented are the assumed system age, the calculated absolute magnitude as well as the derived masses, employing different evolutionary models, the final estimated mass and the mass-ratio of the companion assuming it is physical.

**Table A6**: – Summary of the most relevant data for each detected co-moving, refute or candidate companion, evaluated in this thesis. The estimated probability of being a chance projection as well as the assigned companion status are presented in the last two columns.

**Table A7**: – List of previous registered companions to the investigated B-type sample, found in the literature and not resolved in the study. Depending on availability either orbital periods or separations are given, along with the corresponding reference.

**Table A1.** B-type star target sample information

| HIP | Spectral[a] type | Plx (mas) | $\mu_\alpha \cos\delta$ (mas/yr) | $\mu_\delta$ (mas/yr) | $B$ (mag) | $V$ (mag) | $J$ (mag) | $H$ (mag) | $K$ (mag) | Age (Myr) | ≈Mass ($M_\odot$) | 2MASS sources[c] (arcmin$^{-2}$) |
|---|---|---|---|---|---|---|---|---|---|---|---|---|
| 145 | B6V | 7.18±0.3 | 19.1±0.29 | -9.67±0.16 | 5.005±0.002 | 5.12±0.002 | 5.399±0.019 | 5.453±0.043 | 5.438±0.019 | 80±9 | 4.0 | 0.115 |
| 377 | B8IV/V | 5.7±0.24 | 29.78±0.23 | -12.85±0.19 | 5.486±0.002 | 5.584±0.003 | 5.775±0.018 | 5.835±0.032 | 5.822±0.026 | 152±9 | 3.4 | 0.196 |
| 1191 | B9V | 9.63±0.39 | 23.65±0.43 | -7.8±0.2 | 5.695±0.004 | 5.756±0.003 | 5.929±0.026 | 5.972±0.037 | 5.94±0.017 | 182±75 | 2.5 | 0.104 |
| 1830 | B9 IV | 5.79±0.47 | 22.04±0.48 | 3±0.42 | 6.491±0.004 | 6.553±0.004 | 6.635±0.019 | 6.645±0.02 | 6.656±0.017 | 146±25 | 2.7 | 0.103 |
| 2548 | B9.5V | 12.35±0.55 | 31.9±0.8 | 4.1±0.8 | 5.686±0.003 | 5.693±0.002 | 5.677±0.037 | 5.681±0.039 | 5.637±0.019 | 1139±93 | 2.0 | 0.117 |
| 3678 | B0 (PG1159)[b] | 2.12±3.01 | -18.1±1.9 | -9.8±1.9 | 11.47±0.01 | 11.769±0.01 | 12.612±0.057 | 12.795±0.029 | 12.869±0.029 | 200±10 | 0.8 | 0.102 |
| 3741 | B9Va | 9.51±0.77 | 24.5±0.8 | -11.2±0.8 | 5.514±0.002 | 5.559±0.004 | 5.647±0.026 | 5.686±0.026 | 5.644±0.02 | 210±58 | 2.5 | 0.097 |
| 5778 | B8IV HgMn metallic lines | 7.17±0.44 | -29.8±0.8 | -24.3±0.8 | 5.876±0.003 | 5.958±0.004 | 6.065±0.024 | 6.21±0.028 | 6.212±0.016 | 84±26 | 3.2 | 0.149 |
| 10602 | B6V | 21.22±0.12 | 92.5±0.9 | -24±0.9 | 3.453±0.002 | 3.546±0.002 | 4.026±0.298 | 3.95±0.261 | 4.126±0.268 | 58±12 | 4.0 | 0.119 |
| 13951 | B8 V | 9±0.43 | -5.62±0.5 | -22.11±0.51 | 5.493±0.008 | 5.543±0.004 | 5.688±0.032 | 5.686±0.024 | 5.664±0.02 | 87±26 | 3.2 | 0.120 |
| 14131 | B9V | 6.34±0.2 | 26.2±0.7 | 14.6±0.7 | 5.38±0.002 | 5.5±0.003 | 5.761±0.026 | 5.863±0.027 | 5.837±0.026 | 282±8 | 3.1 | 0.197 |
| 15627 | B5III | 6.41±0.73 | 25.7±1.1 | -25.2±1.1 | 5.225±0.008 | 5.306±0.004 | 5.388±0.028 | 5.439±0.017 | 5.436±0.02 | 44±8 | 4.4 | 0.210 |
| 16511 | B9IV | 9.31±0.38 | 31.38±0.39 | -48.67±0.31 | 5.69±0.003 | 5.75±0.003 | 5.809±0.02 | 5.894±0.028 | 5.881±0.017 | 126±37 | 2.7 | 0.172 |
| 16803 | B9Vp lambda Boo | 6.7±0.51 | 28.5±0.7 | -10.3±0.7 | 5.123±0.004 | 5.236±0.004 | 5.459±0.018 | 5.563±0.048 | 5.526±0.024 | 297±22 | 3.1 | 0.128 |
| 17563 | B3V | 6.11±0.29 | 21.3±0.9 | -13.8±1 | 5.236±0.003 | 5.335±0.003 | 5.541±0.048 | 5.625±0.05 | 5.592±0.02 | 13±10 | 5.9 | 0.169 |
| 17921 | B9IVpHgMnSi sn | 8.86±0.42 | 23.73±0.4 | -44.68±0.34 | 6.06±0.004 | 6.067±0.004 | 5.967±0.018 | 6.051±0.061 | 5.975±0.02 | 113±39 | 2.6 | 0.289 |
| 18213 | B6/7 V | 9.42±0.22 | 32.12±0.17 | -0.92±0.22 | 4.969±0.002 | 5.092±0.002 | 5.39±0.024 | 5.446±0.037 | 5.454±0.017 | 36±12 | 3.7 | 0.130 |
| 18788 | B5V | 7.88±0.27 | 27.84±0.32 | -14.32±0.31 | 5.138±0.003 | 5.269±0.003 | 5.57±0.024 | 5.647±0.028 | 5.662±0.02 | 29±10 | 4.0 | 0.164 |
| 19720 | B8Vn | 7.56±0.81 | 22.49±0.92 | -23.94±0.76 | 6.272±0.004 | 6.243±0.007 | 6.046±0.02 | 6.041±0.041 | 6.028±0.019 | 83±24 | 3.2 | 0.219 |
| 19860 | B3IV | 7.16±0.34 | 19.73±0.31 | -22.04±0.27 | 4.217±0.004 | 4.28±0.003 | 4.684±0.252 | 4.413±0.035 | 4.433±0.034 | 54±10 | 6.0 | 0.218 |
| 20020 | B9 IV | 7.08±0.33 | 5.4±1.5 | 7.7±1.5 | 5.938±0.004 | 6.012±0.007 | 6.126±0.026 | 6.153±0.048 | 6.178±0.024 | 184±14 | 2.8 | 0.200 |
| 20042 | B6V | 18.33±0.15 | 62.52±0.11 | -7.24±0.16 | 3.453±0.002 | 3.546±0.002 | 3.864±0.314 | 3.857±0.268 | 3.954±0.244 | 25±13 | 4.0 | 0.150 |
| 20171 | B9Vsp | 12.08±0.36 | 29.65±0.33 | -42.09±0.28 | 5.425±0.003 | 5.489±0.003 | 5.572±0.026 | 5.609±0.017 | 5.611±0.016 | 116±45 | 2.5 | 0.319 |
| 20554 | B6V | 4.55±0.51 | 2.3±1.1 | 11.7±1.1 | 7.263±0.004 | 7.361±0.008 | 7.557±0.027 | 7.622±0.046 | 7.625±0.024 | 59±15 | 4.0 | 0.152 |
| 20804 | B8IV | 5.55±0.73 | -1.8±1.4 | -10.6±1.3 | 5.916±0.004 | 5.864±0.004 | 5.625±0.023 | 5.677±0.043 | 5.644±0.023 | 152±18 | 3.8 | 0.257 |
| 21177 | B8 V | 5.04±0.55 | 11.52±0.5 | -13.99±0.53 | 7.197±0.008 | 7.242±0.009 | 7.315±0.023 | 7.413±0.046 | 7.372±0.017 | 54±15 | 3.2 | 0.219 |
| 21192 | B9IIIpHg | 6.86±0.35 | 18±1.1 | -15.7±1.1 | 5.64±0.008 | 5.752±0.007 | 5.993±0.024 | 6.087±0.039 | 6.072±0.019 | 190±15 | 3.0 | 0.202 |
| 21640 | B9 V | 7.94±0.61 | 22.84±0.46 | -17.88±0.48 | 7.252±0.004 | 7.263±0.009 | 7.261±0.023 | 7.298±0.037 | 7.296±0.037 | 101±39 | 2.5 | 0.208 |
| 21735 | B6Vp | 7.83±0.32 | -0.9±0.8 | -14.9±0.8 | 5.331±0.004 | 5.447±0.004 | 5.576±0.018 | 5.653±0.016 | 5.657±0.02 | 35±11 | 4.0 | 0.296 |
| 21949 | B9V | 6.64±0.23 | 9.28±0.23 | 34.91±0.25 | 5.407±0.003 | 5.517±0.003 | 5.725±0.02 | 5.79±0.027 | 5.823±0.017 | 274±9 | 3.1 | 0.701 |
| 22913 | B7V | 8.97±0.33 | -3.47±0.3 | -11.38±0.23 | 5.703±0.004 | 5.783±0.004 | 5.861±0.017 | 5.941±0.019 | 5.969±0.026 | 17±15 | 3.2 | 0.398 |
| 23419 | B7V | 6.42±1.71 | -2.5±1.3 | 7.2±1.1 | 6.421±0.004 | 6.505±0.008 | 6.678±0.026 | 6.781±0.048 | 6.731±0.027 | 16±16 | 3.2 | 0.306 |

*Continued on next page*

Table A1 – *Continued from previous page*

| HIP | Spectral[a] type | Plx (mas) | $\mu_\alpha \cos\delta$ (mas/yr) | $\mu_\delta$ (mas/yr) | *B* (mag) | *V* (mag) | *J* (mag) | *H* (mag) | *K* (mag) | Age (Myr) | ≈Mass ($M_\odot$) | 2MASS sources[c] (arcmin$^{-2}$) |
|---|---|---|---|---|---|---|---|---|---|---|---|---|
| 23745 | B9.5 V | 5.32±0.76 | 13.43±0.69 | -13.39±0.57 | 7.657±0.008 | 7.637±0.008 | 7.584±0.017 | 7.656±0.037 | 7.625±0.016 | 567±268 | 2.0 | 0.289 |
| 23794 | B9.5 V | 10.56±0.34 | 10.7±0.38 | -0.78±0.35 | 5.053±0.004 | 5.096±0.003 | 5.228±0.037 | 5.221±0.019 | 5.203±0.023 | 533±27 | 2.5 | 0.275 |
| 24196 | B7V | 2.54±0.73 | 4.8±1.1 | -0.4±1.1 | 6.606±0.004 | 6.664±0.008 | 6.787±0.017 | 6.839±0.026 | 6.859±0.019 | 136±3 | 4.0 | 0.330 |
| 24244 | B6V | 14.07±0.16 | 28±0.9 | -26.8±0.9 | 4.367±0.004 | 4.456±0.002 | 4.985±0.291 | 4.752±0.026 | 4.651±0.016 | 27±25 | 4.0 | 0.246 |
| 24305 | B7IV | 17.54±0.55 | 47.09±0.47 | -16.39±0.39 | 3.19±0.002 | 3.279±0.002 | 3.463±0.246 | 3.469±0.233 | 3.523±0.236 | 99±1 | 4.0 | 0.243 |
| 24505 | B9IV | 11.73±0.27 | 10.11±0.17 | -29.56±0.3 | 4.991±0.002 | 5.053±0.002 | 5.21±0.037 | 5.296±0.028 | 5.217±0.023 | 168±24 | 2.7 | 0.221 |
| 24552 | B9.5 V | 5.24±1.67 | 0.31±0.85 | -3.3±0.83 | 10.152±0.03 | 9.828±0.035 | 9.255±0.026 | 8.475±0.032 | 7.677±0.023 | 143±29 | 2.0 | 0.266 |
| 24740 | B8 V | 8.19±0.47 | 15.2±1.2 | -25.1±1.2 | 6.104±0.004 | 6.142±0.008 | 6.19±0.018 | 6.254±0.017 | 6.264±0.023 | 53±15 | 3.2 | 1.148 |
| 24825 | B5 IV/V | 3.8±0.47 | 1.94±0.43 | 9.34±0.4 | 6.217±0.004 | 6.342±0.008 | 6.662±0.024 | 6.728±0.043 | 6.79±0.037 | 30±12 | 4.5 | 0.242 |
| 24925 | B8 III | 3.55±1.28 | 0.4±1.1 | -4.6±1.2 | 6.368±0.004 | 6.413±0.007 | 6.389±0.024 | 6.467±0.037 | 6.433±0.019 | 133±14 | 3.8 | 0.318 |
| 25365 | B3 V | 4.65±0.58 | -4.2±1.1 | -5.7±1.1 | 6.525±0.004 | 6.559±0.004 | 6.576±0.018 | 6.644±0.037 | 6.6±0.02 | 19±7 | 5.1 | 0.420 |
| 25657 | B9 | 5.8±0.69 | 9.1±1.6 | -9.3±1.5 | 7.678±0.008 | 7.616±0.008 | 7.446±0.023 | 7.454±0.02 | 7.454±0.027 | 85±22 | 2.5 | 0.711 |
| 26215 | B9(III) | 2.91±0.67 | -1.9±2.7 | -16.4±2.4 | 5.739±0.004 | 5.619±0.004 | 5.168±0.019 | 5.133±0.059 | 4.959±0.02 | 159±32 | 3.6 | 0.674 |
| 26235 | O9.5Vp | 2.11±0.41 | 3.7±0.8 | 4±0.8 | 4.981±0.008 | 5.018±0.009 | 4.912±0.037 | 4.922±0.063 | 4.836±0.02 | 11±1 | 13.2 | 0.624 |
| 26237 | B1V | 3.69±1.2 | -6.7±2.8 | 0.4±2.8 | 4.41±0.002 | 4.598±0.004 | 5.361±0.257 | 5.053±0.052 | 5.056±0.017 | 10±1 | 10.9 | 0.614 |
| 26545 | B7V | 7.42±0.48 | -10.3±0.9 | 16.5±0.9 | 5.73±0.003 | 5.804±0.003 | 5.922±0.019 | 5.991±0.041 | 5.939±0.017 | 19±17 | 3.2 | 0.239 |
| 26549 | O9.5V | 2.84±0.91 | 4.61±0.88 | -0.4±0.53 | 3.578±0.003 | 3.793±0.003 | 4.751±0.259 | 4.64±0.252 | 4.489±0.016 | 10±1 | 13.3 | 0.495 |
| 26602 | B8V | 2.11±0.73 | -6.23±0.47 | 1.46±0.51 | 6.304±0.003 | 6.402±0.004 | 6.512±0.024 | 6.578±0.02 | 6.578±0.02 | 143±3 | 3.8 | 0.302 |
| 26634 | B9Ve | 12.48±0.36 | 1.58±0.28 | -24.82±0.5 | 2.565±0.002 | 2.65±0.004 | 2.703±0.275 | 2.815±0.225 | 2.829±0.261 | 176±2 | 4.0 | 0.258 |
| 26836 | B7III | 4.12±0.49 | 9.97±0.43 | -17.84±0.31 | 6.502±0.004 | 6.573±0.004 | 6.631±0.017 | 6.695±0.014 | 6.709±0.017 | 143±22 | 3.3 | 0.997 |
| 26868 | B9/9.5 V | 7.61±0.2 | 4.99±0.13 | 50.77±0.2 | 5.256±0.002 | 5.283±0.002 | 5.333±0.023 | 5.309±0.032 | 5.285±0.017 | 322±20 | 3.1 | 0.259 |
| 27265 | B8IIIpHg(Mn) | 4.44±0.8 | 5.08±0.65 | -2.65±0.49 | 5.923±0.003 | 5.992±0.004 | 6.061±0.026 | 6.093±0.016 | 6.127±0.017 | 136±26 | 3.8 | 0.936 |
| 27534 | B6V | 5.68±0.15 | -21.81±0.11 | 17.39±0.16 | 4.969±0.002 | 5.094±0.003 | 5.368±0.024 | 5.488±0.041 | 5.421±0.019 | 103±18 | 4.3 | 0.827 |
| 27566 | B9V | 11.44±0.2 | -4.23±0.23 | 65.78±0.22 | 5.387±0.003 | 5.452±0.003 | 5.594±0.018 | 5.635±0.024 | 5.642±0.02 | 180±79 | 2.5 | 0.325 |
| 27810 | B5 V | 9.75±0.21 | -4.73±0.15 | 31.31±0.19 | 4.736±0.003 | 4.866±0.003 | 5.23±0.035 | 5.354±0.068 | 5.251±0.024 | 29±10 | 4.0 | 0.291 |
| 28691 | B7 V | 4.54±0.29 | 9.5±0.7 | -20.8±0.7 | 5.04±0.003 | 5.136±0.003 | 5.311±0.037 | 5.429±0.061 | 5.359±0.019 | 150±8 | 4.2 | 1.173 |
| 28744 | B2IVe | 2.48±0.75 | -2.8±0.9 | 3.1±0.9 | 5.173±0.004 | 5.249±0.004 | 5.087±0.019 | 5.067±0.052 | 4.781±0.019 | 20±2 | 9.5 | 0.577 |
| 28992 | B5Ve | 3.2±0.27 | 2.39±0.19 | -0.11±0.29 | 5.717±0.003 | 5.846±0.003 | 5.866±0.019 | 5.837±0.03 | 5.698±0.019 | 89±3 | 5.0 | 0.324 |
| 29134 | B9.5III | 10.88±0.13 | -50.84±0.15 | 18.99±0.16 | 4.989±0.002 | 5.044±0.002 | 5.153±0.019 | 5.196±0.023 | 5.193±0.017 | 591±25 | 2.5 | 0.643 |
| 29401 | B8 II/III | 5.68±0.69 | -7.03±0.66 | -2.3±0.6 | 6.118±0.004 | 6.199±0.008 | 6.269±0.02 | 6.337±0.023 | 6.326±0.026 | 46±10 | 3.2 | 0.686 |
| 29728 | B6Ve | 4.99±0.43 | -0.36±0.41 | -17.41±0.31 | 5.94±0.004 | 6.053±0.004 | 6.284±0.027 | 6.335±0.035 | 6.381±0.027 | 57±12 | 4.0 | 1.084 |
| 29941 | B2/3 V | 4.1±0.28 | -5.71±0.21 | 7.08±0.21 | 5.34±0.002 | 5.5±0.002 | 5.876±0.029 | 5.988±0.039 | 5.975±0.02 | 19±5 | 6.7 | 0.485 |
| 30143 | B3V | 1.68±0.22 | 0.31±0.17 | 20.19±0.27 | 5.353±0.003 | 5.528±0.003 | 5.956±0.027 | 6.072±0.034 | 6.111±0.023 | 33±3 | 7.9 | 0.375 |

*Continued on next page*

Table A1 – *Continued from previous page*

| HIP | Spectral[a] type | Plx (mas) | $\mu_\alpha \cos\delta$ (mas/yr) | $\mu_\delta$ (mas/yr) | *B* (mag) | *V* (mag) | *J* (mag) | *H* (mag) | *K* (mag) | Age (Myr) | ≈Mass ($M_\odot$) | 2MASS sources[c] (arcmin$^{-2}$) |
|---|---|---|---|---|---|---|---|---|---|---|---|---|
| 30180 | B6V | 3.05±0.66 | 2.37±0.64 | -16.15±0.46 | 7.225±0.008 | 7.33±0.012 | 7.551±0.037 | 7.577±0.035 | 7.618±0.017 | 47±12 | 4.0 | 1.291 |
| 30468 | B6/7V | 3.46±0.42 | -2.78±0.36 | 4.12±0.33 | 6.039±0.004 | 6.119±0.004 | 6.206±0.024 | 6.302±0.057 | 6.269±0.017 | 124±11 | 4.1 | 0.679 |
| 30493 | B9III | 4.13±0.82 | 5.7±1.3 | -15.9±1.3 | 6.632±0.008 | 6.731±0.008 | 6.854±0.018 | 6.918±0.054 | 6.926±0.02 | 200±55 | 2.9 | 0.980 |
| 30772 | B3 V | 3±0.24 | -4.2±0.4 | -2.5±0.4 | 4.872±0.002 | 5.041±0.004 | 5.459±0.017 | 5.587±0.037 | 5.565±0.019 | 39±2 | 7.0 | 0.988 |
| 30867 | B4Ve shell | 4.72±1.1 | -2.8±3.4 | -21.7±3.5 | 4.511±0.004 | 4.624±0.004 | 3.72 | 3.517 | 4.079 | 42±3 | 6.6 | 0.860 |
| 31137 | B9IVn | 4.31±0.38 | -0.8±1.1 | 3.2±1.1 | 5.645±0.004 | 5.695±0.004 | 5.721±0.018 | 5.765±0.032 | 5.719±0.023 | 235±20 | 3.4 | 0.336 |
| 31190 | B2 V | 1.86±0.27 | -2.83±0.21 | 4.29±0.25 | 5.532±0.002 | 5.708±0.003 | 5.929±0.019 | 5.98±0.041 | 5.914±0.026 | 20±2 | 9.4 | 0.456 |
| 31278 | B5 V | 5.89±0.24 | 2.09±0.22 | -17.77±0.19 | 4.956±0.003 | 5.085±0.004 | 5.383±0.023 | 5.439±0.02 | 5.46±0.028 | 45±6 | 5.0 | 1.143 |
| 31959 | B3 V | 1.63±0.67 | -2.73±0.46 | 5.28±0.59 | 7.977±0.008 | 8.086±0.008 | 8.31±0.023 | 8.388±0.046 | 8.395±0.023 | 21±7 | 5.8 | 0.556 |
| 32417 | B9IV: | 2.91±1.11 | -4.45±0.84 | -1.11±0.82 | 8.864±0.013 | 8.824±0.018 | 8.92±0.023 | 8.975±0.023 | 8.979±0.023 | 88±23 | 2.5 | 0.860 |
| 32753 | B7 III | 3.8±0.42 | -15.7±0.7 | -10.9±0.7 | 5.73±0.01 | 5.844±0.008 | 6.034±0.019 | 6.135±0.016 | 6.15±0.017 | 155±22 | 4.0 | 0.842 |
| 32823 | B5 V | 1.3±1.26 | -2.24±0.66 | 4.08±0.84 | 9.229±0.012 | 9.329±0.016 | 9.593±0.026 | 9.637±0.021 | 9.685±0.023 | 19±15 | 15.7 | 0.774 |
| 32827 | B2 III/IV | 2.07±0.37 | -4.19±0.24 | 5.5±0.34 | 6.132±0.002 | 6.314±0.004 | 6.743±0.028 | 6.816±0.034 | 6.823±0.017 | 20±2 | 7.7 | 0.751 |
| 32912 | B7III | 5.79±0.19 | 3.65±0.2 | 26.07±0.19 | 5.295±0.002 | 5.394±0.003 | 5.561±0.018 | 5.598±0.02 | 5.59±0.017 | 124±11 | 4.0 | 0.372 |
| 33211 | B3 V | 3.08±0.95 | -3.23±0.57 | 1.98±0.79 | 8.965±0.008 | 9.137±0.014 | 9.435±0.026 | 9.515±0.024 | 9.55±0.02 | 13±6 | 16.4 | 0.871 |
| 33276 | B5/7 V | 1.17±1.09 | -1.73±0.67 | 5.72±0.83 | 9.376±0.014 | 9.475±0.019 | 9.75±0.023 | 9.852±0.024 | 9.821±0.021 | 56±13 | 3.5 | 0.943 |
| 33343 | B5 V | 3.15±1.21 | -3.1±1.4 | 4.7±1.4 | 9.071±0.008 | 9.173±0.01 | 9.458±0.027 | 9.555±0.028 | 9.541±0.028 | 14±13 | 19.5 | 1.022 |
| 33611 | B2 V | 2.33±0.6 | -4.7±1.4 | 2.6±1.3 | 7±0.004 | 7.172±0.004 | 7.532±0.026 | 7.54±0.057 | 7.643±0.03 | 6±3 | 7.0 | 0.911 |
| 33650 | B8II/III | 2.73±0.48 | -5.4±0.8 | -8.3±0.7 | 6.288±0.003 | 6.393±0.004 | 6.544±0.028 | 6.625±0.017 | 6.635±0.027 | 157±10 | 3.9 | 0.510 |
| 33769 | B2/3 V | 1.07±0.66 | -2.89±0.4 | 4.01±0.57 | 7.699±0.004 | 7.823±0.008 | 7.923±0.02 | 7.926±0.028 | 7.771±0.027 | 28±3 | 7.2 | 0.975 |
| 33814 | B3 V | 2.65±0.77 | -2.41±0.49 | 2.8±0.63 | 7.934±0.01 | 8.081±0.01 | 8.472±0.019 | 8.538±0.067 | 8.578±0.02 | 11±4 | 5.0 | 0.911 |
| 33846 | B2 V | 1.51±0.57 | -2.98±0.39 | 3.77±0.49 | 6.778±0.004 | 6.94±0.004 | 7.284±0.026 | 7.423±0.052 | 7.435±0.027 | 16±2 | 8.3 | 0.943 |
| 34041 | B2/3 V | 1.97±0.41 | -3.45±0.22 | 3.26±0.38 | 6.678±0.004 | 6.852±0.004 | 7.225±0.034 | 7.326±0.035 | 7.314±0.027 | 25±4 | 6.8 | 1.086 |
| 34045 | B6III | 7.38±0.21 | -0.28±0.17 | -11.26±0.19 | 3.993±0.002 | 4.099±0.002 | 4.585±0.254 | 4.548±0.224 | 4.366±0.035 | 86±2 | 5.0 | 1.372 |
| 34153 | B8 V | 2.06±0.9 | -3.6±0.57 | 4.31±0.78 | 8.998±0.01 | 9.045±0.014 | 9.128±0.024 | 9.201±0.026 | 9.203±0.023 | 62±18 | 3.2 | 1.053 |
| 34281 | B5 V | 1.68±0.95 | -3.59±0.47 | 4.26±0.75 | 8.711±0.008 | 8.831±0.009 | 9.036±0.034 | 9.097±0.024 | 9.121±0.023 | 24±11 | 4.0 | 1.140 |
| 34338 | B9.5III | 4.91±0.33 | -15.78±0.35 | -7.13±0.25 | 5.977±0.003 | 6.092±0.004 | 6.308±0.019 | 6.373±0.034 | 6.368±0.017 | 431±66 | 2.8 | 0.957 |
| 34579 | B3 V | 1.77±0.44 | -6.5±1 | 4.5±1 | 5.521±0.002 | 5.682±0.002 | 5.98±0.018 | 6.043±0.039 | 6.086±0.023 | 34±3 | 7.6 | 1.255 |
| 34758 | B9.5III | 6.98±0.38 | -9.41±0.27 | 21.14±0.36 | 5.802±0.002 | 5.831±0.004 | 5.861±0.019 | 5.905±0.043 | 5.844±0.017 | 595±25 | 2.5 | 1.402 |
| 34898 | B5 V | 1.6±0.7 | -34.6±1.7 | 8.5±1.7 | 7.71±0.008 | 7.803±0.008 | 8.064±0.027 | 8.149±0.037 | 8.199±0.028 | 56±5 | 4.7 | 0.999 |
| 34968 | B8 V | 2.26±0.9 | -3.14±0.56 | 3.97±0.79 | 8.92±0.01 | 8.982±0.012 | 9.079±0.02 | 9.128±0.021 | 9.159±0.02 | 61±18 | 3.2 | 1.093 |
| 35037 | B2.5Ve | 3.58±0.17 | -11.88±0.11 | 6.89±0.17 | 3.877±0.003 | 4.032±0.003 | 4.543±0.241 | 4.493±0.075 | 4.374±0.017 | 25±1 | 8.8 | 1.292 |
| 35110 | B8 V | 3.42±0.82 | -3.58±0.47 | 4.22±0.59 | 7.946±0.008 | 8.012±0.008 | 8.116±0.043 | 8.154±0.057 | 8.097±0.02 | 62±18 | 3.2 | 1.520 |

*Continued on next page*

Table A1 – *Continued from previous page*

| HIP | Spectral[a] type | Plx (mas) | $\mu_\alpha \cos\delta$ (mas/yr) | $\mu_\delta$ (mas/yr) | $B$ (mag) | $V$ (mag) | $J$ (mag) | $H$ (mag) | $K$ (mag) | Age (Myr) | ≈Mass ($M_\odot$) | 2MASS sources[c] (arcmin$^{-2}$) |
|---|---|---|---|---|---|---|---|---|---|---|---|---|
| 35168 | B2III/IV | 2.02±0.49 | -2.42±0.33 | 3.77±0.4 | 6.973±0.004 | 7.14±0.008 | 7.499±0.02 | 7.589±0.043 | 7.671±0.02 | 10±5 | 7.0 | 1.105 |
| 35267 | B5 V | 2.31±0.77 | -2.33±0.46 | 3.51±0.55 | 7.69±0.004 | 7.828±0.008 | 8.119±0.024 | 8.237±0.054 | 8.204±0.017 | 27±12 | 4.3 | 1.514 |
| 35413 | B3 V | 3.38±1.2 | -4.61±0.75 | 4.42±0.87 | 8.532±0.008 | 8.633±0.01 | 8.8±0.026 | 8.862±0.043 | 8.842±0.023 | 16±6 | 14.6 | 1.620 |
| 35920 | B8 V | 5.66±0.4 | -5.89±0.39 | 3.19±0.42 | 6.11±0.004 | 6.203±0.004 | 6.337±0.02 | 6.405±0.041 | 6.402±0.024 | 110±41 | 3.2 | 1.616 |
| 35951 | B3 Ve | 3.48±0.58 | -4.6±0.42 | -20.35±0.4 | 5.163±0.008 | 5.199±0.008 | 5.418±0.023 | 5.455±0.039 | 5.416±0.027 | 36±2 | 6.8 | 1.583 |
| 36009 | B5 V | 1.87±1 | -0.5±1.6 | 1.4±1.4 | 7.736±0.008 | 7.875±0.008 | 8.137±0.024 | 8.232±0.063 | 8.263±0.032 | 39±6 | 4.5 | 1.492 |
| 36345 | B2.5 V | 4.38±0.61 | -9.4±1.2 | 6.7±1.2 | 6.215±0.004 | 6.372±0.004 | 6.729±0.018 | 6.802±0.046 | 6.816±0.023 | 14±3 | 13.5 | 1.401 |
| 36363 | B3 V | 6.06±0.22 | -21.97±0.17 | 16.13±0.21 | 5.25±0.002 | 5.396±0.003 | 5.714±0.023 | 5.806±0.035 | 5.822±0.027 | 15±11 | 5.5 | 0.936 |
| 36944 | B5 V | 1.42±0.81 | -5.32±0.4 | 2.41±0.67 | 8.527±0.008 | 8.628±0.01 | 8.847±0.026 | 8.975±0.021 | 8.965±0.018 | 35±8 | 4.4 | 1.826 |
| 37322 | B5 V | 5.7±0.27 | -22.1±0.26 | 16.49±0.25 | 5.627±0.004 | 5.752±0.004 | 5.919±0.019 | 6.005±0.034 | 5.982±0.017 | 28±14 | 4.4 | 1.263 |
| 37345 | B4III | 2.33±0.23 | -0.85±0.18 | -4.4±0.2 | 5.956±0.003 | 6.001±0.004 | 5.933±0.018 | 5.934±0.046 | 5.934±0.02 | 56±1 | 6.3 | 1.311 |
| 37450 | B3 V | 5.5±0.23 | -20.95±0.21 | 16.25±0.22 | 5.274±0.002 | 5.401±0.003 | 5.71±0.019 | 5.802±0.026 | 5.783±0.026 | 12±10 | 5.9 | 1.275 |
| 37623 | B5 V | 5.21±0.22 | -20.81±0.17 | 13.85±0.19 | 5.461±0.002 | 5.59±0.003 | 5.855±0.027 | 5.951±0.041 | 5.934±0.023 | 28±14 | 4.6 | 1.506 |
| 37752 | B8 V | 4.85±0.26 | -21.59±0.22 | 15.51±0.3 | 5.775±0.003 | 5.877±0.004 | 6.063±0.017 | 6.177±0.037 | 6.145±0.023 | 150±9 | 3.5 | 1.433 |
| 37915 | B5 V | 5.52±0.24 | -19.69±0.22 | 12.98±0.24 | 5.762±0.004 | 5.859±0.004 | 6.03±0.018 | 6.099±0.039 | 6.106±0.017 | 31±12 | 4.0 | 1.496 |
| 38373 | B8 V | 5.23±0.36 | -14.85±0.36 | -2.64±0.29 | 5.008±0.004 | 5.117±0.004 | 5.321 | 5.426±0.037 | 5.372±0.017 | 169±4 | 4.0 | 0.494 |
| 38906 | B8.5IIIMn | 2.95±0.41 | -3.98±0.41 | 11.95±0.47 | 6.855±0.007 | 6.86±0.008 | 6.747±0.024 | 6.782±0.046 | 6.763±0.023 | 160±9 | 3.9 | 0.706 |
| 39331 | B2 III | 2.31±0.89 | -2.96±0.68 | 4.77±0.59 | 8.821±0.008 | 8.946±0.013 | 9.203±0.029 | 9.298±0.021 | 9.303±0.02 | 22±2 | 9.2 | 1.260 |
| 39184 | B3 III | 4.25±0.25 | -25.47±0.29 | 8.76±0.2 | 5.722±0.002 | 5.844±0.004 | 6.085±0.023 | 6.143±0.03 | 6.179±0.03 | 43±10 | 5.0 | 0.799 |
| 39906 | B4IV | 7.01±0.22 | -13.9±0.9 | -5.4±1 | 4.854±0.004 | 4.401±0.003 | 4.987±0.282 | 4.802±0.02 | 4.769±0.023 | 46±4 | 5.0 | 0.909 |
| 39970 | B2V | 2.95±0.19 | -5.85±0.19 | 9.68±0.18 | 5.028±0.002 | 5.222±0.003 | 5.709±0.037 | 5.765±0.048 | 5.808±0.017 | 17±2 | 8.6 | 1.425 |
| 40085 | B8III | 3.72±0.39 | -8.29±0.39 | -16.17±0.38 | 5.969±0.004 | 6.079±0.004 | 6.223±0.018 | 6.275±0.035 | 6.347±0.017 | 154±18 | 3.9 | 0.312 |
| 40321 | B2 V | 3.21±0.21 | -7.76±0.17 | 7.84±0.19 | 4.89±0.002 | 5.074±0.004 | 5.486±0.018 | 5.613±0.017 | 5.617±0.02 | 17±3 | 8.5 | 2.219 |
| 40787 | B8 Ib/II | 4.25±0.37 | -9.37±0.27 | 5.09±0.28 | 6.357±0.003 | 6.434±0.004 | 6.514±0.017 | 6.606±0.024 | 6.585±0.017 | 170±11 | 3.2 | 2.037 |
| 40817 | B9III/IV | 7.5±0.35 | -18±1 | 35.2±1.2 | 5.268±0.003 | 5.328±0.003 | 5.414±0.032 | 5.427±0.039 | 5.401±0.024 | 267±18 | 3.1 | 0.544 |
| 40834 | B9/A0IV | 7.79±0.21 | -17.7±0.25 | 34.08±0.2 | 5.52±0.003 | 5.618±0.003 | 5.798±0.023 | 5.859±0.043 | 5.842±0.017 | 579±24 | 2.5 | 0.546 |
| 41049 | B9 V | 1.5±0.79 | -7.8±1.4 | 3.3±1.4 | 8.986±0.01 | 9±0.012 | 9.079±0.024 | 9.109±0.023 | 9.123±0.027 | 168±59 | 2.7 | 2.287 |
| 41296 | B2V | 4.69±0.22 | -14.32±0.23 | 17.04±0.2 | 5.006±0.004 | 5.165±0.004 | 5.527±0.024 | 5.624±0.041 | 5.633±0.02 | 7±4 | 7.4 | 1.361 |
| 41603 | B8 III | 2.24±0.48 | 0.08±0.45 | -15.86±0.35 | 6.618±0.007 | 6.676±0.007 | 6.741±0.02 | 6.856±0.037 | 6.777±0.027 | 145±10 | 4.0 | 0.716 |
| 41674 | B3 III | 5.66±0.24 | -25.45±0.24 | 14.77±0.21 | 5.854±0.003 | 5.974±0.004 | 6.228±0.023 | 6.306±0.024 | 6.316±0.019 | 12±11 | 4.9 | 2.281 |
| 41817 | B9Vp | 9.45±0.6 | -35.6±1 | -12.3±1.1 | 5.363±0.004 | 5.414±0.004 | 5.513±0.018 | 5.572±0.024 | 5.565±0.019 | 228±31 | 2.6 | 0.637 |
| 41843 | B9.5Vp HgMnEu | 4.49±0.4 | -8.1±0.4 | -14.87±0.32 | 6.737±0.007 | 6.768±0.008 | 6.794±0.026 | 6.844±0.032 | 6.834±0.032 | 569±27 | 2.5 | 0.242 |
| 42001 | B5 III | 3.91±0.23 | -21.35±0.17 | 8.18±0.24 | 5.802±0.002 | 5.914±0.003 | 6.127±0.027 | 6.225±0.041 | 6.216±0.02 | 67±0 | 4.9 | 2.060 |

*Continued on next page*

Table A1 – *Continued from previous page*

| HIP | Spectral[a] type | Plx (mas) | $\mu_\alpha \cos\delta$ (mas/yr) | $\mu_\delta$ (mas/yr) | *B* (mag) | *V* (mag) | *J* (mag) | *H* (mag) | *K* (mag) | Age (Myr) | ≈Mass ($M_\odot$) | 2MASS sources[c] (arcmin$^{-2}$) |
|---|---|---|---|---|---|---|---|---|---|---|---|---|
| 42129 | B3V | 3.64±0.29 | -21.71±0.27 | 11.32±0.27 | 5.12±0.002 | 5.244±0.002 | 5.506±0.019 | 5.598±0.026 | 5.602±0.017 | 41±10 | 6.6 | 1.068 |
| 42177 | B8p (SI) | 7.31±0.25 | -13.37±0.22 | 11.17±0.2 | 5.664±0.003 | 5.785±0.003 | 6.019±0.027 | 6.033±0.03 | 6.041±0.017 | 158±14 | 3.1 | 1.789 |
| 42334 | B9.5Vn | 14.07±0.21 | -24.51±0.19 | -13.03±0.16 | 5.216±0.002 | 5.241±0.003 | 5.283±0.039 | 5.349±0.041 | 5.321±0.019 | 1168±43 | 2.0 | 0.866 |
| 42459 | B6V | 7.33±0.24 | -23.9±0.24 | 23.46±0.22 | 5.311±0.003 | 5.44±0.003 | 5.77±0.017 | 5.814±0.041 | 5.802±0.017 | 37±10 | 4.0 | 1.611 |
| 42504 | B4III | 7.37±0.34 | -25.5±1.2 | 20.8±1 | 5.046±0.004 | 5.17±0.004 | 5.544±0.054 | 5.539±0.046 | 5.532±0.016 | 17±10 | 5.0 | 1.684 |
| 42535 | B6Vn | 6.79±0.26 | -25.3±0.27 | 23.14±0.24 | 5.432±0.003 | 5.546±0.004 | 5.822±0.023 | 5.925±0.054 | 5.894±0.026 | 45±9 | 4.0 | 1.708 |
| 42540 | B9 V | 11.68±0.5 | -62.4±1 | 5.4±1 | 5.195±0.002 | 5.203±0.004 | 5.265±0.023 | 5.323±0.032 | 5.288±0.02 | 215±64 | 2.5 | 1.925 |
| 42637 | B8V | 10.53±0.16 | -28.88±0.16 | 27.22±0.15 | 5.362±0.004 | 5.456±0.004 | 5.688±0.018 | 5.721±0.039 | 5.717±0.017 | 48±13 | 3.2 | 0.481 |
| 42715 | B9IV(Si) | 6.53±0.26 | -21.8±1.2 | 24.3±1.1 | 5.356±0.003 | 5.479±0.004 | 5.743±0.019 | 5.807±0.037 | 5.809±0.019 | 265±15 | 3.0 | 1.782 |
| 43073 | B9V | 4.55±0.43 | -20.6±0.32 | 5.04±0.35 | 6.158±0.003 | 6.203±0.003 | 6.184±0.02 | 6.243±0.043 | 6.199±0.023 | 307±16 | 3.1 | 1.966 |
| 43305 | B8IIIp HgMn | 7.24±0.24 | -20.2±0.6 | -21.7±0.6 | 5.214±0.002 | 5.291±0.002 | 5.447±0.026 | 5.447±0.037 | 5.435±0.023 | 104±11 | 3.5 | 0.288 |
| 43499 | B7III | 4.42±0.2 | -14.85±0.23 | 15.79±0.18 | 5.486±0.003 | 5.585±0.003 | 5.774±0.023 | 5.82±0.032 | 5.817±0.02 | 155±23 | 4.2 | 1.460 |
| 43689 | B4III | 2.65±0.49 | -11.63±0.46 | 7.69±0.4 | 7.481±0.007 | 7.572±0.008 | 7.709±0.027 | 7.818±0.041 | 7.77±0.023 | 27±9 | 5.0 | 2.355 |
| 43792 | B2 Vn | 1.02±1 | -3±2.3 | 8.7±2.1 | 8.482±0.014 | 8.369±0.013 | 7.817±0.024 | 7.857±0.039 | 7.803±0.014 | 33±3 | 6.5 | 2.147 |
| 44299 | B5V | 7.6±0.45 | -18.41±0.31 | 15.18±0.35 | 5.421±0.004 | 5.545±0.004 | 5.821±0.028 | 5.927±0.032 | 5.927±0.026 | 26±10 | 4.0 | 1.781 |
| 44798 | B8IIIpHgMnEu | 6.14±0.26 | -20.5±0.3 | -10.7±0.3 | 5.147±0.002 | 5.236±0.002 | 5.418±0.028 | 5.443±0.037 | 5.462±0.023 | 137±9 | 3.9 | 0.175 |
| 44883 | B8III | 5.31±0.61 | -19.4±0.9 | -1.9±1 | 5.552±0.004 | 5.605±0.004 | 5.614±0.024 | 5.651±0.028 | 5.64±0.023 | 143±21 | 3.9 | 0.267 |
| 45189 | B8V | 4.71±0.46 | -1±1.1 | 10±1.1 | 5.816±0.004 | 5.927±0.004 | 5.774±0.028 | 5.867±0.032 | 5.862±0.03 | 159±9 | 3.9 | 1.853 |
| 45270 | B9V | 6.4±0.25 | -25.23±0.25 | 14.24±0.23 | 5.87±0.003 | 5.903±0.003 | 5.889±0.023 | 5.953±0.037 | 5.893±0.02 | 268±9 | 3.1 | 2.385 |
| 45314 | B7.5V | 6.2±0.27 | -24.9±0.26 | 13.13±0.19 | 5.731±0.003 | 5.842±0.003 | 6.06±0.018 | 6.153±0.032 | 6.133±0.027 | 45±7 | 3.4 | 1.908 |
| 45344 | B3/5V | 5.33±0.26 | -23.6±0.9 | 8.7±0.9 | 5.11±0.002 | 5.239±0.004 | 5.502±0.023 | 5.574±0.046 | 5.59±0.019 | 69±3 | 4.9 | 1.692 |
| 45631 | B9V | 7.45±0.18 | -20.42±0.18 | 14.68±0.15 | 5.197±0.003 | 5.256±0.003 | 5.394±0.032 | 5.381±0.048 | 5.388±0.019 | 292±9 | 3.2 | 3.575 |
| 45941 | B2IV | 5.7±0.3 | -11.4±0.32 | 11.52±0.27 | 2.331±0.003 | 2.469±0.003 | 2.861±0.263 | 2.928±0.202 | 3.029±0.259 | 20±2 | 10.2 | 3.510 |
| 46283 | B5V | 7.6±0.18 | -19.59±0.19 | 11.35±0.17 | 4.989±0.002 | 5.09±0.002 | 5.298±0.019 | 5.383±0.037 | 5.385±0.024 | 33±13 | 4.0 | 4.261 |
| 46329 | B5V | 1.59±0.67 | -14.7±1 | -4.9±1 | 6.021±0.004 | 6.111±0.004 | 6.177±0.017 | 6.191±0.037 | 6.09±0.017 | 61±5 | 5.5 | 0.485 |
| 46594 | B8III | 7.54±0.2 | -19.7±1 | 10.6±0.9 | 5.367±0.002 | 5.441±0.003 | 5.616±0.027 | 5.689±0.046 | 5.625±0.02 | 74±7 | 3.2 | 3.803 |
| 46914 | B5IV | 3.93±0.49 | -11±2.4 | 11±2.1 | 5.252±0.01 | 5.434±0.008 | 5.315±0.019 | 5.406±0.028 | 5.396±0.02 | 89±5 | 5.0 | 2.623 |
| 46928 | B5V | 5.7±0.15 | -34.84±0.17 | 14.17±0.15 | 4.933±0.003 | 5.063±0.003 | 5.406±0.017 | 5.385±0.046 | 5.426±0.017 | 55±5 | 5.0 | 0.498 |
| 47452 | B5V | 7.48±0.3 | -27.6±0.7 | -19±0.6 | 4.919±0.003 | 5.05±0.002 | 5.355±0.026 | 5.418±0.05 | 5.427±0.017 | 31±13 | 4.0 | 0.237 |
| 47522 | B5 Ve | 6.44±0.2 | -29.3±0.17 | 2.72±0.14 | 4.636±0.002 | 4.757±0.002 | 4.755±0.037 | 4.743±0.075 | 4.54±0.016 | 82±12 | 5.0 | 0.325 |
| 48224 | B7III | 3.87±0.26 | -26.8±0.9 | 10.2±0.9 | 5±0.002 | 5.09±0.002 | 5.313±0.037 | 5.482±0.023 | 5.25±0.019 | 98±2 | 4.9 | 1.429 |
| 48943 | B5 Ve | 4.09±0.55 | -22.6±1.4 | 3.7±1.4 | 6.065±0.004 | 6.156±0.004 | 6.315±0.02 | 6.35±0.027 | 6.231±0.02 | 45±5 | 4.7 | 0.291 |
| 49712 | B3III/IV | 2.45±0.19 | -14.97±0.18 | 0.43±0.16 | 4.729±0.002 | 4.853±0.002 | 5.032±0.043 | 5.166±0.05 | 5.102±0.023 | 38±3 | 7.5 | 2.596 |

*Continued on next page*

Table A1 – *Continued from previous page*

| HIP | Spectral[a] type | Plx (mas) | $\mu_\alpha \cos\delta$ (mas/yr) | $\mu_\delta$ (mas/yr) | *B* (mag) | *V* (mag) | *J* (mag) | *H* (mag) | *K* (mag) | Age (Myr) | ≈Mass ($M_\odot$) | 2MASS sources[c] (arcmin$^{-2}$) |
|---|---|---|---|---|---|---|---|---|---|---|---|---|
| 50044 | B5 (III)E | 1.34±0.29 | -14.83±0.28 | 2.87±0.26 | 6.007±0.003 | 6.091±0.004 | 6.081±0.017 | 6.078±0.02 | 6.024±0.032 | 60±14 | 5.6 | 5.111 |
| 50480 | B9V | 6.13±0.32 | -28.12±0.2 | 3.66±0.23 | 5.903±0.002 | 5.96±0.002 | 6.041±0.018 | 6.142±0.041 | 6.098±0.017 | 263±5 | 3.0 | 0.675 |
| 50847 | B8V | 8.12±0.18 | -22.34±0.2 | 11.5±0.18 | 4.842±0.002 | 4.958±0.002 | 5.203±0.017 | 5.291±0.028 | 5.314±0.024 | 162±16 | 3.3 | 1.733 |
| 51362 | B9.5 V | 10.13±0.23 | -48.88±0.21 | -13.31±0.18 | 5.144±0.002 | 5.178±0.003 | 5.223±0.027 | 5.256±0.032 | 5.238±0.016 | 563±25 | 2.5 | 0.147 |
| 51376 | B9.5 V | 7.51±0.48 | -30.7±0.9 | 5.9±0.9 | 5.533±0.002 | 5.568±0.002 | 5.625±0.029 | 5.638±0.048 | 5.597±0.026 | 578±32 | 2.5 | 0.328 |
| 51437 | B6 V | 8.06±0.36 | -39.12±0.45 | -23.49±0.55 | 4.943±0.003 | 5.063±0.003 | 5.35±0.041 | 5.41±0.039 | 5.386±0.017 | 54±10 | 4.0 | 0.131 |
| 51491 | B9 IV | 6.24±0.32 | -33.96±0.21 | -1.09±0.26 | 5.565±0.003 | 5.589±0.004 | 5.52±0.018 | 5.517±0.019 | 5.517±0.023 | 276±29 | 3.1 | 0.180 |
| 52221 | B5III | 6.23±0.24 | -16.92±0.27 | 13±0.2 | 5.355±0.003 | 5.501±0.003 | 5.789±0.024 | 5.867±0.037 | 5.875±0.023 | 24±13 | 4.0 | 2.930 |
| 52742 | B8III(e) shell | 6.2±0.19 | -20.81±0.21 | -0.32±0.16 | 5.059±0.002 | 5.137±0.002 | 5.199±0.017 | 5.304±0.03 | 5.224±0.019 | 149±15 | 4.0 | 4.503 |
| 53272 | B6 V | 4.29±0.42 | -19±2 | 1.5±2 | 6.061±0.009 | 6.215±0.009 | 5.954±0.02 | 5.998±0.032 | 5.98±0.023 | 93±14 | 4.1 | 1.370 |
| 53762 | B8/9V | 10.69±0.34 | -62.95±0.21 | 9.93±0.24 | 5.738±0.002 | 5.8±0.003 | 5.915±0.024 | 6.033±0.032 | 5.96±0.017 | 103±52 | 2.5 | 0.609 |
| 54255 | B8 V | 4.71±0.27 | 34.74±0.22 | -17.06±0.2 | 5.651±0.013 | 5.714±0.008 | 5.742±0.02 | 5.783±0.037 | 5.764±0.017 | 162±7 | 3.9 | 0.239 |
| 54257 | B7V | 7.04±0.45 | -22.24±0.46 | 1.06±0.41 | 7.84±0.008 | 7.681±0.008 | 7.153±0.02 | 7.09±0.03 | 6.969±0.023 | 15±9 | 3.1 | 0.819 |
| 54413 | B9 III | 6.31±0.62 | -19.07±0.64 | 1.79±0.57 | 8.798±0.014 | 8.449±0.014 | 7.267±0.023 | 6.664±0.048 | 5.94±0.028 | 148±37 | 2.7 | 0.689 |
| 54557 | B9V | 5.6±0.88 | -20.84±0.78 | -0.57±0.68 | 9.395±0.017 | 9.01±0.016 | 7.64±0.026 | 7.347±0.054 | 7.149±0.019 | 98±31 | 2.5 | 0.780 |
| 54767 | B8III | 10.43±0.19 | -47.69±0.2 | 4.95±0.18 | 5.145±0.002 | 5.217±0.002 | 5.414±0.029 | 5.441±0.046 | 5.418±0.034 | 46±5 | 3.2 | 5.309 |
| 54829 | B2III | 1.48±0.22 | -6.87±0.23 | -0.66±0.21 | 5.63±0.003 | 5.734±0.003 | 5.893±0.017 | 5.953±0.043 | 5.931±0.02 | 24±2 | 9.1 | 7.624 |
| 55597 | B5IV | 8.08±0.38 | -15.4±3 | 12.6±2.9 | 5.294±0.004 | 5.388±0.004 | 5.242±0.018 | 5.314±0.035 | 5.282±0.023 | 26±13 | 4.0 | 4.820 |
| 55657 | B2/3V | 3.28±0.21 | -25.84±0.19 | -2.24±0.2 | 5.598±0.003 | 5.578±0.003 | 5.41±0.026 | 5.441±0.028 | 5.408±0.017 | 31±3 | 7.5 | 1.303 |
| 55667 | B2V | 1.18±0.57 | -9.13±0.29 | 0.38±0.31 | 5.947±0.004 | 6.118±0.004 | 6.548±0.028 | 6.644±0.046 | 6.65±0.016 | 19±2 | 9.7 | 0.524 |
| 56000 | B9IV | 4.66±0.7 | -38.7±1.1 | 5.2±1.1 | 5.107±0.002 | 5.131±0.002 | 5.182±0.024 | 5.204±0.026 | 5.173±0.032 | 198±15 | 3.6 | 0.519 |
| 56379 | B9 VNE | 10.32±0.43 | -37.6±1.3 | -0.6±1.2 | 6.712±0.004 | 6.696±0.004 | 6.425±0.019 | 5.961±0.03 | 5.418±0.023 | 117±42 | 2.5 | 1.791 |
| 56480 | B9 V | 7.65±0.22 | -56.17±0.18 | 16.19±0.2 | 4.552±0.002 | 4.613±0.002 | 4.743±0.273 | 4.788±0.023 | 4.721±0.035 | 318±4 | 3.2 | 1.718 |
| 56709 | B5 | 8.93±0.87 | -46.97±0.49 | 34.53±0.55 | 8.76±0.009 | 8.008±0.008 | 7.11±0.018 | 6.942±0.024 | 6.919±0.023 | 7±5 | 23.5 | 0.687 |
| 56754 | B9 IV | 11.44±0.42 | -65.1±1 | 10.6±1 | 5.107±0.002 | 5.137±0.002 | 5.172±0.037 | 5.236±0.072 | 5.125±0.02 | 171±16 | 2.8 | 10.196 |
| 57371 | B6III | 4.72±0.26 | -41.63±0.16 | 5.01±0.2 | 5.159±0.002 | 5.27±0.003 | 5.492±0.027 | 5.538±0.028 | 5.55±0.019 | 87±4 | 4.8 | 0.617 |
| 58326 | B3V | 5.34±0.25 | -23.76±0.24 | -4.32±0.21 | 5.409±0.002 | 5.557±0.003 | 5.879±0.019 | 6.014±0.028 | 5.994±0.02 | 13±10 | 5.7 | 12.266 |
| 58379 | B7III | 4.28±0.34 | -21.69±0.28 | 1.16±0.21 | 5.376±0.003 | 5.435±0.003 | 5.499±0.017 | 5.55±0.027 | 5.51±0.019 | 137±14 | 4.3 | 2.311 |
| 58587 | B2 V | 1.03±0.53 | -16.4±0.37 | 6.73±0.28 | 5.083±0.003 | 5.268±0.003 | 5.676±0.02 | 5.817±0.03 | 5.822±0.019 | 16±1 | 10.9 | 0.164 |
| 58720 | B9V | 9.46±0.21 | -38.84±0.19 | -6.58±0.16 | 5.813±0.002 | 5.879±0.003 | 6.01±0.02 | 6.079±0.028 | 6.085±0.024 | 183±78 | 2.5 | 2.540 |
| 59607 | B4 IV | 2.29±0.29 | -28.27±0.23 | -11±0.15 | 5.619±0.002 | 5.76±0.002 | 6.031±0.02 | 6.085±0.046 | 6.094±0.027 | 52±6 | 6.3 | 0.372 |
| 60189 | B8 Ve | 7.85±0.22 | -108.97±0.22 | -27.31±0.11 | 5.11±0.003 | 5.196±0.003 | 5.313±0.018 | 5.335±0.026 | 5.317±0.019 | 161±16 | 3.3 | 0.182 |
| 60379 | B7Vn | 9.02±0.29 | -37.12±0.2 | -12.44±0.19 | 5.281±0.002 | 5.372±0.002 | 5.591±0.017 | 5.594±0.028 | 5.636±0.016 | 20±17 | 3.2 | 2.979 |

*Continued on next page*

Table A1 – *Continued from previous page*

| HIP | Spectral[a] type | Plx (mas) | $\mu_\alpha \cos\delta$ (mas/yr) | $\mu_\delta$ (mas/yr) | $B$ (mag) | $V$ (mag) | $J$ (mag) | $H$ (mag) | $K$ (mag) | Age (Myr) | ≈Mass ($M_\odot$) | 2MASS sources[c] (arcmin$^{-2}$) |
|---|---|---|---|---|---|---|---|---|---|---|---|---|
| 60449 | B9III | 7.34±0.26 | -41.16±0.2 | -7.44±0.15 | 5.25±0.002 | 5.311±0.002 | 5.414±0.018 | 5.46±0.023 | 5.427±0.017 | 292±31 | 3.1 | 0.315 |
| 60463 | B8/9 V | 9.73±0.32 | -61.3±1.5 | -16±1.2 | 5.723±0.003 | 5.784±0.003 | 5.925±0.029 | 5.995±0.032 | 5.964±0.026 | 108±40 | 2.5 | 0.388 |
| 60610 | B9 IV/V | 7.43±0.33 | -40.57±0.25 | -6.28±0.18 | 5.65±0.004 | 5.702±0.004 | 5.815±0.019 | 5.844±0.028 | 5.847±0.016 | 249±1 | 2.9 | 0.311 |
| 60735 | B9 V | 6.43±0.25 | -6.14±0.17 | -30.44±0.15 | 5.577±0.003 | 5.56±0.003 | 5.478±0.018 | 5.475±0.03 | 5.443±0.02 | 314±8 | 3.2 | 0.269 |
| 60851 | B9.5V | 10.21±0.33 | -36.21±0.32 | -12.34±0.25 | 6.076±0.004 | 6.047±0.003 | 5.973±0.018 | 6.002±0.041 | 5.96±0.024 | 1168±44 | 2.0 | 11.821 |
| 60855 | B8/9 V | 7.47±0.28 | -27.9±0.23 | -13.75±0.15 | 5.383±0.004 | 5.446±0.004 | 5.514±0.019 | 5.578±0.03 | 5.54±0.017 | 176±28 | 3.1 | 0.386 |
| 61318 | B9.5 V | 12.62±0.28 | -83.27±0.22 | 0.23±0.16 | 5.461±0.004 | 5.489±0.004 | 5.56±0.017 | 5.636±0.024 | 5.585±0.017 | 1168±43 | 2.0 | 0.133 |
| 61789 | B8IIIMn (metallic lines) | 8.94±0.24 | -41.5±1 | -24.8±0.8 | 4.55±0.002 | 4.629±0.002 | 4.88±0.037 | 4.902±0.075 | 4.784±0.017 | 114±5 | 3.7 | 0.414 |
| 61966 | B6IVe | 3.41±0.25 | -24.66±0.18 | -3.66±0.18 | 4.876±0.002 | 4.916±0.002 | 4.855±0.037 | 4.933±0.017 | 4.79±0.019 | 90±5 | 5.0 | 5.613 |
| 62026 | B9V | 9.22±0.4 | -34.98±0.28 | -16.44±0.25 | 6.043±0.002 | 6.059±0.002 | 6.026±0.019 | 6.034±0.039 | 6.014±0.017 | 178±76 | 2.5 | 2.098 |
| 62058 | B7/8V | 8.54±0.35 | -31.8±0.26 | -11.91±0.23 | 5.914±0.002 | 5.986±0.002 | 6.118±0.023 | 6.149±0.034 | 6.172±0.035 | 46±14 | 3.2 | 2.236 |
| 62786 | B7/8 V | 7±0.37 | -26±0.3 | -19.2±0.2 | 5.893±0.003 | 5.974±0.003 | 6.156±0.023 | 6.21±0.035 | 6.223±0.02 | 64±16 | 3.2 | 0.407 |
| 63005 | B5Vne | 8.01±0.29 | -27.9±1.3 | -15±1.3 | 5.013±0.004 | 5.096±0.004 | 5.315±0.017 | 5.382±0.046 | 5.313±0.02 | 30±12 | 4.0 | 2.848 |
| 63210 | B8/9 V | 8.85±0.27 | -30.09±0.18 | -14.65±0.17 | 5.105±0.002 | 5.164±0.002 | 5.327±0.017 | 5.361±0.028 | 5.342±0.027 | 196±45 | 3.1 | 1.070 |
| 63945 | B2.5 V | 8.36±0.25 | -31.4±0.9 | -17.5±0.8 | 4.568±0.002 | 4.697±0.002 | 5.02±0.037 | 5.139±0.016 | 5.045±0.024 | 12±1 | 15.2 | 0.828 |
| 64053 | B8/9 V | 9.99±0.32 | -37.38±0.27 | -20.23±0.22 | 5.644±0.002 | 5.702±0.002 | 5.815±0.019 | 5.745±0.026 | 5.729±0.026 | 94±24 | 2.8 | 1.433 |
| 64515 | B9.5 V | 8.91±0.71 | -34.4±0.9 | -18.7±0.8 | 5.899±0.004 | 5.905±0.004 | 5.912±0.02 | 5.984±0.043 | 5.947±0.02 | 645±56 | 2.3 | 1.053 |
| 65688 | B8 V | 4.68±0.77 | -14.55±0.65 | 1.47±0.5 | 8.345±0.008 | 8.354±0.01 | 8.423±0.023 | 8.467±0.039 | 8.446±0.02 | 18±13 | 20.6 | 0.324 |
| 66454 | B8 V | 7.91±0.53 | -27.27±0.47 | -16.95±0.42 | 5.796±0.003 | 5.893±0.004 | 6.085±0.018 | 6.178±0.039 | 6.136±0.019 | 67±23 | 3.2 | 0.759 |
| 66849 | B8.5III | 4.17±0.57 | -29.6±1.1 | -10.3±1 | 5.353±0.003 | 5.377±0.003 | 5.348±0.018 | 5.379±0.039 | 5.322±0.017 | 161±8 | 3.9 | 6.265 |
| 67472 | B2Vnep | 6.45±0.16 | -24.24±0.14 | -18.64±0.08 | 3.28±0.003 | 3.46±0.003 | 3.707±0.211 | 3.74±0.2 | 4.006±0.035 | 19±4 | 8.7 | 0.607 |
| 67669 | B5 III | 10.96±0.88 | -69.6±1.1 | -22.1±1.3 | 4.4±0.007 | 4.528±0.007 | 4.129±0.829 | 4.946±0.017 | 4.971±0.027 | 24±11 | 4.0 | 0.347 |
| 67703 | B8Vnn | 12.55±0.79 | -37.6±1.1 | -27.7±1.1 | 5.166±0.002 | 5.25±0.003 | 5.46±0.018 | 5.508±0.023 | 5.514±0.023 | 41±15 | 3.2 | 1.677 |
| 68002 | B2.5 III | 8.54±0.13 | -57.37±0.1 | -44.55±0.08 | 2.351±0.004 | 2.523±0.004 | 3.022±0.254 | 3.082±0.211 | 3.22±0.25 | 35±3 | 7.4 | 0.935 |
| 68269 | B7 V | 9.8±0.19 | -49.36±0.21 | -29.53±0.15 | 5.116±0.003 | 5.201±0.003 | 5.366±0.018 | 5.368±0.024 | 5.38±0.014 | 20±18 | 3.2 | 0.247 |
| 69113 | B9 V | 6.21±0.41 | -20.8±1 | -18.1±0.9 | 6.135±0.004 | 6.177±0.004 | 6.276±0.017 | 6.352±0.043 | 6.311±0.023 | 230±17 | 2.8 | 0.721 |
| 69174 | B8 V | 3.98±0.39 | -32.7±0.8 | -12.6±0.8 | 5.921±0.003 | 5.956±0.003 | 6.021±0.02 | 6.076±0.043 | 6.079±0.023 | 163±9 | 3.9 | 1.593 |
| 69491 | B5V | 3.17±0.36 | -18.71±0.3 | -11.14±0.23 | 6.15±0.008 | 6.094±0.008 | 6.019±0.02 | 6.085±0.061 | 6.002±0.035 | 88±6 | 5.0 | 2.832 |
| 69618 | B4Ve | 6.77±0.24 | -23.82±0.22 | -20.92±0.18 | 4.973±0.002 | 5.045±0.002 | 5.033±0.017 | 4.992±0.024 | 4.765±0.02 | 24±12 | 5.0 | 5.521 |
| 69658 | B9.5V | 13.22±0.21 | -45.76±0.27 | -12.1±0.16 | 5.535±0.004 | 5.527±0.003 | 5.543±0.017 | 5.547±0.017 | 5.552±0.014 | 1168±51 | 2.0 | 0.215 |
| 70574 | B2 IV | 2.99±0.21 | -15.6±0.7 | -14.2±0.7 | 4.406±0.004 | 4.552±0.004 | 5.078±0.257 | 4.994±0.039 | 4.956±0.019 | 24±2 | 8.8 | 0.954 |
| 70915 | B8 V | 6.84±0.41 | -37.3±0.9 | -29.1±0.9 | 5.423±0.002 | 5.5±0.004 | 5.635±0.019 | 5.676±0.048 | 5.65±0.023 | 158±21 | 3.2 | 0.990 |
| 71353 | B7 V | 8.89±0.66 | -22.04±0.47 | -23.38±0.45 | 5.804±0.004 | 5.87±0.004 | 5.987±0.019 | 6.008±0.043 | 6.03±0.019 | 17±14 | 3.2 | 0.738 |

*Continued on next page*

Table A1 – *Continued from previous page*

| HIP | Spectral[a] type | Plx (mas) | $\mu_\alpha \cos\delta$ (mas/yr) | $\mu_\delta$ (mas/yr) | $B$ (mag) | $V$ (mag) | $J$ (mag) | $H$ (mag) | $K$ (mag) | Age (Myr) | ≈Mass ($M_\odot$) | 2MASS sources[c] (arcmin$^{-2}$) |
|---|---|---|---|---|---|---|---|---|---|---|---|---|
| 71762 | B9III- HgMn metallic lines | 10.28±0.91 | 10.6±0.8 | 16.4±0.8 | 4.78±0.008 | 4.875±0.008 | 4.353 | 4.195 | 5.051±0.017 | 213±34 | 3.0 | 0.115 |
| 71783 | B9.5III | 5.27±0.31 | -31.84±0.27 | -5.93±0.22 | 5.58±0.003 | 5.659±0.003 | 5.775±0.024 | 5.815±0.03 | 5.806±0.019 | 322±16 | 3.1 | 0.535 |
| 71974 | B9.5 V | 6.56±0.23 | -22.19±0.21 | -8.88±0.16 | 5.706±0.003 | 5.692±0.004 | 5.623±0.018 | 5.609±0.039 | 5.572±0.02 | 532±67 | 2.6 | 0.308 |
| 72154 | B9.5V | 6.61±0.84 | -41.15±0.54 | -6.55±0.53 | 5.665±0.008 | 5.668±0.007 | 5.618±0.018 | 5.618±0.02 | 5.602±0.017 | 524±52 | 2.6 | 0.145 |
| 73111 | B8.5 IV | 5.91±0.65 | -22.6±2 | -20.6±1.8 | 5.727±0.013 | 5.822±0.009 | 5.646±0.017 | 5.767±0.032 | 5.683±0.017 | 153±28 | 3.2 | 1.721 |
| 73865 | B8.5 V | 6.07±0.49 | 0.54±0.53 | -18.45±0.38 | 6.631±0.007 | 6.644±0.008 | 6.583±0.023 | 6.625±0.037 | 6.623±0.023 | 90±29 | 2.9 | 0.382 |
| 74750 | B0.5V | 1.94±0.38 | -1.87±0.36 | -3.1±0.33 | 5.658±0.004 | 5.762±0.004 | 5.863±0.019 | 5.929±0.034 | 5.938±0.023 | 8±1 | 12.9 | 10.387 |
| 74911 | B7 V | 9.72±0.71 | -23.3±2.1 | -41.4±1.9 | 4.225±0.004 | 4.392±0.004 | 4.513±0.254 | 4.572±0.211 | 4.427±0.017 | 123±13 | 3.9 | 2.403 |
| 75264 | B2 IV/V | 6.47±0.61 | -17.9±1 | -23.4±1.3 | 3.203±0.002 | 3.369±0.004 | 3.987±0.252 | 3.93±0.233 | 4.127±0.277 | 18±3 | 8.6 | 1.733 |
| 76243 | B5 V | 8.17±0.58 | -33±0.9 | -29.4±0.9 | 5.063±0.004 | 5.146±0.004 | 5.324±0.02 | 5.433±0.037 | 5.368±0.019 | 28±12 | 4.0 | 0.253 |
| 76503 | B7IV | 5.25±0.35 | -10.04±0.36 | -23.49±0.33 | 6.177±0.003 | 6.188±0.004 | 6.165±0.019 | 6.223±0.035 | 6.184±0.019 | 97±6 | 3.9 | 0.470 |
| 76591 | B9 V | 6.66±0.45 | -20.77±0.4 | -22.68±0.37 | 6.52±0.004 | 6.578±0.004 | 6.683±0.024 | 6.738±0.039 | 6.763±0.026 | 135±52 | 2.5 | 1.248 |
| 77227 | B8 V | 7.25±0.31 | -20.8±0.9 | -31.1±0.9 | 5.354±0.004 | 5.385±0.004 | 5.396±0.024 | 5.42±0.027 | 5.402±0.019 | 157±14 | 3.3 | 0.231 |
| 77562 | B9 Vn | 10.58±0.34 | -27.3±0.37 | -38.88±0.34 | 5.71±0.003 | 5.768±0.004 | 5.907±0.035 | 5.922±0.027 | 5.945±0.028 | 110±41 | 2.5 | 18.070 |
| 77634 | B9III | 16.71±0.27 | -7.2±0.7 | -28.4±0.7 | 3.93±0.002 | 3.956±0.002 | 4.053±0.266 | 4.004±0.219 | 3.99±0.035 | 209±16 | 3.1 | 0.932 |
| 77635 | B2 V | 6.59±0.27 | -14.1±0.31 | -25.06±0.25 | 4.568±0.002 | 4.637±0.003 | 4.802±0.228 | 4.86±0.075 | 4.782±0.02 | 8±4 | 7.6 | 0.565 |
| 77840 | B2.5 Vn | 6.49±0.51 | -14.4±0.8 | -23.5±0.8 | 4.578±0.008 | 4.677±0.008 | 4.739±0.037 | 4.814±0.014 | 4.789±0.017 | 12±5 | 7.0 | 0.573 |
| 77900 | B7 V | 6.32±0.46 | -12.54±0.44 | -26.19±0.38 | 6.078±0.004 | 6.143±0.004 | 6.234±0.018 | 6.311±0.032 | 6.3±0.016 | 20±18 | 3.2 | 0.648 |
| 78168 | B3.5 IV | 7.08±0.33 | -9.05±0.4 | -23.27±0.32 | 5.856±0.003 | 5.836±0.003 | 5.763±0.02 | 5.767±0.035 | 5.734±0.032 | 9±8 | 5.0 | 0.480 |
| 78265 | B1.5 V | 5.57±0.64 | -11.42±0.78 | -26.83±0.74 | 2.733±0.002 | 2.884±0.002 | 3.464±0.317 | 3.5±0.275 | 3.686±0.324 | 10±2 | 11.3 | 0.660 |
| 78933 | B1 V | 6.92±0.26 | -8.98±0.23 | -23.48±0.16 | 3.904±0.003 | 3.944±0.003 | 4.159±0.282 | 4.188±0.228 | 4.008±0.035 | 7±3 | 9.6 | 0.530 |
| 78968 | B9 V | 6.27±1.04 | -7.02±0.87 | -21.78±0.71 | 7.926±0.014 | 7.801±0.014 | 7.434±0.034 | 7.456±0.043 | 7.401±0.023 | 83±23 | 2.5 | 0.465 |
| 79005 | B9Vnnp lambda Boo | 8.9±0.6 | -40.7±0.8 | -25±0.8 | 5.768±0.004 | 5.756±0.004 | 5.58±0.019 | 5.577±0.03 | 5.528±0.017 | 226±25 | 2.7 | 0.376 |
| 79031 | B8V | 8.37±0.41 | -14.7±1.1 | -24.7±1.1 | 6.275±0.004 | 6.311±0.004 | 6.379±0.017 | 6.436±0.028 | 6.433±0.017 | 120±42 | 3.2 | 0.676 |
| 79098 | B9IV | 7.35±0.31 | -9.5±0.7 | -26±0.7 | 5.881±0.004 | 5.854±0.004 | 5.736±0.02 | 5.741±0.035 | 5.706±0.017 | 231±12 | 3.0 | 0.659 |
| 79153 | B9.5V | 11.65±0.57 | -13.47±0.42 | -59.41±0.41 | 5.551±0.002 | 5.568±0.002 | 5.63±0.029 | 5.587±0.027 | 5.599±0.016 | 523±202 | 2.0 | 6.538 |
| 79199 | B8 V | 8±0.32 | -25.32±0.43 | -44.92±0.37 | 5.423±0.003 | 5.497±0.003 | 5.64±0.017 | 5.656±0.035 | 5.649±0.019 | 121±35 | 3.2 | 1.331 |
| 79230 | B3 Vne | 3.61±1.06 | -5.2±1.1 | -6.4±1.2 | 7.218±0.004 | 7.107±0.007 | 6.494±0.019 | 6.413±0.039 | 6.242±0.023 | 9±3 | 7.4 | 2.516 |
| 79399 | B9 III/IV | 10.75±0.8 | -24.8±1 | -44.5±1.1 | 5.736±0.008 | 5.756±0.008 | 5.656±0.023 | 5.644±0.037 | 5.599±0.017 | 114±40 | 2.6 | 0.917 |
| 79404 | B2 V | 6.81±0.16 | -10.39±0.17 | -23.98±0.14 | 4.427±0.002 | 4.572±0.002 | 4.98±0.25 | 5.01±0.028 | 4.975±0.027 | 5±4 | 7.0 | 0.872 |
| 79410 | B9Van | 7.12±1.13 | -9.86±0.85 | -23.8±0.66 | 7.789±0.014 | 7.64±0.017 | 7.173±0.024 | 7.171±0.057 | 7.071±0.028 | 84±24 | 2.5 | 0.520 |
| 79622 | B7IV | 6.72±0.4 | -9.64±0.34 | -21.83±0.3 | 6.089±0.003 | 6.052±0.004 | 5.86±0.023 | 5.903±0.037 | 5.822±0.024 | 64±7 | 3.6 | 0.756 |
| 79653 | B8 V | 8.46±0.26 | -36.9±0.9 | -47.8±0.9 | 5.022±0.002 | 5.126±0.002 | 5.393±0.037 | 5.449±0.026 | 5.422±0.027 | 159±24 | 3.2 | 11.951 |

*Continued on next page*

Table A1 – *Continued from previous page*

| HIP | Spectral[a] type | Plx (mas) | $\mu_\alpha \cos\delta$ (mas/yr) | $\mu_\delta$ (mas/yr) | $B$ (mag) | $V$ (mag) | $J$ (mag) | $H$ (mag) | $K$ (mag) | Age (Myr) | ≈Mass ($M_\odot$) | 2MASS sources[c] (arcmin$^{-2}$) |
|---|---|---|---|---|---|---|---|---|---|---|---|---|
| 79739 | B8V | 6.66±0.9 | -13.7±1.6 | -24.9±1.6 | 8.14±0.01 | 7.926±0.009 | 7.239±0.018 | 7.173±0.035 | 7.025±0.017 | 121±46 | 3.2 | 0.758 |
| 79771 | B9 V | 6.16±0.76 | -10.8±0.71 | -23.43±0.59 | 8.71±0.014 | 8.392±0.014 | 7.324±0.018 | 7.19±0.028 | 7.098±0.02 | 93±28 | 2.5 | 0.796 |
| 80066 | B9 V | 7.1±0.43 | -13.7±0.48 | -45.02±0.38 | 6.045±0.004 | 6.105±0.004 | 6.228±0.02 | 6.315±0.027 | 6.289±0.02 | 218±55 | 2.5 | 3.076 |
| 80126 | B8Vnn | 6.64±0.57 | -10.78±0.51 | -25.4±0.43 | 7.192±0.004 | 7.041±0.007 | 6.565±0.039 | 6.506±0.028 | 6.418±0.02 | 76±24 | 3.2 | 0.716 |
| 80142 | B7 V | 7.29±0.49 | -13.21±0.41 | -23±0.36 | 6.462±0.004 | 6.499±0.004 | 6.583±0.02 | 6.644±0.035 | 6.618±0.026 | 16±12 | 3.2 | 22.021 |
| 80461 | B3 V | 8.01±0.8 | -6.9±1.1 | -23.4±1.2 | 7.046±0.007 | 6.77±0.007 | 5.696±0.024 | 5.551±0.034 | 5.427±0.023 | 15±6 | 5.1 | 0.699 |
| 80473 | B2.5 V | 9.03±0.9 | 35.1±4.1 | -31.9±4 | 5.151±0.009 | 4.977±0.008 | 3.569±0.287 | 3.348±0.252 | 3.173±0.518 | 22±4 | 7.8 | 0.701 |
| 80474 | B7V | 7.4±0.59 | -10.5±1.1 | -26.6±1.2 | 7.548±0.008 | 7.26±0.008 | 6.107±0.019 | 5.921±0.037 | 5.775±0.02 | 21±16 | 3.2 | 0.705 |
| 80493 | B9 V | 7.43±0.89 | -10.3±1.3 | -22.3±1.3 | 8.317±0.009 | 8.085±0.009 | 7.297±0.019 | 7.175±0.046 | 7.076±0.017 | 76±18 | 2.5 | 1.187 |
| 81472 | B2 V | 5.2±0.77 | -12.6±0.9 | -20.3±0.9 | 5.798±0.007 | 5.842±0.008 | 5.863±0.024 | 5.908±0.034 | 5.933±0.023 | 5±3 | 7.0 | 13.850 |
| 81474 | B9.5 IV | 7.4±0.55 | -13.09±0.48 | -20.21±0.43 | 6.992±0.004 | 6.734±0.008 | 5.895±0.023 | 5.782±0.039 | 5.69±0.017 | 566±31 | 2.5 | 0.732 |
| 81972 | B3 V | 6.11±0.31 | -11.46±0.3 | -20.94±0.25 | 5.578±0.008 | 5.636±0.007 | 5.811±0.018 | 5.848±0.034 | 5.842±0.017 | 15±11 | 5.5 | 11.098 |
| 82902 | B9 V | 8.61±0.4 | -34.83±0.51 | -42.91±0.39 | 5.864±0.004 | 5.929±0.004 | 6.068±0.026 | 6.118±0.03 | 6.144±0.024 | 189±70 | 2.5 | 5.274 |
| 83336 | B8 V | 7.29±0.45 | -9.8±0.7 | -50.5±0.6 | 4.928±0.004 | 5.015±0.004 | 5.19±0.02 | 5.284±0.035 | 5.256±0.017 | 150±11 | 3.5 | 10.073 |
| 85442 | B9.5III | 4.42±0.43 | -8.5±0.8 | -31.7±0.8 | 5.994±0.004 | 5.98±0.004 | 5.808±0.023 | 5.847±0.027 | 5.782±0.017 | 333±17 | 3.1 | 31.669 |
| 85727 | B7V | 16.48±0.34 | -56.8±0.9 | -100±0.8 | 3.506±0.002 | 3.589±0.002 | 3.697±0.231 | 3.651±0.224 | 3.71±0.197 | 92±7 | 4.0 | 1.214 |
| 85755 | B9.5IIIe | 8.04±0.24 | 2.6±0.5 | -25.8±0.5 | 4.813±0.003 | 4.789±0.003 | 4.9±0.186 | 4.711±0.206 | 4.296±0.028 | 324±12 | 3.1 | 20.299 |
| 85783 | B9 II/III | 8.36±0.67 | -3.1±0.8 | -23.9±0.8 | 6.002±0.108 | 5.992±0.068 | 6.152±0.023 | 6.196±0.037 | 6.151±0.017 | 127±35 | 2.5 | 28.532 |
| 87163 | B4IV | 2.69±0.38 | -1.1±0.44 | -5.21±0.32 | 6.425±0.008 | 6.317±0.008 | 5.908±0.032 | 5.848±0.032 | 5.861±0.024 | 52±5 | 6.3 | 35.478 |
| 87220 | B8III-IV | 5.86±0.26 | 5.47±0.33 | -9.09±0.23 | 4.769±0.003 | 4.803±0.004 | 4.481±0.197 | 4.785±0.028 | 4.752±0.017 | 169±5 | 4.0 | 30.731 |
| 88012 | B3 II/III | 1.8±0.41 | -1.62±0.46 | -4.87±0.24 | 5.914±0.01 | 5.978±0.007 | 6.114±0.019 | 6.181±0.026 | 6.151±0.02 | 46±4 | 6.5 | 36.907 |
| 88149 | B2Ve | 5.01±0.26 | 1.34±0.29 | -12.69±0.18 | 4.685±0.004 | 4.776±0.007 | 4.986±0.017 | 5.078±0.061 | 5.03±0.024 | 13±2 | 8.1 | 1.158 |
| 88859 | B8 III | 3.68±0.6 | 0.4±1.2 | -19.1±1.1 | 6.067±0.003 | 6.156±0.004 | 6.297±0.024 | 6.361±0.048 | 6.328±0.023 | 149±22 | 3.9 | 1.910 |
| 89684 | B9V | 4.94±0.39 | -3.26±0.34 | 2.4±0.27 | 6.236±0.003 | 6.232±0.003 | 6.092±0.018 | 6.138±0.02 | 6.122±0.016 | 298±22 | 3.1 | 0.823 |
| 89956 | B9Iaep | 1.85±1.29 | 1.28±0.99 | -0.57±0.75 | 9.562±0.032 | 8.243±0.016 | 4.596±0.261 | – | 3.51±0.263 | 220±10 | 3.4 | 27.790 |
| 89963 | B6Iap | 2.52±1.1 | 0±0.85 | -0.41±0.63 | 9.692±0.037 | 8.44±0.019 | 5.136±0.273 | 4.537±0.075 | 4.105±0.293 | 113±7 | 4.5 | 27.730 |
| 89977 | B2.5Ve | 3.08±0.62 | -0.37±0.51 | -10.75±0.49 | 6.102±0.004 | 6.144±0.004 | 6.127±0.026 | 6.171±0.03 | 6.156±0.026 | 16±3 | 7.1 | 1.979 |
| 90096 | B8Ve | 5.3±0.37 | -8.49±0.3 | -18.34±0.23 | 5.716±0.004 | 5.702±0.004 | 5.605±0.018 | 5.592±0.034 | 5.526±0.02 | 160±9 | 3.9 | 28.865 |
| 90336 | B7 III | 3.67±0.66 | 0.33±0.65 | -11.02±0.51 | 6.236±0.004 | 6.303±0.008 | 6.35±0.017 | 6.401±0.039 | 6.403±0.019 | 124±20 | 3.9 | 4.259 |
| 90766 | B9IVn | 4.61±0.78 | -2.9±1.5 | -0.5±1.5 | 7.796±0.008 | 7.816±0.009 | 7.769±0.017 | 7.809±0.017 | 7.807±0.017 | 98±30 | 2.5 | 0.584 |
| 91014 | B2 III/IV | 2.47±0.25 | 1.91±0.25 | -10.73±0.18 | 5.164±0.002 | 5.276±0.002 | 5.479±0.063 | 5.553±0.041 | 5.537±0.023 | 24±2 | 8.7 | 3.286 |
| 93368 | B9V | 23.39±6.47 | 8.4±3.3 | -29.3±3.3 | 6.671±0.007 | 6.669±0.008 | 6.718±0.026 | 6.777±0.028 | 6.739±0.02 | 138±13 | 7.0 | 0.998 |
| 93371 | B9V | 12.92±3.91 | -5.45±3.01 | -20.61±2.49 | 6.395±0.008 | 6.388±0.008 | 6.331±0.023 | 6.333±0.039 | 6.263±0.019 | 121±65 | 2.5 | 0.998 |

*Continued on next page*

Table A1 – *Continued from previous page*

| HIP | Spectral[a] type | Plx (mas) | $\mu_\alpha \cos\delta$ (mas/yr) | $\mu_\delta$ (mas/yr) | $B$ (mag) | $V$ (mag) | $J$ (mag) | $H$ (mag) | $K$ (mag) | Age (Myr) | ≈Mass ($M_\odot$) | 2MASS sources[c] (arcmin$^{-2}$) |
|---|---|---|---|---|---|---|---|---|---|---|---|---|
| 93542 | B9.5Vann | 16.89±0.28 | 56.41±0.27 | -46.39±0.19 | 4.719±0.004 | 4.73±0.002 | 4.717±0.208 | 4.96±0.075 | 4.752±0.019 | 1167±48 | 2.0 | 0.802 |
| 93805 | B9IV | 26.37±0.64 | -18.69±0.63 | -91.02±0.44 | 3.352±0.002 | 3.427±0.002 | 3.522±0.303 | 3.476±0.272 | 3.563±0.289 | 147±35 | 2.7 | 4.437 |
| 93892 | B9 II | 3.25±0.67 | -2.8±0.9 | -13.9±1.1 | 6.599±0.004 | 6.55±0.004 | 6.347±0.02 | 6.38±0.028 | 6.348±0.02 | 230±29 | 3.2 | 8.619 |
| 93996 | B2Ve | 2.52±0.33 | 5.14±0.39 | -0.25±0.26 | 5.486±0.004 | 5.568±0.004 | 5.392±0.019 | 5.386±0.034 | 5.313±0.017 | 20±2 | 9.2 | 1.778 |
| 95347 | B8Vs | 17.94±0.22 | 33.1±0.8 | -120.7±0.8 | 3.865±0.004 | 3.95±0.004 | 4.172±0.247 | 4.195±0.208 | 4.195±0.035 | 101±36 | 3.2 | 0.613 |
| 97607 | B2IVe | 1.89±0.45 | -1.3±0.8 | -2.6±0.8 | 6.401±0.003 | 6.482±0.004 | 6.116±0.02 | 6.074±0.041 | 5.967±0.019 | 23±2 | 8.5 | 1.769 |
| 99457 | B0 I | 1.4±0.44 | 0.98±0.47 | -1.75±0.48 | 6.295±0.004 | 6.448±0.007 | 6.793±0.024 | 6.933±0.034 | 6.947±0.024 | 12±2 | 10.9 | 0.586 |
| 100751 | B3V | 18.24±0.52 | 6.9±0.44 | -86.02±0.32 | 1.799±0.007 | 1.917±0.006 | 2.303±0.312 | 2.457±0.217 | 2.479±0.282 | 32±12 | 6.4 | 0.291 |
| 100881 | B8II | 5.98±0.58 | 11±0.5 | -12.2±0.4 | 5.103±0.004 | 5.15±0.004 | 5.164±0.023 | 5.217±0.023 | 5.21±0.017 | 160±7 | 3.9 | 0.399 |
| 102157 | B9.5III | 4.15±0.27 | 9.14±0.15 | -23.76±0.19 | 5.079±0.001 | 5.138±0.001 | 5.223±0.037 | 5.218±0.017 | 5.168±0.023 | 186±16 | 3.9 | 0.281 |
| 105164 | B5 V | 3.21±0.28 | 12.05±0.29 | 12.99±0.2 | 5.699±0.004 | 5.817±0.004 | 6.039±0.018 | 6.166±0.034 | 6.139±0.03 | 87±11 | 5.0 | 0.277 |
| 105842 | B9.5V | 3.89±1.27 | 7.7±1.4 | -4.2±1.5 | 8.904±0.01 | 8.911±0.013 | 8.906±0.027 | 8.93±0.046 | 8.956±0.034 | 358±184 | 1.8 | 0.234 |
| 108874 | B7 III | 7.49±0.23 | 24.69±0.22 | -11.16±0.14 | 4.678±0.017 | 4.767±0.009 | 4.864±0.184 | 4.809±0.03 | 4.66±0.016 | 155±23 | 4.0 | 0.197 |
| 109139 | B8V | 18.62±0.22 | 39.9±0.4 | -57.7±0.4 | 4.221±0.003 | 4.28±0.003 | 4.376±0.272 | 4.58±0.075 | 4.431±0.014 | 50±14 | 3.2 | 0.171 |
| 110672 | B1III-IVe | 4.17±0.28 | 17.76±0.24 | 2.39±0.18 | 4.631±0.003 | 4.797±0.003 | 5.304±0.037 | 5.364±0.048 | 5.35±0.019 | 8±3 | 9.3 | 0.180 |
| 112542 | B9 III | 10.27±0.46 | 30.64±0.4 | -9.33±0.3 | 5.665±0.003 | 5.676±0.004 | 5.745±0.019 | 5.785±0.039 | 5.727±0.019 | 110±45 | 2.5 | 0.136 |
| 112781 | B5/7V | 6.62±0.19 | 19.99±0.21 | -12.18±0.17 | 5.195±0.002 | 5.316±0.002 | 5.668±0.043 | 5.649±0.027 | 5.65±0.019 | 87±10 | 4.0 | 0.278 |
| 113031 | B7 III | 3.95±0.4 | 22±0.7 | 2±0.6 | 5.714±0.004 | 5.782±0.004 | 5.899±0.017 | 5.962±0.02 | 5.925±0.019 | 156±20 | 4.1 | 0.134 |
| 113889 | B6Ve | 7.99±0.22 | 11.88±0.21 | -9.75±0.21 | 4.38±0.003 | 4.487±0.003 | 4.763±0.037 | 4.808±0.026 | 4.75±0.019 | 98±13 | 4.0 | 0.150 |
| 116231 | B9.5IIIpHgMnSi | 18.74±0.15 | 89.8±0.7 | 33.2±0.7 | 4.29±0.002 | 4.37±0.002 | 4.477±0.256 | 4.669±0.039 | 4.611±0.027 | 847±339 | 2.4 | 0.116 |
| 117089 | B8.5Vnn | 8.61±0.54 | 27.23±0.62 | -2.94±0.55 | 5.16±0.003 | 5.236±0.003 | 5.381±0.019 | 5.42±0.032 | 5.381±0.02 | 143±28 | 3.1 | 0.108 |
| 117315 | B3Ve | 5.4±0.25 | 9.04±0.19 | -23.21±0.17 | 5.006±0.002 | 5.166±0.002 | 5.533±0.017 | 5.644±0.028 | 5.675±0.026 | 15±10 | 5.9 | 0.120 |
| 117629 | B6.5V | 10.23±0.31 | 26.82±0.38 | -4.27±0.3 | 5.059±0.004 | 5.178±0.004 | 5.415±0.024 | 5.506±0.017 | 5.505±0.017 | 41±39 | 4.0 | 0.107 |
| 120402 | B9III | 2.98±1.46 | -3.2±3.24 | 7.25±3.24 | 8.331±0.013 | 8.35±0.012 | 8.328±0.019 | 8.364±0.028 | 8.368±0.018 | 107±42 | 2.6 | 0.713 |

**Notes.** The age estimates and associated errors are rounded to nearest integer value.

[a] Most recent spectral type as given in the Catalogue of Stellar Classifications (Skiff 2014)

[b] HIP 3678 is a white dwarf and the central star of the planetary nebula NGC 246, a hierarchical triple found in this study.

The actual suggested spectral type of HIP 3678 A is PG1159 (Lamontagne et al. 2000).

[c] Total number of 2MASS point sources within a $2^\circ \times 2^\circ$ box surrounding each sample star scaled to one square arc minute.

**Table A2.** Observation log and astrometric calibration results of the investigated target sample.

| HIP | MJD (days) | Observation date | Programme ID | PI | Exposure time (s) | Filter | Camera | FWHM (mas) | Pixel scale (mas/pixel) | Orientation (degree) | Method[a] |
|---|---|---|---|---|---|---|---|---|---|---|---|
| 145 | 53349.04 | 2004-12-10 | 074.D-0180(A) | IVANOV | 2.5×10×21 | *IB*2.18 | S27 | 74.1 | 27.110±0.021 | -0.020±0.046 | A |
| | 53690.07 | 2005-11-16 | 076.C-0170(A) | HUBRIG | 1.8×40×10 | *Ks* | S13 | 76.6 | 13.266±0.023 | -0.013±0.097 | A |
| 377 | 53698.02 | 2005-11-24 | 076.D-0108(A) | IVANOV | 0.3454×149×9 | *Ks* | S27 | 82.0 | 27.144±0.032 | -0.009±0.060 | A |
| 1191 | 53698.05 | 2005-11-24 | 076.D-0108(A) | IVANOV | 0.3454×149×9 | *Ks* | S27 | 74.8 | 27.161±0.040 | 0.042±0.088 | A |
| 1830 | 53284.15 | 2004-10-06 | 074.D-0374(A) | HUBRIG | 10.0×5×20 | *Ks* | S13 | 70.1 | 13.261±0.014 | -0.000±0.057 | A |
| 2548 | 53710.05 | 2005-12-06 | 076.D-0108(A) | IVANOV | 1.0×50×9 | *Ks* | S27 | 80.8 | 27.174±0.042 | -0.029±0.092 | A |
| | 54359.25 | 2007-09-16 | 080.D-0348(A) | IVANOV | 1.0×51×9 | *Ks* | S27 | 85.7 | 27.160±0.055 | 0.017±0.115 | A |
| 3678 | 53331.09 | 2004-11-22 | 074.D-0315(A) | POLLACCO | 6.1×20×5 | *Ks* | S13 | 75.7 | 13.269±0.066 | -0.003±0.295 | A |
| | 54265.40 | 2007-06-14 | 079.D-0546(A) | WERNER | 40.0×5×15 | *Ks* | S27 | 97.1 | 27.136±0.063 | -0.050±0.132 | A |
| 3741 | 53710.07 | 2005-12-06 | 076.D-0108(A) | IVANOV | 1.0×50×9 | *Ks* | S27 | 79.5 | 27.127±0.038 | -0.038±0.081 | A |
| 5778 | 53285.21 | 2004-10-07 | 074.D-0374(A) | HUBRIG | 6.0×9×20 | *Ks* | S13 | 72.4 | 13.263±0.020 | 0.007±0.084 | A |
| 10602 | 53710.10 | 2005-12-06 | 076.C-0170(A) | HUBRIG | 0.65×200×10 | *Ks* | S13 | 83.2 | 13.276±0.019 | -0.049±0.076 | A |
| | 53712.09 | 2005-12-08 | 076.C-0170(A) | HUBRIG | 0.65×200×10 | *Ks* | S13 | 70.1 | 13.264±0.019 | -0.030±0.079 | A |
| 13951 | 53358.10 | 2004-12-19 | 074.D-0180(A) | IVANOV | 0.3454×149×9 | *Ks* | S27 | 84.5 | 27.092±0.040 | -0.023±0.086 | A |
| | 54370.30 | 2007-09-27 | 080.D-0348(A) | IVANOV | 2.0×26×9 | *Ks* | S27 | 89.3 | 27.140±0.045 | -0.006±0.097 | A |
| 14131 | 53284.28 | 2004-10-06 | 074.D-0374(A) | HUBRIG | 3.8×4×64 | *Ks* | S13 | 78.0 | 13.257±0.003 | 0.002±0.012 | A |
| | 54357.39 | 2007-09-14 | 080.D-0348(A) | IVANOV | 1.0×51×13 | *Ks* | S27 | 96.0 | 27.144±0.012 | 0.013±0.026 | A |
| 15627 | 54024.21 | 2006-10-16 | 078.D-0639(A) | BOUY | 4.4×12×128 | *H* | SDI | 76.5 | 17.250±0.060 | 0.000±0.500 | U |
| 16511 | 53376.05 | 2005-01-06 | 074.D-0374(A) | HUBRIG | 3.8×13×20 | *Ks* | S13 | 73.8 | 13.264±0.013 | -0.012±0.054 | A |
| | 53700.14 | 2005-11-26 | 076.C-0170(A) | HUBRIG | 1.0×60×10 | *Ks* | S13 | 69.1 | 13.287±0.026 | -0.013±0.121 | A |
| | 55798.41 | 2011-08-25 | 087.D-0197(A) | SCHOELLER | 15.0×4×16 | *Ks* | S13 | 85.8 | 13.268±0.015 | 0.045±0.065 | A |
| 16803 | 53379.10 | 2005-01-09 | 074.D-0180(A) | IVANOV | 10.0×5×12 | *IB*2.18 | S27 | 90.4 | 27.104±0.032 | -0.013±0.066 | A |
| | 54363.35 | 2007-09-20 | 080.D-0348(A) | IVANOV | 10.0×5×9 | *IB*2.18 | S27 | 126.7 | 27.151±0.043 | 0.009±0.089 | A |
| | 54373.25 | 2007-09-30 | 080.D-0348(A) | IVANOV | 10.0×5×15 | *IB*2.18 | S27 | 86.3 | 27.140±0.024 | 0.003±0.050 | A |
| 17563 | 53380.09 | 2005-01-10 | 074.D-0180(A) | IVANOV | 10.0×5×13 | *IB*2.18 | S27 | 83.3 | 27.094±0.031 | -0.003±0.066 | A |

*Continued on next page*

Table A2 – *Continued from previous page*

| HIP | MJD (days) | Observation date | Programme ID | PI | Exposure time (s) | Filter | Camera | FWHM (mas) | Pixel scale (mas/pixel) | Orientation (degree) | Method[a] |
|---|---|---|---|---|---|---|---|---|---|---|---|
| 17921 | 53700.19 | 2005-11-26 | 076.C-0170(A) | HUBRIG | 1.0×60×10 | *Ks* | S13 | 74.4 | 13.277±0.022 | 0.016±0.098 | A |
| | 53728.11 | 2005-12-24 | 076.C-0170(A) | HUBRIG | 0.6×100×10 | *Ks* | S13 | 73.6 | 13.265±0.023 | 0.001±0.098 | A |
| 18213 | 53379.12 | 2005-01-09 | 074.D-0180(A) | IVANOV | 5.0×10×9 | *IB*2.18 | S27 | 82.7 | 27.169±0.034 | -0.004±0.072 | A |
| | 54357.37 | 2007-09-14 | 080.D-0348(A) | IVANOV | 5.0×10×11 | *IB*2.18 | S27 | 83.3 | 27.169±0.034 | -0.004±0.072 | A |
| 18788 | 53683.27 | 2005-11-09 | 076.D-0108(A) | IVANOV | 5.0×10×9 | *IB*2.18 | S27 | 78.8 | 27.168±0.041 | -0.022±0.085 | A |
| | 54363.36 | 2007-09-20 | 080.D-0348(A) | IVANOV | 10.0×5×9 | *IB*2.18 | S27 | 162.5 | 27.147±0.040 | -0.009±0.080 | A |
| | 54370.34 | 2007-09-27 | 080.D-0348(A) | IVANOV | 10.0×5×9 | *IB*2.18 | S27 | 92.7 | 27.138±0.044 | -0.018±0.093 | A |
| 19720 | 54024.32 | 2006-10-16 | 078.D-0639(A) | BOUY | 13.0×4×128 | *H* | SDI | 125.7 | 17.250±0.060 | 0.000±0.500 | U |
| 19860 | 54059.19 | 2006-11-20 | 078.D-0639(A) | BOUY | 1.0×53×128 | *H* | SDI | 82.8 | 17.250±0.060 | 0.000±0.500 | U |
| 20020 | 53347.15 | 2004-12-08 | 074.D-0180(A) | IVANOV | 0.3454×149×9 | *Ks* | S27 | 88.1 | 27.095±0.025 | 0.003±0.057 | A |
| | 54363.37 | 2007-09-20 | 080.D-0348(A) | IVANOV | 0.3454×148×9 | *Ks* | S27 | 165.6 | 27.155±0.043 | 0.006±0.083 | A |
| | 54373.29 | 2007-09-30 | 080.D-0348(A) | IVANOV | 4.0×13×18 | *Ks* | S27 | 96.0 | 27.148±0.012 | -0.008±0.027 | A |
| 20042 | 53690.20 | 2005-11-16 | 076.C-0170(A) | HUBRIG | 0.5×120×20 | *Ks* | S13 | 79.6 | 13.269±0.013 | -0.013±0.054 | A |
| | 56189.19 | 2012-09-19 | 089.D-0366(A) | ADAM | 0.5×120×6 | *Ks* | S13 | 80.2 | 13.273±0.011 | 0.679±0.046 | C |
| 20171 | 53404.04 | 2005-02-03 | 074.D-0374(A) | HUBRIG | 3.8×13×20 | *Ks* | S13 | 70.3 | 13.274±0.014 | -0.025±0.058 | A |
| 20554 | 53266.31 | 2004-09-18 | 60.A-9026(A) | NACO TEAM | 1.0×10×5 | *IB*2.06 | S27 | 153.6 | 27.206±0.020 | -0.190±0.116 | A |
| 20804 | 53409.03 | 2005-02-08 | 074.D-0374(A) | HUBRIG | 3.8×13×15 | *Ks* | S13 | 81.9 | 13.265±0.018 | 0.015±0.078 | A |
| | 56189.33 | 2012-09-19 | 089.D-0366(A) | ADAM | 5.0×12×5 | *Ks* | S13 | 86.1 | 13.273±0.011 | 0.679±0.046 | C |
| | 56296.08 | 2013-01-04 | 090.D-0038(A) | SCHOELLER | 6.0×8×20 | *Ks* | S13 | 77.2 | 13.263±0.013 | -0.027±0.054 | A |
| 21177 | 54096.13 | 2006-12-27 | 078.D-0639(A) | BOUY | 17.5×6×128 | *H* | SDI | 83.7 | 17.250±0.060 | 0.000±0.500 | U |
| 21192 | 53413.07 | 2005-02-12 | 074.D-0180(A) | IVANOV | 0.3454×149×9 | *Ks* | S27 | 89.3 | 27.154±0.042 | -0.014±0.087 | A |
| 21640 | 54131.05 | 2007-01-31 | 078.D-0639(A) | BOUY | 5.0×3×96 | *H* | SDI | 77.7 | 17.250±0.060 | 0.000±0.500 | U |
| 21735 | 53404.07 | 2005-02-03 | 074.D-0374(A) | HUBRIG | 2.4×22×20 | *Ks* | S13 | 69.8 | 13.270±0.012 | -0.013±0.055 | A |
| | 56189.28 | 2012-09-19 | 089.D-0366(A) | ADAM | 6.0×10×4 | *Ks* | S13 | 106.3 | 13.291±0.126 | -0.233±0.525 | A |
| 21949 | 53379.14 | 2005-01-09 | 074.D-0180(A) | IVANOV | 2.0×26×9 | *Ks* | S27 | 83.3 | 27.100±0.017 | -0.003±0.035 | A |
| | 53415.05 | 2005-02-14 | 074.D-0180(A) | IVANOV | 0.3454×149×9 | *Ks* | S27 | 82.0 | 27.139±0.018 | 0.013±0.036 | A |

*Continued on next page*

Table A2 – *Continued from previous page*

| HIP | MJD (days) | Observation date | Programme ID | PI | Exposure time (s) | Filter | Camera | FWHM (mas) | Pixel scale (mas/pixel) | Orientation (degree) | Method[a] |
|---|---|---|---|---|---|---|---|---|---|---|---|
| 22913 | 53409.05 | 2005-02-08 | 074.D-0374(A) | HUBRIG | 3.8×13×20 | *Ks* | S13 | 80.6 | 13.279±0.013 | -0.038±0.055 | A |
| 23419 | 53470.97 | 2005-04-10 | 075.C-0475(A) | OUDMAIJER | 1.0×12×5 | *NB*2.17 | S13 | 75.7 | 13.240±0.083 | 0.130±0.379 | A |
| 23745 | 54128.05 | 2007-01-28 | 078.D-0639(A) | BOUY | 17.4×3×128 | *H* | SDI | 79.2 | 17.250±0.060 | 0.000±0.500 | U |
| 23794 | 53286.34 | 2004-10-08 | 074.D-0374(A) | HUBRIG | 4.8×11×20 | *Ks* | S13 | 84.7 | 13.261±0.030 | -0.020±0.130 | A |
| | 56296.10 | 2013-01-04 | 090.D-0038(A) | SCHOELLER | 4.5×10×20 | *Ks* | S13 | 73.3 | 13.275±0.013 | -0.026±0.058 | A |
| 24196 | 53347.21 | 2004-12-08 | 074.D-0374(A) | HUBRIG | 10.0×5×21 | *Ks* | S13 | 69.4 | 13.243±0.019 | 0.025±0.081 | A |
| 24244 | 55173.23 | 2009-12-08 | 084.C-0364(A) | VOGT | 0.347×126×41 | *Ks* | S13 | 68.5 | 13.271±0.039 | 0.006±0.178 | A |
| 24305 | 53374.16 | 2005-01-04 | 074.D-0374(A) | HUBRIG | 0.5×100×20 | *Ks* | S13 | 83.4 | 13.265±0.014 | 0.027±0.061 | A |
| | 56269.31 | 2012-12-08 | 090.D-0038(A) | SCHOELLER | 1.0×45×20 | *Ks* | S13 | 70.0 | 13.269±0.013 | -0.000±0.057 | A |
| 24505 | 53284.40 | 2004-10-06 | 074.D-0180(A) | IVANOV | 1.0×50×7 | *IB*2.18 | S27 | 83.3 | 27.116±0.107 | 0.025±0.235 | A |
| | 53415.06 | 2005-02-14 | 074.D-0180(A) | IVANOV | 1.0×50×9 | *IB*2.18 | S27 | 78.2 | 27.148±0.040 | 0.009±0.088 | A |
| 24552 | 52959.32 | 2003-11-16 | 072.C-0624(B) | MOUILLET | 10.0×6×30 | *Ks* | S27 | 517.3 | 27.053±0.019 | 0.000±0.500 | U |
| 24740 | 53700.23 | 2005-11-26 | 076.C-0170(A) | HUBRIG | 2.4×25×10 | *Ks* | S13 | 73.9 | 13.296±0.022 | -0.014±0.093 | A |
| 24825 | 53471.97 | 2005-04-11 | 075.C-0475(A) | OUDMAIJER | 1.0×12×5 | *NB*2.17 | S13 | 70.5 | 13.255±0.085 | 0.008±0.383 | A |
| | 56189.40 | 2012-09-19 | 089.D-0366(A) | ADAM | 5.0×12×5 | *Ks* | S13 | 70.1 | 13.273±0.011 | 0.679±0.046 | C |
| 24925 | 53379.16 | 2005-01-09 | 074.D-0374(A) | HUBRIG | 6.0×9×20 | *Ks* | S13 | 69.6 | 13.255±0.018 | 0.019±0.075 | A |
| | 56189.34 | 2012-09-19 | 089.D-0366(A) | ADAM | 6.0×10×5 | *Ks* | S13 | 82.6 | 13.273±0.011 | 0.679±0.046 | C |
| | 56296.12 | 2013-01-04 | 090.D-0038(A) | SCHOELLER | 10.0×5×20 | *Ks* | S13 | 72.2 | 13.270±0.013 | -0.002±0.058 | A |
| 25365 | 53380.14 | 2005-01-10 | 074.D-0374(A) | HUBRIG | 25.0×2×22 | *Ks* | S13 | 75.3 | 13.249±0.013 | 0.028±0.056 | A |
| | 56189.30 | 2012-09-19 | 089.D-0366(A) | ADAM | 5.0×6×5 | *Ks* | S13 | 134.1 | 13.273±0.011 | 0.679±0.046 | C |
| 25657 | 54097.21 | 2006-12-28 | 078.D-0639(A) | BOUY | 52.2×1×128 | *H* | SDI | 103.0 | 17.250±0.060 | 0.000±0.500 | U |
| | 56189.31 | 2012-09-19 | 089.D-0366(A) | ADAM | 15.0×4×5 | *Ks* | S13 | 275.2 | 17.250±0.060 | 0.000±0.500 | U |
| 26215 | 53348.20 | 2004-12-09 | 074.D-0374(A) | HUBRIG | 4.0×6×34 | *Ks* | S13 | 77.0 | 13.252±0.008 | -0.012±0.033 | A |
| 26235 | 54452.07 | 2007-12-18 | 080.D-0532(A) | BOUY | 1.0×30×128 | *H* | SDI | 63.6 | 17.250±0.060 | 0.000±0.500 | U |
| 26237 | 53469.98 | 2005-04-09 | 075.C-0475(A) | OUDMAIJER | 0.35×35×5 | *NB*2.17 | S13 | 74.9 | 13.241±0.098 | 0.093±0.426 | A |
| | 56189.39 | 2012-09-19 | 089.D-0366(A) | ADAM | 2.0×30×5 | *Ks* | S13 | 71.0 | 13.273±0.011 | 0.679±0.046 | C |

*Continued on next page*

Table A2 – *Continued from previous page*

| HIP | MJD (days) | Observation date | Programme ID | PI | Exposure time (s) | Filter | Camera | FWHM (mas) | Pixel scale (mas/pixel) | Orientation (degree) | Method[a] |
|---|---|---|---|---|---|---|---|---|---|---|---|
| 26545 | 53409.08 | 2005-02-08 | 074.D-0180(A) | IVANOV | 0.3454×149×9 | *Ks* | S27 | 81.4 | 27.148±0.032 | -0.062±0.066 | A |
| 26551 | 53289.40 | 2004-10-11 | 074.C-0084(B) | NEUHAEUSER | 0.3×100×4 | *Ks* | S27 | 72.0 | 27.098±0.070 | -0.026±0.152 | A |
| 26602 | 53434.07 | 2005-03-05 | 60.A-9026(A) | NACO TEAM | 3.0×2×0 | *Ks* | S27 | 121.3 | 27.053±0.019 | 0.000±0.500 | U |
| | 56189.38 | 2012-09-19 | 089.D-0366(A) | ADAM | 8.0×7×5 | *Ks* | S13 | 71.2 | 13.273±0.011 | 0.679±0.046 | C |
| 26634 | 53455.99 | 2005-03-26 | 075.C-0475(A) | OUDMAIJER | 1.0×12×5 | *NB*2.17 | S13 | 68.5 | 13.275±0.193 | -0.039±0.801 | A |
| 26836 | 53728.16 | 2005-12-24 | 076.C-0170(A) | HUBRIG | 0.9×67×10 | *Ks* | S13 | 68.7 | 13.266±0.023 | -0.012±0.100 | A |
| | 56189.37 | 2012-09-19 | 089.D-0366(A) | ADAM | 10.0×6×5 | *Ks* | S13 | 82.0 | 13.256±0.089 | 0.070±0.370 | A |
| 26868 | 53375.15 | 2005-01-05 | 074.D-0180(A) | IVANOV | 1.0×50×9 | *IB*2.18 | S27 | 84.5 | 27.116±0.035 | 0.004±0.071 | A |
| 27265 | 53738.15 | 2006-01-03 | 076.C-0170(A) | HUBRIG | 1.0×60×10 | *Ks* | S13 | 69.4 | 13.273±0.023 | -0.025±0.102 | A |
| 27534 | 53380.11 | 2005-01-10 | 074.D-0180(A) | IVANOV | 5.0×10×9 | *IB*2.18 | S27 | 82.7 | 27.117±0.022 | 0.042±0.051 | A |
| 27566 | 53733.20 | 2005-12-29 | 076.D-0108(A) | IVANOV | 5.0×10×9 | *IB*2.18 | S27 | 83.9 | 27.156±0.011 | -0.013±0.019 | A |
| 27810 | 53454.00 | 2005-03-25 | 075.C-0475(A) | OUDMAIJER | 0.35×35×5 | *NB*2.17 | S13 | 68.5 | 13.297±0.094 | -0.054±0.378 | A |
| 28691 | 53348.24 | 2004-12-09 | 074.D-0374(A) | HUBRIG | 2.4×22×20 | *Ks* | S13 | 81.4 | 13.257±0.012 | -0.040±0.053 | A |
| 28744 | 53456.00 | 2005-03-27 | 075.C-0475(A) | OUDMAIJER | 0.35×35×5 | *NB*2.17 | S13 | 68.9 | 13.269±0.076 | -0.041±0.339 | A |
| | 56189.32 | 2012-09-19 | 089.D-0366(A) | ADAM | 5.0×6×6 | *Ks* | S13 | 87.0 | 13.273±0.011 | 0.679±0.046 | C |
| 28992 | 53454.01 | 2005-03-25 | 075.C-0475(A) | OUDMAIJER | 1.0×12×5 | *NB*2.17 | S13 | 68.4 | 13.297±0.089 | 0.147±0.385 | A |
| 29134 | 53690.27 | 2005-11-16 | 076.D-0108(A) | IVANOV | 5.0×10×9 | *IB*2.18 | S27 | 85.7 | 27.143±0.020 | -0.010±0.039 | A |
| | 54373.32 | 2007-09-30 | 080.D-0348(A) | IVANOV | 10.0×5×18 | *IB*2.18 | S27 | 105.7 | 27.146±0.010 | 0.007±0.020 | A |
| | 54387.27 | 2007-10-14 | 080.D-0348(A) | IVANOV | 20.0×3×19 | *IB*2.18 | S27 | 158.6 | 27.153±0.014 | 0.017±0.029 | A |
| | 54407.33 | 2007-11-03 | 080.D-0348(A) | IVANOV | 1.0×50×11 | *IB*2.18 | S27 | 104.3 | 27.156±0.018 | 0.004±0.035 | A |
| | 54408.30 | 2007-11-04 | 080.D-0348(A) | IVANOV | 1.0×50×9 | *IB*2.18 | S27 | 147.1 | 27.140±0.025 | 0.034±0.058 | A |
| 29401 | 53741.18 | 2006-01-06 | 076.C-0170(A) | HUBRIG | 2.0×30×10 | *Ks* | S13 | 69.4 | 13.279±0.024 | 0.015±0.105 | A |
| | 56269.32 | 2012-12-08 | 090.D-0038(A) | SCHOELLER | 10.0×5×20 | *Ks* | S13 | 69.8 | 13.268±0.013 | 0.028±0.056 | A |
| 29728 | 53470.97 | 2005-04-10 | 075.C-0475(A) | OUDMAIJER | 1.0×12×5 | *NB*2.17 | S13 | 71.2 | 13.274±0.112 | 0.272±0.471 | A |
| | 56189.36 | 2012-09-19 | 089.D-0366(A) | ADAM | 6.0×10×6 | *Ks* | S13 | 77.5 | 13.273±0.011 | 0.679±0.046 | C |
| 29941 | 53454.02 | 2005-03-25 | 075.C-0475(A) | OUDMAIJER | 1.0×12×5 | *NB*2.17 | S13 | 67.1 | 13.277±0.089 | -0.037±0.377 | A |

*Continued on next page*

Table A2 – *Continued from previous page*

| HIP | MJD (days) | Observation date | Programme ID | PI | Exposure time (s) | Filter | Camera | FWHM (mas) | Pixel scale (mas/pixel) | Orientation (degree) | Method[a] |
|---|---|---|---|---|---|---|---|---|---|---|---|
| 30143 | 53459.02 | 2005-03-30 | 075.C-0475(A) | OUDMAIJER | 1.0×12×5 | *NB*2.17 | S13 | 70.3 | 13.274±0.081 | -0.090±0.369 | A |
| 30180 | 54056.30 | 2006-11-17 | 078.D-0639(A) | BOUY | 17.4×3×128 | *H* | SDI | 72.5 | 17.250±0.060 | 0.000±0.500 | U |
| 30468 | 53471.98 | 2005-04-11 | 075.C-0475(A) | OUDMAIJER | 1.0×12×5 | *NB*2.17 | S13 | 72.2 | 13.293±0.076 | 0.042±0.315 | A |
| 30493 | 56189.39 | 2012-09-19 | 089.D-0366(A) | ADAM | 10.0×3×5 | *K*s | S13 | 74.9 | 13.273±0.011 | 0.679±0.046 | C |
| 30772 | 53472.98 | 2005-04-12 | 075.C-0475(A) | OUDMAIJER | 0.35×35×5 | *NB*2.17 | S13 | 72.1 | 13.244±0.099 | -0.112±0.428 | A |
| 30867 | 53469.98 | 2005-04-09 | 075.C-0475(A) | OUDMAIJER | 0.35×35×5 | *NB*2.17 | S13 | 74.9 | 13.264±0.102 | -0.226±0.452 | A |
| | 56189.32 | 2012-09-19 | 089.D-0366(A) | ADAM | 3.0×10×5 | *K*s | S13 | 85.3 | 13.273±0.011 | 0.679±0.046 | C |
| 31137 | 53470.98 | 2005-04-10 | 075.C-0475(A) | OUDMAIJER | 1.0×12×5 | *NB*2.17 | S13 | 78.9 | 13.229±0.073 | 0.029±0.283 | A |
| | 56189.35 | 2012-09-19 | 089.D-0366(A) | ADAM | 5.0×10×6 | *K*s | S13 | 106.0 | 13.273±0.011 | 0.679±0.046 | C |
| 31190 | 53471.98 | 2005-04-11 | 075.C-0475(A) | OUDMAIJER | 1.0×12×5 | *NB*2.17 | S13 | 72.1 | 13.285±0.081 | -0.088±0.349 | A |
| 31278 | 54056.35 | 2006-11-17 | 078.D-0639(A) | BOUY | 2.0×26×128 | *H* | SDI | 72.4 | 17.250±0.060 | 0.000±0.500 | U |
| 31959 | 54470.13 | 2008-01-05 | 080.D-0532(A) | BOUY | 36.0×1×128 | *H* | SDI | 70.8 | 17.250±0.060 | 0.000±0.500 | U |
| | 56266.10 | 2012-12-05 | 090.C-0448(A) | VOGT | 1.5×40×7 | *K*s | S13 | 70.1 | 13.265±0.072 | 0.154±0.303 | A |
| 32417 | 53072.02 | 2004-03-08 | 60.A-9026(A) | NACO TEAM | 0.5×40×4 | *NB*2.17 | S13 | 73.8 | 13.221±0.017 | 0.000±0.500 | U |
| 32753 | 53404.10 | 2005-02-03 | 074.D-0374(A) | HUBRIG | 3.8×13×20 | *K*s | S13 | 68.7 | 13.267±0.015 | -0.029±0.063 | A |
| 32823 | 54458.27 | 2007-12-24 | 080.D-0532(A) | BOUY | 50.0×1×128 | *H* | SDI | 61.0 | 17.250±0.060 | 0.000±0.500 | U |
| 32827 | 53507.96 | 2005-05-17 | 075.C-0475(A) | OUDMAIJER | 3.0×4×5 | *NB*2.17 | S13 | 76.4 | 13.245±0.095 | 0.089±0.406 | A |
| 32912 | 53733.23 | 2005-12-29 | 076.D-0108(A) | IVANOV | 5.0×10×9 | *IB*2.18 | S27 | 76.8 | 27.156±0.019 | -0.003±0.036 | A |
| 33211 | 54476.20 | 2008-01-11 | 080.D-0532(A) | BOUY | 45.0×1×128 | *H* | SDI | 59.6 | 17.250±0.060 | 0.000±0.500 | U |
| 33276 | 54481.10 | 2008-01-16 | 080.D-0532(A) | BOUY | 47.0×1×160 | *H* | SDI | 70.6 | 17.250±0.060 | 0.000±0.500 | U |
| 33343 | 54483.02 | 2008-01-18 | 080.D-0532(A) | BOUY | 46.0×1×128 | *H* | SDI | 60.3 | 17.250±0.060 | 0.000±0.500 | U |
| 33611 | 54485.18 | 2008-01-20 | 080.D-0532(A) | BOUY | 8.0×4×128 | *H* | SDI | 66.6 | 17.250±0.060 | 0.000±0.500 | U |
| 33650 | 53731.31 | 2005-12-27 | 076.C-0170(A) | HUBRIG | 0.75×80×10 | *K*s | S13 | 75.7 | 13.271±0.021 | 0.058±0.092 | A |
| 33769 | 54421.35 | 2007-11-17 | 080.D-0532(A) | BOUY | 19.0×1×128 | *H* | SDI | 78.4 | 17.250±0.060 | 0.000±0.500 | U |
| 33814 | 54477.22 | 2008-01-12 | 080.D-0532(A) | BOUY | 40.0×1×128 | *H* | SDI | 72.7 | 17.250±0.060 | 0.000±0.500 | U |
| 33846 | 54485.20 | 2008-01-20 | 080.D-0532(A) | BOUY | 6.6×4×128 | *H* | SDI | 61.0 | 17.250±0.060 | 0.000±0.500 | U |

*Continued on next page*

Table A2 – *Continued from previous page*

| HIP | MJD (days) | Observation date | Programme ID | PI | Exposure time (s) | Filter | Camera | FWHM (mas) | Pixel scale (mas/pixel) | Orientation (degree) | Method[a] |
|---|---|---|---|---|---|---|---|---|---|---|---|
| 34041 | 54497.14 | 2008-02-01 | 080.D-0532(A) | BOUY | 6.0×4×128 | *H* | SDI | 59.4 | 17.250±0.060 | 0.000±0.500 | U |
| 34045 | 53408.13 | 2005-02-07 | 074.D-0374(A) | HUBRIG | 0.9×55×15 | *K*s | S13 | 71.2 | 13.261±0.017 | 0.021±0.076 | A |
| | 56298.14 | 2013-01-06 | 090.D-0038(A) | SCHOELLER | 2.0×22×20 | *K*s | S13 | 69.1 | 13.270±0.020 | 0.056±0.087 | A |
| 34153 | 54499.15 | 2008-02-03 | 080.D-0532(A) | BOUY | 35.0×1×128 | *H* | SDI | 63.6 | 17.250±0.060 | 0.000±0.500 | U |
| 34281 | 54499.02 | 2008-02-03 | 080.D-0532(A) | BOUY | 53.0×1×128 | *H* | SDI | 67.8 | 17.250±0.060 | 0.000±0.500 | U |
| 34338 | 53408.16 | 2005-02-07 | 074.D-0374(A) | HUBRIG | 6.0×9×20 | *K*s | S13 | 73.4 | 13.279±0.014 | 0.052±0.058 | A |
| | 56296.21 | 2013-01-04 | 090.D-0038(A) | SCHOELLER | 10.0×5×20 | *K*s | S13 | 70.1 | 13.259±0.014 | -0.027±0.060 | A |
| 34579 | 53507.97 | 2005-05-17 | 075.C-0475(A) | OUDMAIJER | 1.0×12×5 | *NB*2.17 | S13 | 74.8 | 13.280±0.091 | -0.113±0.416 | A |
| 34758 | 53413.19 | 2005-02-12 | 074.D-0180(A) | IVANOV | 0.3454×149×9 | *K*s | S27 | 97.6 | 27.151±0.041 | -0.027±0.086 | A |
| | 54425.35 | 2007-11-21 | 080.D-0348(A) | IVANOV | 1.0362×49×9 | *K*s | S27 | 80.8 | 27.145±0.040 | 0.005±0.082 | A |
| 34898 | 54482.23 | 2008-01-17 | 080.D-0532(A) | BOUY | 28.0×1×128 | *H* | SDI | 62.0 | 17.250±0.060 | 0.000±0.500 | U |
| 34968 | 54497.08 | 2008-02-01 | 080.D-0532(A) | BOUY | 31.6×1×128 | *H* | SDI | 61.5 | 17.250±0.060 | 0.000±0.500 | U |
| 35037 | 53470.99 | 2005-04-10 | 075.C-0475(A) | OUDMAIJER | 0.35×36×5 | *NB*2.17 | S13 | 78.9 | 13.255±0.074 | 0.097±0.314 | A |
| 35110 | 54497.11 | 2008-02-01 | 080.D-0532(A) | BOUY | 24.0×1×128 | *H* | SDI | 67.9 | 17.250±0.060 | 0.000±0.500 | U |
| 35168 | 54481.16 | 2008-01-16 | 080.D-0532(A) | BOUY | 34.8×1×128 | *H* | SDI | 107.8 | 17.250±0.060 | 0.000±0.500 | U |
| 35267 | 54482.26 | 2008-01-17 | 080.D-0532(A) | BOUY | 27.4×1×128 | *H* | SDI | 61.7 | 17.250±0.060 | 0.000±0.500 | U |
| 35413 | 54477.30 | 2008-01-12 | 080.D-0532(A) | BOUY | 48.0×1×128 | *H* | SDI | 71.7 | 17.250±0.060 | 0.000±0.500 | U |
| 35920 | 54481.22 | 2008-01-16 | 080.D-0532(A) | BOUY | 21.0×1×128 | *H* | SDI | 134.0 | 17.250±0.060 | 0.000±0.500 | U |
| 35951 | 53454.04 | 2005-03-25 | 075.C-0475(A) | OUDMAIJER | 0.35×35×5 | *NB*2.17 | S13 | 67.6 | 13.266±0.109 | 0.135±0.459 | A |
| 36009 | 54477.26 | 2008-01-12 | 080.D-0532(A) | BOUY | 30.0×1×128 | *H* | SDI | 79.2 | 17.250±0.060 | 0.000±0.500 | U |
| 36345 | 54839.34 | 2009-01-08 | 482.L-0802(A) | FORVEILLE | 0.6×20×12 | *NB*2.12 | S27 | 75.4 | 27.053±0.019 | 0.000±0.500 | U |
| 36363 | 53384.19 | 2005-01-14 | 074.D-0180(A) | IVANOV | 1.0×50×9 | *IB*2.18 | S27 | 82.0 | 27.094±0.063 | 0.020±0.140 | A |
| | 54427.20 | 2007-11-23 | 080.D-0348(A) | IVANOV | 5.0×10×9 | *IB*2.18 | S27 | 83.3 | 27.151±0.035 | -0.007±0.076 | A |
| 36944 | 54458.32 | 2007-12-24 | 080.D-0532(A) | BOUY | 52.0×1×128 | *H* | SDI | 76.8 | 17.250±0.060 | 0.000±0.500 | U |
| 37322 | 53384.20 | 2005-01-14 | 074.D-0180(A) | IVANOV | 0.3454×149×9 | *K*s | S27 | 78.8 | 27.122±0.035 | 0.013±0.076 | A |
| | 54412.36 | 2007-11-08 | 080.D-0348(A) | IVANOV | 1.0×52×18 | *K*s | S27 | 121.7 | 27.147±0.026 | 0.002±0.059 | A |

*Continued on next page*

Table A2 – *Continued from previous page*

| HIP | MJD (days) | Observation date | Programme ID | PI | Exposure time (s) | Filter | Camera | FWHM (mas) | Pixel scale (mas/pixel) | Orientation (degree) | Method[a] |
|---|---|---|---|---|---|---|---|---|---|---|---|
| 37345 | 53471.99 | 2005-04-11 | 075.C-0475(A) | OUDMAIJER | 1.0×12×5 | *NB*2.17 | S13 | 74.1 | 13.292±0.093 | 0.035±0.414 | A |
| 37450 | 53384.22 | 2005-01-14 | 074.D-0180(A) | IVANOV | 1.0×50×9 | *IB*2.18 | S27 | 78.8 | 27.076±0.062 | -0.040±0.118 | A |
| 37623 | 53384.23 | 2005-01-14 | 074.D-0180(A) | IVANOV | 0.3454×149×9 | *Ks* | S27 | 76.1 | 27.107±0.033 | 0.012±0.065 | A |
| 37752 | 53384.24 | 2005-01-14 | 074.D-0180(A) | IVANOV | 0.3454×149×9 | *Ks* | S27 | 76.1 | 27.107±0.036 | -0.040±0.078 | A |
| 37915 | 53384.26 | 2005-01-14 | 074.D-0180(A) | IVANOV | 0.3454×149×9 | *Ks* | S27 | 78.2 | 27.119±0.037 | 0.058±0.079 | A |
| | 54427.18 | 2007-11-23 | 080.D-0348(A) | IVANOV | 2.0×25×9 | *Ks* | S27 | 86.9 | 27.146±0.035 | -0.001±0.075 | A |
| 38373 | 53380.21 | 2005-01-10 | 074.D-0374(A) | HUBRIG | 5.0×11×20 | *Ks* | S13 | 74.8 | 13.259±0.016 | 0.012±0.065 | A |
| 38906 | 53331.33 | 2004-11-22 | 074.D-0374(A) | HUBRIG | 10.0×5×20 | *Ks* | S13 | 97.4 | 13.262±0.012 | -0.004±0.048 | A |
| 39184 | 53384.27 | 2005-01-14 | 074.D-0180(A) | IVANOV | 0.3454×149×5 | *Ks* | S27 | 78.2 | 27.114±0.161 | 0.061±0.283 | A |
| | 53414.21 | 2005-02-13 | 074.D-0180(A) | IVANOV | 0.3454×149×9 | *Ks* | S27 | 81.4 | 27.147±0.029 | -0.040±0.057 | A |
| 39331 | 54120.30 | 2007-01-20 | 60.A-9026(A) | NACO TEAM | 0.5×24×5 | *Ks* | S27 | 93.8 | 27.152±0.067 | 0.076±0.139 | A |
| 39906 | 53523.98 | 2005-06-02 | 075.C-0475(A) | OUDMAIJER | 0.35×35×5 | *NB*2.17 | S13 | 69.8 | 13.309±0.096 | -0.102±0.419 | A |
| 39970 | 53523.96 | 2005-06-02 | 075.C-0475(A) | OUDMAIJER | 0.35×35×5 | *NB*2.17 | S13 | 67.8 | 13.309±0.073 | -0.040±0.314 | A |
| 40085 | 53711.34 | 2005-12-07 | 076.C-0170(A) | HUBRIG | 0.6×100×10 | *Ks* | S13 | 66.3 | 13.270±0.023 | -0.006±0.095 | A |
| 40321 | 53523.98 | 2005-06-02 | 075.C-0475(A) | OUDMAIJER | 0.35×35×5 | *NB*2.17 | S13 | 68.2 | 13.260±0.071 | 0.054±0.324 | A |
| 40787 | 53374.21 | 2005-01-04 | 074.D-0374(A) | HUBRIG | 6.0×9×20 | *Ks* | S13 | 86.0 | 13.249±0.012 | 0.047±0.055 | A |
| | 53380.24 | 2005-01-10 | 074.D-0374(A) | HUBRIG | 9.0×6×20 | *Ks* | S13 | 73.8 | 13.256±0.013 | -0.027±0.055 | A |
| 40817 | 53415.17 | 2005-02-14 | 074.D-0180(A) | IVANOV | 1.0×50×9 | *IB*2.18 | S27 | 82.0 | 27.150±0.019 | -0.020±0.042 | A |
| | 54451.32 | 2007-12-17 | 080.D-0348(A) | IVANOV | 1.0×50×9 | *IB*2.18 | S27 | 133.1 | 27.127±0.034 | 0.015±0.057 | A |
| | 54467.29 | 2008-01-02 | 080.D-0348(A) | IVANOV | 5.0×10×9 | *IB*2.18 | S27 | 78.8 | 27.155±0.018 | -0.007±0.034 | A |
| 40834 | 53404.22 | 2005-02-03 | 074.D-0374(A) | HUBRIG | 3.8×13×20 | *Ks* | S13 | 76.6 | 13.268±0.006 | 0.011±0.026 | A |
| | 54425.31 | 2007-11-21 | 080.D-0348(A) | IVANOV | 0.6908×74×9 | *Ks* | S27 | 89.9 | 27.166±0.017 | -0.005±0.039 | A |
| 41049 | 53100.00 | 2004-04-04 | 60.A-9026(A) | NACO TEAM | 0.5×40×4 | *NB*2.17 | S13 | 70.3 | 13.221±0.017 | 0.000±0.500 | U |
| 41296 | 53526.97 | 2005-06-05 | 075.C-0475(A) | OUDMAIJER | 0.35×35×5 | *NB*2.17 | S13 | 74.3 | 13.259±0.073 | -0.135±0.334 | A |
| | 53684.37 | 2005-11-10 | 076.D-0108(A) | IVANOV | 5.0×10×9 | *IB*2.18 | S27 | 82.0 | 27.153±0.029 | -0.018±0.063 | A |
| | 54425.33 | 2007-11-21 | 080.D-0348(A) | IVANOV | 10.0×5×9 | *IB*2.18 | S27 | 81.4 | 27.166±0.029 | -0.005±0.064 | A |

*Continued on next page*

Table A2 – *Continued from previous page*

| HIP | MJD (days) | Observation date | Programme ID | PI | Exposure time (s) | Filter | Camera | FWHM (mas) | Pixel scale (mas/pixel) | Orientation (degree) | Method[a] |
|---|---|---|---|---|---|---|---|---|---|---|---|
| 41603 | 53403.31 | 2005-02-02 | 074.D-0374(A) | HUBRIG | 10.0×5×20 | *Ks* | S13 | 72.2 | 13.262±0.013 | -0.002±0.057 | A |
| 41674 | 53342.37 | 2004-12-03 | 074.D-0180(A) | IVANOV | 2.0×25×11 | *Ks* | S27 | 89.3 | 27.116±0.030 | 0.015±0.060 | A |
| 41817 | 53413.22 | 2005-02-12 | 074.D-0180(A) | IVANOV | 1.0×50×9 | *IB*2.18 | S27 | 77.5 | 27.151±0.097 | -0.042±0.198 | A |
| | 54425.30 | 2007-11-21 | 080.D-0348(A) | IVANOV | 3.0×16×9 | *IB*2.18 | S27 | 87.5 | 27.162±0.062 | -0.003±0.132 | A |
| 41843 | 53404.24 | 2005-02-03 | 074.D-0374(A) | HUBRIG | 10.0×5×20 | *Ks* | S13 | 71.2 | 13.278±0.013 | 0.002±0.057 | A |
| | 56326.14 | 2013-02-03 | 090.D-0038(A) | SCHOELLER | 15.0×3×20 | *Ks* | S13 | 73.9 | 13.279±0.013 | -0.010±0.057 | A |
| 42001 | 53354.33 | 2004-12-15 | 074.D-0180(A) | IVANOV | 0.3454×149×9 | *Ks* | S27 | 106.2 | 27.089±0.038 | -0.027±0.085 | A |
| | 53414.23 | 2005-02-13 | 074.D-0180(A) | IVANOV | 0.3454×149×9 | *Ks* | S27 | 80.8 | 27.162±0.036 | 0.005±0.077 | A |
| | 54501.21 | 2008-02-05 | 080.D-0348(A) | IVANOV | 0.3454×148×9 | *Ks* | S27 | 89.9 | 27.165±0.041 | -0.029±0.084 | A |
| 42129 | 53738.19 | 2006-01-03 | 076.D-0108(A) | IVANOV | 10.0×5×9 | *IB*2.18 | S27 | 75.5 | 27.143±0.029 | 0.025±0.057 | A |
| | 54451.33 | 2007-12-17 | 080.D-0348(A) | IVANOV | 1.0×49×9 | *IB*2.18 | S27 | 94.9 | 27.166±0.030 | -0.019±0.070 | A |
| 42177 | 53404.27 | 2005-02-03 | 074.D-0374(A) | HUBRIG | 3.8×13×20 | *Ks* | S13 | 72.7 | 13.278±0.010 | -0.012±0.044 | A |
| 42334 | 53434.19 | 2005-03-05 | 074.D-0180(A) | IVANOV | 5.0×10×9 | *IB*2.18 | S27 | 78.2 | 27.130±0.041 | -0.004±0.084 | A |
| | 54508.15 | 2008-02-12 | 080.D-0348(A) | IVANOV | 1.0×49×9 | *IB*2.18 | S27 | 78.2 | 27.161±0.035 | 0.013±0.076 | A |
| 42459 | 53526.98 | 2005-06-05 | 075.C-0475(A) | OUDMAIJER | 1.0×12×5 | *NB*2.17 | S13 | 75.3 | 13.257±0.072 | -0.077±0.315 | A |
| | 53738.21 | 2006-01-03 | 076.D-0108(A) | IVANOV | 10.0×5×9 | *IB*2.18 | S27 | 75.5 | 27.141±0.029 | -0.009±0.059 | A |
| 42504 | 53742.18 | 2006-01-07 | 076.D-0108(A) | IVANOV | 10.0×5×18 | *IB*2.18 | S27 | 92.1 | 27.148±0.015 | 0.028±0.033 | A |
| 42535 | 53742.20 | 2006-01-07 | 076.D-0108(A) | IVANOV | 3.5×15×9 | *Ks* | S27 | 86.9 | 27.152±0.029 | 0.035±0.058 | A |
| 42540 | 53375.26 | 2005-01-05 | 074.D-0180(A) | IVANOV | 1.0×50×9 | *IB*2.18 | S27 | 86.9 | 27.108±0.038 | -0.045±0.081 | A |
| | 54451.34 | 2007-12-17 | 080.D-0348(A) | IVANOV | 1.0×49×9 | *IB*2.18 | S27 | 94.9 | 27.128±0.038 | -0.017±0.086 | A |
| 42637 | 53742.31 | 2006-01-07 | 076.D-0108(A) | IVANOV | 25.0×2×9 | *IB*2.18 | S27 | 180.6 | 27.142±0.014 | -0.007±0.024 | A |
| 42715 | 53742.22 | 2006-01-07 | 076.D-0108(A) | IVANOV | 10.0×5×9 | *IB*2.18 | S27 | 97.1 | 27.147±0.032 | 0.058±0.063 | A |
| | 54509.21 | 2008-02-13 | 080.D-0348(A) | IVANOV | 10.0×5×9 | *IB*2.18 | S27 | 86.9 | 27.168±0.030 | 0.017±0.063 | A |
| 43073 | 53454.10 | 2005-03-25 | 075.C-0475(A) | OUDMAIJER | 1.0×12×5 | *NB*2.17 | S13 | 73.6 | 13.270±0.076 | 0.088±0.320 | A |
| 43305 | 53379.29 | 2005-01-09 | 074.D-0374(A) | HUBRIG | 2.4×22×20 | *Ks* | S13 | 68.7 | 13.261±0.013 | 0.014±0.057 | A |
| | 54509.23 | 2008-02-13 | 080.D-0348(A) | IVANOV | 5.0×10×9 | *IB*2.18 | S27 | 83.3 | 27.157±0.042 | -0.003±0.084 | A |

*Continued on next page*

Table A2 – *Continued from previous page*

| HIP | MJD (days) | Observation date | Programme ID | PI | Exposure time (s) | Filter | Camera | FWHM (mas) | Pixel scale (mas/pixel) | Orientation (degree) | Method[a] |
|---|---|---|---|---|---|---|---|---|---|---|---|
| 43499 | 53750.08 | 2006-01-15 | 076.D-0108(A) | IVANOV | 0.3454×149×9 | *Ks* | S27 | 81.4 | 27.142±0.026 | 0.008±0.058 | A |
| 43689 | 53044.20 | 2004-02-09 | 60.A-9026(A) | NACO TEAM | 10.0×6×6 | *NB*2.17 | S27 | 30.5 | 27.080±0.085 | 0.055±0.190 | A |
| 43792 | 52659.32 | 2003-01-20 | 70.C-0701(A) | ZINNECKER | 0.6×20×3 | *NB*2.12 | S13 | 71.9 | 14.400±0.000 | -0.024±0.000 | A |
| 44299 | 53750.09 | 2006-01-15 | 076.D-0108(A) | IVANOV | 2.0×25×9 | *Ks* | S27 | 86.9 | 27.160±0.035 | 0.015±0.071 | A |
| | 54451.35 | 2007-12-17 | 080.D-0348(A) | IVANOV | 0.3454×148×9 | *Ks* | S27 | 98.7 | 27.174±0.034 | 0.026±0.071 | A |
| 44798 | 53380.28 | 2005-01-10 | 074.D-0374(A) | HUBRIG | 20.0×3×22 | *Ks* | S13 | 74.4 | 13.260±0.014 | -0.022±0.061 | A |
| 44883 | 53382.27 | 2005-01-12 | 074.D-0180(A) | IVANOV | 0.3454×149×9 | *Ks* | S27 | 84.5 | 27.094±0.040 | -0.022±0.083 | A |
| | 54468.30 | 2008-01-03 | 080.D-0348(A) | IVANOV | 0.3454×148×9 | *Ks* | S27 | 86.3 | 27.131±0.038 | -0.016±0.082 | A |
| 45189 | 53382.32 | 2005-01-12 | 074.D-0180(A) | IVANOV | 0.3454×149×9 | *Ks* | S27 | 92.7 | 27.095±0.032 | 0.009±0.067 | A |
| | 54467.30 | 2008-01-02 | 080.D-0348(A) | IVANOV | 1.0×52×9 | *Ks* | S27 | 80.1 | 27.138±0.034 | 0.043±0.073 | A |
| 45270 | 53355.38 | 2004-12-16 | 074.D-0180(A) | IVANOV | 0.3454×149×9 | *Ks* | S27 | 81.4 | 27.095±0.034 | 0.014±0.068 | A |
| | 53493.01 | 2005-05-03 | 075.C-0475(A) | OUDMAIJER | 2.0×6×5 | *NB*2.17 | S13 | 72.1 | 13.311±0.061 | -0.074±0.300 | A |
| 45314 | 53355.36 | 2004-12-16 | 074.D-0180(A) | IVANOV | 0.3454×149×9 | *Ks* | S27 | 78.8 | 27.082±0.031 | 0.001±0.065 | A |
| | 54511.14 | 2008-02-15 | 080.D-0348(A) | IVANOV | 1.0×50×9 | *Ks* | S27 | 79.5 | 27.147±0.034 | -0.028±0.075 | A |
| | 56265.36 | 2012-12-04 | 090.C-0448(A) | VOGT | 1.0×30×12 | *NB*2.17 | S13 | 68.7 | 13.267±0.011 | 0.572±0.049 | C |
| 45344 | 53349.38 | 2004-12-10 | 074.D-0180(A) | IVANOV | 2.0×25×9 | *IB*2.18 | S27 | 78.8 | 27.097±0.033 | 0.012±0.068 | A |
| | 54511.16 | 2008-02-15 | 080.D-0348(A) | IVANOV | 2.0×25×9 | *IB*2.18 | S27 | 72.7 | 27.151±0.031 | -0.015±0.068 | A |
| 45631 | 53750.10 | 2006-01-15 | 076.D-0108(A) | IVANOV | 5.0×10×9 | *IB*2.18 | S27 | 83.9 | 27.147±0.028 | -0.014±0.065 | A |
| 45941 | 53507.98 | 2005-05-17 | 075.C-0475(A) | OUDMAIJER | 6.0×2×5 | *NB*2.17 | S13 | 73.6 | 13.276±0.067 | 0.014±0.281 | A |
| 46283 | 53750.26 | 2006-01-15 | 076.D-0108(A) | IVANOV | 5.0×10×9 | *IB*2.18 | S27 | 82.7 | 27.147±0.033 | -0.020±0.061 | A |
| | 54475.31 | 2008-01-10 | 080.D-0348(A) | IVANOV | 5.0×10×9 | *IB*2.18 | S27 | 86.3 | 27.152±0.028 | -0.050±0.061 | A |
| 46329 | 53454.11 | 2005-03-25 | 075.C-0475(A) | OUDMAIJER | 1.0×12×5 | *NB*2.17 | S13 | 70.7 | 13.305±0.082 | -0.126±0.347 | A |
| 46594 | 53753.23 | 2006-01-18 | 076.D-0108(A) | IVANOV | 5.0×10×9 | *IB*2.18 | S27 | 74.1 | 27.146±0.029 | 0.009±0.059 | A |
| | 54535.10 | 2008-03-10 | 080.D-0348(A) | IVANOV | 4.0×13×9 | *IB*2.18 | S27 | 80.8 | 27.133±0.031 | -0.007±0.063 | A |
| 46914 | 53442.14 | 2005-03-13 | 074.D-0180(A) | IVANOV | 5.0×10×9 | *IB*2.18 | S27 | 92.1 | 27.155±0.036 | 0.026±0.076 | A |
| | 54535.11 | 2008-03-10 | 080.D-0348(A) | IVANOV | 1.0×49×9 | *IB*2.18 | S27 | 78.8 | 27.142±0.022 | -0.015±0.020 | A |

*Continued on next page*

Table A2 – *Continued from previous page*

| HIP | MJD (days) | Observation date | Programme ID | PI | Exposure time (s) | Filter | Camera | FWHM (mas) | Pixel scale (mas/pixel) | Orientation (degree) | Method[a] |
|---|---|---|---|---|---|---|---|---|---|---|---|
| 46928 | 53778.24 | 2006-02-12 | 076.D-0108(A) | IVANOV | 25.0×2×9 | *IB*2.18 | S27 | 85.7 | 27.154±0.009 | 0.001±0.019 | A |
| | 54475.33 | 2008-01-10 | 080.D-0348(A) | IVANOV | 10.0×1×9 | *IB*2.18 | S27 | 92.7 | 27.156±0.009 | -0.007±0.020 | A |
| 47452 | 53347.39 | 2004-12-08 | 074.D-0180(A) | IVANOV | 5.0×10×8 | *IB*2.18 | S27 | 74.8 | 27.125±0.051 | 0.026±0.102 | A |
| | 54511.25 | 2008-02-15 | 080.D-0348(A) | IVANOV | 2.0×25×9 | *IB*2.18 | S27 | 81.4 | 27.128±0.038 | 0.032±0.081 | A |
| 47522 | 53523.99 | 2005-06-02 | 075.C-0475(A) | OUDMAIJER | 0.35×35×5 | *NB*2.17 | S13 | 69.8 | 13.290±0.181 | -0.192±0.732 | A |
| 48224 | 53380.32 | 2005-01-10 | 074.D-0180(A) | IVANOV | 10.0×5×9 | *IB*2.18 | S27 | 83.3 | 27.098±0.032 | -0.009±0.062 | A |
| 48943 | 53493.02 | 2005-05-03 | 075.C-0475(A) | OUDMAIJER | 1.0×12×5 | *NB*2.17 | S13 | 72.6 | 13.248±0.091 | -0.011±0.396 | A |
| 49712 | 53527.00 | 2005-06-05 | 075.C-0475(A) | OUDMAIJER | 0.35×35×5 | *NB*2.17 | S13 | 72.6 | 13.251±0.064 | -0.021±0.275 | A |
| 50044 | 53523.99 | 2005-06-02 | 075.C-0475(A) | OUDMAIJER | 1.0×12×5 | *NB*2.17 | S13 | 70.1 | 13.246±0.065 | -0.136±0.252 | A |
| 50480 | 53442.16 | 2005-03-13 | 074.D-0180(A) | IVANOV | 0.3454×149×9 | *Ks* | S27 | 85.7 | 27.139±0.033 | 0.038±0.078 | A |
| 50847 | 53779.20 | 2006-02-13 | 076.C-0170(A) | HUBRIG | 5.4×15×10 | *Ks* | S13 | 75.9 | 13.273±0.013 | 0.022±0.053 | A |
| | 55673.11 | 2011-04-22 | 087.D-0197(A) | SCHOELLER | 5.0×12×18 | *Ks* | S13 | 79.4 | 13.272±0.007 | 0.005±0.028 | A |
| 51362 | 53185.02 | 2004-06-29 | 272.D-5068(A) | IVANOV | 5.0×9×9 | *IB*2.18 | S27 | 79.5 | 27.095±0.040 | 0.043±0.088 | A |
| | 53846.12 | 2006-04-21 | 077.D-0147(A) | IVANOV | 24.0×4×7 | *IB*2.18 | S27 | 88.7 | 27.151±0.051 | 0.010±0.110 | A |
| 51376 | 53405.28 | 2005-02-04 | 074.D-0180(A) | IVANOV | 0.3454×149×9 | *Ks* | S27 | 101.8 | 27.157±0.041 | -0.029±0.088 | A |
| | 53415.32 | 2005-02-14 | 074.D-0180(A) | IVANOV | 0.3454×149×9 | *Ks* | S27 | 81.4 | 27.159±0.047 | -0.050±0.098 | A |
| | 54521.20 | 2008-02-25 | 080.D-0348(A) | IVANOV | 0.3454×148×9 | *Ks* | S27 | 83.3 | 27.166±0.036 | -0.013±0.074 | A |
| 51437 | 53368.38 | 2004-12-29 | 074.D-0180(A) | IVANOV | 1.0×50×9 | *IB*2.18 | S27 | 69.8 | 27.122±0.042 | -0.020±0.090 | A |
| 51491 | 53787.19 | 2006-02-21 | 076.D-0108(A) | IVANOV | 1.0×52×9 | *Ks* | S27 | 92.1 | 27.151±0.036 | -0.004±0.078 | A |
| 52221 | 53779.24 | 2006-02-13 | 076.D-0108(A) | IVANOV | 2.0×26×9 | *Ks* | S27 | 81.4 | 27.137±0.022 | -0.008±0.043 | A |
| 52742 | 53794.08 | 2006-02-28 | 076.D-0108(A) | IVANOV | 10.0×5×10 | *IB*2.18 | S27 | 85.1 | 27.151±0.027 | 0.012±0.052 | A |
| | 54483.36 | 2008-01-18 | 080.D-0348(A) | IVANOV | 5.0×10×9 | *IB*2.18 | S27 | 88.1 | 27.150±0.025 | -0.025±0.055 | A |
| 53272 | 53779.26 | 2006-02-13 | 076.D-0108(A) | IVANOV | 4.0×13×9 | *Ks* | S27 | 82.0 | 27.152±0.019 | -0.011±0.036 | A |
| | 54511.30 | 2008-02-15 | 080.D-0348(A) | IVANOV | 2.0×26×9 | *Ks* | S27 | 85.1 | 27.158±0.016 | -0.011±0.038 | A |
| 53762 | 53406.33 | 2005-02-05 | 074.D-0180(A) | IVANOV | 0.3454×149×9 | *Ks* | S27 | 84.5 | 27.155±0.032 | 0.003±0.070 | A |
| | 53489.12 | 2005-04-29 | 075.C-0475(A) | OUDMAIJER | 1.0×12×5 | *NB*2.17 | S13 | 72.1 | 13.245±0.082 | -0.100±0.389 | A |

*Continued on next page*

Table A2 – *Continued from previous page*

| HIP | MJD (days) | Observation date | Programme ID | PI | Exposure time (s) | Filter | Camera | FWHM (mas) | Pixel scale (mas/pixel) | Orientation (degree) | Method[a] |
|---|---|---|---|---|---|---|---|---|---|---|---|
| 54255 | 53789.11 | 2006-02-23 | 076.D-0108(A) | IVANOV | 1.0×52×9 | *Ks* | S27 | 81.4 | 27.150±0.047 | -0.001±0.094 | A |
| 54257 | 53820.41 | 2006-03-26 | 076.C-0579(A) | BRANDEKER | 0.3454×15×6 | *Ks* | S13 | 123.6 | 13.275±0.060 | 0.033±0.253 | A |
| 54413 | 54882.15 | 2009-02-20 | 082.C-0489(A) | VOGT | 0.3454×87×44 | *Ks* | S13 | 92.1 | 13.275±0.045 | 0.428±0.109 | B |
| | 55555.33 | 2010-12-25 | 086.C-0638(A) | VOGT | 0.5×120×25 | *Ks* | S13 | 88.5 | 13.271±0.016 | 0.599±0.069 | C |
| | 55645.12 | 2011-03-25 | 086.C-0600(B) | VOGT | 0.3454×87×62 | *Ks* | S13 | 79.6 | 13.274±0.045 | 0.639±0.118 | B |
| 54557 | 53794.13 | 2006-02-28 | 076.C-0708(A) | THOMAS | 2.0×100×5 | *NB*2.12 | S13 | 77.5 | 13.272±0.020 | -0.017±0.078 | A |
| | 53820.40 | 2006-03-26 | 076.C-0579(A) | BRANDEKER | 0.3454×15×6 | *Ks* | S13 | 85.3 | 13.268±0.040 | -0.014±0.177 | A |
| | 54160.10 | 2007-03-01 | 078.C-0535(A) | VOGT | 0.5×110×20 | *Ks* | S13 | 76.9 | 13.268±0.045 | 0.040±0.101 | B |
| | 54516.21 | 2008-02-20 | 080.C-0424(A) | VOGT | 0.5×120×5 | *Ks* | S13 | 76.6 | 13.279±0.045 | 0.347±0.105 | B |
| | 55605.34 | 2011-02-13 | 086.C-0762(D) | DAEMGEN | 1.0×13×5 | *Ks* | S13 | 70.5 | 13.280±0.019 | -0.000±0.114 | A |
| 54767 | 53779.27 | 2006-02-13 | 076.D-0108(A) | IVANOV | 10.0×5×9 | *IB*2.18 | S27 | 82.0 | 27.148±0.025 | 0.002±0.048 | A |
| 54829 | 55675.97 | 2011-04-24 | 60.A-9800(J) | OBSERVATORY, P | 1.0×10×6 | *NB*2.17 | S13 | 76.6 | 13.269±0.044 | -0.106±0.227 | A |
| 55597 | 53752.37 | 2006-01-17 | 076.D-0108(A) | IVANOV | 10.0×5×9 | *IB*2.18 | S27 | 76.1 | 27.154±0.023 | 0.024±0.047 | A |
| | 54520.28 | 2008-02-24 | 080.D-0348(A) | IVANOV | 0.5×100×9 | *IB*2.18 | S27 | 91.0 | 27.109±0.012 | -0.007±0.006 | A |
| 55657 | 53741.38 | 2006-01-06 | 076.D-0108(A) | IVANOV | 0.7×74×9 | *Ks* | S27 | 81.4 | 27.144±0.018 | 0.005±0.038 | A |
| 55667 | 53459.09 | 2005-03-30 | 075.C-0475(A) | OUDMAIJER | 3.0×4×5 | *NB*2.17 | S13 | 77.2 | 13.290±0.103 | -0.120±0.379 | A |
| 56000 | 53408.25 | 2005-02-07 | 074.D-0180(A) | IVANOV | 1.0×50×9 | *IB*2.18 | S27 | 85.7 | 27.146±0.033 | 0.043±0.075 | A |
| | 54520.30 | 2008-02-24 | 080.D-0348(A) | IVANOV | 1.0×49×9 | *IB*2.18 | S27 | 86.3 | 27.142±0.033 | -0.023±0.070 | A |
| 56379 | 53171.00 | 2004-06-15 | 073.C-0178(A) | FELDT | 0.3×35×12 | *Ks* | S13 | 101.9 | 13.266±0.010 | 0.035±0.034 | A |
| 56480 | 53454.18 | 2005-03-25 | 075.C-0475(A) | OUDMAIJER | 0.35×35×5 | *NB*2.17 | S13 | 76.2 | 13.266±0.065 | 0.070±0.255 | A |
| 56754 | 53403.36 | 2005-02-02 | 074.D-0374(A) | HUBRIG | 2.4×22×20 | *Ks* | S13 | 75.7 | 13.278±0.008 | 0.022±0.036 | A |
| | 54475.35 | 2008-01-10 | 080.D-0348(A) | IVANOV | 5.0×10×9 | *IB*2.18 | S27 | 82.7 | 27.137±0.028 | 0.021±0.064 | A |
| | 55673.08 | 2011-04-22 | 087.D-0197(A) | SCHOELLER | 4.0×15×16 | *Ks* | S13 | 75.6 | 13.270±0.010 | 0.021±0.047 | A |
| 57371 | 53441.22 | 2005-03-12 | 074.D-0180(A) | IVANOV | 10.0×10×9 | *IB*2.18 | S27 | 86.3 | 27.155±0.032 | 0.015±0.064 | A |
| | 53796.33 | 2006-03-02 | 076.D-0108(A) | IVANOV | 10.0×5×9 | *IB*2.18 | S27 | 84.5 | 27.159±0.033 | 0.040±0.073 | A |
| 58326 | 53779.31 | 2006-02-13 | 076.D-0108(A) | IVANOV | 2.0×26×9 | *Ks* | S27 | 82.7 | 27.155±0.024 | -0.026±0.046 | A |

*Continued on next page*

Table A2 – *Continued from previous page*

| HIP | MJD (days) | Observation date | Programme ID | PI | Exposure time (s) | Filter | Camera | FWHM (mas) | Pixel scale (mas/pixel) | Orientation (degree) | Method[a] |
|---|---|---|---|---|---|---|---|---|---|---|---|
| | 54475.34 | 2008-01-10 | 080.D-0348(A) | IVANOV | 0.3454×148×9 | *Ks* | S27 | 82.7 | 27.159±0.025 | 0.005±0.054 | A |
| 58379 | 53768.35 | 2006-02-02 | 076.D-0108(A) | IVANOV | 5.0×10×9 | *IB*2.18 | S27 | 83.3 | 27.136±0.028 | -0.022±0.058 | A |
| 58587 | 53454.19 | 2005-03-25 | 075.C-0475(A) | OUDMAIJER | 0.35×35×5 | *NB*2.17 | S13 | 73.8 | 13.251±0.080 | 0.114±0.369 | A |
| 58720 | 53442.22 | 2005-03-13 | 074.D-0180(A) | IVANOV | 0.3454×75×18 | *Ks* | S27 | 87.5 | 27.158±0.010 | -0.012±0.021 | A |
| 59607 | 53459.09 | 2005-03-30 | 075.C-0475(A) | OUDMAIJER | 1.0×12×5 | *NB*2.17 | S13 | 75.3 | 13.274±0.086 | -0.016±0.355 | A |
| 60189 | 53407.38 | 2005-02-06 | 074.D-0180(A) | IVANOV | 1.0×50×9 | *IB*2.18 | S27 | 82.7 | 27.148±0.039 | 0.009±0.083 | A |
| 60379 | 53408.33 | 2005-02-07 | 074.D-0180(A) | IVANOV | 1.0×50×9 | *IB*2.18 | S27 | 83.3 | 27.135±0.071 | -0.075±0.127 | A |
| 60449 | 53413.29 | 2005-02-12 | 074.D-0180(A) | IVANOV | 1.0×50×9 | *IB*2.18 | S27 | 83.9 | 27.082±0.037 | -0.009±0.023 | A |
| | 54510.35 | 2008-02-14 | 080.D-0348(A) | IVANOV | 5.0×10×9 | *IB*2.18 | S27 | 75.5 | 27.172±0.036 | -0.012±0.074 | A |
| 60463 | 53165.03 | 2004-06-09 | 272.D-5068(A) | IVANOV | 0.3×140×9 | *Ks* | S27 | 86.9 | 27.094±0.033 | 0.025±0.073 | A |
| | 53413.30 | 2005-02-12 | 074.D-0180(A) | IVANOV | 0.3454×149×9 | *Ks* | S27 | 80.1 | 27.157±0.034 | -0.035±0.075 | A |
| 60610 | 53413.31 | 2005-02-12 | 074.D-0180(A) | IVANOV | 0.3454×149×9 | *Ks* | S27 | 83.3 | 27.149±0.038 | 0.001±0.080 | A |
| 60735 | 53413.33 | 2005-02-12 | 074.D-0180(A) | IVANOV | 0.3454×149×9 | *Ks* | S27 | 80.1 | 27.132±0.038 | 0.023±0.077 | A |
| 60851 | 53102.08 | 2004-04-07 | 073.D-0534(A) | KOUWENHOVEN | 1.3×35×3 | *Ks* | S13 | 69.8 | 13.276±0.117 | -0.106±0.571 | A |
| 60855 | 53413.34 | 2005-02-12 | 074.D-0180(A) | IVANOV | 1.0×50×9 | *IB*2.18 | S27 | 81.4 | 27.153±0.045 | -0.020±0.093 | A |
| 61318 | 53750.37 | 2006-01-15 | 076.D-0108(A) | IVANOV | 10.0×5×9 | *IB*2.18 | S27 | 74.8 | 27.155±0.040 | -0.021±0.083 | A |
| 61789 | 53404.30 | 2005-02-03 | 074.D-0374(A) | HUBRIG | 1.5×35×19 | *Ks* | S13 | 70.1 | 13.259±0.011 | 0.021±0.051 | A |
| 61966 | 53454.20 | 2005-03-25 | 075.C-0475(A) | OUDMAIJER | 0.35×35×5 | *NB*2.17 | S13 | 76.7 | 13.269±0.059 | 0.003±0.337 | A |
| 62026 | 53102.13 | 2004-04-07 | 073.D-0534(A) | KOUWENHOVEN | 2.6×15×3 | *Ks* | S13 | 66.5 | 13.271±0.137 | 0.010±0.794 | A |
| 62058 | 53415.33 | 2005-02-14 | 074.D-0180(A) | IVANOV | 0.3454×149×9 | *Ks* | S27 | 80.8 | 27.170±0.029 | -0.001±0.056 | A |
| 62786 | 53415.36 | 2005-02-14 | 074.D-0180(A) | IVANOV | 0.3454×149×9 | *Ks* | S27 | 81.4 | 27.134±0.032 | 0.017±0.071 | A |
| | 55689.99 | 2011-05-08 | 087.D-0261(A) | ADAM | 6.0×9×10 | *Ks* | S13 | 72.2 | 13.262±0.046 | 0.064±0.201 | A |
| 63005 | 55690.05 | 2011-05-09 | 087.D-0261(A) | ADAM | 6.0×7×6 | *Ks* | S13 | 72.1 | 13.275±0.045 | 0.604±0.119 | B |
| 63210 | 53398.40 | 2005-01-28 | 074.D-0180(A) | IVANOV | 5.0×10×9 | *IB*2.18 | S27 | 82.7 | 27.162±0.037 | -0.031±0.071 | A |
| 63945 | 53454.21 | 2005-03-25 | 075.C-0475(A) | OUDMAIJER | 0.35×35×5 | *NB*2.17 | S13 | 75.7 | 13.299±0.061 | -0.006±0.322 | A |
| 64053 | 53779.32 | 2006-02-13 | 076.D-0108(A) | IVANOV | 2.0×26×9 | *Ks* | S27 | 85.1 | 27.151±0.030 | -0.013±0.065 | A |

*Continued on next page*

Table A2 – *Continued from previous page*

| HIP | MJD (days) | Observation date | Programme ID | PI | Exposure time (s) | Filter | Camera | FWHM (mas) | Pixel scale (mas/pixel) | Orientation (degree) | Method[a] |
|---|---|---|---|---|---|---|---|---|---|---|---|
| 64515 | 53436.29 | 2005-03-07 | 074.D-0180(A) | IVANOV | 5.0×1×90 | *Ks* | S27 | 107.7 | 27.132±0.018 | 0.011±0.042 | A |
| | 53778.37 | 2006-02-12 | 076.D-0108(A) | IVANOV | 4.0×13×9 | *Ks* | S27 | 82.7 | 27.144±0.032 | -0.019±0.066 | A |
| 65688 | 53915.95 | 2006-06-29 | 60.A-9026(A) | NACO TEAM | 0.3454×40×5 | *Ks* | S27 | 92.7 | 27.153±0.148 | -0.009±0.300 | A |
| 66454 | 53413.39 | 2005-02-12 | 074.D-0180(A) | IVANOV | 0.3454×149×9 | *Ks* | S27 | 83.3 | 27.139±0.034 | 0.008±0.069 | A |
| 66849 | 53415.40 | 2005-02-14 | 074.D-0180(A) | IVANOV | 1.0×50×9 | *IB*2.18 | S27 | 82.7 | 27.148±0.024 | -0.027±0.050 | A |
| 67472 | 53454.22 | 2005-03-25 | 075.C-0475(A) | OUDMAIJER | 1.0×12×5 | *Ks* | S13 | 81.9 | 13.254±0.072 | 0.100±0.337 | A |
| | 55690.02 | 2011-05-09 | 087.D-0261(A) | ADAM | 1.5×35×10 | *Ks* | S13 | 75.1 | 13.275±0.045 | 0.604±0.119 | B |
| 67669 | 53404.33 | 2005-02-03 | 074.D-0374(A) | HUBRIG | 1.5×35×20 | *Ks* | S13 | 71.7 | 13.269±0.021 | 0.006±0.087 | A |
| 67703 | 53185.16 | 2004-06-29 | 272.D-5068(A) | IVANOV | 6.0×8×9 | *IB*2.18 | S27 | 80.1 | 27.091±0.072 | 0.050±0.135 | A |
| 68002 | 53454.24 | 2005-03-25 | 075.C-0475(A) | OUDMAIJER | 0.5×24×5 | *Ks* | S13 | 72.6 | 13.284±0.071 | 0.123±0.348 | A |
| 68269 | 53185.17 | 2004-06-29 | 272.D-5068(A) | IVANOV | 10.0×5×9 | *IB*2.18 | S27 | 82.0 | 27.102±0.039 | 0.031±0.077 | A |
| 69113 | 53126.08 | 2004-05-01 | 073.D-0534(A) | KOUWENHOVEN | 2.3×25×3 | *Ks* | S13 | 123.7 | 13.304±0.178 | 0.012±0.720 | A |
| 69174 | 53774.40 | 2006-02-08 | 076.D-0108(A) | IVANOV | 2.1×25×234 | *Ks* | S27 | 80.1 | 27.139±0.031 | 0.028±0.067 | A |
| | 54518.39 | 2008-02-22 | 080.D-0348(A) | IVANOV | 0.3454×148×9 | *Ks* | S27 | 75.5 | 27.171±0.030 | -0.025±0.064 | A |
| 69491 | 53454.25 | 2005-03-25 | 075.C-0475(A) | OUDMAIJER | 1.0×12×5 | *NB*2.17 | S13 | 75.1 | 13.263±0.055 | 0.026±0.220 | A |
| 69618 | 53442.29 | 2005-03-13 | 074.D-0180(A) | IVANOV | 1.0×25×18 | *IB*2.18 | S27 | 91.0 | 27.156±0.013 | -0.019±0.026 | A |
| 69658 | 53407.39 | 2005-02-06 | 074.D-0180(A) | IVANOV | 0.3454×149×9 | *Ks* | S27 | 80.8 | 27.155±0.044 | -0.029±0.091 | A |
| 70574 | 53454.26 | 2005-03-25 | 075.C-0475(A) | OUDMAIJER | 0.35×35×5 | *NB*2.17 | S13 | 74.6 | 13.278±0.061 | -0.002±0.289 | A |
| 70915 | 53791.38 | 2006-02-25 | 076.D-0108(A) | IVANOV | 1.0×52×9 | *Ks* | S27 | 86.9 | 27.145±0.034 | -0.021±0.072 | A |
| | 54518.40 | 2008-02-22 | 080.D-0348(A) | IVANOV | 0.3454×148×9 | *Ks* | S27 | 76.1 | 27.158±0.031 | -0.003±0.068 | A |
| 71353 | 53804.26 | 2006-03-10 | 076.D-0108(A) | IVANOV | 0.3454×149×18 | *Ks* | S27 | 92.7 | 27.162±0.025 | -0.028±0.055 | A |
| 71762 | 53404.39 | 2005-02-03 | 074.D-0374(A) | HUBRIG | 1.5×35×20 | *Ks* | S13 | 70.3 | 13.274±0.016 | 0.001±0.068 | A |
| 71783 | 53806.34 | 2006-03-12 | 076.D-0108(A) | IVANOV | 0.3454×149×18 | *Ks* | S27 | 88.1 | 27.149±0.021 | -0.010±0.042 | A |
| 71974 | 53806.28 | 2006-03-12 | 076.D-0108(A) | IVANOV | 0.3454×149×9 | *Ks* | S27 | 92.1 | 27.167±0.039 | 0.022±0.078 | A |
| 72154 | 53787.31 | 2006-02-21 | 076.D-0108(A) | IVANOV | 1.0×52×9 | *Ks* | S27 | 83.9 | 27.140±0.039 | -0.014±0.085 | A |
| 73111 | 53454.27 | 2005-03-25 | 075.C-0475(A) | OUDMAIJER | 1.0×12×5 | *NB*2.17 | S13 | 71.4 | 13.277±0.072 | -0.201±0.304 | A |

*Continued on next page*

Table A2 – *Continued from previous page*

| HIP | MJD (days) | Observation date | Programme ID | PI | Exposure time (s) | Filter | Camera | FWHM (mas) | Pixel scale (mas/pixel) | Orientation (degree) | Method[a] |
|---|---|---|---|---|---|---|---|---|---|---|---|
| 73865 | 53454.28 | 2005-03-25 | 075.C-0475(A) | OUDMAIJER | 3.0×4×5 | *NB*2.17 | S13 | 71.4 | 13.279±0.088 | 0.007±0.387 | A |
| 74750 | 53454.29 | 2005-03-25 | 075.C-0475(A) | OUDMAIJER | 1.0×12×5 | *NB*2.17 | S13 | 75.4 | 13.283±0.068 | -0.101±0.291 | A |
| 74911 | 53454.30 | 2005-03-25 | 075.C-0475(A) | OUDMAIJER | 0.35×35×8 | *NB*2.17 | S13 | 74.8 | 13.250±0.050 | 0.036±0.214 | A |
| 75264 | 53454.31 | 2005-03-25 | 075.C-0475(A) | OUDMAIJER | 1.0×12×5 | *K*s | S13 | 75.1 | 13.290±0.140 | -0.057±0.626 | A |
| | 55690.09 | 2011-05-09 | 087.D-0261(A) | ADAM | 2.0×15×9 | *K*s | S13 | 72.2 | 13.275±0.045 | 0.604±0.119 | B |
| 76243 | 53787.37 | 2006-02-21 | 076.D-0108(A) | IVANOV | 5.0×10×9 | *IB*2.18 | S27 | 78.2 | 27.136±0.044 | 0.010±0.096 | A |
| 76503 | 56121.08 | 2012-07-13 | 089.C-0494(B) | KURTEV | 0.5×50×10 | *K*s | S13 | 100.4 | 13.265±0.035 | 0.037±0.144 | A |
| 76591 | 53454.32 | 2005-03-25 | 075.C-0475(A) | OUDMAIJER | 3.0×4×5 | *NB*2.17 | S13 | 74.6 | 13.289±0.081 | 0.025±0.343 | A |
| 77227 | 53804.33 | 2006-03-10 | 076.D-0108(A) | IVANOV | 1.0×50×9 | *IB*2.18 | S27 | 86.9 | 27.179±0.040 | -0.004±0.084 | A |
| 77562 | 53186.14 | 2004-06-30 | 272.D-5068(A) | IVANOV | 10.0×5×9 | *K*s | S27 | 101.8 | 27.114±0.031 | 0.008±0.059 | A |
| | 53853.26 | 2006-04-28 | 077.D-0147(A) | IVANOV | 1.0×84×7 | *K*s | S27 | 88.1 | 27.150±0.040 | -0.013±0.081 | A |
| 77634 | 53406.40 | 2005-02-05 | 074.D-0374(A) | HUBRIG | 0.9×55×15 | *K*s | S13 | 75.1 | 13.279±0.042 | 0.050±0.180 | A |
| 77635 | 56121.12 | 2012-07-13 | 089.C-0494(B) | KURTEV | 2.5×10×10 | *K*s | S13 | 97.1 | 13.283±0.033 | -0.016±0.136 | A |
| 77840 | 56121.12 | 2012-07-13 | 089.C-0494(B) | KURTEV | 2.5×10×6 | *K*s | S13 | 94.7 | 13.311±0.102 | -0.113±0.429 | A |
| 77900 | 55743.02 | 2011-07-01 | 60.A-9800(J) | OBSERVATORY, P | 5.0×2×54 | *K*s | S13 | 71.0 | 13.166±0.598 | -2.975±5.380 | A |
| | 56121.20 | 2012-07-13 | 089.C-0494(B) | KURTEV | 2.5×10×6 | *K*s | S13 | 82.2 | 13.270±0.093 | 0.117±0.406 | A |
| 78168 | 53435.42 | 2005-03-06 | 074.D-0180(A) | IVANOV | 0.7×75×9 | *K*s | S27 | 78.2 | 27.163±0.037 | 0.003±0.080 | A |
| | 53454.33 | 2005-03-25 | 075.C-0475(A) | OUDMAIJER | 1.0×12×5 | *NB*2.17 | S13 | 71.0 | 13.287±0.094 | 0.087±0.410 | A |
| 78265 | 56121.18 | 2012-07-13 | 089.C-0494(B) | KURTEV | 0.5×50×6 | *K*s | S13 | 102.3 | 13.244±0.103 | -0.099±0.451 | A |
| 78933 | 53454.35 | 2005-03-25 | 075.C-0475(A) | OUDMAIJER | 0.35×35×5 | *NB*2.17 | S13 | 70.9 | 13.274±0.100 | 0.114±0.427 | A |
| 78968 | 53130.20 | 2004-05-05 | 073.D-0534(A) | KOUWENHOVEN | 0.35×35×3 | *K*s | S13 | 69.4 | 13.245±0.165 | -0.047±0.734 | A |
| 79005 | 53190.13 | 2004-07-04 | 272.D-5068(A) | IVANOV | 1.0×50×9 | *K*s | S27 | 86.3 | 27.117±0.038 | 0.024±0.081 | A |
| | 53852.27 | 2006-04-27 | 077.D-0147(A) | IVANOV | 1.0×84×7 | *K*s | S27 | 105.3 | 27.176±0.050 | 0.009±0.105 | A |
| | 53887.16 | 2006-06-01 | 077.D-0147(A) | IVANOV | 2.0×42×7 | *K*s | S27 | 81.4 | 27.148±0.065 | 0.026±0.138 | A |
| 79031 | 53408.39 | 2005-02-07 | 074.D-0374(A) | HUBRIG | 6.0×9×15 | *K*s | S13 | 78.9 | 13.270±0.017 | -0.019±0.070 | A |
| | 53435.35 | 2005-03-06 | 074.D-0374(A) | HUBRIG | 6.0×9×20 | *K*s | S13 | 70.7 | 13.274±0.013 | 0.028±0.056 | A |

*Continued on next page*

Table A2 – *Continued from previous page*

| HIP | MJD (days) | Observation date | Programme ID | PI | Exposure time (s) | Filter | Camera | FWHM (mas) | Pixel scale (mas/pixel) | Orientation (degree) | Method[a] |
|---|---|---|---|---|---|---|---|---|---|---|---|
| 79098 | 53442.27 | 2005-03-13 | 074.D-0374(A) | HUBRIG | 3.8×13×20 | *Ks* | S13 | 83.1 | 13.268±0.013 | -0.031±0.055 | A |
| 79153 | 53186.19 | 2004-06-30 | 272.D-5068(A) | IVANOV | 2.0×25×9 | *Ks* | S27 | 87.5 | 27.099±0.029 | -0.004±0.063 | A |
| | 53853.27 | 2006-04-28 | 077.D-0147(A) | IVANOV | 1.0×84×7 | *Ks* | S27 | 83.3 | 27.162±0.036 | 0.054±0.077 | A |
| 79199 | 53191.12 | 2004-07-05 | 272.D-5068(A) | IVANOV | 0.3×140×9 | *Ks* | S27 | 85.7 | 27.102±0.038 | 0.015±0.078 | A |
| | 55690.12 | 2011-05-09 | 087.D-0261(A) | ADAM | 6.0×9×9 | *Ks* | S13 | 71.0 | 13.275±0.045 | 0.604±0.119 | B |
| 79230 | 53105.33 | 2004-04-10 | 073.C-0379(A) | ZINNECKER | 0.6×45×0 | *NB*1.64 | S13 | 70.0 | 13.260±0.005 | 0.019±0.004 | A |
| 79399 | 53185.25 | 2004-06-29 | 272.D-5068(A) | IVANOV | 10.0×5×9 | *Ks* | S27 | 118.2 | 27.090±0.040 | -0.018±0.081 | A |
| | 53852.25 | 2006-04-27 | 077.D-0147(A) | IVANOV | 0.3454×243×7 | *Ks* | S27 | 80.8 | 27.131±0.050 | 0.000±0.105 | A |
| 79404 | 56179.02 | 2012-09-09 | 089.C-0494(C) | KURTEV | 0.1091×200×16 | *Ks* | S13 | 91.1 | 13.253±0.055 | 0.040±0.222 | A |
| 79410 | 53176.09 | 2004-06-20 | 073.D-0534(A) | KOUWENHOVEN | 0.35×35×3 | *Ks* | S13 | 71.7 | 13.238±0.186 | -0.067±0.784 | A |
| 79622 | 56121.21 | 2012-07-13 | 089.C-0494(B) | KURTEV | 2.5×10×6 | *Ks* | S13 | 97.6 | 13.278±0.101 | -0.051±0.414 | A |
| 79653 | 53177.28 | 2004-06-21 | 272.D-5068(A) | IVANOV | 15.0×3×9 | *IB*2.18 | S27 | 94.9 | 27.097±0.032 | -0.026±0.068 | A |
| 79739 | 53176.17 | 2004-06-20 | 073.D-0534(A) | KOUWENHOVEN | 4.0×15×3 | *Ks* | S13 | 76.9 | 13.274±0.196 | 0.010±0.924 | A |
| 79771 | 53176.21 | 2004-06-20 | 073.D-0534(A) | KOUWENHOVEN | 2.6×15×3 | *Ks* | S13 | 74.8 | 13.338±0.218 | -0.189±0.919 | A |
| | 56121.25 | 2012-07-13 | 089.C-0494(B) | KURTEV | 0.5×50×10 | *Ks* | S13 | 79.1 | 13.259±0.035 | -0.072±0.151 | A |
| 80066 | 53454.36 | 2005-03-25 | 075.C-0475(A) | OUDMAIJER | 1.0×12×5 | *NB*2.17 | S13 | 71.2 | 13.267±0.081 | 0.005±0.367 | A |
| 80126 | 54994.25 | 2009-06-12 | 083.C-0459(A) | SCHREIBER | 0.5×2×10 | *J* | S13 | 66.5 | 13.274±0.032 | 0.103±0.132 | A |
| 80142 | 53130.25 | 2004-05-05 | 073.D-0534(A) | KOUWENHOVEN | 2.8×15×3 | *Ks* | S13 | 71.4 | 13.251±0.008 | -0.107±0.063 | A |
| 80461 | 56179.04 | 2012-09-09 | 089.C-0494(C) | KURTEV | 0.2×200×21 | *Ks* | S13 | 81.1 | 13.262±0.086 | 0.042±0.395 | A |
| 80473 | 56089.35 | 2012-06-11 | 089.C-0494(A) | KURTEV | 0.2×100×4 | *Ks* | S27 | 330.3 | 27.198±0.117 | 0.050±0.240 | A |
| 80474 | 53184.17 | 2004-06-28 | 073.D-0534(A) | KOUWENHOVEN | 0.35×35×3 | *Ks* | S13 | 114.7 | 13.230±0.275 | -0.250±1.190 | A |
| | 55690.15 | 2011-05-09 | 087.D-0261(A) | ADAM | 8.0×6×10 | *Ks* | S13 | 72.9 | 13.275±0.045 | 0.604±0.119 | B |
| 80493 | 56179.06 | 2012-09-09 | 089.C-0494(C) | KURTEV | 0.4×100×16 | *Ks* | S13 | 77.4 | 13.221±0.017 | 0.000±0.500 | U |
| 81472 | 53454.37 | 2005-03-25 | 075.C-0475(A) | OUDMAIJER | 1.0×12×5 | *NB*2.17 | S13 | 71.5 | 13.276±0.084 | -0.162±0.335 | A |
| | 55690.19 | 2011-05-09 | 087.D-0261(A) | ADAM | 6.0×9×9 | *Ks* | S13 | 69.1 | 13.275±0.045 | 0.604±0.119 | B |
| 81474 | 56179.08 | 2012-09-09 | 089.C-0494(C) | KURTEV | 0.2×200×17 | *Ks* | S13 | 81.6 | 13.309±0.090 | 0.102±0.375 | A |

*Continued on next page*

Table A2 – *Continued from previous page*

| HIP | MJD (days) | Observation date | Programme ID | PI | Exposure time (s) | Filter | Camera | FWHM (mas) | Pixel scale (mas/pixel) | Orientation (degree) | Method[a] |
|---|---|---|---|---|---|---|---|---|---|---|---|
| 81972 | 53184.20 | 2004-06-28 | 073.D-0534(A) | KOUWENHOVEN | 0.35×35×3 | *Ks* | S13 | 101.4 | 13.249±0.254 | 0.200±1.200 | A |
| 82902 | 53177.30 | 2004-06-21 | 272.D-5068(A) | IVANOV | 3.45×14×9 | *Ks* | S27 | 98.1 | 27.113±0.033 | 0.045±0.074 | A |
| | 53895.29 | 2006-06-09 | 077.D-0147(A) | IVANOV | 6.0×2×49 | *Ks* | S27 | 100.2 | 27.162±0.007 | -0.034±0.015 | A |
| 83336 | 53182.27 | 2004-06-26 | 272.D-5068(A) | IVANOV | 10.0×5×9 | *IB*2.18 | S27 | 86.3 | 27.111±0.038 | -0.043±0.084 | A |
| | 53912.13 | 2006-06-26 | 077.D-0147(A) | IVANOV | 12.0×7×7 | *IB*2.18 | S27 | 84.5 | 27.158±0.051 | -0.004±0.105 | A |
| 85442 | 53454.42 | 2005-03-25 | 075.C-0475(A) | OUDMAIJER | 1.0×12×5 | *NB*2.17 | S13 | 72.1 | 13.258±0.060 | -0.178±0.046 | A |
| 85727 | 54699.06 | 2008-08-21 | 081.C-0653(A) | LAGRANGE | 1.0×10×10 | *Ks* | S27 | 92.7 | 27.157±0.026 | -0.008±0.051 | A |
| 85755 | 53455.44 | 2005-03-26 | 075.C-0475(A) | OUDMAIJER | 0.35×35×5 | *NB*2.17 | S13 | 72.9 | 13.277±0.094 | 0.142±0.382 | A |
| | 53489.37 | 2005-04-29 | 075.C-0475(A) | OUDMAIJER | 0.35×35×5 | *NB*2.17 | S13 | 70.9 | 13.263±0.078 | -0.032±0.339 | A |
| 85783 | 53442.33 | 2005-03-13 | 074.D-0374(A) | HUBRIG | 6.0×9×20 | *Ks* | S13 | 87.0 | 13.270±0.015 | 0.023±0.068 | A |
| | 55655.36 | 2011-04-04 | 087.D-0197(A) | SCHOELLER | 7.5×8×18 | *Ks* | S13 | 89.9 | 13.285±0.014 | -0.027±0.060 | A |
| | 55690.35 | 2011-05-09 | 087.D-0261(A) | ADAM | 12.0×3×4 | *Ks* | S13 | 71.4 | 13.275±0.045 | 0.604±0.119 | B |
| 87163 | 53457.37 | 2005-03-28 | 075.C-0475(A) | OUDMAIJER | 1.0×12×5 | *NB*2.17 | S13 | 69.6 | 13.272±0.022 | -0.111±0.056 | A |
| | 55690.27 | 2011-05-09 | 087.D-0261(A) | ADAM | 5.0×7×9 | *Ks* | S13 | 67.6 | 13.275±0.045 | 0.604±0.119 | B |
| 87220 | 53454.43 | 2005-03-25 | 075.C-0475(A) | OUDMAIJER | 0.35×35×5 | *NB*2.17 | S13 | 72.2 | 13.299±0.089 | -0.124±0.378 | A |
| | 55690.24 | 2011-05-09 | 087.D-0261(A) | ADAM | 2.0×20×9 | *Ks* | S13 | 70.0 | 13.275±0.045 | 0.604±0.119 | B |
| 88012 | 53456.43 | 2005-03-27 | 075.C-0475(A) | OUDMAIJER | 1.0×12×5 | *NB*2.17 | S13 | 75.1 | 13.271±0.084 | -0.039±0.371 | A |
| 88149 | 53455.43 | 2005-03-26 | 075.C-0475(A) | OUDMAIJER | 0.35×35×5 | *NB*2.17 | S13 | 67.6 | 13.261±0.093 | -0.135±0.402 | A |
| | 55690.29 | 2011-05-09 | 087.D-0261(A) | ADAM | 3.5×12×9 | *Ks* | S13 | 70.9 | 13.275±0.045 | 0.604±0.119 | B |
| 88859 | 53442.36 | 2005-03-13 | 074.D-0374(A) | HUBRIG | 6.0×9×20 | *Ks* | S13 | 96.3 | 13.271±0.011 | -0.037±0.047 | A |
| 89684 | 53570.20 | 2005-07-19 | 075.C-0668(A) | DOUCET | 4.0×5×8 | *Ks* | S13 | 68.3 | 13.221±0.017 | 0.000±0.500 | U |
| | 55690.31 | 2011-05-09 | 087.D-0261(A) | ADAM | 10.0×4×9 | *Ks* | S13 | 74.4 | 13.275±0.045 | 0.604±0.119 | B |
| 89956 | 55761.05 | 2011-07-19 | 087.D-0426(C) | MARTAYAN | 0.2×100×8 | *Ks* | S27 | 361.5 | 27.160±0.115 | -0.043±0.232 | A |
| 89963 | 55761.01 | 2011-07-19 | 087.D-0426(C) | MARTAYAN | 0.6×25×5 | *Ks* | S27 | 84.5 | 27.149±0.086 | -0.039±0.186 | A |
| 89977 | 53472.33 | 2005-04-12 | 075.C-0475(A) | OUDMAIJER | 1.0×12×5 | *NB*2.17 | S13 | 68.7 | 13.241±0.100 | 0.005±0.425 | A |
| 90096 | 53458.39 | 2005-03-29 | 075.C-0475(A) | OUDMAIJER | 1.0×12×5 | *NB*2.17 | S13 | 70.9 | 13.296±0.077 | -0.119±0.334 | A |

*Continued on next page*

Table A2 – *Continued from previous page*

| HIP | MJD (days) | Observation date | Programme ID | PI | Exposure time (s) | Filter | Camera | FWHM (mas) | Pixel scale (mas/pixel) | Orientation (degree) | Method[a] |
|---|---|---|---|---|---|---|---|---|---|---|---|
| | 55690.37 | 2011-05-09 | 087.D-0261(A) | ADAM | 4.0×8×9 | *K*s | S13 | 71.7 | 13.275±0.045 | 0.604±0.119 | B |
| 90336 | 53472.32 | 2005-04-12 | 075.C-0475(A) | OUDMAIJER | 1.0×12×5 | *NB*2.17 | S13 | 73.3 | 13.268±0.078 | 0.081±0.330 | A |
| 90766 | 55372.17 | 2010-06-25 | 485.L-0725(A) | FORVEILLE | 0.3×20×7 | *K*s | S27 | 161.8 | 27.075±0.126 | 0.043±0.257 | A |
| 91014 | 53472.34 | 2005-04-12 | 075.C-0475(A) | OUDMAIJER | 0.35×35×5 | *NB*2.17 | S13 | 71.5 | 13.300±0.100 | -0.088±0.426 | A |
| 93368 | 53472.35 | 2005-04-12 | 075.C-0475(A) | OUDMAIJER | 3.0×4×5 | *NB*2.17 | S13 | 71.4 | 13.242±0.080 | 0.019±0.312 | A |
| 93542 | 53577.16 | 2005-07-26 | 075.D-0660(A) | DE LAVERNY | 1.8×6×61 | *K*s | S13 | 78.5 | 13.280±0.013 | 0.005±0.055 | A |
| | 53958.15 | 2006-08-11 | 077.D-0606(A) | LEAO | 2.0×7×40 | *K*s | S13 | 85.6 | 13.246±0.015 | -0.028±0.066 | A |
| 93805 | 54699.07 | 2008-08-21 | 081.C-0653(A) | LAGRANGE | 1.0×10×10 | *K*s | S27 | 102.3 | 27.137±0.057 | 0.017±0.118 | A |
| | 54947.29 | 2009-04-26 | 083.C-0151(B) | LAGRANGE | 4.0×20×8 | *NB*2.17 | S27 | 80.1 | 27.155±0.084 | -0.089±0.181 | A |
| 93892 | 53286.00 | 2004-10-08 | 074.D-0374(A) | HUBRIG | 10.0×5×20 | *K*s | S13 | 74.6 | 13.267±0.020 | 0.053±0.086 | A |
| | 55799.14 | 2011-08-26 | 087.D-0197(A) | SCHOELLER | 15.0×4×18 | *K*s | S13 | 75.4 | 13.267±0.013 | 0.028±0.057 | A |
| 93996 | 53489.39 | 2005-04-29 | 075.C-0475(A) | OUDMAIJER | 0.6×20×5 | *NB*2.17 | S13 | 71.0 | 13.312±0.078 | 0.013±0.328 | A |
| 95347 | 53519.38 | 2005-05-29 | 075.C-0475(A) | OUDMAIJER | 0.35×35×5 | *NB*2.17 | S13 | 72.6 | 13.292±0.083 | 0.110±0.334 | A |
| 97607 | 53511.37 | 2005-05-21 | 075.C-0475(A) | OUDMAIJER | 1.0×12×5 | *NB*2.17 | S13 | 72.2 | 13.231±0.100 | 0.236±0.423 | A |
| 99457 | 53512.40 | 2005-05-22 | 075.C-0475(A) | OUDMAIJER | 3.0×4×7 | *NB*2.17 | S13 | 72.4 | 13.254±0.057 | 0.033±0.266 | A |
| 100751 | 53601.10 | 2005-08-19 | 075.C-0521(B) | CHAUVIN | 0.5×20×8 | *NB*2.17 | S27 | 69.0 | 27.167±0.051 | -0.023±0.090 | A |
| 100881 | 54769.99 | 2008-10-30 | 60.A-9800(J) | OBSERVATORY, P | 1.0×1×30 | *K*s | S13 | 250.1 | 13.280±0.014 | 0.021±0.060 | A |
| | 56189.16 | 2012-09-19 | 089.D-0366(A) | ADAM | 3.0×10×5 | *K*s | S13 | 71.9 | 13.273±0.011 | 0.679±0.046 | C |
| 102157 | 53353.03 | 2004-12-14 | 074.D-0180(A) | IVANOV | 1.0×50×9 | *IB*2.18 | S27 | 86.9 | 27.103±0.019 | -0.025±0.048 | A |
| 105164 | 53511.39 | 2005-05-21 | 075.C-0475(A) | OUDMAIJER | 1.0×12×5 | *NB*2.17 | S13 | 70.3 | 13.269±0.080 | -0.202±0.334 | A |
| | 53512.42 | 2005-05-22 | 075.C-0475(A) | OUDMAIJER | 1.0×12×7 | *NB*2.17 | S13 | 77.0 | 13.288±0.073 | -0.024±0.309 | A |
| 105842 | 54685.22 | 2008-08-07 | 081.C-0519(A) | PATIENCE | 3.0×3×6 | *H* | S13 | 65.2 | 13.270±0.000 | 0.025±0.014 | A |
| 108874 | 53510.42 | 2005-05-20 | 075.C-0475(A) | OUDMAIJER | 0.35×35×5 | *NB*2.17 | S13 | 73.1 | 13.243±0.094 | -0.007±0.401 | A |
| 109139 | 54699.27 | 2008-08-21 | 081.C-0653(A) | LAGRANGE | 0.35×30×10 | *K*s | S27 | 77.5 | 27.152±0.038 | 0.006±0.081 | A |
| | 55070.18 | 2009-08-27 | 083.C-0151(A) | LAGRANGE | 0.35×30×10 | *K*s | S27 | 82.0 | 27.155±0.039 | 0.007±0.081 | A |
| 110672 | 53510.43 | 2005-05-20 | 075.C-0475(A) | OUDMAIJER | 0.35×35×5 | *NB*2.17 | S13 | 71.7 | 13.253±0.093 | -0.033±0.412 | A |

*Continued on next page*

Table A2 – *Continued from previous page*

| HIP | MJD (days) | Observation date | Programme ID | PI | Exposure time (s) | Filter | Camera | FWHM (mas) | Pixel scale (mas/pixel) | Orientation (degree) | Method[a] |
|---|---|---|---|---|---|---|---|---|---|---|---|
| 112542 | 53741.03 | 2006-01-06 | 076.D-0108(A) | IVANOV | 4.0×15×9 | *Ks* | S27 | 159.6 | 27.145±0.038 | 0.067±0.081 | A |
| | 54359.14 | 2007-09-16 | 080.D-0348(A) | IVANOV | 0.3454×148×9 | *Ks* | S27 | 86.3 | 27.178±0.039 | 0.017±0.081 | A |
| 112781 | 53742.03 | 2006-01-07 | 076.D-0108(A) | IVANOV | 10.0×5×9 | *IB*2.18 | S27 | 80.8 | 27.156±0.011 | 0.013±0.023 | A |
| 113031 | 53298.07 | 2004-10-20 | 074.D-0374(A) | HUBRIG | 3.8×13×25 | *Ks* | S13 | 94.5 | 13.251±0.011 | -0.040±0.048 | A |
| | 54363.15 | 2007-09-20 | 080.D-0348(A) | IVANOV | 0.3454×148×9 | *Ks* | S27 | 106.2 | 27.169±0.035 | 0.003±0.073 | A |
| 113889 | 53510.44 | 2005-05-20 | 075.C-0475(A) | OUDMAIJER | 0.35×35×5 | *NB*2.17 | S13 | 71.2 | 13.255±0.087 | -0.075±0.356 | A |
| 116231 | 53296.13 | 2004-10-18 | 074.D-0374(A) | HUBRIG | 1.5×35×20 | *Ks* | S13 | 77.0 | 13.261±0.012 | -0.020±0.052 | A |
| | 53297.11 | 2004-10-19 | 074.D-0374(A) | HUBRIG | 1.5×35×20 | *Ks* | S13 | 82.9 | 13.257±0.013 | -0.025±0.054 | A |
| | 56188.16 | 2012-09-18 | 089.D-0366(A) | ADAM | 1.5×35×20 | *Ks* | S13 | 80.3 | 13.285±0.019 | 0.006±0.081 | A |
| 117089 | 53699.02 | 2005-11-25 | 076.D-0108(A) | IVANOV | 1.0×50×9 | *IB*2.18 | S27 | 76.1 | 27.168±0.037 | 0.029±0.080 | A |
| 117315 | 53700.04 | 2005-11-26 | 076.D-0108(A) | IVANOV | 2.0×25×9 | *IB*2.18 | S27 | 76.1 | 27.144±0.038 | -0.049±0.081 | A |
| 117629 | 53285.16 | 2004-10-07 | 074.D-0180(A) | IVANOV | 2.5×20×9 | *IB*2.18 | S27 | 77.5 | 27.104±0.038 | 0.003±0.079 | A |
| 120402 | 53731.36 | 2005-12-27 | 076.C-0170(A) | HUBRIG | 0.5×120×10 | *Ks* | S13 | 72.9 | 13.260±0.016 | 0.021±0.065 | A |

**Note.** The total exposure time is the product of DIT(s)×NDIT×NExp.

[a] Used method for astrometric calibration: A–Auto-calibration; B–Binary; C–Cluster; U–Uncalibrated, i.e. reference value from literature given

**Table A3.** Absolute astrometric results for stars with more than one observation

| HIP | MJD (days) | Ref. | Sep (arcsec) $\Theta \pm \delta_\Theta$ | $\text{Sep}_{\text{bg}}$ (arcsec) $\Theta_{\text{bg}} \pm \delta_{\Theta,\text{bg}}$ | Sign.[a] not Backg. $\sigma_{\Theta,\text{bg}}$ | Sign. orb. motion $\sigma_{\Theta,\text{orb.}}$ | PA[b] (deg) PA$\pm\delta_{\text{PA}}$ | $\text{PA}_{\text{bg}}$ (deg) $\text{PA}_{\text{bg}} \pm \delta_{\text{PA, bg}}$ | Sign.[a] not Backg. $\sigma_{\text{PA,bg}}$ | Sign. orb. motion $\sigma_{\text{PA,orb.}}$ | $P_{\chi,\text{bg}}$ (%) | $P_{\chi,\text{cmv}}$ (%) |
|---|---|---|---|---|---|---|---|---|---|---|---|---|
| | | | | | Binaries | | | | | | | |
| 2548 | 51065.000 | Mason et al. (2001) | 0.274±0.001 | 0.489±0.005 | 45.5 | 51.3 | 284.4±0.1 | 335.9±0.6 | 86.5 | 88.8 | 0.00 | 0.00 |
| | 51466.000 | Horch et al. (2000) | 0.29±0.01 | 0.445±0.004 | 14.4 | 6.8 | 278.1±0.1 | 333.4±0.6 | 93.3 | 53.8 | | |
| | 51477.000 | Mason et al. (2001) | 0.270±0.001 | 0.444±0.004 | 41.3 | 47.4 | 283.1±0.1 | 333.4±0.6 | 84.8 | 81.5 | | |
| | 52872.000 | Horch et al. (2008) | 0.283±0.001 | 0.310±0.002 | 11.0 | 60.1 | 279.4±0.1 | 316.5±0.5 | 67.7 | 61.0 | | |
| | 53297.000 | Mason et al. (2006) | 0.30±0.05 | 0.273±0.002 | 0.5 | 1.6 | 281.4±0.1 | 309.3±0.5 | 54.4 | 72.1 | | |
| | 53710.049 | (1) | 0.2710±0.0009 | 0.245±0.001 | 17.3 | 52.6 | 278.0±0.2 | 299.9±0.4 | 45.5 | 38.9 | | |
| | 54359.246 | (1) | 0.241±0.001 | 0.2247±0.0004 | 14.8 | 18.7 | 275.6±0.2 | 280.6±0.3 | 15.4 | 31.2 | | |
| | 54746.000 | Tokovinin et al. (2010) | 0.2217±0.0002 | c | c | c | 268.4±0.1 | c | c | c | | |
| 15627 | 48475.000 | Fabricius et al. (2002) | 0.990±0.007 | 1.04±0.01 | 3.2 | 13.2 | 228.2±0.6 | 192.4±0.9 | 32.8 | 12.3 | 0.00 | 0.00 |
| | 54024.221 | (1) | 0.874±0.005 | c | c | c | 218.4±0.5 | c | c | c | | |
| 16511 | 53376.049 | (1) | 0.128±0.003 | 0.541±0.005 | 75.2 | 13.6 | 110.1±1.0 | 133.0±0.2 | 20.2 | 1.7 | 0.00 | 0.00 |
| | 53700.139 | (1) | 0.143±0.002 | 0.493±0.005 | 69.7 | 11.0 | 112.6±0.3 | 131.9±0.3 | 46.0 | 5.9 | | |
| | 55798.407 | (1) | 0.189±0.004 | c | c | c | 107.8±0.7 | c | c | c | | |
| 16803 | 48348.000 | ESA (1997) | 0.15±0.01 | 0.61±0.01 | 22.1 | 2.4 | 65.0±0.5 | -0.9±0.9 | 65.8 | 22.9 | 0.00 | 0.00 |
| | 53379.102 | (1) | 0.195±0.001 | 0.213±0.007 | 2.7 | 0.9 | 84.0±0.2 | 40.7±0.6 | 72.4 | 38.7 | | |
| | 54105.000 | Horch et al. (2010) | 0.193±0.005 | 0.188±0.006 | 0.7 | 0.4 | 79.6±0.1 | 58.6±0.3 | 57.8 | 20.5 | | |
| | 54363.350 | (1) | 0.229±0.005 | 0.189±0.005 | 5.2 | 5.3 | 80.9±1.0 | 66.6±0.2 | 14.3 | 4.3 | | |
| | 54373.246 | (1) | 0.198±0.001 | 0.188±0.005 | 1.8 | 1.6 | 78.4±0.3 | 66.8±0.2 | 28.1 | 4.7 | | |
| | 54722.000 | Horch et al. (2012) | 0.190±0.005 | c | c | c | 76.7±0.1 | c | c | c | | |
| 20020 | 48348.000 | Fabricius et al. (2002) | 4.130±0.006 | 4.322±0.008 | 19.6 | 7.8 | 3.0±0.1 | 13.3±0.1 | 63.6 | 6.7 | 0.00 | 0.00 |
| | 53347.154 | (1) | 4.102±0.005 | 4.167±0.004 | 11.1 | 4.2 | 2.56±0.06 | 7.21±0.06 | 57.3 | 4.0 | | |
| | 54363.374 | (1) | 4.115±0.007 | 4.142±0.003 | 3.7 | 4.6 | 1.94±0.08 | 5.87±0.04 | 42.5 | 4.7 | | |
| | 54373.288 | (1) | 4.113±0.004 | 4.142±0.003 | 6.0 | 7.7 | 1.94±0.03 | 5.87±0.04 | 76.4 | 12.4 | | |
| | 57023.000 | GAIA | 4.0830±0.0006 | c | c | c | 2.329±0.006 | c | c | c | | |
| 20042 | 51268.000 | Hubrig et al. (2001) | 5.32±0.05 | 5.848±0.009 | 10.4 | 2.2 | 162.5±0.1 | 154.94±0.06 | 64.9 | 0.1 | 0.00 | 0.68 |
| | 53690.201 | (1) | 5.389±0.005 | 5.638±0.009 | 23.4 | 3.9 | 162.16±0.06 | 158.58±0.05 | 43.9 | 4.4 | | |
| | 56189.188 | (1) | 5.431±0.009 | c | c | c | 162.51±0.05 | c | c | c | | |
| 20554 | 38782.000 | Knipe et al. (1969) | 6.17±0.05 | d | d | d | 42.5±0.1 | d | d | d | 0.00 | 8.39 |

*Continued on next page*

Table A3 – *Continued from previous page*

| HIP | MJD (days) | Ref. | Sep (arcsec) $\Theta \pm \delta_\Theta$ | $\mathrm{Sep_{bg}}$ (arcsec) $\Theta_{\rm bg} \pm \delta_{\Theta,\rm bg}$ | Sign.[a] not Backg. $\sigma_{\Theta,\rm bg}$ | Sign. orb. motion $\sigma_{\Theta,\rm orb.}$ | PA[b] (deg) PA$\pm\delta_{\rm PA}$ | $\mathrm{PA_{bg}}$ (deg) $\mathrm{PA_{bg}} \pm \delta_{\rm PA,\ bg}$ | Sign.[a] not Backg. $\sigma_{\rm PA,bg}$ | Sign. orb. motion $\sigma_{\rm PA,orb.}$ | $\mathrm{P_{\chi,bg}}$ (%) | $\mathrm{P_{\chi,cmv}}$ (%) |
|---|---|---|---|---|---|---|---|---|---|---|---|---|
| | 51171.000 | Cutri et al. (2003) | 6.2±0.1 | 5.81±0.07 | 3.2 | 0.3 | 42.4±0.1 | 39.5±0.3 | 10.0 | 0.7 | | |
| | 53266.307 | (1) | 6.319±0.005 | 5.75±0.07 | 8.0 | 3.0 | 42.0±0.1 | 39.0±0.3 | 9.2 | 3.5 | | |
| 20804 | 48585.000 | Hartkopf et al. (1994) | 0.148±0.005 | 0.13±0.02 | 1.3 | 1.1 | 108.1±0.1 | 203.1±9.0 | 11.1 | 513.8 | 0.00 | 0.00 |
| | 53409.032 | (1) | 0.112±0.003 | 0.057±0.007 | 7.4 | 7.1 | 25.1±0.9 | 321.1±7.0 | 42.4 | 310.9 | | |
| | 56189.333 | (1) | 0.127±0.005 | 0.138±0.003 | 1.9 | 2.5 | 351.0±0.4 | 348.0±0.5 | 4.7 | 3.9 | | |
| | 56296.083 | (1) | 0.142±0.003 | c | c | c | 348.6±0.5 | c | c | c | | |
| 23794 | 51268.000 | Hubrig et al. (2001) | 1.61±0.05 | 1.466±0.006 | 2.9 | 0.5 | 307.4±0.1 | 312.7±0.2 | 23.1 | 18.0 | 0.00 | 0.05 |
| | 53286.342 | (1) | 1.600±0.005 | 1.519±0.004 | 13.9 | 2.4 | 308.3±0.2 | 311.6±0.1 | 16.2 | 7.3 | | |
| | 56296.100 | (1) | 1.588±0.002 | c | c | c | 309.50±0.06 | c | c | c | | |
| 24196 | 47307.000 | Wycoff et al. (2006) | 0.101±0.005 | d | d | d | 333.4±0.1 | d | d | d | 0.00 | 0.00 |
| | 51096.000 | Balega et al. (2002) | 0.14±0.02 | 0.06±0.01 | 3.2 | 1.6 | 351.4±0.5 | 295.0±7.0 | 8.4 | 35.3 | | |
| | 53347.205 | (1) | 0.1456±0.0005 | 0.06±0.01 | 5.6 | 8.9 | 345.1±0.2 | 257.9±10.0 | 8.1 | 49.5 | | |
| | 54748.000 | Tokovinin et al. (2010) | 0.2±0.1 | 0.07±0.02 | 0.8 | 0.5 | 341.6±0.2 | 239.8±10.0 | 9.3 | 36.7 | | |
| | 55549.000 | Hartkopf et al. (2012) | 0.2±0.2 | 0.08±0.02 | 0.4 | 0.3 | 339.8±0.1 | 232.4±10.0 | 10.3 | 45.3 | | |
| 24305 | 53374.161 | (1) | 0.370±0.003 | 0.590±0.003 | 46.5 | 70.5 | 250.2±0.2 | 183.7±0.4 | 151.8 | 130.0 | 0.00 | 0.00 |
| | 56269.305 | (1) | 0.6172±0.0009 | c | c | c | 221.93±0.07 | c | c | c | | |
| 24825 | 53471.968 | (1) | 0.287±0.004 | d | d | d | 297.0±0.6 | d | d | d | 0.24 | 0.00 |
| | 56189.401 | (1) | 0.299±0.001 | 0.276±0.005 | 4.2 | 2.9 | 289.1±0.2 | 282.5±0.9 | 6.9 | 12.7 | | |
| 25365 | 53380.142 | (1) | 0.2994±0.0003 | 0.353±0.005 | 10.6 | 7.0 | 174.15±0.06 | 179.4±0.8 | 6.9 | 28.0 | 0.00 | 0.00 |
| | 54747.000 | Tokovinin et al. (2010) | 0.3±0.1 | 0.341±0.004 | 0.3 | 0.1 | 175.4±0.1 | 178.6±0.4 | 7.6 | 14.6 | | |
| | 55220.000 | Mason et al. (2011) | 0.322±0.005 | 0.334±0.004 | 1.9 | 0.8 | 176.1±0.1 | 178.1±0.3 | 6.8 | 9.7 | | |
| | 56189.297 | (1) | 0.327±0.004 | c | c | c | 177.5±0.1 | c | c | c | | |
| 26215 | 48348.000 | Fabricius et al. (2002) | 2.82±0.04 | 2.723±0.006 | 2.7 | 0.6 | 351.6±0.7 | 352.0±0.2 | 0.5 | 0.4 | 7.09 | 82.16 |
| | 53348.200 | (1) | 2.799±0.002 | c | c | c | 351.90±0.04 | c | c | c | | |
| 26235 | 51477.000 | Mason et al. (2001) | 0.38±0.01 | 0.41±0.01 | 2.2 | 2.3 | 293.0±0.1 | 298.1±0.6 | 8.0 | 9.2 | 0.00 | 0.00 |
| | 53687.000 | Mason et al. (2009) | 0.39±0.01 | 0.41±0.01 | 1.3 | 1.4 | 278.9±0.1 | 296.0±0.3 | 48.6 | 108.9 | | |
| | 53805.000 | Mason et al. (2009) | 0.38±0.01 | 0.41±0.01 | 2.0 | 2.2 | 293.3±0.1 | 296.0±0.3 | 8.1 | 7.1 | | |
| | 54452.075 | (1) | 0.403±0.002 | 0.41±0.01 | 0.8 | 0.8 | 292.4±0.5 | 295.3±0.2 | 5.1 | 3.5 | | |
| | 54482.000 | Maiz Apellaniz (2010) | 0.40±0.02 | 0.41±0.01 | 0.8 | 0.8 | 295.1±0.6 | 295.3±0.2 | 0.4 | 1.4 | | |
| | 55549.000 | Hartkopf et al. (2012) | 0.41±0.01 | c | c | c | 294.3±0.1 | c | c | c | | |
| 26602 | 48475.000 | Fabricius et al. (2002) | 0.600±0.006 | 0.53±0.01 | 4.9 | 1.5 | 153.8±0.6 | 171.7±1.0 | 12.6 | 8.9 | 0.00 | 0.00 |

*Continued on next page*

Table A3 – *Continued from previous page*

| HIP | MJD (days) | Ref. | Sep (arcsec) $\Theta \pm \delta_\Theta$ | $\text{Sep}_{\text{bg}}$ (arcsec) $\Theta_{\text{bg}} \pm \delta_{\Theta,\text{bg}}$ | Sign.[a] not Backg. $\sigma_{\Theta,\text{bg}}$ | Sign. orb. motion $\sigma_{\Theta,\text{orb.}}$ | PA[b] (deg) PA$\pm\delta_{\text{PA}}$ | $\text{PA}_{\text{bg}}$ (deg) $\text{PA}_{\text{bg}} \pm \delta_{\text{PA, bg}}$ | Sign.[a] not Backg. $\sigma_{\text{PA,bg}}$ | Sign. orb. motion $\sigma_{\text{PA,orb.}}$ | $P_{\chi,\text{bg}}$ (%) | $P_{\chi,\text{cmv}}$ (%) |
|---|---|---|---|---|---|---|---|---|---|---|---|---|
| | 53434.070 | (1) | 0.598±0.003 | 0.566±0.005 | 5.8 | 2.5 | 157.5±0.6 | 163.4±0.4 | 8.2 | 2.9 | | |
| | 56189.379 | (1) | 0.5907±0.0005 | c | c | c | 159.18±0.05 | c | c | c | | |
| 28744 | 48348.000 | ESA (1997) | 0.57±0.04 | 0.65±0.02 | 1.7 | 0.2 | 274.0±0.1 | 280.6±1.0 | 4.8 | 20.8 | 0.00 | 0.00 |
| | 51185.000 | Horch et al. (2002) | 0.585±0.005 | 0.62±0.01 | 2.7 | 4.8 | 270.8±0.1 | 277.4±0.9 | 7.1 | 2.7 | | |
| | 53456.004 | (1) | 0.582±0.003 | 0.589±0.006 | 1.1 | 6.1 | 271.0±0.3 | 274.7±0.5 | 6.0 | 0.5 | | |
| | 56189.324 | (1) | 0.560±0.001 | c | c | c | 271.17±0.09 | c | c | c | | |
| 29401 | 48578.000 | Fabricius et al. (2002) | 0.720±0.008 | 0.77±0.02 | 3.0 | 7.6 | 199.4±0.6 | 212.0±1.0 | 9.4 | 6.8 | 0.00 | 0.00 |
| | 53741.177 | (1) | 0.689±0.001 | 0.693±0.005 | 0.9 | 17.9 | 203.0±0.1 | 206.6±0.4 | 8.0 | 4.2 | | |
| | 56269.323 | (1) | 0.659±0.001 | c | c | c | 203.48±0.06 | c | c | c | | |
| 29728 | 53470.975 | (1) | 0.395±0.003 | 0.388±0.003 | 1.6 | 1.3 | 277.8±0.5 | 263.3±0.4 | 24.0 | 9.5 | 0.00 | 0.00 |
| | 56189.360 | (1) | 0.3905±0.0007 | c | c | c | 282.5±0.1 | c | c | c | | |
| 30493 | 48512.000 | Fabricius et al. (2002) | 0.80±0.01 | 0.73±0.02 | 3.6 | 11.7 | 271.2±0.8 | 261.8±1.0 | 6.8 | 3.2 | 0.00 | 0.00 |
| | 53435.117 | (1) | 0.714±0.002 | 0.696±0.006 | 2.8 | 15.7 | 273.0±0.5 | 269.3±0.4 | 5.6 | 1.4 | | |
| | 56189.395 | (1) | 0.6829±0.0006 | c | c | c | 273.78±0.06 | c | c | c | | |
| 30867 | 48541.000 | Fabricius et al. (2002) | 7.150±0.005 | 7.05±0.03 | 3.8 | 4.2 | 132.7±0.1 | 133.8±0.2 | 4.6 | 0.7 | 0.00 | 0.00 |
| | 48559.000 | Jasinta et al. (1995) | 7.166±0.008 | 7.05±0.03 | 4.3 | 4.8 | 132.70±0.07 | 133.7±0.2 | 4.8 | 0.9 | | |
| | 53469.984 | (1) | 7.14±0.06 | 7.09±0.01 | 0.8 | 0.3 | 132.4±0.5 | 133.03±0.09 | 1.3 | 0.4 | | |
| | 54140.000 | Mason et al. (2008) | 7.13±0.01 | 7.097±0.009 | 2.4 | 1.1 | 132.6±0.1 | 132.91±0.07 | 2.6 | 0.2 | | |
| | 54779.000 | Hartkopf et al. (2011) | 7.103±0.005 | 7.103±0.008 | 0.1 | 1.8 | 132.4±0.1 | 132.82±0.06 | 3.6 | 2.1 | | |
| | 55851.000 | Mason et al. (2012) | 6.89±0.01 | 7.114±0.006 | 19.0 | 19.5 | 132.8±0.1 | 132.67±0.05 | 1.2 | 1.6 | | |
| | 56189.317 | (1) | 7.117±0.006 | c | c | c | 132.63±0.05 | c | c | c | | |
| 31137 | 28534.000 | WDS | 2.4±0.1 | 2.44±0.03 | 0.4 | 0.5 | 231.0±0.5 | 233.1±0.8 | 2.2 | 3.8 | 90.44 | 73.07 |
| | 48348.000 | Fabricius et al. (2002) | 2.48±0.02 | 2.442±0.008 | 1.6 | 1.3 | 229.9±0.5 | 230.4±0.2 | 0.8 | 1.6 | | |
| | 53470.984 | (1) | 2.45±0.01 | 2.444±0.003 | 0.4 | 0.1 | 229.5±0.3 | 229.6±0.1 | 0.4 | 1.4 | | |
| | 56189.351 | (1) | 2.451±0.002 | c | c | c | 229.10±0.08 | c | c | c | | |
| 31959 | 54409.342 | (1) | 1.695±0.006 | 1.73±0.01 | 3.0 | 0.5 | 326.8±0.5 | 327.5±0.3 | 1.0 | 0.9 | 65.09 | 91.68 |
| | 54470.143 | (1) | 1.695±0.006 | 1.73±0.01 | 3.0 | 0.5 | 326.7±0.5 | 327.5±0.3 | 1.3 | 1.1 | | |
| | 56266.100 | (1) | 1.70±0.01 | c | c | c | 327.4±0.3 | c | c | c | | |
| 34045 | 53408.131 | (1) | 0.3353±0.0006 | 0.359±0.002 | 12.2 | 2.9 | 114.9±0.2 | 115.0±0.3 | 0.3 | 61.4 | 0.00 | 0.00 |
| | 56298.140 | (1) | 0.3321±0.0009 | c | c | c | 100.6±0.1 | c | c | c | | |
| 34338 | 53408.163 | (1) | 3.664±0.004 | 3.680±0.005 | 2.6 | 7.0 | 345.52±0.06 | 344.39±0.08 | 11.4 | 11.1 | 0.00 | 0.00 |

*Continued on next page*

Table A3 – *Continued from previous page*

| HIP | MJD (days) | Ref. | Sep (arcsec) $\Theta \pm \delta_\Theta$ | $\mathrm{Sep_{bg}}$ (arcsec) $\Theta_{\mathrm{bg}} \pm \delta_{\Theta,\mathrm{bg}}$ | Sign.[a] not Backg. $\sigma_{\Theta,\mathrm{bg}}$ | Sign. orb. motion $\sigma_{\Theta,\mathrm{orb.}}$ | PA[b] (deg) PA$\pm\delta_{\mathrm{PA}}$ | $\mathrm{PA_{bg}}$ (deg) $\mathrm{PA_{bg}} \pm \delta_{\mathrm{PA,\ bg}}$ | Sign.[a] not Backg. $\sigma_{\mathrm{PA,bg}}$ | Sign. orb. motion $\sigma_{\mathrm{PA,orb.}}$ | $\mathrm{P_{\chi,bg}}$ (%) | $\mathrm{P_{\chi,cmv}}$ (%) |
|---|---|---|---|---|---|---|---|---|---|---|---|---|
| | 56296.212 | (1) | 3.704±0.004 | c | c | c | 346.48±0.06 | c | c | c | | |
| 34758 | 53413.189 | (1) | 13.72±0.02 | 13.72±0.02 | 0.1 | 2.3 | 348.03±0.09 | 347.50±0.08 | 4.4 | 4.0 | 17.03 | 2.42 |
| | 54425.348 | (1) | 13.65±0.02 | c | c | c | 347.55±0.08 | c | c | c | | |
| 36345 | 48475.000 | Fabricius et al. (2002) | 8.90±0.06 | 8.82±0.01 | 1.3 | 0.3 | 53.6±0.1 | 52.2±0.5 | 2.7 | 0.9 | 69.26 | 97.54 |
| | 51216.000 | Hartkopf et al. (2013) | 9.0±0.2 | 8.87±0.01 | 0.5 | 0.2 | 53.5±2.0 | 52.6±0.5 | 0.5 | 0.2 | | |
| | 54839.338 | (1) | 8.919±0.009 | c | c | c | 53.1±0.5 | c | c | c | | |
| 36363 | 53384.187 | (1) | 5.49±0.01 | 5.54±0.01 | 2.6 | 1.8 | 299.6±0.2 | 299.08±0.08 | 2.8 | 3.5 | 27.91 | 11.57 |
| | 54427.198 | (1) | 5.46±0.01 | c | c | c | 298.96±0.08 | c | c | c | | |
| 37322 | 48530.000 | Fabricius et al. (2002) | 1.320±0.008 | 0.891±0.005 | 46.4 | 4.6 | 151.7±0.4 | 160.4±0.3 | 17.6 | 5.9 | 0.00 | 0.00 |
| | 50141.000 | Horch et al. (2001) | 1.22±0.01 | 0.988±0.004 | 22.2 | 5.7 | 149.2±0.1 | 156.4±0.2 | 32.5 | 0.8 | | |
| | 53384.200 | (1) | 1.281±0.002 | 1.207±0.002 | 26.7 | 0.3 | 149.81±0.08 | 150.63±0.07 | 7.5 | 5.0 | | |
| | 54412.365 | (1) | 1.282±0.002 | c | c | c | 149.29±0.06 | c | c | c | | |
| 37915 | 53384.257 | (1) | 0.1821±0.0006 | 0.225±0.004 | 9.6 | 0.4 | 15.3±0.3 | -10.3±0.5 | 48.8 | 18.1 | 0.00 | 0.00 |
| | 54427.184 | (1) | 0.184±0.004 | c | c | c | 4.9±0.5 | c | c | c | | |
| 40817 | 53415.171 | (1) | 1.417±0.001 | 1.500±0.002 | 33.2 | 6.4 | 9.33±0.06 | 6.14±0.07 | 36.1 | 10.6 | 0.00 | 0.00 |
| | 54451.318 | (1) | 1.401±0.003 | 1.405±0.002 | 1.3 | 0.5 | 8.6±0.1 | 8.47±0.05 | 1.3 | 0.9 | | |
| | 54467.291 | (1) | 1.403±0.002 | c | c | c | 8.52±0.05 | c | c | c | | |
| 41049 | 48348.000 | Fabricius et al. (2002) | 10.31±0.03 | d | d | d | 54.5±0.1 | d | d | d | 71.74 | 96.69 |
| | 51204.000 | Hartkopf et al. (2013) | 10.32±0.05 | 10.34±0.03 | 0.4 | 0.1 | 54.9±0.4 | 54.2±0.1 | 1.7 | 1.0 | | |
| | 53099.999 | (1) | 10.30±0.01 | 10.36±0.03 | 1.6 | 0.3 | 54.7±0.5 | 54.0±0.1 | 1.4 | 0.5 | | |
| 41817 | 53413.218 | (1) | 0.322±0.001 | 0.432±0.009 | 12.4 | 7.9 | 302.8±0.2 | 251.6±0.7 | 68.2 | 50.5 | 0.00 | 0.00 |
| | 54425.296 | (1) | 0.3379±0.0008 | 0.380±0.007 | 5.8 | 4.9 | 297.8±0.1 | 263.1±0.6 | 60.6 | 42.5 | | |
| | 54927.000 | Tokovinin et al. (2010) | 0.344±0.001 | 0.374±0.007 | 4.5 | 3.6 | 295.6±0.2 | 270.0±0.4 | 53.7 | 23.3 | | |
| | 55576.000 | Hartkopf et al. (2012) | 0.354±0.002 | 0.360±0.006 | 0.9 | 1.5 | 293.6±0.1 | 279.2±0.3 | 49.7 | 22.6 | | |
| | 56340.000 | Tokovinin et al. (2014) | 0.363±0.005 | c | c | c | 290.4±0.1 | c | c | c | | |
| 41843 | 53404.245 | (1) | 0.676±0.003 | 0.600±0.006 | 11.2 | 1.8 | 332.1±0.3 | 321.7±0.7 | 13.8 | 0.5 | 0.00 | 64.51 |
| | 56326.142 | (1) | 0.665±0.005 | c | c | c | 332.4±0.5 | c | c | c | | |
| 42129 | 48444.000 | ESA (1997) | 0.63±0.01 | 1.063±0.005 | 35.2 | 2.7 | 294.0±0.1 | 299.6±0.3 | 19.0 | 45.6 | 0.00 | 0.00 |
| | 53738.190 | (1) | 0.6587±0.0009 | 0.711±0.002 | 24.2 | 2.4 | 301.2±0.1 | 301.3±0.1 | 0.4 | 2.4 | | |
| | 54451.330 | (1) | 0.664±0.002 | c | c | c | 301.6±0.1 | c | c | c | | |
| 42177 | 51268.000 | Hubrig et al. (2001) | 0.60±0.05 | 0.580±0.001 | 0.5 | 0.7 | 221.2±0.1 | 229.7±0.1 | 48.5 | 12.5 | 5.74 | 54.49 |

*Continued on next page*

Table A3 – *Continued from previous page*

| HIP | MJD (days) | Ref. | Sep (arcsec) $\Theta \pm \delta_\Theta$ | $\mathrm{Sep_{bg}}$ (arcsec) $\Theta_{\mathrm{bg}} \pm \delta_{\Theta,\mathrm{bg}}$ | Sign.[a] not Backg. $\sigma_{\Theta,\mathrm{bg}}$ | Sign. orb. motion $\sigma_{\Theta,\mathrm{orb.}}$ | PA[b] (deg) PA$\pm\delta_{\mathrm{PA}}$ | $\mathrm{PA_{bg}}$ (deg) $\mathrm{PA_{bg}} \pm \delta_{\mathrm{PA,\ bg}}$ | Sign.[a] not Backg. $\sigma_{\mathrm{PA,bg}}$ | Sign. orb. motion $\sigma_{\mathrm{PA,orb.}}$ | $\mathrm{P_{\chi,bg}}$ (%) | $\mathrm{P_{\chi,cmv}}$ (%) |
|---|---|---|---|---|---|---|---|---|---|---|---|---|
| | 53404.271 | (1) | 0.5679±0.0005 | c | c | c | 219.79±0.05 | c | c | c | | |
| 42334 | 53434.185 | (1) | 3.210±0.006 | 3.153±0.006 | 6.4 | 0.5 | 10.9±0.1 | 9.6±0.1 | 7.0 | 0.8 | 0.05 | 85.09 |
| | 54508.151 | (1) | 3.205±0.007 | c | c | c | 10.8±0.1 | c | c | c | | |
| 42540 | 48348.000 | Fabricius et al. (2002) | 4.47±0.01 | 3.803±0.009 | 38.2 | 6.7 | 66.7±0.2 | 59.7±0.1 | 28.5 | 1.7 | 0.00 | 0.00 |
| | 51237.000 | Cutri et al. (2003) | 4.120±0.005 | 4.161±0.007 | 4.7 | 55.6 | 66.4±0.1 | 63.6±0.1 | 19.2 | 5.0 | | |
| | 53375.255 | (1) | 4.564±0.007 | 4.437±0.006 | 13.6 | 1.7 | 67.43±0.09 | 65.99±0.09 | 11.1 | 2.8 | | |
| | 54451.341 | (1) | 4.580±0.007 | c | c | c | 67.08±0.09 | c | c | c | | |
| 42715 | 53742.219 | (1) | 0.587±0.001 | 0.528±0.001 | 32.8 | 1.8 | 162.28±0.08 | 166.5±0.1 | 29.5 | 5.3 | 0.00 | 1.70 |
| | 54509.215 | (1) | 0.590±0.001 | c | c | c | 162.93±0.09 | c | c | c | | |
| 43305 | 51268.000 | Hubrig et al. (2001) | 1.34±0.05 | 1.481±0.003 | 2.8 | 0.6 | 165.8±0.1 | 176.2±0.1 | 63.8 | 17.2 | 0.00 | 0.00 |
| | 53379.290 | (1) | 1.315±0.001 | 1.363±0.002 | 17.4 | 2.0 | 167.48±0.06 | 171.1±0.1 | 32.5 | 5.9 | | |
| | 54509.232 | (1) | 1.309±0.002 | c | c | c | 168.11±0.09 | c | c | c | | |
| 43792 | 48501.000 | Fabricius et al. (2002) | 2.05±0.01 | 2.34±0.01 | 17.6 | 15.6 | 305.5±0.4 | 303.4±0.2 | 4.4 | 4.7 | 0.00 | 0.00 |
| | 52659.321 | (1) | 2.2523±0.0004 | c | c | c | 303.61±0.02 | c | c | c | | |
| 44299 | 53750.090 | (1) | 10.47±0.01 | 10.51±0.01 | 2.0 | 1.9 | 222.84±0.07 | 222.49±0.09 | 3.0 | 5.2 | 46.15 | 1.96 |
| | 54451.354 | (1) | 10.51±0.01 | c | c | c | 222.24±0.09 | c | c | c | | |
| 44798 | 49670.000 | Mason et al. (1999) | 0.311±0.005 | 0.424±0.008 | 12.2 | 16.3 | 106.2±0.1 | 173.0±0.4 | 180.6 | 37.5 | 0.00 | 0.00 |
| | 49772.000 | Mason et al. (1999) | 0.310±0.005 | 0.419±0.008 | 11.9 | 16.1 | 106.9±0.1 | 172.4±0.4 | 177.0 | 32.5 | | |
| | 50052.000 | Mason et al. (1999) | 0.304±0.005 | 0.404±0.007 | 11.1 | 15.1 | 106.6±0.1 | 171.3±0.4 | 174.3 | 34.6 | | |
| | 50400.000 | Mason et al. (1999) | 0.300±0.005 | 0.385±0.007 | 9.8 | 14.4 | 107.6±0.1 | 169.5±0.4 | 166.1 | 27.6 | | |
| | 50496.000 | Mason et al. (1999) | 0.301±0.005 | 0.380±0.007 | 9.2 | 14.6 | 106.4±0.1 | 168.8±0.4 | 167.2 | 36.1 | | |
| | 53380.279 | (1) | 0.2684±0.0004 | 0.252±0.004 | 3.7 | 17.3 | 109.47±0.08 | 144.6±0.4 | 95.0 | 16.0 | | |
| | 55167.000 | Balega et al. (2012) | 0.222±0.002 | 0.216±0.003 | 1.5 | 1.7 | 112.2±0.5 | 118.0±0.2 | 10.9 | 1.4 | | |
| | 55550.000 | Hartkopf et al. (2012) | 0.216±0.003 | c | c | c | 111.5±0.1 | c | c | c | | |
| 44883 | 48348.000 | Fabricius et al. (2002) | 1.28±0.04 | 1.60±0.01 | 7.7 | 0.5 | 296.0±1.0 | 291.5±0.3 | 3.7 | 2.9 | 0.00 | 66.84 |
| | 51268.000 | Hubrig et al. (2001) | 1.30±0.05 | 1.454±0.007 | 3.1 | 0.0 | 298.5±0.2 | 294.8±0.2 | 13.1 | 4.4 | | |
| | 53382.271 | (1) | 1.293±0.002 | 1.352±0.003 | 15.1 | 2.5 | 299.34±0.09 | 297.8±0.1 | 10.3 | 1.1 | | |
| | 53516.000 | Hubrig et al. (2007) | 1.30±0.07 | 1.345±0.003 | 0.6 | 0.0 | 299.0±2.0 | 298.0±0.1 | 0.5 | 0.2 | | |
| | 54468.304 | (1) | 1.301±0.002 | c | c | c | 299.5±0.1 | c | c | c | | |
| 45189 | 44339.000 | Jasinta et al. (1995) | 2.74±0.01 | d | d | d | 282.0±0.2 | d | d | d | 0.00 | 0.00 |
| | 47878.000 | Jasinta et al. (1994) | 2.782±0.008 | 2.92±0.02 | 7.0 | 2.5 | 281.3±0.1 | 285.8±0.3 | 14.3 | 3.1 | | |

*Continued on next page*

Table A3 – *Continued from previous page*

| HIP | MJD (days) | Ref. | Sep (arcsec) $\Theta \pm \delta_\Theta$ | $\mathrm{Sep_{bg}}$ (arcsec) $\Theta_{\rm bg} \pm \delta_{\Theta,\rm bg}$ | Sign.[a] not Backg. $\sigma_{\Theta,\rm bg}$ | Sign. orb. motion $\sigma_{\Theta,\rm orb.}$ | PA[b] (deg) PA$\pm\delta_{\rm PA}$ | $\mathrm{PA_{bg}}$ (deg) $\mathrm{PA_{bg}} \pm \delta_{\rm PA,\ bg}$ | Sign.[a] not Backg. $\sigma_{\rm PA,bg}$ | Sign. orb. motion $\sigma_{\rm PA,orb.}$ | $\mathrm{P_{\chi,bg}}$ (%) | $\mathrm{P_{\chi,cmv}}$ (%) |
|---|---|---|---|---|---|---|---|---|---|---|---|---|
| | 47973.000 | Jasinta et al. (1995) | 2.77±0.01 | 2.92±0.02 | 7.3 | 1.6 | 281.7±0.2 | 285.8±0.3 | 12.9 | 1.5 | | |
| | 48505.000 | Fabricius et al. (2002) | 2.810±0.005 | 2.94±0.02 | 7.0 | 4.6 | 281.5±0.1 | 286.4±0.3 | 15.8 | 2.5 | | |
| | 53382.319 | (1) | 2.842±0.004 | 3.21±0.02 | 15.4 | 7.0 | 281.24±0.08 | 290.7±0.4 | 23.5 | 3.9 | | |
| | 54467.304 | (1) | 2.860±0.004 | 3.27±0.02 | 16.3 | 8.2 | 280.57±0.08 | 291.6±0.4 | 26.0 | 7.1 | | |
| | 54927.000 | Tokovinin et al. (2010) | 2.861±0.001 | 3.29±0.03 | 17.1 | 8.5 | 280.4±0.1 | 291.9±0.4 | 26.5 | 7.6 | | |
| | 55994.000 | Tokovinin (2012) | 2.883±0.001 | 3.35±0.03 | 17.8 | 10.1 | 280.6±0.1 | 292.7±0.4 | 26.8 | 6.7 | | |
| | 56340.000 | Tokovinin et al. (2014) | 2.887±0.001 | 3.37±0.03 | 18.2 | 10.4 | 280.6±0.1 | 293.0±0.4 | 27.0 | 6.7 | | |
| 45314 | 53355.364 | (1) | 2.726±0.004 | 2.917±0.004 | 32.1 | 1.9 | 337.00±0.07 | 333.53±0.07 | 33.2 | 8.3 | 0.00 | 0.08 |
| | 54511.144 | (1) | 2.736±0.006 | 2.850±0.004 | 15.6 | 0.1 | 336.3±0.1 | 334.60±0.07 | 14.4 | 0.9 | | |
| | 56265.357 | (1) | 2.737±0.004 | c | c | c | 336.21±0.06 | c | c | c | | |
| 45344 | 53349.377 | (1) | 5.907±0.009 | 5.919±0.007 | 1.1 | 0.6 | 13.65±0.07 | 12.32±0.07 | 13.2 | 4.9 | 0.00 | 1.67 |
| | 54511.158 | (1) | 5.900±0.007 | c | c | c | 13.16±0.07 | c | c | c | | |
| 46283 | 53750.263 | (1) | 0.341±0.002 | 0.312±0.005 | 5.6 | 1.5 | 159.2±0.3 | 160.1±0.3 | 2.4 | 10.7 | 2.33 | 0.00 |
| | 54475.312 | (1) | 0.348±0.005 | c | c | c | 155.4±0.2 | c | c | c | | |
| 46329 | 48497.000 | Fabricius et al. (2002) | 0.540±0.005 | 0.79±0.01 | 19.2 | 1.3 | 275.9±0.6 | 271.8±0.6 | 4.8 | 7.1 | 0.00 | 0.00 |
| | 53454.111 | (1) | 0.548±0.003 | c | c | c | 280.8±0.3 | c | c | c | | |
| 46914 | 48512.000 | Fabricius et al. (2002) | 2.020±0.004 | 2.217±0.008 | 22.3 | 0.5 | 217.8±0.2 | 229.3±0.2 | 39.4 | 8.9 | 0.00 | 0.00 |
| | 49396.000 | Abad et al. (1995) | 1.89±0.08 | 2.182±0.007 | 3.6 | 1.7 | 216.7±3.0 | 228.0±0.2 | 4.4 | 1.2 | | |
| | 53442.136 | (1) | 2.018±0.003 | 2.052±0.003 | 8.0 | 1.1 | 219.76±0.08 | 221.54±0.06 | 17.3 | 1.3 | | |
| | 54535.108 | (1) | 2.022±0.002 | c | c | c | 219.64±0.05 | c | c | c | | |
| 46928 | 53778.238 | (1) | 0.594±0.001 | 0.591±0.004 | 0.6 | 3.2 | 189.6±0.1 | 194.9±0.3 | 17.3 | 4.4 | 0.00 | 0.16 |
| | 54475.332 | (1) | 0.606±0.004 | c | c | c | 188.2±0.3 | c | c | c | | |
| 48943 | 48348.000 | ESA (1997) | 0.53±0.03 | 0.715±0.009 | 5.3 | 0.6 | 360.0±0.1 | 324.6±0.8 | 45.1 | 19.5 | 0.00 | 0.00 |
| | 53493.025 | (1) | 0.507±0.004 | c | c | c | 351.8±0.4 | c | c | c | | |
| 50847 | 53779.196 | (1) | 2.222±0.002 | 2.306±0.002 | 26.7 | 0.2 | 350.18±0.06 | 347.60±0.06 | 31.0 | 0.4 | 0.00 | 96.08 |
| | 55673.115 | (1) | 2.221±0.002 | c | c | c | 350.22±0.06 | c | c | c | | |
| 51362 | 53185.016 | (1) | 5.155±0.009 | 5.07±0.01 | 5.8 | 0.8 | 70.4±0.1 | 70.3±0.1 | 0.4 | 0.2 | 12.11 | 92.29 |
| | 53846.122 | (1) | 5.17±0.01 | c | c | c | 70.4±0.1 | c | c | c | | |
| 52742 | 53794.080 | (1) | 1.056±0.005 | 1.055±0.005 | 0.3 | 0.4 | 8.49±0.07 | 6.10±0.06 | 27.2 | 3.4 | 0.00 | 35.24 |
| | 54483.355 | (1) | 1.059±0.004 | c | c | c | 8.19±0.06 | c | c | c | | |
| 53272 | 48531.000 | Fabricius et al. (2002) | 1.510±0.005 | 1.980±0.009 | 45.9 | 2.9 | 287.9±0.2 | 283.4±0.2 | 15.3 | 0.6 | 0.00 | 0.06 |

*Continued on next page*

Table A3 – *Continued from previous page*

| HIP | MJD (days) | Ref. | Sep (arcsec) $\Theta \pm \delta_\Theta$ | $\text{Sep}_{\text{bg}}$ (arcsec) $\Theta_{\text{bg}} \pm \delta_{\Theta,\text{bg}}$ | Sign.[a] not Backg. $\sigma_{\Theta,\text{bg}}$ | Sign. orb. motion $\sigma_{\Theta,\text{orb.}}$ | PA[b] (deg) PA$\pm\delta_{\text{PA}}$ | $\text{PA}_{\text{bg}}$ (deg) $\text{PA}_{\text{bg}} \pm \delta_{\text{PA, bg}}$ | Sign.[a] not Backg. $\sigma_{\text{PA,bg}}$ | Sign. orb. motion $\sigma_{\text{PA,orb.}}$ | $P_{\chi,\text{bg}}$ (%) | $P_{\chi,\text{cmv}}$ (%) |
|---|---|---|---|---|---|---|---|---|---|---|---|---|
| | 53779.256 | (1) | 1.521±0.001 | 1.580±0.002 | 28.4 | 2.3 | 288.27±0.06 | 287.13±0.06 | 13.5 | 6.3 | | |
| | 54511.296 | (1) | 1.525±0.001 | c | c | c | 287.78±0.05 | c | c | c | | |
| 54557 | 53794.134 | (1) | 0.786±0.002 | d | d | d | 327.08±0.09 | d | d | d | 0.00 | 0.00 |
| | 53820.400 | (1) | 0.787±0.002 | 0.786±0.002 | 0.4 | 0.4 | 326.8±0.2 | 327.15±0.09 | 1.7 | 1.4 | | |
| | 54160.099 | (1) | 0.784±0.003 | 0.775±0.002 | 2.9 | 0.5 | 326.6±0.1 | 328.4±0.1 | 12.5 | 3.4 | | |
| | 54516.213 | (1) | 0.783±0.003 | 0.765±0.002 | 5.2 | 0.9 | 326.1±0.1 | 329.8±0.1 | 19.8 | 6.6 | | |
| | 55605.340 | (1) | 0.783±0.002 | 0.736±0.004 | 10.6 | 1.3 | 324.3±0.1 | 334.3±0.3 | 27.5 | 19.0 | | |
| 55597 | 44268.000 | Jasinta et al. (1995) | 2.42±0.01 | 3.11±0.01 | 45.8 | 7.1 | 306.5±0.2 | 304.4±0.2 | 7.1 | 10.7 | 0.00 | 0.00 |
| | 47214.000 | Jasinta et al. (1994) | 2.356±0.009 | 2.933±0.008 | 46.7 | 14.2 | 307.6±0.2 | 305.6±0.1 | 7.5 | 5.7 | | |
| | 48521.000 | Fabricius et al. (2002) | 2.430±0.005 | 2.860±0.007 | 49.5 | 10.5 | 308.4±0.1 | 306.2±0.1 | 14.4 | 5.7 | | |
| | 53752.367 | (1) | 2.488±0.002 | 2.534±0.003 | 13.2 | 0.1 | 309.33±0.05 | 308.54±0.03 | 13.4 | 6.1 | | |
| | 54520.280 | (1) | 2.488±0.002 | c | c | c | 308.98±0.02 | c | c | c | | |
| 55657 | 53741.381 | (1) | 6.168±0.004 | 6.136±0.008 | 3.7 | 1.8 | 115.52±0.06 | 115.5±0.1 | 0.4 | 2.4 | 61.73 | 17.52 |
| | 54520.291 | (1) | 6.183±0.008 | c | c | c | 115.2±0.1 | c | c | c | | |
| 58326 | 51690.000 | Shatsky et al. (2002) | 4.94±0.05 | 4.854±0.005 | 1.8 | 0.1 | 138.6±0.1 | 138.77±0.06 | 1.5 | 14.5 | 15.62 | 0.00 |
| | 53779.305 | (1) | 4.950±0.005 | 4.927±0.005 | 3.4 | 0.1 | 137.71±0.05 | 137.41±0.06 | 4.0 | 10.4 | | |
| | 54475.341 | (1) | 4.950±0.005 | c | c | c | 136.95±0.05 | c | c | c | | |
| 60189 | 31821.000 | Dommanget et al. (2000) | 11.2±0.1 | 10.10±0.03 | 10.6 | 53.7 | 66.0±0.5 | 71.4±0.1 | 10.6 | 14.2 | 0.00 | 0.00 |
| | 53407.377 | (1) | 16.73±0.02 | c | c | c | 73.21±0.09 | c | c | c | | |
| 60449 | 53413.287 | (1) | 0.684±0.006 | 0.788±0.002 | 16.9 | 5.4 | 320.4±0.7 | 311.0±0.1 | 13.3 | 2.1 | 0.00 | 1.43 |
| | 54510.354 | (1) | 0.716±0.002 | c | c | c | 318.9±0.1 | c | c | c | | |
| 61789 | 51268.000 | Hubrig et al. (2001) | 1.19±0.05 | 0.921±0.002 | 5.4 | 0.2 | 75.0±0.1 | 78.4±0.1 | 24.1 | 9.3 | 0.00 | 31.13 |
| | 53404.299 | (1) | 1.202±0.001 | c | c | c | 73.90±0.06 | c | c | c | | |
| 62026 | 51664.000 | Kouwenhoven et al. (2005) | 0.22±0.05 | 0.199±0.003 | 0.4 | 0.2 | 12.5±0.3 | -34.0±1.0 | 42.9 | 7.2 | 0.00 | 34.64 |
| | 53102.133 | (1) | 0.232±0.002 | c | c | c | 6.3±0.8 | c | c | c | | |
| 63005 | 53397.384 | (1) | 0.192±0.009 | 0.216±0.007 | 2.0 | 1.0 | 88.9±1.0 | 196.0±0.4 | 86.4 | 36.0 | 0.00 | 0.00 |
| | 55690.051 | (1) | 0.204±0.006 | c | c | c | 134.3±0.4 | c | c | c | | |
| 63945 | 51690.000 | Shatsky et al. (2002) | 1.55±0.02 | 1.698±0.008 | 8.3 | 0.1 | 268.2±0.2 | 264.3±0.3 | 10.1 | 4.0 | 0.00 | 2.31 |
| | 53454.210 | (1) | 1.550±0.007 | c | c | c | 266.7±0.3 | c | c | c | | |
| 64515 | 51696.000 | Kouwenhoven et al. (2005) | 0.31±0.01 | 0.407±0.003 | 9.2 | 1.6 | 165.7±0.1 | 188.5±0.4 | 55.6 | 52.3 | 0.00 | 0.00 |
| | 53436.294 | (1) | 0.323±0.002 | 0.3336±0.0008 | 5.5 | 1.8 | 159.7±0.3 | 163.6±0.1 | 11.8 | 6.7 | | |

*Continued on next page*

Table A3 – *Continued from previous page*

| HIP | MJD (days) | Ref. | Sep (arcsec) $\Theta \pm \delta_\Theta$ | $\mathrm{Sep_{bg}}$ (arcsec) $\Theta_{\mathrm{bg}} \pm \delta_{\Theta,\mathrm{bg}}$ | Sign.[a] not Backg. $\sigma_{\Theta,\mathrm{bg}}$ | Sign. orb. motion $\sigma_{\Theta,\mathrm{orb.}}$ | PA[b] (deg) PA$\pm\delta_{\mathrm{PA}}$ | $\mathrm{PA_{bg}}$ (deg) $\mathrm{PA_{bg}} \pm \delta_{\mathrm{PA,\ bg}}$ | Sign.[a] not Backg. $\sigma_{\mathrm{PA,bg}}$ | Sign. orb. motion $\sigma_{\mathrm{PA,orb.}}$ | $\mathrm{P_{\chi,bg}}$ (%) | $\mathrm{P_{\chi,cmv}}$ (%) |
|---|---|---|---|---|---|---|---|---|---|---|---|---|
| | 53778.374 | (1) | 0.3265±0.0006 | c | c | c | 157.5±0.1 | c | c | c | | |
| 67472 | 51634.000 | Shatsky et al. (2002) | 4.64±0.05 | 4.76±0.02 | 2.5 | 0.0 | 304.2±0.1 | 300.1±0.1 | 26.0 | 1.6 | 0.00 | 97.66 |
| | 53454.224 | (1) | 4.62±0.03 | 4.70±0.02 | 2.8 | 0.6 | 304.3±0.3 | 301.8±0.1 | 6.8 | 0.9 | | |
| | 55690.020 | (1) | 4.64±0.02 | c | c | c | 304.0±0.1 | c | c | c | | |
| 67669 | 44369.000 | Jasinta et al. (1995) | 7.859±0.005 | 7.26±0.02 | 25.2 | 1.7 | 106.55±0.04 | 112.7±0.2 | 36.8 | 10.6 | 0.00 | 0.00 |
| | 48348.000 | Fabricius et al. (2002) | 7.850±0.005 | 7.50±0.02 | 20.2 | 1.1 | 106.0±0.1 | 109.4±0.1 | 22.4 | 3.6 | | |
| | 53404.327 | (1) | 7.84±0.01 | c | c | c | 105.53±0.09 | c | c | c | | |
| 67703 | 48348.000 | Fabricius et al. (2002) | 18.11±0.02 | 18.49±0.05 | 6.9 | 0.5 | 288.7±0.1 | 287.2±0.1 | 8.7 | 0.5 | 0.00 | 0.00 |
| | 50948.000 | Hartkopf et al. (2013) | 17.88±0.01 | 18.27±0.05 | 7.7 | 4.0 | 286.9±0.1 | 288.0±0.1 | 6.8 | 11.2 | | |
| | 53144.000 | Sinachopoulos et al. (2007) | 18.35±0.03 | 18.09±0.05 | 4.8 | 4.9 | 288.53±0.02 | 288.8±0.1 | 1.8 | 1.9 | | |
| | 53185.155 | (1) | 18.08±0.05 | c | c | c | 288.8±0.1 | c | c | c | | |
| 70915 | 51317.000 | Cutri et al. (2003) | 10.72±0.05 | 10.86±0.01 | 2.6 | 0.6 | 309.5±0.5 | 307.22±0.07 | 4.5 | 0.4 | 0.00 | 14.83 |
| | 53791.380 | (1) | 10.74±0.01 | 10.77±0.01 | 1.7 | 0.5 | 309.82±0.08 | 308.83±0.07 | 9.6 | 5.0 | | |
| | 54518.402 | (1) | 10.75±0.01 | c | c | c | 309.30±0.07 | c | c | c | | |
| 71762 | 48348.000 | Fabricius et al. (2002) | 5.550±0.004 | d | d | d | 109.8±0.1 | d | d | d | 0.00 | 0.15 |
| | 49876.000 | Popovic et al. (1997) | 5.56±0.01 | 5.532±0.008 | 2.1 | 0.9 | 109.71±0.05 | 110.4±0.1 | 4.4 | 0.8 | | |
| | 52381.000 | Mason et al. (2004) | 5.49±0.01 | 5.50±0.02 | 0.4 | 5.6 | 109.8±0.1 | 111.4±0.2 | 6.3 | 0.0 | | |
| | 53404.392 | (1) | 5.542±0.008 | 5.48±0.02 | 3.0 | 0.9 | 110.47±0.07 | 111.8±0.3 | 4.9 | 5.5 | | |
| 73111 | 48494.000 | Fabricius et al. (2002) | 2.190±0.005 | 2.52±0.02 | 18.0 | 5.1 | 277.8±0.1 | 269.4±0.4 | 21.9 | 0.7 | 0.00 | 0.20 |
| | 53454.267 | (1) | 2.13±0.01 | c | c | c | 277.6±0.3 | c | c | c | | |
| 74750 | 48497.000 | Fabricius et al. (2002) | 1.31±0.01 | 1.253±0.008 | 4.4 | 7.8 | 163.3±0.4 | 165.4±0.4 | 3.8 | 0.8 | 2.05 | 0.00 |
| | 53454.289 | (1) | 1.218±0.006 | c | c | c | 163.7±0.3 | c | c | c | | |
| 75264 | 53454.311 | (1) | 0.279±0.003 | d | d | d | 131.6±0.6 | d | d | d | 0.00 | 0.00 |
| | 54666.000 | Tokovinin et al. (2010) | 0.2688±0.0001 | 0.308±0.004 | 8.7 | 3.5 | 119.9±0.1 | 112.9±0.8 | 8.8 | 18.2 | | |
| | 54927.000 | Tokovinin et al. (2010) | 0.2639±0.0005 | 0.320±0.005 | 11.1 | 5.0 | 117.5±0.1 | 110.0±0.8 | 8.8 | 22.0 | | |
| | 55690.093 | (1) | 0.2454±0.0009 | 0.355±0.007 | 16.1 | 10.7 | 109.4±0.1 | 101.3±1.0 | 8.1 | 34.3 | | |
| 77840 | 44338.000 | Jasinta et al. (1995) | 2.18±0.02 | 2.68±0.03 | 14.1 | 6.2 | 271.6±0.2 | 249.9±0.7 | 30.8 | 9.8 | 0.00 | 0.00 |
| | 48475.000 | Fabricius et al. (2002) | 2.130±0.005 | 2.43±0.02 | 12.3 | 5.8 | 269.3±0.2 | 254.8±0.6 | 24.0 | 5.0 | | |
| | 56121.124 | (1) | 2.04±0.02 | c | c | c | 266.9±0.4 | c | c | c | | |
| 78968 | 51664.000 | Kouwenhoven et al. (2005) | 2.75±0.01 | 2.73±0.03 | 0.6 | 0.5 | 321.1±0.3 | 320.6±0.7 | 0.6 | 1.5 | 96.41 | 66.06 |
| | 53130.200 | (1) | 2.77±0.03 | c | c | c | 322.3±0.7 | c | c | c | | |

*Continued on next page*

Table A3 – *Continued from previous page*

| HIP | MJD (days) | Ref. | Sep (arcsec) $\Theta \pm \delta_\Theta$ | $\text{Sep}_{\text{bg}}$ (arcsec) $\Theta_{\text{bg}} \pm \delta_{\Theta,\text{bg}}$ | Sign.[a] not Backg. $\sigma_{\Theta,\text{bg}}$ | Sign. orb. motion $\sigma_{\Theta,\text{orb.}}$ | PA[b] (deg) PA$\pm\delta_{\text{PA}}$ | $\text{PA}_{\text{bg}}$ (deg) $\text{PA}_{\text{bg}} \pm \delta_{\text{PA, bg}}$ | Sign.[a] not Backg. $\sigma_{\text{PA,bg}}$ | Sign. orb. motion $\sigma_{\text{PA,orb.}}$ | $P_{\chi,\text{bg}}$ (%) | $P_{\chi,\text{cmv}}$ (%) |
|---|---|---|---|---|---|---|---|---|---|---|---|---|
| 79005 | 48348.000 | Fabricius et al. (2002) | 3.34±0.04 | 4.04±0.01 | 16.2 | 0.2 | 259.0±0.7 | 255.2±0.2 | 5.2 | 0.2 | 0.00 | 99.99 |
| | 53190.133 | (1) | 3.333±0.005 | 3.421±0.009 | 8.9 | 0.1 | 258.90±0.09 | 258.3±0.1 | 3.5 | 0.1 | | |
| | 53852.267 | (1) | 3.336±0.006 | 3.337±0.008 | 0.0 | 0.4 | 258.8±0.1 | 258.9±0.1 | 0.5 | 0.5 | | |
| | 53887.160 | (1) | 3.332±0.008 | c | c | c | 258.9±0.1 | c | c | c | | |
| 79098 | 51634.000 | Shatsky et al. (2002) | 2.36±0.03 | 2.364±0.006 | 0.2 | 0.2 | 116.6±0.8 | 120.0±0.2 | 4.2 | 0.1 | 4.09 | 98.73 |
| | 53442.268 | (1) | 2.350±0.005 | c | c | c | 116.7±0.2 | c | c | c | | |
| 79230 | 49819.000 | Ghez et al. (1997) | 2.7±0.1 | 2.65±0.01 | 0.5 | 1.0 | 142.0±2.0 | 142.7±0.2 | 0.3 | 0.6 | 92.39 | 73.20 |
| | 53105.328 | (1) | 2.601±0.005 | c | c | c | 140.8±0.1 | c | c | c | | |
| 79739 | 51696.000 | Kouwenhoven et al. (2005) | 0.94±0.01 | 0.97±0.02 | 1.7 | 1.1 | 118.6±0.1 | 124.4±1.0 | 6.0 | 0.3 | 12.95 | 80.62 |
| | 53176.174 | (1) | 0.96±0.01 | c | c | c | 118.3±0.9 | c | c | c | | |
| 80142 | 51696.000 | Kouwenhoven et al. (2005) | 9.32±0.01 | 9.360±0.006 | 3.4 | 5.4 | 216.2±0.1 | 215.96±0.06 | 2.0 | 1.4 | 50.17 | 2.19 |
| | 51712.000 | Shatsky et al. (2002) | 9.33±0.01 | 9.359±0.006 | 2.4 | 6.3 | 216.1±0.1 | 215.96±0.06 | 1.1 | 0.5 | | |
| | 53130.250 | (1) | 9.257±0.006 | c | c | c | 216.04±0.06 | c | c | c | | |
| 80461 | 51696.000 | Kouwenhoven et al. (2005) | 0.27±0.01 | 0.50±0.01 | 14.0 | 2.8 | 285.64±0.05 | 211.4±0.9 | 79.4 | 116.2 | 0.00 | 0.00 |
| | 56179.046 | (1) | 0.239±0.005 | c | c | c | 223.8±0.5 | c | c | c | | |
| 80473 | 44309.000 | Jasnita et al. (1995) | 3.117±0.006 | 2.50±0.03 | 18.0 | 6.8 | 340.6±0.1 | 324.5±0.7 | 21.3 | 20.1 | 0.00 | 0.00 |
| | 48029.000 | Jasnita et al. (1995) | 3.067±0.007 | 2.65±0.02 | 16.1 | 3.2 | 338.9±0.1 | 328.3±0.5 | 20.0 | 13.9 | | |
| | 48348.000 | Fabricius et al. (2002) | 3.080±0.004 | 2.67±0.02 | 17.0 | 4.5 | 339.4±0.1 | 328.6±0.5 | 21.4 | 16.5 | | |
| | 48395.000 | Jasnita et al. (1995) | 3.06±0.01 | 2.67±0.02 | 13.9 | 2.1 | 339.6±0.2 | 328.7±0.5 | 20.5 | 14.1 | | |
| | 56089.350 | (1) | 3.02±0.01 | c | c | c | 335.1±0.2 | c | c | c | | |
| 80474 | 51696.000 | Kouwenhoven et al. (2005) | 4.83±0.01 | 5.12±0.02 | 13.8 | 0.5 | 206.2±0.1 | 205.9±0.1 | 1.5 | 2.3 | 0.00 | 87.03 |
| | 53184.170 | (1) | 4.8±0.1 | 5.01±0.02 | 1.8 | 0.0 | 206.0±1.0 | 206.2±0.1 | 0.1 | 0.5 | | |
| | 55690.150 | (1) | 4.82±0.02 | c | c | c | 206.6±0.1 | c | c | c | | |
| 82902 | 53177.300 | (1) | 4.04±0.01 | 4.049±0.007 | 0.5 | 2.5 | 151.4±0.2 | 151.6±0.1 | 0.5 | 5.9 | 95.98 | 0.18 |
| | 53895.286 | (1) | 4.008±0.007 | c | c | c | 150.1±0.1 | c | c | c | | |
| 87220 | 53454.427 | (1) | 7.78±0.05 | 7.74±0.03 | 0.7 | 0.5 | 327.2±0.4 | 327.0±0.1 | 0.3 | 0.3 | 93.89 | 95.61 |
| | 55690.243 | (1) | 7.80±0.03 | c | c | c | 327.0±0.1 | c | c | c | | |
| 88149 | 53455.426 | (1) | 0.108±0.003 | 0.209±0.003 | 23.3 | 6.1 | 153.5±0.8 | 169.6±0.7 | 14.7 | 12.4 | 0.00 | 0.00 |
| | 54315.000 | Mason et al. (2009) | 0.121±0.005 | 0.183±0.003 | 10.7 | 2.1 | 155.4±0.1 | 169.0±0.6 | 21.5 | 17.1 | | |
| | 54748.000 | Tokovinin et al. (2010) | 0.131±0.002 | 0.167±0.003 | 10.8 | 0.7 | 160.0±0.1 | 168.5±0.6 | 14.0 | 10.1 | | |
| | 54928.000 | Tokovinin et al. (2010) | 0.132±0.002 | 0.158±0.003 | 7.2 | 0.4 | 161.3±0.1 | 167.9±0.6 | 10.7 | 8.1 | | |

*Continued on next page*

Table A3 – *Continued from previous page*

| HIP | MJD (days) | Ref. | Sep (arcsec) $\Theta \pm \delta_\Theta$ | $\text{Sep}_{\text{bg}}$ (arcsec) $\Theta_{\text{bg}} \pm \delta_{\Theta,\text{bg}}$ | Sign.[a] not Backg. $\sigma_{\Theta,\text{bg}}$ | Sign. orb. motion $\sigma_{\Theta,\text{orb.}}$ | PA[b] (deg) $\text{PA} \pm \delta_{\text{PA}}$ | $\text{PA}_{\text{bg}}$ (deg) $\text{PA}_{\text{bg}} \pm \delta_{\text{PA, bg}}$ | Sign.[a] not Backg. $\sigma_{\text{PA,bg}}$ | Sign. orb. motion $\sigma_{\text{PA,orb.}}$ | $P_{\chi,\text{bg}}$ (%) | $P_{\chi,\text{cmv}}$ (%) |
|---|---|---|---|---|---|---|---|---|---|---|---|---|
| | 55690.288 | (1) | 0.133±0.003 | c | c | c | 166.5±0.6 | c | c | c | | |
| 88859 | 48348.000 | Fabricius et al. (2002) | 4.05±0.02 | 4.14±0.01 | 3.9 | 0.2 | 257.5±0.2 | 254.23±0.09 | 15.0 | 0.7 | 0.00 | 90.23 |
| | 53442.364 | (1) | 4.046±0.004 | c | c | c | 257.35±0.05 | c | c | c | | |
| 89684 | 53570.203 | (1) | 6.47±0.01 | 6.48±0.02 | 0.5 | 1.3 | 90.8±0.5 | 90.7±0.1 | 0.3 | 0.0 | 95.69 | 66.57 |
| | 55690.313 | (1) | 6.50±0.02 | c | c | c | 90.8±0.1 | c | c | c | | |
| 90096 | 53458.392 | (1) | 4.10±0.02 | 4.08±0.01 | 0.7 | 3.7 | 20.8±0.3 | 20.7±0.1 | 0.1 | 0.3 | 94.20 | 8.72 |
| | 55690.366 | (1) | 4.20±0.01 | c | c | c | 20.9±0.1 | c | c | c | | |
| 90766 | 48501.000 | Fabricius et al. (2002) | 6.35±0.01 | d | d | d | 333.5±0.1 | d | d | d | 9.64 | 5.91 |
| | 52442.000 | Hartkopf et al. (2013) | 6.6±0.2 | 6.35±0.02 | 1.6 | 1.6 | 333.9±0.8 | 333.7±0.2 | 0.2 | 0.5 | | |
| | 55372.167 | (1) | 6.46±0.03 | 6.35±0.02 | 2.7 | 3.3 | 332.6±0.3 | 333.9±0.2 | 3.8 | 3.2 | | |
| 93805 | 54699.074 | (1) | 12.47±0.03 | d | d | d | 30.5±0.1 | d | d | d | 37.20 | 12.65 |
| | 54947.291 | (1) | 12.51±0.04 | 12.54±0.03 | 0.5 | 0.8 | 29.7±0.2 | 30.4±0.1 | 3.4 | 3.8 | | |
| 100881 | 44383.000 | Jasinta et al. (1995) | 3.364±0.008 | 3.99±0.02 | 32.6 | 12.0 | 146.3±0.2 | 145.7±0.3 | 2.1 | 6.1 | 0.00 | 0.00 |
| | 54769.988 | (1) | 3.45±0.01 | 3.529±0.004 | 6.9 | 1.2 | 146.9±0.1 | 147.11±0.06 | 1.2 | 3.0 | | |
| | 56189.158 | (1) | 3.467±0.003 | c | c | c | 147.34±0.05 | c | c | c | | |
| 105842 | 48348.000 | Fabricius et al. (2002) | 4.68±0.02 | 4.94±0.02 | 10.2 | 0.5 | 130.9±0.2 | 131.2±0.2 | 1.1 | 2.3 | 0.00 | 35.26 |
| | 54685.224 | (1) | 4.6892±0.0006 | c | c | c | 131.36±0.02 | c | c | c | | |
| 113031 | 53298.075 | (1) | 0.083±0.002 | 0.036±0.003 | 13.4 | 1.6 | 284.3±1.0 | 351.4±10.0 | 6.0 | 2.6 | 0.00 | 20.52 |
| | 54363.151 | (1) | 0.073±0.006 | c | c | c | 294.5±4.0 | c | c | c | | |
| 116231 | 53296.128 | (1) | 0.642±0.001 | 0.040±0.002 | 310.9 | 112.0 | 240.74±0.07 | 331.0±3.0 | 34.3 | 85.6 | 0.00 | 0.00 |
| | 53297.113 | (1) | 0.6417±0.0009 | 0.040±0.002 | 317.6 | 115.6 | 240.74±0.08 | 330.7±3.0 | 34.3 | 80.2 | | |
| | 56188.158 | (1) | 0.825±0.001 | c | c | c | 251.1±0.1 | c | c | c | | |
| | | | | | Higher-order multiple systems | | | | | | | |
| 24925AB | 48348.000 | ESA (1997) | 0.53±0.01 | d | d | d | 196.0±0.5 | d | d | d | 0.00 | 0.00 |
| | 53379.159 | (1) | 0.5102±0.0008 | 0.48±0.02 | 1.3 | 1.5 | 199.66±0.08 | 189.8±2.0 | 5.6 | 7.2 | | |
| | 56189.342 | (1) | 0.5084±0.0008 | 0.45±0.03 | 1.7 | 1.7 | 200.39±0.06 | 185.4±3.0 | 5.8 | 8.7 | | |
| | 56296.120 | (1) | 0.5086±0.0006 | 0.45±0.03 | 1.7 | 1.7 | 199.49±0.06 | 185.4±3.0 | 5.4 | 6.9 | | |
| 24925AC | 27073.000 | WDS | 4.4±0.1 | d | d | d | 285.0±0.5 | d | d | d | 7.97 | 19.72 |
| | 53379.159 | (1) | 4.570±0.006 | 4.1±0.2 | 2.9 | 1.7 | 284.94±0.08 | 288.7±1.0 | 2.6 | 0.1 | | |
| | 56189.342 | (1) | 4.579±0.004 | 4.1±0.2 | 3.0 | 1.8 | 284.79±0.05 | 289.2±2.0 | 2.8 | 0.4 | | |
| | 56296.120 | (1) | 4.586±0.005 | 4.1±0.2 | 3.0 | 1.9 | 283.93±0.06 | 289.2±2.0 | 3.3 | 2.1 | | |

*Continued on next page*

Table A3 – *Continued from previous page*

| HIP | MJD (days) | Ref. | Sep (arcsec) $\Theta \pm \delta_\Theta$ | $\text{Sep}_{\text{bg}}$ (arcsec) $\Theta_{\text{bg}} \pm \delta_{\Theta,\text{bg}}$ | Sign.[a] not Backg. $\sigma_{\Theta,\text{bg}}$ | Sign. orb. motion $\sigma_{\Theta,\text{orb.}}$ | PA[b] (deg) PA$\pm\delta_{\text{PA}}$ | $\text{PA}_{\text{bg}}$ (deg) $\text{PA}_{\text{bg}} \pm \delta_{\text{PA, bg}}$ | Sign.[a] not Backg. $\sigma_{\text{PA,bg}}$ | Sign. orb. motion $\sigma_{\text{PA,orb.}}$ | $P_{\chi,\text{bg}}$ (%) | $P_{\chi,\text{cmv}}$ (%) |
|---|---|---|---|---|---|---|---|---|---|---|---|---|
| 26237AB | 53469.976 | (1) | 0.151±0.001 | 0.21±0.02 | 3.8 | 1.6 | 330.1±0.6 | 345.1±2.0 | 8.3 | 62.1 | 0.01 | 0.00 |
| | 56189.387 | (1) | 0.1586±0.0006 | 0.168±0.007 | 1.3 | 0.1 | 358.2±0.1 | 361.0±0.5 | 5.9 | 56.9 | | |
| | 56970.000 | Tokovinin et al. (2015) | 0.159±0.005 | c | c | c | 366.2±0.1 | c | c | c | | |
| 26237AC | 48485.000 | Fabricius et al. (2002) | 1.430±0.006 | 1.31±0.01 | 7.2 | 36.9 | 208.3±0.3 | 197.8±1.0 | 10.3 | 13.3 | 0.00 | 0.00 |
| | 53469.976 | (1) | 1.233±0.009 | 1.243±0.005 | 0.9 | 3.0 | 206.4±0.4 | 201.8±0.4 | 8.2 | 5.0 | | |
| | 56189.387 | (1) | 1.205±0.001 | c | c | c | 204.27±0.05 | c | c | c | | |
| 26549AB | 51465.000 | Horch (2000) | 0.24±0.05 | 0.6±0.1 | 2.8 | 0.4 | 106.5±0.5 | 52.0±10.0 | 4.4 | 49.2 | 0.00 | 0.00 |
| | 53289.404 | (1) | 0.254±0.002 | 0.43±0.06 | 3.1 | 2.3 | 101.0±0.4 | 58.3±10.0 | 4.1 | 44.9 | | |
| | 54482.000 | Maiz Apellaniz, J. (2010) | 0.26±0.02 | 0.36±0.03 | 2.9 | 0.1 | 94.5±0.6 | 64.6±8.0 | 3.7 | 21.8 | | |
| | 54747.000 | Tokovinin (2010) | 0.2568±0.0001 | 0.34±0.02 | 3.5 | 8.9 | 91.3±0.1 | 66.5±7.0 | 3.4 | 70.0 | | |
| | 56340.000 | Tokovinin (2014) | 0.2588±0.0002 | c | c | c | 81.4±0.1 | c | c | c | | |
| 26549AC | 48348.000 | Fabricius (2002) | 12.94±0.03 | 13.3±0.1 | 3.4 | 2.9 | 84.0±0.1 | 82.5±0.9 | 1.8 | 0.1 | 0.21 | 0.75 |
| | 52603.000 | Mason (2004) | 12.73±0.05 | 13.11±0.04 | 5.8 | 5.6 | 83.8±0.5 | 83.5±0.3 | 0.5 | 0.4 | | |
| | 53289.404 | (1) | 13.00±0.03 | 13.08±0.03 | 1.9 | 0.9 | 84.0±0.2 | 83.7±0.2 | 1.2 | 0.2 | | |
| | 54482.000 | Maiz Apellaniz, J. (2010) | 13.03±0.02 | c | c | c | 83.99±0.08 | c | c | c | | |
| 26549AD | 53289.404 | (1) | 3.224±0.009 | 3.31±0.08 | 1.1 | 0.0 | 20.5±0.2 | 20.6±0.9 | 0.1 | 0.2 | 86.39 | 99.31 |
| | 54482.000 | Maiz Apellaniz, J. (2010) | 3.22±0.04 | c | c | c | 20.3±0.7 | c | c | c | | |
| 46594AB | 53753.228 | (1) | 12.61±0.02 | 12.62±0.02 | 0.2 | 1.8 | 167.68±0.06 | 167.15±0.07 | 5.9 | 7.7 | 5.87 | 0.00 |
| | 54535.097 | (1) | 12.65±0.02 | c | c | c | 166.99±0.07 | c | c | c | | |
| 46594AC | 53753.228 | (1) | 17.48±0.02 | 17.48±0.02 | 0.2 | 1.6 | 130.90±0.06 | 130.38±0.06 | 5.8 | 5.5 | 13.30 | 1.60 |
| | 54535.097 | (1) | 17.43±0.02 | c | c | c | 130.40±0.06 | c | c | c | | |
| 51376AB | 51268.000 | Hubrig et al. (2001) | 11.084±0.005 | 11.27±0.02 | 9.8 | 0.4 | 225.8±0.2 | 225.97±0.08 | 0.8 | 3.8 | 16.56 | 0.88 |
| | 53405.279 | (1) | 11.09±0.02 | 11.15±0.02 | 2.3 | 0.1 | 225.54±0.09 | 225.33±0.08 | 1.8 | 4.7 | | |
| | 53415.316 | (1) | 11.09±0.02 | 11.15±0.02 | 2.3 | 0.1 | 225.5±0.1 | 225.32±0.08 | 1.3 | 4.1 | | |
| | 54521.197 | (1) | 11.09±0.02 | c | c | c | 224.98±0.08 | c | c | c | | |
| 51376AC | 51268.000 | Hubrig et al. (2001) | 11.084±0.005 | 11.12±0.02 | 1.9 | 8.1 | 225.8±0.2 | 226.47±0.08 | 3.1 | 1.5 | 41.16 | 2.82 |
| | 53405.279 | (1) | 10.93±0.02 | 11.00±0.02 | 2.8 | 0.5 | 225.92±0.09 | 225.83±0.08 | 0.7 | 3.7 | | |
| | 53415.316 | (1) | 10.92±0.02 | 11.00±0.02 | 2.7 | 0.5 | 225.9±0.1 | 225.82±0.08 | 0.4 | 3.1 | | |
| | 54521.197 | (1) | 10.94±0.02 | c | c | c | 225.47±0.08 | c | c | c | | |
| 54413AB | 54158.304 | (1) | 6.823±0.007 | 6.82±0.02 | 0.0 | 0.3 | 13.62±0.06 | 13.5±0.1 | 0.6 | 4.1 | 100.00 | 36.56 |
| | 54516.365 | (1) | 6.83±0.02 | 6.82±0.02 | 0.2 | 0.0 | 13.7±0.1 | 13.7±0.1 | 0.1 | 3.2 | | |

*Continued on next page*

Table A3 – *Continued from previous page*

| HIP | MJD (days) | Ref. | Sep (arcsec) $\Theta \pm \delta_\Theta$ | $\text{Sep}_{\text{bg}}$ (arcsec) $\Theta_{\text{bg}} \pm \delta_{\Theta,\text{bg}}$ | Sign.[a] not Backg. $\sigma_{\Theta,\text{bg}}$ | Sign. orb. motion $\sigma_{\Theta,\text{orb.}}$ | PA[b] (deg) PA$\pm\delta_{\text{PA}}$ | $\text{PA}_{\text{bg}}$ (deg) $\text{PA}_{\text{bg}} \pm \delta_{\text{PA, bg}}$ | Sign.[a] not Backg. $\sigma_{\text{PA,bg}}$ | Sign. orb. motion $\sigma_{\text{PA,orb.}}$ | $P_{\chi,\text{bg}}$ (%) | $P_{\chi,\text{cmv}}$ (%) |
|---|---|---|---|---|---|---|---|---|---|---|---|---|
| | 54882.153 | (1) | 6.82±0.02 | 6.83±0.02 | 0.1 | 0.2 | 13.9±0.1 | 13.8±0.1 | 0.7 | 1.4 | | |
| | 55555.332 | (1) | 6.820±0.009 | 6.84±0.02 | 0.6 | 0.4 | 14.07±0.08 | 14.1±0.1 | 0.3 | 0.7 | | |
| | 55645.122 | (1) | 6.83±0.02 | c | c | c | 14.2±0.1 | c | c | c | | |
| 54413AC | 54158.304 | (1) | 4.395±0.006 | 4.43±0.02 | 2.3 | 2.0 | 302.2±0.1 | 302.3±0.1 | 0.2 | 2.8 | 99.07 | 83.95 |
| | 54516.365 | (1) | 4.37±0.02 | 4.42±0.02 | 1.9 | 0.6 | 302.3±0.1 | 302.4±0.1 | 0.2 | 1.9 | | |
| | 54882.153 | (1) | 4.38±0.02 | 4.40±0.02 | 1.0 | 0.8 | 302.5±0.1 | 302.5±0.1 | 0.3 | 1.0 | | |
| | 55555.332 | (1) | 4.366±0.006 | 4.37±0.02 | 0.3 | 0.2 | 302.7±0.1 | 302.7±0.1 | 0.4 | 0.3 | | |
| | 55645.122 | (1) | 4.36±0.02 | c | c | c | 302.7±0.1 | c | c | c | | |
| 56000AB | 53408.250 | (1) | 13.06±0.02 | 13.02±0.02 | 1.6 | 0.1 | 168.56±0.08 | 168.33±0.07 | 2.2 | 6.2 | 55.48 | 0.14 |
| | 54520.301 | (1) | 13.06±0.02 | c | c | c | 167.90±0.07 | c | c | c | | |
| 56000AC | 53408.250 | (1) | 13.06±0.02 | 12.98±0.02 | 2.6 | 1.2 | 168.02±0.08 | 167.87±0.07 | 1.4 | 5.5 | 47.38 | 0.56 |
| | 54520.301 | (1) | 13.02±0.02 | c | c | c | 167.44±0.07 | c | c | c | | |
| 56754AB | 53403.363 | (1) | 0.3364±0.0003 | 0.156±0.003 | 56.1 | 39.6 | 104.06±0.05 | 180.4±1.0 | 75.2 | 40.1 | 0.00 | 0.00 |
| | 54475.353 | (1) | 0.3698±0.0005 | 0.223±0.002 | 65.6 | 15.1 | 107.54±0.09 | 130.6±0.4 | 52.7 | 19.0 | | |
| | 55673.077 | (1) | 0.392±0.001 | c | c | c | 111.3±0.2 | c | c | c | | |
| 56754AC | 53403.363 | (1) | 8.432±0.005 | 8.477±0.008 | 4.8 | 0.4 | 184.97±0.04 | 186.65±0.05 | 26.2 | 13.0 | 0.00 | 0.00 |
| | 54475.353 | (1) | 8.46±0.01 | 8.448±0.008 | 1.1 | 2.6 | 184.61±0.07 | 185.49±0.05 | 10.6 | 5.2 | | |
| | 55673.077 | (1) | 8.428±0.008 | c | c | c | 184.17±0.05 | c | c | c | | |
| 60851AB | 51696.000 | Kouwenhoven et al. (2005) | 2.01±0.05 | 1.96±0.02 | 1.0 | 1.6 | 44.1±0.1 | 43.0±0.6 | 1.8 | 1.2 | 75.89 | 41.44 |
| | 53102.079 | (1) | 2.09±0.02 | c | c | c | 44.8±0.6 | c | c | c | | |
| 60851AC | 51696.000 | Kouwenhoven et al. (2005) | 6.92±0.05 | 6.96±0.06 | 0.5 | 0.2 | 181.1±0.1 | 181.3±0.6 | 0.4 | 1.6 | 96.24 | 39.60 |
| | 53102.079 | (1) | 6.90±0.06 | c | c | c | 180.2±0.6 | c | c | c | | |
| 69113AB | 51664.000 | Kouwenhoven et al. (2005) | 5.33±0.01 | 5.232±0.008 | 7.8 | 0.2 | 64.8±0.3 | 65.5±0.5 | 1.2 | 0.6 | 47.49 | 87.17 |
| | 53126.078 | (1) | 5.332±0.008 | c | c | c | 65.2±0.5 | c | c | c | | |
| 69113AC | 51664.000 | Kouwenhoven et al. (2005) | 5.52±0.01 | 5.402±0.008 | 9.3 | 1.4 | 66.9±0.3 | 67.5±0.5 | 1.0 | 0.4 | 32.86 | 92.31 |
| | 53126.078 | (1) | 5.502±0.008 | c | c | c | 67.1±0.5 | c | c | c | | |
| 74911AB | 48457.000 | Fabricius et al. (2002) | 1.110±0.004 | 1.18±0.01 | 5.3 | 30.1 | 331.4±0.3 | 272.8±0.5 | 98.8 | 72.1 | 0.00 | 0.00 |
| | 51268.000 | Hubrig et al. (2001) | 1.04±0.05 | 1.011±0.006 | 0.5 | 1.8 | 322.5±0.2 | 289.2±0.3 | 87.3 | 60.3 | | |
| | 53454.299 | (1) | 0.948±0.004 | c | c | c | 304.8±0.2 | c | c | c | | |
| 74911AC | 51268.000 | Hubrig et al. (2001) | 6.15±0.05 | 6.17±0.02 | 0.5 | 1.8 | 156.9±0.2 | 158.4±0.2 | 5.1 | 2.6 | 22.41 | 30.68 |
| | 53454.299 | (1) | 6.05±0.02 | c | c | c | 156.1±0.2 | c | c | c | | |

*Continued on next page*

Table A3 – *Continued from previous page*

| HIP | MJD (days) | Ref. | Sep (arcsec) $\Theta \pm \delta_\Theta$ | $\text{Sep}_{\text{bg}}$ (arcsec) $\Theta_{\text{bg}} \pm \delta_{\Theta,\text{bg}}$ | Sign.[a] not Backg. $\sigma_{\Theta,\text{bg}}$ | Sign. orb. motion $\sigma_{\Theta,\text{orb.}}$ | PA[b] (deg) PA$\pm\delta_{\text{PA}}$ | $\text{PA}_{\text{bg}}$ (deg) $\text{PA}_{\text{bg}} \pm \delta_{\text{PA, bg}}$ | Sign.[a] not Backg. $\sigma_{\text{PA,bg}}$ | Sign. orb. motion $\sigma_{\text{PA,orb.}}$ | $P_{\chi,\text{bg}}$ (%) | $P_{\chi,\text{cmv}}$ (%) |
|---|---|---|---|---|---|---|---|---|---|---|---|---|
| 77562AB | 53186.143 | (1) | 9.97±0.01 | 9.98±0.02 | 0.1 | 4.5 | 38.36±0.07 | 38.20±0.09 | 1.4 | 1.8 | 89.15 | 4.99 |
| | 53853.258 | (1) | 10.06±0.02 | c | c | c | 38.16±0.09 | c | c | c | | |
| 77562AC | 53186.143 | (1) | 6.11±0.01 | 6.11±0.01 | 0.5 | 5.6 | 43.6±0.1 | 43.4±0.1 | 1.1 | 2.1 | 91.08 | 1.56 |
| | 53853.258 | (1) | 6.19±0.01 | c | c | c | 43.3±0.1 | c | c | c | | |
| 77562AD | 53186.143 | (1) | 9.25±0.01 | 9.26±0.02 | 0.7 | 4.9 | 41.52±0.08 | 41.3±0.1 | 1.3 | 1.9 | 87.93 | 3.12 |
| | 53853.258 | (1) | 9.35±0.02 | c | c | c | 41.3±0.1 | c | c | c | | |
| 77562AE | 53186.143 | (1) | 11.38±0.01 | 11.37±0.02 | 0.6 | 2.1 | 76.77±0.08 | 76.5±0.1 | 2.1 | 4.5 | 68.75 | 1.44 |
| | 53853.258 | (1) | 11.43±0.02 | c | c | c | 76.2±0.1 | c | c | c | | |
| 79153AB | 53186.190 | (1) | 11.71±0.02 | 11.79±0.02 | 3.0 | 0.5 | 230.00±0.09 | 229.7±0.1 | 1.8 | 0.5 | 53.06 | 93.57 |
| | 53853.271 | (1) | 11.70±0.02 | c | c | c | 230.1±0.1 | c | c | c | | |
| 79153AC | 53186.190 | (1) | 6.66±0.01 | 6.68±0.01 | 1.1 | 5.9 | 324.5±0.1 | 324.2±0.1 | 1.4 | 3.3 | 82.93 | 0.35 |
| | 53853.271 | (1) | 6.75±0.01 | c | c | c | 325.0±0.1 | c | c | c | | |
| 79199AB | 51634.000 | Shatsky et al. (2002) | 1.12±0.01 | 1.177±0.008 | 3.5 | 4.1 | 116.9±0.3 | 146.6±0.3 | 66.4 | 1.6 | 0.00 | 0.00 |
| | 53191.122 | (1) | 1.093±0.002 | 1.096±0.005 | 0.5 | 9.4 | 117.20±0.09 | 136.1±0.2 | 75.4 | 1.4 | | |
| | 55690.119 | (1) | 1.055±0.004 | c | c | c | 117.4±0.1 | c | c | c | | |
| 79199AC | 51634.000 | Shatsky et al. (2002) | 3.06±0.03 | 3.64±0.01 | 16.7 | 1.0 | 228.0±0.2 | 225.6±0.2 | 9.6 | 1.7 | 0.00 | 68.54 |
| | 53191.122 | (1) | 3.069±0.005 | 3.43±0.01 | 26.7 | 1.7 | 228.16±0.09 | 226.6±0.1 | 9.6 | 1.6 | | |
| | 55690.119 | (1) | 3.09±0.01 | c | c | c | 228.4±0.1 | c | c | c | | |
| 79399AB | 53185.247 | (1) | 3.698±0.006 | 3.629±0.007 | 7.6 | 0.2 | 69.98±0.08 | 70.5±0.1 | 4.1 | 2.8 | 0.53 | 29.76 |
| | 53852.251 | (1) | 3.696±0.007 | c | c | c | 69.6±0.1 | c | c | c | | |
| 79399AC | 53185.247 | (1) | 3.896±0.006 | 3.815±0.007 | 8.6 | 1.4 | 69.32±0.09 | 70.3±0.1 | 6.8 | 0.5 | 0.02 | 71.96 |
| | 53852.251 | (1) | 3.883±0.007 | c | c | c | 69.4±0.1 | c | c | c | | |
| 79399AD | 53185.247 | (1) | 11.80±0.02 | 11.86±0.02 | 2.0 | 0.4 | 250.23±0.08 | 250.1±0.1 | 1.1 | 1.0 | 70.53 | 82.53 |
| | 53852.251 | (1) | 11.79±0.02 | c | c | c | 250.4±0.1 | c | c | c | | |
| 79771AB | 51696.000 | Kouwenhoven et al. (2005) | 3.66±0.01 | 3.57±0.01 | 5.5 | 0.6 | 313.6±0.1 | 308.0±0.2 | 24.0 | 4.7 | 0.00 | 29.41 |
| | 53176.206 | (1) | 3.68±0.06 | 3.59±0.01 | 1.5 | 0.5 | 313.2±0.9 | 309.6±0.2 | 3.9 | 0.5 | | |
| | 56121.247 | (1) | 3.65±0.01 | c | c | c | 312.7±0.2 | c | c | c | | |
| 79771AC | 53176.206 | (1) | 0.435±0.007 | 0.528±0.006 | 10.2 | 0.5 | 128.4±0.9 | 150.8±0.8 | 18.7 | 0.1 | 0.00 | 94.60 |
| | 56121.247 | (1) | 0.438±0.001 | c | c | c | 128.3±0.2 | c | c | c | | |
| 81472AB | 51696.000 | Kouwenhoven et al. (2005) | 4.52±0.01 | 4.54±0.02 | 1.1 | 5.7 | 274.4±0.1 | 274.4±0.2 | 0.0 | 16.0 | 97.09 | 0.00 |
| | 53454.368 | (1) | 4.49±0.03 | 4.49±0.02 | 0.2 | 2.4 | 275.2±0.3 | 275.5±0.2 | 0.8 | 4.9 | | |

*Continued on next page*

Table A3 – *Continued from previous page*

| HIP | MJD (days) | Ref. | Sep (arcsec) $\Theta \pm \delta_\Theta$ | $\text{Sep}_{\text{bg}}$ (arcsec) $\Theta_{\text{bg}} \pm \delta_{\Theta,\text{bg}}$ | Sign.[a] not Backg. $\sigma_{\Theta,\text{bg}}$ | Sign. orb. motion $\sigma_{\Theta,\text{orb.}}$ | PA[b] (deg) PA$\pm\delta_{\text{PA}}$ | $\text{PA}_{\text{bg}}$ (deg) $\text{PA}_{\text{bg}} \pm \delta_{\text{PA, bg}}$ | Sign.[a] not Backg. $\sigma_{\text{PA,bg}}$ | Sign. orb. motion $\sigma_{\text{PA,orb.}}$ | $P_{\chi,\text{bg}}$ (%) | $P_{\chi,\text{cmv}}$ (%) |
|---|---|---|---|---|---|---|---|---|---|---|---|---|
| | 55690.189 | (1) | 4.42±0.02 | c | c | c | 277.0±0.1 | c | c | c | | |
| 81472AC | 51696.000 | Kouwenhoven et al. (2005) | 5.21±0.01 | 5.19±0.02 | 0.9 | 7.5 | 357.5±0.1 | 356.6±0.2 | 4.7 | 4.9 | 21.62 | 0.00 |
| | 53454.368 | (1) | 5.27±0.03 | 5.27±0.02 | 0.1 | 2.5 | 357.6±0.3 | 357.3±0.1 | 0.7 | 1.9 | | |
| | 55690.189 | (1) | 5.37±0.02 | c | c | c | 358.3±0.1 | c | c | c | | |
| 81972AB | 51690.000 | Shatsky et al. (2002) | 2.02±0.02 | d | d | d | 311.3±0.3 | d | d | d | 91.92 | 49.40 |
| | 53184.214 | (1) | 2.02±0.04 | 1.98±0.02 | 0.8 | 0.1 | 314.0±1.0 | 314.0±0.3 | 0.0 | 2.2 | | |
| 81972AC | 51690.000 | Shatsky et al. (2002) | 7.11±0.07 | d | d | d | 258.3±0.1 | d | d | d | 94.97 | 79.90 |
| | 53184.214 | (1) | 7.0±0.1 | 7.02±0.07 | 0.1 | 0.7 | 259.1±1.0 | 258.5±0.1 | 0.4 | 0.6 | | |
| 81972AD | 51690.000 | Shatsky et al. (2002) | 5.06±0.05 | d | d | d | 213.9±0.2 | d | d | d | 95.17 | 98.47 |
| | 53184.214 | (1) | 5.0±0.1 | 4.97±0.05 | 0.5 | 0.3 | 213.7±1.0 | 213.4±0.2 | 0.3 | 0.2 | | |
| 83336AB | 53182.267 | (1) | 8.92±0.01 | 8.83±0.02 | 4.1 | 0.4 | 25.60±0.08 | 25.8±0.1 | 1.2 | 0.2 | 32.39 | 96.98 |
| | 53912.135 | (1) | 8.92±0.02 | c | c | c | 25.6±0.1 | c | c | c | | |
| 83336AC | 53182.267 | (1) | 8.89±0.01 | 8.90±0.02 | 0.6 | 2.5 | 302.27±0.09 | 302.2±0.1 | 0.4 | 3.9 | 97.35 | 5.91 |
| | 53912.135 | (1) | 8.94±0.02 | c | c | c | 302.8±0.1 | c | c | c | | |
| 83336AD | 53182.267 | (1) | 9.23±0.01 | 9.26±0.02 | 1.1 | 1.7 | 137.61±0.09 | 137.6±0.1 | 0.2 | 3.3 | 93.53 | 16.36 |
| | 53912.135 | (1) | 9.19±0.02 | c | c | c | 137.1±0.1 | c | c | c | | |
| 85442AB | 53454.417 | (1) | 3.00±0.01 | 2.97±0.01 | 1.6 | 6.9 | 329.42±0.06 | 328.7±0.1 | 4.6 | 11.4 | 43.59 | 0.00 |
| | 55690.216 | (1) | 3.12±0.01 | c | c | c | 331.1±0.1 | c | c | c | | |
| 85442AC | 53454.417 | (1) | 6.05±0.03 | 6.07±0.02 | 0.6 | 1.2 | 261.39±0.05 | 261.2±0.1 | 1.7 | 11.6 | 77.14 | 0.00 |
| | 55690.216 | (1) | 6.01±0.02 | c | c | c | 262.9±0.1 | c | c | c | | |
| 85442AD | 53454.417 | (1) | 5.78±0.03 | 5.77±0.02 | 0.4 | 5.0 | 33.79±0.06 | 34.0±0.1 | 1.2 | 4.5 | 95.25 | 0.12 |
| | 55690.216 | (1) | 5.95±0.02 | c | c | c | 33.2±0.1 | c | c | c | | |
| 85442AE | 53454.417 | (1) | 5.23±0.02 | 5.27±0.02 | 1.3 | 3.3 | 145.91±0.07 | 146.4±0.1 | 3.3 | 7.0 | 61.20 | 0.97 |
| | 55690.216 | (1) | 5.13±0.02 | c | c | c | 144.9±0.1 | c | c | c | | |
| 85727AB | 54699.057 | (1) | 2.834±0.006 | 3.01±0.01 | 14.6 | 24.3 | 58.6±0.1 | 67.4±0.3 | 30.2 | 29.8 | 0.00 | 0.00 |
| | 55070.000 | Ehrenreich et al. (2010) | 3.12±0.01 | c | c | c | 67.2±0.3 | c | c | c | | |
| 85727AC | 54699.057 | (1) | 12.21±0.02 | 12.20±0.01 | 0.3 | 5.1 | 62.8±0.1 | 62.07±0.08 | 5.4 | 5.5 | 5.26 | 0.05 |
| | 55070.000 | Ehrenreich et al. (2010) | 12.32±0.01 | c | c | c | 62.06±0.08 | c | c | c | | |
| 85783AB | 53442.335 | (1) | 0.433±0.003 | 0.618±0.003 | 44.9 | 12.5 | 192.8±0.4 | 191.4±0.4 | 2.6 | 1.2 | 0.00 | 0.00 |
| | 55655.363 | (1) | 0.4719±0.0008 | 0.474±0.002 | 1.4 | 0.0 | 192.64±0.07 | 193.3±0.1 | 4.6 | 4.8 | | |
| | 55690.353 | (1) | 0.472±0.002 | c | c | c | 193.3±0.1 | c | c | c | | |

*Continued on next page*

Table A3 – *Continued from previous page*

| HIP | MJD (days) | Ref. | Sep (arcsec) $\Theta \pm \delta_\Theta$ | $Sep_{bg}$ (arcsec) $\Theta_{bg} \pm \delta_{\Theta,bg}$ | Sign.[a] not Backg. $\sigma_{\Theta,bg}$ | Sign. orb. motion $\sigma_{\Theta,orb.}$ | PA[b] (deg) PA$\pm\delta_{PA}$ | $PA_{bg}$ (deg) $PA_{bg} \pm \delta_{PA,\ bg}$ | Sign.[a] not Backg. $\sigma_{PA,bg}$ | Sign. orb. motion $\sigma_{PA,orb.}$ | $P_{\chi,bg}$ (%) | $P_{\chi,cmv}$ (%) |
|---|---|---|---|---|---|---|---|---|---|---|---|---|
| 85783AC | 53442.335 | (1) | 1.624±0.005 | 1.635±0.007 | 1.4 | 7.6 | 123.5±0.2 | 123.7±0.2 | 0.5 | 14.9 | 87.20 | 0.00 |
| | 55655.363 | (1) | 1.555±0.005 | 1.570±0.005 | 2.1 | 2.0 | 118.6±0.2 | 119.1±0.2 | 1.7 | 1.4 | | |
| | 55690.353 | (1) | 1.569±0.005 | c | c | c | 119.0±0.2 | c | c | c | | |
| 87163AB | 53457.375 | (1) | 7.35±0.01 | 7.35±0.03 | 0.2 | 0.2 | 107.67±0.06 | 108.1±0.1 | 3.2 | 1.4 | 62.86 | 77.41 |
| | 55690.267 | (1) | 7.35±0.02 | c | c | c | 107.9±0.1 | c | c | c | | |
| 87163AC | 53457.375 | (1) | 6.77±0.01 | 6.75±0.02 | 1.0 | 0.0 | 47.51±0.06 | 47.5±0.1 | 0.1 | 1.1 | 92.87 | 89.74 |
| | 55690.267 | (1) | 6.77±0.02 | c | c | c | 47.4±0.1 | c | c | c | | |
| 87163AD | 53457.375 | (1) | 2.103±0.005 | 2.053±0.008 | 5.5 | 2.5 | 37.7±0.1 | 38.2±0.2 | 2.4 | 0.9 | 9.51 | 34.82 |
| | 55690.267 | (1) | 2.081±0.007 | c | c | c | 37.9±0.1 | c | c | c | | |
| 87163AE | 53457.375 | (1) | 4.280±0.008 | 4.31±0.02 | 2.0 | 0.3 | 170.50±0.07 | 170.7±0.1 | 1.1 | 0.0 | 66.82 | 97.48 |
| | 55690.267 | (1) | 4.29±0.01 | c | c | c | 170.5±0.1 | c | c | c | | |
| 87163AF | 53457.375 | (1) | 6.78±0.01 | 6.78±0.02 | 0.0 | 0.4 | 123.50±0.08 | 124.1±0.1 | 4.1 | 2.5 | 55.16 | 57.21 |
| | 55690.267 | (1) | 6.77±0.02 | c | c | c | 123.9±0.1 | c | c | c | | |
| 87163AG | 53457.375 | (1) | 1.515±0.005 | 1.484±0.007 | 3.6 | 2.2 | 77.5±0.3 | 78.8±0.2 | 3.2 | 0.6 | 9.85 | 45.60 |
| | 55690.267 | (1) | 1.498±0.006 | c | c | c | 77.7±0.2 | c | c | c | | |
| 89963AB | 54930.000 | Aldoretta et al. (2015) | 1.134±0.001 | 1.148±0.004 | 3.4 | 3.6 | 201.86±0.07 | 201.2±0.2 | 2.8 | 3.8 | 26.53 | 0.66 |
| | 55761.007 | (1) | 1.148±0.004 | c | c | c | 201.1±0.2 | c | c | c | | |
| 93892AB | 53286.002 | (1) | 6.43±0.01 | 6.485±0.008 | 3.9 | 3.0 | 204.16±0.09 | 203.81±0.09 | 2.9 | 5.2 | 8.55 | 0.50 |
| | 55799.136 | (1) | 6.395±0.006 | c | c | c | 203.61±0.06 | c | c | c | | |
| 93892AC | 53286.002 | (1) | 3.327±0.006 | 3.282±0.008 | 4.5 | 5.1 | 65.0±0.1 | 64.8±0.2 | 1.3 | 6.1 | 13.14 | 0.02 |
| | 55799.136 | (1) | 3.364±0.004 | c | c | c | 64.1±0.1 | c | c | c | | |

**Note.** Designation given in column 1 assigned by decreasing magnitude and not necessarily tally with designations given in the WDS catalogue.

[a] Assuming the fainter component is a non-moving background star.

[b] Position angle (PA) is measured from N over E to S.

[c] Significances are given relative to the last epoch.

[d] Significances are given relative to the first epoch.

**References.** (1) This work; otherwise given in the table

**Table A4.** Measured brightness differences, apparent and absolute magnitudes for the visual companions identified in this study.

| HIP | Distance (pc) | Date | Band | $\Delta m^{a}$ (mag) | $m_{\rm system}$ (mag) | $m_{\rm prim}$ (mag) | $m_{\rm comp}$ (mag) | $M_{\rm prim}$ (mag) | $M_{\rm comp}$ (mag) |
|---|---|---|---|---|---|---|---|---|---|
| | | | | | Binaries | | | | |
| 2548 | $81.0^{+3.8}_{-3.5}$ | 2005-12-06 | $Ks$ | 1.1620±0.0044 | 5.637±0.019 | 5.96±0.02 | 7.119±0.022 | $1.415^{+0.103}_{-0.095}$ | $2.577^{+0.104}_{-0.095}$ |
| | | 2007-09-16 | $Ks$ | 1.1400±0.0054 | 5.637±0.019 | 5.96±0.02 | 7.103±0.023 | $1.421^{+0.103}_{-0.095}$ | $2.561^{+0.104}_{-0.095}$ |
| 15627 | $156.0^{+20.1}_{-16.0}$ | 2006-10-16 | $H$ | 2.166±0.049 | 5.439±0.017 | 5.578±0.025 | 7.743±0.075 | $-0.44^{+0.28}_{-0.22}$ | $1.73^{+0.29}_{-0.23}$ |
| 16511 | $107.4^{+4.6}_{-4.2}$ | 2005-01-06 | $Ks$ | 2.547±0.025 | 5.881±0.017 | 5.980±0.019 | 8.53±0.04 | $0.824^{+0.094}_{-0.087}$ | $3.371^{+0.101}_{-0.094}$ |
| | | 2005-11-26 | $Ks$ | 2.710±0.025 | 5.881±0.017 | 5.967±0.019 | 8.68±0.04 | $0.811^{+0.094}_{-0.087}$ | $3.521^{+0.101}_{-0.094}$ |
| | | 2011-08-25 | $Ks$ | 2.353±0.029 | 5.881±0.017 | 6.00±0.02 | 8.351±0.043 | $0.843^{+0.095}_{-0.087}$ | $3.195^{+0.102}_{-0.095}$ |
| 16803 | $149.3^{+12.3}_{-10.6}$ | 2005-01-09 | $Ks$ | 0.884±0.012 | 5.526±0.024 | 5.924±0.028 | 6.808±0.032 | $0.07^{+0.18}_{-0.16}$ | $0.96^{+0.18}_{-0.16}$ |
| | | 2007-09-20 | $Ks$ | 0.812±0.026 | 5.526±0.024 | 5.947±0.032 | 6.759±0.042 | $0.09^{+0.18}_{-0.16}$ | $0.91^{+0.18}_{-0.16}$ |
| | | 2007-09-30 | $Ks$ | 0.798±0.013 | 5.526±0.024 | 5.951±0.028 | 6.749±0.033 | $0.10^{+0.18}_{-0.16}$ | $0.90^{+0.18}_{-0.16}$ |
| 17563 | $163.7^{+8.2}_{-7.4}$ | 2005-01-10 | $Ks$ | 5.88±0.13 | 5.592±0.02 | 5.597±0.021 | 11.48±0.16 | $-0.5^{+0.1}_{-0.1}$ | $5.38^{+0.19}_{-0.18}$ |
| 18213 | $106.2^{+2.5}_{-2.4}$ | 2007-09-14 | $Ks$ | 4.78±0.12 | 5.454±0.017 | 5.467±0.019 | 10.25±0.19 | $0.337^{+0.055}_{-0.053}$ | $5.1^{+0.2}_{-0.2}$ |
| 20020 | $141.2^{+6.9}_{-6.3}$ | 2004-12-08 | $Ks$ | 1.331±0.028 | 6.178±0.024 | 6.457±0.035 | 7.79±0.06 | $0.7^{+0.1}_{-0.1}$ | $2.04^{+0.12}_{-0.11}$ |
| | | 2007-09-20 | $Ks$ | 1.355±0.034 | 6.178±0.024 | 6.452±0.037 | 7.807±0.068 | $0.7^{+0.1}_{-0.1}$ | $2.06^{+0.13}_{-0.12}$ |
| | | 2007-09-30 | $Ks$ | 1.3306±0.0095 | 6.178±0.024 | 6.457±0.028 | 7.788±0.036 | $0.7^{+0.1}_{-0.1}$ | $2.0^{+0.1}_{-0.1}$ |
| 20042 | $54.6^{+0.5}_{-0.4}$ | 2005-11-16 | $Ks$ | 6.208±0.067 | 3.954±0.244 | 3.96±0.24 | 10.17±0.32 | $0.27^{+0.24}_{-0.24}$ | $6.48^{+0.32}_{-0.32}$ |
| | | 2012-09-19 | $Ks$ | 7.0±0.1 | 3.954±0.244 | 3.96±0.24 | 10.92±0.35 | $0.27^{+0.24}_{-0.24}$ | $7.24^{+0.35}_{-0.35}$ |
| 20554 | $219.8^{+27.7}_{-22.2}$ | 2004-09-18 | $Ks$ | 2.472±0.025 | 7.625±0.024 | 7.731±0.028 | 10.203±0.058 | $1.01^{+0.28}_{-0.22}$ | $3.49^{+0.28}_{-0.23}$ |
| 20804 | $180.2^{+27.3}_{-20.9}$ | 2005-02-08 | $Ks$ | 1.284±0.021 | 5.644±0.023 | 5.934±0.028 | 7.219±0.039 | $-0.40^{+0.33}_{-0.25}$ | $0.89^{+0.33}_{-0.26}$ |
| | | 2012-09-19 | $Ks$ | 1.349±0.021 | 5.644±0.023 | 5.919±0.028 | 7.268±0.039 | $-0.41^{+0.33}_{-0.25}$ | $0.94^{+0.33}_{-0.26}$ |
| | | 2013-01-04 | $Ks$ | 1.359±0.015 | 5.644±0.023 | 5.917±0.026 | 7.276±0.034 | $-0.42^{+0.33}_{-0.25}$ | $0.94^{+0.33}_{-0.25}$ |
| 23794 | $94.7^{+3.2}_{-3.0}$ | 2004-10-08 | $Ks$ | 3.8271±0.0011 | 5.203±0.023 | 5.235±0.023 | 9.062±0.024 | $0.367^{+0.076}_{-0.072}$ | $4.194^{+0.076}_{-0.072}$ |
| | | 2013-01-04 | $Ks$ | 3.7869±0.0012 | 5.203±0.023 | 5.236±0.023 | 9.023±0.024 | $0.368^{+0.076}_{-0.072}$ | $4.155^{+0.076}_{-0.072}$ |
| 24196 | $393.7^{+158.8}_{-87.9}$ | 2004-12-08 | $Ks$ | 0.806±0.021 | 6.859±0.019 | 7.282±0.031 | 8.088±0.044 | $-0.71^{+0.88}_{-0.49}$ | $0.10^{+0.88}_{-0.49}$ |
| 24305 | $57.0^{+1.8}_{-1.7}$ | 2005-01-04 | $Ks$ | 2.034±0.045 | 3.523±0.236 | 3.68±0.24 | 5.71±0.28 | $-0.11^{+0.25}_{-0.25}$ | $1.92^{+0.28}_{-0.28}$ |

*Continued on next page*

Table A4 – *Continued from previous page*

| HIP | Distance (pc) | Date | Band | $\Delta m^{a}$ (mag) | $m_{\mathrm{system}}$ (mag) | $m_{\mathrm{prim}}$ (mag) | $m_{\mathrm{comp}}$ (mag) | $M_{\mathrm{prim}}$ (mag) | $M_{\mathrm{comp}}$ (mag) |
|---|---|---|---|---|---|---|---|---|---|
| | | 2012-12-08 | *Ks* | 4.9289±0.0044 | 3.523±0.236 | 3.53±0.24 | 8.46±0.24 | $-0.25^{+0.25}_{-0.25}$ | $4.67^{+0.25}_{-0.25}$ |
| 24825 | $263.2^{+37.1}_{-29.0}$ | 2005-04-11 | *Ks* | 4.0077±0.0086 | 6.79±0.037 | 6.817±0.037 | 10.824±0.045 | $-0.28^{+0.31}_{-0.24}$ | $3.72^{+0.31}_{-0.24}$ |
| | | 2012-09-19 | *Ks* | 4.157±0.014 | 6.79±0.037 | 6.813±0.037 | 10.970±0.051 | $-0.29^{+0.31}_{-0.24}$ | $3.87^{+0.31}_{-0.24}$ |
| 25365 | $215.1^{+30.6}_{-23.8}$ | 2005-01-10 | *Ks* | 0.77417±0.00064 | 6.6±0.02 | 7.03±0.02 | 7.81±0.02 | $0.32^{+0.31}_{-0.24}$ | $1.09^{+0.31}_{-0.24}$ |
| | | 2012-09-19 | *Ks* | 0.8243±0.0043 | 6.6±0.02 | 7.017±0.021 | 7.841±0.023 | $0.30^{+0.31}_{-0.24}$ | $1.12^{+0.31}_{-0.24}$ |
| 25657 | $172.4^{+23.3}_{-18.3}$ | 2006-10-16 | *H* | 4.4210±0.0054 | 7.454±0.02 | 7.47±0.02 | 11.893±0.025 | $1.24^{+0.29}_{-0.23}$ | $5.66^{+0.29}_{-0.23}$ |
| | | 2006-12-28 | *H* | 4.4793±0.0091 | 7.454±0.02 | 7.47±0.02 | 11.951±0.029 | $1.24^{+0.29}_{-0.23}$ | $5.72^{+0.29}_{-0.23}$ |
| 26215 | $343.6^{+102.8}_{-64.3}$ | 2004-12-09 | *Ks* | 4.166±0.017 | 4.959±0.02 | 4.98±0.02 | 9.15±0.04 | $-2.78^{+0.65}_{-0.41}$ | $1.39^{+0.65}_{-0.41}$ |
| 26235 | $473.9^{+114.3}_{-77.1}$ | 2007-12-18 | *H* | 2.7250±0.0056 | 4.922±0.063 | 5.007±0.063 | 7.732±0.068 | $-3.53^{+0.53}_{-0.36}$ | $-0.81^{+0.53}_{-0.36}$ |
| 26602 | $473.9^{+250.7}_{-121.8}$ | 2005-03-05 | *Ks* | 0.789±0.016 | 6.578±0.02 | 7.006±0.025 | 7.795±0.031 | $-1.38^{+1.15}_{-0.56}$ | $-0.59^{+1.15}_{-0.56}$ |
| | | 2012-09-19 | *Ks* | 1.0376±0.0012 | 6.578±0.02 | 6.93±0.02 | 7.969±0.021 | $-1.45^{+1.15}_{-0.56}$ | $-0.42^{+1.15}_{-0.56}$ |
| 27810 | $102.6^{+2.3}_{-2.2}$ | 2005-03-25 | *Ks* | 5.1701±0.0031 | 5.251±0.024 | 5.260±0.024 | 10.430±0.027 | $0.205^{+0.054}_{-0.052}$ | $5.375^{+0.055}_{-0.053}$ |
| 28744 | $403.2^{+174.8}_{-93.6}$ | 2005-03-27 | *Ks* | 4.6603±0.0029 | 4.781±0.019 | 4.796±0.019 | 9.456±0.022 | $-3.33^{+0.94}_{-0.51}$ | $1.33^{+0.94}_{-0.51}$ |
| | | 2012-09-19 | *Ks* | 4.55±0.02 | 4.781±0.019 | 4.797±0.019 | 9.350±0.039 | $-3.33^{+0.94}_{-0.51}$ | $1.23^{+0.94}_{-0.51}$ |
| 29401 | $176.1^{+24.3}_{-19.1}$ | 2006-01-06 | *Ks* | 1.3978±0.0048 | 6.326±0.026 | 6.591±0.027 | 7.99±0.03 | $0.35^{+0.30}_{-0.24}$ | $1.74^{+0.30}_{-0.24}$ |
| | | 2012-12-08 | *Ks* | 1.4168±0.0038 | 6.326±0.026 | 6.587±0.027 | 8.003±0.029 | $0.34^{+0.30}_{-0.24}$ | $1.76^{+0.30}_{-0.24}$ |
| 29728 | $200.4^{+18.9}_{-15.9}$ | 2005-04-10 | *Ks* | 3.8528±0.0071 | 6.381±0.027 | 6.412±0.027 | 10.265±0.034 | $-0.10^{+0.21}_{-0.17}$ | $3.75^{+0.21}_{-0.18}$ |
| | | 2012-09-19 | *Ks* | 3.85±0.01 | 6.381±0.027 | 6.412±0.027 | 10.263±0.037 | $-0.10^{+0.21}_{-0.17}$ | $3.75^{+0.21}_{-0.18}$ |
| 30493 | $242.1^{+60.0}_{-40.1}$ | 2005-03-06 | *Ks* | 1.4331±0.0058 | 6.926±0.02 | 7.183±0.021 | 8.616±0.025 | $0.26^{+0.54}_{-0.36}$ | $1.70^{+0.54}_{-0.36}$ |
| | | 2012-09-19 | *Ks* | 1.4073±0.0014 | 6.926±0.02 | 7.19±0.02 | 8.596±0.021 | $0.27^{+0.54}_{-0.36}$ | $1.68^{+0.54}_{-0.36}$ |
| 30867 | $207.5^{+62.8}_{-39.1}$ | 2005-04-09 | *Ks* | 1.4915±0.0045 | 4.079±0.204 | 4.32±0.21 | 5.82±0.21 | $-2.38^{+0.69}_{-0.46}$ | $-0.89^{+0.69}_{-0.46}$ |
| | | 2012-09-19 | *Ks* | 1.5867±0.0081 | 4.079±0.204 | 4.31±0.21 | 5.89±0.21 | $-2.40^{+0.69}_{-0.46}$ | $-0.82^{+0.69}_{-0.46}$ |
| 31137 | $232.0^{+22.4}_{-18.8}$ | 2005-04-10 | *Ks* | 2.749±0.011 | 5.719±0.023 | 5.802±0.024 | 8.551±0.037 | $-1.04^{+0.21}_{-0.18}$ | $1.71^{+0.21}_{-0.18}$ |
| | | 2012-09-19 | *Ks* | 2.804±0.018 | 5.719±0.023 | 5.798±0.025 | 8.602±0.046 | $-1.04^{+0.21}_{-0.18}$ | $1.76^{+0.22}_{-0.18}$ |
| 31959 | $613.5^{+428.2}_{-178.7}$ | 2007-11-05 | *H* | 5.3509±0.0053 | 8.388±0.046 | 8.396±0.046 | 13.747±0.051 | $-0.59^{+1.52}_{-0.63}$ | $4.77^{+1.52}_{-0.63}$ |
| | | 2008-01-05 | *H* | 5.248±0.037 | 8.388±0.046 | 8.397±0.046 | 13.644±0.086 | $-0.58^{+1.52}_{-0.63}$ | $4.66^{+1.52}_{-0.64}$ |

*Continued on next page*

Table A4 – *Continued from previous page*

| HIP | Distance (pc) | Date | Band | $\Delta m^a$ (mag) | $m_{system}$ (mag) | $m_{prim}$ (mag) | $m_{comp}$ (mag) | $M_{prim}$ (mag) | $M_{comp}$ (mag) |
|---|---|---|---|---|---|---|---|---|---|
| | | 2012-12-05 | *Ks* | 5.1416±0.0042 | 8.395±0.023 | 8.404±0.023 | 13.546±0.027 | $-0.56^{+1.52}_{-0.63}$ | $4.58^{+1.52}_{-0.63}$ |
| 32823 | $769.2^{+24230.8}_{-378.6}$ | 2007-12-24 | *H* | 5.277±0.021 | 9.637±0.021 | 9.645±0.021 | 14.922±0.045 | $0.2^{+68.4}_{-1.1}$ | $5.5^{+68.4}_{-1.1}$ |
| 34041 | $507.6^{+133.4}_{-87.4}$ | 2008-02-01 | *H* | 2.095±0.064 | 7.326±0.035 | 7.473±0.045 | 9.57±0.11 | $-1.07^{+0.57}_{-0.38}$ | $1.02^{+0.58}_{-0.39}$ |
| 34045 | $135.5^{+4.0}_{-3.7}$ | 2005-02-07 | *Ks* | 4.6730±0.0075 | 4.366±0.035 | 4.381±0.035 | 9.054±0.042 | $-1.29^{+0.07}_{-0.07}$ | $3.386^{+0.076}_{-0.074}$ |
| | | 2013-01-06 | *Ks* | 4.690±0.011 | 4.366±0.035 | 4.380±0.035 | 9.070±0.046 | $-1.29^{+0.07}_{-0.07}$ | $3.403^{+0.078}_{-0.075}$ |
| 34153 | $485.4^{+376.6}_{-147.6}$ | 2008-02-03 | *H* | 1.39±0.11 | 9.201±0.026 | 9.47±0.05 | 10.86±0.11 | $1.02^{+1.69}_{-0.66}$ | $2.41^{+1.69}_{-0.67}$ |
| 34338 | $203.7^{+14.7}_{-12.8}$ | 2005-02-07 | *Ks* | 3.759±0.017 | 6.368±0.017 | 6.402±0.018 | 10.160±0.038 | $-0.12^{+0.16}_{-0.14}$ | $3.64^{+0.16}_{-0.14}$ |
| | | 2013-01-04 | *Ks* | 3.760±0.014 | 6.368±0.017 | 6.402±0.018 | 10.161±0.034 | $-0.12^{+0.16}_{-0.14}$ | $3.64^{+0.16}_{-0.14}$ |
| 34758 | $143.3^{+8.2}_{-7.4}$ | 2005-02-12 | *Ks* | 5.62±0.15 | 5.844±0.017 | 5.850±0.018 | 11.47±0.18 | $0.07^{+0.13}_{-0.11}$ | $5.69^{+0.22}_{-0.21}$ |
| | | 2007-11-21 | *Ks* | 5.699±0.084 | 5.844±0.017 | 5.850±0.017 | 11.55±0.11 | $0.07^{+0.13}_{-0.11}$ | $5.77^{+0.17}_{-0.16}$ |
| 35110 | $292.4^{+92.2}_{-56.5}$ | 2008-02-01 | *H* | 3.610±0.036 | 8.154±0.057 | 8.192±0.058 | 11.803±0.098 | $0.84^{+0.69}_{-0.42}$ | $4.45^{+0.69}_{-0.43}$ |
| 35413 | $295.9^{+162.9}_{-77.5}$ | 2008-01-12 | *H* | 2.155±0.017 | 8.862±0.043 | 9.002±0.046 | 11.157±0.062 | $1.59^{+1.20}_{-0.57}$ | $3.75^{+1.20}_{-0.57}$ |
| 36345 | $228.3^{+36.9}_{-27.9}$ | 2009-01-08 | *Ks* | 0.8353±0.0088 | 6.816±0.023 | 7.229±0.028 | 8.065±0.034 | $0.42^{+0.35}_{-0.27}$ | $1.26^{+0.35}_{-0.27}$ |
| 36363 | $165.0^{+6.2}_{-5.8}$ | 2005-01-14 | *Ks* | 5.85±0.23 | 5.822±0.027 | 5.827±0.028 | 11.68±0.28 | $-0.274^{+0.087}_{-0.081}$ | $5.58^{+0.29}_{-0.29}$ |
| | | 2007-11-23 | *Ks* | 6.20±0.14 | 5.822±0.027 | 5.826±0.027 | 12.02±0.18 | $-0.275^{+0.086}_{-0.081}$ | $5.92^{+0.19}_{-0.19}$ |
| 37322 | $175.4^{+8.7}_{-7.9}$ | 2005-01-14 | *Ks* | 2.1630±0.0029 | 5.982±0.017 | 6.121±0.017 | 8.28±0.02 | $-0.1^{+0.1}_{-0.1}$ | $2.0^{+0.1}_{-0.1}$ |
| | | 2007-11-08 | *Ks* | 2.1677±0.0019 | 5.982±0.017 | 6.120±0.017 | 8.288±0.019 | $-0.1^{+0.1}_{-0.1}$ | $2.0^{+0.1}_{-0.1}$ |
| 37915 | $181.2^{+8.2}_{-7.5}$ | 2005-01-14 | *Ks* | 2.129±0.013 | 6.106±0.017 | 6.249±0.019 | 8.378±0.029 | $-0.060^{+0.100}_{-0.092}$ | $2.069^{+0.103}_{-0.095}$ |
| | | 2007-11-23 | *Ks* | 1.929±0.041 | 6.106±0.017 | 6.276±0.023 | 8.204±0.052 | $-0.033^{+0.101}_{-0.093}$ | $1.9^{+0.1}_{-0.1}$ |
| 39906 | $142.7^{+4.6}_{-4.3}$ | 2005-06-02 | *Ks* | 6.332±0.093 | 4.769±0.023 | 4.772±0.023 | 11.10±0.12 | $-1.024^{+0.075}_{-0.071}$ | $5.31^{+0.14}_{-0.13}$ |
| 40817 | $133.3^{+6.5}_{-5.9}$ | 2005-02-14 | *Ks* | 2.7743±0.0095 | 5.401±0.024 | 5.482±0.025 | 8.257±0.033 | $-0.1^{+0.1}_{-0.1}$ | $2.6^{+0.1}_{-0.1}$ |
| | | 2007-12-17 | *Ks* | 2.6843±0.0099 | 5.401±0.024 | 5.489±0.025 | 8.173±0.033 | $-0.1^{+0.1}_{-0.1}$ | $2.5^{+0.1}_{-0.1}$ |
| | | 2008-01-02 | *Ks* | 2.7328±0.0053 | 5.401±0.024 | 5.485±0.024 | 8.218±0.029 | $-0.1^{+0.1}_{-0.1}$ | $2.6^{+0.1}_{-0.1}$ |
| 41049 | $666.7^{+741.8}_{-230.0}$ | 2004-04-04 | *Ks* | 1.173±0.022 | 9.123±0.027 | 9.440±0.036 | 10.613±0.055 | $0.32^{+2.42}_{-0.75}$ | $1.49^{+2.42}_{-0.75}$ |
| 41817 | $105.8^{+7.2}_{-6.3}$ | 2005-02-12 | *Ks* | 0.5936±0.0018 | 5.565±0.019 | 6.06±0.02 | 6.65±0.02 | $0.94^{+0.15}_{-0.13}$ | $1.53^{+0.15}_{-0.13}$ |
| | | 2007-11-21 | *Ks* | 0.5980±0.0027 | 5.565±0.019 | 6.06±0.02 | 6.657±0.021 | $0.94^{+0.15}_{-0.13}$ | $1.53^{+0.15}_{-0.13}$ |

*Continued on next page*

Table A4 – *Continued from previous page*

| HIP | Distance (pc) | Date | Band | $\Delta m$[a] (mag) | $m_{\text{system}}$ (mag) | $m_{\text{prim}}$ (mag) | $m_{\text{comp}}$ (mag) | $M_{\text{prim}}$ (mag) | $M_{\text{comp}}$ (mag) |
|---|---|---|---|---|---|---|---|---|---|
| 41843 | $222.7^{+21.8}_{-18.2}$ | 2005-02-03 | $K$s | 7.026±0.018 | 6.834±0.032 | 6.836±0.032 | 13.86±0.05 | $0.11^{+0.21}_{-0.18}$ | $7.13^{+0.22}_{-0.18}$ |
| | | 2013-02-03 | $K$s | 7.133±0.044 | 6.834±0.032 | 6.836±0.032 | 13.968±0.076 | $0.10^{+0.21}_{-0.18}$ | $7.24^{+0.23}_{-0.19}$ |
| 42129 | $274.7^{+23.8}_{-20.3}$ | 2006-01-03 | $K$s | 2.7735±0.0036 | 5.602±0.017 | 5.683±0.017 | 8.46±0.02 | $-1.53^{+0.19}_{-0.16}$ | $1.24^{+0.19}_{-0.16}$ |
| | | 2007-12-17 | $K$s | 2.833±0.012 | 5.602±0.017 | 5.679±0.018 | 8.512±0.028 | $-1.54^{+0.19}_{-0.16}$ | $1.30^{+0.19}_{-0.16}$ |
| 42177 | $136.8^{+4.8}_{-4.5}$ | 2005-02-03 | $K$s | 2.4106±0.0022 | 6.041±0.017 | 6.153±0.017 | 8.56±0.02 | $0.480^{+0.079}_{-0.074}$ | $2.890^{+0.079}_{-0.074}$ |
| 42334 | $71.1^{+1.1}_{-1.0}$ | 2005-03-05 | $K$s | 7.8±0.2 | 5.321±0.019 | 5.322±0.019 | 13.13±0.23 | $1.072^{+0.038}_{-0.037}$ | $8.88^{+0.23}_{-0.23}$ |
| | | 2008-02-12 | $K$s | 7.31±0.37 | 5.321±0.019 | 5.322±0.019 | 12.6±0.4 | $1.073^{+0.038}_{-0.037}$ | $8.4^{+0.4}_{-0.4}$ |
| 42540 | $85.6^{+3.8}_{-3.5}$ | 2005-01-05 | $K$s | 2.263±0.045 | 5.288±0.02 | 5.415±0.027 | 7.679±0.079 | $0.751^{+0.101}_{-0.093}$ | $3.01^{+0.13}_{-0.12}$ |
| | | 2007-12-17 | $K$s | 2.250±0.049 | 5.288±0.02 | 5.417±0.028 | 7.666±0.084 | $0.752^{+0.101}_{-0.093}$ | $3.00^{+0.13}_{-0.12}$ |
| 42715 | $153.1^{+6.4}_{-5.9}$ | 2006-01-07 | $K$s | 1.632±0.004 | 5.809±0.019 | 6.03±0.02 | 7.659±0.022 | $0.121^{+0.092}_{-0.086}$ | $1.753^{+0.093}_{-0.086}$ |
| | | 2008-02-13 | $K$s | 1.6177±0.0034 | 5.809±0.019 | 6.03±0.02 | 7.647±0.022 | $0.123^{+0.092}_{-0.086}$ | $1.741^{+0.093}_{-0.086}$ |
| 43305 | $138.1^{+4.7}_{-4.4}$ | 2005-01-09 | $K$s | 3.94±0.01 | 5.435±0.023 | 5.463±0.023 | 9.402±0.033 | $-0.248^{+0.078}_{-0.073}$ | $3.691^{+0.082}_{-0.077}$ |
| | | 2008-02-13 | $K$s | 3.7493±0.0082 | 5.435±0.023 | 5.469±0.023 | 9.218±0.031 | $-0.243^{+0.078}_{-0.073}$ | $3.507^{+0.081}_{-0.076}$ |
| 43792 | $980.4^{+49019.6}_{-485.3}$ | 2003-01-20 | $K$s | 1.212±0.028 | 7.803±0.014 | 8.111±0.026 | 9.322±0.049 | $-2.0^{+108.6}_{-1.1}$ | $-0.8^{+108.6}_{-1.1}$ |
| 44299 | $131.6^{+8.3}_{-7.4}$ | 2006-01-15 | $K$s | 7.54±0.16 | 5.927±0.026 | 5.928±0.026 | 13.47±0.19 | $0.33^{+0.14}_{-0.12}$ | $7.87^{+0.24}_{-0.23}$ |
| | | 2007-12-17 | $K$s | 6.69±0.31 | 5.927±0.026 | 5.929±0.027 | 12.62±0.35 | $0.33^{+0.14}_{-0.12}$ | $7.02^{+0.38}_{-0.37}$ |
| 44798 | $162.9^{+7.2}_{-6.6}$ | 2005-01-10 | $K$s | 2.6738±0.0095 | 5.462±0.023 | 5.551±0.024 | 8.225±0.033 | $-0.515^{+0.099}_{-0.091}$ | $2.159^{+0.102}_{-0.094}$ |
| 44883 | $188.3^{+24.4}_{-19.4}$ | 2005-01-12 | $K$s | 2.9970±0.0049 | 5.64±0.023 | 5.707±0.023 | 8.704±0.028 | $-0.69^{+0.28}_{-0.23}$ | $2.30^{+0.28}_{-0.23}$ |
| | | 2008-01-03 | $K$s | 3.0014±0.0058 | 5.64±0.023 | 5.706±0.023 | 8.708±0.028 | $-0.69^{+0.28}_{-0.23}$ | $2.31^{+0.28}_{-0.23}$ |
| 45189 | $212.3^{+23.0}_{-18.9}$ | 2005-01-12 | $K$s | 0.634±0.029 | 5.862±0.03 | 6.343±0.049 | 6.977±0.064 | $-0.3^{+0.2}_{-0.2}$ | $0.3^{+0.2}_{-0.2}$ |
| | | 2008-01-02 | $K$s | 0.619±0.012 | 5.862±0.03 | 6.349±0.038 | 6.967±0.044 | $-0.3^{+0.2}_{-0.2}$ | $0.3^{+0.2}_{-0.2}$ |
| 45314 | $161.3^{+7.3}_{-6.7}$ | 2004-12-16 | $K$s | 6.37±0.17 | 6.133±0.027 | 6.136±0.028 | 12.51±0.21 | $0.098^{+0.103}_{-0.095}$ | $6.47^{+0.24}_{-0.23}$ |
| | | 2008-02-15 | $K$s | 6.36±0.13 | 6.133±0.027 | 6.136±0.027 | 12.49±0.16 | $0.098^{+0.103}_{-0.095}$ | $6.45^{+0.19}_{-0.19}$ |
| | | 2012-12-04 | $K$s | 6.232±0.055 | 6.133±0.027 | 6.136±0.027 | 12.368±0.086 | $0.098^{+0.103}_{-0.095}$ | $6.33^{+0.13}_{-0.12}$ |
| 45344 | $187.6^{+9.6}_{-8.7}$ | 2004-12-10 | $K$s | 3.317±0.039 | 5.59±0.019 | 5.640±0.021 | 8.957±0.067 | $-0.7^{+0.1}_{-0.1}$ | $2.57^{+0.13}_{-0.12}$ |
| | | 2008-02-15 | $K$s | 3.355±0.047 | 5.59±0.019 | 5.638±0.022 | 8.994±0.078 | $-0.7^{+0.1}_{-0.1}$ | $2.61^{+0.14}_{-0.13}$ |

*Continued on next page*

Table A4 – *Continued from previous page*

| HIP | Distance (pc) | Date | Band | $\Delta m^{a}$ (mag) | $m_{\mathrm{system}}$ (mag) | $m_{\mathrm{prim}}$ (mag) | $m_{\mathrm{comp}}$ (mag) | $M_{\mathrm{prim}}$ (mag) | $M_{\mathrm{comp}}$ (mag) |
|---|---|---|---|---|---|---|---|---|---|
| 46283 | $131.6^{+3.2}_{-3.0}$ | 2006-01-15 | $K$s | 4.625±0.033 | 5.385±0.024 | 5.400±0.024 | 10.025±0.056 | $-0.209^{+0.058}_{-0.056}$ | $4.417^{+0.077}_{-0.075}$ |
| | | 2008-01-10 | $K$s | 4.783±0.053 | 5.385±0.024 | 5.398±0.025 | 10.181±0.076 | $-0.211^{+0.058}_{-0.056}$ | $4.572^{+0.093}_{-0.091}$ |
| 46329 | $628.9^{+458.0}_{-186.5}$ | 2005-03-25 | $K$s | 1.0107±0.0016 | 6.09±0.017 | 6.451±0.018 | 7.462±0.019 | $-2.58^{+1.58}_{-0.64}$ | $-1.57^{+1.58}_{-0.64}$ |
| 46914 | $254.5^{+36.2}_{-28.2}$ | 2005-03-13 | $K$s | 0.775±0.016 | 5.396±0.02 | 5.829±0.029 | 6.604±0.039 | $-1.24^{+0.31}_{-0.24}$ | $-0.47^{+0.31}_{-0.24}$ |
| | | 2008-03-10 | $K$s | 0.709±0.023 | 5.396±0.02 | 5.851±0.035 | 6.560±0.048 | $-1.22^{+0.31}_{-0.24}$ | $-0.51^{+0.31}_{-0.25}$ |
| 46928 | $175.4^{+4.7}_{-4.5}$ | 2006-02-12 | $K$s | 4.373±0.017 | 5.426±0.017 | 5.445±0.017 | 9.818±0.034 | $-0.783^{+0.061}_{-0.058}$ | $3.590^{+0.068}_{-0.065}$ |
| | | 2008-01-10 | $K$s | 4.37±0.02 | 5.426±0.017 | 5.445±0.017 | 9.817±0.037 | $-0.783^{+0.061}_{-0.058}$ | $3.589^{+0.069}_{-0.067}$ |
| 48943 | $244.5^{+38.0}_{-29.0}$ | 2005-05-03 | $K$s | 3.1781±0.0021 | 6.231±0.02 | 6.29±0.02 | 9.466±0.022 | $-0.68^{+0.34}_{-0.26}$ | $2.50^{+0.34}_{-0.26}$ |
| 49712 | $408.2^{+34.3}_{-29.4}$ | 2005-06-05 | $K$s | 4.364±0.018 | 5.102±0.023 | 5.121±0.023 | 9.48±0.04 | $-2.96^{+0.18}_{-0.16}$ | $1.41^{+0.19}_{-0.16}$ |
| 50044 | $746.3^{+206.1}_{-132.8}$ | 2005-06-02 | $K$s | 8.10±0.11 | 6.024±0.032 | 6.025±0.032 | 14.12±0.15 | $-3.38^{+0.60}_{-0.39}$ | $4.72^{+0.62}_{-0.41}$ |
| 50847 | $123.2^{+2.8}_{-2.7}$ | 2006-02-13 | $K$s | 5.513±0.042 | 5.314±0.024 | 5.321±0.024 | 10.834±0.071 | $-0.123^{+0.055}_{-0.053}$ | $5.390^{+0.086}_{-0.085}$ |
| | | 2011-04-22 | $K$s | 5.553±0.035 | 5.314±0.024 | 5.321±0.024 | 10.873±0.063 | $-0.124^{+0.055}_{-0.053}$ | $5.429^{+0.080}_{-0.079}$ |
| 51362 | $98.7^{+2.3}_{-2.2}$ | 2004-06-29 | $K$s | 8.11±0.28 | 5.238±0.016 | 5.239±0.016 | 13.3±0.3 | $0.275^{+0.053}_{-0.051}$ | $8.4^{+0.3}_{-0.3}$ |
| | | 2006-04-21 | $K$s | 8.08±0.22 | 5.238±0.016 | 5.239±0.016 | 13.32±0.24 | $0.275^{+0.053}_{-0.051}$ | $8.35^{+0.25}_{-0.25}$ |
| 52742 | $161.3^{+5.1}_{-4.8}$ | 2006-02-28 | $K$s | 6.737±0.033 | 5.224±0.019 | 5.226±0.019 | 11.963±0.052 | $-0.826^{+0.071}_{-0.067}$ | $5.911^{+0.086}_{-0.083}$ |
| | | 2008-01-18 | $K$s | 6.92±0.06 | 5.224±0.019 | 5.226±0.019 | 12.146±0.079 | $-0.827^{+0.071}_{-0.067}$ | $6.1^{+0.1}_{-0.1}$ |
| 53272 | $233.1^{+25.3}_{-20.8}$ | 2006-02-13 | $K$s | 0.6051±0.0015 | 5.98±0.023 | 6.472±0.024 | 7.077±0.024 | $-0.4^{+0.2}_{-0.2}$ | $0.2^{+0.2}_{-0.2}$ |
| | | 2008-02-15 | $K$s | 0.594±0.001 | 5.98±0.023 | 6.476±0.023 | 7.070±0.024 | $-0.4^{+0.2}_{-0.2}$ | $0.2^{+0.2}_{-0.2}$ |
| 54557 | $178.6^{+33.3}_{-24.3}$ | 2006-02-28 | $K$s | 3.0676±0.0019 | 7.149±0.019 | 7.212±0.019 | 10.279±0.021 | $0.8^{+0.4}_{-0.3}$ | $3.8^{+0.4}_{-0.3}$ |
| | | 2006-03-26 | $K$s | 3.1159±0.0026 | 7.149±0.019 | 7.209±0.019 | 10.325±0.021 | $0.8^{+0.4}_{-0.3}$ | $3.9^{+0.4}_{-0.3}$ |
| | | 2007-03-01 | $K$s | 2.9545±0.0012 | 7.149±0.019 | 7.218±0.019 | 10.17±0.02 | $0.8^{+0.4}_{-0.3}$ | $3.7^{+0.4}_{-0.3}$ |
| | | 2008-02-20 | $K$s | 2.9758±0.0015 | 7.149±0.019 | 7.217±0.019 | 10.19±0.02 | $0.8^{+0.4}_{-0.3}$ | $3.7^{+0.4}_{-0.3}$ |
| | | 2011-02-13 | $J$ | 3.890±0.014 | 7.64±0.026 | 7.670±0.026 | 11.559±0.041 | $0.94^{+0.41}_{-0.31}$ | $4.83^{+0.41}_{-0.31}$ |
| | | | $K$s | 3.0289±0.0021 | 7.149±0.019 | 7.214±0.019 | 10.243±0.021 | $0.8^{+0.4}_{-0.3}$ | $3.8^{+0.4}_{-0.3}$ |
| 54829 | $675.7^{+118.0}_{-87.4}$ | 2011-04-24 | $K$s | 7.064±0.099 | 5.931±0.02 | 5.93±0.02 | 13.00±0.12 | $-3.26^{+0.38}_{-0.28}$ | $3.81^{+0.40}_{-0.31}$ |
| 55597 | $123.8^{+6.1}_{-5.6}$ | 2006-01-17 | $K$s | 0.8758±0.0083 | 5.282±0.023 | 5.683±0.028 | 6.558±0.033 | $0.2^{+0.1}_{-0.1}$ | $1.0^{+0.1}_{-0.1}$ |

*Continued on next page*

Table A4 – *Continued from previous page*

| HIP | Distance (pc) | Date | Band | $\Delta m^{a}$ (mag) | $m_{\mathrm{system}}$ (mag) | $m_{\mathrm{prim}}$ (mag) | $m_{\mathrm{comp}}$ (mag) | $M_{\mathrm{prim}}$ (mag) | $M_{\mathrm{comp}}$ (mag) |
|---|---|---|---|---|---|---|---|---|---|
| | | 2008-02-24 | $Ks$ | 0.952±0.044 | 5.282±0.023 | 5.660±0.046 | 6.612±0.078 | $0.14^{+0.12}_{-0.11}$ | $1.10^{+0.13}_{-0.13}$ |
| 55657 | $304.9^{+20.9}_{-18.3}$ | 2006-01-06 | $Ks$ | 8.16±0.24 | 5.408±0.017 | 5.409±0.017 | 13.57±0.26 | $-2.10^{+0.15}_{-0.13}$ | $6.06^{+0.30}_{-0.29}$ |
| | | 2008-02-24 | $Ks$ | 8.2±0.4 | 5.408±0.017 | 5.409±0.017 | 13.57±0.43 | $-2.10^{+0.15}_{-0.13}$ | $6.07^{+0.46}_{-0.45}$ |
| 58326 | $187.3^{+9.2}_{-8.4}$ | 2006-02-13 | $Ks$ | 7.24±0.14 | 5.994±0.02 | 6.00±0.02 | 13.24±0.17 | $-0.376^{+0.109}_{-0.099}$ | $6.9^{+0.2}_{-0.2}$ |
| | | 2008-01-10 | $Ks$ | 7.24±0.32 | 5.994±0.02 | 6.00±0.02 | 13.24±0.35 | $-0.376^{+0.109}_{-0.099}$ | $6.86^{+0.37}_{-0.36}$ |
| 60189 | $127.4^{+3.7}_{-3.5}$ | 2005-02-06 | $Ks$ | 6.40±0.26 | 5.317±0.019 | 5.32±0.02 | 11.7±0.3 | $-0.217^{+0.066}_{-0.062}$ | $6.2^{+0.3}_{-0.3}$ |
| 60449 | $136.2^{+5.0}_{-4.7}$ | 2005-02-12 | $Ks$ | 5.973±0.097 | 5.427±0.017 | 5.431±0.017 | 11.40±0.11 | $-0.245^{+0.082}_{-0.076}$ | $5.73^{+0.14}_{-0.14}$ |
| | | 2008-02-14 | $Ks$ | 5.987±0.025 | 5.427±0.017 | 5.431±0.017 | 11.419±0.042 | $-0.245^{+0.082}_{-0.076}$ | $5.743^{+0.090}_{-0.086}$ |
| 61789 | $111.9^{+3.1}_{-2.9}$ | 2005-02-03 | $Ks$ | 3.096±0.001 | 4.784±0.017 | 4.845±0.017 | 7.941±0.018 | $-0.40^{+0.06}_{-0.06}$ | $2.69^{+0.06}_{-0.06}$ |
| 62026 | $108.5^{+4.9}_{-4.5}$ | 2004-04-07 | $Ks$ | 1.5421±0.0047 | 6.014±0.017 | 6.249±0.018 | 7.791±0.022 | $1.056^{+0.100}_{-0.092}$ | $2.598^{+0.101}_{-0.093}$ |
| 63005 | $124.8^{+4.7}_{-4.4}$ | 2011-05-09 | $Ks$ | 4.128±0.053 | 5.313±0.02 | 5.337±0.021 | 9.465±0.072 | $-0.163^{+0.084}_{-0.079}$ | $4.0^{+0.1}_{-0.1}$ |
| 63945 | $119.6^{+3.7}_{-3.5}$ | 2005-03-25 | $Ks$ | 3.2052±0.0015 | 5.045±0.024 | 5.100±0.024 | 8.305±0.025 | $-0.308^{+0.071}_{-0.068}$ | $2.897^{+0.072}_{-0.068}$ |
| 64053 | $100.1^{+3.3}_{-3.1}$ | 2006-02-13 | $Ks$ | 8.36±0.26 | 5.729±0.026 | 5.729±0.026 | 14.09±0.29 | $0.711^{+0.077}_{-0.072}$ | $9.1^{+0.3}_{-0.3}$ |
| 64515 | $112.2^{+9.7}_{-8.3}$ | 2005-03-07 | $Ks$ | 0.2271±0.0031 | 5.947±0.02 | 6.592±0.021 | 6.819±0.022 | $1.35^{+0.19}_{-0.16}$ | $1.58^{+0.19}_{-0.16}$ |
| | | 2006-02-12 | $Ks$ | 0.2340±0.0021 | 5.947±0.02 | 6.589±0.021 | 6.823±0.021 | $1.34^{+0.19}_{-0.16}$ | $1.58^{+0.19}_{-0.16}$ |
| 67472 | $155.0^{+3.9}_{-3.8}$ | 2005-03-25 | $Ks$ | 5.827±0.047 | 4.006±0.035 | 4.011±0.035 | 9.838±0.086 | $-1.958^{+0.066}_{-0.063}$ | $3.9^{+0.1}_{-0.1}$ |
| | | 2011-05-09 | $Ks$ | 6.039±0.038 | 4.006±0.035 | 4.010±0.035 | 10.049±0.076 | $-1.959^{+0.066}_{-0.063}$ | $4.079^{+0.094}_{-0.093}$ |
| 67669 | $105.4^{+10.9}_{-9.0}$ | 2005-02-03 | $Ks$ | 1.5305±0.0075 | 4.971±0.027 | 5.208±0.029 | 6.739±0.037 | $0.09^{+0.23}_{-0.19}$ | $1.63^{+0.23}_{-0.19}$ |
| 67703 | $79.7^{+5.4}_{-4.7}$ | 2004-06-29 | $Ks$ | 2.059±0.015 | 5.514±0.023 | 5.666±0.026 | 7.725±0.043 | $1.16^{+0.15}_{-0.13}$ | $3.22^{+0.15}_{-0.14}$ |
| 70915 | $146.2^{+9.3}_{-8.3}$ | 2006-02-25 | $Ks$ | 4.40±0.05 | 5.65±0.023 | 5.669±0.024 | 10.072±0.081 | $-0.16^{+0.14}_{-0.13}$ | $4.24^{+0.16}_{-0.15}$ |
| | | 2008-02-22 | $Ks$ | 4.049±0.053 | 5.65±0.023 | 5.676±0.025 | 9.725±0.086 | $-0.16^{+0.14}_{-0.13}$ | $3.89^{+0.16}_{-0.15}$ |
| 71762 | $93.7^{+13.6}_{-10.5}$ | 2005-02-03 | $Ks$ | 0.2723±0.0047 | 5.051±0.017 | 5.676±0.021 | 5.948±0.022 | $0.81^{+0.32}_{-0.24}$ | $1.08^{+0.32}_{-0.24}$ |
| 73111 | $169.2^{+20.9}_{-16.8}$ | 2005-03-25 | $Ks$ | 0.8017±0.0056 | 5.683±0.017 | 6.11±0.02 | 6.909±0.024 | $-0.06^{+0.27}_{-0.22}$ | $0.74^{+0.27}_{-0.22}$ |
| 74750 | $515.5^{+125.6}_{-84.4}$ | 2005-03-25 | $Ks$ | 2.6362±0.0011 | 5.938±0.023 | 6.030±0.023 | 8.666±0.024 | $-2.60^{+0.53}_{-0.36}$ | $0.04^{+0.53}_{-0.36}$ |
| 75264 | $157.0^{+19.4}_{-15.5}$ | 2005-03-25 | $Ks$ | 1.2803±0.0015 | 4.127±0.277 | 4.42±0.28 | 5.70±0.28 | $-1.57^{+0.39}_{-0.35}$ | $-0.29^{+0.39}_{-0.35}$ |
| | | 2011-05-09 | $Ks$ | 1.2497±0.0015 | 4.127±0.277 | 4.43±0.28 | 5.68±0.28 | $-1.56^{+0.39}_{-0.35}$ | $-0.31^{+0.39}_{-0.35}$ |

*Continued on next page*

Table A4 – *Continued from previous page*

| HIP | Distance (pc) | Date | Band | $\Delta m^a$ (mag) | $m_{system}$ (mag) | $m_{prim}$ (mag) | $m_{comp}$ (mag) | $M_{prim}$ (mag) | $M_{comp}$ (mag) |
|---|---|---|---|---|---|---|---|---|---|
| 76503 | $190.5^{+13.6}_{-11.9}$ | 2012-07-13 | *Ks* | 9.73±0.11 | 6.184±0.019 | 6.184±0.019 | 15.92±0.13 | $-0.25^{+0.16}_{-0.14}$ | $9.49^{+0.20}_{-0.19}$ |
| 77634 | $59.8^{+1.0}_{-1.0}$ | 2005-02-05 | *Ks* | 8.16±0.14 | 3.99±0.035 | 3.991±0.035 | 12.15±0.18 | $0.091^{+0.050}_{-0.049}$ | $8.25^{+0.18}_{-0.18}$ |
| 77840 | $154.1^{+13.1}_{-11.2}$ | 2012-07-13 | *Ks* | 1.9672±0.0087 | 4.789±0.017 | 4.953±0.019 | 6.921±0.028 | $-1.03^{+0.19}_{-0.16}$ | $0.93^{+0.19}_{-0.16}$ |
| 78968 | $122.7^{+20.2}_{-15.2}$ | 2004-05-05 | *Ks* | 6.843±0.069 | 7.401±0.023 | 7.403±0.023 | 14.246±0.096 | $1.90^{+0.36}_{-0.27}$ | $8.75^{+0.37}_{-0.29}$ |
| 79005 | $112.4^{+8.1}_{-7.1}$ | 2004-07-04 | *Ks* | 2.733±0.021 | 5.528±0.017 | 5.612±0.019 | 8.345±0.044 | $0.33^{+0.16}_{-0.14}$ | $3.06^{+0.16}_{-0.14}$ |
| | | 2006-04-27 | *Ks* | 2.585±0.034 | 5.528±0.017 | 5.624±0.021 | 8.209±0.061 | $0.34^{+0.16}_{-0.14}$ | $2.92^{+0.17}_{-0.15}$ |
| | | 2006-06-01 | *Ks* | 2.634±0.013 | 5.528±0.017 | 5.620±0.019 | 8.254±0.034 | $0.33^{+0.16}_{-0.14}$ | $2.97^{+0.16}_{-0.14}$ |
| 79098 | $136.1^{+6.0}_{-5.5}$ | 2005-03-13 | *Ks* | 8.16±0.19 | 5.706±0.017 | 5.707±0.017 | 13.87±0.21 | $0.01^{+0.10}_{-0.09}$ | $8.17^{+0.23}_{-0.23}$ |
| 79230 | $277.0^{+115.1}_{-62.9}$ | 2004-04-10 | *H* | 2.651±0.015 | 6.413±0.039 | 6.504±0.041 | 9.155±0.059 | $-0.9^{+0.9}_{-0.5}$ | $1.7^{+0.9}_{-0.5}$ |
| 79410 | $140.4^{+26.5}_{-19.2}$ | 2004-06-20 | *Ks* | 8.125±0.078 | 7.071±0.028 | 7.072±0.028 | 15.20±0.11 | $1.3^{+0.4}_{-0.3}$ | $9.39^{+0.42}_{-0.32}$ |
| 79622 | $148.8^{+9.4}_{-8.4}$ | 2012-07-13 | *Ks* | 3.9±1.4 | 5.822±0.024 | 5.852±0.063 | 9.7±1.4 | $-0.07^{+0.15}_{-0.14}$ | $3.8^{+1.4}_{-1.4}$ |
| 79739 | $150.2^{+23.5}_{-17.9}$ | 2004-06-20 | *Ks* | 4.30±0.02 | 7.025±0.017 | 7.045±0.017 | 11.346±0.036 | $1.05^{+0.34}_{-0.26}$ | $5.35^{+0.34}_{-0.26}$ |
| 80142 | $137.2^{+9.9}_{-8.6}$ | 2004-05-05 | *Ks* | 2.899±0.023 | 6.618±0.026 | 6.691±0.028 | 9.589±0.055 | $0.98^{+0.16}_{-0.14}$ | $3.88^{+0.17}_{-0.15}$ |
| 80461 | $124.8^{+13.9}_{-11.3}$ | 2012-09-09 | *Ks* | 1.181±0.013 | 5.427±0.023 | 5.742±0.028 | 6.923±0.038 | $0.1^{+0.2}_{-0.2}$ | $1.3^{+0.2}_{-0.2}$ |
| 80473 | $110.7^{+12.3}_{-10.0}$ | 2012-06-11 | *Ks* | 0.2642±0.0011 | 3.173±0.518 | 3.80±0.52 | 4.07±0.52 | $-1.68^{+0.57}_{-0.56}$ | $-1.41^{+0.57}_{-0.56}$ |
| 80474 | $135.1^{+11.7}_{-10.0}$ | 2004-06-28 | *Ks* | 5.563±0.013 | 5.775±0.02 | 5.78±0.02 | 11.344±0.034 | $-0.05^{+0.19}_{-0.17}$ | $5.51^{+0.19}_{-0.17}$ |
| | | 2011-05-09 | *Ks* | 5.838±0.032 | 5.775±0.02 | 5.78±0.02 | 11.618±0.055 | $-0.05^{+0.19}_{-0.17}$ | $5.79^{+0.20}_{-0.17}$ |
| 80493 | $134.6^{+18.3}_{-14.4}$ | 2012-09-09 | *Ks* | 0.7131±0.0072 | 7.076±0.017 | 7.530±0.021 | 8.243±0.025 | $1.77^{+0.30}_{-0.23}$ | $2.49^{+0.30}_{-0.23}$ |
| 82902 | $116.1^{+5.7}_{-5.2}$ | 2004-06-21 | *Ks* | 8.13±0.23 | 6.144±0.024 | 6.145±0.024 | 14.28±0.26 | $0.826^{+0.109}_{-0.099}$ | $8.96^{+0.28}_{-0.28}$ |
| | | 2006-06-09 | *Ks* | 8.0±0.2 | 6.144±0.024 | 6.145±0.024 | 14.19±0.23 | $0.826^{+0.109}_{-0.099}$ | $8.87^{+0.25}_{-0.25}$ |
| 87220 | $170.6^{+7.9}_{-7.2}$ | 2005-03-25 | *Ks* | 8.20±0.13 | 4.752±0.017 | 4.753±0.017 | 12.95±0.15 | $-1.442^{+0.102}_{-0.094}$ | $6.76^{+0.18}_{-0.18}$ |
| | | 2011-05-09 | *Ks* | 8.44±0.13 | 4.752±0.017 | 4.752±0.017 | 13.19±0.15 | $-1.442^{+0.102}_{-0.094}$ | $6.99^{+0.18}_{-0.18}$ |
| 88149 | $199.6^{+10.9}_{-9.8}$ | 2005-03-26 | *Ks* | 2.010±0.029 | 5.03±0.024 | 5.188±0.028 | 7.199±0.049 | $-1.35^{+0.12}_{-0.11}$ | $0.66^{+0.13}_{-0.12}$ |
| | | 2011-05-09 | *Ks* | 1.882±0.022 | 5.03±0.024 | 5.207±0.027 | 7.089±0.043 | $-1.33^{+0.12}_{-0.11}$ | $0.55^{+0.13}_{-0.12}$ |
| 88859 | $271.7^{+52.9}_{-38.1}$ | 2005-03-13 | *Ks* | 2.954±0.022 | 6.328±0.023 | 6.397±0.025 | 9.352±0.051 | $-0.78^{+0.42}_{-0.31}$ | $2.17^{+0.43}_{-0.31}$ |
| 89684 | $202.4^{+17.4}_{-14.8}$ | 2005-07-19 | *Ks* | 5.212±0.037 | 6.122±0.016 | 6.131±0.016 | 11.343±0.058 | $-0.42^{+0.19}_{-0.16}$ | $4.79^{+0.19}_{-0.17}$ |

*Continued on next page*

Table A4 – *Continued from previous page*

| HIP | Distance (pc) | Date | Band | $\Delta m^{a}$ (mag) | $m_{\mathrm{system}}$ (mag) | $m_{\mathrm{prim}}$ (mag) | $m_{\mathrm{comp}}$ (mag) | $M_{\mathrm{prim}}$ (mag) | $M_{\mathrm{comp}}$ (mag) |
|---|---|---|---|---|---|---|---|---|---|
| | | 2011-05-09 | *Ks* | 5.327±0.027 | 6.122±0.016 | 6.130±0.016 | 11.457±0.046 | $-0.42^{+0.19}_{-0.16}$ | $4.90^{+0.19}_{-0.17}$ |
| 90096 | $188.7^{+14.2}_{-12.3}$ | 2005-03-29 | *Ks* | 4.081±0.016 | 5.526±0.02 | 5.55±0.02 | 9.632±0.039 | $-0.87^{+0.16}_{-0.14}$ | $3.21^{+0.17}_{-0.15}$ |
| | | 2011-05-09 | *Ks* | 4.048±0.016 | 5.526±0.02 | 5.55±0.02 | 9.599±0.039 | $-0.87^{+0.16}_{-0.14}$ | $3.18^{+0.17}_{-0.15}$ |
| 90766 | $216.9^{+44.2}_{-31.4}$ | 2010-06-25 | *Ks* | 1.182±0.018 | 7.807±0.017 | 8.122±0.025 | 9.30±0.04 | $1.42^{+0.44}_{-0.32}$ | $2.61^{+0.44}_{-0.32}$ |
| 91014 | $404.9^{+45.6}_{-37.2}$ | 2005-04-12 | *Ks* | 4.32±0.02 | 5.537±0.023 | 5.557±0.023 | 9.881±0.043 | $-2.5^{+0.2}_{-0.2}$ | $1.8^{+0.2}_{-0.2}$ |
| 93805 | $37.9^{+0.9}_{-0.9}$ | 2008-08-21 | *Ks* | 3.976±0.016 | 3.563±0.289 | 3.59±0.29 | 7.57±0.31 | $0.70^{+0.29}_{-0.29}$ | $4.67^{+0.31}_{-0.31}$ |
| | | 2009-04-26 | *Ks* | 3.818±0.023 | 3.563±0.289 | 3.59±0.29 | 7.41±0.32 | $0.70^{+0.29}_{-0.29}$ | $4.52^{+0.32}_{-0.32}$ |
| 99457 | $714.3^{+327.4}_{-170.8}$ | 2005-05-22 | *Ks* | 4.856±0.021 | 6.947±0.024 | 6.959±0.024 | 11.816±0.048 | $-2.34^{+1.00}_{-0.52}$ | $2.52^{+1.00}_{-0.52}$ |
| 100751 | $54.8^{+1.6}_{-1.5}$ | 2005-08-19 | *Ks* | 8.07±0.26 | 2.479±0.282 | 2.48±0.28 | 10.55±0.55 | $-1.22^{+0.29}_{-0.29}$ | $6.86^{+0.55}_{-0.55}$ |
| 100881 | $167.2^{+18.0}_{-14.8}$ | 2008-10-30 | *Ks* | 2.4867±0.0016 | 5.21±0.017 | 5.315±0.017 | 7.801±0.019 | $-0.83^{+0.23}_{-0.19}$ | $1.66^{+0.23}_{-0.19}$ |
| | | 2012-09-19 | *Ks* | 2.9387±0.0098 | 5.21±0.017 | 5.280±0.018 | 8.219±0.029 | $-0.86^{+0.23}_{-0.19}$ | $2.07^{+0.24}_{-0.19}$ |
| 105842 | $257.1^{+124.6}_{-63.3}$ | 2008-08-07 | *H* | 1.818±0.024 | 8.93±0.046 | 9.116±0.052 | 10.935±0.078 | $2.07^{+1.05}_{-0.54}$ | $3.88^{+1.06}_{-0.54}$ |
| 113031 | $253.2^{+28.5}_{-23.3}$ | 2004-10-20 | *Ks* | 0.520±0.054 | 5.925±0.019 | 6.45±0.04 | 6.968±0.053 | $-0.6^{+0.2}_{-0.2}$ | $-0.06^{+0.25}_{-0.21}$ |
| | | 2007-09-20 | *Ks* | 0.83±0.11 | 5.925±0.019 | 6.341±0.054 | 7.169±0.093 | $-0.69^{+0.25}_{-0.21}$ | $0.14^{+0.26}_{-0.22}$ |
| 116231 | $53.4^{+0.4}_{-0.4}$ | 2004-10-18 | *Ks* | 4.0844±0.0063 | 4.611±0.027 | 4.636±0.027 | 8.720±0.033 | $1.019^{+0.032}_{-0.032}$ | $5.104^{+0.038}_{-0.038}$ |
| | | 2004-10-19 | *Ks* | 4.034±0.012 | 4.611±0.027 | 4.637±0.027 | 8.671±0.039 | $1.021^{+0.033}_{-0.032}$ | $5.055^{+0.043}_{-0.043}$ |
| | | 2012-09-18 | *Ks* | 4.1627±0.0031 | 4.611±0.027 | 4.634±0.027 | 8.80±0.03 | $1.018^{+0.032}_{-0.032}$ | $5.180^{+0.035}_{-0.035}$ |
| | | | | | Higher-order multiple systems | | | | |
| 24925AB | $281.7^{+158.8}_{-74.7}$ | 2005-01-09 | *Ks* | 2.27637±0.00077 | 6.433±0.019 | 6.62±0.02 | 8.899±0.021 | $-0.65^{+1.22}_{-0.58}$ | $1.62^{+1.22}_{-0.58}$ |
| | | 2012-09-19 | *Ks* | 2.2885±0.0043 | 6.433±0.019 | 6.618±0.021 | 8.906±0.024 | $-0.66^{+1.22}_{-0.58}$ | $1.63^{+1.22}_{-0.58}$ |
| | | 2013-01-04 | *Ks* | 2.258±0.001 | 6.433±0.019 | 6.62±0.02 | 8.878±0.021 | $-0.66^{+1.22}_{-0.58}$ | $1.60^{+1.22}_{-0.58}$ |
| 24925AC | | 2005-01-09 | *Ks* | 2.920±0.015 | 6.433±0.019 | 6.62±0.02 | 9.542±0.034 | $-0.65^{+1.22}_{-0.58}$ | $2.27^{+1.22}_{-0.58}$ |
| | | 2012-09-19 | *Ks* | 2.988±0.022 | 6.433±0.019 | 6.618±0.021 | 9.605±0.041 | $-0.66^{+1.22}_{-0.58}$ | $2.33^{+1.23}_{-0.58}$ |
| | | 2013-01-04 | *Ks* | 3.001±0.012 | 6.433±0.019 | 6.62±0.02 | 9.62±0.03 | $-0.66^{+1.22}_{-0.58}$ | $2.35^{+1.22}_{-0.58}$ |
| 26237AB | $271.0^{+130.6}_{-66.5}$ | 2005-04-09 | *Ks* | 0.9890±0.0089 | 5.056±0.017 | 5.536±0.025 | 6.525±0.029 | $-1.67^{+1.05}_{-0.53}$ | $-0.68^{+1.05}_{-0.53}$ |
| | | 2012-09-19 | *Ks* | 1.0510±0.0058 | 5.056±0.017 | 5.516±0.018 | 6.567±0.021 | $-1.69^{+1.05}_{-0.53}$ | $-0.63^{+1.05}_{-0.53}$ |

*Continued on next page*

Table A4 – *Continued from previous page*

| HIP | Distance (pc) | Date | Band | $\Delta m^a$ (mag) | $m_{system}$ (mag) | $m_{prim}$ (mag) | $m_{comp}$ (mag) | $M_{prim}$ (mag) | $M_{comp}$ (mag) |
|---|---|---|---|---|---|---|---|---|---|
| 26237AC | | 2005-04-09 | *Ks* | 2.036±0.054 | 5.056±0.017 | 5.536±0.025 | 7.572±0.068 | $-1.67^{+1.05}_{-0.53}$ | $0.37^{+1.05}_{-0.54}$ |
| | | 2012-09-19 | *Ks* | 2.07312±0.00018 | 5.056±0.017 | 5.516±0.018 | 7.589±0.019 | $-1.69^{+1.05}_{-0.53}$ | $0.39^{+1.05}_{-0.53}$ |
| 26549AB | $328.9^{+499.0}_{-245.3}$ | 2004-10-11 | *Ks* | 1.174±0.012 | 4.489±0.016 | 4.886±0.023 | 6.060±0.032 | $-2.7^{+3.3}_{-1.6}$ | $-1.5^{+3.3}_{-1.6}$ |
| 26549AC | | 2004-10-11 | *Ks* | 2.602±0.016 | 4.489±0.016 | 4.886±0.023 | 7.49±0.04 | $-2.7^{+3.3}_{-1.6}$ | $-0.1^{+3.3}_{-1.6}$ |
| 26549AD | | 2004-10-11 | *Ks* | 5.347±0.055 | 4.489±0.016 | 4.886±0.023 | 10.23±0.08 | $-2.7^{+3.3}_{-1.6}$ | $2.6^{+3.3}_{-1.6}$ |
| 26549AE | | 2004-10-11 | *Ks* | 6.7±0.1 | 4.489±0.016 | 4.886±0.023 | 11.59±0.13 | $-2.7^{+3.3}_{-1.6}$ | $4.0^{+3.3}_{-1.6}$ |
| 26549AF | | 2004-10-11 | *Ks* | 7.32±0.14 | 4.489±0.016 | 4.886±0.023 | 12.20±0.16 | $-2.7^{+3.3}_{-1.6}$ | $4.6^{+3.3}_{-1.6}$ |
| 26549AG | | 2004-10-11 | *Ks* | 7.59±0.16 | 4.489±0.016 | 4.886±0.023 | 12.47±0.18 | $-2.7^{+3.3}_{-1.6}$ | $4.9^{+3.3}_{-1.6}$ |
| 39331AB | $432.9^{+271.3}_{-120.4}$ | 2007-01-20 | *Ks* | 6.147±0.076 | 9.303±0.02 | 9.310±0.021 | 15.5±0.1 | $1.1^{+1.4}_{-0.6}$ | $7.25^{+1.36}_{-0.61}$ |
| 39331AC | | 2007-01-20 | *Ks* | 6.388±0.087 | 9.303±0.02 | 9.310±0.021 | 15.70±0.11 | $1.1^{+1.4}_{-0.6}$ | $7.49^{+1.37}_{-0.61}$ |
| 42504AB | $135.7^{+6.6}_{-6.0}$ | 2006-01-07 | *Ks* | 2.677±0.027 | 5.532±0.016 | 5.633±0.019 | 8.309±0.041 | $-0.040^{+0.107}_{-0.098}$ | $2.6^{+0.1}_{-0.1}$ |
| 42504AC | | 2006-01-07 | *Ks* | 4.790±0.039 | 5.532±0.016 | 5.633±0.019 | 10.422±0.057 | $-0.040^{+0.107}_{-0.098}$ | $4.75^{+0.12}_{-0.11}$ |
| 46594AB | $132.6^{+3.6}_{-3.4}$ | 2006-01-18 | *Ks* | 4.594±0.055 | 5.625±0.02 | 5.651±0.022 | 10.245±0.084 | $0.03^{+0.06}_{-0.06}$ | $4.6^{+0.1}_{-0.1}$ |
| | | 2008-03-10 | *Ks* | 4.463±0.056 | 5.625±0.02 | 5.654±0.022 | 10.117±0.086 | $0.03^{+0.06}_{-0.06}$ | $4.5^{+0.1}_{-0.1}$ |
| 46594AC | | 2006-01-18 | *Ks* | 5.040±0.072 | 5.625±0.02 | 5.651±0.022 | 10.7±0.1 | $0.03^{+0.06}_{-0.06}$ | $5.07^{+0.12}_{-0.12}$ |
| | | 2008-03-10 | *Ks* | 4.944±0.071 | 5.625±0.02 | 5.654±0.022 | 10.6±0.1 | $0.03^{+0.06}_{-0.06}$ | $4.98^{+0.12}_{-0.12}$ |
| 51376AB | $133.2^{+9.1}_{-8.0}$ | 2005-02-04 | *Ks* | 3.219±0.073 | 5.597±0.026 | 5.699±0.035 | 8.92±0.12 | $0.08^{+0.15}_{-0.14}$ | $3.30^{+0.19}_{-0.18}$ |
| | | 2005-02-14 | *Ks* | 3.493±0.041 | 5.597±0.026 | 5.68±0.03 | 9.169±0.078 | $0.06^{+0.15}_{-0.13}$ | $3.55^{+0.17}_{-0.15}$ |
| | | 2008-02-25 | *Ks* | 3.335±0.045 | 5.597±0.026 | 5.689±0.031 | 9.023±0.083 | $0.07^{+0.15}_{-0.13}$ | $3.41^{+0.17}_{-0.15}$ |
| 51376AC | | 2005-02-04 | *Ks* | 3.310±0.076 | 5.597±0.026 | 5.699±0.035 | 9.01±0.12 | $0.08^{+0.15}_{-0.14}$ | $3.39^{+0.19}_{-0.18}$ |
| | | 2005-02-14 | *Ks* | 3.614±0.043 | 5.597±0.026 | 5.68±0.03 | 9.29±0.08 | $0.06^{+0.15}_{-0.13}$ | $3.67^{+0.17}_{-0.15}$ |
| | | 2008-02-25 | *Ks* | 3.452±0.048 | 5.597±0.026 | 5.689±0.031 | 9.141±0.086 | $0.07^{+0.15}_{-0.13}$ | $3.52^{+0.17}_{-0.16}$ |
| 54413AB | $158.5^{+17.3}_{-14.2}$ | 2007-02-27 | *Ks* | 10.0±0.2 | 5.94±0.028 | 5.940±0.028 | 15.90±0.23 | $-0.28^{+0.25}_{-0.21}$ | $9.68^{+0.34}_{-0.31}$ |
| | | 2008-02-20 | *Ks* | 10.21±0.21 | 5.94±0.028 | 5.940±0.028 | 16.15±0.24 | $-0.28^{+0.25}_{-0.21}$ | $9.93^{+0.34}_{-0.32}$ |
| | | 2009-02-20 | *Ks* | 9.76±0.11 | 5.94±0.028 | 5.940±0.028 | 15.70±0.14 | $-0.28^{+0.25}_{-0.21}$ | $9.48^{+0.28}_{-0.25}$ |
| | | 2010-12-25 | *Ks* | 9.86±0.13 | 5.94±0.028 | 5.940±0.028 | 15.80±0.16 | $-0.28^{+0.25}_{-0.21}$ | $9.58^{+0.30}_{-0.26}$ |

*Continued on next page*

Table A4 – *Continued from previous page*

| HIP | Distance (pc) | Date | Band | $\Delta m^{a}$ (mag) | $m_{\mathrm{system}}$ (mag) | $m_{\mathrm{prim}}$ (mag) | $m_{\mathrm{comp}}$ (mag) | $M_{\mathrm{prim}}$ (mag) | $M_{\mathrm{comp}}$ (mag) |
|---|---|---|---|---|---|---|---|---|---|
| | | 2011-03-25 | $Ks$ | 9.44±0.13 | 5.94±0.028 | 5.940±0.028 | 15.38±0.16 | $-0.28^{+0.25}_{-0.21}$ | $9.16^{+0.29}_{-0.26}$ |
| 54413AC | | 2007-02-27 | $Ks$ | 9.9±0.2 | 5.94±0.028 | 5.940±0.028 | 15.89±0.23 | $-0.28^{+0.25}_{-0.21}$ | $9.67^{+0.34}_{-0.31}$ |
| | | 2008-02-20 | $Ks$ | 10.07±0.19 | 5.94±0.028 | 5.940±0.028 | 16.01±0.23 | $-0.28^{+0.25}_{-0.21}$ | $9.79^{+0.33}_{-0.31}$ |
| | | 2009-02-20 | $Ks$ | 9.96±0.12 | 5.94±0.028 | 5.940±0.028 | 15.90±0.15 | $-0.28^{+0.25}_{-0.21}$ | $9.68^{+0.29}_{-0.26}$ |
| | | 2010-12-25 | $Ks$ | 9.87±0.13 | 5.94±0.028 | 5.940±0.028 | 15.81±0.16 | $-0.28^{+0.25}_{-0.21}$ | $9.59^{+0.30}_{-0.26}$ |
| | | 2011-03-25 | $Ks$ | 9.55±0.13 | 5.94±0.028 | 5.940±0.028 | 15.49±0.16 | $-0.28^{+0.25}_{-0.21}$ | $9.27^{+0.30}_{-0.26}$ |
| 56000AB | $214.6^{+37.9}_{-28.0}$ | 2005-02-07 | $Ks$ | 2.648±0.037 | 5.173±0.032 | 5.310±0.039 | 7.958±0.082 | $-1.36^{+0.39}_{-0.29}$ | $1.3^{+0.4}_{-0.3}$ |
| | | 2008-02-24 | $Ks$ | 2.987±0.055 | 5.173±0.032 | 5.28±0.04 | 8.3±0.1 | $-1.38^{+0.39}_{-0.29}$ | $1.6^{+0.4}_{-0.3}$ |
| 56000AC | | 2005-02-07 | $Ks$ | 3.325±0.051 | 5.173±0.032 | 5.310±0.039 | 8.634±0.097 | $-1.36^{+0.39}_{-0.29}$ | $2.0^{+0.4}_{-0.3}$ |
| | | 2008-02-24 | $Ks$ | 3.421±0.068 | 5.173±0.032 | 5.28±0.04 | 8.70±0.12 | $-1.38^{+0.39}_{-0.29}$ | $2.04^{+0.40}_{-0.31}$ |
| 56754AB | $87.4^{+3.3}_{-3.1}$ | 2005-02-02 | $Ks$ | 1.82548±0.00097 | 5.125±0.02 | 5.31±0.02 | 7.139±0.021 | $0.59^{+0.09}_{-0.08}$ | $2.42^{+0.09}_{-0.08}$ |
| | | 2008-01-10 | $Ks$ | 1.813±0.011 | 5.125±0.02 | 5.315±0.023 | 7.128±0.034 | $0.60^{+0.09}_{-0.08}$ | $2.408^{+0.090}_{-0.084}$ |
| | | 2011-04-22 | $Ks$ | 1.8215±0.0034 | 5.125±0.02 | 5.314±0.021 | 7.135±0.024 | $0.59^{+0.09}_{-0.08}$ | $2.416^{+0.086}_{-0.081}$ |
| 56754AC | | 2005-02-02 | $Ks$ | 6.10±0.05 | 5.125±0.02 | 5.31±0.02 | 11.41±0.07 | $0.59^{+0.09}_{-0.08}$ | $6.7^{+0.1}_{-0.1}$ |
| | | 2008-01-10 | $Ks$ | 6.19±0.11 | 5.125±0.02 | 5.315±0.023 | 11.50±0.14 | $0.60^{+0.09}_{-0.08}$ | $6.78^{+0.16}_{-0.16}$ |
| | | 2011-04-22 | $Ks$ | 6.269±0.066 | 5.125±0.02 | 5.314±0.021 | 11.583±0.088 | $0.59^{+0.09}_{-0.08}$ | $6.86^{+0.12}_{-0.12}$ |
| 60851AB | $97.9^{+3.3}_{-3.1}$ | 2004-04-07 | $Ks$ | 5.294±0.077 | 5.96±0.024 | 5.976±0.026 | 11.27±0.11 | $1.020^{+0.077}_{-0.073}$ | $6.31^{+0.13}_{-0.13}$ |
| 60851AC | | 2004-04-07 | $Ks$ | 5.37±0.21 | 5.96±0.024 | 5.976±0.026 | 11.35±0.24 | $1.020^{+0.077}_{-0.073}$ | $6.39^{+0.25}_{-0.25}$ |
| 62058AB | $117.1^{+5.0}_{-4.6}$ | 2005-02-14 | $Ks$ | 7.34±0.34 | 6.172±0.035 | 6.174±0.036 | 13.51±0.39 | $0.819^{+0.099}_{-0.093}$ | $8.2^{+0.4}_{-0.4}$ |
| 62058AC | | 2005-02-14 | $Ks$ | 8.10±0.47 | 6.172±0.035 | 6.174±0.036 | 14.27±0.52 | $0.819^{+0.099}_{-0.093}$ | $8.92^{+0.53}_{-0.53}$ |
| 69113AB | $161.0^{+11.4}_{-10.0}$ | 2004-05-01 | $Ks$ | 3.997±0.047 | 6.311±0.023 | 6.363±0.026 | 10.360±0.079 | $0.33^{+0.16}_{-0.14}$ | $4.33^{+0.17}_{-0.16}$ |
| 69113AC | | 2004-05-01 | $Ks$ | 4.063±0.049 | 6.311±0.023 | 6.363±0.026 | 10.426±0.081 | $0.33^{+0.16}_{-0.14}$ | $4.39^{+0.17}_{-0.16}$ |
| 74911AB | $102.9^{+8.1}_{-7.0}$ | 2005-03-25 | $Ks$ | 0.30719±0.00013 | 4.427±0.017 | 5.037±0.017 | 5.344±0.017 | $-0.04^{+0.17}_{-0.15}$ | $0.27^{+0.17}_{-0.15}$ |
| 74911AC | | 2005-03-25 | $Ks$ | 7.82±0.13 | 4.427±0.017 | 5.037±0.017 | 12.85±0.15 | $-0.04^{+0.17}_{-0.15}$ | $7.78^{+0.23}_{-0.21}$ |
| 77562AB | $94.5^{+3.1}_{-2.9}$ | 2004-06-30 | $Ks$ | 7.380±0.092 | 5.945±0.028 | 5.948±0.028 | 13.33±0.12 | $1.075^{+0.077}_{-0.073}$ | $8.45^{+0.14}_{-0.14}$ |
| | | 2006-04-28 | $Ks$ | 7.31±0.23 | 5.945±0.028 | 5.948±0.029 | 13.25±0.27 | $1.075^{+0.078}_{-0.074}$ | $8.38^{+0.28}_{-0.28}$ |

*Continued on next page*

Table A4 – *Continued from previous page*

| HIP | Distance (pc) | Date | Band | $\Delta m^{a}$ (mag) | $m_{\mathrm{system}}$ (mag) | $m_{\mathrm{prim}}$ (mag) | $m_{\mathrm{comp}}$ (mag) | $M_{\mathrm{prim}}$ (mag) | $M_{\mathrm{comp}}$ (mag) |
|---|---|---|---|---|---|---|---|---|---|
| 77562AC | | 2004-06-30 | $Ks$ | 7.93±0.12 | 5.945±0.028 | 5.948±0.028 | 13.88±0.15 | $1.075^{+0.077}_{-0.073}$ | $9.00^{+0.17}_{-0.17}$ |
| | | 2006-04-28 | $Ks$ | 7.74±0.28 | 5.945±0.028 | 5.948±0.029 | 13.69±0.32 | $1.075^{+0.078}_{-0.074}$ | $8.81^{+0.33}_{-0.33}$ |
| 77562AD | | 2004-06-30 | $Ks$ | 8.11±0.13 | 5.945±0.028 | 5.948±0.028 | 14.06±0.16 | $1.075^{+0.077}_{-0.073}$ | $9.19^{+0.18}_{-0.18}$ |
| | | 2006-04-28 | $Ks$ | 8.04±0.33 | 5.945±0.028 | 5.948±0.029 | 13.99±0.36 | $1.075^{+0.078}_{-0.074}$ | $9.11^{+0.37}_{-0.37}$ |
| 77562AE | | 2004-06-30 | $Ks$ | 8.00±0.13 | 5.945±0.028 | 5.948±0.028 | 13.95±0.16 | $1.075^{+0.077}_{-0.073}$ | $9.07^{+0.18}_{-0.18}$ |
| | | 2006-04-28 | $Ks$ | 8.65±0.47 | 5.945±0.028 | 5.948±0.029 | 14.60±0.51 | $1.075^{+0.078}_{-0.074}$ | $9.73^{+0.51}_{-0.51}$ |
| 79153AB | $85.8^{+4.4}_{-4.0}$ | 2004-06-30 | $Ks$ | 8.4±0.2 | 5.599±0.016 | 5.600±0.016 | 14.04±0.23 | $0.9^{+0.1}_{-0.1}$ | $9.38^{+0.25}_{-0.25}$ |
| | | 2006-04-28 | $Ks$ | 8.29±0.29 | 5.599±0.016 | 5.600±0.016 | 13.89±0.32 | $0.9^{+0.1}_{-0.1}$ | $9.23^{+0.34}_{-0.33}$ |
| 79153AC | | 2004-06-30 | $Ks$ | 8.79±0.24 | 5.599±0.016 | 5.600±0.016 | 14.39±0.27 | $0.9^{+0.1}_{-0.1}$ | $9.73^{+0.29}_{-0.28}$ |
| | | 2006-04-28 | $Ks$ | 8.75±0.36 | 5.599±0.016 | 5.600±0.016 | 14.35±0.39 | $0.9^{+0.1}_{-0.1}$ | $9.7^{+0.4}_{-0.4}$ |
| 79199AB | $125.0^{+5.2}_{-4.8}$ | 2004-07-05 | $Ks$ | 3.9243±0.0053 | 5.649±0.019 | 5.680±0.019 | 9.604±0.024 | $0.187^{+0.093}_{-0.086}$ | $4.111^{+0.094}_{-0.087}$ |
| | | 2011-05-09 | $Ks$ | 3.9053±0.0016 | 5.649±0.019 | 5.680±0.019 | 9.586±0.021 | $0.187^{+0.093}_{-0.086}$ | $4.092^{+0.093}_{-0.086}$ |
| 79199AC | | 2004-07-05 | $Ks$ | 6.74±0.18 | 5.649±0.019 | 5.680±0.019 | 12.4±0.2 | $0.187^{+0.093}_{-0.086}$ | $6.93^{+0.22}_{-0.21}$ |
| | | 2011-05-09 | $Ks$ | 6.881±0.055 | 5.649±0.019 | 5.680±0.019 | 12.561±0.074 | $0.187^{+0.093}_{-0.086}$ | $7.07^{+0.12}_{-0.11}$ |
| 79399AB | $93.0^{+7.5}_{-6.4}$ | 2004-06-29 | $Ks$ | 0.927±0.013 | 5.599±0.017 | 6.188±0.029 | 7.116±0.037 | $1.32^{+0.18}_{-0.15}$ | $2.24^{+0.18}_{-0.15}$ |
| | | 2006-04-27 | $Ks$ | 1.058±0.021 | 5.599±0.017 | 6.087±0.031 | 7.144±0.047 | $1.21^{+0.18}_{-0.15}$ | $2.27^{+0.18}_{-0.16}$ |
| 79399AC | | 2004-06-29 | $Ks$ | 1.336±0.027 | 5.599±0.017 | 6.188±0.029 | 7.524±0.048 | $1.32^{+0.18}_{-0.15}$ | $2.65^{+0.18}_{-0.16}$ |
| | | 2006-04-27 | $Ks$ | 1.825±0.028 | 5.599±0.017 | 6.087±0.031 | 7.912±0.057 | $1.21^{+0.18}_{-0.15}$ | $3.04^{+0.18}_{-0.16}$ |
| 79399AD | | 2004-06-29 | $Ks$ | 6.393±0.073 | 5.599±0.017 | 6.188±0.029 | 12.6±0.1 | $1.32^{+0.18}_{-0.15}$ | $7.71^{+0.20}_{-0.18}$ |
| | | 2006-04-27 | $Ks$ | 6.3±0.2 | 5.599±0.017 | 6.087±0.031 | 12.35±0.23 | $1.21^{+0.18}_{-0.15}$ | $7.48^{+0.29}_{-0.28}$ |
| 79771AB | $162.3^{+22.8}_{-17.8}$ | 2004-06-20 | $Ks$ | 3.781±0.038 | 7.098±0.02 | 7.149±0.021 | 10.930±0.057 | $0.96^{+0.31}_{-0.24}$ | $4.74^{+0.31}_{-0.25}$ |
| | | 2012-07-13 | $Ks$ | 4.080±0.013 | 7.098±0.02 | 7.14±0.02 | 11.224±0.033 | $0.95^{+0.31}_{-0.24}$ | $5.03^{+0.31}_{-0.24}$ |
| 79771AC | | 2004-06-20 | $Ks$ | 4.375±0.013 | 7.098±0.02 | 7.149±0.021 | 11.524±0.034 | $0.96^{+0.31}_{-0.24}$ | $5.33^{+0.31}_{-0.24}$ |
| | | 2012-07-13 | $Ks$ | 4.274±0.004 | 7.098±0.02 | 7.14±0.02 | 11.418±0.024 | $0.95^{+0.31}_{-0.24}$ | $5.22^{+0.31}_{-0.24}$ |
| 81472AB | $192.3^{+33.4}_{-24.8}$ | 2005-03-25 | $Ks$ | 7.408±0.083 | 5.933±0.023 | 5.935±0.023 | 13.34±0.11 | $-0.55^{+0.38}_{-0.28}$ | $6.9^{+0.4}_{-0.3}$ |
| | | 2011-05-09 | $Ks$ | 7.336±0.072 | 5.933±0.023 | 5.936±0.023 | 13.271±0.099 | $-0.55^{+0.38}_{-0.28}$ | $6.8^{+0.4}_{-0.3}$ |

*Continued on next page*

Table A4 – *Continued from previous page*

| HIP | Distance (pc) | Date | Band | $\Delta m$[a] (mag) | $m_{\mathrm{system}}$ (mag) | $m_{\mathrm{prim}}$ (mag) | $m_{\mathrm{comp}}$ (mag) | $M_{\mathrm{prim}}$ (mag) | $M_{\mathrm{comp}}$ (mag) |
|---|---|---|---|---|---|---|---|---|---|
| 81472AC | | 2005-03-25 | $Ks$ | 7.403±0.084 | 5.933±0.023 | 5.935±0.023 | 13.34±0.11 | $-0.55^{+0.38}_{-0.28}$ | $6.9^{+0.4}_{-0.3}$ |
| | | 2011-05-09 | $Ks$ | 7.310±0.071 | 5.933±0.023 | 5.936±0.023 | 13.246±0.098 | $-0.55^{+0.38}_{-0.28}$ | $6.8^{+0.4}_{-0.3}$ |
| 81972AB | $163.7^{+8.7}_{-7.9}$ | 2004-06-28 | $Ks$ | 4.3885±0.0084 | 5.842±0.017 | 5.887±0.017 | 10.276±0.027 | $-0.22^{+0.12}_{-0.11}$ | $4.17^{+0.12}_{-0.11}$ |
| 81972AC | | 2004-06-28 | $Ks$ | 4.4177±0.0085 | 5.842±0.017 | 5.887±0.017 | 10.305±0.027 | $-0.22^{+0.12}_{-0.11}$ | $4.20^{+0.12}_{-0.11}$ |
| 81972AD | | 2004-06-28 | $Ks$ | 5.376±0.013 | 5.842±0.017 | 5.887±0.017 | 11.263±0.032 | $-0.22^{+0.12}_{-0.11}$ | $5.16^{+0.12}_{-0.11}$ |
| 81972AE | | 2004-06-28 | $Ks$ | 7.816±0.041 | 5.842±0.017 | 5.887±0.017 | 13.70±0.06 | $-0.22^{+0.12}_{-0.11}$ | $7.60^{+0.13}_{-0.12}$ |
| 81972AF | | 2004-06-28 | $Ks$ | 8.848±0.073 | 5.842±0.017 | 5.887±0.017 | 14.735±0.091 | $-0.22^{+0.12}_{-0.11}$ | $8.63^{+0.15}_{-0.14}$ |
| 83336AB | $137.2^{+9.0}_{-8.0}$ | 2004-06-26 | $Ks$ | 6.624±0.075 | 5.256±0.017 | 5.262±0.017 | 11.886±0.098 | $-0.43^{+0.14}_{-0.13}$ | $6.20^{+0.17}_{-0.16}$ |
| | | 2006-06-26 | $Ks$ | 6.474±0.077 | 5.256±0.017 | 5.262±0.018 | 11.7±0.1 | $-0.42^{+0.14}_{-0.13}$ | $6.05^{+0.17}_{-0.16}$ |
| 83336AC | | 2004-06-26 | $Ks$ | 6.603±0.075 | 5.256±0.017 | 5.262±0.017 | 11.865±0.097 | $-0.43^{+0.14}_{-0.13}$ | $6.18^{+0.17}_{-0.16}$ |
| | | 2006-06-26 | $Ks$ | 6.468±0.078 | 5.256±0.017 | 5.262±0.018 | 11.7±0.1 | $-0.42^{+0.14}_{-0.13}$ | $6.04^{+0.17}_{-0.16}$ |
| 83336AD | | 2004-06-26 | $Ks$ | 7.86±0.14 | 5.256±0.017 | 5.262±0.017 | 13.12±0.17 | $-0.43^{+0.14}_{-0.13}$ | $7.44^{+0.22}_{-0.21}$ |
| | | 2006-06-26 | $Ks$ | 8.22±0.18 | 5.256±0.017 | 5.262±0.018 | 13.48±0.21 | $-0.42^{+0.14}_{-0.13}$ | $7.79^{+0.25}_{-0.24}$ |
| 85442AB | $226.2^{+24.4}_{-20.1}$ | 2005-03-25 | $Ks$ | 6.916±0.062 | 5.782±0.017 | 5.787±0.017 | 12.703±0.082 | $-1.01^{+0.23}_{-0.19}$ | $5.91^{+0.25}_{-0.21}$ |
| | | 2011-05-09 | $Ks$ | 7.040±0.059 | 5.782±0.017 | 5.786±0.017 | 12.83±0.08 | $-1.01^{+0.23}_{-0.19}$ | $6.03^{+0.25}_{-0.21}$ |
| 85442AC | | 2005-03-25 | $Ks$ | 7.407±0.085 | 5.782±0.017 | 5.787±0.017 | 13.19±0.11 | $-1.01^{+0.23}_{-0.19}$ | $6.40^{+0.26}_{-0.22}$ |
| | | 2011-05-09 | $Ks$ | 7.604±0.078 | 5.782±0.017 | 5.786±0.017 | 13.391±0.098 | $-1.01^{+0.23}_{-0.19}$ | $6.60^{+0.25}_{-0.22}$ |
| 85442AD | | 2005-03-25 | $Ks$ | 7.788±0.097 | 5.782±0.017 | 5.787±0.017 | 13.57±0.12 | $-1.01^{+0.23}_{-0.19}$ | $6.78^{+0.26}_{-0.23}$ |
| | | 2011-05-09 | $Ks$ | 7.844±0.088 | 5.782±0.017 | 5.786±0.017 | 13.63±0.11 | $-1.01^{+0.23}_{-0.19}$ | $6.84^{+0.26}_{-0.22}$ |
| 85442AE | | 2005-03-25 | $Ks$ | 7.89±0.11 | 5.782±0.017 | 5.787±0.017 | 13.68±0.13 | $-1.01^{+0.23}_{-0.19}$ | $6.89^{+0.27}_{-0.23}$ |
| | | 2011-05-09 | $Ks$ | 7.917±0.092 | 5.782±0.017 | 5.786±0.017 | 13.70±0.11 | $-1.01^{+0.23}_{-0.19}$ | $6.91^{+0.26}_{-0.22}$ |
| 85727AB | $60.7^{+1.3}_{-1.2}$ | 2008-08-21 | $Ks$ | 8.29±0.12 | 3.71±0.197 | 3.7±0.2 | 12.00±0.32 | $-0.2^{+0.2}_{-0.2}$ | $8.06^{+0.32}_{-0.32}$ |
| 85727AC | | 2008-08-21 | $Ks$ | 10.0±0.3 | 3.71±0.197 | 3.7±0.2 | 13.7±0.5 | $-0.2^{+0.2}_{-0.2}$ | $9.7^{+0.5}_{-0.5}$ |
| 85783AB | $119.6^{+10.4}_{-8.9}$ | 2005-03-13 | $Ks$ | 1.2545±0.0017 | 6.151±0.017 | 6.450±0.017 | 7.705±0.018 | $1.06^{+0.19}_{-0.16}$ | $2.32^{+0.19}_{-0.16}$ |
| | | 2011-04-04 | $Ks$ | 1.2575±0.0014 | 6.151±0.017 | 6.450±0.017 | 7.708±0.018 | $1.06^{+0.19}_{-0.16}$ | $2.32^{+0.19}_{-0.16}$ |
| | | 2011-05-09 | $Ks$ | 1.23246±0.00053 | 6.151±0.017 | 6.456±0.017 | 7.688±0.017 | $1.07^{+0.19}_{-0.16}$ | $2.30^{+0.19}_{-0.16}$ |

*Continued on next page*

Table A4 – *Continued from previous page*

| HIP | Distance (pc) | Date | Band | $\Delta m$[a] (mag) | $m_{\mathrm{system}}$ (mag) | $m_{\mathrm{prim}}$ (mag) | $m_{\mathrm{comp}}$ (mag) | $M_{\mathrm{prim}}$ (mag) | $M_{\mathrm{comp}}$ (mag) |
|---|---|---|---|---|---|---|---|---|---|
| 85783AC | | 2005-03-13 | $Ks$ | 6.630±0.033 | 6.151±0.017 | 6.450±0.017 | 13.08±0.05 | $1.06^{+0.19}_{-0.16}$ | $7.69^{+0.20}_{-0.17}$ |
| | | 2011-04-04 | $Ks$ | 6.309±0.028 | 6.151±0.017 | 6.450±0.017 | 12.759±0.045 | $1.06^{+0.19}_{-0.16}$ | $7.37^{+0.19}_{-0.17}$ |
| | | 2011-05-09 | $Ks$ | 6.50±0.02 | 6.151±0.017 | 6.456±0.017 | 12.957±0.037 | $1.07^{+0.19}_{-0.16}$ | $7.57^{+0.19}_{-0.17}$ |
| 87163AB | $371.7^{+61.2}_{-46.0}$ | 2005-03-28 | $Ks$ | 1.6187±0.0064 | 5.861±0.024 | 6.086±0.026 | 7.71±0.03 | $-1.87^{+0.36}_{-0.27}$ | $-0.25^{+0.36}_{-0.27}$ |
| | | 2011-05-09 | $Ks$ | 1.900±0.007 | 5.861±0.024 | 6.040±0.026 | 7.941±0.031 | $-1.91^{+0.36}_{-0.27}$ | $-0.01^{+0.36}_{-0.27}$ |
| 87163AC | | 2005-03-28 | $Ks$ | 6.423±0.054 | 5.861±0.024 | 6.086±0.026 | 12.509±0.079 | $-1.87^{+0.36}_{-0.27}$ | $4.56^{+0.37}_{-0.28}$ |
| | | 2011-05-09 | $Ks$ | 6.487±0.054 | 5.861±0.024 | 6.040±0.026 | 12.53±0.08 | $-1.91^{+0.36}_{-0.27}$ | $4.57^{+0.37}_{-0.28}$ |
| 87163AD | | 2005-03-28 | $Ks$ | 7.6±0.1 | 5.861±0.024 | 6.086±0.026 | 13.72±0.13 | $-1.87^{+0.36}_{-0.27}$ | $5.8^{+0.4}_{-0.3}$ |
| | | 2011-05-09 | $Ks$ | 7.581±0.094 | 5.861±0.024 | 6.040±0.026 | 13.62±0.12 | $-1.91^{+0.36}_{-0.27}$ | $5.67^{+0.38}_{-0.29}$ |
| 87163AE | | 2005-03-28 | $Ks$ | 7.6±0.1 | 5.861±0.024 | 6.086±0.026 | 13.69±0.13 | $-1.87^{+0.36}_{-0.27}$ | $5.7^{+0.4}_{-0.3}$ |
| | | 2011-05-09 | $Ks$ | 7.577±0.095 | 5.861±0.024 | 6.040±0.026 | 13.62±0.12 | $-1.91^{+0.36}_{-0.27}$ | $5.7^{+0.4}_{-0.3}$ |
| 87163AF | | 2005-03-28 | $Ks$ | 7.93±0.12 | 5.861±0.024 | 6.086±0.026 | 14.02±0.14 | $-1.87^{+0.36}_{-0.27}$ | $6.06^{+0.39}_{-0.31}$ |
| | | 2011-05-09 | $Ks$ | 7.83±0.11 | 5.861±0.024 | 6.040±0.026 | 13.87±0.13 | $-1.91^{+0.36}_{-0.27}$ | $5.9^{+0.4}_{-0.3}$ |
| 87163AG | | 2005-03-28 | $Ks$ | 8.33±0.17 | 5.861±0.024 | 6.086±0.026 | 14.4±0.2 | $-1.87^{+0.36}_{-0.27}$ | $6.47^{+0.41}_{-0.33}$ |
| | | 2011-05-09 | $Ks$ | 7.68±0.34 | 5.861±0.024 | 6.040±0.026 | 13.72±0.37 | $-1.91^{+0.36}_{-0.27}$ | $5.77^{+0.51}_{-0.46}$ |
| 88012AB | $555.6^{+163.9}_{-103.1}$ | 2005-03-27 | $Ks$ | 6.538±0.068 | 6.151±0.02 | 6.15±0.02 | 12.693±0.092 | $-2.6^{+0.6}_{-0.4}$ | $3.94^{+0.65}_{-0.41}$ |
| 88012AC | | 2005-03-27 | $Ks$ | 7.34±0.11 | 6.151±0.02 | 6.15±0.02 | 13.50±0.13 | $-2.6^{+0.6}_{-0.4}$ | $4.74^{+0.65}_{-0.42}$ |
| 89963AB | $396.8^{+307.4}_{-120.6}$ | 2011-07-19 | $Ks$ | 4.985±0.016 | 4.105±0.293 | 4.12±0.29 | 9.10±0.31 | $-4.35^{+1.71}_{-0.73}$ | $0.63^{+1.71}_{-0.73}$ |
| 89963AC | | 2011-07-19 | $Ks$ | 6.620±0.078 | 4.105±0.293 | 4.12±0.29 | 10.74±0.37 | $-4.35^{+1.71}_{-0.73}$ | $2.27^{+1.72}_{-0.76}$ |
| 93892AB | $307.7^{+79.9}_{-52.6}$ | 2004-10-08 | $Ks$ | 6.853±0.054 | 6.348±0.02 | 6.35±0.02 | 13.203±0.077 | $-1.13^{+0.56}_{-0.37}$ | $5.73^{+0.57}_{-0.38}$ |
| | | 2011-08-26 | $Ks$ | 6.96±0.05 | 6.348±0.02 | 6.35±0.02 | 13.312±0.073 | $-1.13^{+0.56}_{-0.37}$ | $5.83^{+0.57}_{-0.38}$ |
| 93892AC | | 2004-10-08 | $Ks$ | 9.06±0.16 | 6.348±0.02 | 6.35±0.02 | 15.41±0.19 | $-1.13^{+0.56}_{-0.37}$ | $7.94^{+0.59}_{-0.42}$ |
| | | 2011-08-26 | $Ks$ | 8.75±0.12 | 6.348±0.02 | 6.35±0.02 | 15.10±0.15 | $-1.13^{+0.56}_{-0.37}$ | $7.6^{+0.6}_{-0.4}$ |

**Notes.** The given companion identification AB, AC, etc. for visual higher-order multiples indicates the sequences of detection by increasing magnitude difference.

[a] Measured magnitude difference in the given band.

**Table A5.** Estimated masses for the visual companions resolved in this study.

| HIP | log(*Age*[*yr*]) | Date | Band | $M_{X,\mathrm{comp}}$ (mag) | $M_{\mathrm{prim}}$ ($M_\odot$) | $M_{\mathrm{comp}}$ (1) ($M_\odot$) | (2) ($M_\odot$) | (3) ($M_\odot$) | (4) ($M_\odot$) | (5) ($M_\odot$) | (6) ($M_\odot$) | $M_{\mathrm{comp}}$ ($M_\odot$) | $q$ |
|---|---|---|---|---|---|---|---|---|---|---|---|---|---|
| | | | | | | | | Binaries | | | | | |
| 2548 | $9.06^{+0.03}_{-0.04}$ | 2005-12-06 | *Ks* | $2.577^{+0.104}_{-0.095}$ | 2.00±0.01 | | 1.26±0.02 | 1.24±0.03 | 1.28±0.03 | 1.28±0.03 | 1.29±0.03 | 1.27±0.03 | 0.64±0.01 |
| | | 2007-09-16 | *Ks* | $2.561^{+0.104}_{-0.095}$ | | | 1.27±0.03 | 1.24±0.03 | 1.28±0.03 | 1.28±0.03 | 1.30±0.03 | 1.28±0.03 | 0.64±0.01 |
| 15627 | $7.64^{+0.08}_{-0.09}$ | 2006-10-16 | *H* | $1.73^{+0.29}_{-0.23}$ | 4.4±0.1 | | | | 2.1±0.3 | 2.0±0.2 | 2.1±0.2 | 2.1±0.2 | 0.46±0.06 |
| 16511 | $8.1^{+0.1}_{-0.2}$ | 2005-01-06 | *Ks* | $3.371^{+0.101}_{-0.094}$ | 2.65±0.07 | | 1.06±0.02 | 1.03±0.02 | 1.07±0.02 | 1.06±0.02 | 1.07±0.03 | 1.06±0.02 | 0.40±0.01 |
| | | 2005-11-26 | *Ks* | $3.521^{+0.101}_{-0.094}$ | | | 1.02±0.02 | 0.99±0.02 | 1.03±0.02 | 1.02±0.02 | 1.03±0.02 | 1.02±0.02 | 0.38±0.01 |
| | | 2011-08-25 | *Ks* | $3.195^{+0.102}_{-0.095}$ | | | 1.12±0.02 | 1.08±0.02 | 1.12±0.03 | 1.11±0.03 | 1.13±0.03 | 1.11±0.03 | 0.42±0.01 |
| 16803 | $8.47^{+0.03}_{-0.03}$ | 2005-01-09 | *Ks* | $0.96^{+0.18}_{-0.16}$ | 3.13±0.04 | | 2.34±0.09 | | 2.5±0.1 | 2.5±0.1 | 2.5±0.1 | 2.4±0.1 | 0.78±0.03 |
| | | 2007-09-20 | *Ks* | $0.91^{+0.18}_{-0.16}$ | | | 2.4±0.1 | | 2.5±0.1 | 2.5±0.1 | 2.5±0.1 | 2.5±0.1 | 0.79±0.03 |
| | | 2007-09-30 | *Ks* | $0.90^{+0.18}_{-0.16}$ | | | 2.38±0.09 | | 2.5±0.1 | 2.5±0.1 | 2.5±0.1 | 2.5±0.1 | 0.79±0.03 |
| 17563 | $7.1^{+0.3}_{-0.7}$ | 2005-01-10 | *Ks* | $5.38^{+0.19}_{-0.18}$ | 5.9±0.3 | 0.58±0.03 | | 0.2±0.1 | 0.2±0.1 | 0.56±0.03 | 0.3±0.1 | 0.39±0.09 | 0.07±0.02 |
| 18213 | $7.6^{+0.1}_{-0.2}$ | 2007-09-14 | *Ks* | $5.1^{+0.2}_{-0.2}$ | 3.7±0.1 | 0.63±0.03 | | 0.51±0.07 | 0.52±0.07 | 0.61±0.03 | 0.54±0.06 | 0.56±0.06 | 0.15±0.02 |
| 20020 | $8.26^{+0.03}_{-0.04}$ | 2004-12-08 | *Ks* | $2.04^{+0.12}_{-0.11}$ | 2.79±0.06 | | 1.61±0.07 | | 1.69±0.07 | 1.65±0.08 | 1.67±0.08 | 1.66±0.08 | 0.59±0.03 |
| | | 2007-09-20 | *Ks* | $2.06^{+0.13}_{-0.12}$ | | | 1.58±0.08 | | 1.68±0.07 | 1.64±0.08 | 1.66±0.08 | 1.64±0.08 | 0.59±0.03 |
| | | 2007-09-30 | *Ks* | $2.0^{+0.1}_{-0.1}$ | | | 1.61±0.07 | | 1.69±0.07 | 1.65±0.08 | 1.67±0.07 | 1.66±0.07 | 0.59±0.03 |
| 20042 | $7.4^{+0.2}_{-0.3}$ | 2005-11-16 | *Ks* | $6.48^{+0.32}_{-0.32}$ | 3.9807±0.0005 | 0.37±0.04 | | 0.17±0.05 | 0.15±0.05 | 0.35±0.05 | 0.19±0.05 | 0.25±0.05 | 0.06±0.01 |
| | | 2012-09-19 | *Ks* | $7.24^{+0.35}_{-0.35}$ | | 0.26±0.04 | | 0.10±0.03 | 0.10±0.01 | 0.24±0.03 | 0.13±0.03 | 0.17±0.03 | 0.042±0.007 |
| 20554 | $7.8^{+0.1}_{-0.1}$ | 2004-09-18 | *Ks* | $3.49^{+0.28}_{-0.23}$ | 3.979±0.001 | | 0.88±0.09 | 0.99±0.07 | 1.04±0.06 | 1.03±0.06 | 1.05±0.07 | 1.00±0.07 | 0.25±0.02 |
| 20804 | $8.18^{+0.05}_{-0.05}$ | 2005-02-08 | *Ks* | $0.89^{+0.33}_{-0.26}$ | 3.8±0.2 | | 2.7±0.2 | | 2.9±0.2 | 2.8±0.2 | 2.8±0.2 | 2.8±0.2 | 0.72±0.07 |
| | | 2012-09-19 | *Ks* | $0.94^{+0.33}_{-0.26}$ | | | 2.6±0.2 | | 2.8±0.2 | 2.7±0.2 | 2.7±0.2 | 2.7±0.2 | 0.71±0.07 |
| | | 2013-01-04 | *Ks* | $0.94^{+0.33}_{-0.25}$ | | | 2.6±0.2 | | 2.8±0.2 | 2.7±0.2 | 2.7±0.2 | 2.7±0.2 | 0.71±0.07 |
| 23794 | $8.73^{+0.02}_{-0.02}$ | 2004-10-08 | *Ks* | $4.194^{+0.076}_{-0.072}$ | 2.497±0.009 | | 0.82±0.02 | 0.80±0.02 | 0.83±0.02 | 0.81±0.02 | 0.82±0.02 | 0.82±0.02 | 0.327±0.007 |
| | | 2013-01-04 | *Ks* | $4.155^{+0.076}_{-0.072}$ | | | 0.83±0.02 | 0.81±0.02 | 0.84±0.02 | 0.82±0.02 | 0.83±0.02 | 0.83±0.02 | 0.332±0.007 |
| 24196 | $8.135^{+0.009}_{-0.009}$ | 2004-12-08 | *Ks* | $0.10^{+0.88}_{-0.49}$ | 3.97±0.05 | | 3.4±0.4 | | 3.6±0.6 | 3.6±0.5 | 3.6±0.4 | 3.6±0.5 | 0.9±0.1 |
| 24305 | $7.995^{+0.006}_{-0.006}$ | 2005-01-04 | *Ks* | $1.92^{+0.28}_{-0.28}$ | 3.97±0.02 | | 1.8±0.2 | | 1.8±0.2 | 1.8±0.2 | 1.8±0.2 | 1.8±0.2 | 0.45±0.06 |
| | | 2012-12-08 | *Ks* | $4.67^{+0.25}_{-0.25}$ | | | 0.71±0.04 | 0.69±0.06 | 0.72±0.04 | 0.70±0.04 | 0.69±0.06 | 0.70±0.05 | 0.18±0.01 |
| 24825 | $7.5^{+0.1}_{-0.2}$ | 2005-04-11 | *Ks* | $3.72^{+0.31}_{-0.24}$ | 4.5±0.1 | | | 0.88±0.07 | 0.93±0.07 | 0.96±0.07 | 0.92±0.08 | 0.92±0.07 | 0.21±0.02 |
| | | 2012-09-19 | *Ks* | $3.87^{+0.31}_{-0.24}$ | | | | 0.84±0.07 | 0.88±0.07 | 0.92±0.07 | 0.87±0.08 | 0.88±0.07 | 0.20±0.02 |
| 25365 | $7.3^{+0.1}_{-0.2}$ | 2005-01-10 | *Ks* | $1.09^{+0.31}_{-0.24}$ | 5.1±0.1 | | | | 3.1±0.3 | 2.9±0.3 | 2.9±0.3 | 2.9±0.3 | 0.58±0.06 |
| | | 2012-09-19 | *Ks* | $1.12^{+0.31}_{-0.24}$ | | | | | 3.0±0.3 | 2.8±0.3 | 2.8±0.3 | 2.9±0.3 | 0.57±0.06 |
| 25657 | $7.9^{+0.1}_{-0.1}$ | 2006-10-16 | *H* | $5.66^{+0.29}_{-0.23}$ | 2.5117±0.0002 | | 0.54±0.04 | 0.53±0.04 | 0.53±0.05 | 0.53±0.04 | 0.54±0.03 | 0.53±0.04 | 0.21±0.02 |

*Continued on next page*

Table A5 – *Continued from previous page*

| HIP | log(*Age*[*yr*]) | Date | Band | $M_{X,\mathrm{comp}}$ (mag) | $M_{\mathrm{prim}}$ ($M_\odot$) | $M_{\mathrm{comp}}$ (1) ($M_\odot$) | (2) ($M_\odot$) | (3) ($M_\odot$) | (4) ($M_\odot$) | (5) ($M_\odot$) | (6) ($M_\odot$) | $M_{\mathrm{comp}}$ ($M_\odot$) | $q$ |
|---|---|---|---|---|---|---|---|---|---|---|---|---|---|
| | | 2006-12-28 | *H* | $5.72^{+0.29}_{-0.23}$ | | | 0.54±0.04 | 0.52±0.04 | 0.52±0.05 | 0.52±0.04 | 0.53±0.04 | 0.52±0.04 | 0.21±0.02 |
| 26215 | $8.20^{+0.08}_{-0.10}$ | 2004-12-09 | *Ks* | $1.39^{+0.65}_{-0.41}$ | 3.6±0.1 | | 2.2±0.4 | | 2.3±0.4 | 2.3±0.4 | 2.3±0.4 | 2.3±0.4 | 0.6±0.1 |
| 26235 | $7.05^{+0.03}_{-0.03}$ | 2007-12-18 | *H* | $-0.81^{+0.53}_{-0.36}$ | 13.2±0.5 | | | | 7.0±0.5 | 7.0±1.0 | 7.0±1.0 | 7.0±0.9 | 0.53±0.07 |
| 26602 | $8.15^{+0.01}_{-0.01}$ | 2005-03-05 | *Ks* | $-0.59^{+1.15}_{-0.56}$ | 3.8±0.2 | | 3.9±0.2 | | 4.1±1.0 | 4.0±0.4 | 4.0±0.3 | 4.0±0.7 | 1.1±0.2 |
| | | 2012-09-19 | *Ks* | $-0.42^{+1.15}_{-0.56}$ | | | 3.8±0.3 | | 3.9±1.0 | 4.0±0.4 | 3.9±0.4 | 3.9±0.7 | 1.0±0.2 |
| 27810 | $7.5^{+0.1}_{-0.2}$ | 2005-03-25 | *Ks* | $5.375^{+0.055}_{-0.053}$ | 3.9807±0.0004 | 0.578±0.009 | | 0.40±0.06 | 0.43±0.06 | 0.558±0.009 | 0.44±0.05 | 0.48±0.05 | 0.12±0.01 |
| 28744 | $7.31^{+0.03}_{-0.04}$ | 2005-03-27 | *Ks* | $1.33^{+0.94}_{-0.51}$ | 9.5±0.4 | | | | 2.7±0.9 | 2.8±0.8 | 2.8±0.8 | 2.8±0.9 | 0.29±0.09 |
| | | 2012-09-19 | *Ks* | $1.23^{+0.94}_{-0.51}$ | | | | | 2.9±1.0 | 2.9±0.9 | 2.9±0.9 | 2.9±0.9 | 0.3±0.1 |
| 29401 | $7.66^{+0.09}_{-0.11}$ | 2006-01-06 | *Ks* | $1.74^{+0.30}_{-0.24}$ | 3.20±0.06 | | | | 2.1±0.3 | 2.0±0.2 | 2.0±0.2 | 2.0±0.3 | 0.64±0.08 |
| | | 2012-12-08 | *Ks* | $1.76^{+0.30}_{-0.24}$ | | | | | 2.0±0.3 | 2.0±0.2 | 2.0±0.2 | 2.0±0.3 | 0.63±0.08 |
| 29728 | $7.75^{+0.08}_{-0.10}$ | 2005-04-10 | *Ks* | $3.75^{+0.21}_{-0.18}$ | 4.0±1.0 | | 0.84±0.07 | 0.90±0.06 | 0.97±0.05 | 0.95±0.05 | 0.95±0.06 | 0.92±0.06 | 0.23±0.01 |
| | | 2012-09-19 | *Ks* | $3.75^{+0.21}_{-0.18}$ | | | 0.84±0.07 | 0.90±0.06 | 0.97±0.05 | 0.95±0.05 | 0.95±0.06 | 0.92±0.06 | 0.23±0.01 |
| 30493 | $8.3^{+0.1}_{-0.1}$ | 2005-03-06 | *Ks* | $1.70^{+0.54}_{-0.36}$ | 2.93±0.08 | | 1.9±0.3 | | 1.9±0.3 | 2.0±0.3 | 2.0±0.3 | 2.0±0.3 | 0.7±0.1 |
| | | 2012-09-19 | *Ks* | $1.68^{+0.54}_{-0.36}$ | | | 1.9±0.3 | | 2.0±0.3 | 2.0±0.3 | 2.0±0.3 | 2.0±0.3 | 0.7±0.1 |
| 30867 | $7.62^{+0.03}_{-0.03}$ | 2005-04-09 | *Ks* | $-0.89^{+0.69}_{-0.46}$ | 6.6±0.2 | | | | 5.9±0.6 | 5.9±0.7 | 5.9±0.7 | 5.9±0.7 | 0.9±0.1 |
| | | 2012-09-19 | *Ks* | $-0.82^{+0.69}_{-0.46}$ | | | | | 5.8±0.6 | 5.8±0.7 | 5.8±0.7 | 5.8±0.7 | 0.9±0.1 |
| 31137 | $8.37^{+0.03}_{-0.04}$ | 2005-04-10 | *Ks* | $1.71^{+0.21}_{-0.18}$ | 3.4±0.1 | | 1.9±0.1 | | 1.9±0.1 | 1.9±0.1 | 1.9±0.1 | 1.9±0.1 | 0.56±0.04 |
| | | 2012-09-19 | *Ks* | $1.76^{+0.22}_{-0.18}$ | | | 1.8±0.1 | | 1.9±0.1 | 1.9±0.1 | 1.9±0.1 | 1.9±0.1 | 0.54±0.04 |
| 31959 | $7.3^{+0.1}_{-0.2}$ | 2007-11-05 | *H* | $4.77^{+1.52}_{-0.63}$ | 5.8±0.3 | | | 0.7±0.3 | 0.6±0.3 | 0.8±0.2 | 0.7±0.3 | 0.7±0.3 | 0.12±0.05 |
| | | 2008-01-05 | *H* | $4.66^{+1.52}_{-0.64}$ | | | | 0.7±0.3 | 0.6±0.3 | 0.8±0.2 | 0.8±0.3 | 0.7±0.3 | 0.12±0.05 |
| | | 2012-12-05 | *Ks* | $4.58^{+1.52}_{-0.63}$ | | | | 0.7±0.3 | 0.6±0.3 | 0.8±0.2 | 0.7±0.3 | 0.7±0.3 | 0.12±0.05 |
| 32823 | $7.4^{+0.2}_{-0.3}$ | 2007-12-24 | *H* | $5.5^{+68.4}_{-1.1}$ | 3.981±0.001 | | | 0.3±0.1 | 0.4±3.0 | 0.5±0.1 | 0.3±0.1 | 0.4±2.0 | 0.1±0.4 |
| 34041 | $7.40^{+0.06}_{-0.07}$ | 2008-02-01 | *H* | $1.02^{+0.58}_{-0.39}$ | 6.77±0.09 | | | | 3.1±0.6 | 3.0±0.6 | 3.0±0.5 | 3.0±0.6 | 0.45±0.08 |
| 34045 | $7.94^{+0.01}_{-0.01}$ | 2005-02-07 | *Ks* | $3.386^{+0.076}_{-0.074}$ | 5.00±0.04 | | 1.05±0.02 | 1.03±0.02 | 1.07±0.02 | 1.06±0.02 | 1.07±0.02 | 1.06±0.02 | 0.211±0.004 |
| | | 2013-01-06 | *Ks* | $3.403^{+0.078}_{-0.075}$ | | | 1.05±0.02 | 1.02±0.02 | 1.07±0.02 | 1.05±0.02 | 1.06±0.02 | 1.05±0.02 | 0.210±0.004 |
| 34153 | $7.8^{+0.1}_{-0.1}$ | 2008-02-03 | *H* | $2.41^{+1.69}_{-0.67}$ | 3.162±0.007 | | 1.0±0.7 | 1.3±0.1 | 2.0±0.9 | 1.9±0.9 | 1.9±0.9 | 1.6±0.8 | 0.5±0.2 |
| 34338 | $8.63^{+0.06}_{-0.07}$ | 2005-02-07 | *Ks* | $3.64^{+0.16}_{-0.14}$ | 2.8±0.1 | | 0.98±0.03 | 0.95±0.03 | 0.99±0.03 | 0.98±0.04 | 0.98±0.04 | 0.98±0.03 | 0.35±0.02 |
| | | 2013-01-04 | *Ks* | $3.64^{+0.16}_{-0.14}$ | | | 0.98±0.03 | 0.95±0.03 | 0.99±0.03 | 0.98±0.04 | 0.98±0.04 | 0.98±0.03 | 0.35±0.02 |
| 34758 | $8.77^{+0.02}_{-0.02}$ | 2005-02-12 | *Ks* | $5.69^{+0.22}_{-0.21}$ | 2.52±0.05 | 0.51±0.04 | 0.51±0.04 | 0.52±0.03 | 0.51±0.03 | 0.50±0.03 | 0.53±0.03 | 0.51±0.03 | 0.20±0.01 |
| | | 2007-11-21 | *Ks* | $5.77^{+0.17}_{-0.16}$ | | 0.50±0.03 | 0.49±0.03 | 0.51±0.02 | 0.50±0.02 | 0.48±0.03 | 0.52±0.02 | 0.50±0.02 | 0.20±0.01 |
| 35110 | $7.8^{+0.1}_{-0.1}$ | 2008-02-01 | *H* | $4.45^{+0.69}_{-0.43}$ | 3.162±0.001 | | 0.7±0.1 | 0.8±0.1 | 0.8±0.1 | 0.8±0.1 | 0.8±0.1 | 0.8±0.1 | 0.24±0.04 |
| 35413 | $7.1^{+0.2}_{-0.6}$ | 2008-01-12 | *H* | $3.75^{+1.20}_{-0.57}$ | 5.0±1.0 | | | 0.8±0.3 | 0.9±0.3 | 1.0±0.2 | 0.9±0.3 | 0.9±0.3 | 0.18±0.06 |

*Continued on next page*

Table A5 – *Continued from previous page*

| HIP | log(*Age*[*yr*]) | Date | Band | $M_{X,\mathrm{comp}}$ (mag) | $M_{\mathrm{prim}}$ ($M_\odot$) | $M_{\mathrm{comp}}$ (1) ($M_\odot$) | (2) ($M_\odot$) | (3) ($M_\odot$) | (4) ($M_\odot$) | (5) ($M_\odot$) | (6) ($M_\odot$) | $M_{\mathrm{comp}}$ ($M_\odot$) | $q$ |
|---|---|---|---|---|---|---|---|---|---|---|---|---|---|
| 36345 | $6.7^{+0.2}_{-0.6}$ | 2009-01-08 | *Ks* | $1.26^{+0.35}_{-0.27}$ | 6.7±0.3 | | | | 2.0±0.7 | | 2.1±0.6 | 2.0±0.6 | 0.30±0.09 |
| 36363 | $7.2^{+0.2}_{-0.6}$ | 2005-01-14 | *Ks* | $5.58^{+0.29}_{-0.29}$ | 5.5±0.2 | 0.54±0.05 | | 0.2±0.1 | 0.2±0.1 | 0.52±0.05 | 0.3±0.1 | 0.36±0.09 | 0.07±0.02 |
| | | 2007-11-23 | *Ks* | $5.92^{+0.19}_{-0.19}$ | | 0.47±0.03 | | 0.18±0.08 | 0.17±0.07 | 0.45±0.03 | 0.26±0.05 | 0.31±0.05 | 0.06±0.01 |
| 37322 | $7.5^{+0.2}_{-0.3}$ | 2005-01-14 | *Ks* | $2.0^{+0.1}_{-0.1}$ | 4.4±0.2 | | | | 1.7±0.1 | 1.69±0.08 | 1.6±0.1 | 1.7±0.1 | 0.38±0.03 |
| | | 2007-11-08 | *Ks* | $2.0^{+0.1}_{-0.1}$ | | | | | 1.7±0.1 | 1.69±0.08 | 1.6±0.1 | 1.7±0.1 | 0.38±0.03 |
| 37915 | $7.5^{+0.1}_{-0.2}$ | 2005-01-14 | *Ks* | $2.069^{+0.103}_{-0.095}$ | 3.99±0.05 | | | 1.329±0.006 | 1.70±0.09 | 1.67±0.08 | 1.67±0.09 | 1.59±0.07 | 0.40±0.02 |
| | | 2007-11-23 | *Ks* | $1.9^{+0.1}_{-0.1}$ | | | | | 1.88±0.09 | 1.84±0.09 | 1.9±0.1 | 1.9±0.1 | 0.47±0.02 |
| 39906 | $7.66^{+0.03}_{-0.03}$ | 2005-06-02 | *Ks* | $5.31^{+0.14}_{-0.13}$ | 5.0±0.1 | 0.59±0.02 | | 0.51±0.03 | 0.53±0.03 | 0.57±0.02 | 0.54±0.03 | 0.55±0.03 | 0.109±0.006 |
| 40817 | $8.43^{+0.03}_{-0.03}$ | 2005-02-14 | *Ks* | $2.6^{+0.1}_{-0.1}$ | 3.06±0.05 | | 1.29±0.03 | 1.26±0.03 | 1.29±0.05 | 1.30±0.03 | 1.32±0.03 | 1.30±0.04 | 0.42±0.01 |
| | | 2007-12-17 | *Ks* | $2.5^{+0.1}_{-0.1}$ | | | 1.32±0.03 | 1.30±0.04 | 1.36±0.06 | 1.34±0.04 | 1.36±0.04 | 1.33±0.04 | 0.44±0.02 |
| | | 2008-01-02 | *Ks* | $2.6^{+0.1}_{-0.1}$ | | | 1.31±0.03 | 1.28±0.04 | 1.32±0.06 | 1.32±0.03 | 1.34±0.03 | 1.31±0.04 | 0.43±0.01 |
| 41049 | $8.2^{+0.1}_{-0.2}$ | 2004-04-04 | *Ks* | $1.49^{+2.42}_{-0.75}$ | 2.7±0.1 | | 2.1±1.0 | | 2.2±1.0 | 2.6±1.0 | 2.6±1.0 | 2.4±1.0 | 0.9±0.4 |
| 41817 | $8.36^{+0.06}_{-0.06}$ | 2005-02-12 | *Ks* | $1.53^{+0.15}_{-0.13}$ | 2.61±0.09 | | 2.0±0.1 | | 2.1±0.1 | 2.1±0.1 | 2.1±0.1 | 2.1±0.1 | 0.79±0.05 |
| | | 2007-11-21 | *Ks* | $1.53^{+0.15}_{-0.13}$ | | | 2.0±0.1 | | 2.1±0.1 | 2.1±0.1 | 2.1±0.1 | 2.1±0.1 | 0.79±0.05 |
| 41843 | $8.76^{+0.02}_{-0.02}$ | 2005-02-03 | *Ks* | $7.13^{+0.22}_{-0.18}$ | 2.51±0.02 | 0.27±0.02 | 0.26±0.02 | 0.28±0.03 | 0.26±0.03 | 0.25±0.02 | 0.32±0.02 | 0.27±0.02 | 0.109±0.009 |
| | | 2013-02-03 | *Ks* | $7.24^{+0.23}_{-0.19}$ | | 0.26±0.02 | 0.25±0.02 | 0.27±0.02 | 0.24±0.03 | 0.24±0.02 | 0.30±0.02 | 0.26±0.02 | 0.103±0.009 |
| 42129 | $7.61^{+0.09}_{-0.12}$ | 2006-01-03 | *Ks* | $1.24^{+0.19}_{-0.16}$ | 6.6±0.3 | | | | 2.8±0.2 | 2.6±0.2 | 2.6±0.2 | 2.7±0.2 | 0.40±0.03 |
| | | 2007-12-17 | *Ks* | $1.30^{+0.19}_{-0.16}$ | | | | | 2.7±0.2 | 2.5±0.2 | 2.5±0.2 | 2.6±0.2 | 0.39±0.03 |
| 42177 | $8.20^{+0.04}_{-0.04}$ | 2005-02-03 | *Ks* | $2.890^{+0.079}_{-0.074}$ | 3.09±0.09 | | 1.20±0.02 | 1.17±0.02 | 1.22±0.02 | 1.21±0.02 | 1.23±0.02 | 1.21±0.02 | 0.39±0.01 |
| 42334 | $9.07^{+0.02}_{-0.02}$ | 2005-03-05 | *Ks* | $8.88^{+0.23}_{-0.23}$ | 1.9943±0.0001 | 0.117±0.009 | | 0.120±0.009 | 0.118±0.005 | | 0.14±0.01 | 0.124±0.009 | 0.062±0.004 |
| | | 2008-02-12 | *Ks* | $8.4^{+0.4}_{-0.4}$ | | 0.15±0.02 | | 0.15±0.02 | 0.13±0.02 | | 0.18±0.03 | 0.15±0.02 | 0.08±0.01 |
| 42540 | $8.3^{+0.1}_{-0.2}$ | 2005-01-05 | *Ks* | $3.01^{+0.13}_{-0.12}$ | 2.5113±0.0008 | | 1.16±0.03 | 1.13±0.03 | 1.18±0.03 | 1.17±0.03 | 1.18±0.04 | 1.17±0.03 | 0.46±0.01 |
| | | 2007-12-17 | *Ks* | $3.00^{+0.13}_{-0.12}$ | | | 1.17±0.03 | 1.13±0.03 | 1.19±0.03 | 1.17±0.03 | 1.19±0.04 | 1.17±0.03 | 0.47±0.01 |
| 42715 | $8.42^{+0.02}_{-0.03}$ | 2006-01-07 | *Ks* | $1.753^{+0.093}_{-0.086}$ | 3.05±0.04 | | 1.83±0.06 | | 1.85±0.03 | 1.87±0.06 | 1.88±0.06 | 1.85±0.05 | 0.61±0.02 |
| | | 2008-02-13 | *Ks* | $1.741^{+0.093}_{-0.086}$ | | | 1.83±0.05 | | 1.85±0.03 | 1.88±0.06 | 1.89±0.06 | 1.86±0.05 | 0.61±0.02 |
| 43305 | $8.21^{+0.04}_{-0.04}$ | 2005-01-09 | *Ks* | $3.691^{+0.082}_{-0.077}$ | 3.3±0.1 | | 0.97±0.02 | 0.94±0.02 | 0.98±0.02 | 0.96±0.02 | 0.97±0.02 | 0.97±0.02 | 0.29±0.01 |
| | | 2008-02-13 | *Ks* | $3.507^{+0.081}_{-0.076}$ | | | 1.02±0.02 | 0.99±0.02 | 1.03±0.02 | 1.02±0.02 | 1.03±0.02 | 1.02±0.02 | 0.31±0.01 |
| 43792 | $7.19^{+0.05}_{-0.05}$ | 2003-01-20 | *Ks* | $-0.8^{+108.6}_{-1.1}$ | 8.2±0.2 | | | | 6.9±1.0 | 5.4±1.0 | 5.4±1.0 | 5.9±1.0 | 0.7±0.2 |
| 44299 | $7.4^{+0.1}_{-0.2}$ | 2006-01-15 | *Ks* | $7.87^{+0.24}_{-0.23}$ | 3.9808±0.0002 | 0.19±0.02 | | 0.07±0.02 | | 0.18±0.01 | | 0.14±0.02 | 0.036±0.004 |
| | | 2007-12-17 | *Ks* | $7.02^{+0.38}_{-0.37}$ | | 0.29±0.04 | | 0.12±0.03 | 0.11±0.02 | 0.27±0.04 | 0.14±0.03 | 0.19±0.03 | 0.047±0.009 |
| 44798 | $8.14^{+0.03}_{-0.03}$ | 2005-01-10 | *Ks* | $2.159^{+0.102}_{-0.094}$ | 3.91±0.08 | | 1.54±0.05 | | 1.62±0.05 | 1.56±0.06 | 1.58±0.06 | 1.58±0.06 | 0.40±0.02 |
| 44883 | $8.16^{+0.06}_{-0.07}$ | 2005-01-12 | *Ks* | $2.30^{+0.28}_{-0.23}$ | 3.9±0.1 | | 1.4±0.1 | 1.308±0.002 | 1.5±0.1 | 1.5±0.1 | 1.5±0.1 | 1.5±0.1 | 0.37±0.03 |

*Continued on next page*

Table A5 – *Continued from previous page*

| HIP | log(*Age*[*yr*]) | Date | Band | $M_{X,\mathrm{comp}}$ (mag) | $M_{\mathrm{prim}}$ ($M_\odot$) | $M_{\mathrm{comp}}$ (1) ($M_\odot$) | (2) ($M_\odot$) | (3) ($M_\odot$) | (4) ($M_\odot$) | (5) ($M_\odot$) | (6) ($M_\odot$) | $M_{\mathrm{comp}}$ ($M_\odot$) | $q$ |
|---|---|---|---|---|---|---|---|---|---|---|---|---|---|
| | | 2008-01-03 | *Ks* | $2.31^{+0.28}_{-0.23}$ | | | 1.4±0.1 | 1.306±0.002 | 1.5±0.1 | 1.5±0.1 | 1.5±0.1 | 1.5±0.1 | 0.37±0.03 |
| 45189 | $8.20^{+0.03}_{-0.03}$ | 2005-01-12 | *Ks* | $0.3^{+0.2}_{-0.2}$ | 3.9±0.1 | | 3.1±0.2 | | 3.3±0.1 | 3.3±0.2 | 3.3±0.2 | 3.2±0.2 | 0.83±0.05 |
| | | 2008-01-02 | *Ks* | $0.3^{+0.2}_{-0.2}$ | | | 3.1±0.2 | | 3.3±0.1 | 3.3±0.2 | 3.3±0.1 | 3.3±0.2 | 0.84±0.05 |
| 45314 | $7.65^{+0.06}_{-0.07}$ | 2004-12-16 | *Ks* | $6.47^{+0.24}_{-0.23}$ | 3.39±0.09 | 0.37±0.03 | | 0.24±0.04 | 0.21±0.04 | 0.35±0.03 | 0.26±0.04 | 0.29±0.04 | 0.08±0.01 |
| | | 2008-02-15 | *Ks* | $6.45^{+0.19}_{-0.19}$ | | 0.37±0.03 | | 0.24±0.03 | 0.22±0.04 | 0.35±0.03 | 0.26±0.03 | 0.29±0.03 | 0.09±0.01 |
| | | 2012-12-04 | *Ks* | $6.33^{+0.13}_{-0.12}$ | | 0.39±0.02 | | 0.26±0.03 | 0.24±0.04 | 0.37±0.02 | 0.28±0.03 | 0.31±0.03 | 0.092±0.008 |
| 45344 | $7.84^{+0.02}_{-0.02}$ | 2004-12-10 | *Ks* | $2.57^{+0.13}_{-0.12}$ | 4.9±0.1 | | 1.32±0.04 | 1.30±0.05 | 1.35±0.07 | 1.34±0.04 | 1.36±0.04 | 1.33±0.05 | 0.27±0.01 |
| | | 2008-02-15 | *Ks* | $2.61^{+0.14}_{-0.13}$ | | | 1.31±0.04 | 1.28±0.05 | 1.32±0.07 | 1.32±0.04 | 1.34±0.04 | 1.31±0.05 | 0.27±0.01 |
| 46283 | $7.5^{+0.1}_{-0.2}$ | 2006-01-15 | *Ks* | $4.417^{+0.077}_{-0.075}$ | 3.98±0.02 | | | 0.69±0.04 | 0.73±0.04 | 0.76±0.01 | 0.71±0.02 | 0.72±0.03 | 0.182±0.008 |
| | | 2008-01-10 | *Ks* | $4.572^{+0.093}_{-0.091}$ | | | | 0.65±0.05 | 0.70±0.06 | 0.72±0.02 | 0.67±0.03 | 0.69±0.04 | 0.17±0.01 |
| 46329 | $7.79^{+0.03}_{-0.03}$ | 2005-03-25 | *Ks* | $-1.57^{+1.58}_{-0.64}$ | 5.5±0.1 | | 0.9±2.0 | | 6.1±0.7 | 5.9±0.4 | 5.8±0.4 | 4.7±1.0 | 0.8±0.2 |
| 46914 | $7.95^{+0.02}_{-0.02}$ | 2005-03-13 | *Ks* | $-0.47^{+0.31}_{-0.24}$ | 4.99±0.06 | | 4.3±0.2 | | 4.4±0.2 | 4.5±0.2 | 4.4±0.2 | 4.4±0.2 | 0.88±0.04 |
| | | 2008-03-10 | *Ks* | $-0.51^{+0.31}_{-0.25}$ | | | 4.3±0.2 | | 4.5±0.2 | 4.5±0.2 | 4.5±0.2 | 4.4±0.2 | 0.89±0.04 |
| 46928 | $7.742^{+0.002}_{-0.002}$ | 2006-02-12 | *Ks* | $3.590^{+0.068}_{-0.065}$ | 4.99±0.02 | | | 0.97±0.02 | 1.01±0.01 | 0.99±0.02 | 1.01±0.02 | 1.00±0.02 | 0.199±0.003 |
| | | 2008-01-10 | *Ks* | $3.589^{+0.069}_{-0.067}$ | | | | 0.97±0.02 | 1.01±0.01 | 1.00±0.02 | 1.01±0.02 | 1.00±0.02 | 0.200±0.003 |
| 48943 | $7.65^{+0.04}_{-0.05}$ | 2005-05-03 | *Ks* | $2.50^{+0.34}_{-0.26}$ | 4.73±0.05 | | | 1.28±0.05 | 1.4±0.2 | 1.4±0.1 | 1.4±0.1 | 1.4±0.1 | 0.29±0.03 |
| 49712 | $7.58^{+0.03}_{-0.03}$ | 2005-06-05 | *Ks* | $1.41^{+0.19}_{-0.16}$ | 7.5±0.2 | | | | 2.6±0.2 | 2.4±0.2 | 2.4±0.2 | 2.5±0.2 | 0.33±0.03 |
| 50044 | $7.78^{+0.09}_{-0.11}$ | 2005-06-02 | *Ks* | $4.72^{+0.62}_{-0.41}$ | 5.6±0.3 | | 0.66±0.09 | 0.68±0.09 | 0.7±0.1 | 0.7±0.1 | 0.7±0.1 | 0.7±0.1 | 0.12±0.02 |
| 50847 | $8.21^{+0.04}_{-0.04}$ | 2006-02-13 | *Ks* | $5.390^{+0.086}_{-0.085}$ | 3.3±0.1 | 0.57±0.01 | 0.57±0.01 | 0.56±0.01 | 0.58±0.01 | 0.55±0.01 | 0.56±0.01 | 0.57±0.01 | 0.174±0.008 |
| | | 2011-04-22 | *Ks* | $5.429^{+0.080}_{-0.079}$ | | 0.57±0.01 | 0.56±0.01 | 0.56±0.01 | 0.57±0.01 | 0.55±0.01 | 0.56±0.01 | 0.56±0.01 | 0.171±0.008 |
| 51362 | $8.75^{+0.02}_{-0.02}$ | 2004-06-29 | *Ks* | $8.4^{+0.3}_{-0.3}$ | 2.49±0.02 | 0.15±0.02 | | 0.15±0.02 | 0.13±0.01 | | 0.17±0.02 | 0.15±0.02 | 0.060±0.007 |
| | | 2006-04-21 | *Ks* | $8.35^{+0.25}_{-0.25}$ | | 0.15±0.01 | | 0.15±0.01 | 0.13±0.01 | | 0.18±0.02 | 0.15±0.01 | 0.061±0.006 |
| 52742 | $8.17^{+0.04}_{-0.05}$ | 2006-02-28 | *Ks* | $5.911^{+0.086}_{-0.083}$ | 3.96±0.02 | 0.47±0.01 | 0.46±0.01 | 0.47±0.01 | 0.47±0.01 | 0.45±0.01 | 0.48±0.01 | 0.47±0.01 | 0.118±0.003 |
| | | 2008-01-18 | *Ks* | $6.1^{+0.1}_{-0.1}$ | | 0.43±0.02 | 0.42±0.02 | 0.44±0.02 | 0.44±0.02 | 0.42±0.01 | 0.45±0.01 | 0.43±0.02 | 0.110±0.004 |
| 53272 | $7.97^{+0.06}_{-0.07}$ | 2006-02-13 | *Ks* | $0.2^{+0.2}_{-0.2}$ | 4.1±0.1 | | 3.6±0.2 | | 3.8±0.2 | 3.7±0.2 | 3.7±0.2 | 3.7±0.2 | 0.89±0.06 |
| | | 2008-02-15 | *Ks* | $0.2^{+0.2}_{-0.2}$ | | | 3.6±0.2 | | 3.8±0.2 | 3.7±0.2 | 3.7±0.2 | 3.7±0.2 | 0.89±0.06 |
| 54557 | $8.0^{+0.1}_{-0.2}$ | 2006-02-28 | *Ks* | $3.8^{+0.4}_{-0.3}$ | 2.512±0.001 | | 0.93±0.08 | 0.91±0.08 | 0.95±0.08 | 0.93±0.09 | 0.94±0.09 | 0.93±0.08 | 0.37±0.03 |
| | | 2006-03-26 | *Ks* | $3.9^{+0.4}_{-0.3}$ | | | 0.92±0.08 | 0.90±0.08 | 0.93±0.08 | 0.92±0.09 | 0.93±0.09 | 0.92±0.08 | 0.37±0.03 |
| | | 2007-03-01 | *Ks* | $3.7^{+0.4}_{-0.3}$ | | | 0.96±0.08 | 0.94±0.08 | 0.98±0.08 | 0.97±0.09 | 0.98±0.09 | 0.96±0.08 | 0.38±0.03 |
| | | 2008-02-20 | *Ks* | $3.7^{+0.4}_{-0.3}$ | | | 0.96±0.08 | 0.94±0.08 | 0.97±0.08 | 0.96±0.09 | 0.97±0.09 | 0.96±0.08 | 0.38±0.03 |
| | | 2011-02-13 | *J* | $4.83^{+0.41}_{-0.31}$ | | | 0.82±0.06 | 0.80±0.06 | 0.84±0.07 | 0.82±0.06 | 0.81±0.07 | 0.88±0.08 | 0.35±0.03 |
| | | | *Ks* | $3.8^{+0.4}_{-0.3}$ | | | 0.94±0.08 | 0.92±0.08 | 0.96±0.08 | 0.95±0.09 | 0.96±0.09 | 0.88±0.08 | 0.35±0.03 |

*Continued on next page*

Table A5 – *Continued from previous page*

| HIP | log(*Age*[*yr*]) | Date | Band | $M_{X,\mathrm{comp}}$ (mag) | $M_{\mathrm{prim}}$ ($M_\odot$) | $M_{\mathrm{comp}}$ (1) ($M_\odot$) | (2) ($M_\odot$) | (3) ($M_\odot$) | (4) ($M_\odot$) | (5) ($M_\odot$) | (6) ($M_\odot$) | $M_{\mathrm{comp}}$ ($M_\odot$) | $q$ |
|---|---|---|---|---|---|---|---|---|---|---|---|---|---|
| 54829 | $7.39^{+0.03}_{-0.04}$ | 2011-04-24 | *Ks* | $3.81^{+0.40}_{-0.31}$ | 9.1±0.4 | | | 0.87±0.09 | 0.92±0.08 | 0.94±0.09 | 0.89±0.08 | 0.90±0.08 | 0.10±0.01 |
| 55597 | $7.4^{+0.2}_{-0.3}$ | 2006-01-17 | *Ks* | $1.0^{+0.1}_{-0.1}$ | 3.99±0.04 | | | | 3.1±0.1 | 2.9±0.1 | 2.9±0.1 | 3.0±0.1 | 0.74±0.03 |
| | | 2008-02-24 | *Ks* | $1.10^{+0.13}_{-0.13}$ | | | | | 3.1±0.1 | 2.8±0.1 | 2.8±0.1 | 2.9±0.1 | 0.73±0.04 |
| 55657 | $7.49^{+0.05}_{-0.05}$ | 2006-01-06 | *Ks* | $6.06^{+0.30}_{-0.29}$ | 7.5±0.1 | 0.44±0.05 | | 0.26±0.05 | 0.24±0.06 | 0.43±0.05 | 0.29±0.05 | 0.33±0.05 | 0.045±0.007 |
| | | 2008-02-24 | *Ks* | $6.07^{+0.46}_{-0.45}$ | | 0.44±0.07 | | 0.27±0.07 | 0.24±0.08 | 0.42±0.07 | 0.29±0.08 | 0.33±0.07 | 0.04±0.01 |
| 58326 | $7.1^{+0.3}_{-0.7}$ | 2006-02-13 | *Ks* | $6.9^{+0.2}_{-0.2}$ | 5.7±0.3 | 0.31±0.02 | | 0.09±0.04 | 0.100±0.009 | 0.29±0.02 | 0.13±0.02 | 0.18±0.03 | 0.032±0.005 |
| | | 2008-01-10 | *Ks* | $6.86^{+0.37}_{-0.36}$ | | 0.31±0.04 | | 0.09±0.04 | 0.10±0.01 | 0.29±0.04 | 0.14±0.03 | 0.18±0.04 | 0.032±0.007 |
| 60189 | $8.21^{+0.04}_{-0.05}$ | 2005-02-06 | *Ks* | $6.2^{+0.3}_{-0.3}$ | 3.3±0.1 | 0.42±0.05 | 0.40±0.05 | 0.43±0.04 | 0.43±0.05 | 0.40±0.05 | 0.44±0.04 | 0.42±0.04 | 0.13±0.01 |
| 60449 | $8.47^{+0.04}_{-0.05}$ | 2005-02-12 | *Ks* | $5.73^{+0.14}_{-0.14}$ | 3.1±0.1 | 0.50±0.02 | 0.50±0.03 | 0.51±0.02 | 0.51±0.02 | 0.49±0.02 | 0.52±0.02 | 0.51±0.02 | 0.164±0.009 |
| | | 2008-02-14 | *Ks* | $5.743^{+0.090}_{-0.086}$ | | 0.50±0.01 | 0.49±0.02 | 0.51±0.01 | 0.50±0.01 | 0.48±0.01 | 0.52±0.01 | 0.50±0.01 | 0.163±0.007 |
| 61789 | $8.06^{+0.02}_{-0.02}$ | 2005-02-03 | *Ks* | $2.69^{+0.06}_{-0.06}$ | 3.68±0.08 | | 1.28±0.02 | 1.25±0.02 | 1.28±0.01 | 1.28±0.02 | 1.31±0.02 | 1.28±0.02 | 0.347±0.009 |
| 62026 | $8.3^{+0.2}_{-0.2}$ | 2004-04-07 | *Ks* | $2.598^{+0.101}_{-0.093}$ | 2.5114±0.0002 | | 1.31±0.03 | 1.28±0.03 | 1.32±0.05 | 1.32±0.03 | 1.34±0.03 | 1.31±0.04 | 0.52±0.01 |
| 63005 | $7.5^{+0.1}_{-0.2}$ | 2011-05-09 | *Ks* | $4.0^{+0.1}_{-0.1}$ | 3.98±0.02 | | | 0.80±0.03 | 0.85±0.03 | 0.88±0.03 | 0.83±0.03 | 0.84±0.03 | 0.211±0.008 |
| 63945 | $6.8^{+0.3}_{-0.8}$ | 2005-03-25 | *Ks* | $2.897^{+0.072}_{-0.068}$ | 6.8±0.3 | | | 1.1±0.1 | 1.1±0.4 | 1.22±0.02 | 1.15±0.07 | 1.1±0.2 | 0.17±0.03 |
| 64053 | $8.0^{+0.1}_{-0.1}$ | 2006-02-13 | *Ks* | $9.1^{+0.3}_{-0.3}$ | 2.777±0.007 | 0.11±0.01 | | 0.06±0.01 | | | | 0.09±0.01 | 0.031±0.004 |
| 64515 | $8.81^{+0.04}_{-0.04}$ | 2005-03-07 | *Ks* | $1.58^{+0.19}_{-0.16}$ | 2.31±0.04 | | 1.73±0.08 | | 1.83±0.07 | 1.82±0.08 | 1.82±0.08 | 1.80±0.08 | 0.78±0.04 |
| | | 2006-02-12 | *Ks* | $1.58^{+0.19}_{-0.16}$ | | | 1.73±0.08 | | 1.83±0.07 | 1.82±0.08 | 1.82±0.08 | 1.80±0.08 | 0.78±0.04 |
| 67472 | $7.28^{+0.08}_{-0.09}$ | 2005-03-25 | *Ks* | $3.9^{+0.1}_{-0.1}$ | 8.7±0.2 | | | 0.82±0.04 | 0.90±0.04 | 0.91±0.02 | 0.85±0.04 | 0.87±0.04 | 0.100±0.005 |
| | | 2011-05-09 | *Ks* | $4.079^{+0.094}_{-0.093}$ | | | | 0.74±0.04 | 0.81±0.05 | 0.85±0.02 | 0.77±0.03 | 0.79±0.04 | 0.091±0.005 |
| 67669 | $7.4^{+0.2}_{-0.3}$ | 2005-02-03 | *Ks* | $1.63^{+0.23}_{-0.19}$ | 3.9808±0.0005 | | | | 2.2±0.3 | 2.2±0.2 | 2.2±0.2 | 2.2±0.3 | 0.55±0.07 |
| 67703 | $7.6^{+0.1}_{-0.2}$ | 2004-06-29 | *Ks* | $3.22^{+0.15}_{-0.14}$ | 3.1621±0.0007 | | | 1.05±0.05 | 1.08±0.05 | 1.11±0.04 | 1.10±0.06 | 1.09±0.05 | 0.34±0.02 |
| 70915 | $8.20^{+0.05}_{-0.06}$ | 2006-02-25 | *Ks* | $4.24^{+0.16}_{-0.15}$ | 3.24±0.08 | | 0.81±0.04 | 0.80±0.03 | 0.82±0.04 | 0.81±0.03 | 0.81±0.04 | 0.81±0.03 | 0.25±0.01 |
| | | 2008-02-22 | *Ks* | $3.89^{+0.16}_{-0.15}$ | | | 0.92±0.03 | 0.89±0.03 | 0.93±0.04 | 0.91±0.04 | 0.91±0.04 | 0.91±0.04 | 0.28±0.01 |
| 71762 | $8.33^{+0.06}_{-0.08}$ | 2005-02-03 | *Ks* | $1.08^{+0.32}_{-0.24}$ | 2.97±0.07 | | 2.4±0.2 | | 2.5±0.2 | 2.5±0.2 | 2.5±0.2 | 2.5±0.2 | 0.83±0.07 |
| 73111 | $8.18^{+0.07}_{-0.09}$ | 2005-03-25 | *Ks* | $0.74^{+0.27}_{-0.22}$ | 3.20±0.08 | | 2.8±0.2 | | 3.0±0.2 | 2.9±0.2 | 2.9±0.2 | 2.9±0.2 | 0.91±0.06 |
| 74750 | $6.92^{+0.04}_{-0.04}$ | 2005-03-25 | *Ks* | $0.04^{+0.53}_{-0.36}$ | 12.9±0.3 | | | | 5.1±0.9 | | 5.0±0.9 | 5.1±0.9 | 0.39±0.07 |
| 75264 | $7.27^{+0.06}_{-0.07}$ | 2005-03-25 | *Ks* | $-0.29^{+0.39}_{-0.35}$ | 8.6±0.2 | | | | 5.6±0.7 | 5.4±0.7 | 5.4±0.7 | 5.5±0.7 | 0.63±0.08 |
| | | 2011-05-09 | *Ks* | $-0.31^{+0.39}_{-0.35}$ | | | | | 5.6±0.7 | 5.5±0.7 | 5.4±0.7 | 5.5±0.7 | 0.64±0.08 |
| 76503 | $7.99^{+0.03}_{-0.03}$ | 2012-07-13 | *Ks* | $9.49^{+0.20}_{-0.19}$ | 3.9±0.1 | | | 0.050±0.004 | | | | 0.050±0.004 | 0.013±0.001 |
| 77634 | $8.32^{+0.03}_{-0.03}$ | 2005-02-05 | *Ks* | $8.25^{+0.18}_{-0.18}$ | 3.05±0.05 | 0.16±0.01 | | 0.14±0.01 | 0.13±0.01 | 0.161±0.007 | 0.16±0.01 | 0.15±0.01 | 0.049±0.004 |
| 77840 | $7.1^{+0.2}_{-0.3}$ | 2012-07-13 | *Ks* | $0.93^{+0.19}_{-0.16}$ | 6.9999±0.0003 | | | | 3.1±0.5 | 3.1±0.2 | 2.9±0.5 | 3.0±0.4 | 0.43±0.06 |
| 78968 | $7.9^{+0.1}_{-0.1}$ | 2004-05-05 | *Ks* | $8.75^{+0.37}_{-0.29}$ | 2.5117±0.0003 | 0.13±0.01 | | 0.07±0.02 | | | 0.101±0.006 | 0.10±0.01 | 0.040±0.005 |

*Continued on next page*

Table A5 – *Continued from previous page*

| HIP | log(*Age*[*yr*]) | Date | Band | $M_{X,\mathrm{comp}}$ (mag) | $M_{\mathrm{prim}}$ ($M_\odot$) | $M_{\mathrm{comp}}$ (1) ($M_\odot$) | (2) ($M_\odot$) | (3) ($M_\odot$) | (4) ($M_\odot$) | (5) ($M_\odot$) | (6) ($M_\odot$) | $M_{\mathrm{comp}}$ ($M_\odot$) | $q$ |
|---|---|---|---|---|---|---|---|---|---|---|---|---|---|
| 79005 | $8.35^{+0.04}_{-0.05}$ | 2004-07-04 | *Ks* | $3.06^{+0.16}_{-0.14}$ | 2.7±0.1 | | 1.15±0.04 | 1.12±0.04 | 1.17±0.04 | 1.16±0.04 | 1.17±0.04 | 1.15±0.04 | 0.43±0.02 |
| | | 2006-04-27 | *Ks* | $2.92^{+0.17}_{-0.15}$ | | | 1.19±0.04 | 1.16±0.04 | 1.21±0.04 | 1.20±0.04 | 1.22±0.05 | 1.20±0.04 | 0.45±0.02 |
| | | 2006-06-01 | *Ks* | $2.97^{+0.16}_{-0.14}$ | | | 1.18±0.04 | 1.15±0.04 | 1.20±0.04 | 1.19±0.04 | 1.20±0.04 | 1.18±0.04 | 0.45±0.02 |
| 79098 | $8.36^{+0.02}_{-0.02}$ | 2005-03-13 | *Ks* | $8.17^{+0.23}_{-0.23}$ | 2.96±0.05 | 0.16±0.01 | | 0.15±0.02 | 0.14±0.01 | 0.168±0.008 | 0.17±0.02 | 0.16±0.01 | 0.054±0.005 |
| 79230 | $6.9^{+0.1}_{-0.2}$ | 2004-04-10 | *H* | $1.7^{+0.9}_{-0.5}$ | 7.4±0.1 | | | | 1.9±0.8 | 2.3±0.7 | 2.1±0.7 | 2.1±0.7 | 0.3±0.1 |
| 79410 | $7.9^{+0.1}_{-0.1}$ | 2004-06-20 | *Ks* | $9.39^{+0.42}_{-0.32}$ | 2.5117±0.0003 | | | 0.05±0.01 | | | | 0.05±0.01 | 0.020±0.004 |
| 79622 | $7.81^{+0.04}_{-0.05}$ | 2012-07-13 | *Ks* | $3.8^{+1.4}_{-1.4}$ | 3.63±0.02 | | 0.9±0.3 | 0.9±0.3 | 0.9±0.4 | 1.0±0.3 | 1.0±0.4 | 1.0±0.3 | 0.26±0.09 |
| 79739 | $8.1^{+0.1}_{-0.2}$ | 2004-06-20 | *Ks* | $5.35^{+0.34}_{-0.26}$ | 3.1611±0.0008 | 0.59±0.05 | 0.58±0.05 | 0.56±0.04 | 0.58±0.06 | 0.57±0.05 | 0.57±0.04 | 0.57±0.05 | 0.18±0.02 |
| 80142 | $7.2^{+0.2}_{-0.6}$ | 2004-05-05 | *Ks* | $3.88^{+0.17}_{-0.15}$ | 3.15±0.07 | | | 0.7±0.2 | 0.8±0.2 | 0.91±0.04 | 0.7±0.2 | 0.8±0.2 | 0.25±0.06 |
| 80461 | $7.51^{+0.09}_{-0.11}$ | 2012-09-09 | *Ks* | $1.3^{+0.2}_{-0.2}$ | 4.84±0.02 | | | | 2.8±0.3 | 2.6±0.2 | 2.6±0.2 | 2.7±0.2 | 0.55±0.05 |
| 80473 | $7.47^{+0.05}_{-0.05}$ | 2012-06-11 | *Ks* | $-1.41^{+0.57}_{-0.56}$ | 7.4±0.1 | | | | 7.0±0.3 | 7.2±0.8 | 7.1±0.8 | 7.1±0.7 | 0.97±0.09 |
| 80474 | $7.3^{+0.3}_{-0.7}$ | 2004-06-28 | *Ks* | $5.51^{+0.19}_{-0.17}$ | 3.2±0.1 | 0.55±0.03 | | 0.3±0.1 | 0.3±0.1 | 0.53±0.03 | 0.3±0.1 | 0.4±0.1 | 0.12±0.03 |
| | | 2011-05-09 | *Ks* | $5.79^{+0.20}_{-0.17}$ | | 0.50±0.03 | | 0.2±0.1 | 0.2±0.1 | 0.48±0.03 | 0.3±0.1 | 0.34±0.09 | 0.11±0.03 |
| 80493 | $7.88^{+0.09}_{-0.11}$ | 2012-09-09 | *Ks* | $2.49^{+0.30}_{-0.23}$ | 2.5117±0.0003 | | 1.3±0.2 | 1.28±0.05 | 1.4±0.1 | 1.4±0.1 | 1.4±0.1 | 1.4±0.1 | 0.54±0.06 |
| 82902 | $8.3^{+0.1}_{-0.2}$ | 2004-06-21 | *Ks* | $8.96^{+0.28}_{-0.28}$ | 2.5114±0.0002 | 0.11±0.01 | | 0.09±0.02 | 0.100±0.004 | | 0.11±0.01 | 0.10±0.01 | 0.041±0.005 |
| | | 2006-06-09 | *Ks* | $8.87^{+0.25}_{-0.25}$ | | 0.12±0.01 | | 0.10±0.02 | 0.100±0.004 | | 0.11±0.01 | 0.11±0.01 | 0.042±0.005 |
| 87220 | $8.23^{+0.01}_{-0.01}$ | 2005-03-25 | *Ks* | $6.76^{+0.18}_{-0.18}$ | 3.98±0.02 | 0.32±0.02 | 0.31±0.02 | 0.33±0.03 | 0.31±0.03 | 0.30±0.02 | 0.35±0.02 | 0.32±0.02 | 0.081±0.006 |
| | | 2011-05-09 | *Ks* | $6.99^{+0.18}_{-0.18}$ | | 0.29±0.02 | 0.28±0.02 | 0.29±0.03 | 0.27±0.03 | 0.27±0.02 | 0.31±0.02 | 0.28±0.02 | 0.071±0.006 |
| 88149 | $7.10^{+0.05}_{-0.06}$ | 2005-03-26 | *Ks* | $0.66^{+0.13}_{-0.12}$ | 8.1±0.1 | | | | 3.8±0.2 | 3.5±0.2 | 3.5±0.2 | 3.6±0.2 | 0.45±0.02 |
| | | 2011-05-09 | *Ks* | $0.55^{+0.13}_{-0.12}$ | | | | | 4.0±0.2 | 3.7±0.2 | 3.7±0.2 | 3.8±0.2 | 0.47±0.02 |
| 88859 | $8.17^{+0.06}_{-0.07}$ | 2005-03-13 | *Ks* | $2.17^{+0.43}_{-0.31}$ | 3.90±0.09 | | 1.5±0.2 | 1.334±0.002 | 1.6±0.2 | 1.6±0.2 | 1.6±0.2 | 1.5±0.2 | 0.40±0.05 |
| 89684 | $8.47^{+0.03}_{-0.03}$ | 2005-07-19 | *Ks* | $4.79^{+0.19}_{-0.17}$ | 3.13±0.04 | 0.70±0.03 | 0.68±0.03 | 0.67±0.03 | 0.70±0.03 | 0.68±0.03 | 0.67±0.03 | 0.69±0.03 | 0.22±0.01 |
| | | 2011-05-09 | *Ks* | $4.90^{+0.19}_{-0.17}$ | | 0.68±0.03 | 0.66±0.03 | 0.65±0.03 | 0.68±0.03 | 0.66±0.03 | 0.65±0.03 | 0.66±0.03 | 0.21±0.01 |
| 90096 | $8.20^{+0.02}_{-0.03}$ | 2005-03-29 | *Ks* | $3.21^{+0.17}_{-0.15}$ | 3.9±0.1 | | 1.10±0.04 | 1.07±0.04 | 1.12±0.04 | 1.11±0.04 | 1.12±0.04 | 1.11±0.04 | 0.28±0.01 |
| | | 2011-05-09 | *Ks* | $3.18^{+0.17}_{-0.15}$ | | | 1.12±0.03 | 1.08±0.04 | 1.13±0.04 | 1.12±0.04 | 1.13±0.04 | 1.12±0.04 | 0.28±0.01 |
| 90766 | $8.0^{+0.1}_{-0.2}$ | 2010-06-25 | *Ks* | $2.61^{+0.44}_{-0.32}$ | 2.516±0.008 | | 1.3±0.1 | 1.22±0.06 | 1.3±0.2 | 1.4±0.1 | 1.4±0.2 | 1.3±0.1 | 0.52±0.06 |
| 91014 | $7.39^{+0.04}_{-0.04}$ | 2005-04-12 | *Ks* | $1.8^{+0.2}_{-0.2}$ | 8.7±0.3 | | | | 2.0±0.3 | 2.0±0.2 | 2.0±0.2 | 2.0±0.2 | 0.23±0.03 |
| 93805 | $8.4^{+0.1}_{-0.1}$ | 2008-08-21 | *Ks* | $4.67^{+0.31}_{-0.31}$ | 2.5113±0.0004 | | 0.71±0.06 | 0.70±0.05 | 0.73±0.05 | 0.70±0.06 | 0.70±0.06 | 0.71±0.05 | 0.28±0.02 |
| | | 2009-04-26 | *Ks* | $4.52^{+0.32}_{-0.32}$ | | | 0.75±0.06 | 0.73±0.06 | 0.76±0.06 | 0.74±0.06 | 0.74±0.07 | 0.74±0.06 | 0.30±0.02 |
| 99457 | $7.06^{+0.06}_{-0.07}$ | 2005-05-22 | *Ks* | $2.52^{+1.00}_{-0.52}$ | | | | 1.2±0.1 | 1.3±0.5 | 1.6±0.5 | 1.6±0.5 | 1.4±0.4 | 0.13±0.04 |
| 100751 | $7.5^{+0.1}_{-0.2}$ | 2005-08-19 | *Ks* | $6.86^{+0.55}_{-0.55}$ | 6.4±0.2 | 0.31±0.07 | | 0.16±0.06 | 0.14±0.05 | 0.29±0.07 | 0.18±0.05 | 0.22±0.06 | 0.034±0.009 |
| 100881 | $8.18^{+0.06}_{-0.06}$ | 2008-10-30 | *Ks* | $1.66^{+0.23}_{-0.19}$ | 3.97±0.02 | | 2.0±0.2 | | 2.1±0.2 | 2.0±0.2 | 2.0±0.2 | 2.0±0.2 | 0.51±0.04 |

*Continued on next page*

Table A5 – *Continued from previous page*

| HIP | log(*Age*[*yr*]) | Date | Band | $M_{X,\mathrm{comp}}$ (mag) | $M_{\mathrm{prim}}$ ($M_\odot$) | $M_{\mathrm{comp}}$ (1) ($M_\odot$) | (2) ($M_\odot$) | (3) ($M_\odot$) | (4) ($M_\odot$) | (5) ($M_\odot$) | (6) ($M_\odot$) | $M_{\mathrm{comp}}$ ($M_\odot$) | $q$ |
|---|---|---|---|---|---|---|---|---|---|---|---|---|---|
| | | 2012-09-19 | *Ks* | $2.07^{+0.24}_{-0.19}$ | | | 1.6±0.1 | | 1.7±0.1 | 1.6±0.1 | 1.7±0.1 | 1.6±0.1 | 0.41±0.04 |
| 105842 | $8.6^{+0.2}_{-0.3}$ | 2008-08-07 | *H* | $3.88^{+1.06}_{-0.54}$ | 1.84±0.03 | | 0.9±0.2 | 1.0±0.2 | 0.9±0.2 | 1.0±0.2 | 1.0±0.2 | 1.0±0.2 | 0.5±0.1 |
| 113031 | $8.19^{+0.05}_{-0.06}$ | 2004-10-20 | *Ks* | $-0.06^{+0.25}_{-0.21}$ | 4.1±0.1 | | 3.4±0.2 | | 3.6±0.2 | 3.6±0.2 | 3.6±0.2 | 3.6±0.2 | 0.88±0.05 |
| | | 2007-09-20 | *Ks* | $0.14^{+0.26}_{-0.22}$ | | | 3.3±0.2 | | 3.5±0.2 | 3.4±0.2 | 3.4±0.2 | 3.4±0.2 | 0.84±0.05 |
| 116231 | $8.9^{+0.1}_{-0.2}$ | 2004-10-18 | *Ks* | $5.104^{+0.038}_{-0.038}$ | 2.4±0.1 | 0.636±0.007 | 0.624±0.006 | 0.612±0.005 | 0.630±0.007 | 0.613±0.006 | 0.614±0.005 | 0.622±0.006 | 0.26±0.01 |
| | | 2004-10-19 | *Ks* | $5.055^{+0.043}_{-0.043}$ | | 0.646±0.007 | 0.632±0.006 | 0.620±0.006 | 0.641±0.008 | 0.623±0.007 | 0.622±0.006 | 0.631±0.007 | 0.27±0.01 |
| | | 2012-09-18 | *Ks* | $5.180^{+0.035}_{-0.035}$ | | 0.619±0.006 | 0.610±0.006 | 0.599±0.005 | 0.613±0.006 | 0.598±0.006 | 0.602±0.005 | 0.607±0.006 | 0.26±0.01 |
| | | | | | | Higher-order multiple systems | | | | | | | |
| 24925AB | $8.12^{+0.04}_{-0.05}$ | 2005-01-09 | *Ks* | $1.62^{+1.22}_{-0.58}$ | 3.8±0.1 | | 2.0±0.7 | | 2.1±0.8 | 2.3±0.7 | 2.3±0.7 | 2.2±0.7 | 0.6±0.2 |
| | | 2012-09-19 | *Ks* | $1.63^{+1.22}_{-0.58}$ | | | 2.0±0.7 | | 2.1±0.8 | 2.3±0.7 | 2.3±0.7 | 2.2±0.7 | 0.6±0.2 |
| | | 2013-01-04 | *Ks* | $1.60^{+1.22}_{-0.58}$ | | | 2.0±0.7 | | 2.1±0.8 | 2.3±0.7 | 2.3±0.7 | 2.2±0.7 | 0.6±0.2 |
| 24925AC | | 2005-01-09 | *Ks* | $2.27^{+1.22}_{-0.58}$ | | | 1.5±0.6 | 1.1874±0.0008 | 1.6±0.7 | 1.8±0.6 | 1.8±0.6 | 1.6±0.5 | 0.4±0.1 |
| | | 2012-09-19 | *Ks* | $2.33^{+1.23}_{-0.58}$ | | | 1.4±0.6 | 1.1654±0.0005 | 1.5±0.6 | 1.7±0.6 | 1.8±0.6 | 1.5±0.5 | 0.4±0.1 |
| | | 2013-01-04 | *Ks* | $2.35^{+1.22}_{-0.58}$ | | | 1.4±0.6 | 1.1601±0.0005 | 1.5±0.6 | 1.7±0.6 | 1.7±0.6 | 1.5±0.5 | 0.4±0.1 |
| 26237AB | $6.98^{+0.05}_{-0.06}$ | 2005-04-09 | *Ks* | $-0.68^{+1.05}_{-0.53}$ | 10.9±0.4 | | | | 7.0±0.7 | 7.3±2.0 | 7.3±2.0 | 7.2±2.0 | 0.7±0.2 |
| | | 2012-09-19 | *Ks* | $-0.63^{+1.05}_{-0.53}$ | | | | | 6.9±0.7 | 7.2±2.0 | 7.2±2.0 | 7.1±2.0 | 0.6±0.2 |
| 26237AC | | 2005-04-09 | *Ks* | $0.37^{+1.05}_{-0.54}$ | | | | | 4.4±2.0 | 4.6±1.0 | 4.6±1.0 | 4.5±2.0 | 0.4±0.1 |
| | | 2012-09-19 | *Ks* | $0.39^{+1.05}_{-0.53}$ | | | | | 4.3±2.0 | 4.6±1.0 | 4.6±1.0 | 4.5±2.0 | 0.4±0.1 |
| 26549AB | $7.02^{+0.02}_{-0.03}$ | 2004-10-11 | *Ks* | $-1.5^{+3.3}_{-1.6}$ | 13.3±0.5 | | | | 6.3±1.0 | 10.6±5.0 | 10.3±5.0 | 9.1±4.0 | 0.7±0.3 |
| 26549AC | | 2004-10-11 | *Ks* | $-0.1^{+3.3}_{-1.6}$ | | | | | 4.9±2.0 | 7.6±6.0 | 7.3±6.0 | 6.6±5.0 | 0.5±0.4 |
| 26549AD | | 2004-10-11 | *Ks* | $2.6^{+3.3}_{-1.6}$ | | | | 0.9±0.4 | 2.9±3.0 | 2.9±3.0 | 2.8±3.0 | 2.4±2.0 | 0.2±0.2 |
| 26549AE | | 2004-10-11 | *Ks* | $4.0^{+3.3}_{-1.6}$ | | | | 0.4±0.2 | 1.5±2.0 | 1.6±1.0 | 1.5±1.0 | 1.2±1.0 | 0.09±0.09 |
| 26549AF | | 2004-10-11 | *Ks* | $4.6^{+3.3}_{-1.6}$ | | | | 0.3±0.1 | 1.1±1.0 | 1.2±1.0 | 1.1±1.0 | 0.9±0.9 | 0.07±0.07 |
| 26549AG | | 2004-10-11 | *Ks* | $4.9^{+3.3}_{-1.6}$ | | | | 0.2±0.1 | 0.8±0.8 | 1.1±0.8 | 0.9±0.9 | 0.7±0.7 | 0.06±0.06 |
| 39331AB | $7.34^{+0.04}_{-0.05}$ | 2007-01-20 | *Ks* | $7.25^{+1.36}_{-0.61}$ | 9.2±0.5 | 0.3±0.1 | | 0.13±0.08 | | 0.3±0.1 | 0.19±0.08 | 0.2±0.1 | 0.02±0.01 |
| 39331AC | | 2007-01-20 | *Ks* | $7.49^{+1.37}_{-0.61}$ | | 0.3±0.1 | | 0.11±0.07 | | 0.3±0.1 | | 0.2±0.1 | 0.02±0.01 |
| 42504AB | $7.2^{+0.2}_{-0.4}$ | 2006-01-07 | *Ks* | $2.6^{+0.1}_{-0.1}$ | 5.0±1.0 | | | 1.23±0.04 | 1.30±0.06 | 1.31±0.04 | 1.30±0.06 | 1.28±0.05 | 0.26±0.01 |
| 42504AC | | 2006-01-07 | *Ks* | $4.75^{+0.12}_{-0.11}$ | | 0.71±0.02 | | 0.5±0.1 | 0.5±0.1 | 0.69±0.02 | 0.5±0.1 | 0.6±0.1 | 0.11±0.02 |
| 46594AB | $7.87^{+0.04}_{-0.04}$ | 2006-01-18 | *Ks* | $4.6^{+0.1}_{-0.1}$ | 3.20±0.09 | 0.74±0.02 | 0.73±0.02 | 0.67±0.02 | 0.72±0.02 | 0.71±0.02 | 0.67±0.02 | 0.71±0.02 | 0.221±0.009 |
| | | 2008-03-10 | *Ks* | $4.5^{+0.1}_{-0.1}$ | | | 0.75±0.02 | 0.70±0.03 | 0.75±0.02 | 0.74±0.02 | 0.71±0.03 | 0.73±0.03 | 0.23±0.01 |
| 46594AC | | 2006-01-18 | *Ks* | $5.07^{+0.12}_{-0.12}$ | | 0.64±0.02 | 0.64±0.02 | 0.59±0.02 | 0.62±0.02 | 0.62±0.02 | 0.60±0.01 | 0.62±0.02 | 0.193±0.008 |
| | | 2008-03-10 | *Ks* | $4.98^{+0.12}_{-0.12}$ | | 0.66±0.02 | 0.65±0.02 | 0.61±0.02 | 0.64±0.02 | 0.64±0.02 | 0.61±0.01 | 0.63±0.02 | 0.198±0.008 |

*Continued on next page*

Table A5 – *Continued from previous page*

| HIP | log(*Age*[*yr*]) | Date | Band | $M_{X,\mathrm{comp}}$ (mag) | $M_{\mathrm{prim}}$ ($M_\odot$) | $M_{\mathrm{comp}}$ (1) ($M_\odot$) | (2) ($M_\odot$) | (3) ($M_\odot$) | (4) ($M_\odot$) | (5) ($M_\odot$) | (6) ($M_\odot$) | $M_{\mathrm{comp}}$ ($M_\odot$) | $q$ |
|---|---|---|---|---|---|---|---|---|---|---|---|---|---|
| 51376AB | $8.76^{+0.02}_{-0.02}$ | 2005-02-04 | *Ks* | $3.30^{+0.19}_{-0.18}$ | 2.53±0.05 | | 1.07±0.04 | 1.04±0.04 | 1.08±0.04 | 1.07±0.04 | 1.08±0.05 | 1.07±0.04 | 0.42±0.02 |
| | | 2005-02-14 | *Ks* | $3.55^{+0.17}_{-0.15}$ | | | 1.01±0.03 | 0.97±0.04 | 1.02±0.04 | 1.00±0.04 | 1.01±0.04 | 1.00±0.04 | 0.40±0.02 |
| | | 2008-02-25 | *Ks* | $3.41^{+0.17}_{-0.15}$ | | | 1.04±0.03 | 1.01±0.04 | 1.05±0.04 | 1.04±0.04 | 1.05±0.04 | 1.04±0.04 | 0.41±0.02 |
| 51376AC | | 2005-02-04 | *Ks* | $3.39^{+0.19}_{-0.18}$ | | | 1.04±0.04 | 1.01±0.04 | 1.06±0.04 | 1.05±0.04 | 1.05±0.05 | 1.04±0.04 | 0.41±0.02 |
| | | 2005-02-14 | *Ks* | $3.67^{+0.17}_{-0.15}$ | | | 0.98±0.04 | 0.94±0.04 | 0.98±0.04 | 0.96±0.04 | 0.97±0.04 | 0.97±0.04 | 0.38±0.02 |
| | | 2008-02-25 | *Ks* | $3.52^{+0.17}_{-0.16}$ | | | 1.02±0.04 | 0.98±0.04 | 1.02±0.04 | 1.01±0.04 | 1.01±0.04 | 1.01±0.04 | 0.40±0.02 |
| 54413AB | $8.2^{+0.1}_{-0.1}$ | 2007-02-27 | *Ks* | $9.68^{+0.34}_{-0.31}$ | 2.71±0.05 | | | 0.056±0.009 | | | | 0.056±0.009 | 0.021±0.003 |
| | | 2008-02-20 | *Ks* | $9.93^{+0.34}_{-0.32}$ | | | | 0.050±0.008 | | | | 0.050±0.008 | 0.018±0.003 |
| | | 2009-02-20 | *Ks* | $9.48^{+0.28}_{-0.25}$ | | | | 0.06±0.01 | | | | 0.06±0.01 | 0.023±0.004 |
| | | 2010-12-25 | *Ks* | $9.58^{+0.30}_{-0.26}$ | | | | 0.059±0.009 | | | | 0.059±0.009 | 0.022±0.003 |
| | | 2011-03-25 | *Ks* | $9.16^{+0.29}_{-0.26}$ | | 0.106±0.009 | | 0.07±0.01 | | | | 0.09±0.01 | 0.033±0.004 |
| 54413AC | | 2007-02-27 | *Ks* | $9.67^{+0.34}_{-0.31}$ | | | | 0.056±0.009 | | | | 0.056±0.009 | 0.021±0.003 |
| | | 2008-02-20 | *Ks* | $9.79^{+0.33}_{-0.31}$ | | | | 0.053±0.008 | | | | 0.053±0.008 | 0.020±0.003 |
| | | 2009-02-20 | *Ks* | $9.68^{+0.29}_{-0.26}$ | | | | 0.056±0.008 | | | | 0.056±0.008 | 0.021±0.003 |
| | | 2010-12-25 | *Ks* | $9.59^{+0.30}_{-0.26}$ | | | | 0.058±0.009 | | | | 0.058±0.009 | 0.022±0.003 |
| | | 2011-03-25 | *Ks* | $9.27^{+0.30}_{-0.26}$ | | | | 0.07±0.01 | | | | 0.07±0.01 | 0.026±0.004 |
| 56000AB | $8.30^{+0.03}_{-0.03}$ | 2005-02-07 | *Ks* | $1.3^{+0.4}_{-0.3}$ | 3.6±0.1 | | 2.2±0.2 | | 2.4±0.3 | 2.3±0.2 | 2.3±0.2 | 2.3±0.2 | 0.65±0.07 |
| | | 2008-02-24 | *Ks* | $1.6^{+0.4}_{-0.3}$ | | | 2.0±0.2 | | 2.1±0.3 | 2.1±0.3 | 2.1±0.2 | 2.1±0.2 | 0.58±0.07 |
| 56000AC | | 2005-02-07 | *Ks* | $2.0^{+0.4}_{-0.3}$ | | | 1.7±0.2 | | 1.8±0.2 | 1.7±0.2 | 1.8±0.2 | 1.7±0.2 | 0.49±0.07 |
| | | 2008-02-24 | *Ks* | $2.04^{+0.40}_{-0.31}$ | | | 1.6±0.2 | | 1.7±0.2 | 1.7±0.2 | 1.7±0.2 | 1.7±0.2 | 0.47±0.06 |
| 56754AB | $8.23^{+0.04}_{-0.04}$ | 2005-02-02 | *Ks* | $2.42^{+0.09}_{-0.08}$ | 2.75±0.05 | | 1.39±0.03 | 1.34±0.02 | 1.46±0.04 | 1.40±0.03 | 1.42±0.03 | 1.40±0.03 | 0.51±0.02 |
| | | 2008-01-10 | *Ks* | $2.408^{+0.090}_{-0.084}$ | | | 1.39±0.03 | 1.35±0.02 | 1.46±0.05 | 1.40±0.04 | 1.42±0.03 | 1.40±0.03 | 0.51±0.02 |
| | | 2011-04-22 | *Ks* | $2.416^{+0.086}_{-0.081}$ | | | 1.39±0.03 | 1.34±0.02 | 1.46±0.04 | 1.40±0.03 | 1.42±0.03 | 1.40±0.03 | 0.51±0.02 |
| 56754AC | | 2005-02-02 | *Ks* | $6.7^{+0.1}_{-0.1}$ | | 0.33±0.01 | 0.32±0.01 | 0.34±0.02 | 0.33±0.02 | 0.31±0.01 | 0.36±0.01 | 0.33±0.01 | 0.121±0.006 |
| | | 2008-01-10 | *Ks* | $6.78^{+0.16}_{-0.16}$ | | 0.32±0.02 | 0.31±0.02 | 0.33±0.02 | 0.31±0.03 | 0.30±0.02 | 0.35±0.02 | 0.32±0.02 | 0.115±0.008 |
| | | 2011-04-22 | *Ks* | $6.86^{+0.12}_{-0.12}$ | | 0.31±0.01 | 0.30±0.01 | 0.31±0.02 | 0.29±0.02 | 0.29±0.01 | 0.33±0.02 | 0.30±0.02 | 0.111±0.006 |
| 60851AB | $9.07^{+0.02}_{-0.02}$ | 2004-04-07 | *Ks* | $6.31^{+0.13}_{-0.13}$ | 1.994±0.003 | 0.39±0.02 | 0.38±0.02 | 0.41±0.02 | 0.40±0.02 | 0.37±0.02 | 0.44±0.02 | 0.40±0.02 | 0.200±0.009 |
| 60851AC | | 2004-04-07 | *Ks* | $6.39^{+0.25}_{-0.25}$ | | 0.38±0.04 | 0.37±0.03 | 0.40±0.03 | 0.39±0.04 | 0.36±0.04 | 0.42±0.03 | 0.39±0.03 | 0.19±0.02 |
| 62058AB | $7.7^{+0.1}_{-0.2}$ | 2005-02-14 | *Ks* | $8.2^{+0.4}_{-0.4}$ | 3.1620±0.0003 | 0.16±0.03 | | 0.08±0.02 | | 0.17±0.01 | | 0.14±0.02 | 0.044±0.006 |
| 62058AC | | 2005-02-14 | *Ks* | $8.92^{+0.53}_{-0.53}$ | | 0.12±0.02 | | 0.05±0.01 | | | | 0.08±0.02 | 0.026±0.006 |
| 69113AB | $8.36^{+0.03}_{-0.03}$ | 2004-05-01 | *Ks* | $4.33^{+0.17}_{-0.16}$ | 2.80±0.09 | | 0.79±0.04 | 0.78±0.03 | 0.79±0.03 | 0.78±0.03 | 0.79±0.04 | 0.79±0.03 | 0.28±0.02 |
| 69113AC | | 2004-05-01 | *Ks* | $4.39^{+0.17}_{-0.16}$ | | | 0.77±0.03 | 0.76±0.03 | 0.78±0.03 | 0.77±0.03 | 0.77±0.04 | 0.77±0.03 | 0.28±0.02 |

*Continued on next page*

Table A5 – *Continued from previous page*

| HIP | log(*Age*[*yr*]) | Date | Band | $M_{X,\mathrm{comp}}$ (mag) | $M_{\mathrm{prim}}$ ($M_\odot$) | $M_{\mathrm{comp}}$ (1) ($M_\odot$) | (2) ($M_\odot$) | (3) ($M_\odot$) | (4) ($M_\odot$) | (5) ($M_\odot$) | (6) ($M_\odot$) | $M_{\mathrm{comp}}$ ($M_\odot$) | $q$ |
|---|---|---|---|---|---|---|---|---|---|---|---|---|---|
| 74911AB | $8.19^{+0.03}_{-0.03}$ | 2005-03-25 | *Ks* | $0.27^{+0.17}_{-0.15}$ | 3.7±0.2 | | 3.2±0.1 | | 3.4±0.1 | 3.3±0.1 | 3.3±0.1 | 3.3±0.1 | 0.88±0.06 |
| 74911AC | | 2005-03-25 | *Ks* | $7.78^{+0.23}_{-0.21}$ | | 0.20±0.02 | 0.19±0.02 | 0.18±0.02 | 0.15±0.02 | 0.19±0.01 | 0.19±0.02 | 0.18±0.02 | 0.049±0.005 |
| 77562AB | $8.0^{+0.1}_{-0.2}$ | 2004-06-30 | *Ks* | $8.45^{+0.14}_{-0.14}$ | 2.5±0.6 | 0.141±0.008 | | 0.10±0.02 | | | 0.11±0.01 | 0.12±0.01 | 0.047±0.005 |
| | | 2006-04-28 | *Ks* | $8.38^{+0.28}_{-0.28}$ | | 0.15±0.02 | | 0.10±0.02 | | | 0.12±0.02 | 0.12±0.02 | 0.049±0.007 |
| 77562AC | | 2004-06-30 | *Ks* | $9.00^{+0.17}_{-0.17}$ | | 0.111±0.006 | | 0.07±0.01 | | | | 0.09±0.01 | 0.036±0.004 |
| | | 2006-04-28 | *Ks* | $8.81^{+0.33}_{-0.33}$ | | 0.12±0.01 | | 0.08±0.02 | | | | 0.10±0.02 | 0.040±0.006 |
| 77562AD | | 2004-06-30 | *Ks* | $9.19^{+0.18}_{-0.18}$ | | 0.104±0.006 | | 0.06±0.01 | | | | 0.082±0.009 | 0.033±0.004 |
| | | 2006-04-28 | *Ks* | $9.11^{+0.37}_{-0.37}$ | | 0.11±0.01 | | 0.07±0.02 | | | | 0.09±0.01 | 0.034±0.006 |
| 77562AE | | 2004-06-30 | *Ks* | $9.07^{+0.18}_{-0.18}$ | | 0.108±0.006 | | 0.07±0.01 | | | | 0.09±0.01 | 0.035±0.004 |
| | | 2006-04-28 | *Ks* | $9.73^{+0.51}_{-0.51}$ | | | | 0.05±0.01 | | | | 0.05±0.01 | 0.019±0.005 |
| 79153AB | $8.7^{+0.1}_{-0.2}$ | 2004-06-30 | *Ks* | $9.38^{+0.25}_{-0.25}$ | 1.99±0.04 | | | 0.097±0.009 | 0.100±0.003 | | 0.111±0.009 | 0.103±0.008 | 0.052±0.004 |
| | | 2006-04-28 | *Ks* | $9.23^{+0.34}_{-0.33}$ | | | | 0.10±0.01 | 0.103±0.006 | | 0.12±0.01 | 0.11±0.01 | 0.055±0.005 |
| 79153AC | | 2004-06-30 | *Ks* | $9.73^{+0.29}_{-0.28}$ | | | | 0.086±0.009 | | | 0.100±0.008 | 0.093±0.008 | 0.047±0.004 |
| | | 2006-04-28 | *Ks* | $9.7^{+0.4}_{-0.4}$ | | | | 0.09±0.01 | 0.100±0.001 | | 0.107±0.008 | 0.098±0.008 | 0.049±0.004 |
| 79199AB | $8.1^{+0.1}_{-0.1}$ | 2004-07-05 | *Ks* | $4.111^{+0.094}_{-0.087}$ | 3.161±0.002 | | 0.85±0.02 | 0.83±0.02 | 0.86±0.02 | 0.84±0.02 | 0.85±0.02 | 0.85±0.02 | 0.268±0.007 |
| | | 2011-05-09 | *Ks* | $4.092^{+0.093}_{-0.086}$ | | | 0.85±0.02 | 0.83±0.02 | 0.87±0.02 | 0.85±0.02 | 0.85±0.02 | 0.85±0.02 | 0.269±0.007 |
| 79199AC | | 2004-07-05 | *Ks* | $6.93^{+0.22}_{-0.21}$ | | 0.30±0.03 | 0.29±0.03 | 0.27±0.04 | 0.26±0.04 | 0.28±0.03 | 0.29±0.04 | 0.28±0.03 | 0.09±0.01 |
| | | 2011-05-09 | *Ks* | $7.07^{+0.12}_{-0.11}$ | | 0.28±0.01 | 0.27±0.01 | 0.25±0.03 | 0.23±0.03 | 0.26±0.01 | 0.27±0.03 | 0.26±0.02 | 0.081±0.007 |
| 79399AB | $8.1^{+0.1}_{-0.2}$ | 2004-06-29 | *Ks* | $2.24^{+0.18}_{-0.15}$ | 2.60±0.05 | | 1.48±0.09 | 1.378±0.002 | 1.57±0.09 | 1.5±0.1 | 1.54±0.09 | 1.50±0.08 | 0.58±0.03 |
| | | 2006-04-27 | *Ks* | $2.27^{+0.18}_{-0.16}$ | | | 1.48±0.08 | 1.362±0.002 | 1.56±0.09 | 1.50±0.09 | 1.52±0.09 | 1.48±0.08 | 0.57±0.03 |
| 79399AC | | 2004-06-29 | *Ks* | $2.65^{+0.18}_{-0.16}$ | | | 1.29±0.05 | 1.27±0.06 | 1.29±0.08 | 1.31±0.05 | 1.33±0.06 | 1.30±0.06 | 0.50±0.03 |
| | | 2006-04-27 | *Ks* | $3.04^{+0.18}_{-0.16}$ | | | 1.16±0.05 | 1.13±0.04 | 1.18±0.05 | 1.17±0.05 | 1.18±0.05 | 1.16±0.05 | 0.45±0.02 |
| 79399AD | | 2004-06-29 | *Ks* | $7.71^{+0.20}_{-0.18}$ | | 0.20±0.02 | 0.19±0.02 | 0.16±0.03 | 0.14±0.02 | 0.19±0.01 | 0.17±0.03 | 0.18±0.02 | 0.068±0.008 |
| | | 2006-04-27 | *Ks* | $7.48^{+0.29}_{-0.28}$ | | 0.23±0.03 | 0.22±0.02 | 0.19±0.04 | 0.17±0.04 | 0.21±0.02 | 0.20±0.04 | 0.20±0.03 | 0.08±0.01 |
| 79771AB | $8.0^{+0.1}_{-0.2}$ | 2004-06-20 | *Ks* | $4.74^{+0.31}_{-0.25}$ | 2.5117±0.0002 | | 0.70±0.05 | 0.67±0.05 | 0.71±0.05 | 0.69±0.05 | 0.67±0.05 | 0.69±0.05 | 0.27±0.02 |
| | | 2012-07-13 | *Ks* | $5.03^{+0.31}_{-0.24}$ | | 0.66±0.05 | 0.64±0.05 | 0.61±0.04 | 0.64±0.05 | 0.63±0.04 | 0.61±0.04 | 0.63±0.05 | 0.25±0.02 |
| 79771AC | | 2004-06-20 | *Ks* | $5.33^{+0.31}_{-0.24}$ | | 0.59±0.05 | 0.58±0.04 | 0.56±0.04 | 0.57±0.06 | 0.57±0.05 | 0.56±0.04 | 0.57±0.05 | 0.23±0.02 |
| | | 2012-07-13 | *Ks* | $5.22^{+0.31}_{-0.24}$ | | 0.61±0.05 | 0.60±0.05 | 0.57±0.04 | 0.60±0.05 | 0.59±0.05 | 0.58±0.04 | 0.59±0.05 | 0.24±0.02 |
| 81472AB | $6.7^{+0.2}_{-0.3}$ | 2005-03-25 | *Ks* | $6.9^{+0.4}_{-0.3}$ | 7.000±0.003 | 0.31±0.04 | | 0.05±0.02 | | | | 0.18±0.03 | 0.026±0.005 |
| | | 2011-05-09 | *Ks* | $6.8^{+0.4}_{-0.3}$ | | 0.32±0.04 | | 0.05±0.02 | | | | 0.19±0.03 | 0.027±0.005 |
| 81472AC | | 2005-03-25 | *Ks* | $6.9^{+0.4}_{-0.3}$ | | 0.31±0.04 | | 0.05±0.02 | | | | 0.18±0.03 | 0.026±0.005 |
| | | 2011-05-09 | *Ks* | $6.8^{+0.4}_{-0.3}$ | | 0.33±0.04 | | 0.05±0.02 | | | | 0.19±0.03 | 0.027±0.005 |

*Continued on next page*

Table A5 – *Continued from previous page*

| HIP | log(*Age*[*yr*]) | Date | Band | $M_{X,\mathrm{comp}}$ (mag) | $M_{\mathrm{prim}}$ ($M_\odot$) | $M_{\mathrm{comp}}$ (1) ($M_\odot$) | (2) ($M_\odot$) | (3) ($M_\odot$) | (4) ($M_\odot$) | (5) ($M_\odot$) | (6) ($M_\odot$) | $M_{\mathrm{comp}}$ ($M_\odot$) | $q$ |
|---|---|---|---|---|---|---|---|---|---|---|---|---|---|
| 81972AB | $7.2^{+0.2}_{-0.5}$ | 2004-06-28 | *Ks* | $4.17^{+0.12}_{-0.11}$ | 5.5±0.2 | | | 0.6±0.2 | 0.6±0.2 | 0.83±0.03 | 0.6±0.2 | 0.7±0.1 | 0.12±0.03 |
| 81972AC | | 2004-06-28 | *Ks* | $4.20^{+0.12}_{-0.11}$ | | | | 0.6±0.2 | 0.6±0.2 | 0.82±0.03 | 0.6±0.2 | 0.7±0.1 | 0.12±0.03 |
| 81972AD | | 2004-06-28 | *Ks* | $5.16^{+0.12}_{-0.11}$ | | 0.63±0.02 | | 0.3±0.1 | 0.3±0.1 | 0.60±0.02 | 0.4±0.1 | 0.4±0.1 | 0.08±0.02 |
| 81972AE | | 2004-06-28 | *Ks* | $7.60^{+0.13}_{-0.12}$ | | 0.21±0.01 | | 0.06±0.02 | | 0.201±0.009 | | 0.16±0.02 | 0.029±0.003 |
| 81972AF | | 2004-06-28 | *Ks* | $8.63^{+0.15}_{-0.14}$ | | 0.131±0.007 | | | | | | 0.131±0.007 | 0.024±0.001 |
| 83336AB | $8.17^{+0.03}_{-0.03}$ | 2004-06-26 | *Ks* | $6.20^{+0.17}_{-0.16}$ | 3.5±0.2 | 0.42±0.02 | 0.40±0.03 | 0.43±0.02 | 0.42±0.02 | 0.40±0.03 | 0.44±0.02 | 0.42±0.02 | 0.120±0.009 |
| | | 2006-06-26 | *Ks* | $6.05^{+0.17}_{-0.16}$ | | 0.44±0.03 | 0.43±0.03 | 0.45±0.02 | 0.45±0.02 | 0.43±0.02 | 0.46±0.02 | 0.44±0.02 | 0.13±0.01 |
| 83336AC | | 2004-06-26 | *Ks* | $6.18^{+0.17}_{-0.16}$ | | 0.42±0.02 | 0.40±0.02 | 0.43±0.02 | 0.43±0.02 | 0.41±0.03 | 0.44±0.02 | 0.42±0.02 | 0.121±0.009 |
| | | 2006-06-26 | *Ks* | $6.04^{+0.17}_{-0.16}$ | | 0.44±0.03 | 0.43±0.03 | 0.45±0.02 | 0.45±0.02 | 0.43±0.02 | 0.46±0.02 | 0.44±0.02 | 0.13±0.01 |
| 83336AD | | 2004-06-26 | *Ks* | $7.44^{+0.22}_{-0.21}$ | | 0.23±0.02 | 0.22±0.02 | 0.21±0.02 | 0.19±0.02 | 0.22±0.02 | 0.23±0.03 | 0.22±0.02 | 0.063±0.007 |
| | | 2006-06-26 | *Ks* | $7.79^{+0.25}_{-0.24}$ | | 0.19±0.02 | 0.19±0.02 | 0.17±0.02 | 0.15±0.02 | 0.19±0.01 | 0.19±0.02 | 0.18±0.02 | 0.052±0.006 |
| 85442AB | $8.52^{+0.02}_{-0.02}$ | 2005-03-25 | *Ks* | $5.91^{+0.25}_{-0.21}$ | 3.11±0.07 | 0.47±0.04 | 0.46±0.04 | 0.49±0.03 | 0.47±0.03 | 0.46±0.03 | 0.50±0.03 | 0.47±0.03 | 0.15±0.01 |
| | | 2011-05-09 | *Ks* | $6.03^{+0.25}_{-0.21}$ | | 0.45±0.04 | 0.43±0.04 | 0.47±0.03 | 0.45±0.03 | 0.43±0.03 | 0.48±0.03 | 0.45±0.03 | 0.15±0.01 |
| 85442AC | | 2005-03-25 | *Ks* | $6.40^{+0.26}_{-0.22}$ | | 0.38±0.03 | 0.37±0.03 | 0.40±0.03 | 0.39±0.03 | 0.36±0.04 | 0.42±0.03 | 0.39±0.03 | 0.12±0.01 |
| | | 2011-05-09 | *Ks* | $6.60^{+0.25}_{-0.22}$ | | 0.35±0.03 | 0.33±0.03 | 0.37±0.03 | 0.35±0.03 | 0.33±0.03 | 0.40±0.03 | 0.36±0.03 | 0.11±0.01 |
| 85442AD | | 2005-03-25 | *Ks* | $6.78^{+0.26}_{-0.23}$ | | 0.32±0.03 | 0.31±0.03 | 0.34±0.03 | 0.32±0.04 | 0.30±0.03 | 0.37±0.03 | 0.33±0.03 | 0.10±0.01 |
| | | 2011-05-09 | *Ks* | $6.84^{+0.26}_{-0.22}$ | | 0.31±0.03 | 0.30±0.03 | 0.33±0.03 | 0.31±0.04 | 0.29±0.03 | 0.36±0.03 | 0.32±0.03 | 0.10±0.01 |
| 85442AE | | 2005-03-25 | *Ks* | $6.89^{+0.27}_{-0.23}$ | | 0.30±0.03 | 0.29±0.03 | 0.32±0.03 | 0.30±0.04 | 0.28±0.03 | 0.35±0.03 | 0.31±0.03 | 0.10±0.01 |
| | | 2011-05-09 | *Ks* | $6.91^{+0.26}_{-0.22}$ | | 0.30±0.03 | 0.29±0.03 | 0.32±0.03 | 0.30±0.04 | 0.28±0.03 | 0.35±0.03 | 0.31±0.03 | 0.10±0.01 |
| 85727AB | $7.96^{+0.03}_{-0.03}$ | 2008-08-21 | *Ks* | $8.06^{+0.32}_{-0.32}$ | 3.95±0.05 | 0.17±0.02 | | 0.12±0.02 | 0.11±0.01 | 0.18±0.01 | 0.12±0.02 | 0.14±0.02 | 0.035±0.005 |
| 85727AC | | 2008-08-21 | *Ks* | $9.7^{+0.5}_{-0.5}$ | | | | 0.044±0.008 | | | | 0.044±0.008 | 0.011±0.002 |
| 85783AB | $8.1^{+0.1}_{-0.1}$ | 2005-03-13 | *Ks* | $2.32^{+0.19}_{-0.16}$ | 2.52±0.03 | | 1.43±0.09 | 1.336±0.003 | 1.53±0.09 | 1.47±0.09 | 1.49±0.09 | 1.45±0.08 | 0.58±0.03 |
| | | 2011-04-04 | *Ks* | $2.32^{+0.19}_{-0.16}$ | | | 1.43±0.08 | 1.335±0.003 | 1.53±0.09 | 1.47±0.09 | 1.49±0.09 | 1.45±0.08 | 0.58±0.03 |
| | | 2011-05-09 | *Ks* | $2.30^{+0.19}_{-0.16}$ | | | 1.45±0.09 | 1.345±0.003 | 1.54±0.09 | 1.48±0.09 | 1.50±0.09 | 1.46±0.08 | 0.58±0.03 |
| 85783AC | | 2005-03-13 | *Ks* | $7.69^{+0.20}_{-0.17}$ | | 0.20±0.02 | 0.20±0.02 | 0.17±0.02 | 0.14±0.02 | 0.19±0.01 | 0.18±0.03 | 0.18±0.02 | 0.072±0.008 |
| | | 2011-04-04 | *Ks* | $7.37^{+0.19}_{-0.17}$ | | 0.24±0.02 | 0.23±0.02 | 0.21±0.03 | 0.18±0.03 | 0.22±0.02 | 0.23±0.03 | 0.22±0.02 | 0.087±0.009 |
| | | 2011-05-09 | *Ks* | $7.57^{+0.19}_{-0.17}$ | | 0.22±0.02 | 0.21±0.02 | 0.18±0.02 | 0.16±0.02 | 0.20±0.01 | 0.20±0.03 | 0.20±0.02 | 0.077±0.008 |
| 87163AB | $7.72^{+0.04}_{-0.05}$ | 2005-03-28 | *Ks* | $-0.25^{+0.36}_{-0.27}$ | 6.27±0.09 | | | | 4.8±0.4 | 4.7±0.4 | 4.7±0.4 | 4.7±0.4 | 0.75±0.06 |
| | | 2011-05-09 | *Ks* | $-0.01^{+0.36}_{-0.27}$ | | | | | 4.5±0.4 | 4.3±0.4 | 4.3±0.4 | 4.4±0.4 | 0.70±0.06 |
| 87163AC | | 2005-03-28 | *Ks* | $4.56^{+0.37}_{-0.28}$ | | | | 0.69±0.05 | 0.72±0.06 | 0.74±0.06 | 0.70±0.06 | 0.71±0.06 | 0.114±0.009 |
| | | 2011-05-09 | *Ks* | $4.57^{+0.37}_{-0.28}$ | | | | 0.69±0.05 | 0.72±0.06 | 0.73±0.06 | 0.70±0.06 | 0.71±0.06 | 0.113±0.009 |
| 87163AD | | 2005-03-28 | *Ks* | $5.8^{+0.4}_{-0.3}$ | | 0.50±0.06 | | 0.42±0.07 | 0.42±0.07 | 0.49±0.05 | 0.44±0.07 | 0.46±0.06 | 0.07±0.01 |

*Continued on next page*

Table A5 – *Continued from previous page*

| HIP | log(*Age*[*yr*]) | Date | Band | $M_{X,\mathrm{comp}}$ (mag) | $M_{\mathrm{prim}}$ ($M_\odot$) | $M_{\mathrm{comp}}$ (1) ($M_\odot$) | (2) ($M_\odot$) | (3) ($M_\odot$) | (4) ($M_\odot$) | (5) ($M_\odot$) | (6) ($M_\odot$) | $M_{\mathrm{comp}}$ ($M_\odot$) | $q$ |
|---|---|---|---|---|---|---|---|---|---|---|---|---|---|
| | | 2011-05-09 | *Ks* | $5.67^{+0.38}_{-0.29}$ | | 0.52±0.06 | | 0.44±0.07 | 0.45±0.07 | 0.51±0.05 | 0.47±0.07 | 0.48±0.06 | 0.08±0.01 |
| 87163AE | | 2005-03-28 | *Ks* | $5.7^{+0.4}_{-0.3}$ | | 0.51±0.06 | | 0.43±0.07 | 0.43±0.07 | 0.49±0.05 | 0.45±0.07 | 0.46±0.06 | 0.07±0.01 |
| | | 2011-05-09 | *Ks* | $5.7^{+0.4}_{-0.3}$ | | 0.52±0.06 | | 0.45±0.07 | 0.45±0.07 | 0.51±0.05 | 0.47±0.07 | 0.48±0.06 | 0.08±0.01 |
| 87163AF | | 2005-03-28 | *Ks* | $6.06^{+0.39}_{-0.31}$ | | 0.45±0.05 | | 0.35±0.07 | 0.36±0.07 | 0.43±0.05 | 0.37±0.07 | 0.39±0.06 | 0.06±0.01 |
| | | 2011-05-09 | *Ks* | $5.9^{+0.4}_{-0.3}$ | | 0.47±0.05 | | 0.38±0.07 | 0.39±0.07 | 0.46±0.05 | 0.41±0.07 | 0.42±0.06 | 0.07±0.01 |
| 87163AG | | 2005-03-28 | *Ks* | $6.47^{+0.41}_{-0.33}$ | | 0.37±0.05 | | 0.27±0.06 | 0.24±0.07 | 0.36±0.05 | 0.29±0.06 | 0.30±0.06 | 0.048±0.009 |
| | | 2011-05-09 | *Ks* | $5.77^{+0.51}_{-0.46}$ | | 0.50±0.08 | | 0.4±0.1 | 0.4±0.1 | 0.49±0.08 | 0.4±0.1 | 0.46±0.09 | 0.07±0.01 |
| 88012AB | $7.67^{+0.04}_{-0.04}$ | 2005-03-27 | *Ks* | $3.94^{+0.65}_{-0.41}$ | 6.5±0.2 | | | 0.9±0.1 | 0.9±0.1 | 0.9±0.1 | 0.9±0.2 | 0.9±0.1 | 0.14±0.02 |
| 88012AC | | 2005-03-27 | *Ks* | $4.74^{+0.65}_{-0.42}$ | | | | 0.66±0.09 | 0.7±0.1 | 0.7±0.1 | 0.68±0.09 | 0.7±0.1 | 0.11±0.02 |
| 89963AB | $8.05^{+0.03}_{-0.03}$ | 2011-07-19 | *Ks* | $0.63^{+1.71}_{-0.73}$ | 4.5±0.1 | | 3.0±0.9 | | 3.2±1.0 | 3.3±0.9 | 3.3±0.9 | 3.2±1.0 | 0.7±0.2 |
| 89963AC | | 2011-07-19 | *Ks* | $2.27^{+1.72}_{-0.76}$ | | | 1.5±0.8 | 1.1274±0.0004 | 1.6±0.9 | 1.9±0.9 | 2.0±0.9 | 1.6±0.8 | 0.4±0.2 |
| 93892AB | $8.36^{+0.05}_{-0.06}$ | 2004-10-08 | *Ks* | $5.73^{+0.57}_{-0.38}$ | 3.22±0.06 | 0.52±0.08 | 0.50±0.08 | 0.52±0.06 | 0.51±0.07 | 0.50±0.08 | 0.53±0.06 | 0.51±0.07 | 0.16±0.02 |
| | | 2011-08-26 | *Ks* | $5.83^{+0.57}_{-0.38}$ | | 0.50±0.08 | 0.48±0.08 | 0.51±0.06 | 0.49±0.07 | 0.48±0.07 | 0.51±0.06 | 0.49±0.07 | 0.15±0.02 |
| 93892AC | | 2004-10-08 | *Ks* | $7.94^{+0.59}_{-0.42}$ | | 0.19±0.04 | | 0.19±0.04 | 0.15±0.04 | 0.20±0.02 | 0.21±0.05 | 0.19±0.04 | 0.06±0.01 |
| | | 2011-08-26 | *Ks* | $7.6^{+0.6}_{-0.4}$ | | 0.22±0.04 | 0.20±0.04 | 0.22±0.05 | 0.18±0.05 | 0.21±0.04 | 0.25±0.05 | 0.21±0.05 | 0.07±0.01 |

**Note.** $M_{\mathrm{comp}}$ is the average mass obtained from available models. $q$ is the mass ratio as function of the primary mass; $q = M_{\mathrm{S}}/M_{\mathrm{P}}$

**References.** (1) Delfosse et al. (2000); empirical mass-luminosity relation for $M \lesssim 1.0\,\mathrm{M}_\odot$. (2) Girardi et al. (2000). (3) Baraffe et al. (2002). (4) Siess et al. (2000). (5) Bertelli et al. (2009). (6) Bressan et al. (2012)

**Table A6.** Result table of visual binaries and multiple systems detected within the investigated VLT/NaCo data sample.

| HIP | CC# | WDS desig. | MJD (days) | Θ (arcsec) | PA[a] (deg) | Band | $\Delta m$ (mag) | $a_{\mathrm{proj.}}$ (au) | $\log(Age[yr])$ | $M_1$ ($M_\odot$) | $M_{\mathrm{comp}}$ ($M_\odot$) | $q$ | Chance proj. prob. (%) | Comp. status[b] |
|---|---|---|---|---|---|---|---|---|---|---|---|---|---|---|
| Visual binaries and multiples with only one observation and without additional data points from literature | | | | | | | | | | | | | | |
| 17563 | 1 | – | 53380.085 | 4.325±0.007 | 277.2±0.1 | *Ks* | 5.88±0.13 | $707.8^{+35.3}_{-32.1}$ | $7.1^{+0.3}_{-0.7}$ | 5.9±0.3 | 0.39±0.09 | 0.07±0.02 | $4.43 \times 10^{-2}$ | nU |
| 18213 | 1 | – | 53266.307 | 0.259±0.004 | 239.0±0.9 | *Ks* | 4.78±0.12 | $27.5^{+0.8}_{-0.7}$ | $7.6^{+0.1}_{-0.2}$ | 3.7±0.1 | 0.56±0.06 | 0.15±0.02 | $4.27 \times 10^{-5}$ | nU |
| 25657 | 1 | – | 54097.209 | 1.070±0.006 | 74.1±0.5 | *H* | 4.4793±0.0091 | $184.5^{+24.9}_{-19.6}$ | $7.9^{+0.1}_{-0.1}$ | 2.5117±0.0002 | 0.52±0.04 | 0.21±0.02 | $1.35 \times 10^{-2}$ | nU |
| 26549 | 4 | – | 53289.404 | 17.44±0.05 | 116.2±0.2 | *Ks* | 6.7±0.1 | $5737.9^{+8704.5}_{-4279.5}$ | $7.02^{+0.02}_{-0.03}$ | 13.3±0.5 | 1.2±1.0 | 0.09±0.09 | $2.66 \times 10^{0}$ | nU |
| 26549 | 5 | – | 53289.404 | 3.35±0.01 | 17.0±0.2 | *Ks* | 7.32±0.14 | $1102.1^{+1671.9}_{-822.0}$ | $7.02^{+0.02}_{-0.03}$ | 13.3±0.5 | 0.9±0.9 | 0.07±0.07 | $1.52 \times 10^{-1}$ | nU |
| 26549 | 6 | – | 53289.404 | 17.20±0.04 | 116.4±0.2 | *Ks* | 7.59±0.16 | $5657.0^{+8581.8}_{-4219.1}$ | $7.02^{+0.02}_{-0.03}$ | 13.3±0.5 | 0.7±0.7 | 0.06±0.06 | $4.70 \times 10^{0}$ | nU |
| 27810 | 1 | – | 53454.001 | 1.037±0.007 | 198.2±0.4 | *Ks* | 5.1701±0.0031 | $106.4^{+2.5}_{-2.4}$ | $7.5^{+0.1}_{-0.2}$ | 3.9807±0.0004 | 0.48±0.05 | 0.12±0.01 | $1.70 \times 10^{-3}$ | U |
| 32823 | 1 | – | 54458.281 | 1.194±0.007 | 250.9±0.5 | *H* | 5.277±0.021 | $918.5^{+28932.7}_{-452.1}$ | $7.4^{+0.2}_{-0.3}$ | 3.981±0.001 | 0.4±2.0 | 0.1±0.4 | $1.73 \times 10^{-1}$ | nU |
| 34041 | 1 | – | 54497.142 | 0.149±0.006 | 134.3±0.7 | *H* | 2.095±0.064 | $75.4^{+20.1}_{-13.4}$ | $7.40^{+0.06}_{-0.07}$ | 6.77±0.09 | 3.0±0.6 | 0.45±0.08 | $6.09 \times 10^{-5}$ | nU |
| 34153 | 1 | – | 54499.151 | 0.070±0.003 | 40.7±3.0 | *H* | 1.39±0.11 | $34.0^{+26.4}_{-10.4}$ | $7.8^{+0.1}_{-0.1}$ | 3.162±0.007 | 1.6±0.8 | 0.5±0.2 | $4.03 \times 10^{-5}$ | nU |
| 35110 | 1 | – | 54497.116 | 0.930±0.004 | 154.0±0.6 | *H* | 3.610±0.036 | $272.0^{+85.8}_{-52.6}$ | $7.8^{+0.1}_{-0.1}$ | 3.162±0.001 | 0.8±0.1 | 0.24±0.04 | $1.91 \times 10^{-2}$ | nU |
| 35413 | 1 | – | 54477.310 | 0.703±0.003 | 155.4±0.5 | *H* | 2.155±0.017 | $207.9^{+114.4}_{-54.5}$ | $7.1^{+0.2}_{-0.6}$ | 5.0±1.0 | 0.9±0.3 | 0.18±0.06 | $7.04 \times 10^{-3}$ | nU |
| 39331 | 1 | – | 54120.299 | 7.44±0.02 | 119.0±0.1 | *Ks* | 6.147±0.076 | $3219.2^{+2017.7}_{-895.4}$ | $7.34^{+0.04}_{-0.05}$ | 9.2±0.5 | 0.2±0.1 | 0.02±0.01 | $1.98 \times 10^{1}$ | B |
| 39331 | 2 | – | 54120.299 | 10.14±0.03 | 163.5±0.1 | *Ks* | 6.388±0.087 | $4390.4^{+2751.8}_{-1221.1}$ | $7.34^{+0.04}_{-0.05}$ | 9.2±0.5 | 0.2±0.1 | 0.02±0.01 | $3.73 \times 10^{1}$ | B |
| 39906 | 1 | – | 53523.981 | 0.336±0.005 | 201.2±0.5 | *Ks* | 6.332±0.093 | $47.9^{+1.7}_{-1.6}$ | $7.66^{+0.03}_{-0.03}$ | 5.0±0.1 | 0.55±0.03 | 0.109±0.006 | $1.02 \times 10^{-3}$ | U |
| 42504 | 1 | * | 53742.180 | 16.79±0.01 | 30.73±0.04 | *Ks* | 2.677±0.027 | $2278.5^{+110.2}_{-100.5}$ | $7.2^{+0.2}_{-0.4}$ | 5.0±1.0 | 1.28±0.05 | 0.26±0.01 | $4.91 \times 10^{-1}$ | U |
| 42504 | 2 | – | 53742.180 | 0.805±0.006 | 0.7±0.3 | *Ks* | 4.790±0.039 | $109.2^{+5.3}_{-4.9}$ | $7.2^{+0.2}_{-0.4}$ | 5.0±1.0 | 0.6±0.1 | 0.11±0.02 | $5.86 \times 10^{-3}$ | nU |
| 49712 | 1 | – | 53526.996 | 0.301±0.002 | 304.7±0.7 | *Ks* | 4.364±0.018 | $122.8^{+10.4}_{-8.9}$ | $7.58^{+0.03}_{-0.03}$ | 7.5±0.2 | 2.5±0.2 | 0.33±0.03 | $3.73 \times 10^{-4}$ | U |
| 50044 | 1 | – | 53523.994 | 5.13±0.03 | 135.8±0.3 | *Ks* | 8.10±0.11 | $3827.4^{+1057.3}_{-681.2}$ | $7.78^{+0.09}_{-0.11}$ | 5.6±0.3 | 0.7±0.1 | 0.12±0.02 | $4.52 \times 10^{0}$ | U |
| 54829 | 1 | – | 55675.969 | 8.21±0.03 | 140.8±0.2 | *Ks* | 7.064±0.099 | $5547.9^{+968.9}_{-718.2}$ | $7.39^{+0.03}_{-0.04}$ | 9.1±0.4 | 0.90±0.08 | 0.10±0.01 | $6.10 \times 10^{0}$ | B |
| 62058 | 1 | – | 53415.333 | 15.16±0.02 | 89.53±0.07 | *Ks* | 7.34±0.34 | $1775.5^{+75.9}_{-70.0}$ | $7.7^{+0.1}_{-0.2}$ | 3.1620±0.0003 | 0.14±0.02 | 0.044±0.006 | $2.02 \times 10^{1}$ | B |
| 62058 | 2 | – | 53415.333 | 3.930±0.008 | 109.6±0.1 | *Ks* | 8.10±0.47 | $460.2^{+19.7}_{-18.1}$ | $7.7^{+0.1}_{-0.2}$ | 3.1620±0.0003 | 0.08±0.02 | 0.026±0.006 | $2.63 \times 10^{0}$ | nU |
| 64053 | 1 | – | 53779.324 | 13.74±0.02 | 106.09±0.08 | *Ks* | 8.36±0.26 | $1375.5^{+45.6}_{-42.7}$ | $8.0^{+0.1}_{-0.1}$ | 2.777±0.007 | 0.09±0.01 | 0.031±0.004 | $2.25 \times 10^{1}$ | B |
| 76503 | 1 | – | 56121.084 | 7.05±0.02 | 225.5±0.2 | *Ks* | 9.73±0.11 | $1342.1^{+95.9}_{-84.0}$ | $7.99^{+0.03}_{-0.03}$ | 3.9±0.1 | 0.050±0.004 | 0.013±0.001 | $9.36 \times 10^{0}$ | B |
| 77634 | 1 | – | 53406.402 | 8.48±0.03 | 180.2±0.2 | *Ks* | 8.16±0.14 | $507.8^{+8.5}_{-8.2}$ | $8.32^{+0.03}_{-0.03}$ | 3.05±0.05 | 0.15±0.01 | 0.049±0.004 | $1.46 \times 10^{0}$ | nU |
| 79410 | 1 | * | 53176.088 | 3.24±0.05 | 340.8±0.8 | *Ks* | 8.125±0.078 | $454.4^{+86.0}_{-62.6}$ | $7.9^{+0.1}_{-0.1}$ | 2.5117±0.0003 | 0.05±0.01 | 0.020±0.004 | $1.29 \times 10^{0}$ | U |
| 79622 | 1 | – | 56121.208 | 0.38±0.01 | 144.9±0.6 | *Ks* | 3.9±1.4 | $56.7^{+4.0}_{-3.6}$ | $7.81^{+0.04}_{-0.05}$ | 3.63±0.02 | 1.0±0.3 | 0.26±0.09 | $4.26 \times 10^{-4}$ | U |
| 80493 | 1 | – | 56179.066 | 0.212±0.002 | 139.0±0.5 | *Ks* | 0.7131±0.0072 | $28.5^{+3.9}_{-3.1}$ | $7.88^{+0.09}_{-0.11}$ | 2.5117±0.0003 | 1.4±0.1 | 0.54±0.06 | $5.77 \times 10^{-5}$ | nU |
| 81972 | 5 | – | 53184.214 | 7.9±0.2 | 49.5±1.0 | *Ks* | 8.848±0.073 | $1292.5^{+73.4}_{-67.2}$ | $7.2^{+0.2}_{-0.5}$ | 5.5±0.2 | 0.131±0.007 | 0.024±0.001 | $2.49 \times 10^{1}$ | B |
| 88012 | 1 | – | 53456.432 | 6.03±0.04 | 56.1±0.4 | *Ks* | 6.538±0.068 | $3349.8^{+988.3}_{-621.8}$ | $7.67^{+0.04}_{-0.04}$ | 6.5±0.2 | 0.9±0.1 | 0.14±0.02 | $1.66 \times 10^{1}$ | B |
| 88012 | 2 | – | 53456.432 | 6.91±0.04 | 244.5±0.4 | *Ks* | 7.34±0.11 | $3839.8^{+1132.9}_{-712.8}$ | $7.67^{+0.04}_{-0.04}$ | 6.5±0.2 | 0.7±0.1 | 0.11±0.02 | $2.49 \times 10^{1}$ | B |
| 89963 | 2 | – | 55761.007 | 7.06±0.02 | 9.8±0.2 | *Ks* | 6.620±0.078 | $2802.9^{+2171.3}_{-851.8}$ | $8.05^{+0.03}_{-0.03}$ | 4.5±0.1 | 1.6±0.8 | 0.4±0.2 | $2.34 \times 10^{0}$ | nU |
| 91014 | 1 | – | 53472.339 | 0.248±0.003 | 183.2±0.5 | *Ks* | 4.32±0.02 | $100.6^{+11.4}_{-9.3}$ | $7.39^{+0.04}_{-0.04}$ | 8.7±0.3 | 2.0±0.2 | 0.23±0.03 | $3.52 \times 10^{-4}$ | U |
| 99457 | 1 | – | 53512.404 | 3.49±0.02 | 150.1±0.3 | *Ks* | 4.856±0.021 | $2492.4^{+1142.4}_{-596.1}$ | $7.06^{+0.06}_{-0.07}$ | 10.9±0.4 | 1.4±0.4 | 0.13±0.04 | $1.11 \times 10^{-1}$ | U |

*Continued on next page*

Table A6 – *Continued from previous page*

| HIP | CC# | WDS desig. | MJD (days) | Θ (arcsec) | PA[a] (deg) | Band | $\Delta m$ (mag) | $a_{\rm proj.}$ (au) | $\log(Age[yr])$ | $M_1$ ($M_\odot$) | $M_{\rm comp}$ ($M_\odot$) | $q$ | Chance proj. prob. (%) | Comp. status[b] |
|---|---|---|---|---|---|---|---|---|---|---|---|---|---|---|
| 100751 | 1 | – | 53601.097 | 2.454±0.007 | 55.9±0.2 | *Ks* | 8.07±0.26 | $134.5^{+4.0}_{-3.7}$ | $7.5^{+0.1}_{-0.2}$ | 6.4±0.2 | 0.22±0.06 | 0.034±0.009 | $1.07\times10^{-2}$ | U |
| Visual binaries and multiples with more than one observation, including data points from literature | | | | | | | | | | | | | | |
| 2548 | 1 | – | 53710.049 | 0.2710±0.0009 | 278.0±0.2 | *Ks* | 1.1620±0.0044 | $21.9^{+1.0}_{-0.9}$ | $9.06^{+0.03}_{-0.04}$ | 2.00±0.01 | 1.27±0.03 | 0.64±0.01 | $3.12\times10^{-6}$ | C |
| | | | 54359.246 | 0.241±0.001 | 275.6±0.2 | *Ks* | 1.1400±0.0054 | $19.5^{+0.9}_{-0.8}$ | | 2.00±0.01 | 1.28±0.03 | 0.64±0.01 | $2.46\times10^{-6}$ | C |
| 15627 | 1 | * | 54024.221 | 0.874±0.005 | 218.4±0.5 | *H* | 2.166±0.049 | $136.3^{+17.5}_{-14.0}$ | $7.64^{+0.08}_{-0.09}$ | 4.4±0.1 | 2.1±0.2 | 0.46±0.06 | $1.11\times10^{-4}$ | U |
| 16511 | 1 | – | 53376.049 | 0.128±0.003 | 110.1±1.0 | *Ks* | 2.547±0.025 | $13.7^{+0.6}_{-0.6}$ | $8.1^{+0.1}_{-0.2}$ | 2.65±0.07 | 1.06±0.02 | 0.40±0.01 | $3.77\times10^{-6}$ | C |
| | | | 53700.139 | 0.143±0.002 | 112.6±0.3 | *Ks* | 2.710±0.025 | $15.3^{+0.7}_{-0.6}$ | | 2.65±0.07 | 1.02±0.02 | 0.38±0.01 | $4.96\times10^{-6}$ | C |
| | | | 55798.407 | 0.189±0.004 | 107.8±0.7 | *Ks* | 2.353±0.029 | $20.3^{+1.0}_{-0.9}$ | | 2.65±0.07 | 1.11±0.03 | 0.42±0.01 | $7.79\times10^{-6}$ | C |
| 16803 | 1 | – | 53379.102 | 0.195±0.001 | 84.0±0.2 | *Ks* | 0.884±0.012 | $29.0^{+2.4}_{-2.1}$ | $8.47^{+0.03}_{-0.03}$ | 3.13±0.04 | 2.4±0.1 | 0.78±0.03 | $9.22\times10^{-7}$ | C |
| | | | 54363.350 | 0.229±0.005 | 80.9±1.0 | *Ks* | 0.812±0.026 | $34.2^{+2.9}_{-2.6}$ | | 3.13±0.04 | 2.5±0.1 | 0.79±0.03 | $1.27\times10^{-6}$ | C |
| | | | 54373.246 | 0.198±0.001 | 78.4±0.3 | *Ks* | 0.798±0.013 | $29.6^{+2.4}_{-2.1}$ | | 3.13±0.04 | 2.5±0.1 | 0.79±0.03 | $9.50\times10^{-7}$ | C |
| 20020 | 1 | – | 53347.154 | 4.102±0.005 | 2.56±0.06 | *Ks* | 1.331±0.028 | $579.4^{+28.3}_{-25.8}$ | $8.26^{+0.03}_{-0.04}$ | 2.79±0.06 | 1.66±0.08 | 0.59±0.03 | $2.65\times10^{-3}$ | C |
| | | | 54363.374 | 4.115±0.007 | 1.94±0.08 | *Ks* | 1.355±0.034 | $581.2^{+28.4}_{-25.9}$ | | 2.79±0.06 | 1.64±0.08 | 0.59±0.03 | $2.67\times10^{-3}$ | C |
| | | | 54373.288 | 4.113±0.004 | 1.94±0.03 | *Ks* | 1.3306±0.0095 | $581.0^{+28.4}_{-25.9}$ | | 2.79±0.06 | 1.66±0.07 | 0.59±0.03 | $2.67\times10^{-3}$ | C |
| 20042 | 1 | AB | 53690.201 | 5.389±0.005 | 162.16±0.06 | *Ks* | 6.208±0.067 | $294.0^{+2.4}_{-2.4}$ | $7.4^{+0.2}_{-0.3}$ | 3.9807±0.0005 | 0.25±0.05 | 0.06±0.01 | $2.01\times10^{-2}$ | C |
| | | | 56189.188 | 5.431±0.009 | 162.51±0.05 | *Ks* | 7.0±0.1 | $296.3^{+2.5}_{-2.5}$ | | 3.9807±0.0005 | 0.17±0.03 | 0.042±0.007 | $4.11\times10^{-2}$ | C |
| 20554 | 1 | * | 53266.307 | 6.319±0.005 | 42.0±0.1 | *Ks* | 2.472±0.025 | $1388.8^{+175.3}_{-140.0}$ | $7.8^{+0.1}_{-0.1}$ | 3.979±0.001 | 1.00±0.07 | 0.25±0.02 | $3.44\times10^{-2}$ | C |
| 20804 | 1 | – | 53409.032 | 0.112±0.003 | 385.1±0.9 | *Ks* | 1.284±0.021 | $20.1^{+3.1}_{-2.4}$ | $8.18^{+0.05}_{-0.05}$ | 3.8±0.2 | 2.8±0.2 | 0.72±0.07 | $1.67\times10^{-6}$ | U |
| | | | 56189.333 | 0.127±0.005 | 351.0±0.4 | *Ks* | 1.349±0.021 | $22.9^{+3.6}_{-2.8}$ | | 3.8±0.2 | 2.7±0.2 | 0.71±0.07 | $2.25\times10^{-6}$ | U |
| | | | 56296.083 | 0.142±0.003 | 348.6±0.5 | *Ks* | 1.359±0.015 | $25.5^{+3.9}_{-3.0}$ | | 3.8±0.2 | 2.7±0.2 | 0.71±0.07 | $2.81\times10^{-6}$ | U |
| 23794 | 1 | AB | 53286.342 | 1.600±0.005 | 308.3±0.2 | *Ks* | 3.8271±0.0011 | $151.5^{+5.1}_{-4.7}$ | $8.73^{+0.02}_{-0.02}$ | 2.497±0.009 | 0.82±0.02 | 0.327±0.007 | $1.54\times10^{-3}$ | C |
| | | | 56296.100 | 1.588±0.002 | 309.50±0.06 | *Ks* | 3.7869±0.0012 | $150.4^{+5.0}_{-4.7}$ | | 2.497±0.009 | 0.83±0.02 | 0.332±0.007 | $1.48\times10^{-3}$ | C |
| 24196 | 1 | * | 53347.205 | 0.1456±0.0005 | 345.1±0.2 | *Ks* | 0.806±0.021 | $57.3^{+23.1}_{-12.8}$ | $8.135^{+0.009}_{-0.009}$ | 3.97±0.05 | 3.6±0.5 | 0.9±0.1 | $8.01\times10^{-6}$ | C |
| 24305 | 1 | – | 53374.161 | 0.370±0.003 | 250.2±0.2 | *Ks* | 2.034±0.045 | $21.1^{+0.7}_{-0.7}$ | $7.995^{+0.006}_{-0.006}$ | 3.97±0.02 | 1.8±0.2 | 0.45±0.06 | $5.81\times10^{-6}$ | U |
| | | | 56269.305 | 0.6172±0.0009 | 221.93±0.07 | *Ks* | 4.9289±0.0044 | $35.2^{+1.1}_{-1.1}$ | | 3.97±0.02 | 0.70±0.05 | 0.18±0.01 | $1.41\times10^{-4}$ | U |
| 24825 | 1 | – | 53471.968 | 0.287±0.004 | 297.0±0.6 | *Ks* | 4.0077±0.0086 | $75.5^{+10.7}_{-8.4}$ | $7.5^{+0.1}_{-0.2}$ | 4.5±0.1 | 0.92±0.07 | 0.21±0.02 | $1.56\times10^{-4}$ | U |
| | | | 56189.401 | 0.299±0.001 | 289.1±0.2 | *Ks* | 4.157±0.014 | $78.6^{+11.1}_{-8.7}$ | | 4.5±0.1 | 0.88±0.07 | 0.20±0.02 | $1.88\times10^{-4}$ | U |
| 24925 | 1 | Aa,Ab | 53379.159 | 0.5102±0.0008 | 199.66±0.08 | *Ks* | 2.27637±0.00077 | $143.7^{+81.0}_{-38.1}$ | $8.12^{+0.04}_{-0.05}$ | 3.8±0.1 | 2.2±0.7 | 0.6±0.2 | $1.69\times10^{-4}$ | C |
| | | | 56189.342 | 0.5084±0.0008 | 200.39±0.06 | *Ks* | 2.2885±0.0043 | $143.2^{+80.8}_{-38.0}$ | | 3.8±0.1 | 2.2±0.7 | 0.6±0.2 | $1.67\times10^{-4}$ | C |
| | | | 56296.120 | 0.5086±0.0006 | 199.49±0.06 | *Ks* | 2.258±0.001 | $143.3^{+80.8}_{-38.0}$ | | 3.8±0.1 | 2.2±0.7 | 0.6±0.2 | $1.63\times10^{-4}$ | C |
| 24925 | 2 | AB | 53379.159 | 4.570±0.006 | 284.94±0.08 | *Ks* | 2.920±0.015 | $1287.4^{+725.9}_{-341.2}$ | $8.12^{+0.04}_{-0.05}$ | 3.8±0.1 | 1.6±0.5 | 0.4±0.1 | $2.18\times10^{-2}$ | C |
| | | | 56189.342 | 4.579±0.004 | 284.79±0.05 | *Ks* | 2.988±0.022 | $1289.8^{+727.3}_{-341.8}$ | | 3.8±0.1 | 1.5±0.5 | 0.4±0.1 | $2.35\times10^{-2}$ | C |
| | | | 56296.120 | 4.586±0.005 | 283.93±0.06 | *Ks* | 3.001±0.012 | $1291.8^{+728.4}_{-342.3}$ | | 3.8±0.1 | 1.5±0.5 | 0.4±0.1 | $2.38\times10^{-2}$ | C |
| 25365 | 1 | – | 53380.142 | 0.2994±0.0003 | 174.15±0.06 | *Ks* | 0.77417±0.00064 | $64.4^{+9.2}_{-7.1}$ | $7.3^{+0.1}_{-0.2}$ | 5.1±0.1 | 2.9±0.3 | 0.58±0.06 | $2.44\times10^{-5}$ | C |
| | | | 56189.297 | 0.327±0.004 | 177.5±0.1 | *Ks* | 0.8243±0.0043 | $70.3^{+10.0}_{-7.8}$ | | 5.1±0.1 | 2.9±0.3 | 0.57±0.06 | $3.05\times10^{-5}$ | C |
| 26215 | 1 | * | 53348.200 | 2.799±0.002 | 351.90±0.04 | *Ks* | 4.166±0.017 | $961.7^{+287.7}_{-180.0}$ | $8.20^{+0.08}_{-0.10}$ | 3.6±0.1 | 2.3±0.4 | 0.6±0.1 | $1.25\times10^{-2}$ | C |
| 26235 | 1 | Aa,Ab | 54452.075 | 0.403±0.002 | 292.4±0.5 | *H* | 2.7250±0.0056 | $191.1^{+46.1}_{-31.1}$ | $7.05^{+0.03}_{-0.03}$ | 13.2±0.5 | 7.0±0.9 | 0.53±0.07 | $6.79\times10^{-5}$ | C |

*Continued on next page*

Table A6 – *Continued from previous page*

| HIP | CC# | WDS desig. | MJD (days) | Θ (arcsec) | PA[a] (deg) | Band | $\Delta m$ (mag) | $a_{\rm proj.}$ (au) | $\log(Age[yr])$ | $M_1$ ($M_\odot$) | $M_{\rm comp}$ ($M_\odot$) | $q$ | Chance proj. prob. (%) | Comp. status[b] |
|---|---|---|---|---|---|---|---|---|---|---|---|---|---|---|
| 26237 | 1 | Aa,Ab | 53469.976 | 0.151±0.001 | 330.1±0.6 | *Ks* | 0.9890±0.0089 | $40.9^{+19.7}_{-10.0}$ | $6.98^{+0.05}_{-0.06}$ | 10.9±0.4 | 7.2±2.0 | 0.7±0.2 | $4.01 \times 10^{-6}$ | U |
| | | | 56189.387 | 0.1586±0.0006 | 358.2±0.1 | *Ks* | 1.0510±0.0058 | $43.0^{+20.7}_{-10.5}$ | | 10.9±0.4 | 7.1±2.0 | 0.6±0.2 | $4.60 \times 10^{-6}$ | U |
| 26237 | 2 | AB | 53469.976 | 1.233±0.009 | 206.4±0.4 | *Ks* | 2.036±0.054 | $334.2^{+161.1}_{-82.1}$ | $6.98^{+0.05}_{-0.06}$ | 10.9±0.4 | 4.5±2.0 | 0.4±0.1 | $7.00 \times 10^{-4}$ | U |
| | | | 56189.387 | 1.205±0.001 | 204.27±0.05 | *Ks* | 2.07312±0.00018 | $326.5^{+157.4}_{-80.1}$ | | 10.9±0.4 | 4.5±2.0 | 0.4±0.1 | $6.86 \times 10^{-4}$ | U |
| 26549 | 1 | – | 53289.404 | 0.254±0.002 | 101.0±0.4 | *Ks* | 1.174±0.012 | $83.7^{+127.0}_{-62.4}$ | $7.02^{+0.02}_{-0.03}$ | 13.3±0.5 | 9.1±4.0 | 0.7±0.3 | $7.43 \times 10^{-6}$ | C |
| 26549 | 2 | AB,D | 53289.404 | 13.00±0.03 | 84.0±0.2 | *Ks* | 2.602±0.016 | $4274.9^{+6485.0}_{-3188.3}$ | $7.02^{+0.02}_{-0.03}$ | 13.3±0.5 | 6.6±5.0 | 0.5±0.4 | $5.83 \times 10^{-2}$ | C |
| 26549 | 3 | AB,G | 53289.404 | 3.224±0.009 | 20.5±0.2 | *Ks* | 5.347±0.055 | $1060.5^{+1608.8}_{-791.0}$ | $7.02^{+0.02}_{-0.03}$ | 13.3±0.5 | 2.4±2.0 | 0.2±0.2 | $3.30 \times 10^{-2}$ | U |
| 26602 | 1 | AB | 53434.070 | 0.598±0.003 | 157.5±0.6 | *Ks* | 0.789±0.016 | $283.2^{+149.8}_{-72.8}$ | $8.15^{+0.01}_{-0.01}$ | 3.8±0.2 | 4.0±0.7 | 1.1±0.2 | $1.02 \times 10^{-4}$ | C |
| | | | 56189.379 | 0.5907±0.0005 | 159.18±0.05 | *Ks* | 1.0376±0.0012 | $279.9^{+148.1}_{-72.0}$ | | 3.8±0.2 | 3.9±0.7 | 1.0±0.2 | $1.16 \times 10^{-4}$ | C |
| 28744 | 1 | * | 53456.004 | 0.582±0.003 | 271.0±0.3 | *Ks* | 4.6603±0.0029 | $234.7^{+101.8}_{-54.5}$ | $7.31^{+0.03}_{-0.04}$ | 9.5±0.4 | 2.8±0.9 | 0.29±0.09 | $5.38 \times 10^{-4}$ | C |
| | | | 56189.324 | 0.560±0.001 | 271.17±0.09 | *Ks* | 4.55±0.02 | $226.0^{+98.0}_{-52.5}$ | | 9.5±0.4 | 2.9±0.9 | 0.3±0.1 | $4.58 \times 10^{-4}$ | C |
| 29401 | 1 | * | 53741.177 | 0.689±0.001 | 203.0±0.1 | *Ks* | 1.3978±0.0048 | $121.3^{+16.8}_{-13.1}$ | $7.66^{+0.09}_{-0.11}$ | 3.20±0.06 | 2.0±0.3 | 0.64±0.08 | $2.73 \times 10^{-4}$ | C |
| | | | 56269.323 | 0.659±0.001 | 203.48±0.06 | *Ks* | 1.4168±0.0038 | $116.0^{+16.0}_{-12.6}$ | | 3.20±0.06 | 2.0±0.3 | 0.63±0.08 | $2.50 \times 10^{-4}$ | C |
| 29728 | 1 | – | 53470.975 | 0.395±0.003 | 277.8±0.5 | *Ks* | 3.8528±0.0071 | $79.2^{+7.5}_{-6.3}$ | $7.75^{+0.08}_{-0.10}$ | 4.0±1.0 | 0.92±0.06 | 0.23±0.01 | $8.60 \times 10^{-4}$ | C |
| | | | 56189.360 | 0.3905±0.0007 | 282.5±0.1 | *Ks* | 3.85±0.01 | $78.2^{+7.4}_{-6.2}$ | | 4.0±1.0 | 0.92±0.06 | 0.23±0.01 | $8.39 \times 10^{-4}$ | C |
| 30493 | 1 | * | 53435.117 | 0.714±0.002 | 273.0±0.5 | *Ks* | 1.4331±0.0058 | $173.0^{+42.9}_{-28.7}$ | $8.3^{+0.1}_{-0.1}$ | 2.93±0.08 | 2.0±0.3 | 0.7±0.1 | $7.54 \times 10^{-4}$ | U |
| | | | 56189.395 | 0.6829±0.0006 | 273.78±0.06 | *Ks* | 1.4073±0.0014 | $165.3^{+41.0}_{-27.4}$ | | 2.93±0.08 | 2.0±0.3 | 0.7±0.1 | $6.76 \times 10^{-4}$ | U |
| 30867 | 1 | AB | 53469.984 | 7.14±0.06 | 132.4±0.5 | *Ks* | 1.4915±0.0045 | $1480.4^{+448.3}_{-279.4}$ | $7.62^{+0.03}_{-0.03}$ | 6.6±0.2 | 5.9±0.7 | 0.9±0.1 | $4.94 \times 10^{-3}$ | C |
| | | | 56189.317 | 7.117±0.006 | 132.63±0.05 | *Ks* | 1.5867±0.0081 | $1476.6^{+447.0}_{-278.4}$ | | 6.6±0.2 | 5.8±0.7 | 0.9±0.1 | $5.22 \times 10^{-3}$ | C |
| 31137 | 1 | * | 53470.984 | 2.45±0.01 | 229.5±0.3 | *Ks* | 2.749±0.011 | $568.3^{+55.0}_{-46.2}$ | $8.37^{+0.03}_{-0.04}$ | 3.4±0.1 | 1.9±0.1 | 0.56±0.04 | $2.94 \times 10^{-3}$ | C |
| | | | 56189.351 | 2.451±0.002 | 229.10±0.08 | *Ks* | 2.804±0.018 | $568.6^{+55.0}_{-46.1}$ | | 3.4±0.1 | 1.9±0.1 | 0.54±0.04 | $2.99 \times 10^{-3}$ | C |
| 31959 | 1 | – | 54409.342 | 1.695±0.006 | 326.8±0.5 | *H* | 5.3509±0.0053 | $1039.9^{+725.8}_{-303.0}$ | $7.3^{+0.1}_{-0.2}$ | 5.8±0.3 | 0.7±0.3 | 0.12±0.05 | $1.06 \times 10^{-1}$ | nC |
| | | | 54470.143 | 1.695±0.006 | 326.7±0.5 | *H* | 5.248±0.037 | $1039.7^{+725.7}_{-302.9}$ | | 5.8±0.3 | 0.7±0.3 | 0.12±0.05 | $9.77 \times 10^{-2}$ | nC |
| | | | 56266.100 | 1.70±0.01 | 327.4±0.3 | *Ks* | 5.1416±0.0042 | $1043.3^{+728.2}_{-304.0}$ | | 5.8±0.3 | 0.7±0.3 | 0.12±0.05 | $9.88 \times 10^{-2}$ | nC |
| 34045 | 1 | – | 53408.131 | 0.3353±0.0006 | 114.9±0.2 | *Ks* | 4.6730±0.0075 | $45.4^{+1.3}_{-1.3}$ | $7.94^{+0.01}_{-0.01}$ | 5.00±0.04 | 1.06±0.02 | 0.211±0.004 | $2.86 \times 10^{-4}$ | U |
| | | | 56298.140 | 0.3321±0.0009 | 100.6±0.1 | *Ks* | 4.690±0.011 | $45.0^{+1.3}_{-1.3}$ | | 5.00±0.04 | 1.05±0.02 | 0.210±0.004 | $2.83 \times 10^{-4}$ | U |
| 34338 | 1 | – | 53408.163 | 3.664±0.004 | 345.52±0.06 | *Ks* | 3.759±0.017 | $746.3^{+53.8}_{-47.0}$ | $8.63^{+0.06}_{-0.07}$ | 2.8±0.1 | | | $6.21 \times 10^{-2}$ | B |
| | | | 56296.212 | 3.704±0.004 | 346.48±0.06 | *Ks* | 3.760±0.014 | $754.4^{+54.4}_{-47.5}$ | | 2.8±0.1 | | | $6.35 \times 10^{-2}$ | B |
| 34758 | 1 | – | 53413.189 | 13.72±0.02 | 348.03±0.09 | *Ks* | 5.62±0.15 | $1965.8^{+113.2}_{-101.5}$ | $8.77^{+0.02}_{-0.02}$ | 2.52±0.05 | | | $3.19 \times 10^{0}$ | nB |
| | | | 54425.348 | 13.65±0.02 | 347.55±0.08 | *Ks* | 5.699±0.084 | $1956.3^{+112.7}_{-101.0}$ | | 2.52±0.05 | | | $3.36 \times 10^{0}$ | nB |
| 36345 | 1 | * | 54839.338 | 8.919±0.009 | 53.1±0.5 | *Ks* | 0.8353±0.0088 | $2036.3^{+329.5}_{-248.9}$ | $6.7^{+0.2}_{-0.6}$ | 6.7±0.3 | 2.0±0.6 | 0.30±0.09 | $9.54 \times 10^{-2}$ | C |
| 36363 | 1 | – | 53384.187 | 5.49±0.01 | 299.6±0.2 | *Ks* | 5.85±0.23 | $906.3^{+34.2}_{-31.8}$ | $7.2^{+0.2}_{-0.6}$ | 5.5±0.2 | 0.36±0.09 | 0.07±0.02 | $4.22 \times 10^{-1}$ | nU |
| | | | 54427.198 | 5.46±0.01 | 298.96±0.08 | *Ks* | 6.20±0.14 | $901.1^{+34.0}_{-31.6}$ | | 5.5±0.2 | 0.31±0.05 | 0.06±0.01 | $5.37 \times 10^{-1}$ | nU |
| 37322 | 1 | * | 53384.200 | 1.281±0.002 | 149.81±0.08 | *Ks* | 2.1630±0.0029 | $224.8^{+11.2}_{-10.2}$ | $7.5^{+0.2}_{-0.3}$ | 4.4±0.2 | 1.7±0.1 | 0.38±0.03 | $2.19 \times 10^{-3}$ | C |
| | | | 54412.365 | 1.282±0.002 | 149.29±0.06 | *Ks* | 2.1677±0.0019 | $224.9^{+11.2}_{-10.2}$ | | 4.4±0.2 | 1.7±0.1 | 0.38±0.03 | $2.19 \times 10^{-3}$ | C |
| 37915 | 1 | – | 53384.257 | 0.1821±0.0006 | 15.3±0.3 | *Ks* | 2.129±0.013 | $33.0^{+1.5}_{-1.4}$ | $7.5^{+0.1}_{-0.2}$ | 3.99±0.05 | 1.59±0.07 | 0.40±0.02 | $5.62 \times 10^{-5}$ | nC |
| | | | 54427.184 | 0.184±0.004 | 4.9±0.5 | *Ks* | 1.929±0.041 | $33.3^{+1.7}_{-1.6}$ | | 3.99±0.05 | 1.9±0.1 | 0.47±0.02 | $5.07 \times 10^{-5}$ | nC |

*Continued on next page*

Table A6 – *Continued from previous page*

| HIP | CC# | WDS desig. | MJD (days) | Θ (arcsec) | PA[a] (deg) | Band | $\Delta m$ (mag) | $a_{\rm proj.}$ (au) | $\log(Age[yr])$ | $M_1$ ($M_\odot$) | $M_{\rm comp}$ ($M_\odot$) | $q$ | Chance proj. prob. (%) | Comp. status[b] |
|---|---|---|---|---|---|---|---|---|---|---|---|---|---|---|
| 40817 | 1 | – | 53415.171 | 1.417±0.001 | 9.33±0.06 | *Ks* | 2.7743±0.0095 | $188.9^{+9.3}_{-8.4}$ | $8.43^{+0.03}_{-0.03}$ | 3.06±0.05 | 1.30±0.04 | 0.42±0.01 | $1.03 \times 10^{-3}$ | nC |
| | | | 54451.318 | 1.401±0.003 | 8.6±0.1 | *Ks* | 2.6843±0.0099 | $186.8^{+9.2}_{-8.3}$ | | 3.06±0.05 | 1.33±0.04 | 0.44±0.02 | $9.16 \times 10^{-4}$ | nC |
| | | | 54467.291 | 1.403±0.002 | 8.52±0.05 | *Ks* | 2.7328±0.0053 | $187.0^{+9.2}_{-8.3}$ | | 3.06±0.05 | 1.31±0.04 | 0.43±0.01 | $9.54 \times 10^{-4}$ | nC |
| 41049 | 1 | * | 53099.999 | 10.30±0.01 | 54.7±0.5 | *Ks* | 1.173±0.022 | $6867.9^{+7641.7}_{-2369.3}$ | $8.2^{+0.1}_{-0.2}$ | 2.7±0.1 | 2.4±1.0 | 0.9±0.4 | $9.62 \times 10^{-1}$ | C |
| 41817 | 1 | – | 53413.218 | 0.322±0.001 | 302.8±0.2 | *Ks* | 0.5936±0.0018 | $34.0^{+2.3}_{-2.0}$ | $8.36^{+0.06}_{-0.06}$ | 2.61±0.09 | 2.1±0.1 | 0.79±0.05 | $1.82 \times 10^{-5}$ | C |
| | | | 54425.296 | 0.3379±0.0008 | 297.8±0.1 | *Ks* | 0.5980±0.0027 | $35.8^{+2.4}_{-2.1}$ | | 2.61±0.09 | 2.1±0.1 | 0.79±0.05 | $2.01 \times 10^{-5}$ | C |
| 41843 | 1 | – | 53404.245 | 0.676±0.003 | 332.1±0.3 | *Ks* | 7.026±0.018 | $150.6^{+14.7}_{-12.3}$ | $8.76^{+0.02}_{-0.02}$ | 2.51±0.02 | 0.27±0.02 | 0.109±0.009 | $8.73 \times 10^{-3}$ | C |
| | | | 56326.142 | 0.665±0.005 | 332.4±0.5 | *Ks* | 7.133±0.044 | $148.2^{+14.5}_{-12.2}$ | | 2.51±0.02 | 0.26±0.02 | 0.103±0.009 | $9.16 \times 10^{-3}$ | C |
| 42129 | 1 | * | 53738.190 | 0.6587±0.0009 | 301.2±0.1 | *Ks* | 2.7735±0.0036 | $181.0^{+15.7}_{-13.4}$ | $7.61^{+0.09}_{-0.12}$ | 6.6±0.3 | 2.7±0.2 | 0.40±0.03 | $6.03 \times 10^{-4}$ | U |
| | | | 54451.330 | 0.664±0.002 | 301.6±0.1 | *Ks* | 2.833±0.012 | $182.3^{+15.8}_{-13.5}$ | | 6.6±0.3 | 2.6±0.2 | 0.39±0.03 | $6.36 \times 10^{-4}$ | U |
| 42177 | 1 | * | 53404.271 | 0.5679±0.0005 | 219.79±0.05 | *Ks* | 2.4106±0.0022 | $77.7^{+2.8}_{-2.6}$ | $8.20^{+0.04}_{-0.04}$ | 3.09±0.09 | 1.21±0.02 | 0.39±0.01 | $6.78 \times 10^{-4}$ | C |
| 42334 | 1 | AD | 53434.185 | 3.210±0.006 | 10.9±0.1 | *Ks* | 7.8±0.2 | $228.1^{+3.5}_{-3.4}$ | $9.07^{+0.02}_{-0.02}$ | 1.9943±0.0001 | 0.124±0.009 | 0.062±0.004 | $3.94 \times 10^{-1}$ | C |
| | | | 54508.151 | 3.205±0.007 | 10.8±0.1 | *Ks* | 7.31±0.37 | $227.8^{+3.5}_{-3.4}$ | | 1.9943±0.0001 | 0.15±0.02 | 0.08±0.01 | $2.71 \times 10^{-1}$ | C |
| 42540 | 1 | * | 53375.255 | 4.564±0.007 | 67.43±0.09 | *Ks* | 2.263±0.045 | $390.8^{+17.5}_{-16.1}$ | $8.3^{+0.1}_{-0.2}$ | 2.5113±0.0008 | 1.17±0.03 | 0.46±0.01 | $2.32 \times 10^{-2}$ | C |
| | | | 54451.341 | 4.580±0.007 | 67.08±0.09 | *Ks* | 2.250±0.049 | $392.1^{+17.5}_{-16.1}$ | | 2.5113±0.0008 | 1.17±0.03 | 0.47±0.01 | $2.33 \times 10^{-2}$ | C |
| 42715 | 1 | BC | 53742.219 | 0.587±0.001 | 162.28±0.08 | *Ks* | 1.632±0.004 | $89.9^{+3.7}_{-3.4}$ | $8.42^{+0.02}_{-0.03}$ | 3.05±0.04 | 1.85±0.05 | 0.61±0.02 | $3.30 \times 10^{-4}$ | C |
| | | | 54509.215 | 0.590±0.001 | 162.93±0.09 | *Ks* | 1.6177±0.0034 | $90.4^{+3.8}_{-3.5}$ | | 3.05±0.04 | 1.86±0.05 | 0.61±0.02 | $3.31 \times 10^{-4}$ | C |
| 43305 | 1 | * | 53379.290 | 1.315±0.001 | 167.48±0.06 | *Ks* | 3.94±0.01 | $181.6^{+6.2}_{-5.8}$ | $8.21^{+0.04}_{-0.04}$ | 3.3±0.1 | 0.97±0.02 | 0.29±0.01 | $1.37 \times 10^{-3}$ | C |
| | | | 54509.232 | 1.309±0.002 | 168.11±0.09 | *Ks* | 3.7493±0.0082 | $180.8^{+6.2}_{-5.8}$ | | 3.3±0.1 | 1.02±0.02 | 0.31±0.01 | $1.12 \times 10^{-3}$ | C |
| 43792 | 1 | * | 52659.321 | 2.2523±0.0004 | 303.61±0.02 | *Ks* | 1.212±0.028 | $2208.2^{+110409.2}_{-1093.2}$ | $7.19^{+0.05}_{-0.05}$ | 8.2±0.2 | | | $2.39 \times 10^{-2}$ | B |
| 44299 | 1 | – | 53750.090 | 10.47±0.01 | 222.84±0.07 | *Ks* | 7.54±0.16 | $1377.6^{+86.7}_{-77.0}$ | $7.4^{+0.1}_{-0.2}$ | 3.9808±0.0002 | | | $1.04 \times 10^{1}$ | nB |
| | | | 54451.354 | 10.51±0.01 | 222.24±0.09 | *Ks* | 6.69±0.31 | $1382.8^{+87.1}_{-77.3}$ | | 3.9808±0.0002 | | | $5.66 \times 10^{0}$ | nB |
| 44798 | 1 | * | 53380.279 | 0.2684±0.0004 | 109.47±0.08 | *Ks* | 2.6738±0.0095 | $43.7^{+1.9}_{-1.8}$ | $8.14^{+0.03}_{-0.03}$ | 3.91±0.08 | 1.58±0.06 | 0.40±0.02 | $1.70 \times 10^{-5}$ | C |
| 44883 | 1 | * | 53382.271 | 1.293±0.002 | 299.34±0.09 | *Ks* | 2.9970±0.0049 | $243.5^{+31.6}_{-25.1}$ | $8.16^{+0.06}_{-0.07}$ | 3.9±0.1 | 1.5±0.1 | 0.37±0.03 | $7.09 \times 10^{-4}$ | C |
| | | | 54468.304 | 1.301±0.002 | 299.5±0.1 | *Ks* | 3.0014±0.0058 | $245.1^{+31.8}_{-25.3}$ | | 3.9±0.1 | 1.5±0.1 | 0.37±0.03 | $7.18 \times 10^{-4}$ | C |
| 45189 | 1 | AB | 53382.319 | 2.842±0.004 | 281.24±0.08 | *Ks* | 0.634±0.029 | $603.4^{+65.3}_{-53.7}$ | $8.20^{+0.03}_{-0.03}$ | 3.9±0.1 | 3.2±0.2 | 0.83±0.05 | $4.65 \times 10^{-3}$ | C |
| | | | 54467.304 | 2.860±0.004 | 280.57±0.08 | *Ks* | 0.619±0.012 | $607.3^{+65.7}_{-54.0}$ | | 3.9±0.1 | 3.3±0.2 | 0.84±0.05 | $4.71 \times 10^{-3}$ | C |
| 45314 | 1 | – | 53355.364 | 2.726±0.004 | 337.00±0.07 | *Ks* | 6.37±0.17 | $439.7^{+20.0}_{-18.4}$ | $7.65^{+0.06}_{-0.07}$ | 3.39±0.09 | 0.29±0.04 | 0.08±0.01 | $3.87 \times 10^{-1}$ | nC |
| | | | 54511.144 | 2.736±0.006 | 336.3±0.1 | *Ks* | 6.36±0.13 | $441.3^{+20.1}_{-18.4}$ | | 3.39±0.09 | 0.29±0.03 | 0.09±0.01 | $3.84 \times 10^{-1}$ | nC |
| | | | 56265.357 | 2.737±0.004 | 336.21±0.06 | *Ks* | 6.232±0.055 | $441.4^{+20.1}_{-18.4}$ | | 3.39±0.09 | 0.31±0.03 | 0.092±0.008 | $3.51 \times 10^{-1}$ | nC |
| 45344 | 1 | – | 53349.377 | 5.907±0.009 | 13.65±0.07 | *Ks* | 3.317±0.039 | $1108.2^{+56.9}_{-51.6}$ | $7.84^{+0.02}_{-0.02}$ | 4.9±0.1 | 1.33±0.05 | 0.27±0.01 | $1.05 \times 10^{-1}$ | C |
| | | | 54511.158 | 5.900±0.007 | 13.16±0.07 | *Ks* | 3.355±0.047 | $1107.0^{+56.8}_{-51.5}$ | | 4.9±0.1 | 1.31±0.05 | 0.27±0.01 | $1.09 \times 10^{-1}$ | C |
| 46283 | 1 | – | 53750.263 | 0.341±0.002 | 159.2±0.3 | *Ks* | 4.625±0.033 | $44.8^{+1.1}_{-1.1}$ | $7.5^{+0.1}_{-0.2}$ | 3.98±0.02 | 0.72±0.03 | 0.182±0.008 | $7.12 \times 10^{-4}$ | nU |
| | | | 54475.312 | 0.348±0.005 | 155.4±0.2 | *Ks* | 4.783±0.053 | $45.8^{+1.3}_{-1.2}$ | | 3.98±0.02 | 0.69±0.04 | 0.17±0.01 | $8.32 \times 10^{-4}$ | nU |
| 46329 | 1 | * | 53454.111 | 0.548±0.003 | 280.8±0.3 | *Ks* | 1.0107±0.0016 | $344.4^{+250.8}_{-102.1}$ | $7.79^{+0.03}_{-0.03}$ | 5.5±0.1 | 4.7±1.0 | 0.8±0.2 | $1.07 \times 10^{-4}$ | U |
| 46594 | 1 | – | 53753.228 | 12.61±0.02 | 167.68±0.06 | *Ks* | 4.594±0.055 | $1672.7^{+45.6}_{-43.3}$ | $7.87^{+0.04}_{-0.04}$ | 3.20±0.09 | | | $1.25 \times 10^{0}$ | nB |
| | | | 54535.097 | 12.65±0.02 | 166.99±0.07 | *Ks* | 4.463±0.056 | $1678.0^{+45.8}_{-43.4}$ | | 3.20±0.09 | | | $1.12 \times 10^{0}$ | nB |

*Continued on next page*

Table A6 – *Continued from previous page*

| HIP | CC# | WDS desig. | MJD (days) | Θ (arcsec) | PA[a] (deg) | Band | $\Delta m$ (mag) | $a_{\rm proj.}$ (au) | $\log(Age[yr])$ | $M_1$ ($M_\odot$) | $M_{\rm comp}$ ($M_\odot$) | $q$ | Chance proj. prob. (%) | Comp. status[b] |
|---|---|---|---|---|---|---|---|---|---|---|---|---|---|---|
| 46594 | 2 | – | 53753.228 | 17.48±0.02 | 130.90±0.06 | *Ks* | 5.040±0.072 | $2318.2^{+63.2}_{-60.0}$ | $7.87^{+0.04}_{-0.04}$ | 3.20±0.09 | | | $3.38 \times 10^{0}$ | nB |
| | | | 54535.097 | 17.43±0.02 | 130.40±0.06 | *Ks* | 4.944±0.071 | $2312.2^{+63.1}_{-59.8}$ | | 3.20±0.09 | | | $3.15 \times 10^{0}$ | nB |
| 46914 | 1 | * | 53442.136 | 2.018±0.003 | 219.76±0.08 | *Ks* | 0.775±0.016 | $513.4^{+73.1}_{-56.9}$ | $7.95^{+0.02}_{-0.02}$ | 4.99±0.06 | 4.4±0.2 | 0.88±0.04 | $1.68 \times 10^{-3}$ | C |
| | | | 54535.108 | 2.022±0.002 | 219.64±0.05 | *Ks* | 0.709±0.023 | $514.5^{+73.3}_{-57.0}$ | | 4.99±0.06 | 4.4±0.2 | 0.89±0.04 | $1.64 \times 10^{-3}$ | C |
| 46928 | 1 | – | 53778.238 | 0.594±0.001 | 189.6±0.1 | *Ks* | 4.373±0.017 | $104.2^{+2.8}_{-2.7}$ | $7.742^{+0.002}_{-0.002}$ | 4.99±0.02 | 1.00±0.02 | 0.199±0.003 | $6.65 \times 10^{-4}$ | nC |
| | | | 54475.332 | 0.606±0.004 | 188.2±0.3 | *Ks* | 4.37±0.02 | $106.2^{+2.9}_{-2.8}$ | | 4.99±0.02 | 1.00±0.02 | 0.200±0.003 | $6.92 \times 10^{-4}$ | nC |
| 48943 | 1 | * | 53493.025 | 0.507±0.004 | 351.8±0.4 | *Ks* | 3.1781±0.0021 | $124.0^{+19.3}_{-14.7}$ | $7.65^{+0.04}_{-0.05}$ | 4.73±0.05 | 1.4±0.1 | 0.29±0.03 | $2.17 \times 10^{-4}$ | C |
| 50847 | 1 | – | 53779.196 | 2.222±0.002 | 350.18±0.06 | *Ks* | 5.513±0.042 | $273.6^{+6.2}_{-5.9}$ | $8.21^{+0.04}_{-0.04}$ | 3.3±0.1 | 0.57±0.01 | 0.174±0.008 | $6.31 \times 10^{-2}$ | C |
| | | | 55673.115 | 2.221±0.002 | 350.22±0.06 | *Ks* | 5.553±0.035 | $273.5^{+6.2}_{-5.9}$ | | 3.3±0.1 | 0.56±0.01 | 0.171±0.008 | $6.46 \times 10^{-2}$ | C |
| 51362 | 1 | – | 53185.016 | 5.155±0.009 | 70.4±0.1 | *Ks* | 8.11±0.28 | $508.9^{+11.9}_{-11.3}$ | $8.75^{+0.02}_{-0.02}$ | 2.49±0.02 | 0.15±0.02 | 0.060±0.007 | $2.15 \times 10^{-1}$ | nC |
| | | | 53846.122 | 5.17±0.01 | 70.4±0.1 | *Ks* | 8.08±0.22 | $509.9^{+11.9}_{-11.4}$ | | 2.49±0.02 | 0.15±0.01 | 0.061±0.006 | $2.11 \times 10^{-1}$ | nC |
| 51376 | 1 | * | 53405.279 | 11.09±0.02 | 225.54±0.09 | *Ks* | 3.219±0.073 | $1476.6^{+100.9}_{-88.7}$ | $8.76^{+0.02}_{-0.02}$ | 2.53±0.05 | 1.07±0.04 | 0.42±0.02 | $7.45 \times 10^{-2}$ | C |
| | | | 53415.316 | 11.09±0.02 | 225.5±0.1 | *Ks* | 3.493±0.041 | $1476.5^{+100.9}_{-88.7}$ | | 2.53±0.05 | 1.00±0.04 | 0.40±0.02 | $8.71 \times 10^{-2}$ | C |
| | | | 54521.197 | 11.09±0.02 | 224.98±0.08 | *Ks* | 3.335±0.045 | $1477.0^{+100.9}_{-88.8}$ | | 2.53±0.05 | 1.04±0.04 | 0.41±0.02 | $7.97 \times 10^{-2}$ | C |
| 51376 | 2 | * | 53405.279 | 10.93±0.02 | 225.92±0.09 | *Ks* | 3.310±0.076 | $1454.8^{+99.4}_{-87.4}$ | $8.76^{+0.02}_{-0.02}$ | 2.53±0.05 | 1.04±0.04 | 0.41±0.02 | $7.52 \times 10^{-2}$ | C |
| | | | 53415.316 | 10.92±0.02 | 225.9±0.1 | *Ks* | 3.614±0.043 | $1454.7^{+99.4}_{-87.4}$ | | 2.53±0.05 | 0.97±0.04 | 0.38±0.02 | $9.11 \times 10^{-2}$ | C |
| | | | 54521.197 | 10.94±0.02 | 225.47±0.08 | *Ks* | 3.452±0.048 | $1456.6^{+99.5}_{-87.5}$ | | 2.53±0.05 | 1.01±0.04 | 0.40±0.02 | $8.26 \times 10^{-2}$ | C |
| 52742 | 1 | – | 53794.080 | 1.056±0.005 | 8.49±0.07 | *Ks* | 6.737±0.033 | $170.4^{+5.4}_{-5.1}$ | $8.17^{+0.04}_{-0.05}$ | 3.96±0.02 | 0.47±0.01 | 0.118±0.003 | $3.88 \times 10^{-2}$ | nC |
| | | | 54483.355 | 1.059±0.004 | 8.19±0.06 | *Ks* | 6.92±0.06 | $170.8^{+5.4}_{-5.1}$ | | 3.96±0.02 | 0.43±0.02 | 0.110±0.004 | $4.48 \times 10^{-2}$ | nC |
| 53272 | 1 | * | 53779.256 | 1.521±0.001 | 288.27±0.06 | *Ks* | 0.6051±0.0015 | $354.5^{+38.5}_{-31.6}$ | $7.97^{+0.06}_{-0.07}$ | 4.1±0.1 | 3.7±0.2 | 0.89±0.06 | $1.26 \times 10^{-3}$ | C |
| | | | 54511.296 | 1.525±0.001 | 287.78±0.05 | *Ks* | 0.594±0.001 | $355.5^{+38.6}_{-31.7}$ | | 4.1±0.1 | 3.7±0.2 | 0.89±0.06 | $1.24 \times 10^{-3}$ | C |
| 54413 | 1 | – | 54158.304 | 6.823±0.007 | 13.62±0.06 | *Ks* | 10.0±0.2 | $1081.3^{+117.8}_{-96.7}$ | $8.2^{+0.1}_{-0.1}$ | 2.71±0.05 | | | $1.05 \times 10^{1}$ | B |
| | | | 54516.365 | 6.83±0.02 | 13.7±0.1 | *Ks* | 10.21±0.21 | $1082.7^{+118.0}_{-96.9}$ | | 2.71±0.05 | | | $1.07 \times 10^{1}$ | B |
| | | | 54882.153 | 6.82±0.02 | 13.9±0.1 | *Ks* | 9.76±0.11 | $1081.6^{+117.9}_{-96.8}$ | | 2.71±0.05 | | | $1.02 \times 10^{1}$ | B |
| | | | 55555.332 | 6.820±0.009 | 14.07±0.08 | *Ks* | 9.86±0.13 | $1080.8^{+117.8}_{-96.7}$ | | 2.71±0.05 | | | $1.04 \times 10^{1}$ | B |
| | | | 55645.122 | 6.83±0.02 | 14.2±0.1 | *Ks* | 9.44±0.13 | $1082.6^{+118.0}_{-96.9}$ | | 2.71±0.05 | | | $8.65 \times 10^{0}$ | B |
| 54413 | 2 | – | 54158.304 | 4.395±0.006 | 302.2±0.1 | *Ks* | 9.9±0.2 | $696.4^{+75.9}_{-62.3}$ | $8.2^{+0.1}_{-0.1}$ | 2.71±0.05 | | | $4.50 \times 10^{0}$ | B |
| | | | 54516.365 | 4.37±0.02 | 302.3±0.1 | *Ks* | 10.07±0.19 | $693.3^{+75.6}_{-62.1}$ | | 2.71±0.05 | | | $4.50 \times 10^{0}$ | B |
| | | | 54882.153 | 4.38±0.02 | 302.5±0.1 | *Ks* | 9.96±0.12 | $693.9^{+75.6}_{-62.1}$ | | 2.71±0.05 | | | $4.47 \times 10^{0}$ | B |
| | | | 55555.332 | 4.366±0.006 | 302.7±0.1 | *Ks* | 9.87±0.13 | $691.9^{+75.4}_{-61.9}$ | | 2.71±0.05 | | | $4.40 \times 10^{0}$ | B |
| | | | 55645.122 | 4.36±0.02 | 302.7±0.1 | *Ks* | 9.55±0.13 | $691.3^{+75.4}_{-61.9}$ | | 2.71±0.05 | | | $3.91 \times 10^{0}$ | B |
| 54557 | 1 | * | 53794.134 | 0.786±0.002 | 327.08±0.09 | *Ks* | 3.0676±0.0019 | $140.3^{+26.2}_{-19.1}$ | $8.0^{+0.1}_{-0.2}$ | 2.512±0.001 | 0.93±0.08 | 0.37±0.03 | $2.81 \times 10^{-3}$ | C |
| | | | 53820.400 | 0.787±0.002 | 326.8±0.2 | *Ks* | 3.1159±0.0026 | $140.5^{+26.2}_{-19.1}$ | | 2.512±0.001 | 0.92±0.08 | 0.37±0.03 | $2.89 \times 10^{-3}$ | C |
| | | | 54160.099 | 0.784±0.003 | 326.6±0.1 | *Ks* | 2.9545±0.0012 | $140.1^{+26.1}_{-19.0}$ | | 2.512±0.001 | 0.96±0.08 | 0.38±0.03 | $2.63 \times 10^{-3}$ | C |
| | | | 54516.213 | 0.783±0.003 | 326.1±0.1 | *Ks* | 2.9758±0.0015 | $139.8^{+26.1}_{-19.0}$ | | 2.512±0.001 | 0.96±0.08 | 0.38±0.03 | $2.65 \times 10^{-3}$ | C |
| | | | 55605.340 | 0.783±0.002 | 324.3±0.1 | *J* | 3.890±0.014 | $139.8^{+26.1}_{-19.0}$ | | 2.512±0.001 | 0.88±0.08 | 0.35±0.03 | $3.76 \times 10^{-3}$ | C |
| | | | 55605.340 | | 324.3±0.1 | *Ks* | 3.0289±0.0021 | $139.8^{+26.1}_{-19.0}$ | | 2.512±0.001 | 0.88±0.08 | 0.35±0.03 | $2.71 \times 10^{-3}$ | C |

*Continued on next page*

Table A6 – *Continued from previous page*

| HIP | CC# | WDS desig. | MJD (days) | Θ (arcsec) | PA[a] (deg) | Band | $\Delta m$ (mag) | $a_{\rm proj.}$ (au) | $\log(Age[yr])$ | $M_1$ ($M_\odot$) | $M_{\rm comp}$ ($M_\odot$) | $q$ | Chance proj. prob. (%) | Comp. status[b] |
|---|---|---|---|---|---|---|---|---|---|---|---|---|---|---|
| 55597 | 1 | * | 53752.367 | 2.488±0.002 | 309.33±0.05 | *Ks* | 0.8758±0.0083 | $308.0^{+15.2}_{-13.8}$ | $7.4^{+0.2}_{-0.3}$ | 3.99±0.04 | 3.0±0.1 | 0.74±0.03 | $2.14 \times 10^{-3}$ | C |
| | | | 54520.280 | 2.488±0.002 | 308.98±0.02 | *Ks* | 0.952±0.044 | $307.9^{+15.2}_{-13.8}$ | | 3.99±0.04 | 2.9±0.1 | 0.73±0.04 | $2.33 \times 10^{-3}$ | C |
| 55657 | 1 | – | 53741.381 | 6.168±0.004 | 115.52±0.06 | *Ks* | 8.16±0.24 | $1880.4^{+128.6}_{-113.2}$ | $7.49^{+0.05}_{-0.05}$ | 7.5±0.1 | 0.33±0.05 | 0.045±0.007 | $3.00 \times 10^{0}$ | nU |
| | | | 54520.291 | 6.183±0.008 | 115.2±0.1 | *Ks* | 8.2±0.4 | $1885.1^{+129.0}_{-113.5}$ | | 7.5±0.1 | 0.33±0.07 | 0.04±0.01 | $3.03 \times 10^{0}$ | nU |
| 56000 | 1 | * | 53408.250 | 13.06±0.02 | 168.56±0.08 | *Ks* | 2.648±0.037 | $2803.3^{+495.5}_{-366.1}$ | $8.30^{+0.03}_{-0.03}$ | 3.6±0.1 | 2.3±0.2 | 0.65±0.07 | $7.75 \times 10^{-2}$ | U |
| | | | 54520.301 | 13.06±0.02 | 167.90±0.07 | *Ks* | 2.987±0.055 | $2802.7^{+495.5}_{-366.1}$ | | 3.6±0.1 | 2.1±0.2 | 0.58±0.07 | $9.71 \times 10^{-2}$ | U |
| 56000 | 2 | * | 53408.250 | 13.06±0.02 | 168.02±0.08 | *Ks* | 3.325±0.051 | $2801.8^{+495.3}_{-365.9}$ | $8.30^{+0.03}_{-0.03}$ | 3.6±0.1 | 1.7±0.2 | 0.49±0.07 | $1.35 \times 10^{-1}$ | U |
| | | | 54520.301 | 13.02±0.02 | 167.44±0.07 | *Ks* | 3.421±0.068 | $2794.5^{+494.0}_{-365.0}$ | | 3.6±0.1 | 1.7±0.2 | 0.47±0.06 | $1.40 \times 10^{-1}$ | U |
| 56754 | 1 | – | 53403.363 | 0.3364±0.0003 | 104.06±0.05 | *Ks* | 1.82548±0.00097 | $29.4^{+1.1}_{-1.0}$ | $8.23^{+0.04}_{-0.04}$ | 2.75±0.05 | 1.40±0.03 | 0.51±0.02 | $8.96 \times 10^{-5}$ | C |
| | | | 54475.353 | 0.3698±0.0005 | 107.54±0.09 | *Ks* | 1.813±0.011 | $32.3^{+1.2}_{-1.1}$ | | 2.75±0.05 | 1.40±0.03 | 0.51±0.02 | $1.07 \times 10^{-4}$ | C |
| | | | 55673.077 | 0.392±0.001 | 111.3±0.2 | *Ks* | 1.8215±0.0034 | $34.2^{+1.3}_{-1.2}$ | | 2.75±0.05 | 1.40±0.03 | 0.51±0.02 | $1.22 \times 10^{-4}$ | C |
| 56754 | 2 | – | 53403.363 | 8.432±0.005 | 184.97±0.04 | *Ks* | 6.10±0.05 | $737.0^{+28.1}_{-26.1}$ | $8.23^{+0.04}_{-0.04}$ | 2.75±0.05 | 0.33±0.01 | 0.121±0.006 | $2.25 \times 10^{0}$ | nU |
| | | | 54475.353 | 8.46±0.01 | 184.61±0.07 | *Ks* | 6.19±0.11 | $739.8^{+28.2}_{-26.2}$ | | 2.75±0.05 | 0.32±0.02 | 0.115±0.008 | $2.45 \times 10^{0}$ | nU |
| | | | 55673.077 | 8.428±0.008 | 184.17±0.05 | *Ks* | 6.269±0.066 | $736.7^{+28.1}_{-26.1}$ | | 2.75±0.05 | 0.30±0.02 | 0.111±0.006 | $2.60 \times 10^{0}$ | nU |
| 58326 | 1 | AE | 53779.305 | 4.950±0.005 | 137.71±0.05 | *Ks* | 7.24±0.14 | $927.0^{+45.5}_{-41.5}$ | $7.1^{+0.3}_{-0.7}$ | 5.7±0.3 | | | $4.25 \times 10^{0}$ | B |
| | | | 54475.341 | 4.950±0.005 | 136.95±0.05 | *Ks* | 7.24±0.32 | $926.9^{+45.5}_{-41.5}$ | | 5.7±0.3 | | | $4.25 \times 10^{0}$ | B |
| 60189 | 1 | – | 53407.377 | 16.73±0.02 | 73.21±0.09 | *Ks* | 6.40±0.26 | $2131.0^{+61.5}_{-58.2}$ | $8.21^{+0.04}_{-0.05}$ | 3.3±0.1 | | | $8.09 \times 10^{-1}$ | B |
| 60449 | 1 | – | 53413.287 | 0.684±0.006 | 320.4±0.7 | *Ks* | 5.973±0.097 | $93.1^{+3.5}_{-3.3}$ | $8.47^{+0.04}_{-0.05}$ | 3.1±0.1 | 0.51±0.02 | 0.164±0.009 | $1.84 \times 10^{-3}$ | nC |
| | | | 54510.354 | 0.716±0.002 | 318.9±0.1 | *Ks* | 5.987±0.025 | $97.6^{+3.6}_{-3.4}$ | | 3.1±0.1 | 0.50±0.01 | 0.163±0.007 | $2.03 \times 10^{-3}$ | nC |
| 60851 | 1 | AB | 53102.079 | 2.09±0.02 | 44.8±0.6 | *Ks* | 5.294±0.077 | $205.0^{+7.1}_{-6.7}$ | $9.07^{+0.02}_{-0.02}$ | 1.994±0.003 | 0.40±0.02 | 0.200±0.009 | $1.50 \times 10^{-1}$ | U |
| 60851 | 2 | AC | 53102.079 | 6.90±0.06 | 180.2±0.6 | *Ks* | 5.37±0.21 | $675.9^{+23.4}_{-22.0}$ | $9.07^{+0.02}_{-0.02}$ | 1.994±0.003 | 0.39±0.03 | 0.19±0.02 | $1.72 \times 10^{0}$ | U |
| 61789 | 1 | * | 53404.299 | 1.202±0.001 | 73.90±0.06 | *Ks* | 3.096±0.001 | $134.5^{+3.7}_{-3.5}$ | $8.06^{+0.02}_{-0.02}$ | 3.68±0.08 | 1.28±0.02 | 0.347±0.009 | $5.95 \times 10^{-4}$ | C |
| 62026 | 1 | * | 53102.133 | 0.232±0.002 | 6.3±0.8 | *Ks* | 1.5421±0.0047 | $25.2^{+1.2}_{-1.1}$ | $8.3^{+0.2}_{-0.2}$ | 2.5114±0.0002 | 1.31±0.04 | 0.52±0.01 | $5.55 \times 10^{-5}$ | C |
| 63005 | 1 | – | 55690.051 | 0.204±0.006 | 134.3±0.4 | *Ks* | 4.128±0.053 | $25.5^{+1.2}_{-1.2}$ | $7.5^{+0.1}_{-0.2}$ | 3.98±0.02 | 0.84±0.03 | 0.211±0.008 | $1.84 \times 10^{-4}$ | nC |
| 63945 | 1 | AC | 53454.210 | 1.550±0.007 | 266.7±0.3 | *Ks* | 3.2052±0.0015 | $185.4^{+5.8}_{-5.4}$ | $6.8^{+0.3}_{-0.8}$ | 6.8±0.3 | 1.1±0.2 | 0.17±0.03 | $2.53 \times 10^{-3}$ | C |
| 64515 | 1 | * | 53436.294 | 0.323±0.002 | 159.7±0.3 | *Ks* | 0.2271±0.0031 | $36.3^{+3.1}_{-2.7}$ | $8.81^{+0.04}_{-0.04}$ | 2.31±0.04 | 1.80±0.08 | 0.78±0.04 | $2.91 \times 10^{-5}$ | C |
| | | | 53778.374 | 0.3265±0.0006 | 157.5±0.1 | *Ks* | 0.2340±0.0021 | $36.6^{+3.2}_{-2.7}$ | | 2.31±0.04 | 1.80±0.08 | 0.78±0.04 | $2.96 \times 10^{-5}$ | C |
| 67472 | 1 | AC | 53454.224 | 4.62±0.03 | 304.3±0.3 | *Ks* | 5.827±0.047 | $716.3^{+18.6}_{-17.8}$ | $7.28^{+0.08}_{-0.09}$ | 8.7±0.2 | 0.87±0.04 | 0.100±0.005 | $4.97 \times 10^{-2}$ | C |
| | | | 55690.020 | 4.64±0.02 | 304.0±0.1 | *Ks* | 6.039±0.038 | $719.2^{+18.5}_{-17.6}$ | | 8.7±0.2 | 0.79±0.04 | 0.091±0.005 | $5.87 \times 10^{-2}$ | C |
| 67669 | 1 | * | 53404.327 | 7.84±0.01 | 105.53±0.09 | *Ks* | 1.5305±0.0075 | $825.6^{+85.5}_{-70.8}$ | $7.4^{+0.2}_{-0.3}$ | 3.9808±0.0005 | 2.2±0.3 | 0.55±0.07 | $1.12 \times 10^{-2}$ | C |
| 67703 | 1 | * | 53185.155 | 18.08±0.05 | 288.8±0.1 | *Ks* | 2.059±0.015 | $1440.7^{+96.9}_{-85.4}$ | $7.6^{+0.1}_{-0.2}$ | 3.1621±0.0007 | 1.09±0.05 | 0.34±0.02 | $3.62 \times 10^{-1}$ | U |
| 69113 | 1 | AD | 53126.078 | 5.332±0.008 | 65.2±0.5 | *Ks* | 3.997±0.047 | $858.7^{+60.7}_{-53.2}$ | $8.36^{+0.03}_{-0.03}$ | 2.80±0.09 | 0.79±0.03 | 0.28±0.02 | $1.13 \times 10^{-1}$ | C |
| 69113 | 2 | AE | 53126.078 | 5.502±0.008 | 67.1±0.5 | *Ks* | 4.063±0.049 | $886.0^{+62.6}_{-54.9}$ | $8.36^{+0.03}_{-0.03}$ | 2.80±0.09 | 0.77±0.03 | 0.28±0.02 | $1.27 \times 10^{-1}$ | C |
| 70915 | 1 | * | 53791.380 | 10.74±0.01 | 309.82±0.08 | *Ks* | 4.40±0.05 | $1570.6^{+100.2}_{-88.8}$ | $8.20^{+0.05}_{-0.06}$ | 3.24±0.08 | 0.81±0.03 | 0.25±0.01 | $5.52 \times 10^{-1}$ | nU |
| | | | 54518.402 | 10.75±0.01 | 309.30±0.07 | *Ks* | 4.049±0.053 | $1572.0^{+100.3}_{-88.9}$ | | 3.24±0.08 | 0.91±0.04 | 0.28±0.01 | $4.13 \times 10^{-1}$ | nU |
| 71762 | 1 | AB | 53404.392 | 5.542±0.008 | 110.47±0.07 | *Ks* | 0.2723±0.0047 | $519.4^{+75.2}_{-58.3}$ | $8.33^{+0.06}_{-0.08}$ | 2.97±0.07 | 2.5±0.2 | 0.83±0.07 | $5.58 \times 10^{-4}$ | C |
| 73111 | 1 | * | 53454.267 | 2.13±0.01 | 277.6±0.3 | *Ks* | 0.8017±0.0056 | $359.6^{+44.5}_{-35.7}$ | $8.18^{+0.07}_{-0.09}$ | 3.20±0.08 | 2.9±0.2 | 0.91±0.06 | $2.33 \times 10^{-3}$ | C |

*Continued on next page*

Table A6 – *Continued from previous page*

| HIP | CC# | WDS desig. | MJD (days) | Θ (arcsec) | PA[a] (deg) | Band | $\Delta m$ (mag) | $a_{\rm proj.}$ (au) | $\log(Age[yr])$ | $M_1$ ($M_\odot$) | $M_{\rm comp}$ ($M_\odot$) | $q$ | Chance proj. prob. (%) | Comp. status[b] |
|---|---|---|---|---|---|---|---|---|---|---|---|---|---|---|
| 74750 | 1 | AB | 53454.289 | 1.218±0.006 | 163.7±0.3 | *Ks* | 2.6362±0.0011 | $627.9^{+153.0}_{-102.9}$ | $6.92^{+0.04}_{-0.04}$ | 12.9±0.3 | 5.1±0.9 | 0.39±0.07 | $5.43 \times 10^{-3}$ | U |
| 74911 | 1 | – | 53454.299 | 0.948±0.004 | 304.8±0.2 | *Ks* | 0.30719±0.00013 | $97.6^{+7.7}_{-6.7}$ | $8.19^{+0.03}_{-0.03}$ | 3.7±0.2 | 3.3±0.1 | 0.88±0.06 | $1.14 \times 10^{-4}$ | U |
| 74911 | 2 | AD | 53454.299 | 6.05±0.02 | 156.1±0.2 | *Ks* | 7.82±0.13 | $622.2^{+49.1}_{-42.4}$ | $8.19^{+0.03}_{-0.03}$ | 3.7±0.2 | 0.18±0.02 | 0.049±0.005 | $1.81 \times 10^{0}$ | U |
| 75264 | 1 | – | 53454.311 | 0.279±0.003 | 131.6±0.6 | *Ks* | 1.2803±0.0015 | $43.9^{+5.4}_{-4.4}$ | $7.27^{+0.06}_{-0.07}$ | 8.6±0.2 | 5.5±0.7 | 0.63±0.08 | $1.18 \times 10^{-5}$ | C |
| | | | 55690.093 | 0.2454±0.0009 | 109.4±0.1 | *Ks* | 1.2497±0.0015 | $38.5^{+4.8}_{-3.8}$ | | 8.6±0.2 | 5.5±0.7 | 0.64±0.08 | $9.09 \times 10^{-6}$ | C |
| 77562 | 1 | – | 53186.143 | 9.97±0.01 | 38.36±0.07 | *Ks* | 7.380±0.092 | $942.8^{+31.3}_{-29.4}$ | $8.0^{+0.1}_{-0.2}$ | 2.5±0.6 | | | $2.06 \times 10^{1}$ | nB |
| | | | 53853.258 | 10.06±0.02 | 38.16±0.09 | *Ks* | 7.31±0.23 | $951.2^{+31.6}_{-29.7}$ | | 2.5±0.6 | | | $1.99 \times 10^{1}$ | nB |
| 77562 | 2 | – | 53186.143 | 6.11±0.01 | 43.6±0.1 | *Ks* | 7.93±0.12 | $577.9^{+19.2}_{-18.0}$ | $8.0^{+0.1}_{-0.2}$ | 2.5±0.6 | | | $1.19 \times 10^{1}$ | nB |
| | | | 53853.258 | 6.19±0.01 | 43.3±0.1 | *Ks* | 7.74±0.28 | $585.4^{+19.5}_{-18.3}$ | | 2.5±0.6 | | | $1.08 \times 10^{1}$ | nB |
| 77562 | 3 | – | 53186.143 | 9.25±0.01 | 41.52±0.08 | *Ks* | 8.11±0.13 | $874.3^{+29.1}_{-27.2}$ | $8.0^{+0.1}_{-0.2}$ | 2.5±0.6 | | | $2.81 \times 10^{1}$ | nB |
| | | | 53853.258 | 9.35±0.02 | 41.3±0.1 | *Ks* | 8.04±0.33 | $883.9^{+29.4}_{-27.6}$ | | 2.5±0.6 | | | $2.74 \times 10^{1}$ | nB |
| 77562 | 4 | – | 53186.143 | 11.38±0.01 | 76.77±0.08 | *Ks* | 8.00±0.13 | $1075.8^{+35.7}_{-33.5}$ | $8.0^{+0.1}_{-0.2}$ | 2.5±0.6 | | | $3.70 \times 10^{1}$ | nB |
| | | | 53853.258 | 11.43±0.02 | 76.2±0.1 | *Ks* | 8.65±0.47 | $1080.5^{+35.9}_{-33.7}$ | | 2.5±0.6 | | | $4.99 \times 10^{1}$ | nB |
| 77840 | 1 | * | 56121.124 | 2.04±0.02 | 266.9±0.4 | *Ks* | 1.9672±0.0087 | $313.6^{+26.8}_{-23.0}$ | $7.1^{+0.2}_{-0.3}$ | 6.9999±0.0003 | 3.0±0.4 | 0.43±0.06 | $1.00 \times 10^{-3}$ | C |
| 78968 | 1 | * | 53130.200 | 2.77±0.03 | 322.3±0.7 | *Ks* | 6.843±0.069 | $339.6^{+55.9}_{-42.2}$ | $7.9^{+0.1}_{-0.1}$ | 2.5117±0.0003 | 0.10±0.01 | 0.040±0.005 | $3.78 \times 10^{-1}$ | U |
| 79005 | 1 | AB | 53190.133 | 3.333±0.005 | 258.90±0.09 | *Ks* | 2.733±0.021 | $374.5^{+27.1}_{-23.7}$ | $8.35^{+0.04}_{-0.05}$ | 2.7±0.1 | 1.15±0.04 | 0.43±0.02 | $5.72 \times 10^{-3}$ | C |
| | | | 53852.267 | 3.336±0.006 | 258.8±0.1 | *Ks* | 2.585±0.034 | $374.9^{+27.1}_{-23.7}$ | | 2.7±0.1 | 1.20±0.04 | 0.45±0.02 | $5.73 \times 10^{-3}$ | C |
| | | | 53887.160 | 3.332±0.008 | 258.9±0.1 | *Ks* | 2.634±0.013 | $374.4^{+27.1}_{-23.7}$ | | 2.7±0.1 | 1.18±0.04 | 0.45±0.02 | $5.72 \times 10^{-3}$ | C |
| 79098 | 1 | * | 53442.268 | 2.350±0.005 | 116.7±0.2 | *Ks* | 8.16±0.19 | $319.7^{+14.1}_{-13.0}$ | $8.36^{+0.02}_{-0.02}$ | 2.96±0.05 | 0.16±0.01 | 0.054±0.005 | $2.88 \times 10^{-1}$ | C |
| 79153 | 1 | – | 53186.190 | 11.71±0.02 | 230.00±0.09 | *Ks* | 8.4±0.2 | $1005.4^{+51.7}_{-46.9}$ | $8.7^{+0.1}_{-0.2}$ | 1.99±0.04 | 0.103±0.008 | 0.052±0.004 | $2.23 \times 10^{1}$ | C |
| | | | 53853.271 | 11.70±0.02 | 230.1±0.1 | *Ks* | 8.29±0.29 | $1004.3^{+51.7}_{-46.9}$ | | 1.99±0.04 | 0.11±0.01 | 0.055±0.005 | $2.01 \times 10^{1}$ | C |
| 79153 | 2 | – | 53186.190 | 6.66±0.01 | 324.5±0.1 | *Ks* | 8.79±0.24 | $571.6^{+29.4}_{-26.7}$ | $8.7^{+0.1}_{-0.2}$ | 1.99±0.04 | | | $1.02 \times 10^{1}$ | nB |
| | | | 53853.271 | 6.75±0.01 | 325.0±0.1 | *Ks* | 8.75±0.36 | $579.7^{+29.8}_{-27.1}$ | | 1.99±0.04 | | | $1.02 \times 10^{1}$ | nB |
| 79199 | 1 | AB | 53191.122 | 1.093±0.002 | 117.20±0.09 | *Ks* | 3.9243±0.0053 | $136.6^{+5.7}_{-5.3}$ | $8.1^{+0.1}_{-0.1}$ | 3.161±0.002 | 0.85±0.02 | 0.268±0.007 | $4.76 \times 10^{-3}$ | C |
| | | | 55690.119 | 1.055±0.004 | 117.4±0.1 | *Ks* | 3.9053±0.0016 | $131.9^{+5.5}_{-5.1}$ | | 3.161±0.002 | 0.85±0.02 | 0.269±0.007 | $4.42 \times 10^{-3}$ | C |
| 79199 | 2 | AC | 53191.122 | 3.069±0.005 | 228.16±0.09 | *Ks* | 6.74±0.18 | $383.6^{+16.0}_{-14.8}$ | $8.1^{+0.1}_{-0.1}$ | 3.161±0.002 | 0.28±0.03 | 0.09±0.01 | $3.27 \times 10^{-1}$ | C |
| | | | 55690.119 | 3.09±0.01 | 228.4±0.1 | *Ks* | 6.881±0.055 | $386.0^{+16.1}_{-14.9}$ | | 3.161±0.002 | 0.26±0.02 | 0.081±0.007 | $3.67 \times 10^{-1}$ | C |
| 79230 | 1 | AB,C | 53105.328 | 2.601±0.005 | 140.8±0.1 | *H* | 2.651±0.015 | $720.6^{+299.5}_{-163.6}$ | $6.9^{+0.1}_{-0.2}$ | 7.4±0.1 | 2.1±0.7 | 0.3±0.1 | $1.86 \times 10^{-2}$ | U |
| 79399 | 1 | AB | 53185.247 | 3.698±0.006 | 69.98±0.08 | *Ks* | 0.927±0.013 | $344.0^{+27.7}_{-23.8}$ | $8.1^{+0.1}_{-0.2}$ | 2.60±0.05 | 1.50±0.08 | 0.58±0.03 | $5.22 \times 10^{-3}$ | C |
| | | | 53852.251 | 3.696±0.007 | 69.6±0.1 | *Ks* | 1.058±0.021 | $343.8^{+27.7}_{-23.8}$ | | 2.60±0.05 | 1.48±0.08 | 0.57±0.03 | $5.30 \times 10^{-3}$ | C |
| 79399 | 2 | AB | 53185.247 | 3.896±0.006 | 69.32±0.09 | *Ks* | 1.336±0.027 | $362.4^{+29.1}_{-25.1}$ | $8.1^{+0.1}_{-0.2}$ | 2.60±0.05 | 1.30±0.06 | 0.50±0.03 | $8.09 \times 10^{-3}$ | C |
| | | | 53852.251 | 3.883±0.007 | 69.4±0.1 | *Ks* | 1.825±0.028 | $361.2^{+29.0}_{-25.0}$ | | 2.60±0.05 | 1.16±0.05 | 0.45±0.02 | $1.06 \times 10^{-2}$ | C |
| 79399 | 3 | – | 53185.247 | 11.80±0.02 | 250.23±0.08 | *Ks* | 6.393±0.073 | $1097.9^{+88.3}_{-76.1}$ | $8.1^{+0.1}_{-0.2}$ | 2.60±0.05 | 0.18±0.02 | 0.068±0.008 | $3.70 \times 10^{0}$ | nU |
| | | | 53852.251 | 11.79±0.02 | 250.4±0.1 | *Ks* | 6.3±0.2 | $1096.9^{+88.2}_{-76.0}$ | | 2.60±0.05 | 0.20±0.03 | 0.08±0.01 | $3.13 \times 10^{0}$ | nU |
| 79739 | 1 | * | 53176.174 | 0.96±0.01 | 118.3±0.9 | *Ks* | 4.30±0.02 | $143.9^{+22.6}_{-17.3}$ | $8.1^{+0.1}_{-0.2}$ | 3.1611±0.0008 | 0.57±0.05 | 0.18±0.02 | $8.73 \times 10^{-3}$ | C |
| 79771 | 1 | * | 53176.206 | 3.68±0.06 | 313.2±0.9 | *Ks* | 3.781±0.038 | $598.0^{+84.7}_{-66.4}$ | $8.0^{+0.1}_{-0.2}$ | 2.5117±0.0002 | 0.69±0.05 | 0.27±0.02 | $1.04 \times 10^{-1}$ | C |
| | | | 56121.247 | 3.65±0.01 | 312.7±0.2 | *Ks* | 4.080±0.013 | $592.9^{+83.5}_{-65.1}$ | | 2.5117±0.0002 | 0.63±0.05 | 0.25±0.02 | $1.24 \times 10^{-1}$ | C |

*Continued on next page*

Table A6 – *Continued from previous page*

| HIP | CC# | WDS desig. | MJD (days) | Θ (arcsec) | PA[a] (deg) | Band | $\Delta m$ (mag) | $a_{\rm proj.}$ (au) | $\log(Age[yr])$ | $M_1$ ($M_\odot$) | $M_{\rm comp}$ ($M_\odot$) | $q$ | Chance proj. prob. (%) | Comp. status[b] |
|---|---|---|---|---|---|---|---|---|---|---|---|---|---|---|
| 79771 | 2 | – | 53176.206 | 0.435±0.007 | 128.4±0.9 | *Ks* | 4.375±0.013 | $70.6^{+10.0}_{-7.8}$ | $8.0^{+0.1}_{-0.2}$ | 2.5117±0.0002 | 0.57±0.05 | 0.23±0.02 | $2.17 \times 10^{-3}$ | C |
| | | | 56121.247 | 0.438±0.001 | 128.3±0.2 | *Ks* | 4.274±0.004 | $71.2^{+10.0}_{-7.8}$ | | 2.5117±0.0002 | 0.59±0.05 | 0.24±0.02 | $2.04 \times 10^{-3}$ | C |
| 80142 | 1 | AH | 53130.250 | 9.257±0.006 | 216.04±0.06 | *Ks* | 2.899±0.023 | $1269.8^{+91.5}_{-80.0}$ | $7.2^{+0.2}_{-0.6}$ | 3.15±0.07 | | | $1.20 \times 10^{0}$ | B |
| 80461 | 1 | – | 56179.046 | 0.239±0.005 | 223.8±0.5 | *Ks* | 1.181±0.013 | $29.8^{+3.4}_{-2.8}$ | $7.51^{+0.09}_{-0.11}$ | 4.84±0.02 | 2.7±0.2 | 0.55±0.05 | $1.97 \times 10^{-5}$ | C |
| 80473 | 1 | AB | 56089.350 | 3.02±0.01 | 335.1±0.2 | *Ks* | 0.2642±0.0011 | $334.3^{+37.0}_{-30.3}$ | $7.47^{+0.05}_{-0.05}$ | 7.4±0.1 | 7.1±0.7 | 0.97±0.09 | $1.66 \times 10^{-4}$ | C |
| 80474 | 1 | CF | 53184.170 | 4.8±0.1 | 206.0±1.0 | *Ks* | 5.563±0.013 | $651.8^{+58.1}_{-50.0}$ | $7.3^{+0.3}_{-0.7}$ | 3.2±0.1 | 0.4±0.1 | 0.12±0.03 | $2.29 \times 10^{-1}$ | C |
| | | | 55690.150 | 4.82±0.02 | 206.6±0.1 | *Ks* | 5.838±0.032 | $651.4^{+56.5}_{-48.1}$ | | 3.2±0.1 | 0.34±0.09 | 0.11±0.03 | $2.71 \times 10^{-1}$ | C |
| 81472 | 1 | AC | 53454.368 | 4.49±0.03 | 275.2±0.3 | *Ks* | 7.408±0.083 | $864.3^{+150.3}_{-111.6}$ | $6.7^{+0.2}_{-0.3}$ | 7.000±0.003 | | | $3.86 \times 10^{0}$ | B |
| | | | 55690.189 | 4.42±0.02 | 277.0±0.1 | *Ks* | 7.336±0.072 | $849.4^{+147.7}_{-109.6}$ | | 7.000±0.003 | | | $3.54 \times 10^{0}$ | B |
| 81472 | 2 | AD | 53454.368 | 5.27±0.03 | 357.6±0.3 | *Ks* | 7.403±0.084 | $1014.1^{+176.4}_{-131.0}$ | $6.7^{+0.2}_{-0.3}$ | 7.000±0.003 | | | $5.27 \times 10^{0}$ | B |
| | | | 55690.189 | 5.37±0.02 | 358.3±0.1 | *Ks* | 7.310±0.071 | $1032.7^{+179.5}_{-133.2}$ | | 7.000±0.003 | | | $5.11 \times 10^{0}$ | B |
| 81972 | 1 | AC | 53184.214 | 2.02±0.04 | 314.0±1.0 | *Ks* | 4.3885±0.0084 | $330.8^{+18.8}_{-17.2}$ | $7.2^{+0.2}_{-0.5}$ | 5.5±0.2 | 0.7±0.1 | 0.12±0.03 | $6.30 \times 10^{-2}$ | U |
| 81972 | 2 | AB | 53184.214 | 7.0±0.1 | 259.1±1.0 | *Ks* | 4.4177±0.0085 | $1147.2^{+65.1}_{-59.6}$ | $7.2^{+0.2}_{-0.5}$ | 5.5±0.2 | 0.7±0.1 | 0.12±0.03 | $7.70 \times 10^{-1}$ | U |
| 81972 | 3 | AE | 53184.214 | 5.0±0.1 | 213.7±1.0 | *Ks* | 5.376±0.013 | $823.0^{+46.7}_{-42.8}$ | $7.2^{+0.2}_{-0.5}$ | 5.5±0.2 | 0.4±0.1 | 0.08±0.02 | $8.68 \times 10^{-1}$ | U |
| 81972 | 4 | AD | 53184.214 | 2.78±0.05 | 106.9±1.0 | *Ks* | 7.816±0.041 | $455.8^{+25.9}_{-23.7}$ | $7.2^{+0.2}_{-0.5}$ | 5.5±0.2 | 0.16±0.02 | 0.029±0.003 | $1.64 \times 10^{0}$ | U |
| 82902 | 1 | – | 53177.300 | 4.04±0.01 | 151.4±0.2 | *Ks* | 8.13±0.23 | $469.5^{+22.9}_{-20.9}$ | $8.3^{+0.1}_{-0.2}$ | 2.5114±0.0002 | | | $3.32 \times 10^{0}$ | nB |
| | | | 53895.286 | 4.008±0.007 | 150.1±0.1 | *Ks* | 8.0±0.2 | $465.5^{+22.7}_{-20.7}$ | | 2.5114±0.0002 | | | $3.06 \times 10^{0}$ | nB |
| 83336 | 1 | – | 53182.267 | 8.92±0.01 | 25.60±0.08 | *Ks* | 6.624±0.075 | $1222.9^{+80.5}_{-71.1}$ | $8.17^{+0.03}_{-0.03}$ | 3.5±0.2 | 0.42±0.02 | 0.120±0.009 | $3.98 \times 10^{0}$ | C |
| | | | 53912.135 | 8.92±0.02 | 25.6±0.1 | *Ks* | 6.474±0.077 | $1224.2^{+80.6}_{-71.2}$ | | 3.5±0.2 | 0.44±0.02 | 0.13±0.01 | $3.59 \times 10^{0}$ | C |
| 83336 | 2 | – | 53182.267 | 8.89±0.01 | 302.27±0.09 | *Ks* | 6.603±0.075 | $1219.4^{+80.2}_{-70.9}$ | $8.17^{+0.03}_{-0.03}$ | 3.5±0.2 | | | $3.89 \times 10^{0}$ | nB |
| | | | 53912.135 | 8.94±0.02 | 302.8±0.1 | *Ks* | 6.468±0.078 | $1226.6^{+80.7}_{-71.4}$ | | 3.5±0.2 | | | $3.59 \times 10^{0}$ | nB |
| 83336 | 3 | – | 53182.267 | 9.23±0.01 | 137.61±0.09 | *Ks* | 7.86±0.14 | $1266.2^{+83.3}_{-73.6}$ | $8.17^{+0.03}_{-0.03}$ | 3.5±0.2 | | | $1.12 \times 10^{1}$ | nB |
| | | | 53912.135 | 9.19±0.02 | 137.1±0.1 | *Ks* | 8.22±0.18 | $1260.9^{+83.0}_{-73.4}$ | | 3.5±0.2 | | | $1.51 \times 10^{1}$ | nB |
| 85442 | 1 | – | 53454.417 | 3.00±0.01 | 329.42±0.06 | *Ks* | 6.916±0.062 | $677.7^{+73.1}_{-60.2}$ | $8.52^{+0.02}_{-0.02}$ | 3.11±0.07 | | | $3.23 \times 10^{0}$ | nB |
| | | | 55690.216 | 3.12±0.01 | 331.1±0.1 | *Ks* | 7.040±0.059 | $705.1^{+76.0}_{-62.6}$ | | 3.11±0.07 | | | $3.83 \times 10^{0}$ | nB |
| 85442 | 2 | – | 53454.417 | 6.05±0.03 | 261.39±0.05 | *Ks* | 7.407±0.085 | $1368.8^{+147.6}_{-121.5}$ | $8.52^{+0.02}_{-0.02}$ | 3.11±0.07 | | | $1.75 \times 10^{1}$ | nB |
| | | | 55690.216 | 6.01±0.02 | 262.9±0.1 | *Ks* | 7.604±0.078 | $1359.7^{+146.6}_{-120.6}$ | | 3.11±0.07 | | | $1.87 \times 10^{1}$ | nB |
| 85442 | 3 | – | 53454.417 | 5.78±0.03 | 33.79±0.06 | *Ks* | 7.788±0.097 | $1308.5^{+141.1}_{-116.2}$ | $8.52^{+0.02}_{-0.02}$ | 3.11±0.07 | | | $1.80 \times 10^{1}$ | nB |
| | | | 55690.216 | 5.95±0.02 | 33.2±0.1 | *Ks* | 7.844±0.088 | $1346.1^{+145.1}_{-119.4}$ | | 3.11±0.07 | | | $1.90 \times 10^{1}$ | nB |
| 85442 | 4 | – | 53454.417 | 5.23±0.02 | 145.91±0.07 | *Ks* | 7.89±0.11 | $1183.4^{+127.7}_{-105.1}$ | $8.52^{+0.02}_{-0.02}$ | 3.11±0.07 | | | $1.51 \times 10^{1}$ | nB |
| | | | 55690.216 | 5.13±0.02 | 144.9±0.1 | *Ks* | 7.917±0.092 | $1161.1^{+125.2}_{-103.0}$ | | 3.11±0.07 | | | $1.46 \times 10^{1}$ | nB |
| 85727 | 1 | AB | 54699.057 | 2.834±0.006 | 58.6±0.1 | *Ks* | 8.29±0.12 | $172.0^{+3.6}_{-3.5}$ | $7.96^{+0.03}_{-0.03}$ | 3.95±0.05 | | | $1.83 \times 10^{-1}$ | B |
| 85727 | 2 | AD | 54699.057 | 12.21±0.02 | 62.8±0.1 | *Ks* | 10.0±0.3 | $740.9^{+15.6}_{-15.0}$ | $7.96^{+0.03}_{-0.03}$ | 3.95±0.05 | | | $1.15 \times 10^{1}$ | B |
| 85783 | 1 | * | 53442.335 | 0.433±0.003 | 192.8±0.4 | *Ks* | 1.2545±0.0017 | $51.8^{+4.5}_{-3.9}$ | $8.1^{+0.1}_{-0.1}$ | 2.52±0.03 | 1.45±0.08 | 0.58±0.03 | $2.98 \times 10^{-4}$ | C |
| | | | 55655.363 | 0.4719±0.0008 | 192.64±0.07 | *Ks* | 1.2575±0.0014 | $56.4^{+4.9}_{-4.2}$ | | 2.52±0.03 | 1.45±0.08 | 0.58±0.03 | $3.55 \times 10^{-4}$ | C |
| | | | 55690.353 | 0.472±0.002 | 193.3±0.1 | *Ks* | 1.23246±0.00053 | $56.5^{+4.9}_{-4.2}$ | | 2.52±0.03 | 1.46±0.08 | 0.58±0.03 | $3.39 \times 10^{-4}$ | C |
| 85783 | 2 | – | 53442.335 | 1.624±0.005 | 123.5±0.2 | *Ks* | 6.630±0.033 | $194.2^{+16.9}_{-14.4}$ | $8.1^{+0.1}_{-0.1}$ | 2.52±0.03 | | | $7.75 \times 10^{-1}$ | B |

*Continued on next page*

Table A6 – *Continued from previous page*

| HIP | CC# | WDS desig. | MJD (days) | Θ (arcsec) | PA[a] (deg) | Band | $\Delta m$ (mag) | $a_{\rm proj.}$ (au) | log(*Age*[*yr*]) | $M_1$ ($M_\odot$) | $M_{\rm comp}$ ($M_\odot$) | $q$ | Chance proj. prob. (%) | Comp. status[b] |
|---|---|---|---|---|---|---|---|---|---|---|---|---|---|---|
| | | | 55655.363 | 1.555±0.005 | 118.6±0.2 | *Ks* | 6.309±0.028 | $186.0^{+16.2}_{-13.8}$ | | 2.52±0.03 | | | $5.32 \times 10^{-1}$ | B |
| | | | 55690.353 | 1.569±0.005 | 119.0±0.2 | *Ks* | 6.50±0.02 | $187.7^{+16.4}_{-13.9}$ | | 2.52±0.03 | | | $6.44 \times 10^{-1}$ | B |
| 87163 | 1 | – | 53457.375 | 7.35±0.01 | 107.67±0.06 | *Ks* | 1.6187±0.0064 | $2733.0^{+449.6}_{-338.3}$ | $7.72^{+0.04}_{-0.05}$ | 6.27±0.09 | 4.7±0.4 | 0.75±0.06 | $1.52 \times 10^{-1}$ | nU |
| | | | 55690.267 | 7.35±0.02 | 107.9±0.1 | *Ks* | 1.900±0.007 | $2730.6^{+449.3}_{-338.1}$ | | 6.27±0.09 | 4.4±0.4 | 0.70±0.06 | $2.24 \times 10^{-1}$ | nU |
| 87163 | 2 | – | 53457.375 | 6.77±0.01 | 47.51±0.06 | *Ks* | 6.423±0.054 | $2517.8^{+414.2}_{-311.7}$ | $7.72^{+0.04}_{-0.05}$ | 6.27±0.09 | 0.71±0.06 | 0.114±0.009 | $1.83 \times 10^{1}$ | nU |
| | | | 55690.267 | 6.77±0.02 | 47.4±0.1 | *Ks* | 6.487±0.054 | $2518.0^{+414.3}_{-311.8}$ | | 6.27±0.09 | 0.71±0.06 | 0.113±0.009 | $1.84 \times 10^{1}$ | nU |
| 87163 | 3 | – | 53457.375 | 2.103±0.005 | 37.7±0.1 | *Ks* | 7.6±0.1 | $781.9^{+128.6}_{-96.8}$ | $7.72^{+0.04}_{-0.05}$ | 6.27±0.09 | 0.46±0.06 | 0.07±0.01 | $2.57 \times 10^{0}$ | nU |
| | | | 55690.267 | 2.081±0.007 | 37.9±0.1 | *Ks* | 7.581±0.094 | $773.7^{+127.3}_{-95.8}$ | | 6.27±0.09 | 0.48±0.06 | 0.08±0.01 | $2.50 \times 10^{0}$ | nU |
| 87163 | 4 | – | 53457.375 | 4.280±0.008 | 170.50±0.07 | *Ks* | 7.6±0.1 | $1591.0^{+261.7}_{-197.0}$ | $7.72^{+0.04}_{-0.05}$ | 6.27±0.09 | 0.46±0.06 | 0.07±0.01 | $1.02 \times 10^{1}$ | nU |
| | | | 55690.267 | 4.29±0.01 | 170.5±0.1 | *Ks* | 7.577±0.095 | $1593.1^{+262.1}_{-197.3}$ | | 6.27±0.09 | 0.48±0.06 | 0.08±0.01 | $1.02 \times 10^{1}$ | nU |
| 87163 | 5 | – | 53457.375 | 6.78±0.01 | 123.50±0.08 | *Ks* | 7.93±0.12 | $2521.0^{+414.7}_{-312.1}$ | $7.72^{+0.04}_{-0.05}$ | 6.27±0.09 | 0.39±0.06 | 0.06±0.01 | $2.39 \times 10^{1}$ | nU |
| | | | 55690.267 | 6.77±0.02 | 123.9±0.1 | *Ks* | 7.83±0.11 | $2516.8^{+414.1}_{-311.6}$ | | 6.27±0.09 | 0.42±0.06 | 0.07±0.01 | $2.37 \times 10^{1}$ | nU |
| 87163 | 6 | – | 53457.375 | 1.515±0.005 | 77.5±0.3 | *Ks* | 8.33±0.17 | $563.1^{+92.7}_{-69.7}$ | $7.72^{+0.04}_{-0.05}$ | 6.27±0.09 | 0.30±0.06 | 0.048±0.009 | $1.38 \times 10^{0}$ | nU |
| | | | 55690.267 | 1.498±0.006 | 77.7±0.2 | *Ks* | 7.68±0.34 | $556.7^{+91.6}_{-69.0}$ | | 6.27±0.09 | 0.46±0.09 | 0.07±0.01 | $1.31 \times 10^{0}$ | nU |
| 87220 | 1 | – | 53454.427 | 7.78±0.05 | 327.2±0.4 | *Ks* | 8.20±0.13 | $1327.3^{+62.3}_{-57.1}$ | $8.23^{+0.01}_{-0.01}$ | 3.98±0.02 | 0.32±0.02 | 0.081±0.006 | $2.56 \times 10^{1}$ | nU |
| | | | 55690.243 | 7.80±0.03 | 327.0±0.1 | *Ks* | 8.44±0.13 | $1331.8^{+62.0}_{-56.8}$ | | 3.98±0.02 | 0.28±0.02 | 0.071±0.006 | $2.81 \times 10^{1}$ | nU |
| 88149 | 1 | * | 53455.426 | 0.108±0.003 | 153.5±0.8 | *Ks* | 2.010±0.029 | $21.6^{+1.3}_{-1.2}$ | $7.10^{+0.05}_{-0.06}$ | 8.1±0.1 | 3.6±0.2 | 0.45±0.02 | $5.87 \times 10^{-6}$ | C |
| | | | 55690.288 | 0.133±0.003 | 166.5±0.6 | *Ks* | 1.882±0.022 | $26.5^{+1.6}_{-1.4}$ | | 8.1±0.1 | 3.8±0.2 | 0.47±0.02 | $8.15 \times 10^{-6}$ | C |
| 88859 | 1 | * | 53442.364 | 4.046±0.004 | 257.35±0.05 | *Ks* | 2.954±0.022 | $1099.5^{+214.2}_{-154.1}$ | $8.17^{+0.06}_{-0.07}$ | 3.90±0.09 | 1.5±0.2 | 0.40±0.05 | $5.86 \times 10^{-2}$ | C |
| 89684 | 1 | – | 53570.203 | 6.47±0.01 | 90.8±0.5 | *Ks* | 5.212±0.037 | $1309.5^{+112.3}_{-95.9}$ | $8.47^{+0.03}_{-0.03}$ | 3.13±0.04 | 0.69±0.03 | 0.22±0.01 | $4.06 \times 10^{-1}$ | nU |
| | | | 55690.313 | 6.50±0.02 | 90.8±0.1 | *Ks* | 5.327±0.027 | $1316.1^{+112.9}_{-96.4}$ | | 3.13±0.04 | 0.66±0.03 | 0.21±0.01 | $4.51 \times 10^{-1}$ | nU |
| 89963 | 1 | * | 55761.007 | 1.148±0.004 | 201.1±0.2 | *Ks* | 4.985±0.016 | $455.5^{+352.9}_{-138.4}$ | $8.05^{+0.03}_{-0.03}$ | 4.5±0.1 | | | $1.51 \times 10^{-2}$ | B |
| 90096 | 1 | – | 53458.392 | 4.10±0.02 | 20.8±0.3 | *Ks* | 4.081±0.016 | $773.3^{+58.2}_{-50.7}$ | $8.20^{+0.02}_{-0.03}$ | 3.9±0.1 | | | $4.53 \times 10^{-1}$ | B |
| | | | 55690.366 | 4.20±0.01 | 20.9±0.1 | *Ks* | 4.048±0.016 | $792.7^{+59.6}_{-51.8}$ | | 3.9±0.1 | | | $4.61 \times 10^{-1}$ | B |
| 90766 | 1 | AB | 55372.167 | 6.46±0.03 | 332.6±0.3 | *Ks* | 1.182±0.018 | $1400.5^{+285.3}_{-202.8}$ | $8.0^{+0.1}_{-0.2}$ | 2.516±0.008 | 1.3±0.1 | 0.52±0.06 | $6.04 \times 10^{-2}$ | U |
| 93805 | 1 | AB | 54699.074 | 12.47±0.03 | 30.5±0.1 | *Ks* | 3.976±0.016 | $473.0^{+11.8}_{-11.3}$ | $8.4^{+0.1}_{-0.1}$ | 2.5113±0.0004 | | | $1.50 \times 10^{-1}$ | B |
| | | | 54947.291 | 12.51±0.04 | 29.7±0.2 | *Ks* | 3.818±0.023 | $474.5^{+11.9}_{-11.3}$ | | 2.5113±0.0004 | | | $1.35 \times 10^{-1}$ | B |
| 93892 | 1 | – | 53286.002 | 6.43±0.01 | 204.16±0.09 | *Ks* | 6.853±0.054 | $1979.1^{+514.0}_{-338.3}$ | $8.36^{+0.05}_{-0.06}$ | 3.22±0.06 | | | $5.43 \times 10^{0}$ | B |
| | | | 55799.136 | 6.395±0.006 | 203.61±0.06 | *Ks* | 6.96±0.05 | $1967.8^{+511.0}_{-336.3}$ | | 3.22±0.06 | | | $5.77 \times 10^{0}$ | B |
| 93892 | 2 | – | 53286.002 | 3.327±0.006 | 65.0±0.1 | *Ks* | 9.06±0.16 | $1023.6^{+265.8}_{-175.0}$ | $8.36^{+0.05}_{-0.06}$ | 3.22±0.06 | | | $5.96 \times 10^{0}$ | B |
| | | | 55799.136 | 3.364±0.004 | 64.1±0.1 | *Ks* | 8.75±0.12 | $1035.0^{+268.8}_{-176.9}$ | | 3.22±0.06 | | | $5.56 \times 10^{0}$ | B |
| 100881 | 1 | AB | 54769.988 | 3.45±0.01 | 146.9±0.1 | *Ks* | 2.4867±0.0016 | $577.6^{+62.1}_{-51.1}$ | $8.18^{+0.06}_{-0.06}$ | 3.97±0.02 | 2.0±0.2 | 0.51±0.04 | $4.12 \times 10^{-3}$ | C |
| | | | 56189.158 | 3.467±0.003 | 147.34±0.05 | *Ks* | 2.9387±0.0098 | $579.8^{+62.3}_{-51.3}$ | | 3.97±0.02 | 1.6±0.1 | 0.41±0.04 | $5.68 \times 10^{-3}$ | C |
| 105842 | 1 | * | 54685.224 | 4.6892±0.0006 | 131.36±0.02 | *H* | 1.818±0.024 | $1205.4^{+584.3}_{-296.7}$ | $8.6^{+0.2}_{-0.3}$ | 1.84±0.03 | 1.0±0.2 | 0.5±0.1 | $3.78 \times 10^{-2}$ | C |
| 113031 | 1 | – | 53298.075 | 0.083±0.002 | 284.3±1.0 | *Ks* | 0.520±0.054 | $21.0^{+2.4}_{-2.0}$ | $8.19^{+0.05}_{-0.06}$ | 4.1±0.1 | 3.6±0.2 | 0.88±0.05 | $3.76 \times 10^{-7}$ | C |
| | | | 54363.151 | 0.073±0.006 | 294.5±4.0 | *Ks* | 0.83±0.11 | $18.5^{+2.5}_{-2.2}$ | | 4.1±0.1 | 3.4±0.2 | 0.84±0.05 | $3.88 \times 10^{-7}$ | C |
| 116231 | 1 | – | 53296.128 | 0.642±0.001 | 240.74±0.07 | *Ks* | 4.0844±0.0063 | $34.2^{+0.3}_{-0.3}$ | $8.9^{+0.1}_{-0.2}$ | 2.4±0.1 | 0.622±0.006 | 0.26±0.01 | $8.49 \times 10^{-5}$ | C |

*Continued on next page*

Table A6 – *Continued from previous page*

| HIP | CC# | WDS desig. | MJD (days) | Θ (arcsec) | PA[a] (deg) | Band | $\Delta m$ (mag) | $a_{\mathrm{proj.}}$ (au) | $\log(Age[yr])$ | $M_1$ ($M_\odot$) | $M_{\mathrm{comp}}$ ($M_\odot$) | $q$ | Chance proj. prob. (%) | Comp. status[b] |
|---|---|---|---|---|---|---|---|---|---|---|---|---|---|---|
| | | | 53297.113 | 0.6417±0.0009 | 240.74±0.08 | *K*s | 4.034±0.012 | $34.2^{+0.3}_{-0.3}$ | | 2.4±0.1 | 0.631±0.007 | 0.27±0.01 | $8.24 \times 10^{-5}$ | C |
| | | | 56188.158 | 0.825±0.001 | 251.1±0.1 | *K*s | 4.1627±0.0031 | $44.0^{+0.4}_{-0.4}$ | | 2.4±0.1 | 0.607±0.006 | 0.26±0.01 | $1.44 \times 10^{-4}$ | C |

**Notes.** Component designation as assigned in the WDS catalogue. –: No WDS entry; *: Companion is listed in WDS certainly without component designation

[a] Position angle (PA) is measured from N over E to S.

[b] Companion status: (B)ackground; (C)o-moving; (U)ndefined; (n)ew detection

**Table A7.** Additional companions listed within the literature.

| HIP | WDS desig. | log($P$[$d$]) | $\rho$ (arcsec) | log($a_{\mathrm{proj.}}$[$au$]) | Reference | HIP | WDS desig. | log($P$[$d$]) | $\rho$ (arcsec) | log($a_{\mathrm{proj.}}$[$au$]) | Reference |
|---|---|---|---|---|---|---|---|---|---|---|---|
| 377[a] | – | – | – | – | Chini et al. (2012) | 26549 | AB,E | – | 41.561 | 6.698 | Jasinta et al. (1995) |
| 2548 | Aa-B | – | 27.5 | 3.35 | Holdenried and Rafferty (1997) | 26549 | AB,F | – | 207.302 | 7.396 | Hartkopf et al. (2013) |
| 2548 | Aa-C | – | 168.1 | 4.13 | Hartkopf et al. (2013) | 26549 | AB,H | – | 306.745 | 7.567 | Hartkopf et al. (2013) |
| 5778 | – | 2.9 | 0.002 | -0.48 | Stickland and Weatherby (1984) | 26549 | AB,I | – | 524.066 | 7.799 | Hartkopf et al. (2013) |
| 10602 | AB | – | 88.21 | 3.62 | Jasinta et al. (1995) | 26602 | AC | – | 89.25 | 4.63 | Hartkopf et al. (2013) |
| 10602 | AC | – | 13733.03 | 5.81 | Shaya and Olling (2011) | 26602 | AE | – | 75.72 | 4.56 | Hartkopf et al. (2013) |
| 10602 | AD | – | 26525.39 | 6.1 | Shaya and Olling (2011) | 26602 | AF | – | 133.5 | 4.8 | Hartkopf et al. (2013) |
| 15627[a] | – | – | – | – | Chini et al. (2012) | 26602 | AG | – | 58.98 | 4.45 | Hartkopf et al. (2013) |
| 17563 | – | 0.23 | – | – | Abt et al. (1990) | 26602 | AH | – | 40.78 | 4.29 | Hartkopf et al. (2013) |
| 17563 | – | – | 65.26 | 4.03 | Hartkopf et al. (2013) | 26602 | AB,I | – | 91.77 | 4.64 | Hartkopf et al. (2013) |
| 18213[a] | – | – | – | – | Chini et al. (2012) | 26634 | – | – | 13.5 | 3.03 | Dommanget and Nys (2000) |
| 20042 | – | 0.7 | – | – | Abt (2005) | 28691 | – | 1.16 | – | – | Scarfe et al. (2000) |
| 20042 | Aa-C | – | 48.95 | 3.43 | Wycoff et al. (2006) | 28691 | – | 3.68 | 0.05 | 1.07 | Scarfe et al. (2000) |
| 20171 | – | 0.65 | – | – | Dworetsky (1972b) | 28744 | – | 1.91 | – | – | Peters (1983) |
| 21192 | – | – | 123.4 | 4.26 | Hartkopf et al. (2013) | 29941 | – | 1.85 | – | – | Abt et al. (1990) |
| 21735 | – | – | 10 | 3.11 | Hubrig et al. (2001) | 30180 | – | 0.91 | – | – | Gies and Bolton (1986) |
| 23419 | A,BC | – | 14.39 | 3.43 | Hartkopf et al. (2013) | 30468 | – | – | 23.04 | 3.82 | Hartkopf et al. (2013) |
| 23419 | AD | – | 131.91 | 4.39 | Hartkopf et al. (2013) | 30772 | AB | – | 77.6 | 4.41 | Hartkopf et al. (2013) |
| 23794 | – | 0.74 | – | – | Catanzaro and Leto (2004) | 30772 | AC | – | 80.89 | 4.43 | Hartkopf et al. (2013) |
| 23794 | AC | – | 52.41 | 3.7 | Hartkopf et al. (2013) | 30867 | AC | – | 9.27 | 3.28 | Mason et al. (2012) |
| 24244 | Aa,Ab | – | 0.37 | 1.42 | Hubrig et al. (2001) | 30867 | AD | – | 24.38 | 3.7 | Hartkopf et al. (2013) |
| 24244 | AB | – | 12.7 | 2.96 | Huélamo et al. (2000) | 31190 | – | – | 24.72 | 4.12 | Hartkopf et al. (2013) |
| 24740 | – | 0.62 | – | – | Wyse (1936) | 31959 | – | – | – | – | Bragança et al. (2012) |
| 24825 | AB | – | 39.38 | 4.02 | Hartkopf et al. (2013) | 32753 | – | – | 28.91 | 3.88 | Hartkopf et al. (2013) |
| 24825 | AC | – | 166.43 | 4.64 | Hartkopf et al. (2013) | 33343 | – | – | 6.5 | 3.32 | Mason et al. (2001) |
| 26215 | – | 3.27 | – | – | Dworetsky (1982) | 33611 | – | – | 3.3 | 3.15 | Dommanget and Nys (2000) |
| 26235 | – | 1.32 | – | – | Stickland and Lloyd (2001) | 33650 | – | – | 0.1 | 1.56 | Dommanget and Nys (2000) |
| 26235 | AB | – | 52.34 | 4.4 | Wycoff et al. (2006) | 34579 | – | – | 0.1 | 1.75 | Mason et al. (2001) |
| 26235 | AC | – | 128.76 | 4.79 | Wycoff et al. (2006) | 34579 | – | – | 8.4 | 3.68 | Mason et al. (2001) |
| 26235 | AD | – | 134.92 | 4.81 | Wycoff et al. (2006) | 34898 | – | – | 6.69 | 3.62 | Hartkopf et al. (2013) |
| 26549[a] | – | – | – | – | Chini et al. (2012) | 36009 | – | – | 11.32 | 3.78 | Hartkopf et al. (2013) |
| 26549 | AB,C | – | 11.443 | 6.138 | Maíz Apellániz (2010) | 36363 | – | – | – | – | Bragança et al. (2012) |

*Continued on next page*

Table A7 – *Continued from previous page*

| HIP | WDS desig. | log($P[d]$) | $\rho$ (arcsec) | log($a_{\text{proj.}}[au]$) | Reference | HIP | WDS desig. | log($P[d]$) | $\rho$ (arcsec) | log($a_{\text{proj.}}[au]$) | Reference |
|---|---|---|---|---|---|---|---|---|---|---|---|
| 37450 | – | – | – | – | Bragança et al. (2012) | 63005 | AB | – | 36.35 | 3.66 | Hartkopf et al. (2013) |
| 37752 | – | – | 176.7 | 4.56 | Mason et al. (2001) | 63210[a] | – | – | – | – | Chini et al. (2012) |
| 39970[a] | – | – | – | – | Chini et al. (2012) | 63945[a] | – | – | – | – | Chini et al. (2012) |
| 40321 | – | – | 66.94 | 4.32 | Hartkopf et al. (2013) | 63945 | AB | – | 11.53 | 3.14 | Wycoff et al. (2006) |
| 40817 | AB | – | 64.9 | 3.84 | Hartkopf et al. (2013) | 63945 | – | – | 37.84 | 3.66 | Rizzuto et al. (2013) |
| 40817 | AC | – | 99.85 | 4.02 | Hartkopf et al. (2013) | 67472 | AB | – | 46.51 | 3.86 | Hartkopf et al. (2013) |
| 40834 | AB | – | 64.83 | 3.92 | Fabricius et al. (2002) | 67669 | – | 1.24 | – | – | Levato et al. (1987) |
| 40834 | BC | – | 37.49 | 3.68 | Hartkopf et al. (2013) | 67703 | – | – | 18.35 | 3.17 | Sinachopoulos et al. (2007) |
| 41296 | AB | – | 26.13 | 3.75 | Hartkopf et al. (2013) | 68002 | – | 0.9 | – | – | Pourbaix et al. (2004) |
| 41296 | AC | – | 34.9 | 3.87 | Huélamo et al. (2000) | 69113 | AB | – | 29.91 | 3.68 | Hartkopf et al. (2013) |
| 41603 | – | – | 18 | 3.91 | Hartkopf et al. (2013) | 69113 | BC | – | 51.94 | 3.92 | Hartkopf et al. (2013) |
| 41843 | – | 1.34 | – | – | Stickland et al. (1984) | 69174 | – | 1.42 | – | – | De Cat et al. (2000) |
| 42129[a] | – | – | – | – | Chini et al. (2012) | 69174 | – | – | 64.14 | 4.21 | Bystrov et al. (1994) |
| 42334 | – | – | 16 | 3.06 | Dommanget and Nys (2000) | 69491 | – | 0.17 | – | – | Malkov et al. (2006) |
| 42504 | – | 0.5 | – | – | Levato et al. (1988) | 69618 | AB | – | 32.45 | 3.68 | Wycoff et al. (2006) |
| 42504 | – | – | 16.6 | 3.35 | Huélamo et al. (2000) | 69618 | AC | – | 36 | 3.73 | Dommanget and Nys (2000) |
| 42637 | AC | – | 501.13 | 4.68 | Hartkopf et al. (2013) | 70574 | AB | – | 157.45 | 4.36 | Hartkopf et al. (2013) |
| 42715 | A,BC | – | 76.03 | 4.07 | Hartkopf et al. (2013) | 71353 | – | – | 25.27 | 3.45 | Hartkopf et al. (2013) |
| 42715 | BC,D | – | 60.43 | 3.97 | Hartkopf et al. (2013) | 71762 | AC | – | 127.77 | 4.08 | Hartkopf et al. (2013) |
| 44798 | – | 0.81 | – | – | Aikman (1976) | 74750[a] | – | – | – | – | Chini et al. (2012) |
| 45189 | Aa,Ab | – | 0.12 | 1.42 | Mason et al. (2009) | 74750 | AC | – | 10.96 | 3.75 | Wycoff et al. (2006) |
| 45941 | – | 2.07 | – | – | Curtis (1907) | 74911 | AC | – | 23.1 | 3.38 | Wycoff et al. (2006) |
| 46283[a] | – | – | – | – | Chini et al. (2012) | 74911 | BC | – | 22.7 | 3.37 | Shatsky (2001) |
| 46283 | AB | – | 3.25 | 2.63 | Hartkopf et al. (2013) | 74911 | AE | – | 102.3 | 4.02 | Mason et al. (2001) |
| 46283 | AC | – | 9.65 | 3.1 | Hartkopf et al. (2013) | 75264 | – | 0.66 | – | – | Thackeray (1970) |
| 46594[a] | – | – | – | – | Chini et al. (2012) | 75264 | AC | – | 26.29 | 3.62 | Wycoff et al. (2006) |
| 46914[a] | – | – | – | – | Chini et al. (2012) | 76503 | – | 0.72 | – | – | Levato et al. (1987) |
| 47522 | – | – | 51.54 | 3.9 | Hartkopf et al. (2013) | 77227 | – | 1.59 | – | – | De Cat et al. (2000) |
| 48224 | – | – | 66.51 | 4.24 | Hartkopf et al. (2013) | 77562 | – | – | 28.82 | 3.44 | Hartkopf et al. (2013) |
| 54255 | – | 0.36 | – | – | Andersen (1975) | 77634 | – | 1.18 | – | – | Dworetsky (1972a) |
| 54767 | – | – | 21.94 | 3.32 | Hartkopf et al. (2013) | 78168 | – | 1 | – | – | Levato et al. (1987) |
| 58587 | – | 0.47 | – | – | Pourbaix et al. (2004) | 78265 | – | 0.2 | – | – | Levato et al. (1987) |
| 60463[a] | – | – | – | – | Chini et al. (2012) | 78265 | AB | – | 50.35 | 3.96 | Hartkopf et al. (2013) |

*Continued on next page*

Table A7 – *Continued from previous page*

| HIP | WDS desig. | log($P$[$d$]) | $\rho$ (arcsec) | log($a_{\mathrm{proj.}}$[$au$]) | Reference | HIP | WDS desig. | log($P$[$d$]) | $\rho$ (arcsec) | log($a_{\mathrm{proj.}}$[$au$]) | Reference |
|---|---|---|---|---|---|---|---|---|---|---|---|
| 79005 | AC | – | 29.53 | 3.52 | Hartkopf et al. (2013) | 90766 | AC | – | 164.37 | 4.55 | Hartkopf et al. (2013) |
| 79404 | – | 0.76 | – | – | Levato et al. (1987) | 90766 | AD | – | 85.84 | 4.27 | Hartkopf et al. (2013) |
| 79622 | – | – | 46.5 | 3.84 | Mason et al. (2001) | 93368[a] | – | – | – | – | Chini et al. (2012) |
| 79653[a] | – | – | – | – | Chini et al. (2012) | 93368 | AB | – | 12.79 | 3.71 | Hartkopf et al. (2013) |
| 80473[a] | – | – | – | – | Chini et al. (2012) | 95347[a] | – | – | – | – | Chini et al. (2012) |
| 80473 | AC | – | 149.23 | 4.22 | Hartkopf et al. (2013) | 100751 | – | 1.07 | – | – | Luyten (1936) |
| 80473 | AD | – | 156.37 | 4.24 | Hartkopf et al. (2013) | 100751 | AB | – | 249.14 | 4.14 | Hartkopf et al. (2013) |
| 81472 | AB | – | 16.12 | 3.49 | Hartkopf et al. (2013) | 100751 | AC | – | 244.5 | 4.13 | Mason et al. (2001) |
| 83336 | AB | – | 22.56 | 3.49 | Hartkopf et al. (2013) | 100751 | AD | – | 58.9 | 3.51 | Mason et al. (2001) |
| 83336 | AC | – | 42.43 | 3.77 | Hartkopf et al. (2013) | 100881 | AC | – | 37.88 | 3.8 | Hartkopf et al. (2013) |
| 83336 | AD | – | 51.43 | 3.85 | Hartkopf et al. (2013) | 110672 | – | 1.93 | – | – | Bjorkman et al. (2002) |
| 85727 | – | 3.02 | 0.01 | -0.39 | Malkov et al. (2012) | 112542[a] | – | – | – | – | Chini et al. (2012) |
| 85727 | AE | – | 49.88 | 3.48 | Wycoff et al. (2006) | 112542 | AB | – | 20.93 | 3.31 | Mason et al. (2007) |
| 87163 | – | 0.42 | – | – | Malkov et al. (2006) | 113031 | – | 0.54 | – | – | Catanzaro and Leto (2004) |
| 88149[a] | – | – | – | – | Chini et al. (2012) | | | | | | |

[a] The primary target star is listed as a spectroscopic binary, but without period given by Chini et al. (2012) or Bragança et al. (2012).

## A.2 Figures

### Detection limits and companion candidates motion on the sky

In this section the astrometric measurements for all point sources detected at several observing epochs, the corresponding detection limits and a NaCo image of the investigated target are illustrated. The background/co-moving probabilities, in per cent, as well as the number of epochs (N) and the resulting degree of freedom (df) defined in section 5.2 are given above each common proper motion diagram, if available.

HIP2548

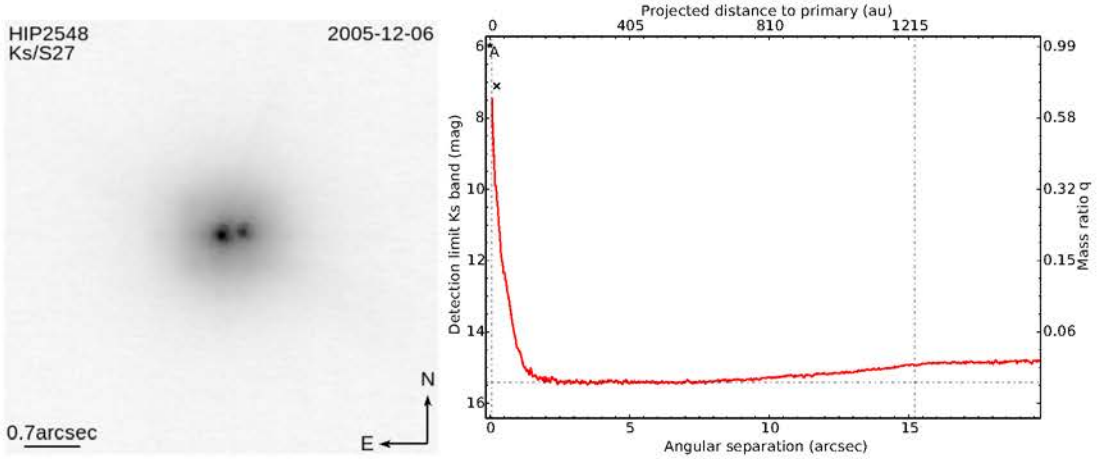


CC1: $P_{bg}$ = 0.00%, $P_{cmv}$ = 0.00%, N=8, df=14

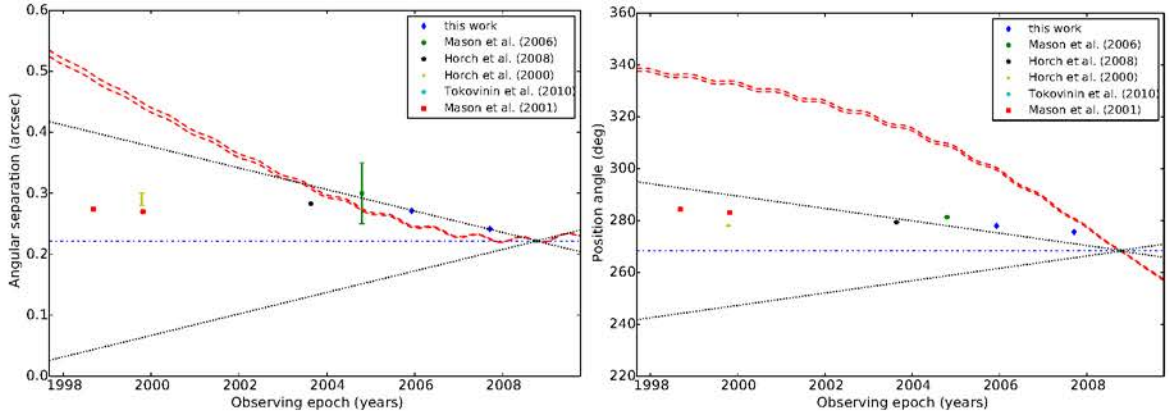


HIP15627

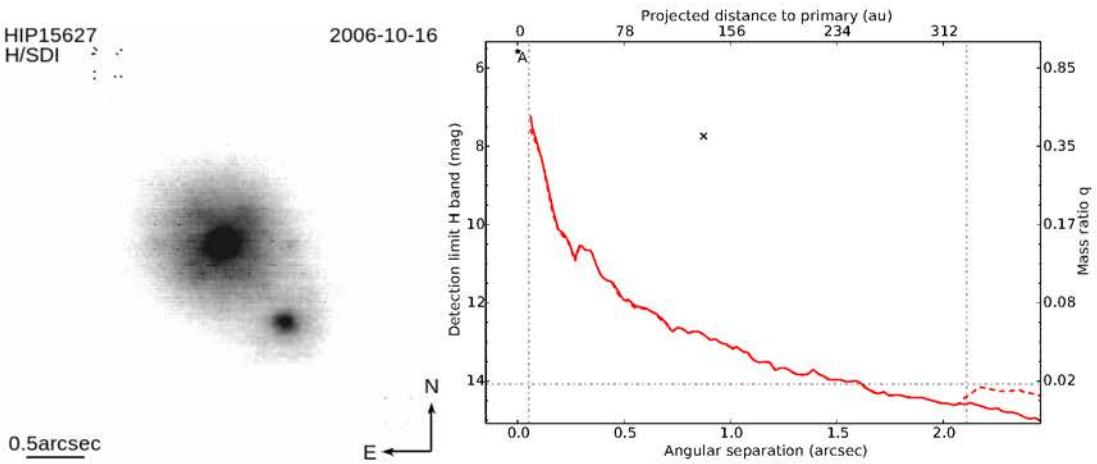

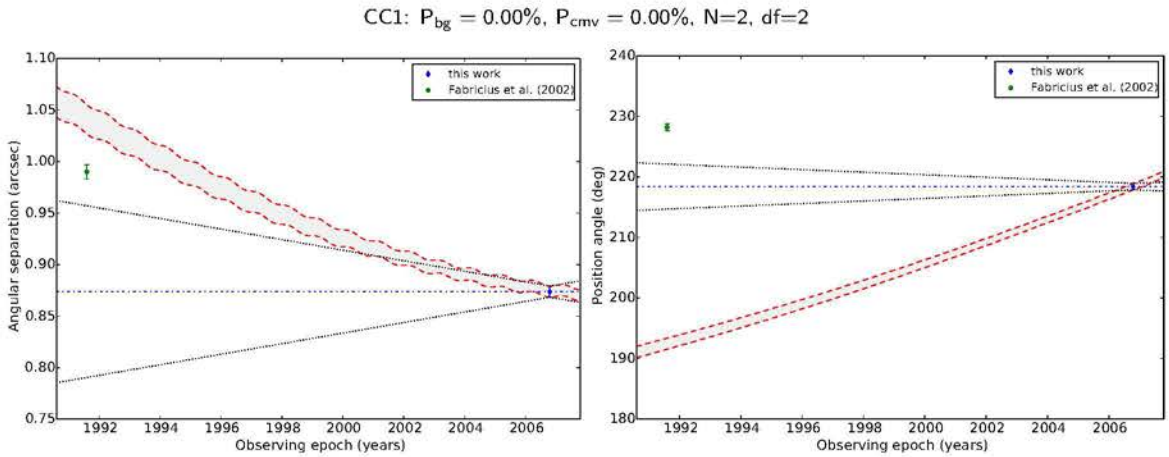


## HIP16511

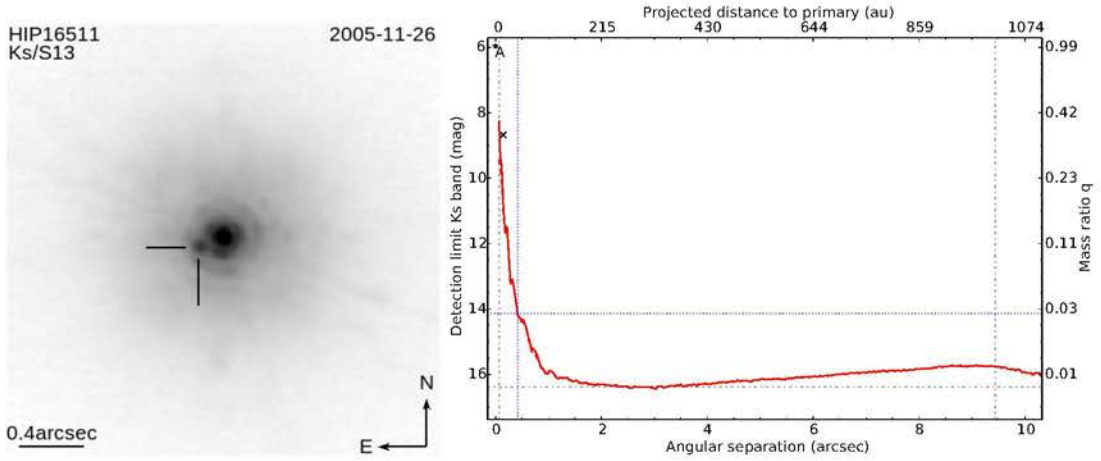


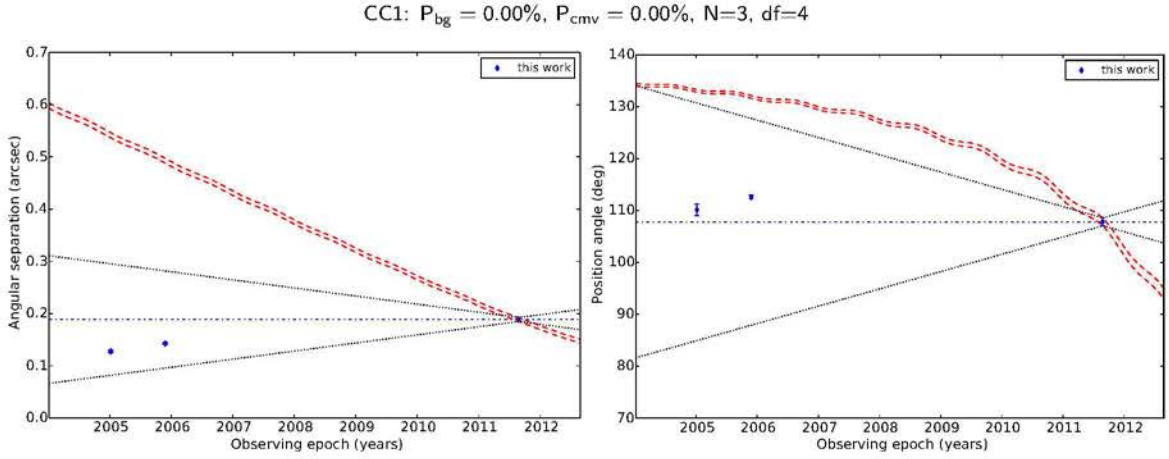


## HIP16803

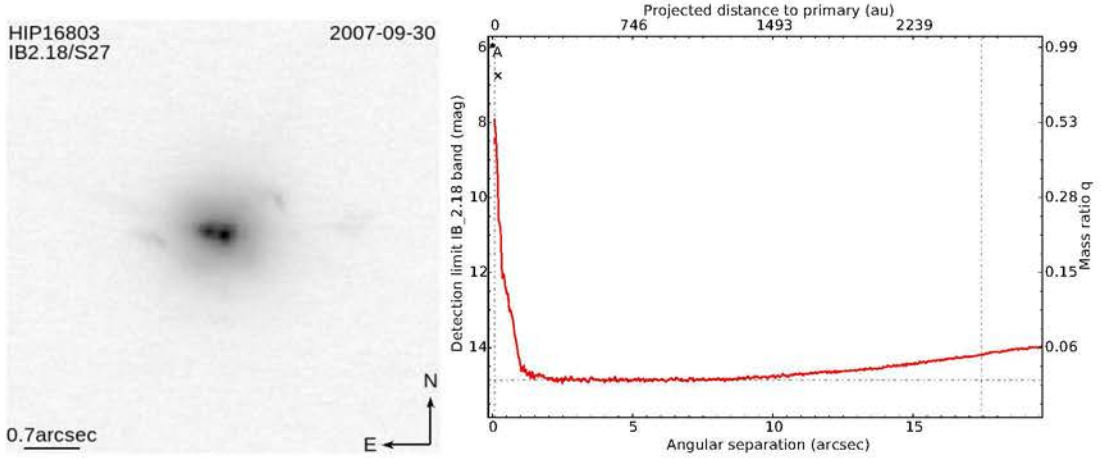

CC1: $P_{bg} = 0.00\%$, $P_{cmv} = 0.00\%$, N=6, df=10

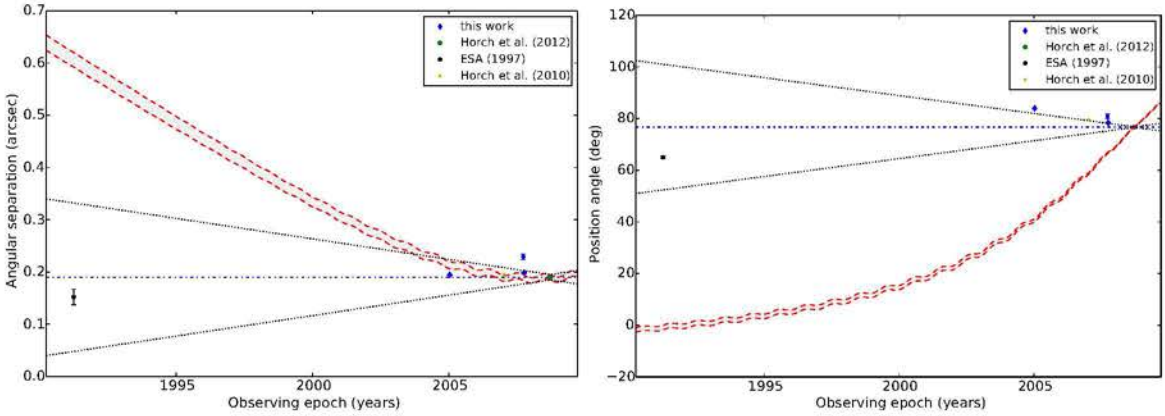


## HIP20020

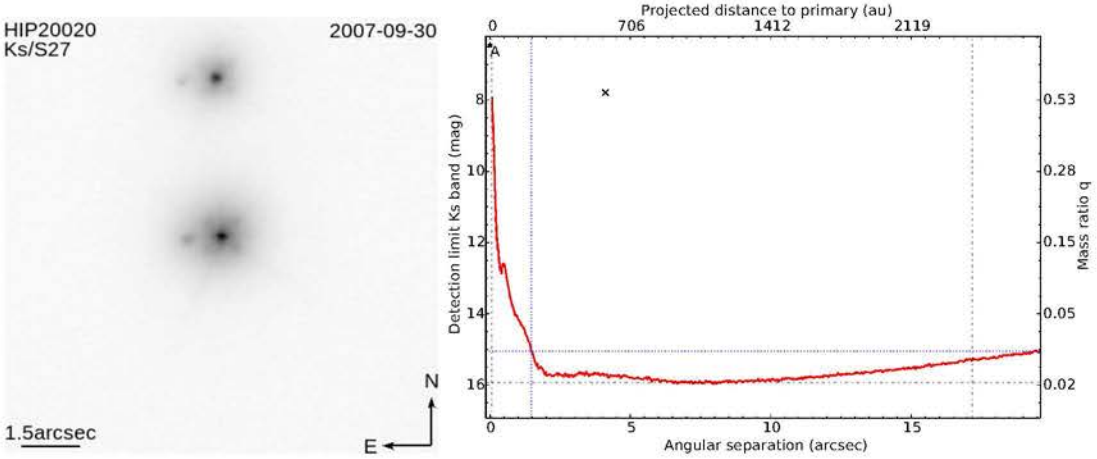


CC1: $P_{bg} = 0.00\%$, $P_{cmv} = 0.00\%$, N=5, df=8

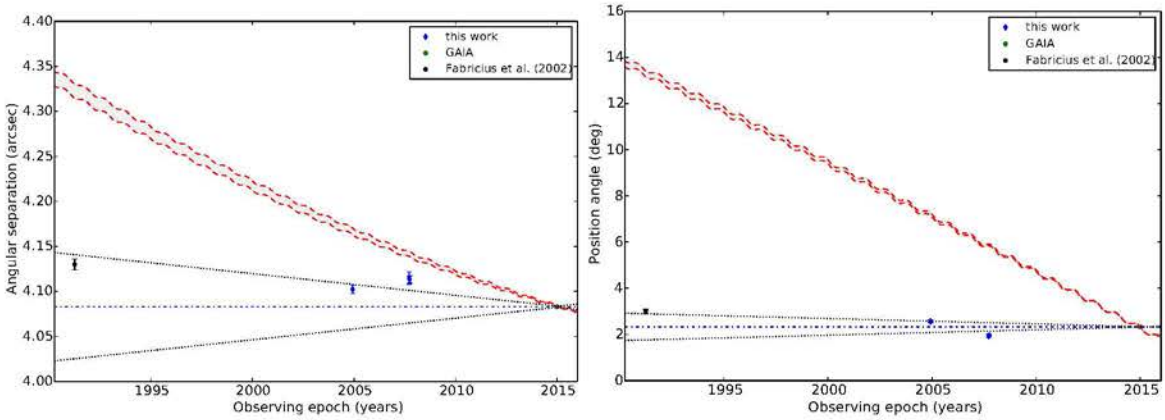


## HIP20042

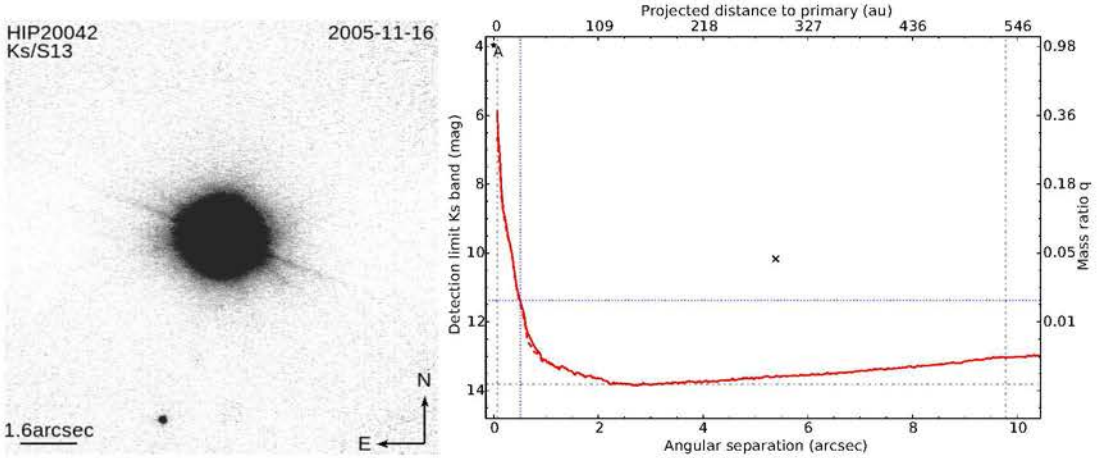

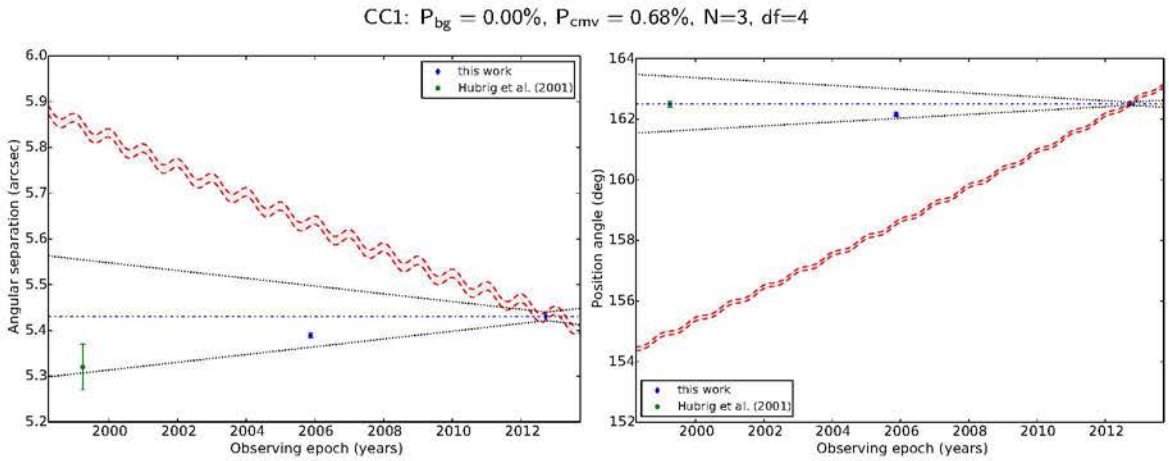


## HIP20554

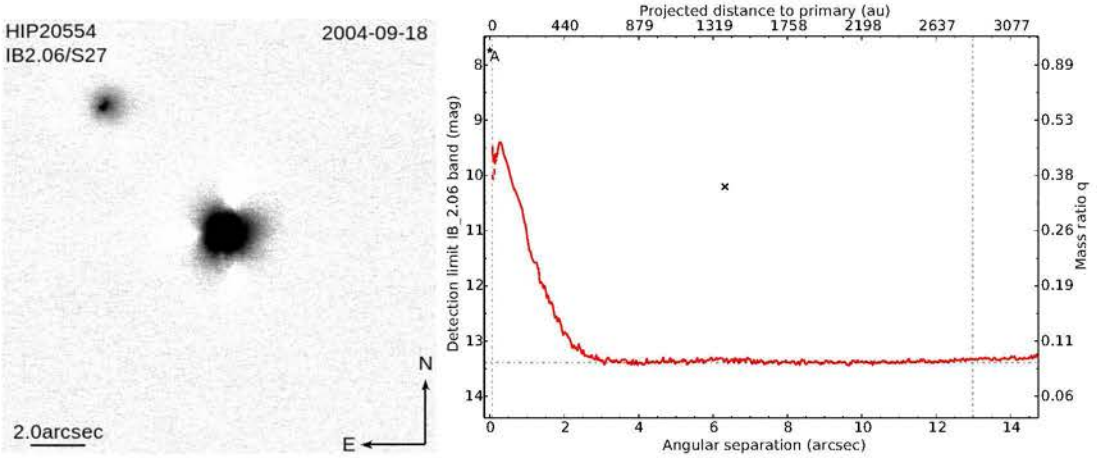


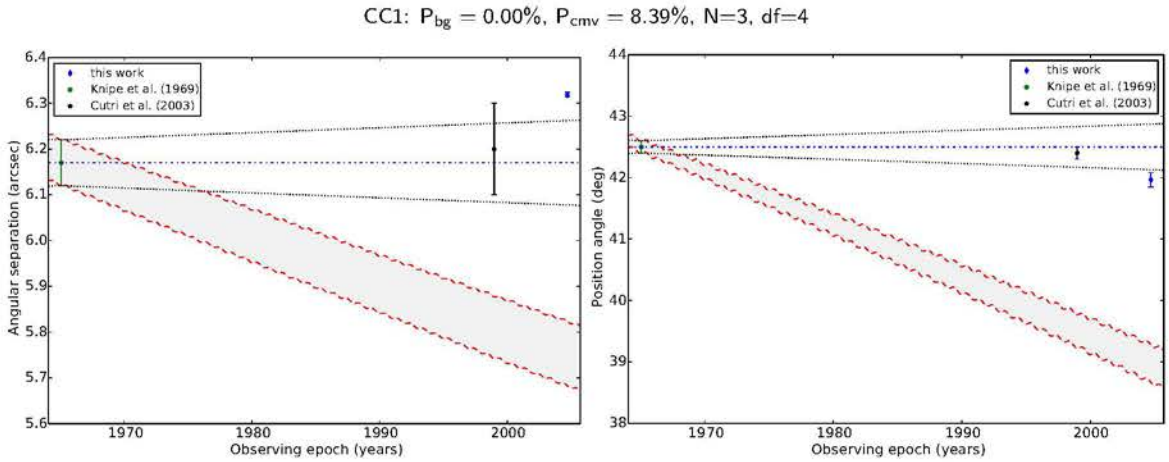


## HIP20804

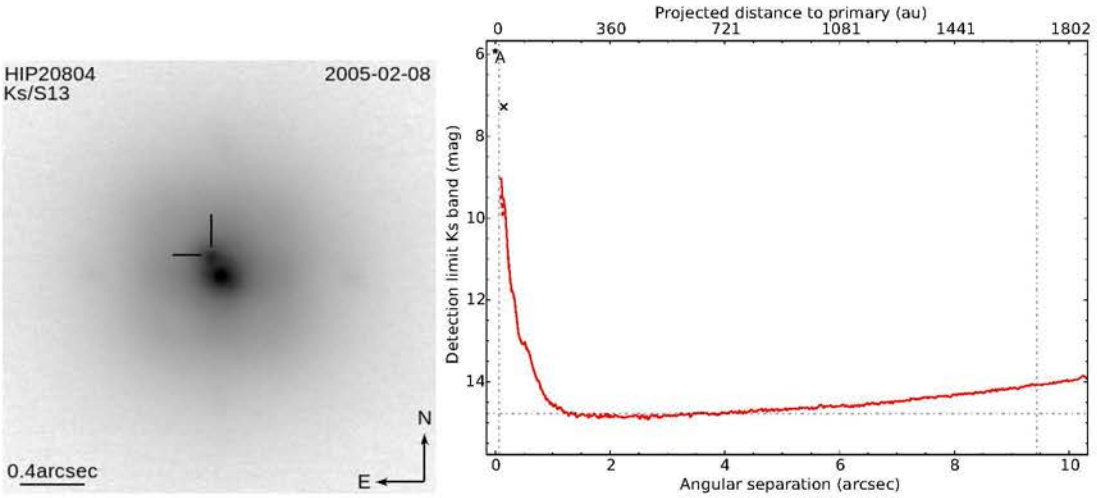

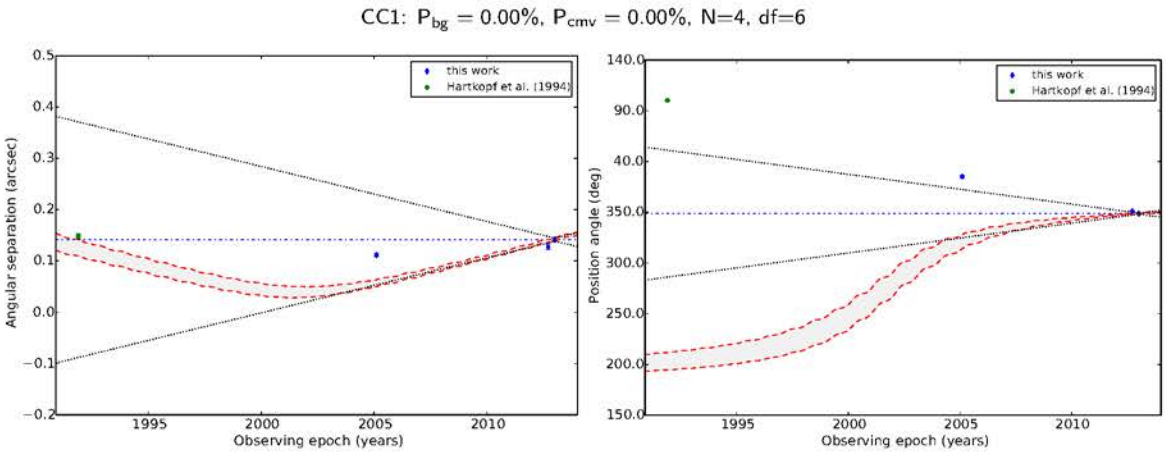


## HIP23794

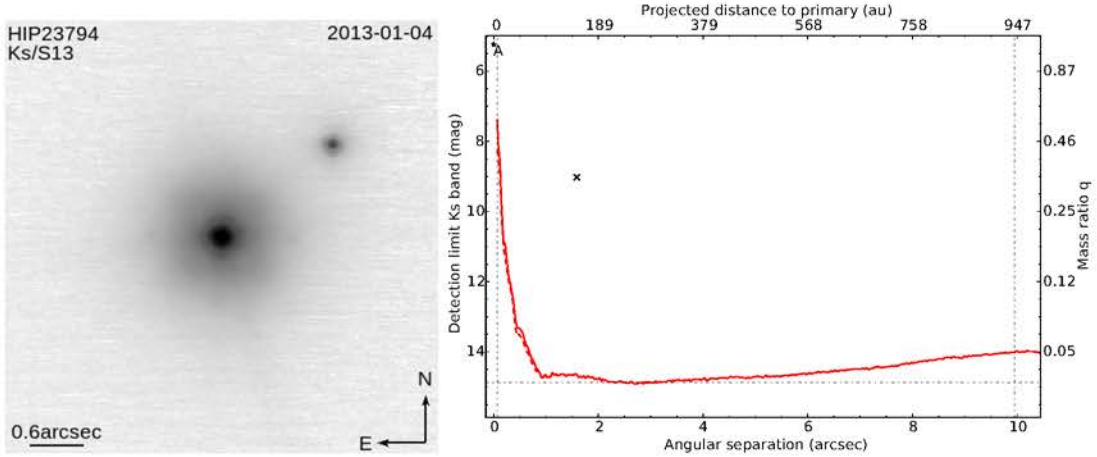


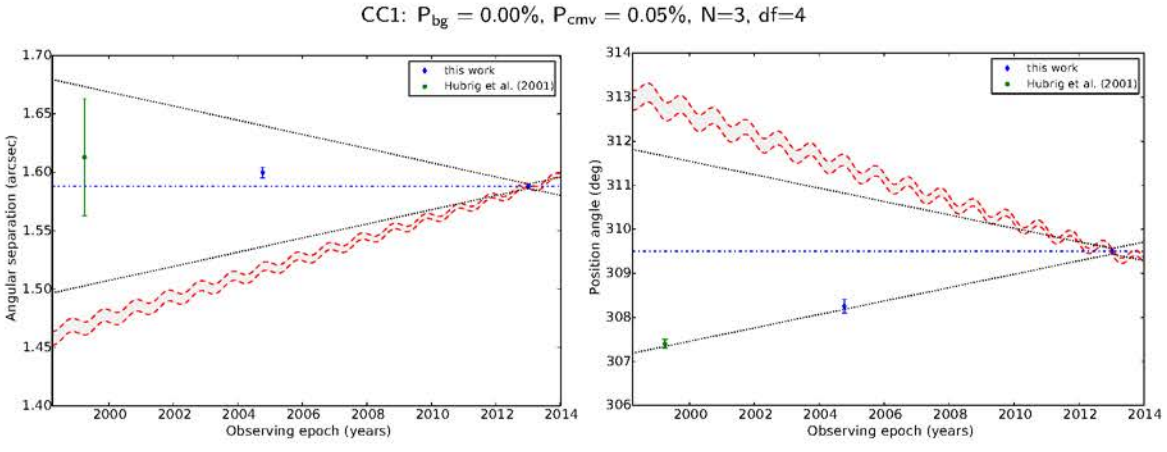


## HIP24196

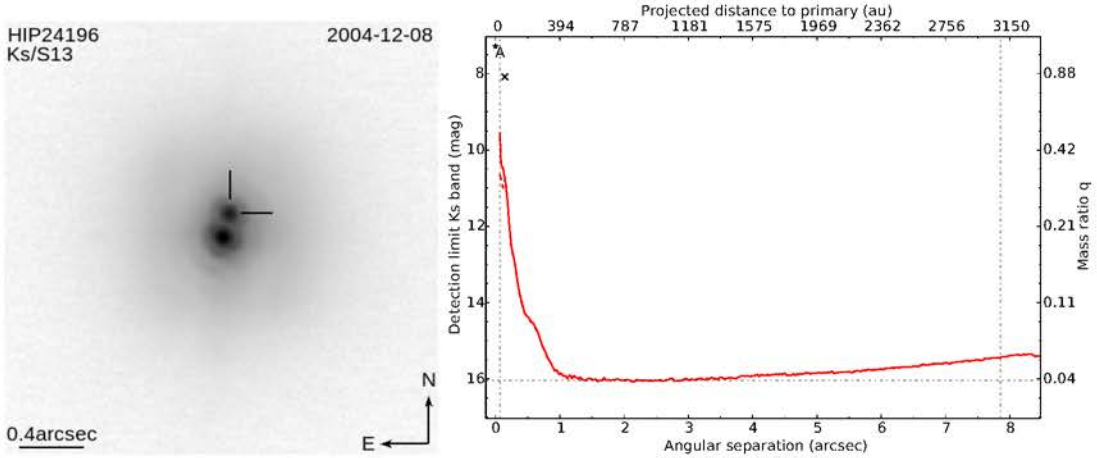

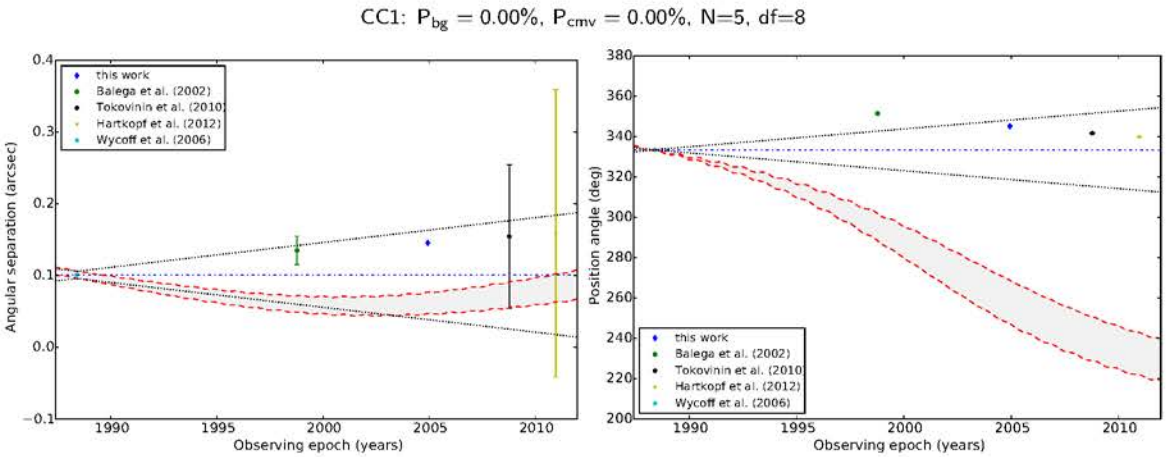


## HIP24305

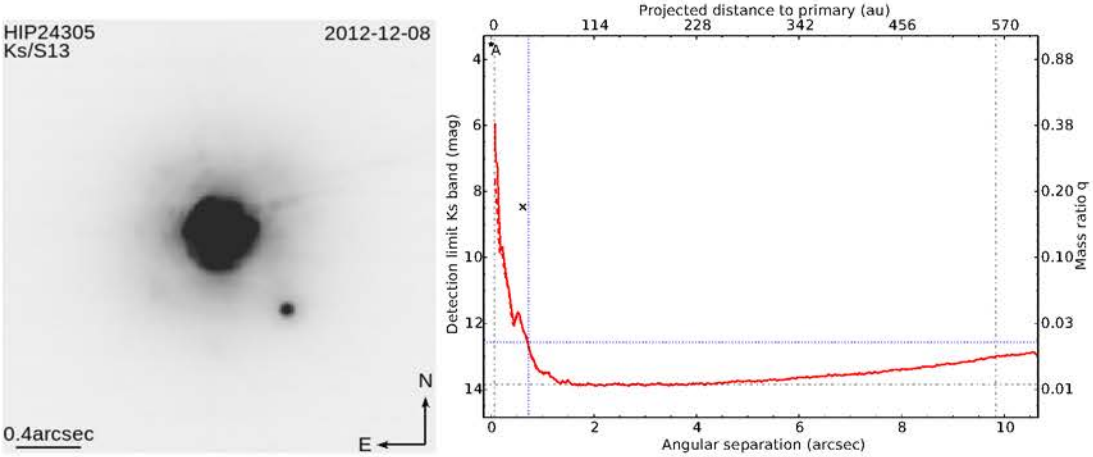


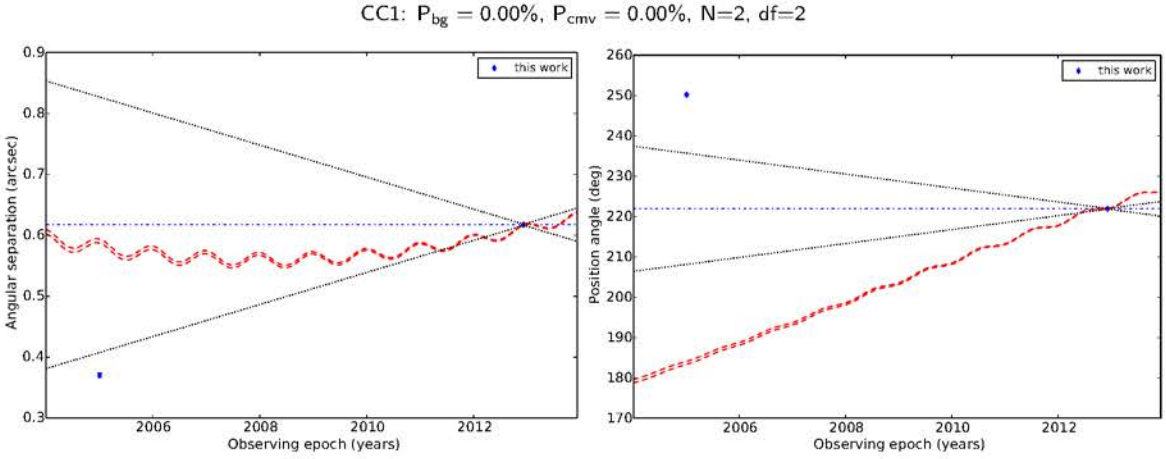


## HIP24825

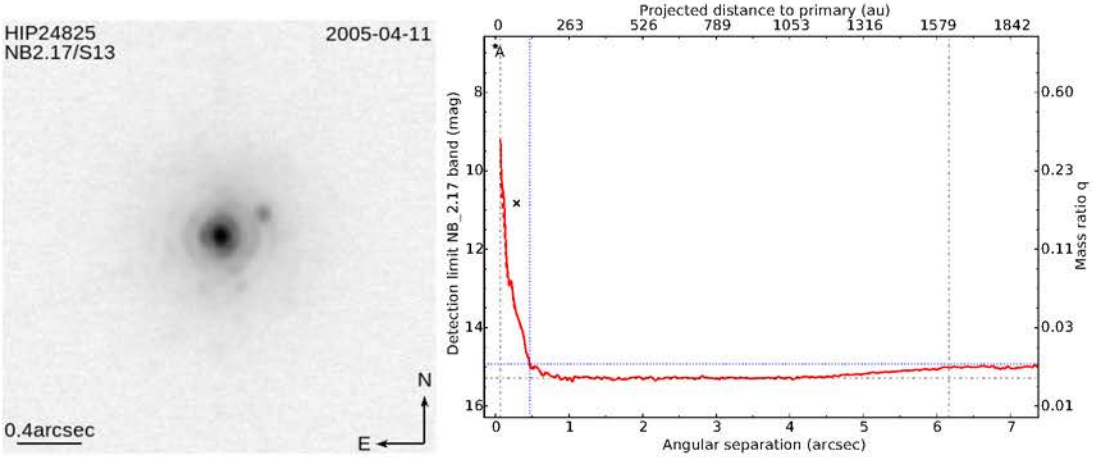

CC1: $P_{bg}$ = 0.24%, $P_{cmv}$ = 0.00%, N=2, df=2

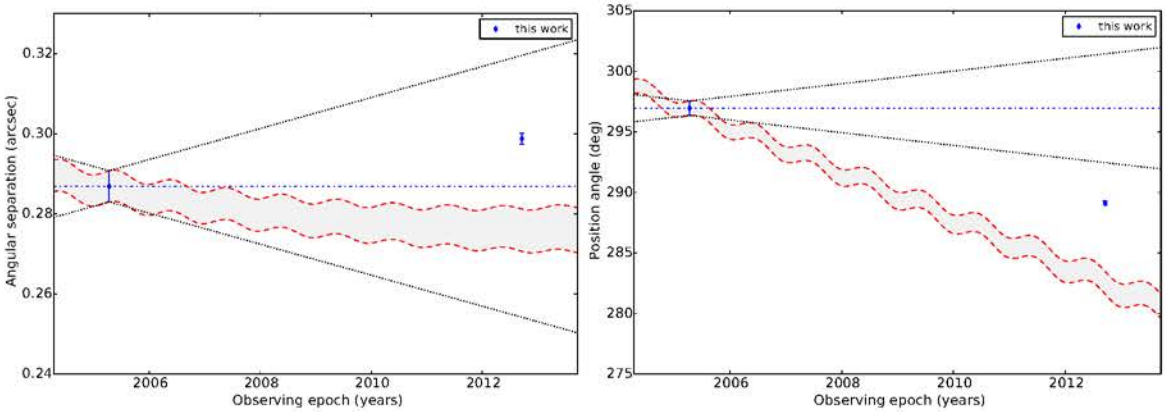


HIP24925

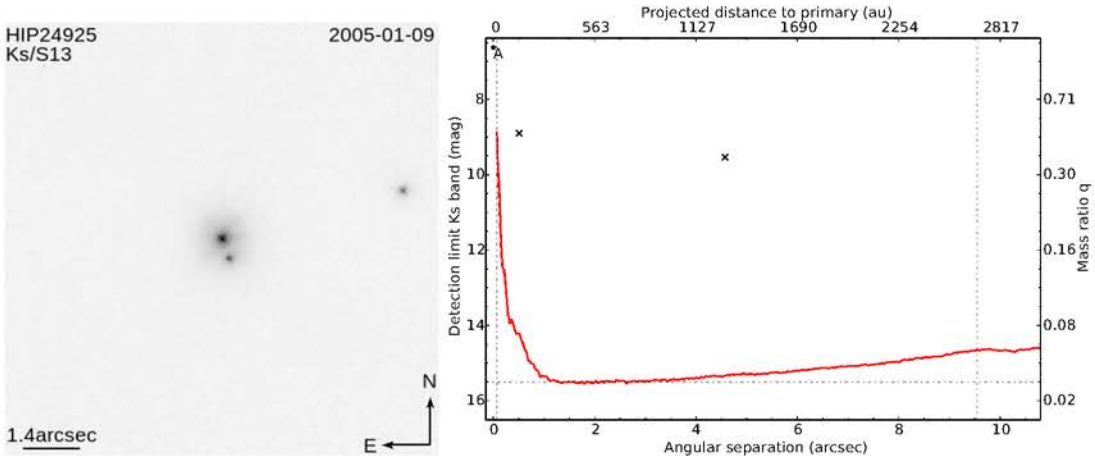


CC1: $P_{bg}$ = 0.00%, $P_{cmv}$ = 0.00%, N=4, df=6

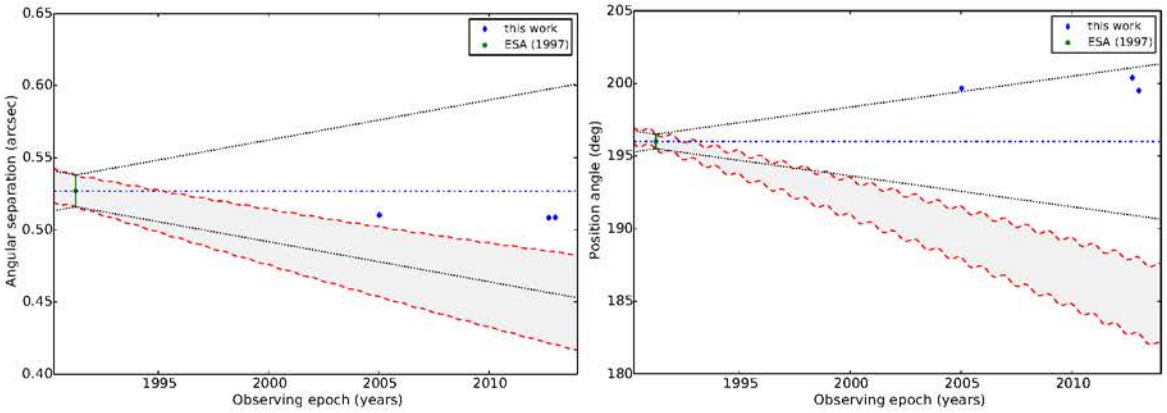


CC2: $P_{bg}$ = 7.97%, $P_{cmv}$ = 19.72%, N=4, df=6

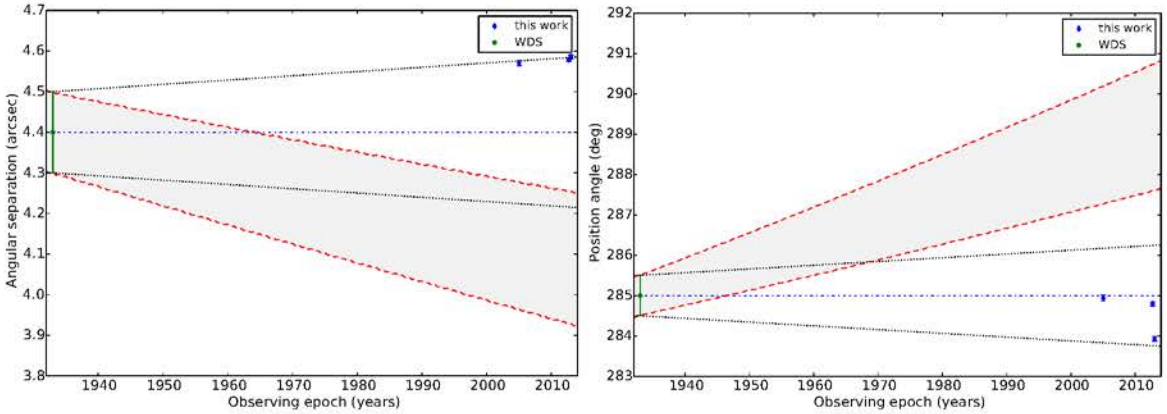

## HIP25365

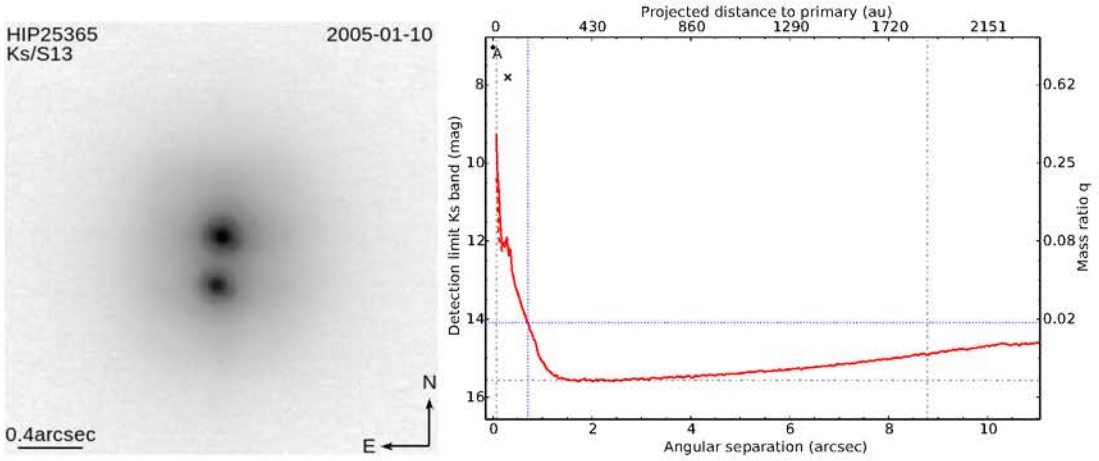


CC1: $P_{bg} = 0.00\%$, $P_{cmv} = 0.00\%$, N=4, df=6

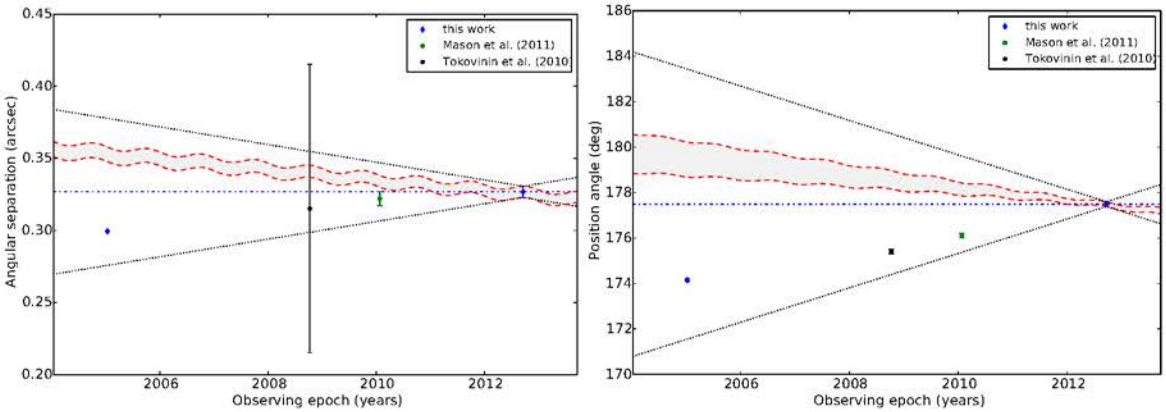


## HIP26215

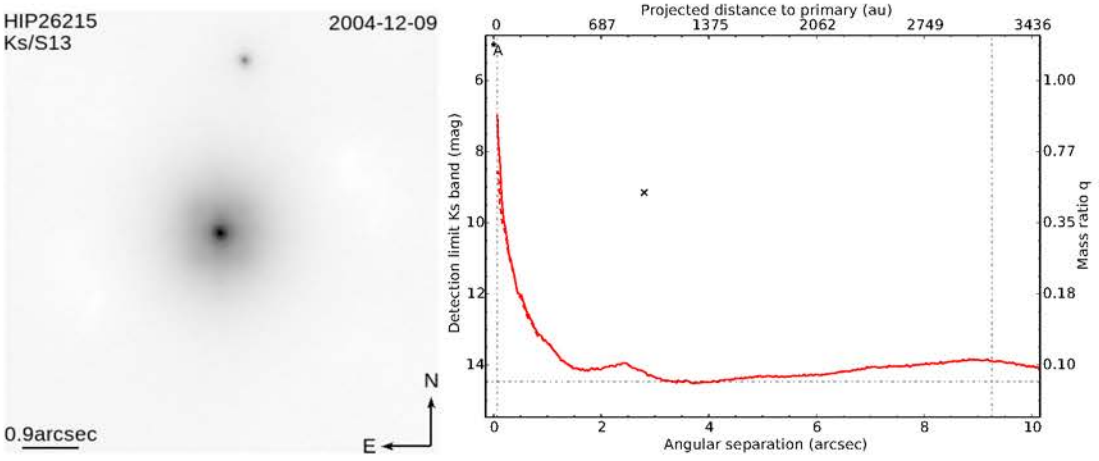


CC1: $P_{bg} = 7.09\%$, $P_{cmv} = 82.16\%$, N=2, df=2

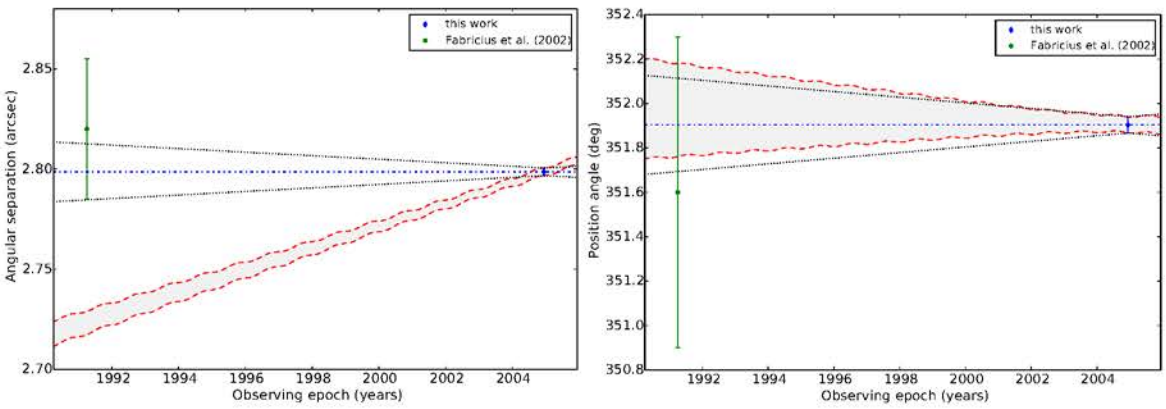

## HIP26235

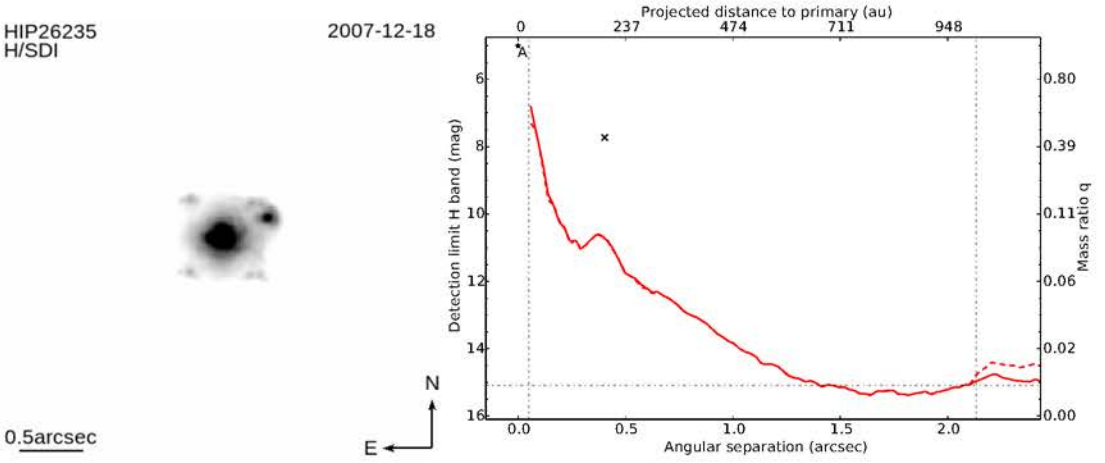


CC1: $P_{bg} = 0.00\%$, $P_{cmv} = 0.00\%$, N=6, df=10

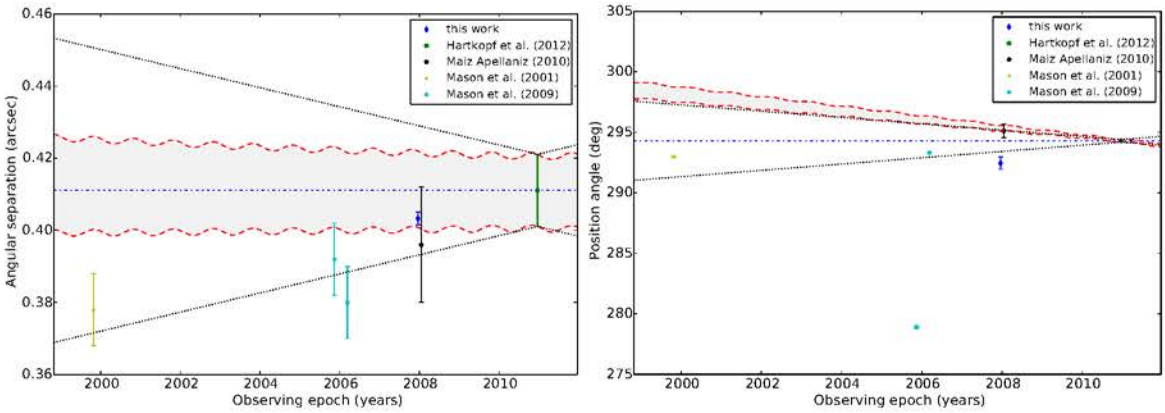


## HIP26237

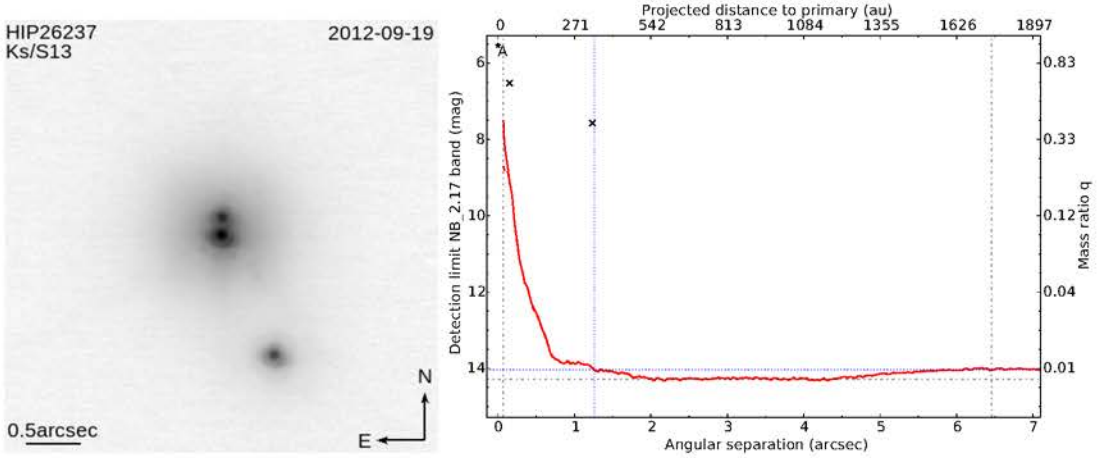


CC1: $P_{bg} = 0.01\%$, $P_{cmv} = 0.00\%$, N=3, df=4

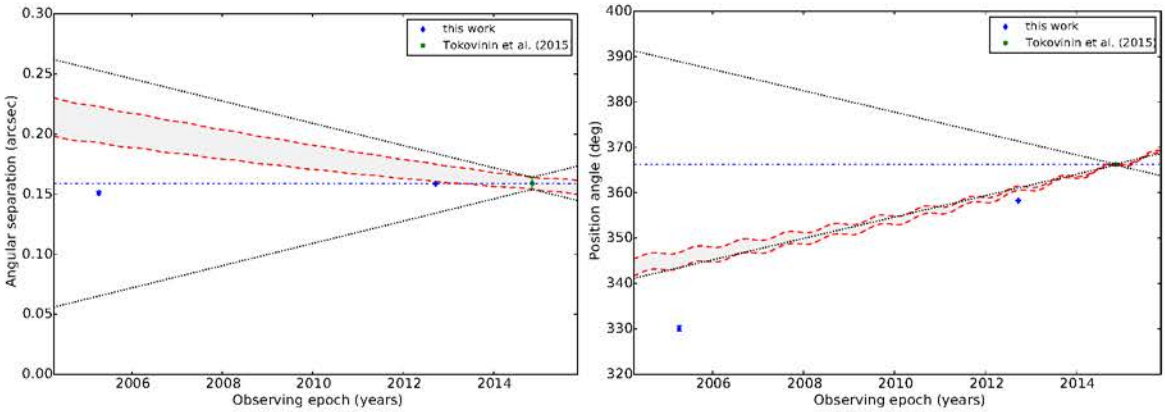

CC2: $P_{bg} = 0.00\%$, $P_{cmv} = 0.00\%$, N=3, df=4

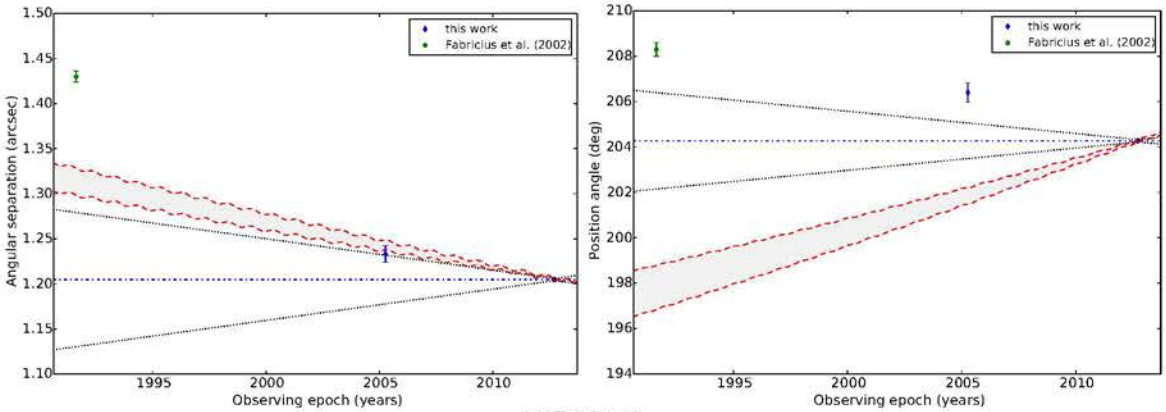


HIP26549

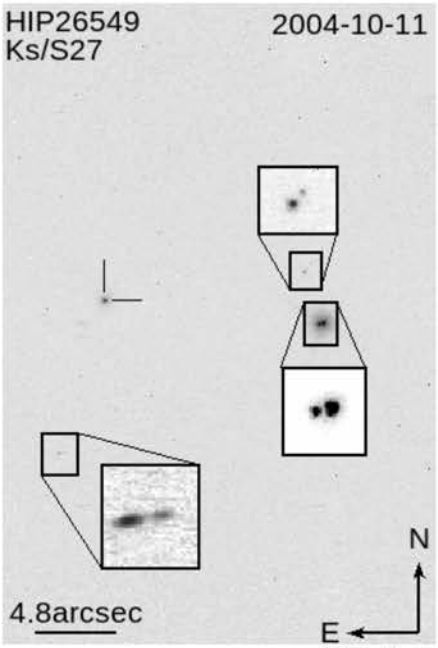


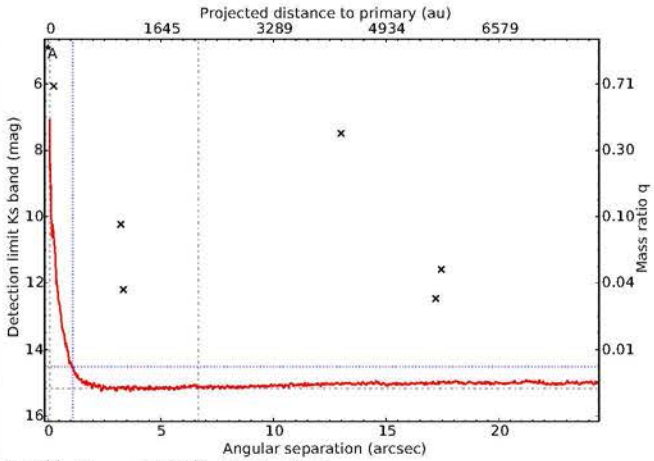


CC1: $P_{bg} = 0.00\%$, $P_{cmv} = 0.00\%$, N=5, df=8

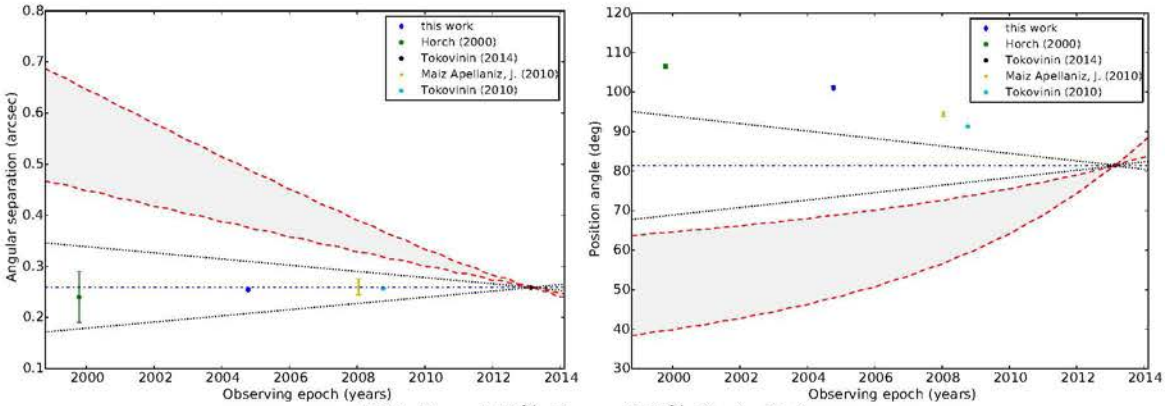


CC2: $P_{bg} = 0.21\%$, $P_{cmv} = 0.75\%$, N=4, df=6

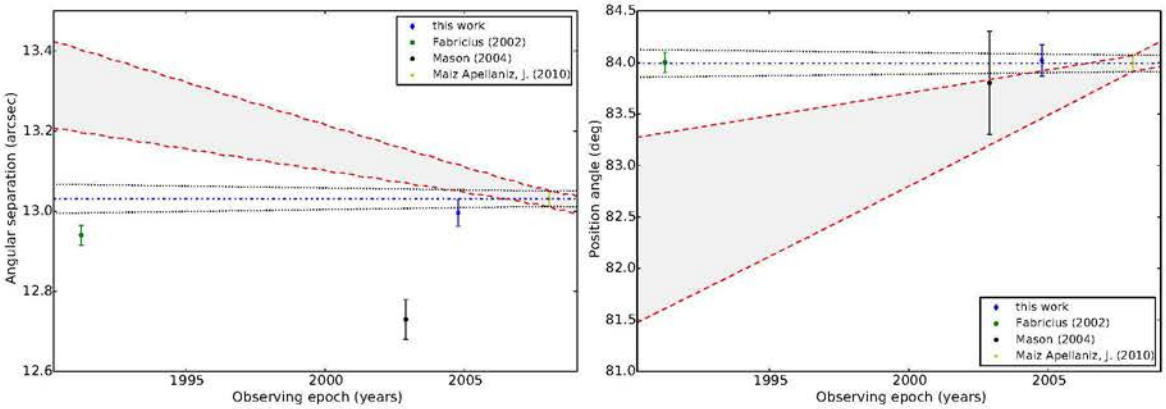

CC3: $P_{bg}$ = 86.39%, $P_{cmv}$ = 99.31%, N=2, df=2

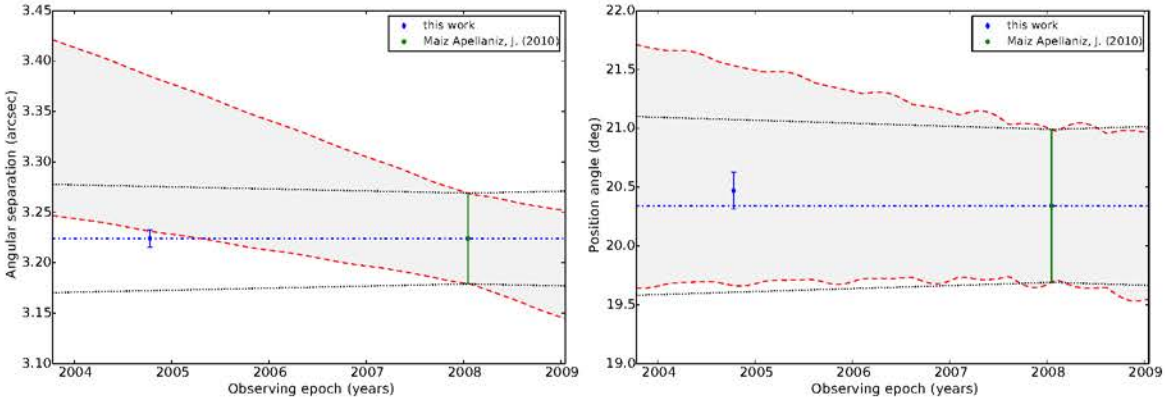


HIP26602

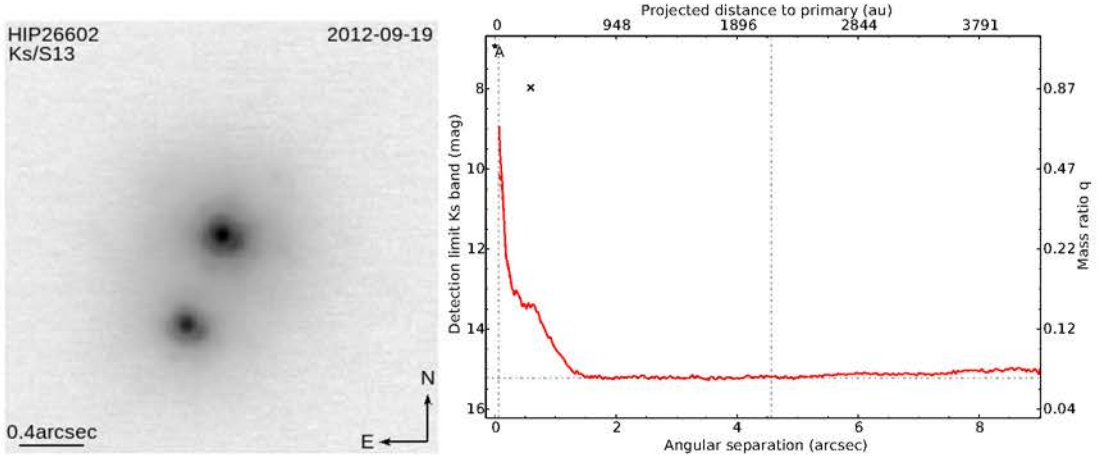


CC1: $P_{bg}$ = 0.00%, $P_{cmv}$ = 0.00%, N=3, df=4

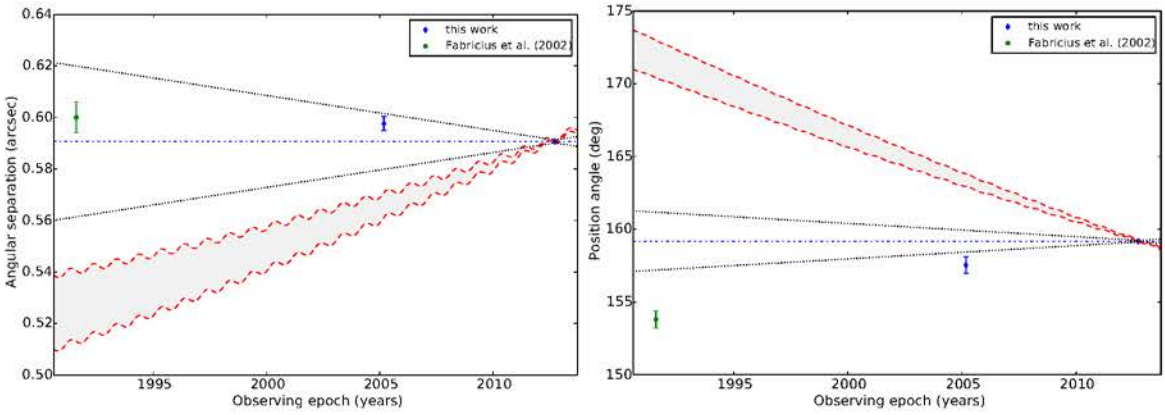


HIP28744

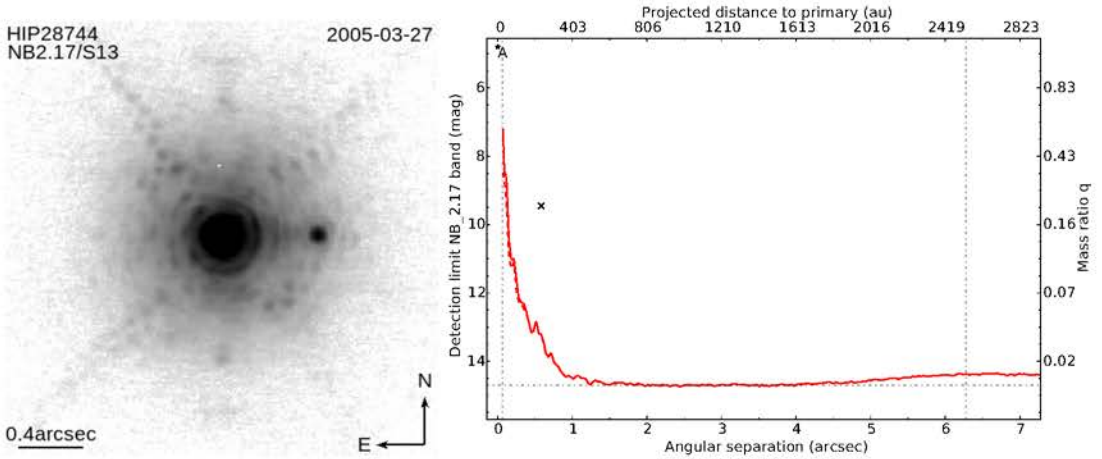

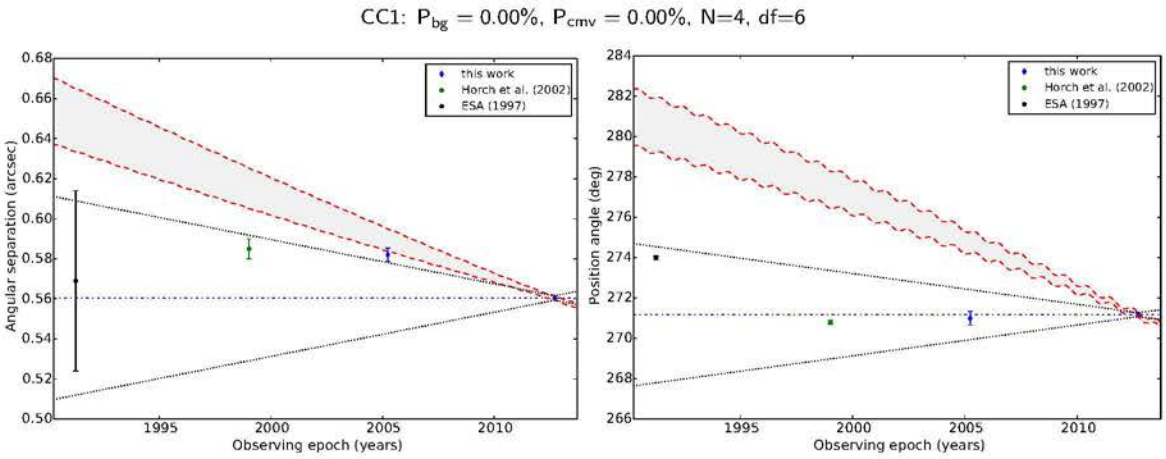


## HIP29401

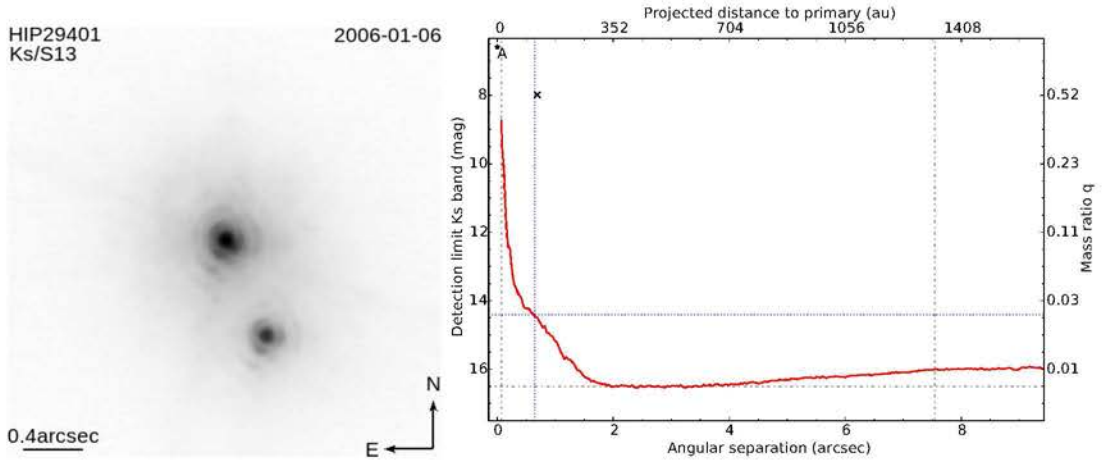


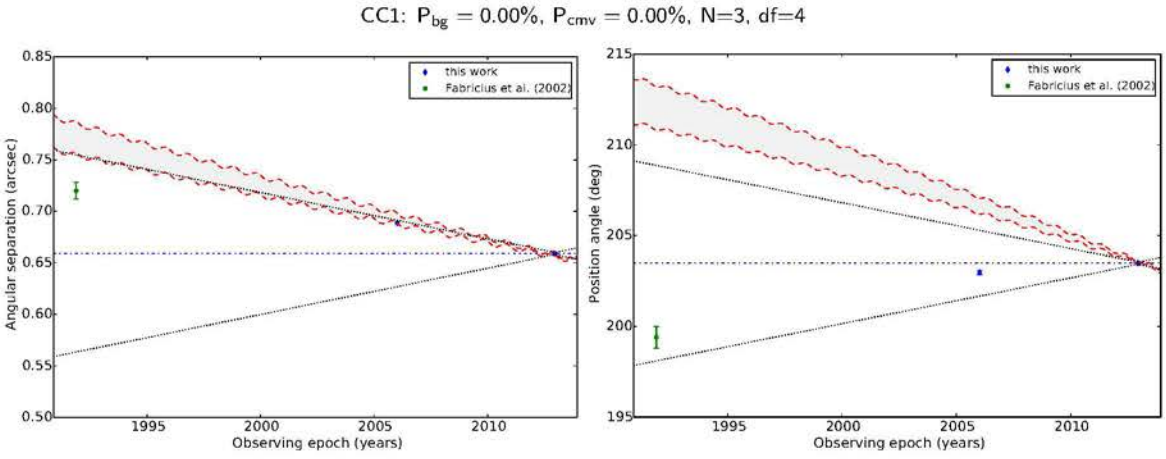


## HIP29728

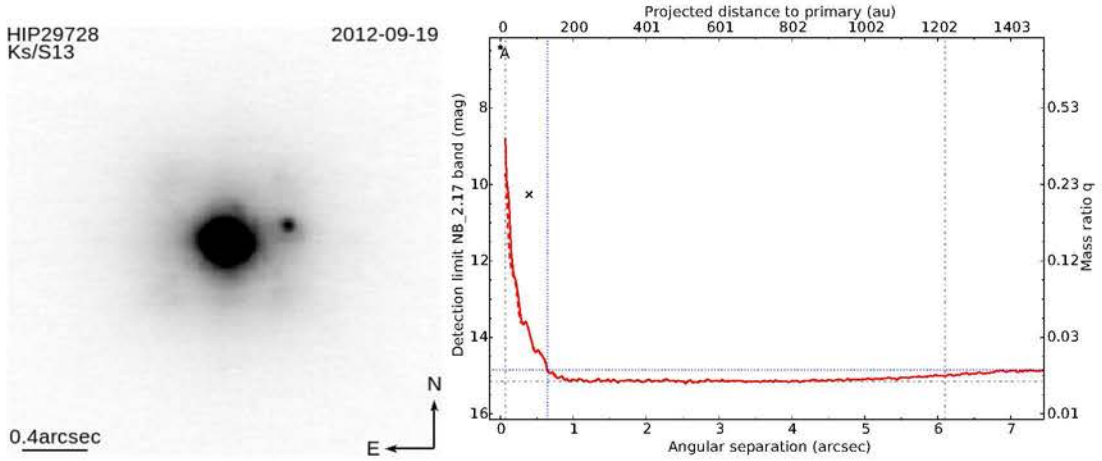

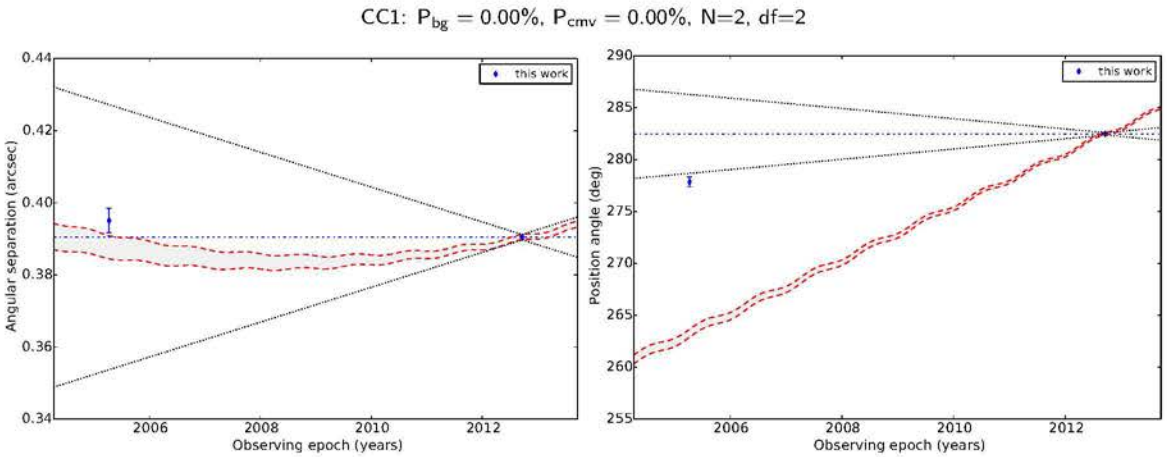


## HIP30493

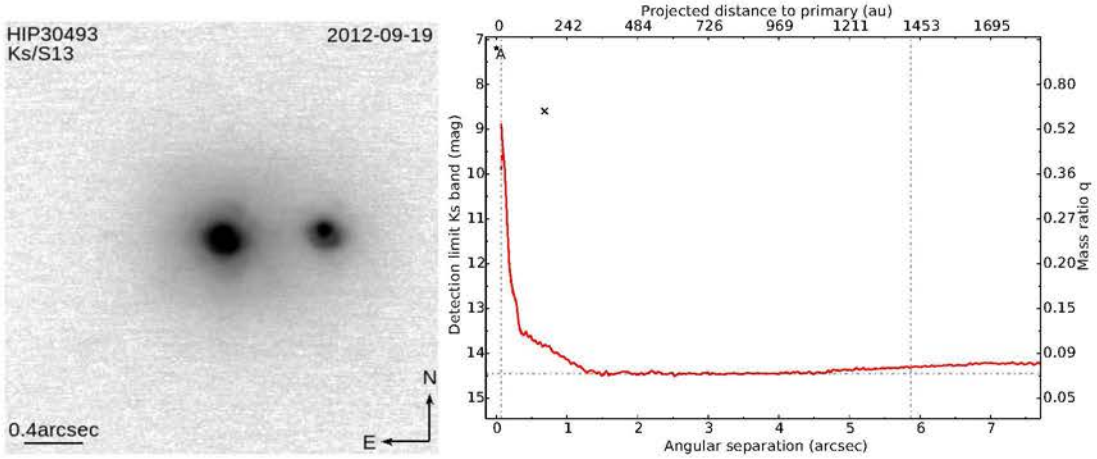


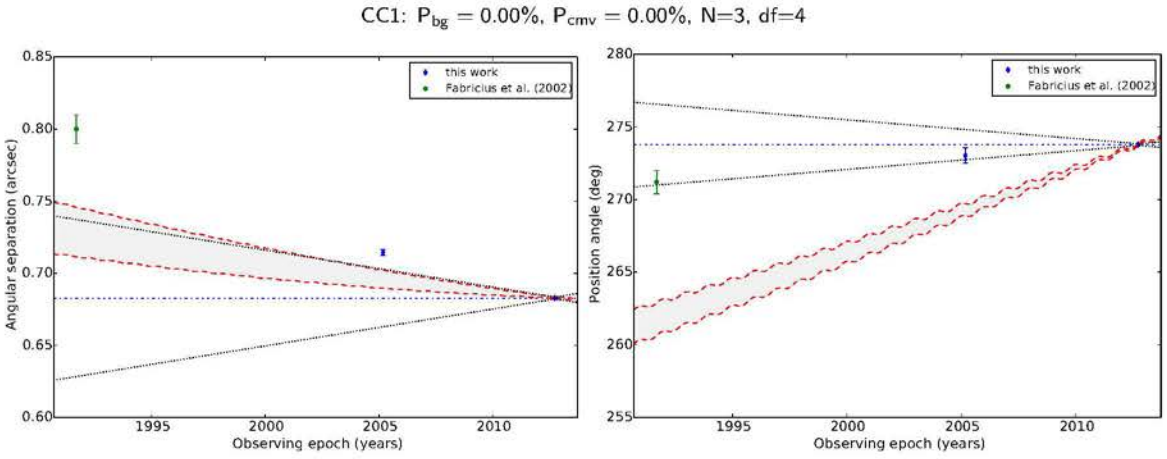


## HIP30867

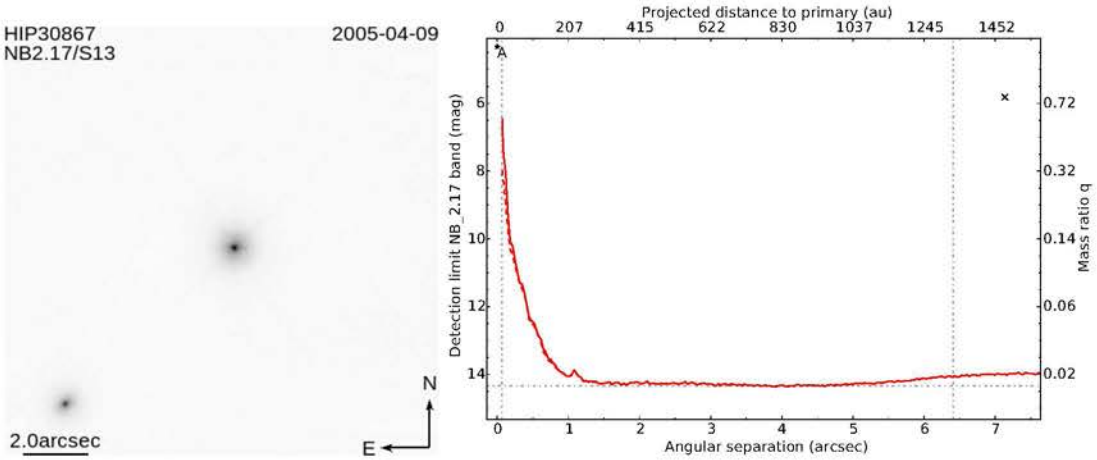

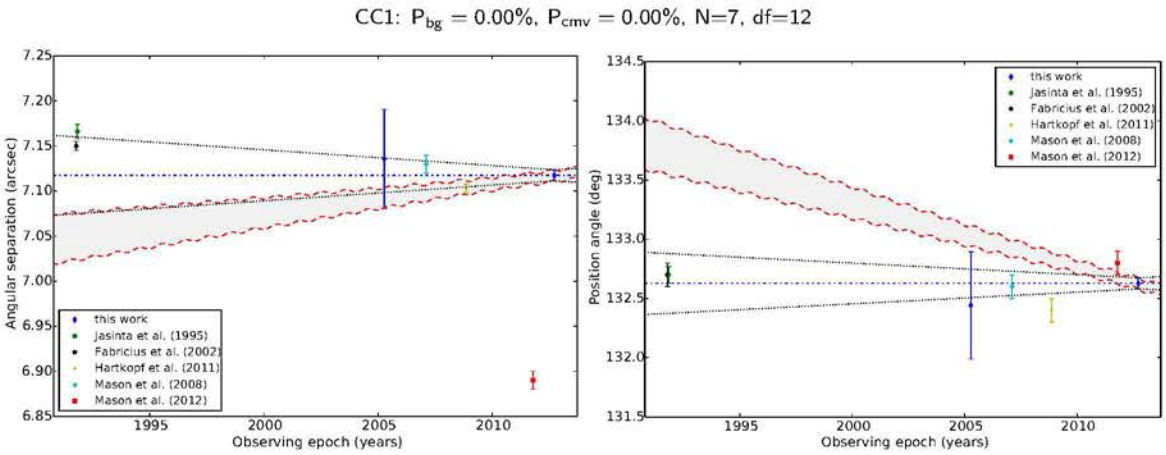


## HIP31137

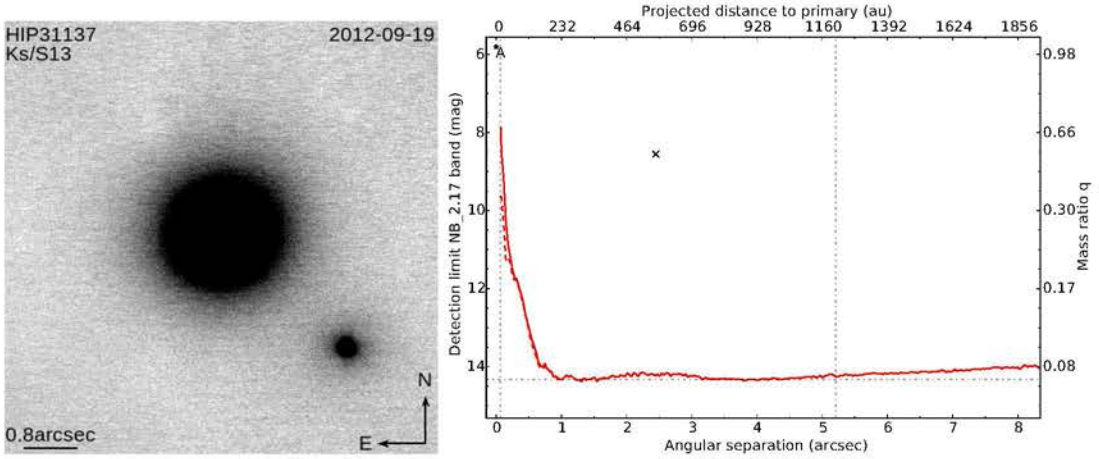


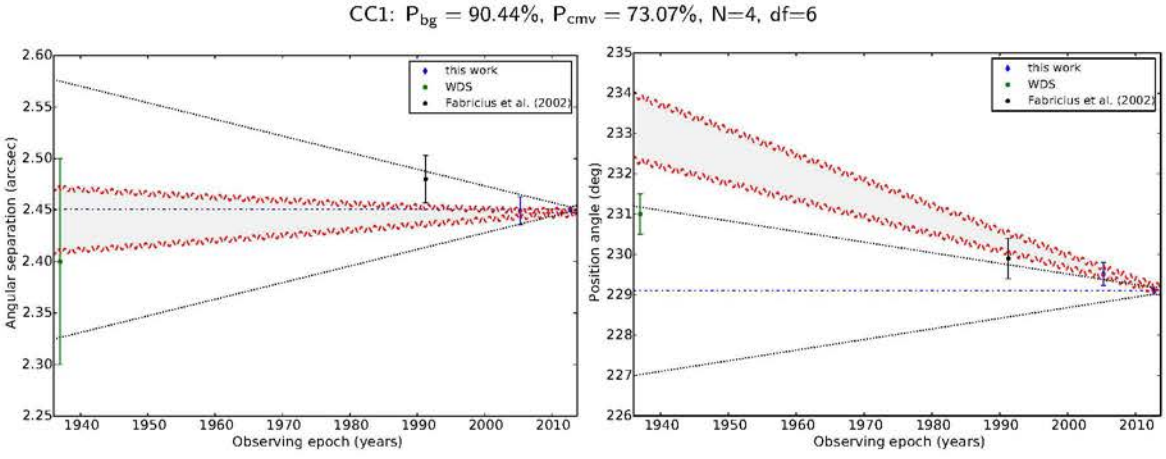


## HIP31959

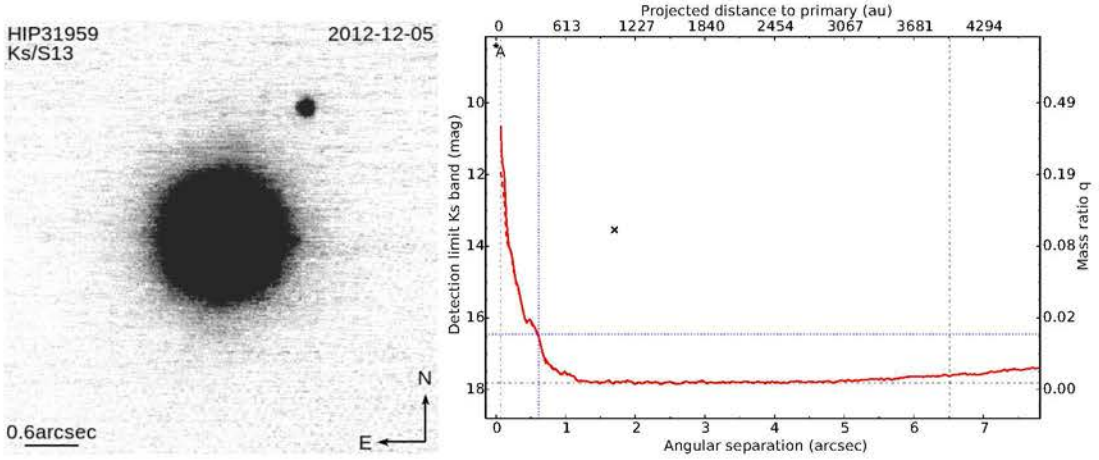

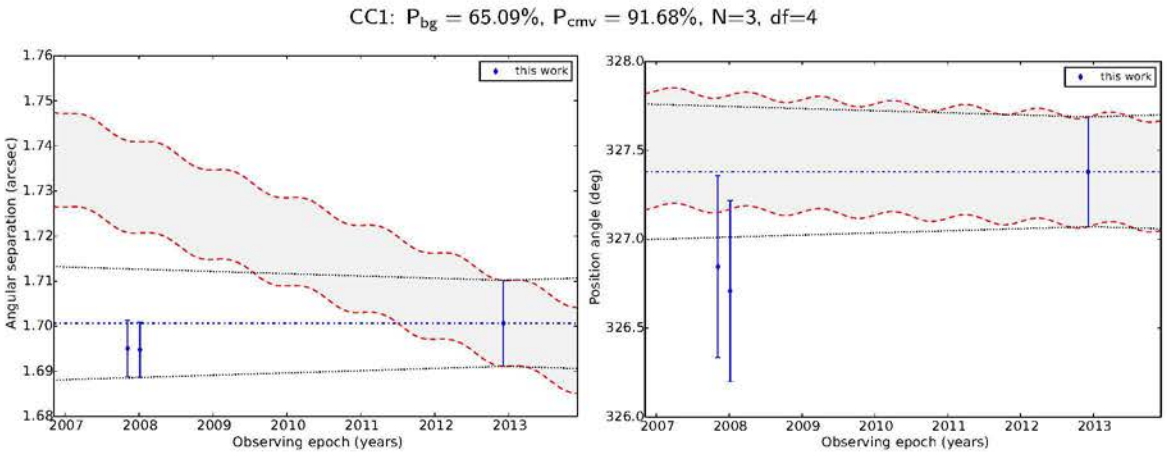


## HIP34045

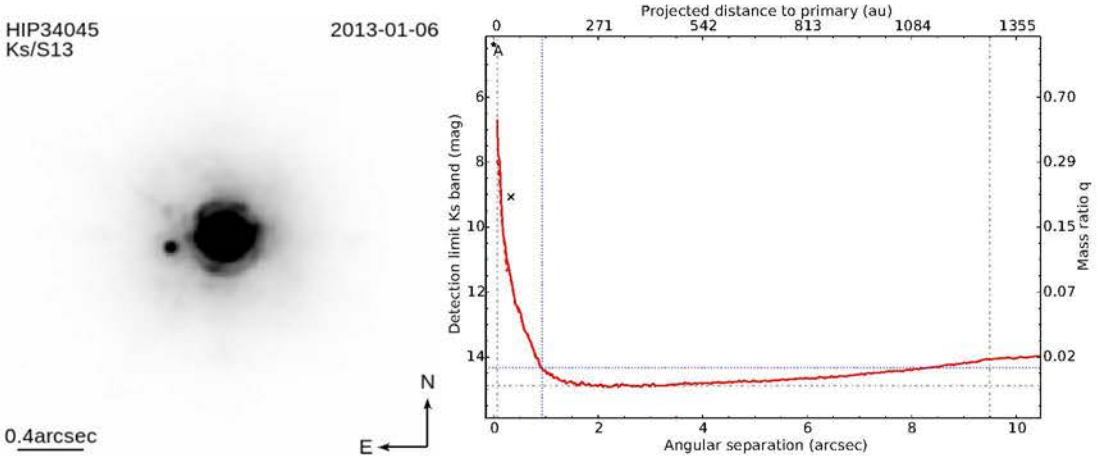


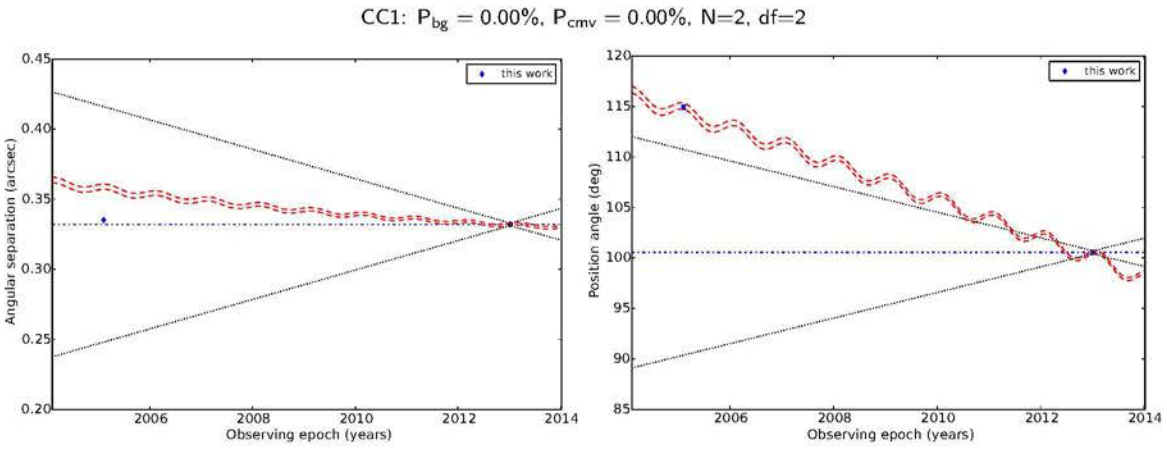


## HIP34338

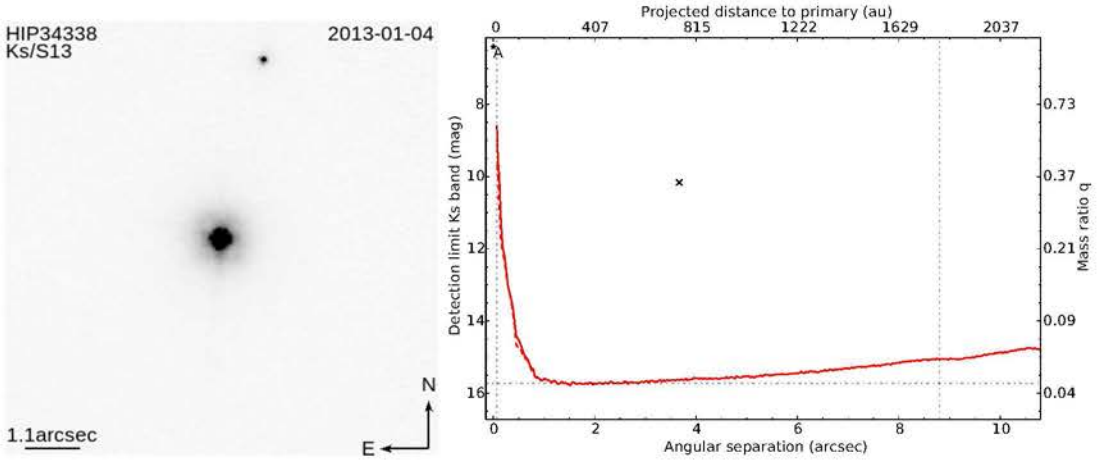

CC1: $P_{bg} = 0.00\%$, $P_{cmv} = 0.00\%$, N=2, df=2

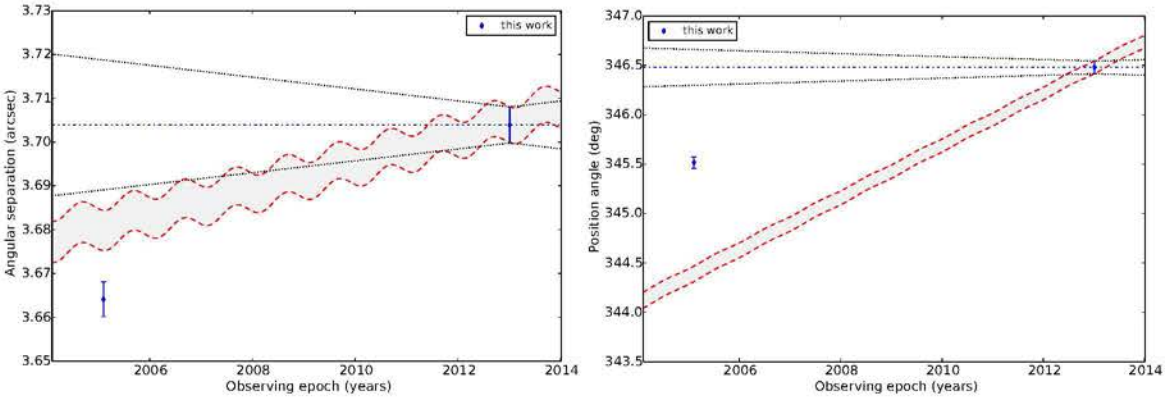


## HIP34758

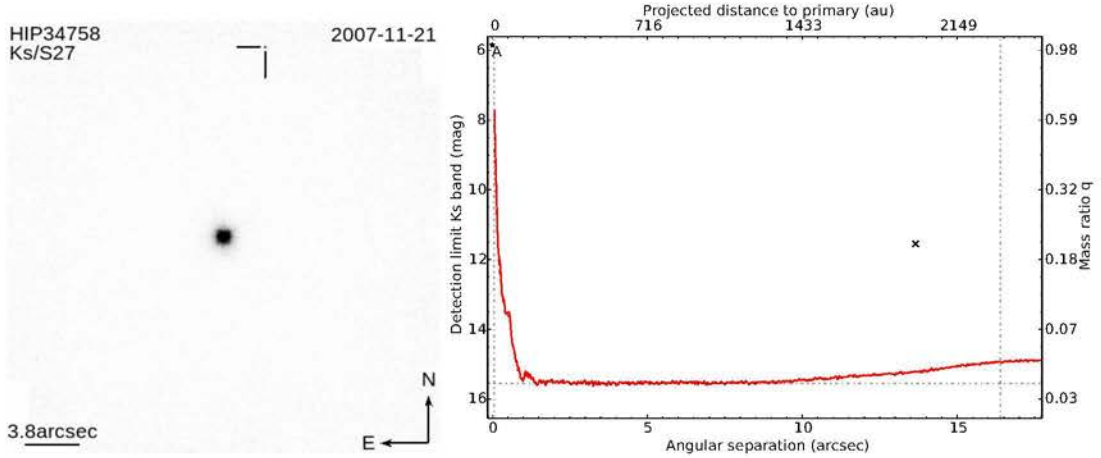


CC1: $P_{bg} = 17.03\%$, $P_{cmv} = 2.42\%$, N=2, df=2

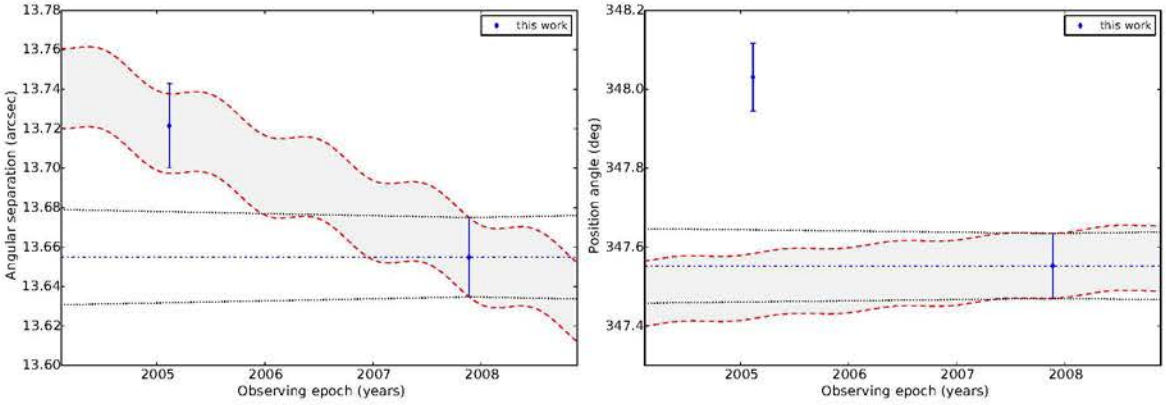


## HIP36345

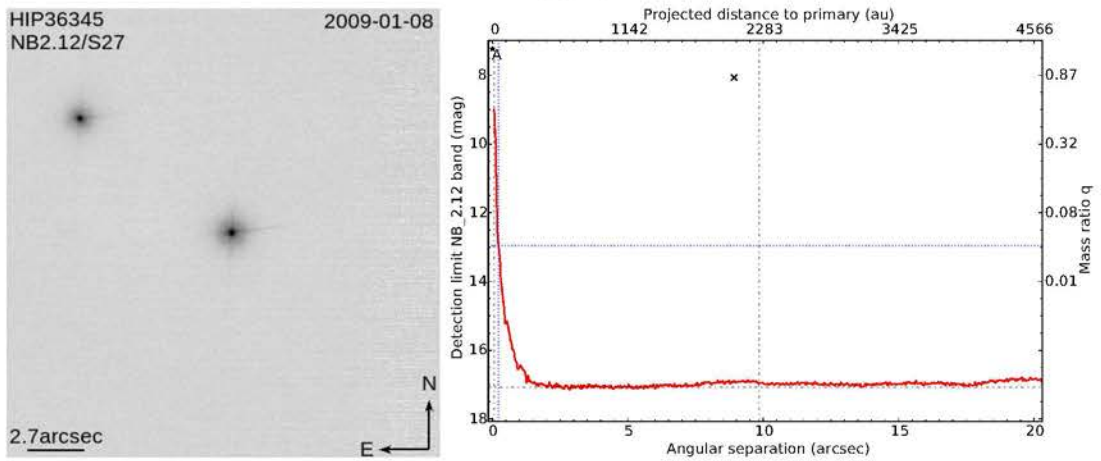

CC1: $P_{bg} = 69.26\%$, $P_{cmv} = 97.54\%$, N=3, df=4

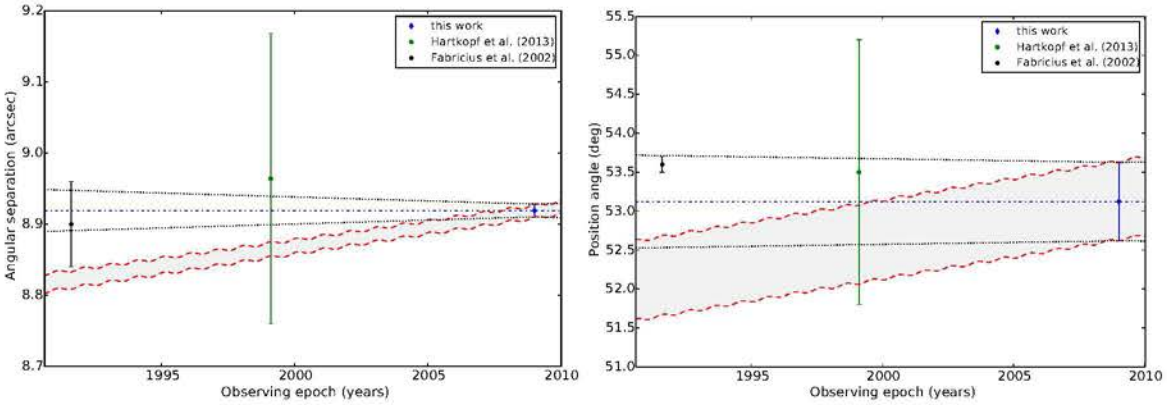


## HIP36363

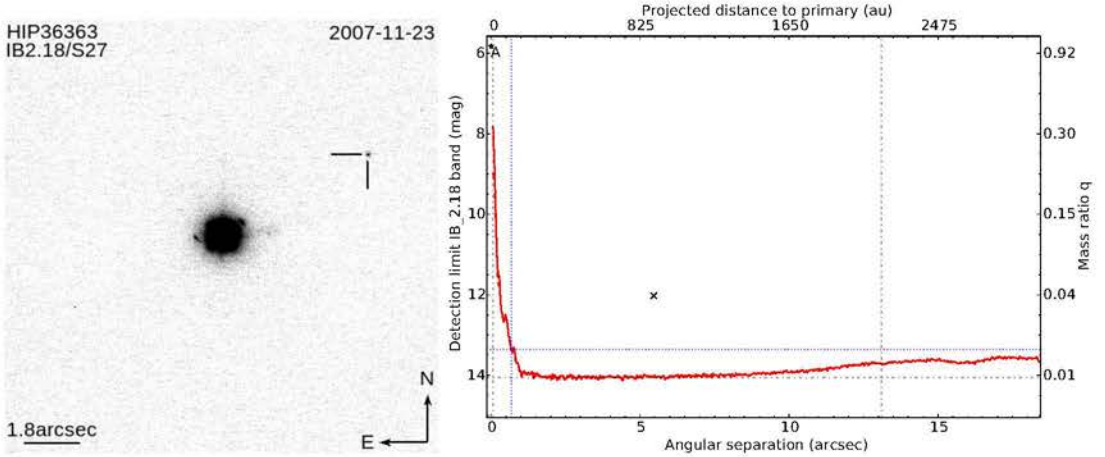


CC1: $P_{bg} = 27.91\%$, $P_{cmv} = 11.57\%$, N=2, df=2

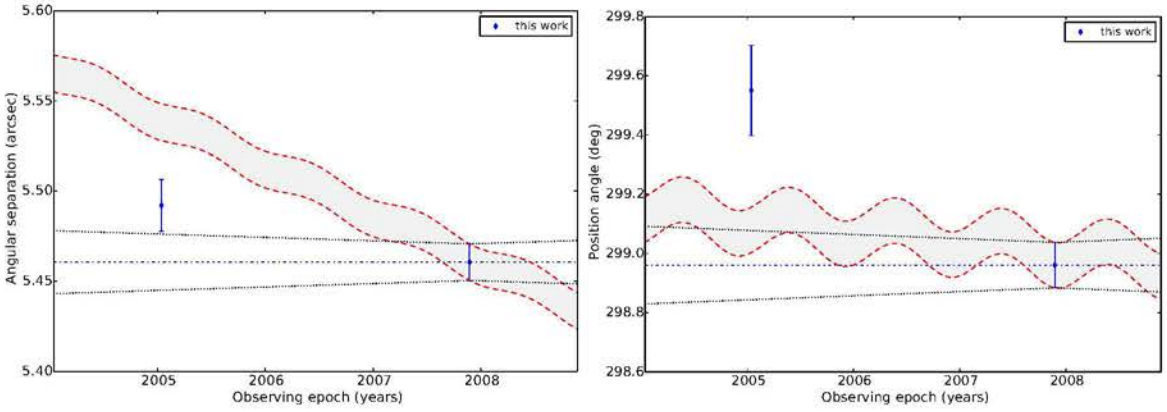


## HIP37322

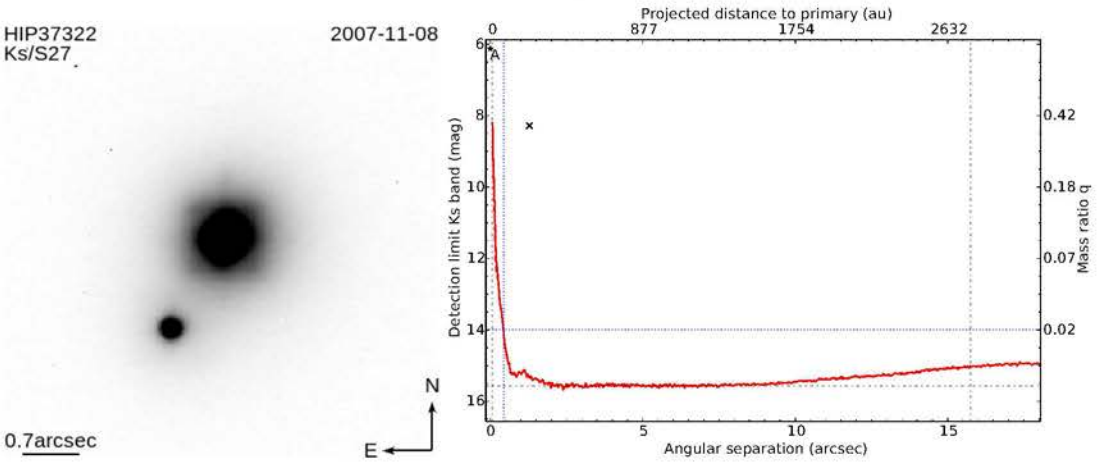

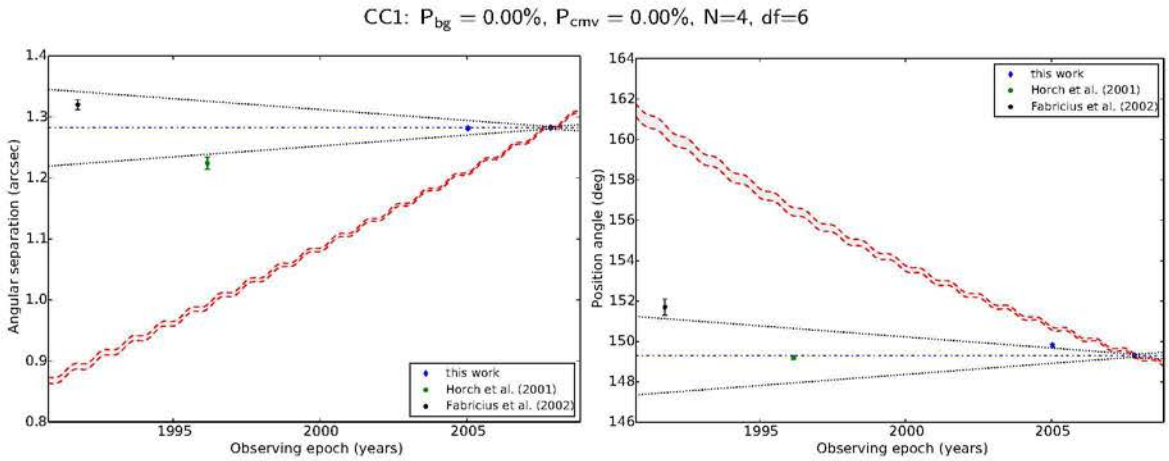


## HIP37915

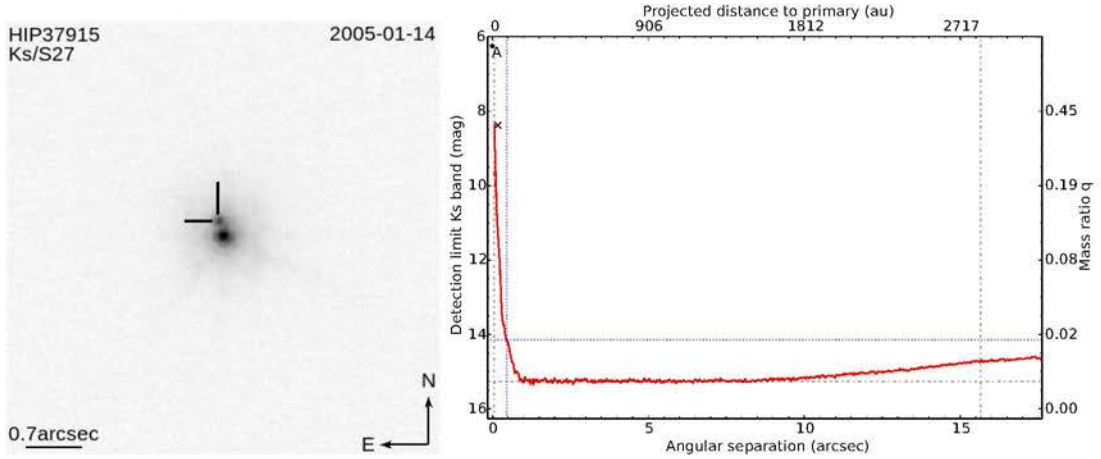


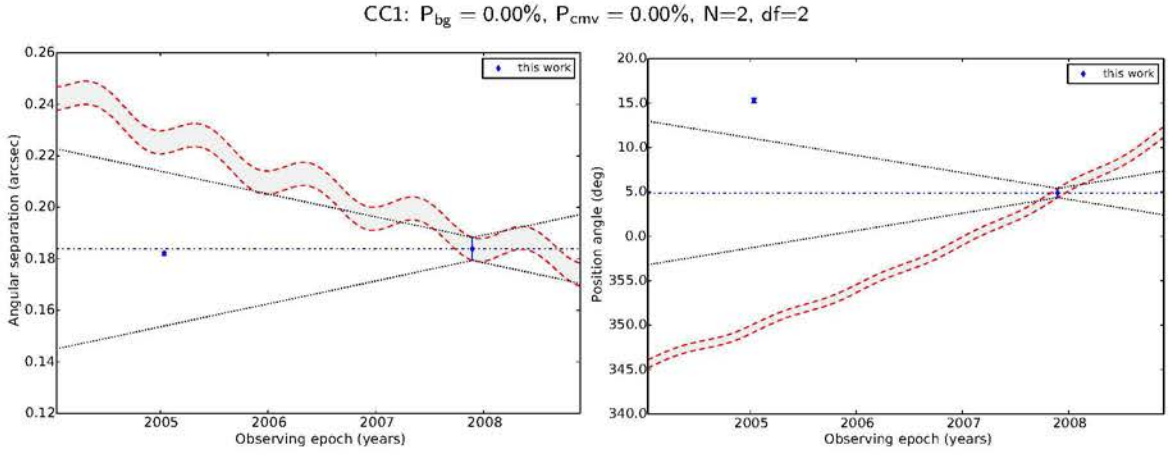


## HIP40817

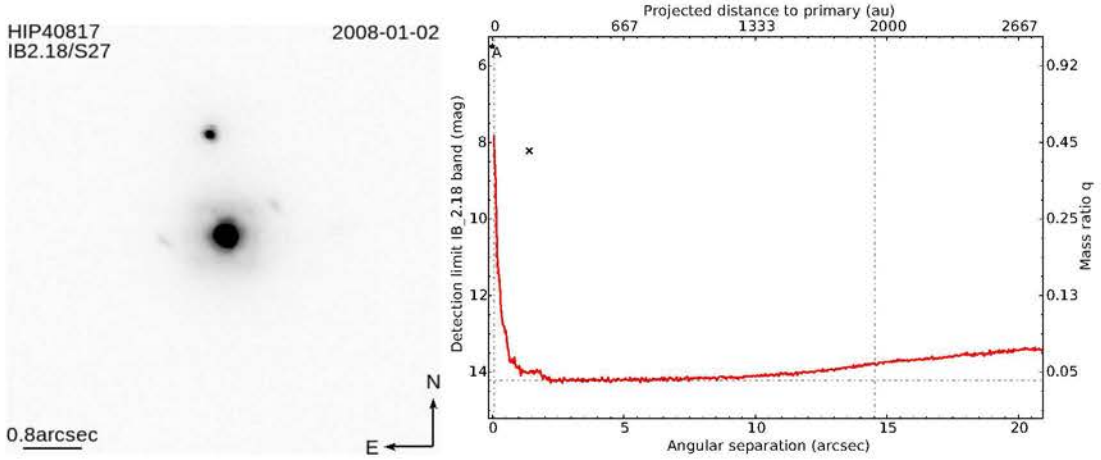

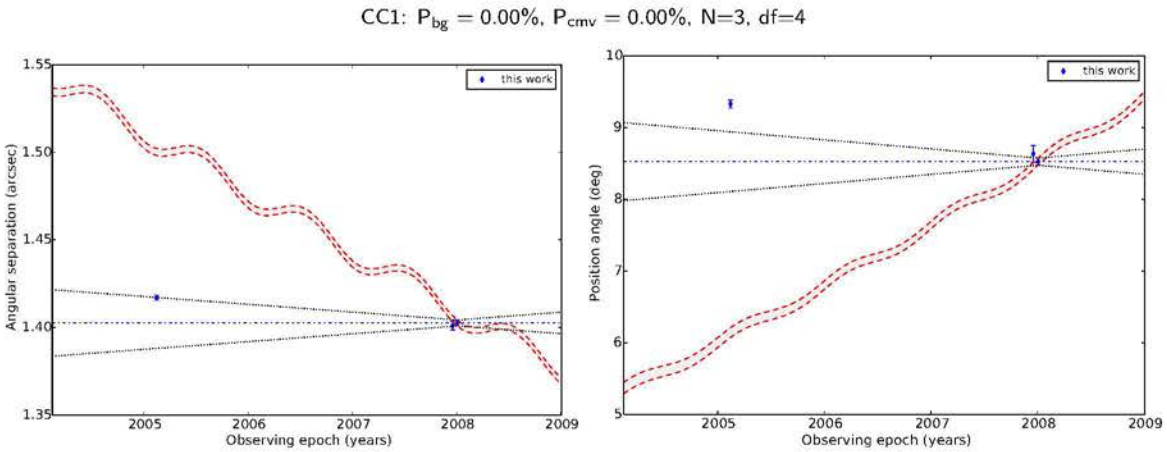


HIP41049

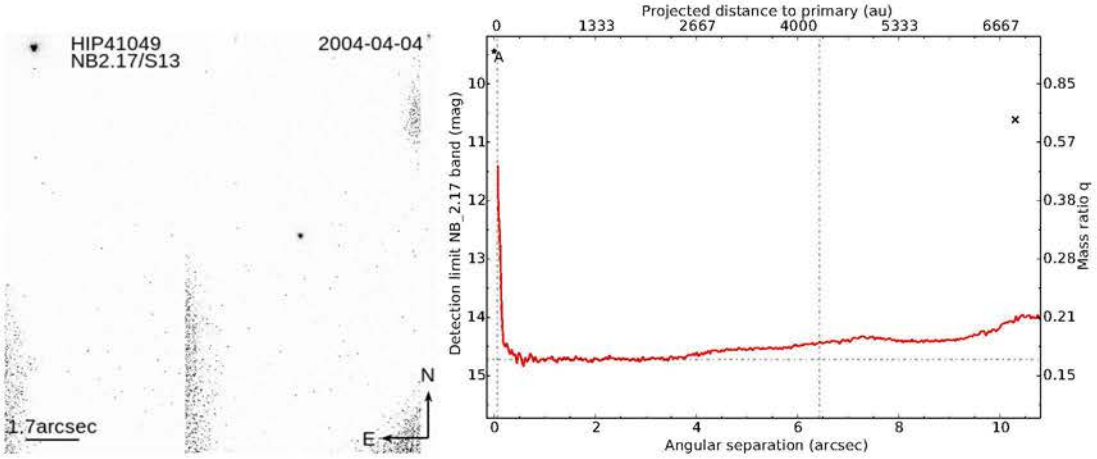


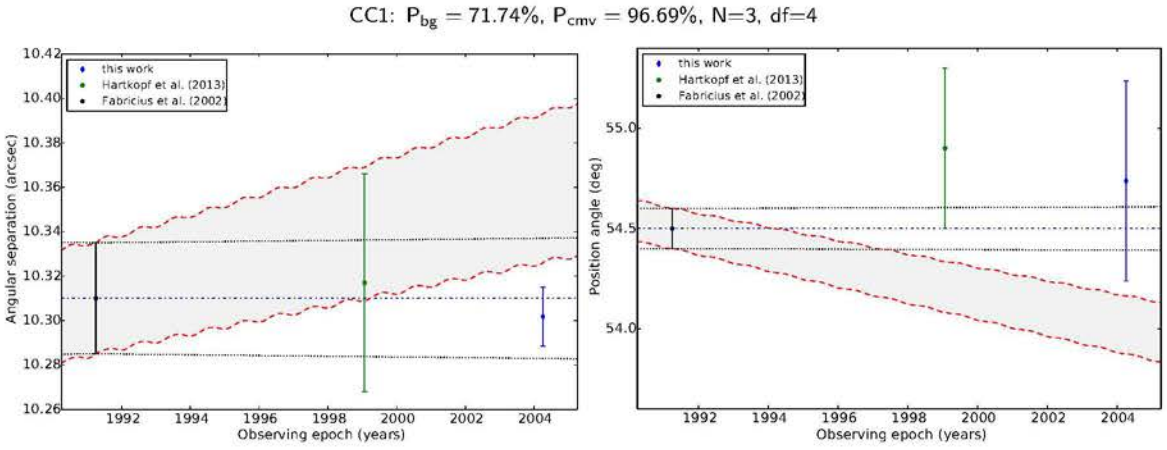


HIP41817

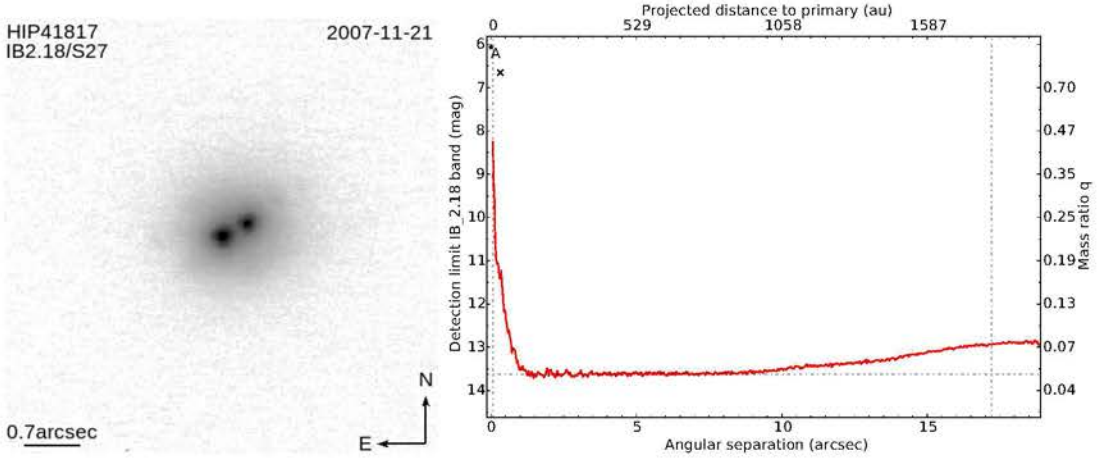

CC1: $P_{bg} = 0.00\%$, $P_{cmv} = 0.00\%$, N=5, df=8

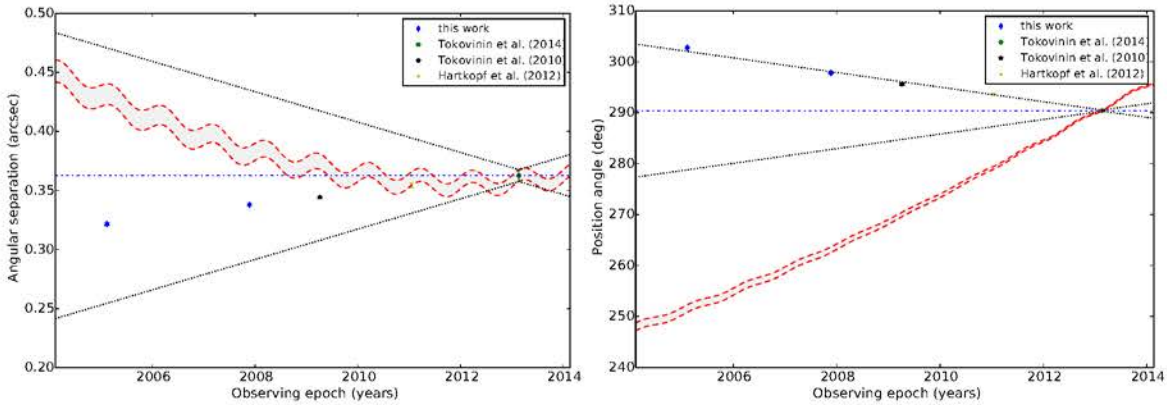


## HIP41843

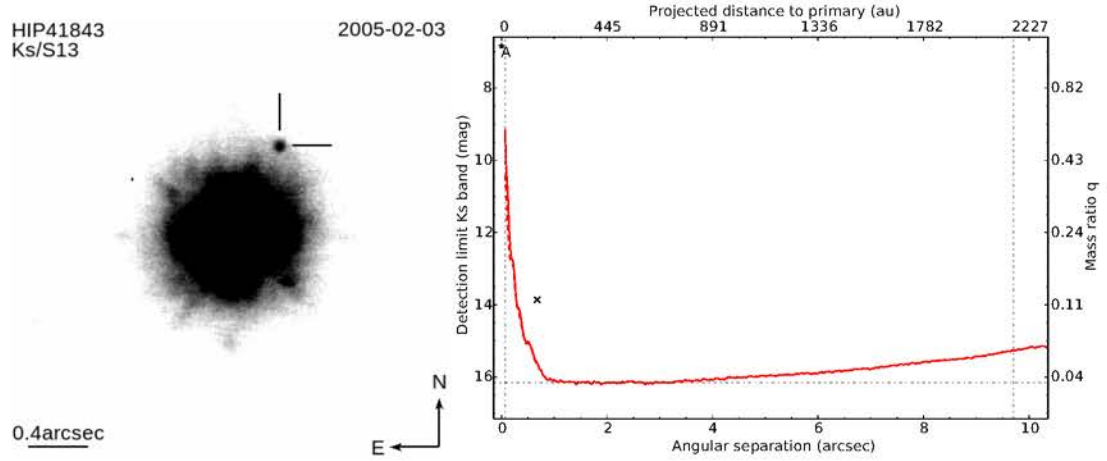


CC1: $P_{bg} = 0.00\%$, $P_{cmv} = 64.51\%$, N=2, df=2

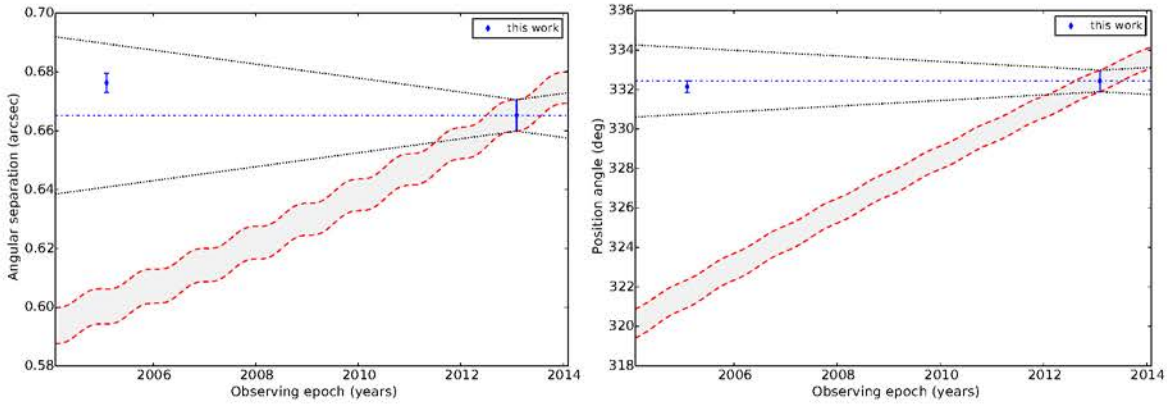


## HIP42129

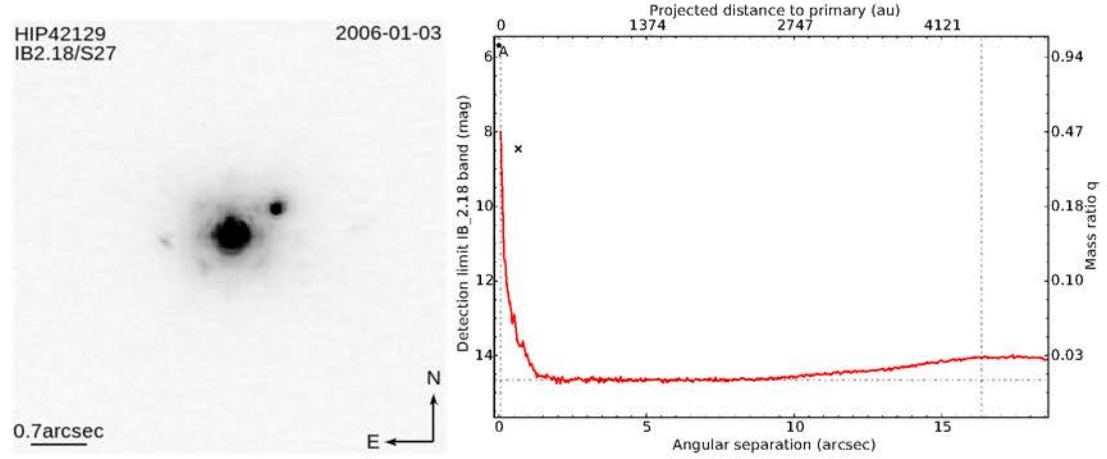

CC1: $P_{bg}$ = 0.00%, $P_{cmv}$ = 0.00%, N=3, df=4

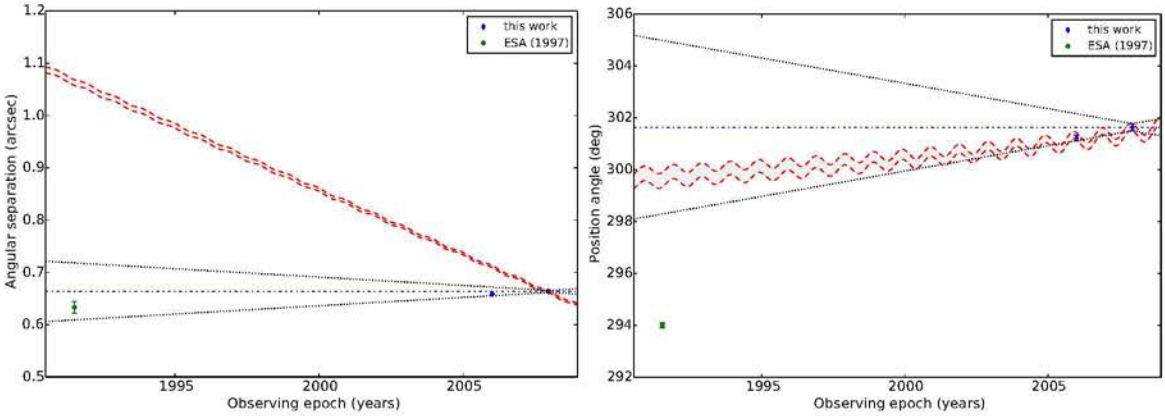


## HIP42177

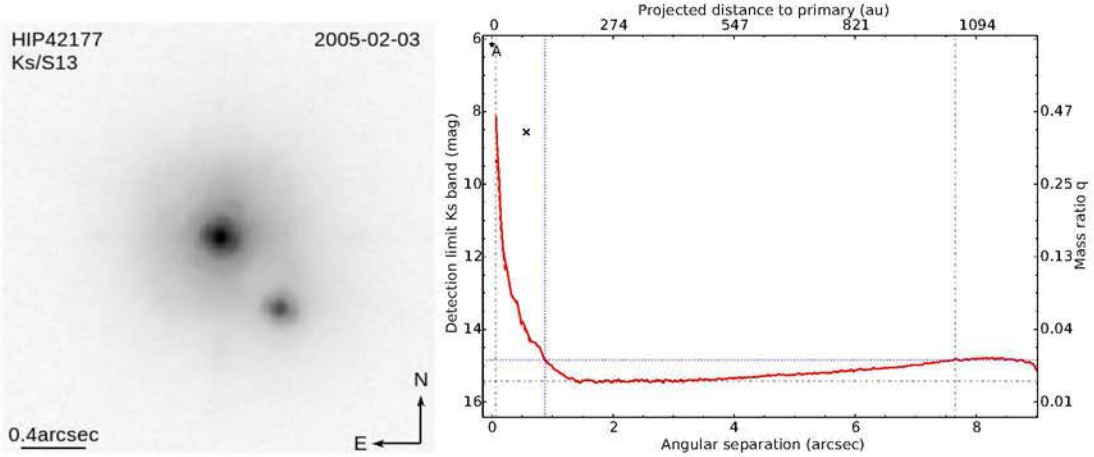


CC1: $P_{bg}$ = 5.74%, $P_{cmv}$ = 54.49%, N=2, df=2

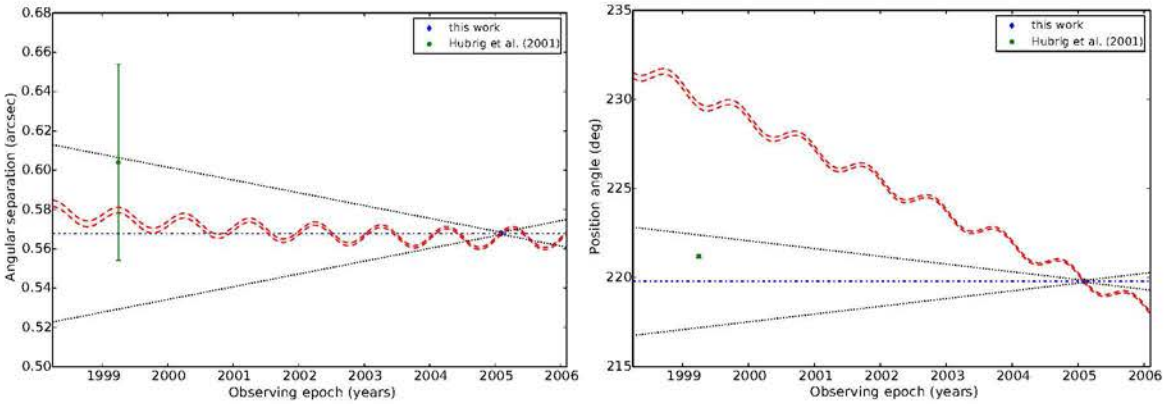


## HIP42334

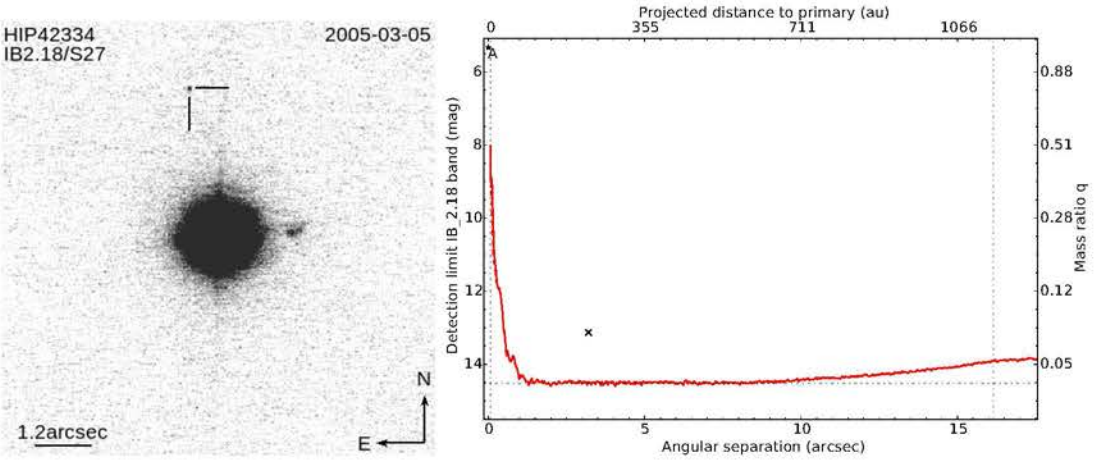

CC1: $P_{bg} = 0.05\%$, $P_{cmv} = 85.09\%$, N=2, df=2

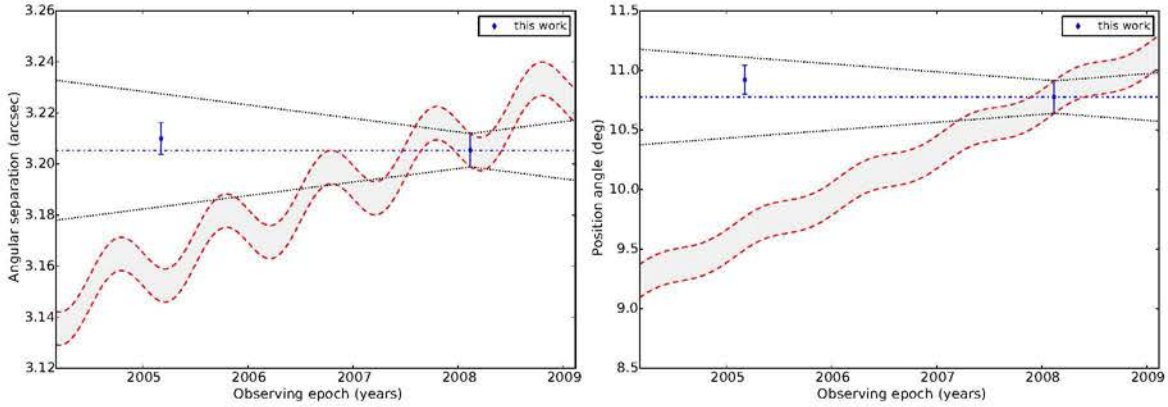


## HIP42540

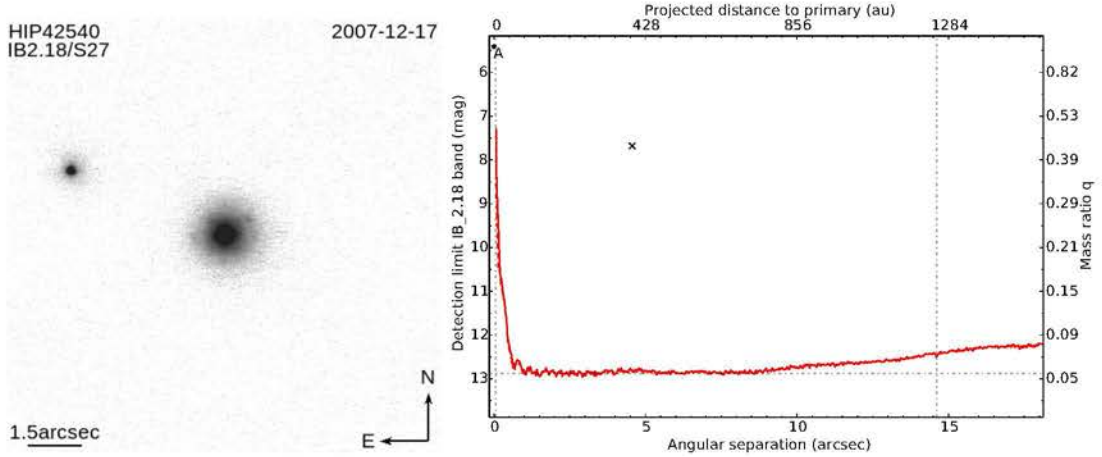


CC1: $P_{bg} = 0.00\%$, $P_{cmv} = 0.00\%$, N=4, df=6

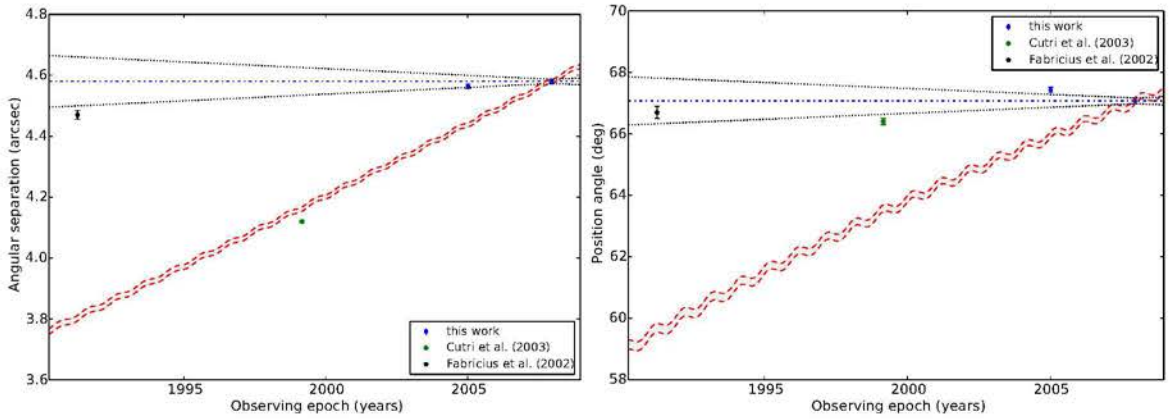


## HIP42715

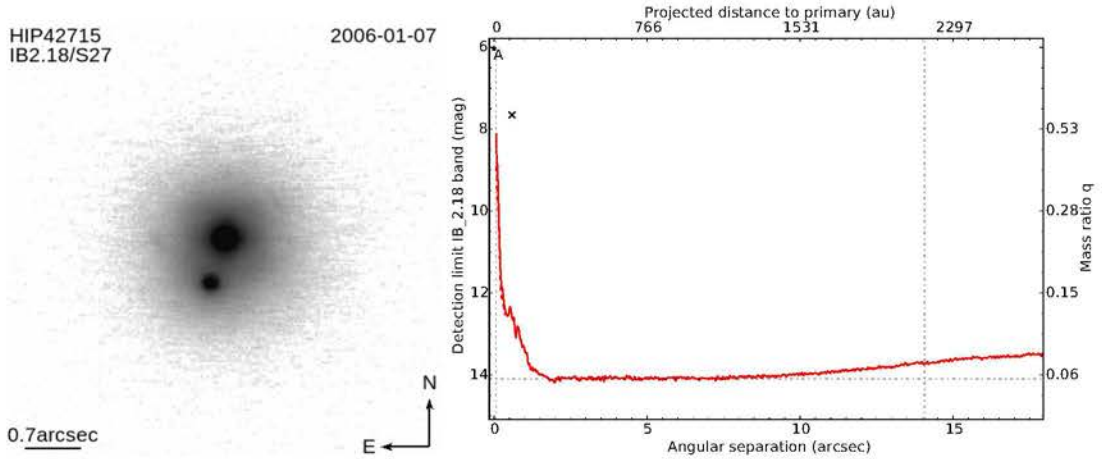

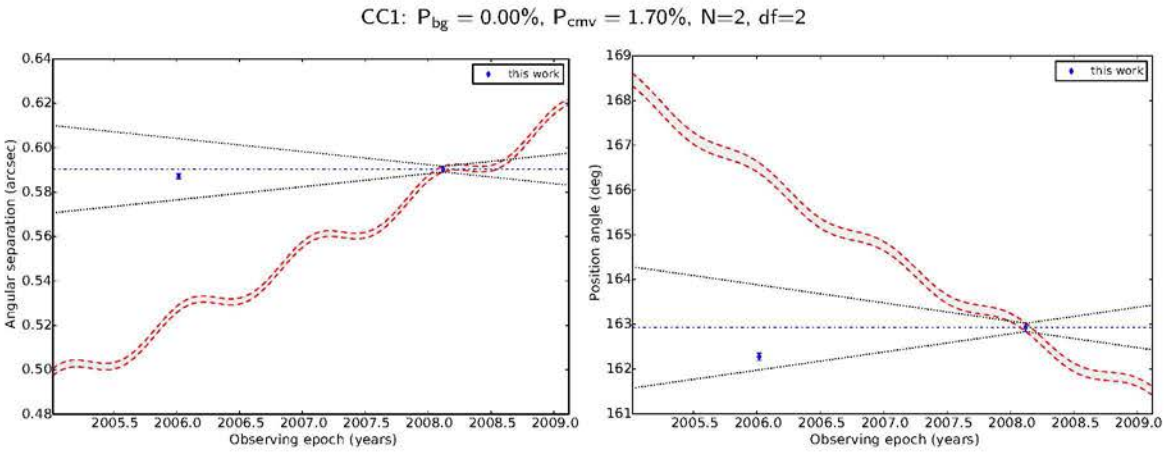


## HIP43305

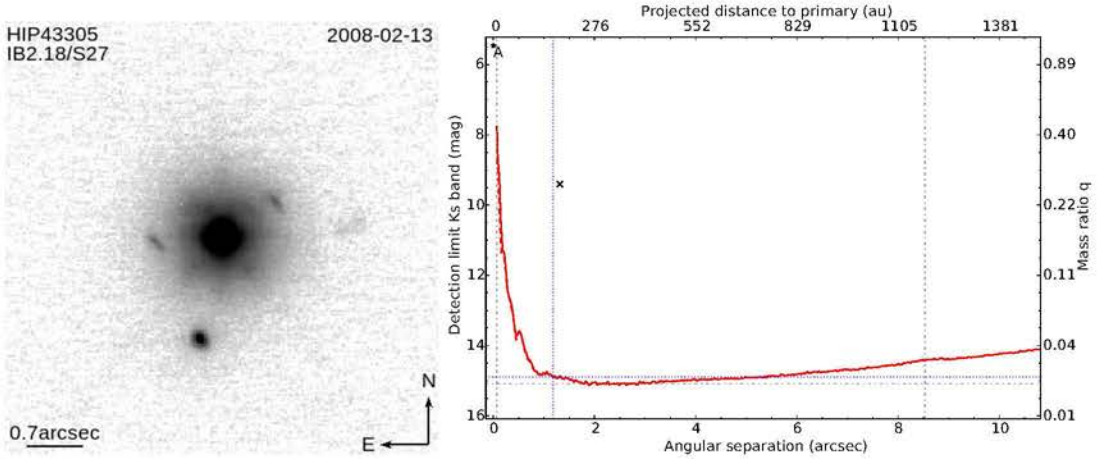


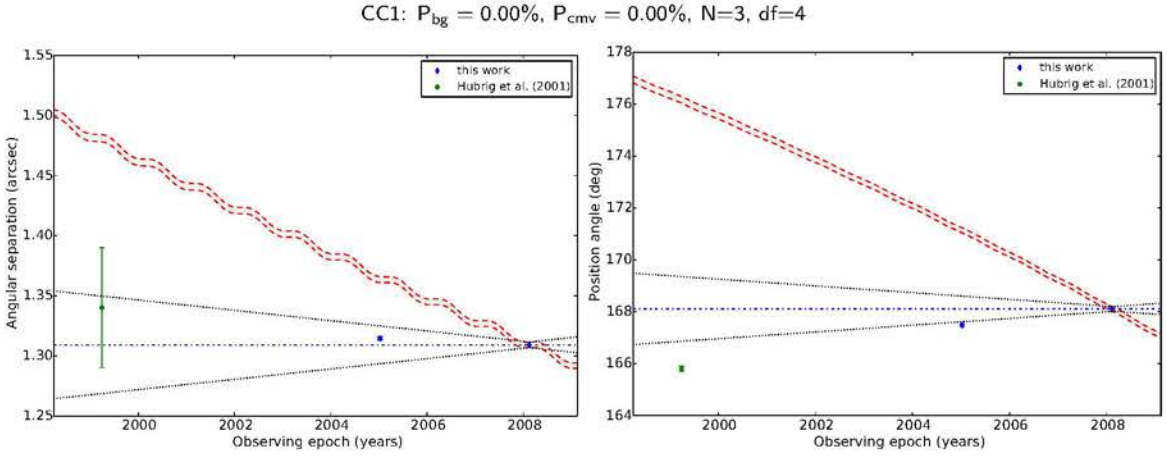


## HIP43792

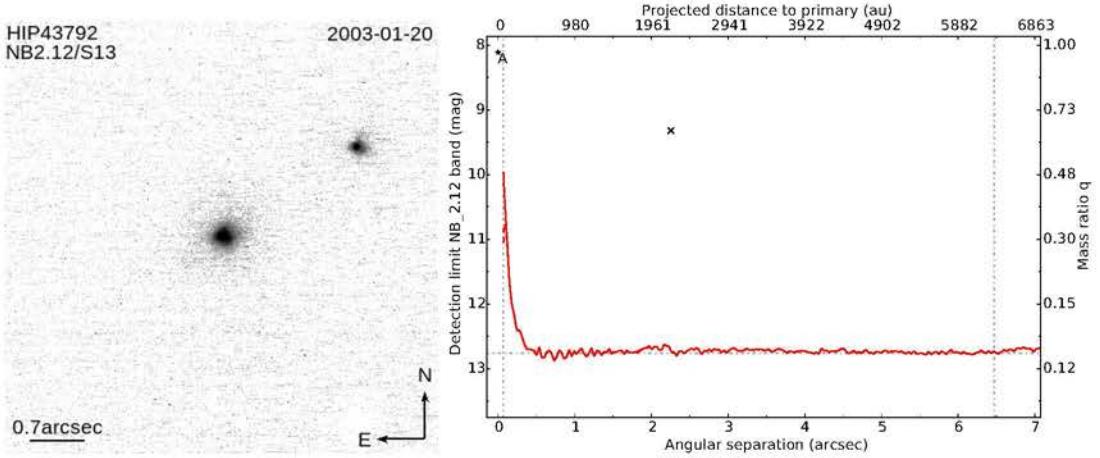

CC1: $P_{bg} = 0.00\%$, $P_{cmv} = 0.00\%$, N=2, df=2

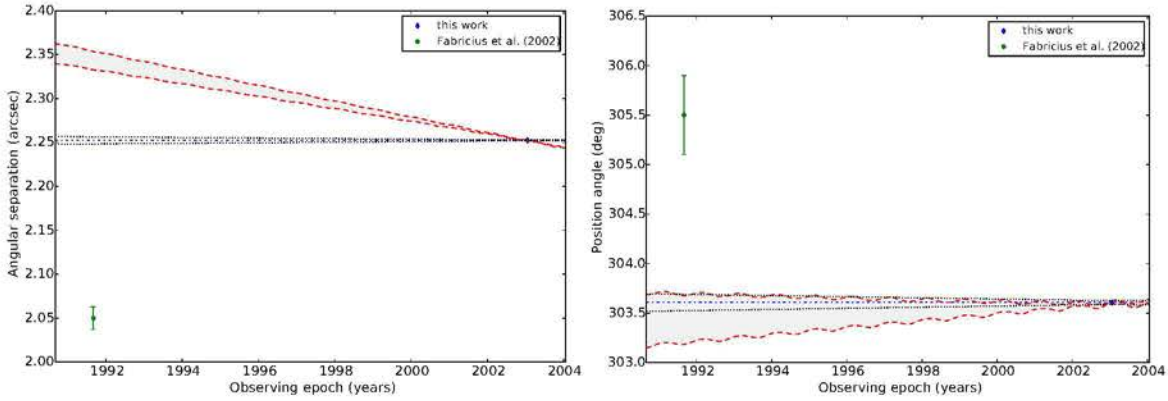


## HIP44299

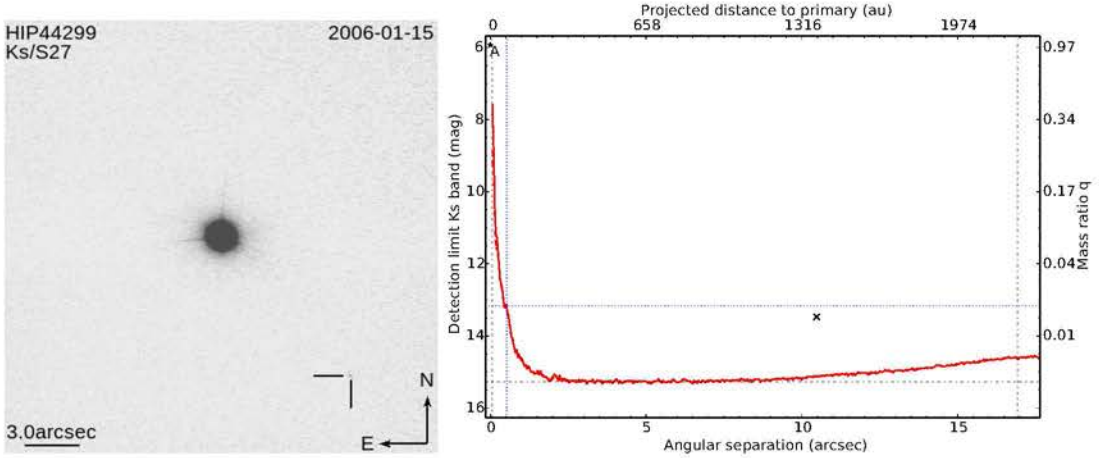


CC1: $P_{bg} = 46.15\%$, $P_{cmv} = 1.96\%$, N=2, df=2

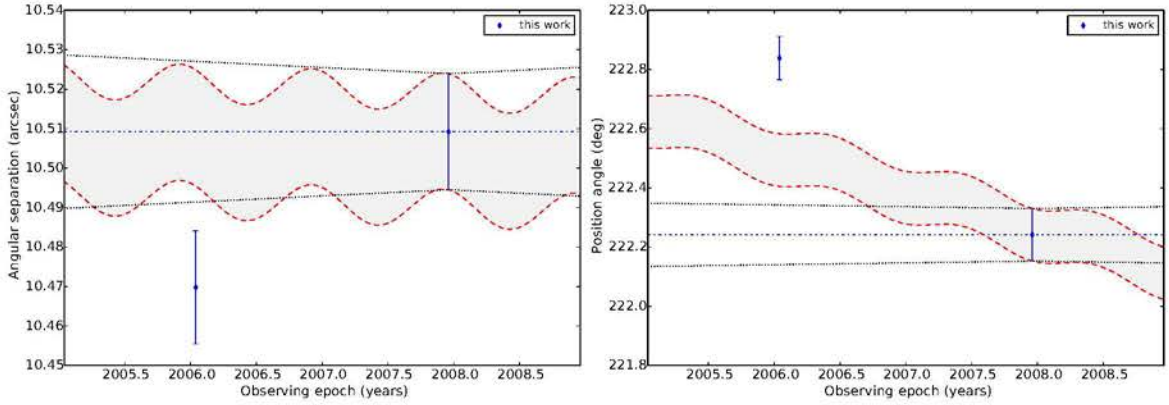


## HIP44798

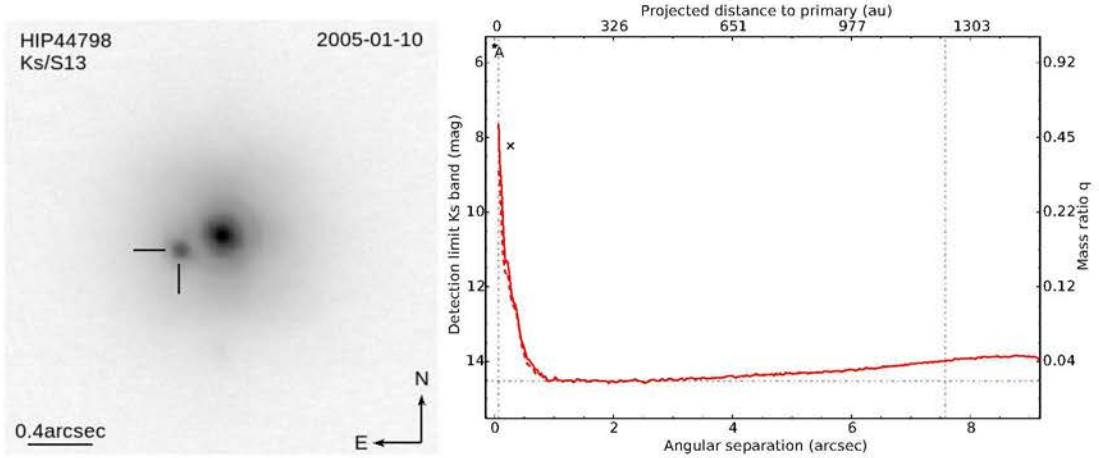

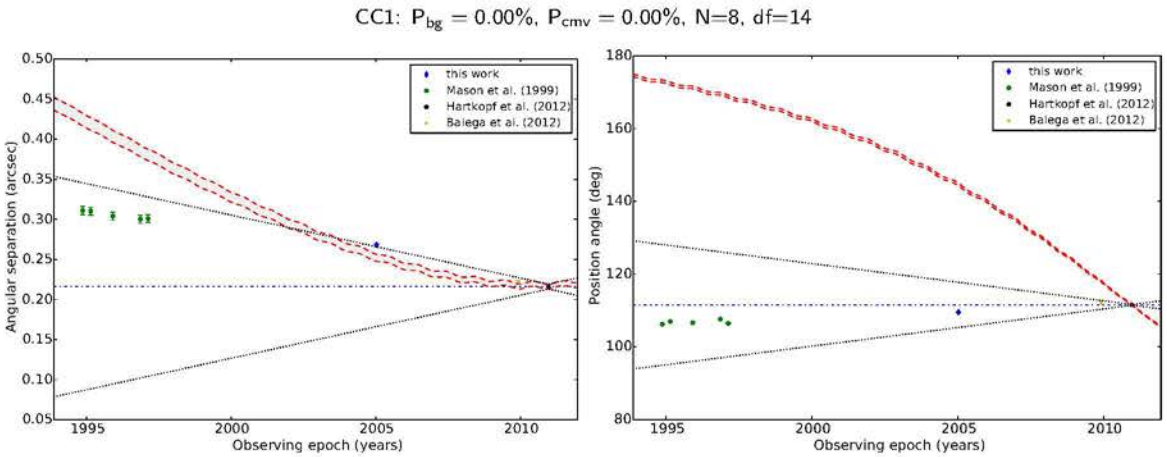
CC1: $P_{bg}$ = 0.00%, $P_{cmv}$ = 0.00%, N=8, df=14
this work
Mason et al. (1999)
Hartkopf et al. (2012)
Balega et al. (2012)
Angular separation (arcsec)
Position angle (deg)
Observing epoch (years)

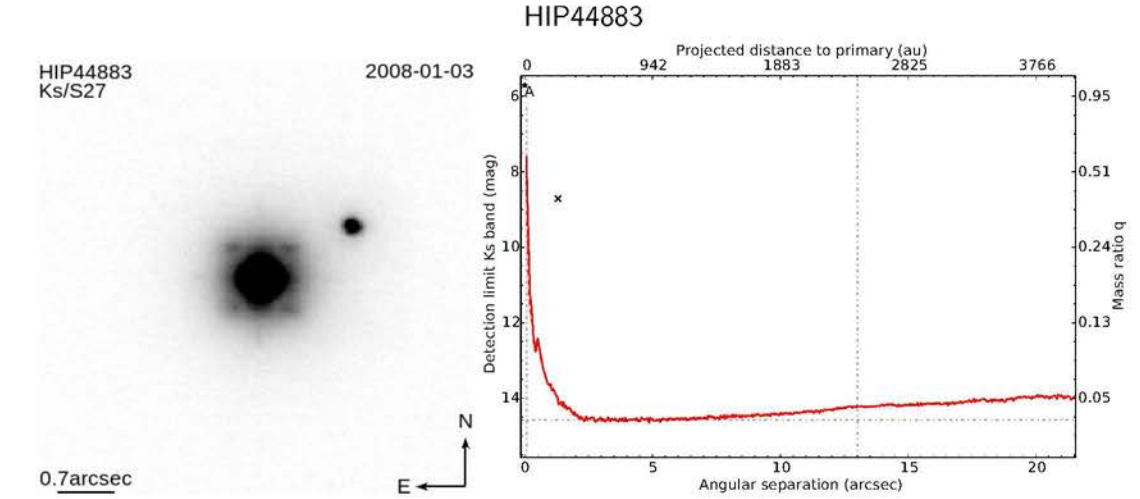
HIP44883
HIP44883
Ks/S27
2008-01-03
0.7arcsec
N
E
Projected distance to primary (au)
Detection limit Ks band (mag)
Mass ratio q
Angular separation (arcsec)

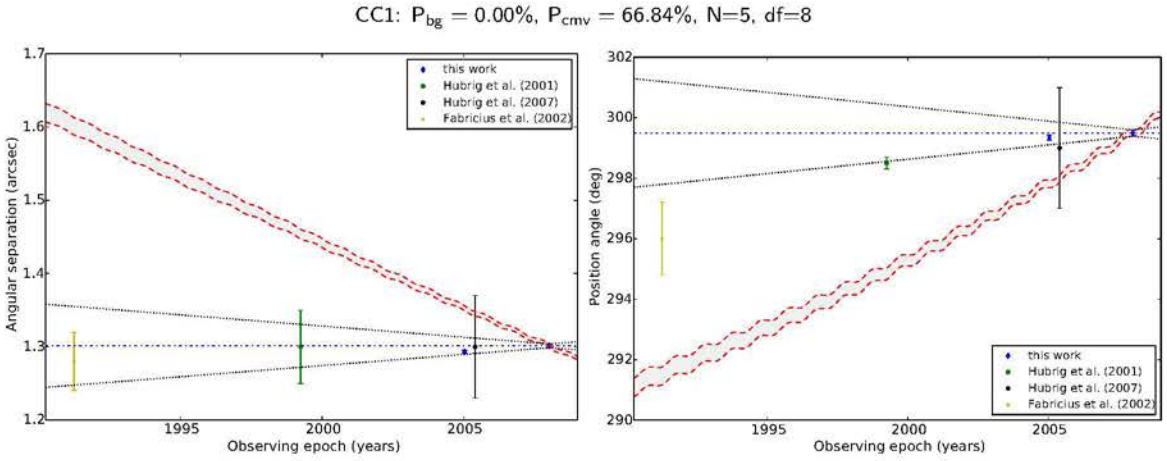
CC1: $P_{bg}$ = 0.00%, $P_{cmv}$ = 66.84%, N=5, df=8
this work
Hubrig et al. (2001)
Hubrig et al. (2007)
Fabricius et al. (2002)
Angular separation (arcsec)
Position angle (deg)
Observing epoch (years)

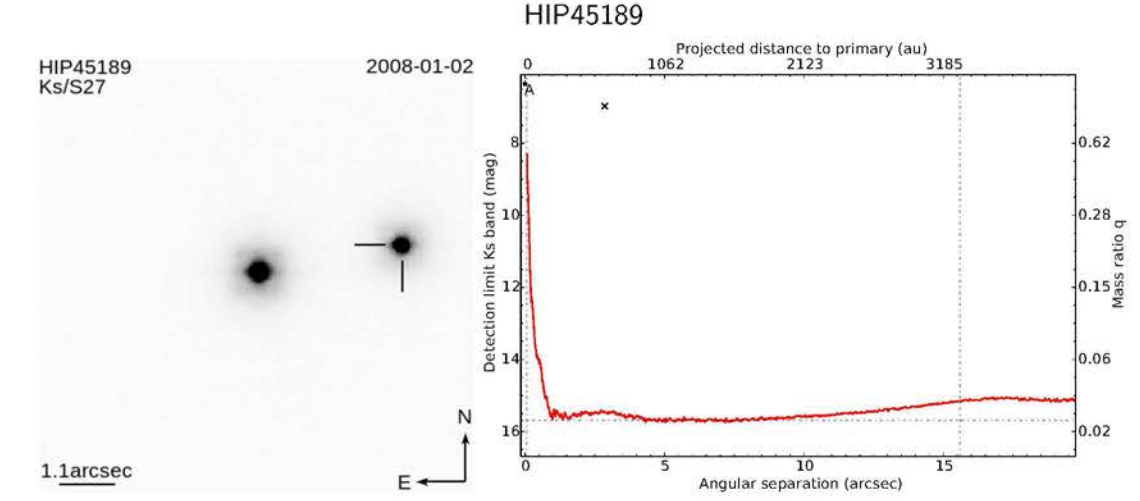
HIP45189
HIP45189
Ks/S27
2008-01-02
1.1arcsec
N
E
Projected distance to primary (au)
Detection limit Ks band (mag)
Mass ratio q
Angular separation (arcsec)

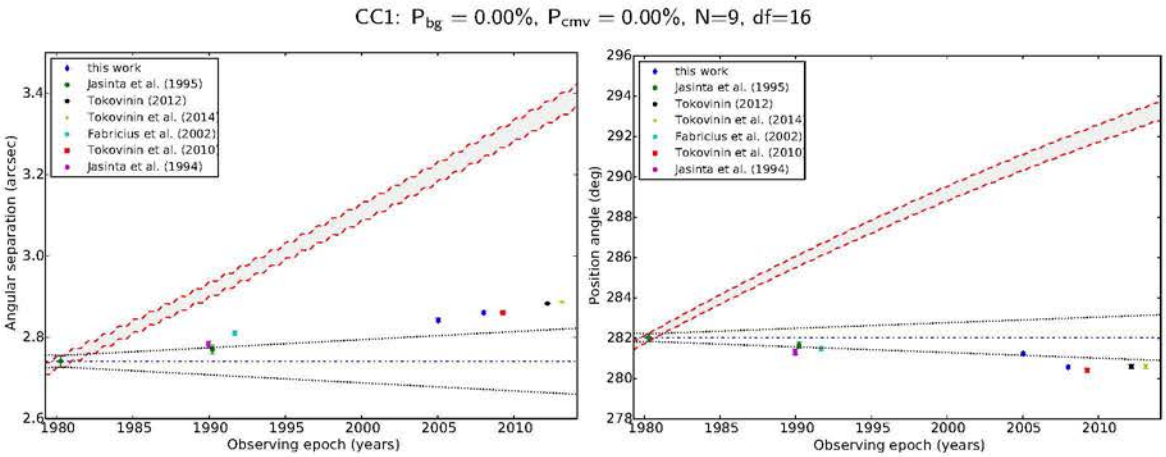


## HIP45314

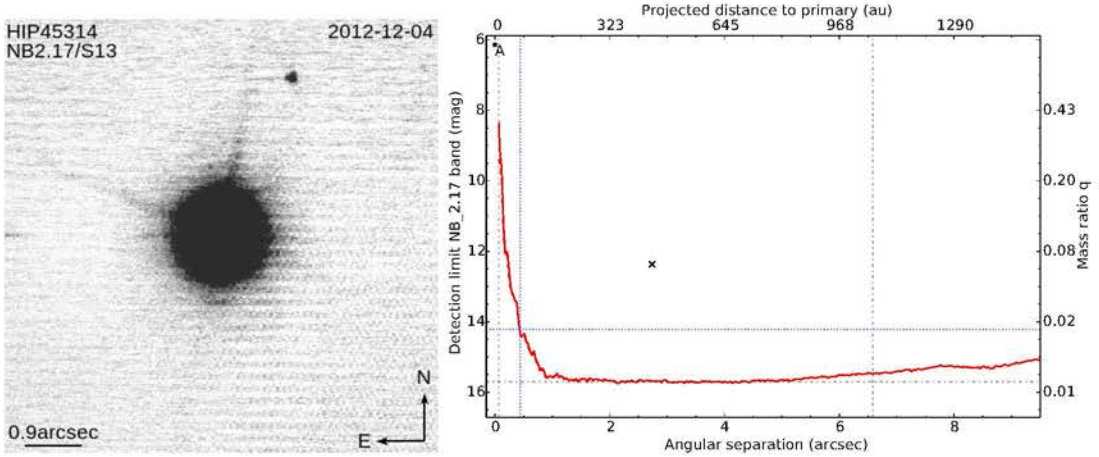


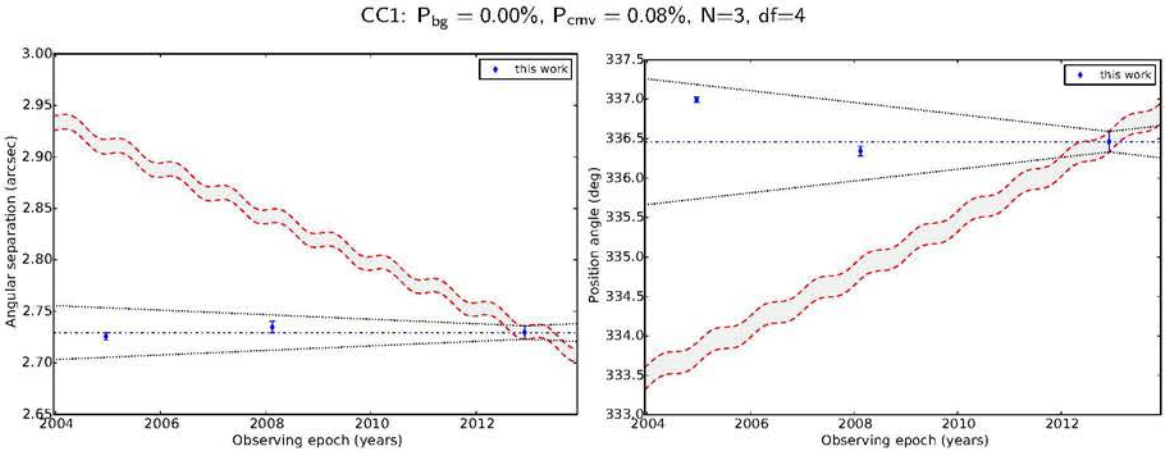


## HIP45344

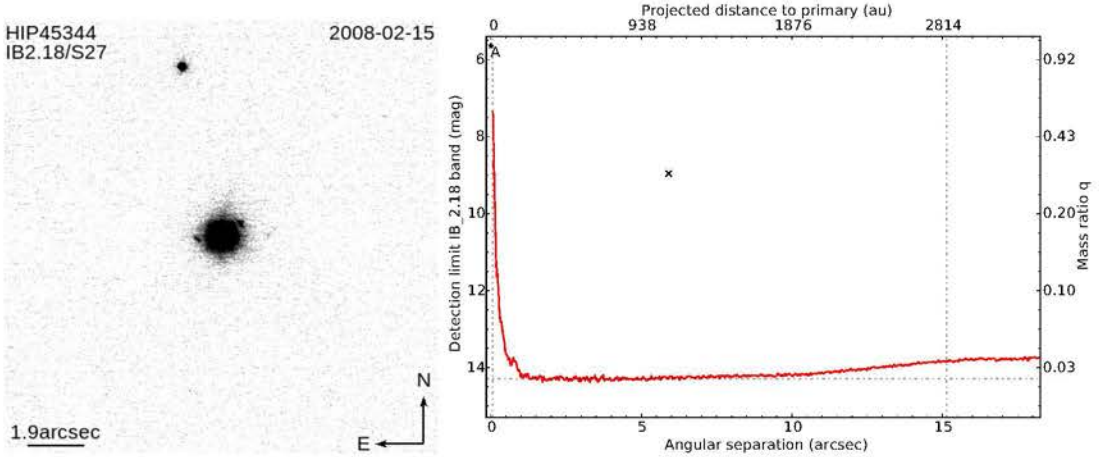

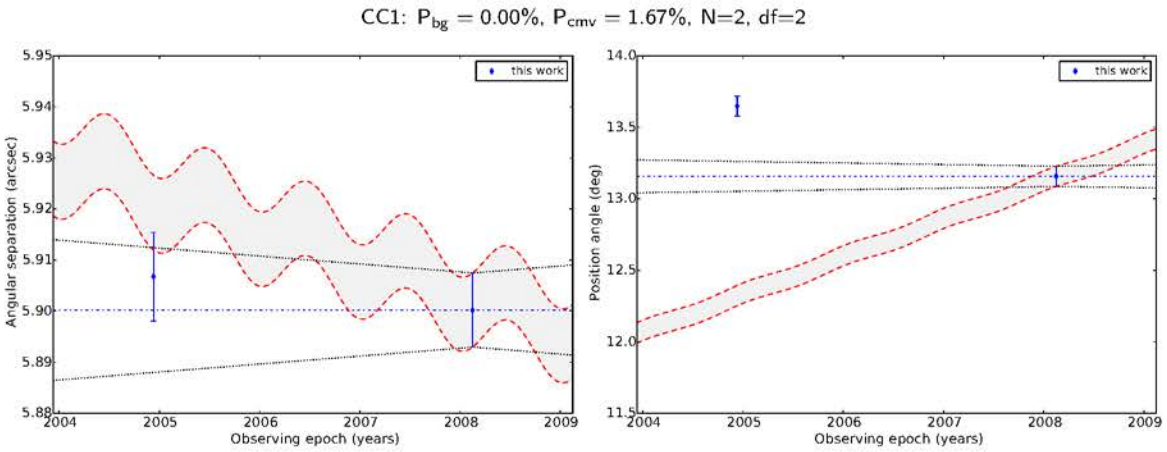
CC1: $P_{bg}$ = 0.00%, $P_{cmv}$ = 1.67%, N=2, df=2
this work
Angular separation (arcsec)
Observing epoch (years)
Position angle (deg)

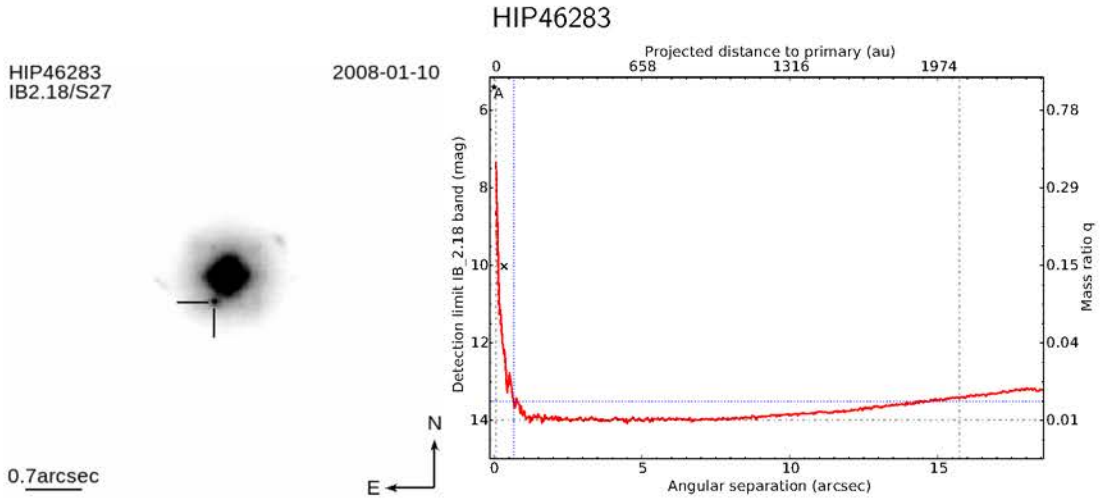
HIP46283
HIP46283
IB2.18/S27
2008-01-10
0.7arcsec
N
E
Projected distance to primary (au)
Detection limit IB_2.18 band (mag)
Mass ratio q
Angular separation (arcsec)

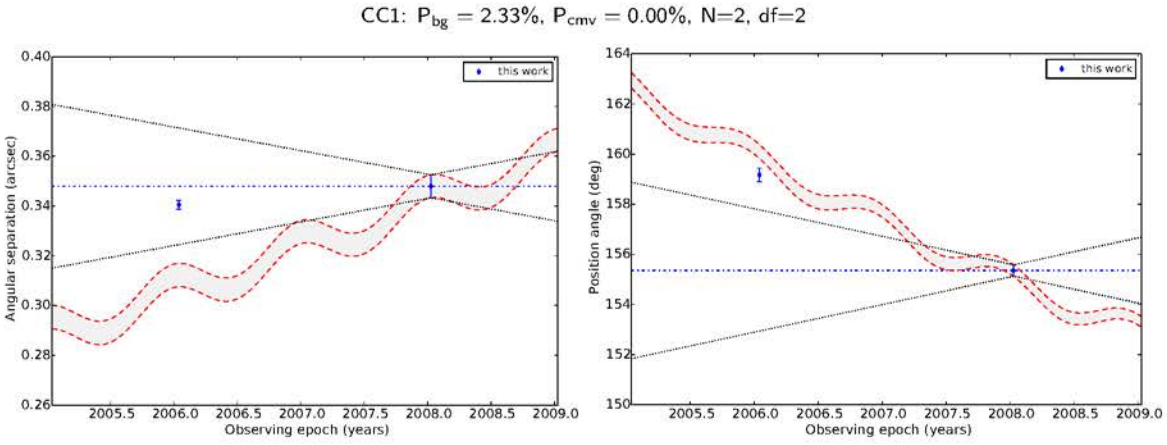
CC1: $P_{bg}$ = 2.33%, $P_{cmv}$ = 0.00%, N=2, df=2
this work
Angular separation (arcsec)
Observing epoch (years)
Position angle (deg)

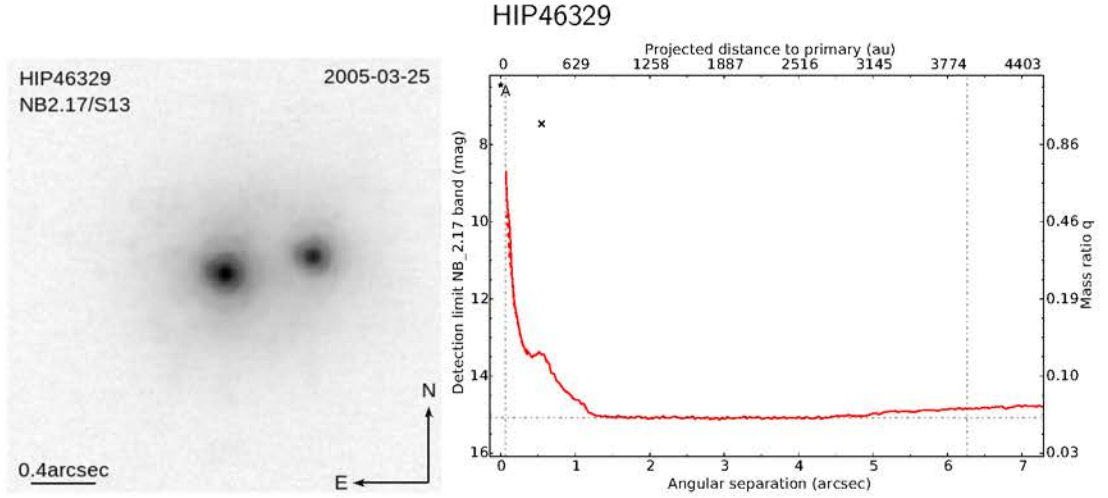
HIP46329
HIP46329
NB2.17/S13
2005-03-25
0.4arcsec
N
E
Projected distance to primary (au)
Detection limit NB_2.17 band (mag)
Mass ratio q
Angular separation (arcsec)

CC1: $P_{bg} = 0.00\%$, $P_{cmv} = 0.00\%$, N=2, df=2

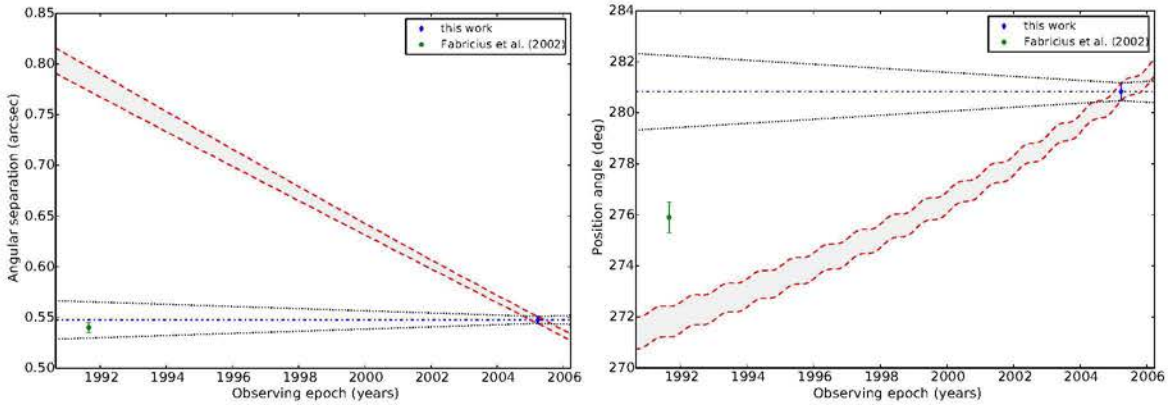


HIP46594

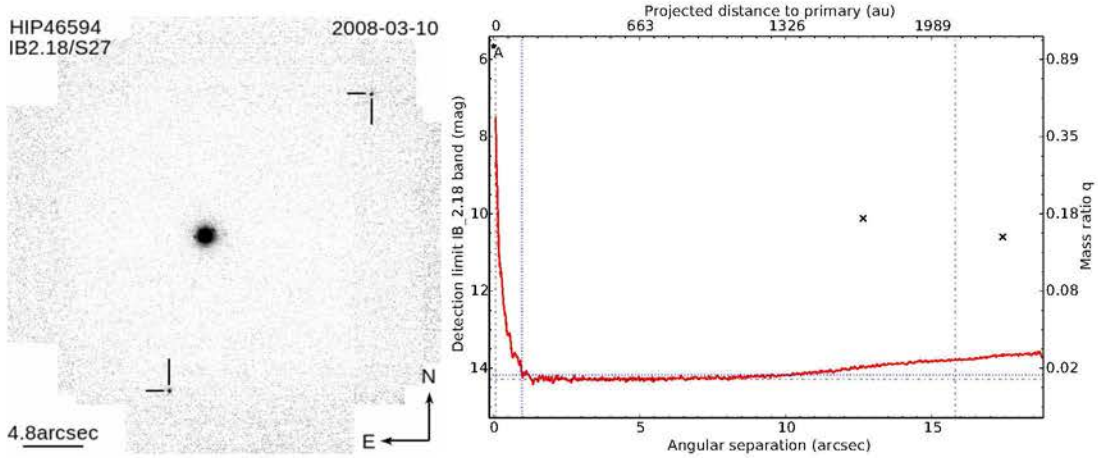


CC1: $P_{bg} = 5.87\%$, $P_{cmv} = 0.00\%$, N=2, df=2

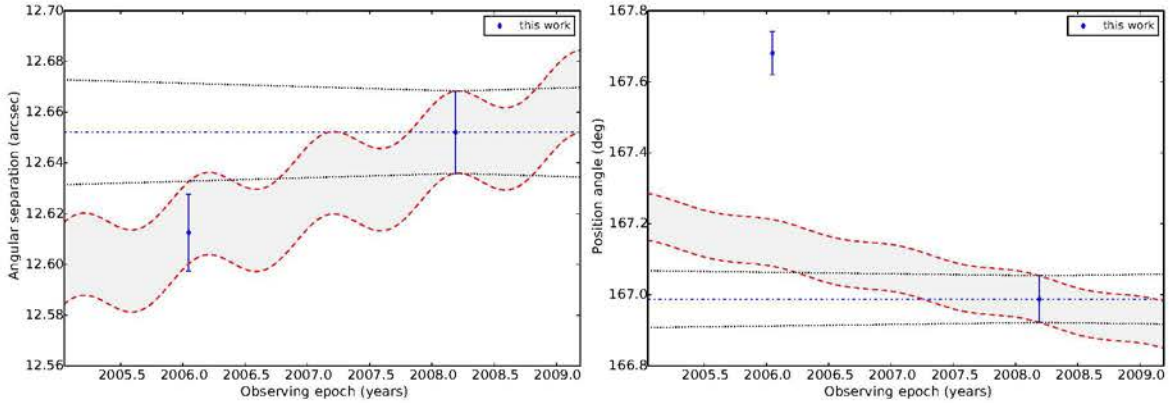


CC2: $P_{bg} = 13.30\%$, $P_{cmv} = 1.60\%$, N=2, df=2

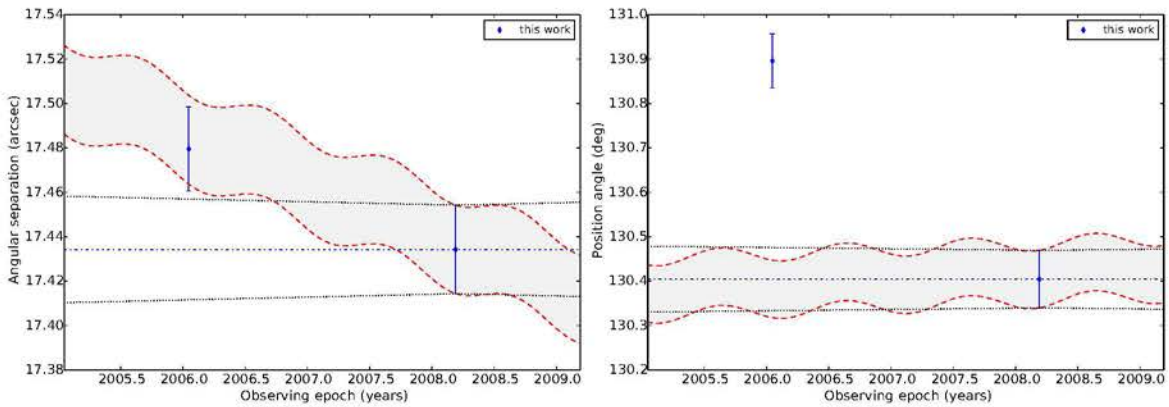

## HIP46914

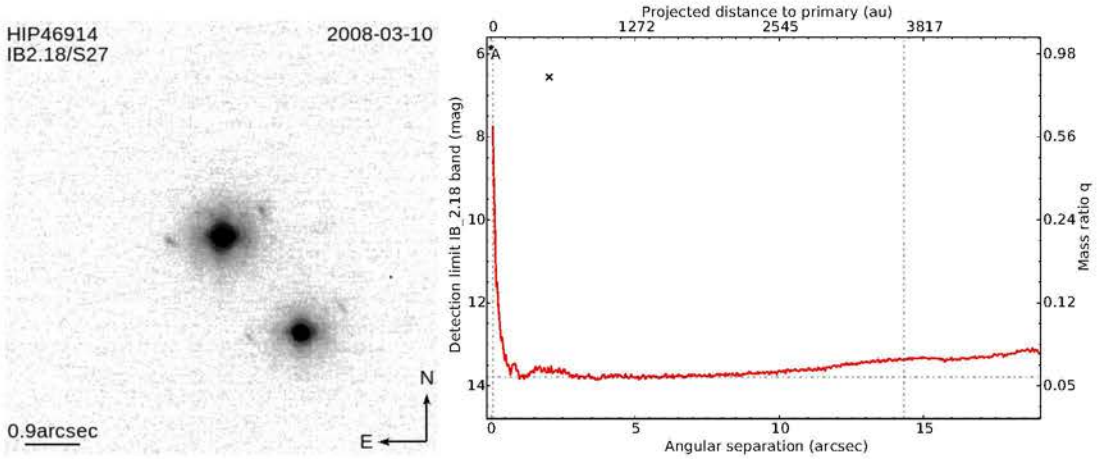


CC1: $P_{bg} = 0.00\%$, $P_{cmv} = 0.00\%$, N=4, df=6

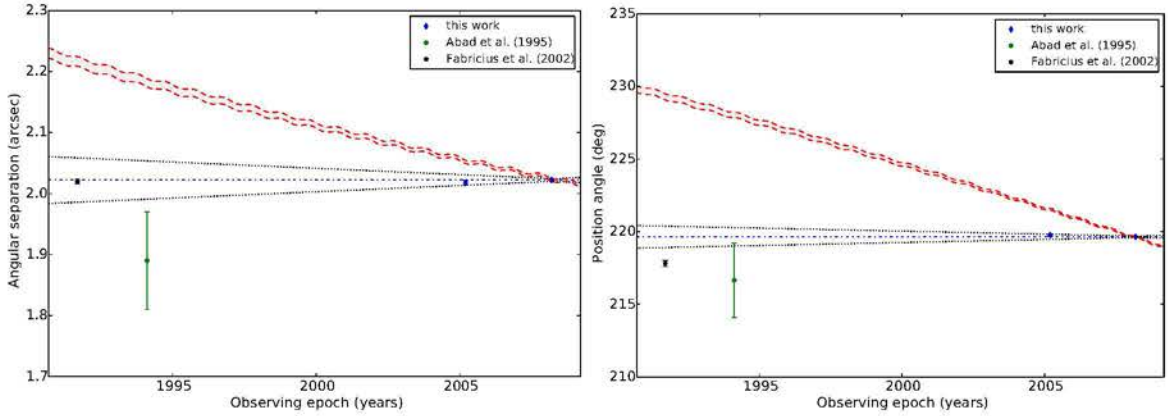


## HIP46928

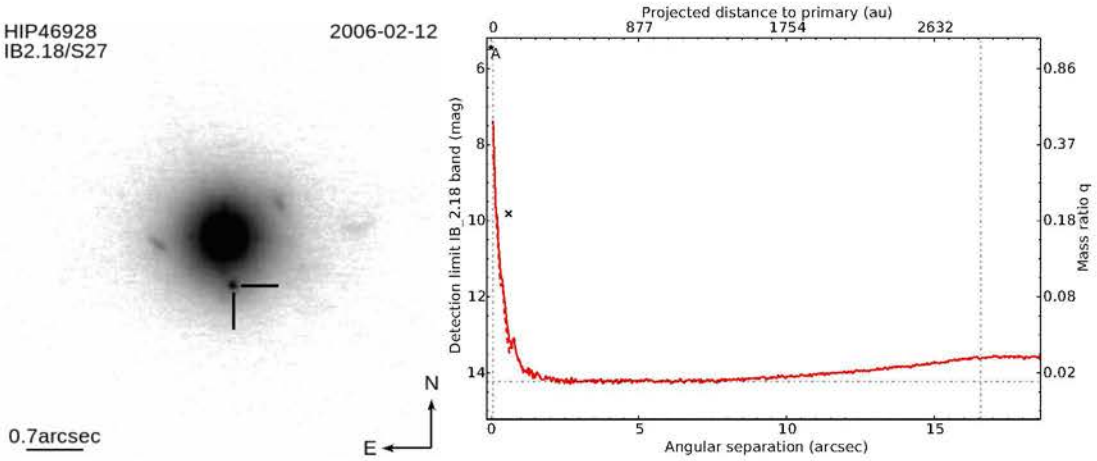


CC1: $P_{bg} = 0.00\%$, $P_{cmv} = 0.16\%$, N=2, df=2

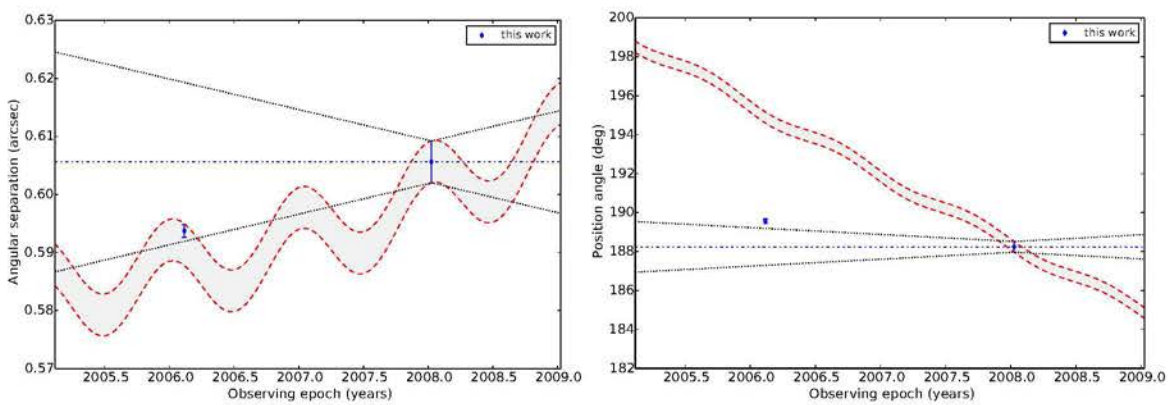

## HIP48943

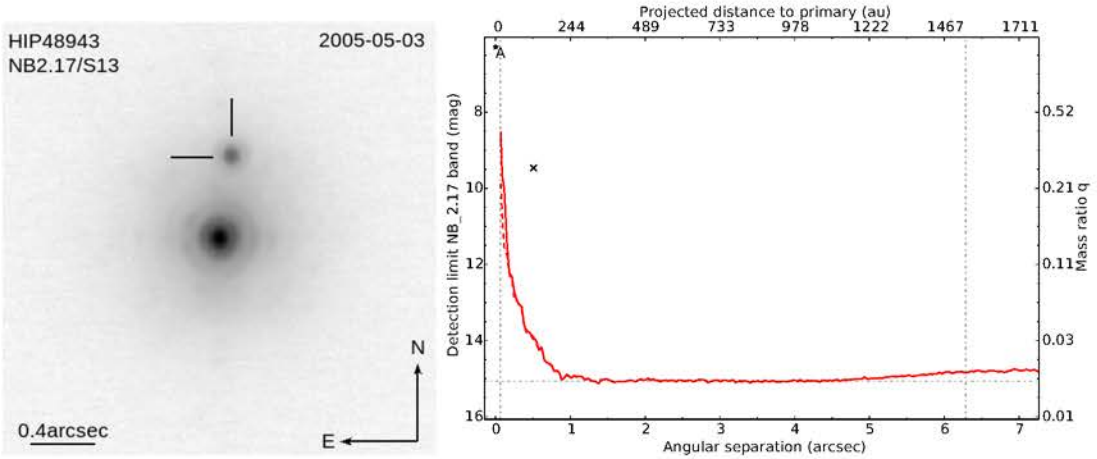


CC1: $P_{bg} = 0.00\%$, $P_{cmv} = 0.00\%$, N=2, df=2

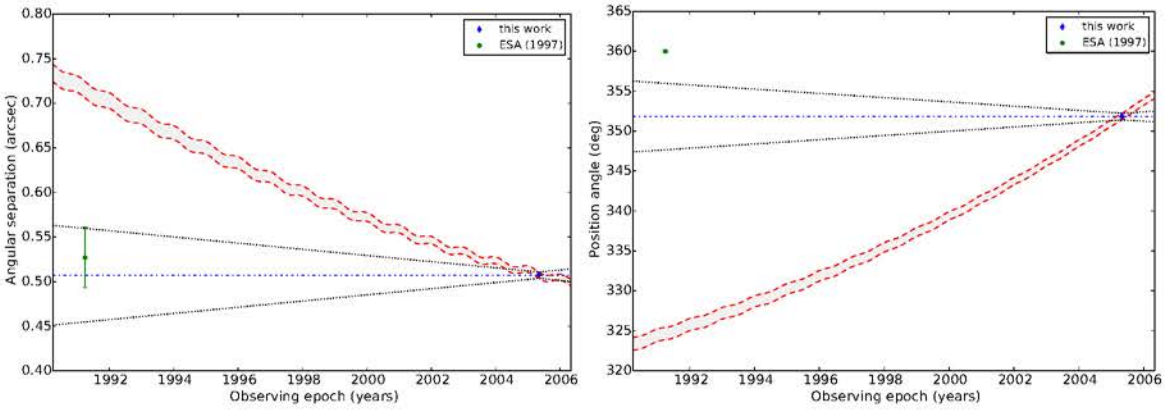


## HIP50847

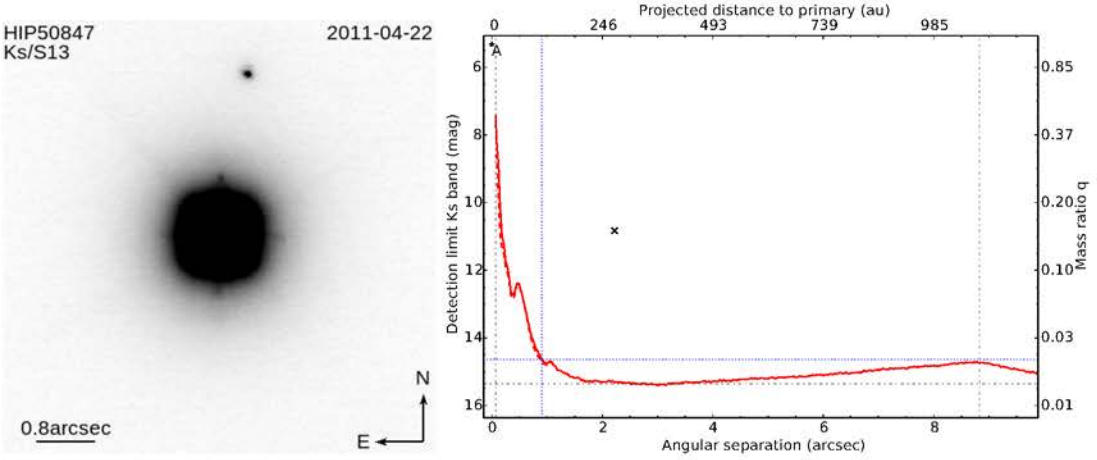


CC1: $P_{bg} = 0.00\%$, $P_{cmv} = 96.08\%$, N=2, df=2

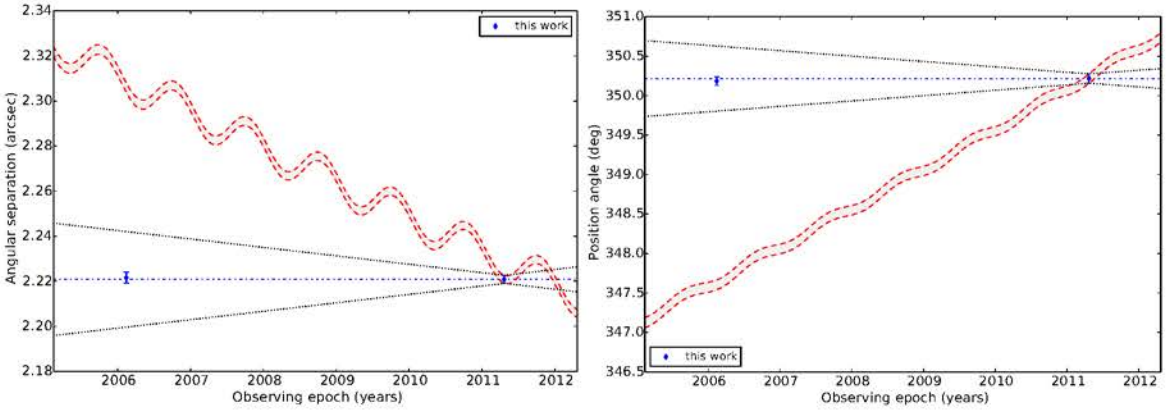

## HIP51362

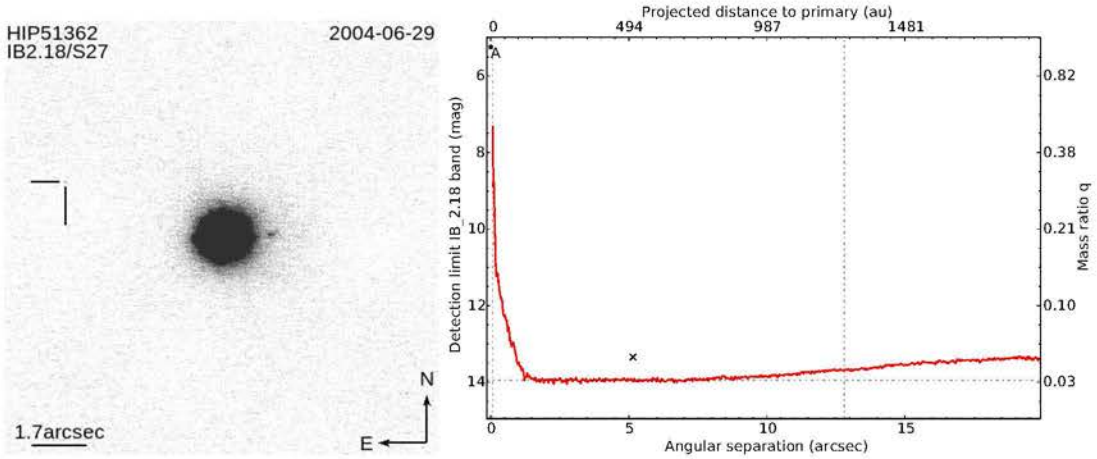


CC1: $P_{bg} = 12.11\%$, $P_{cmv} = 92.29\%$, N=2, df=2

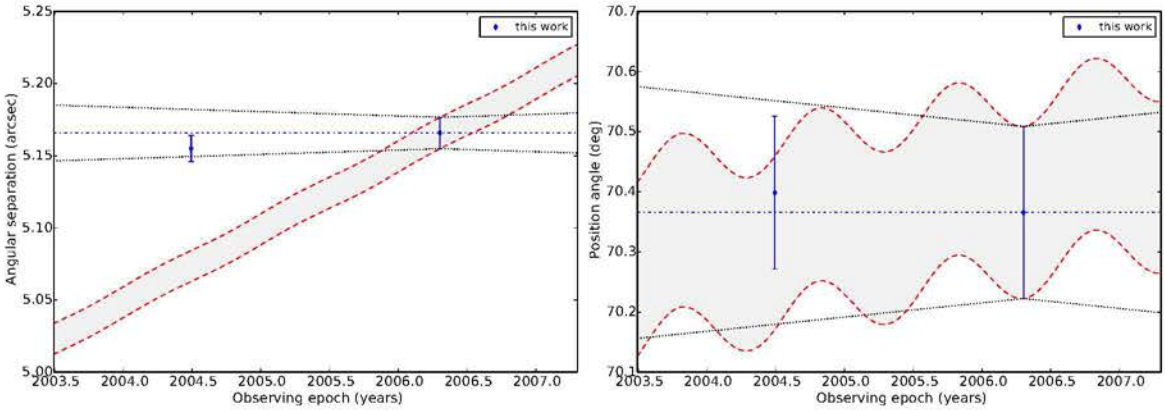


## HIP51376

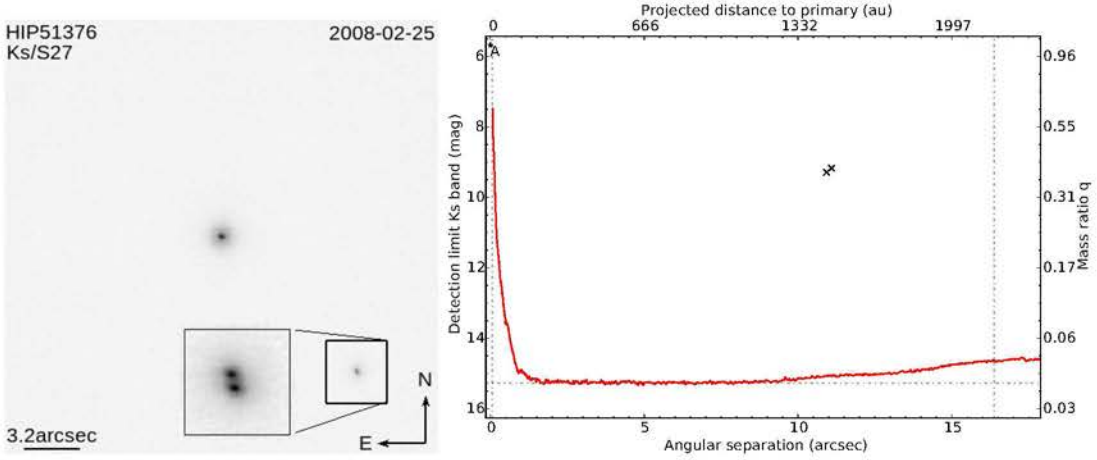


CC1: $P_{bg} = 16.56\%$, $P_{cmv} = 0.88\%$, N=4, df=6

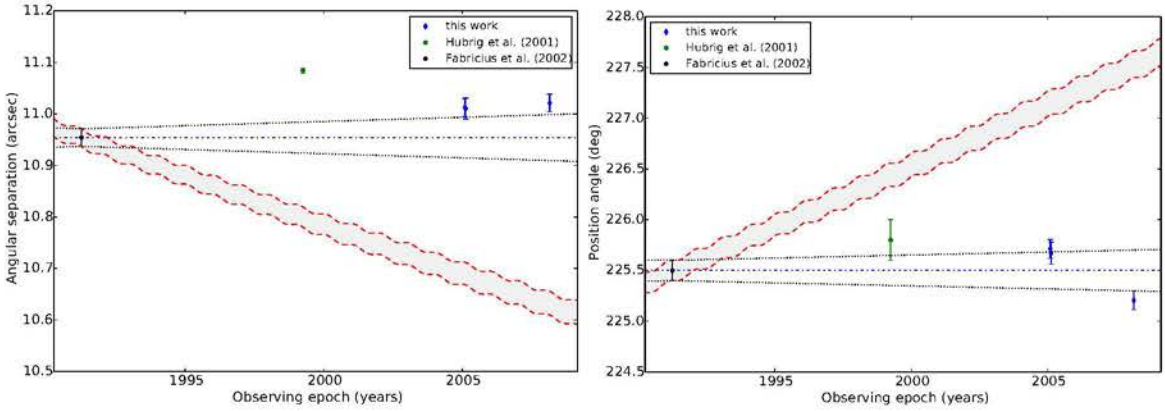

CC2: $P_{bg}$ = 41.16%, $P_{cmv}$ = 2.82%, N=4, df=6

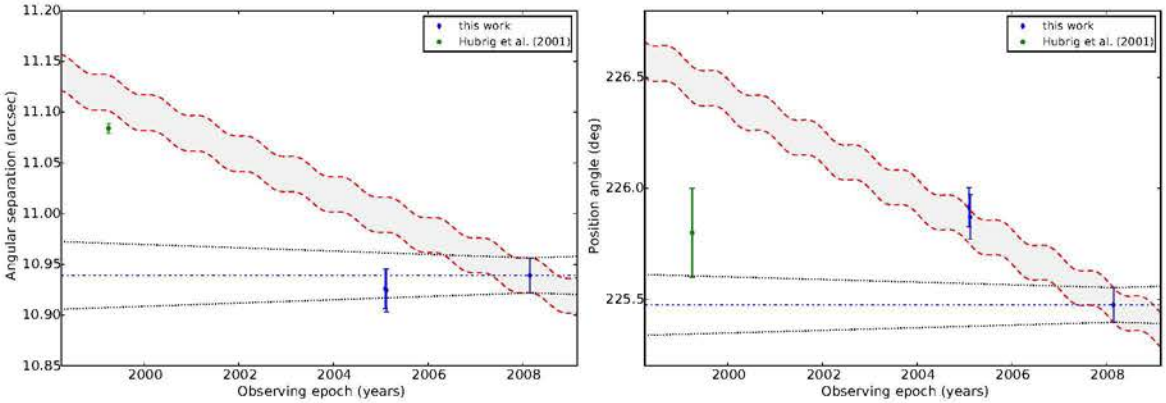


HIP52742

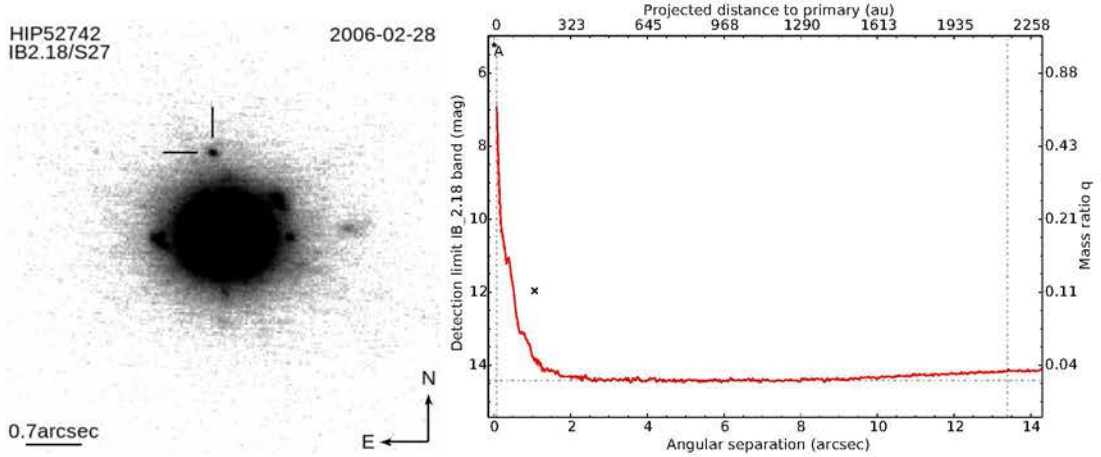


CC1: $P_{bg}$ = 0.00%, $P_{cmv}$ = 35.24%, N=2, df=2

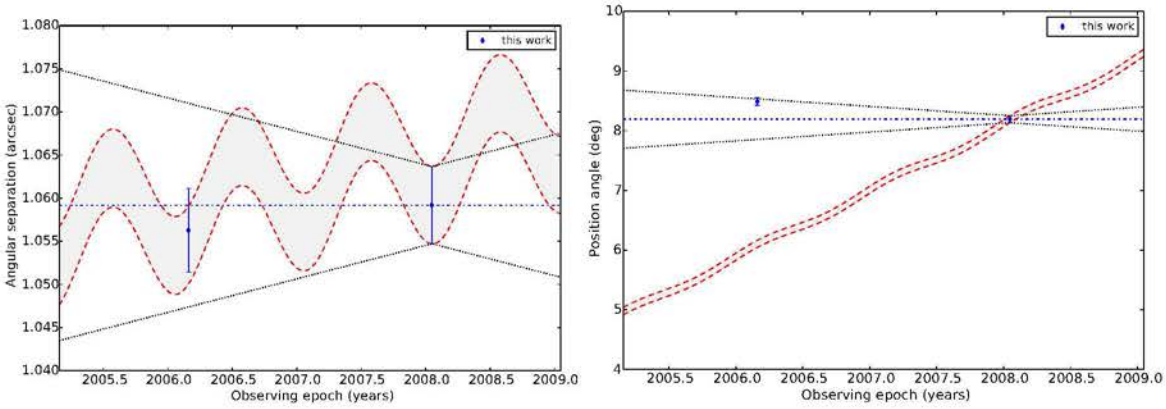


HIP53272

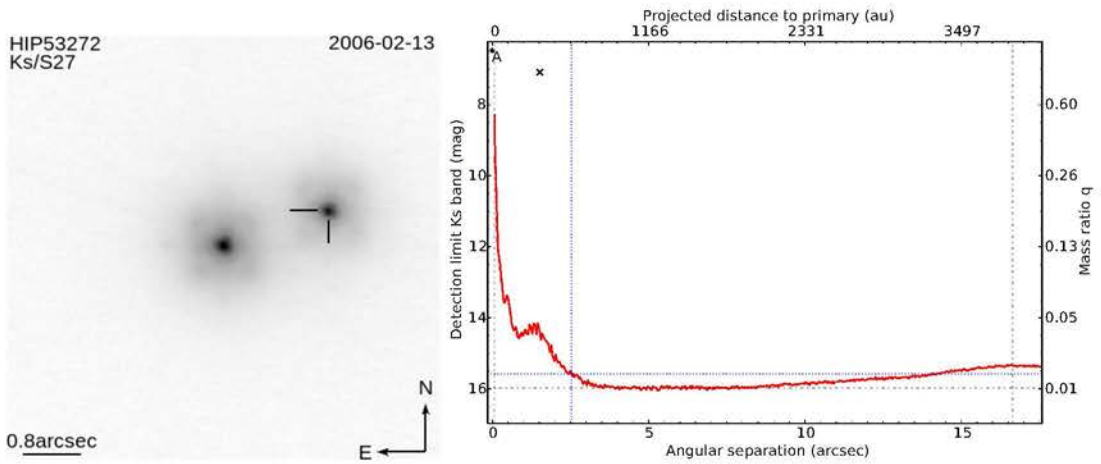

CC1: $P_{bg} = 0.00\%$, $P_{cmv} = 0.06\%$, N=3, df=4

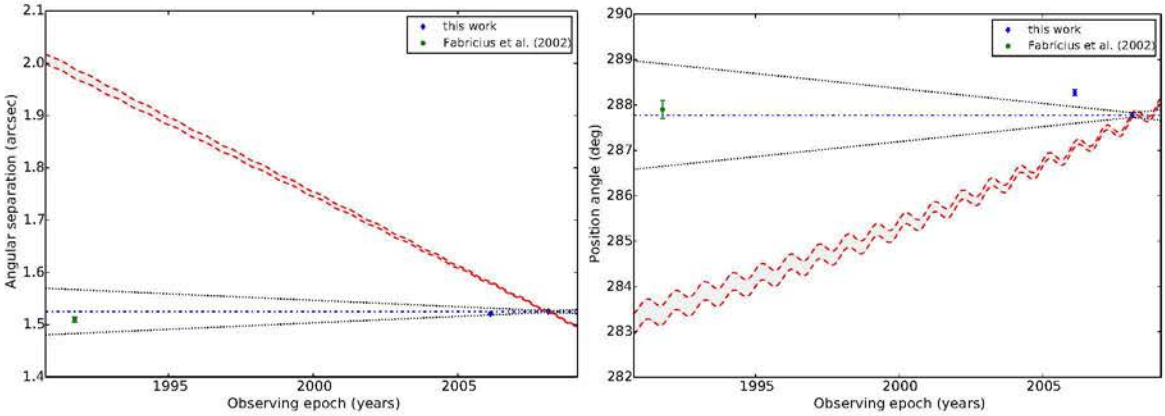


HIP54413

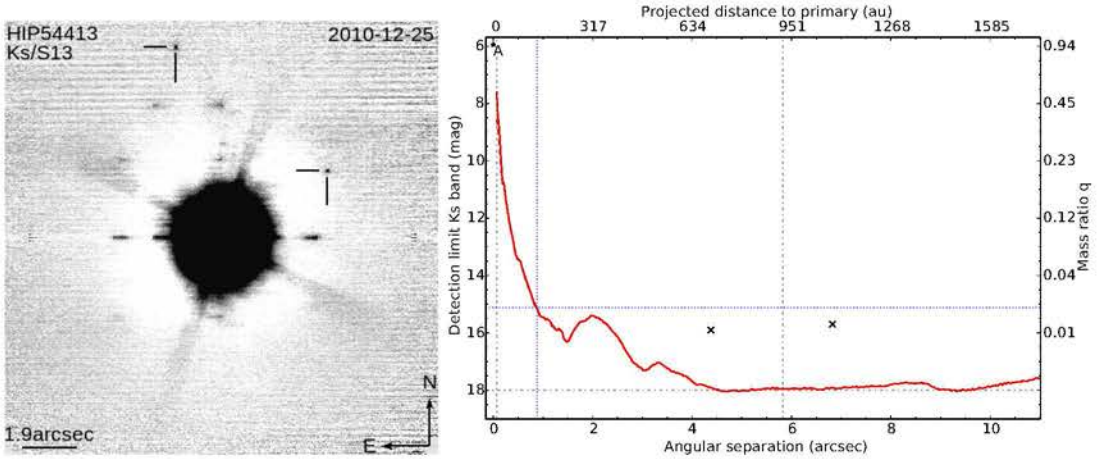


CC1: $P_{bg} = 100.00\%$, $P_{cmv} = 36.56\%$, N=5, df=8

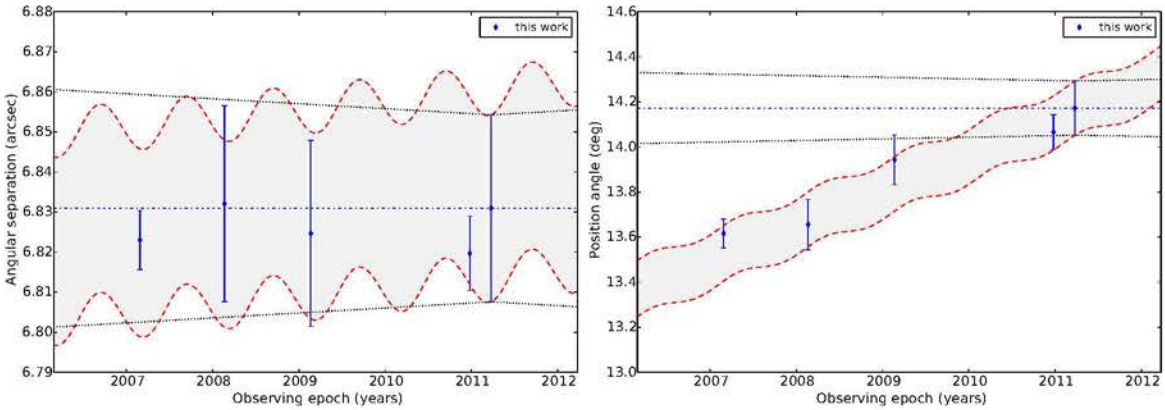


CC2: $P_{bg} = 99.07\%$, $P_{cmv} = 83.95\%$, N=5, df=8

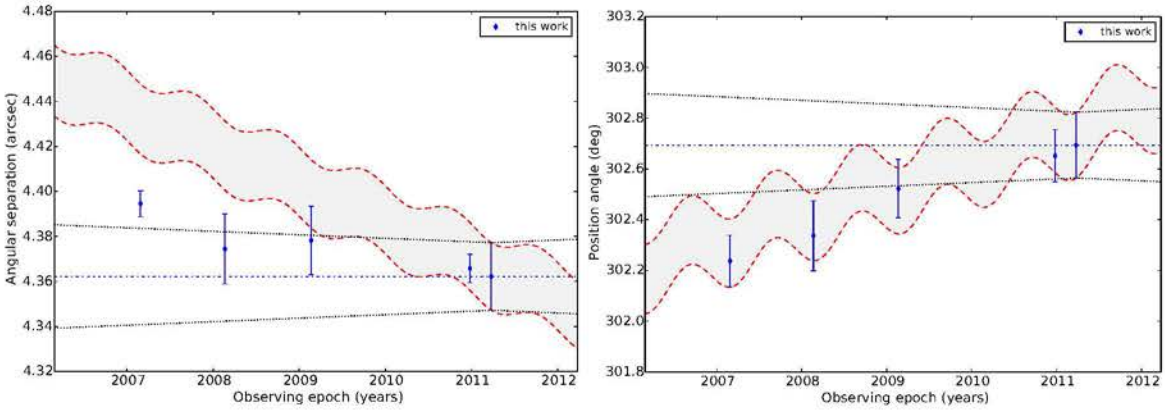

## HIP54557

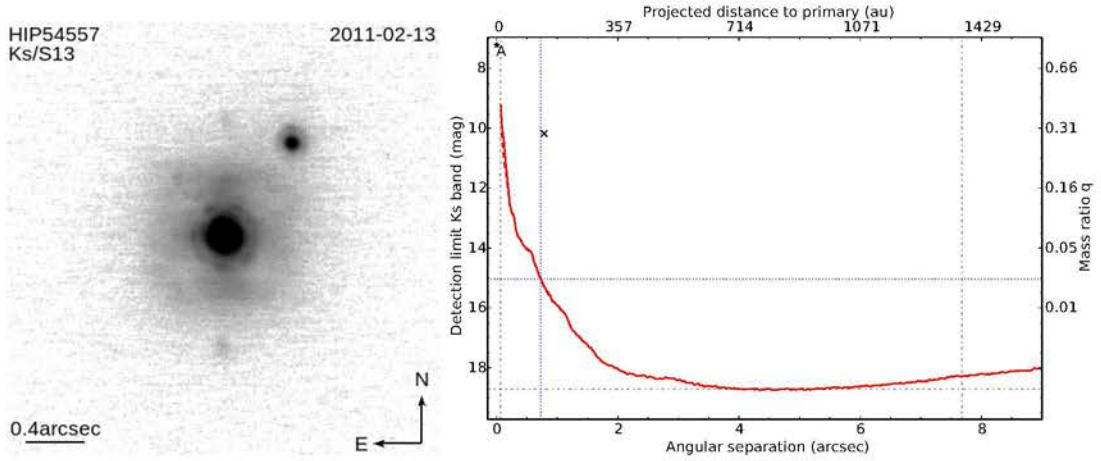


CC1: $P_{bg} = 0.00\%$, $P_{cmv} = 0.00\%$, N=5, df=8

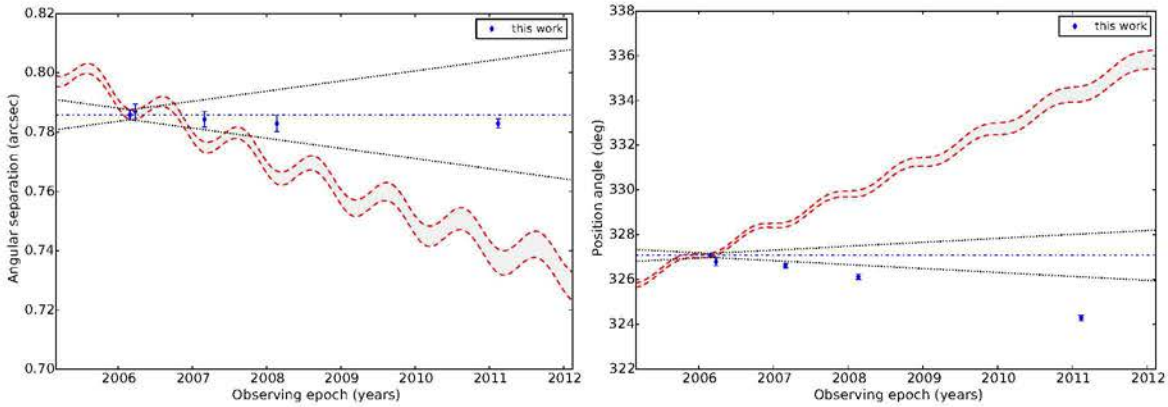


## HIP55597

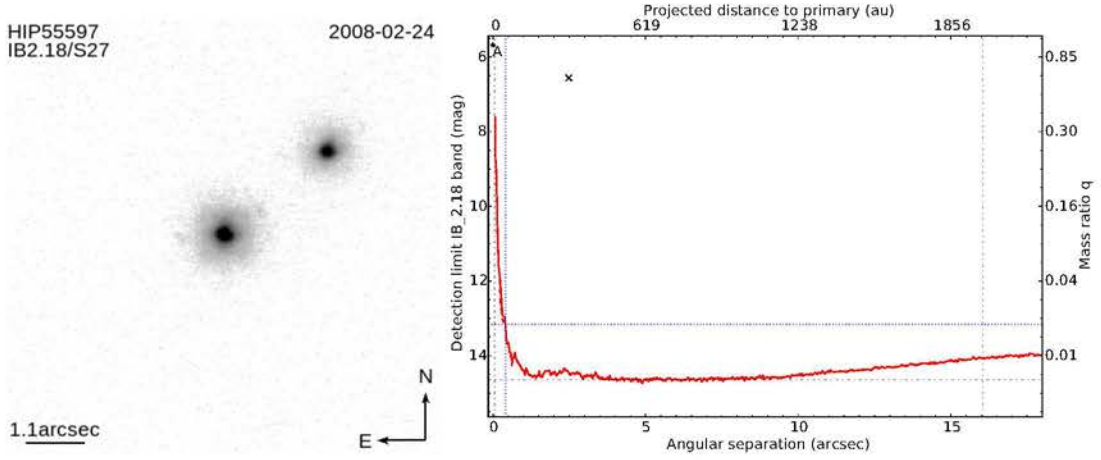


CC1: $P_{bg} = 0.00\%$, $P_{cmv} = 0.00\%$, N=5, df=8

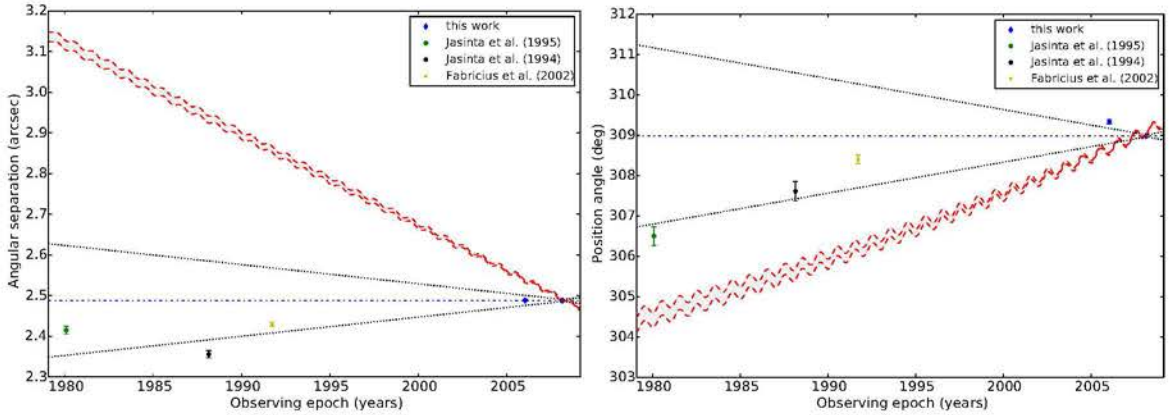

## HIP55657

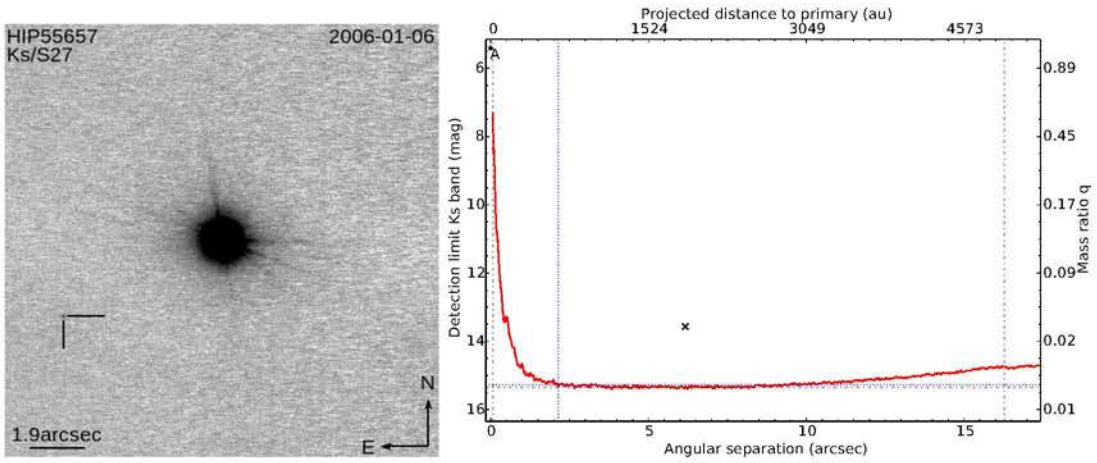


CC1: $P_{bg} = 61.73\%$, $P_{cmv} = 17.52\%$, N=2, df=2

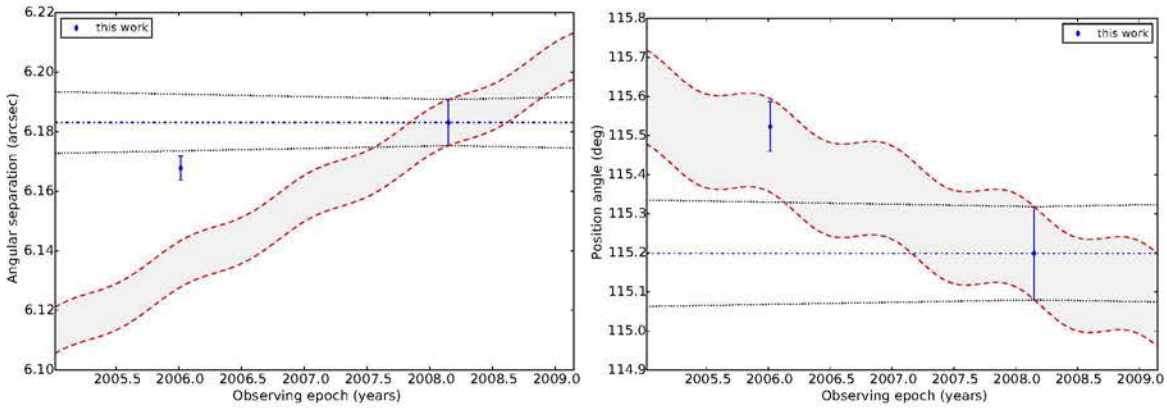


## HIP56000

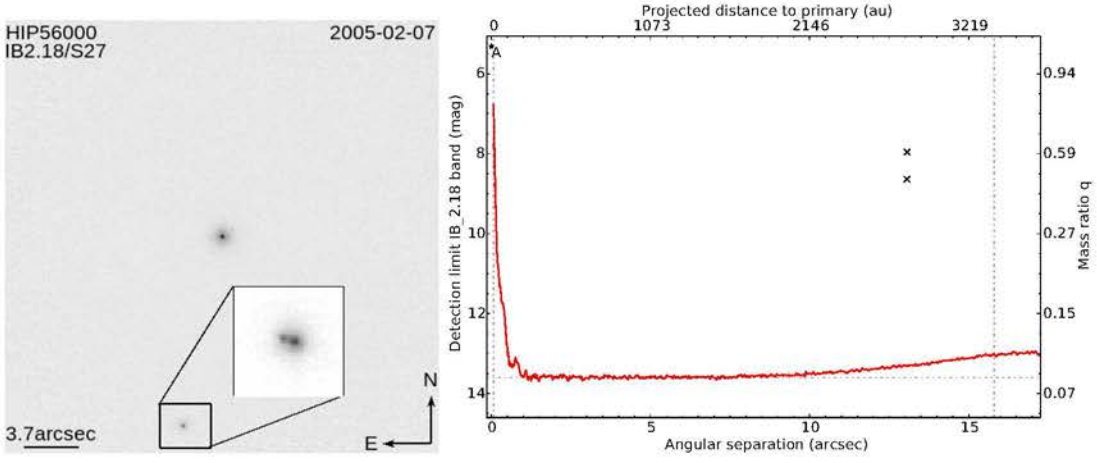


CC1: $P_{bg} = 55.48\%$, $P_{cmv} = 0.14\%$, N=2, df=2

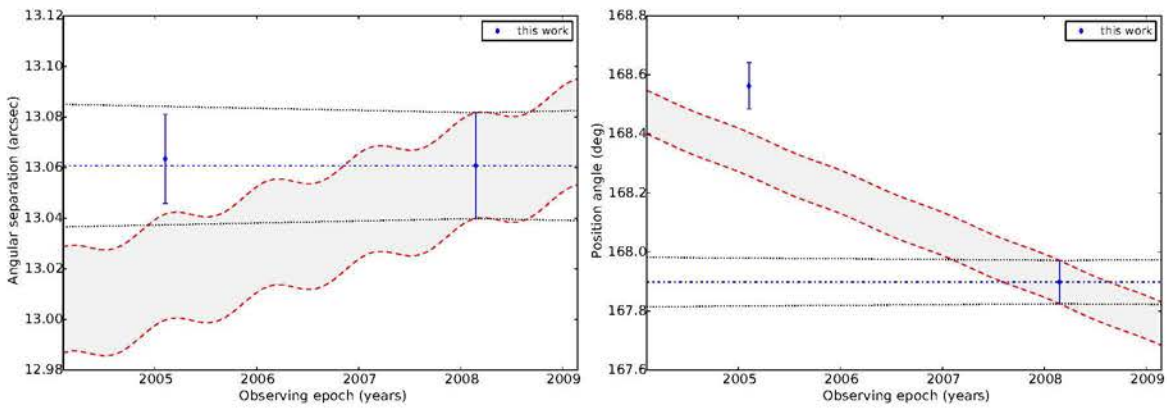

CC2: $P_{bg}$ = 47.38%, $P_{cmv}$ = 0.56%, N=2, df=2

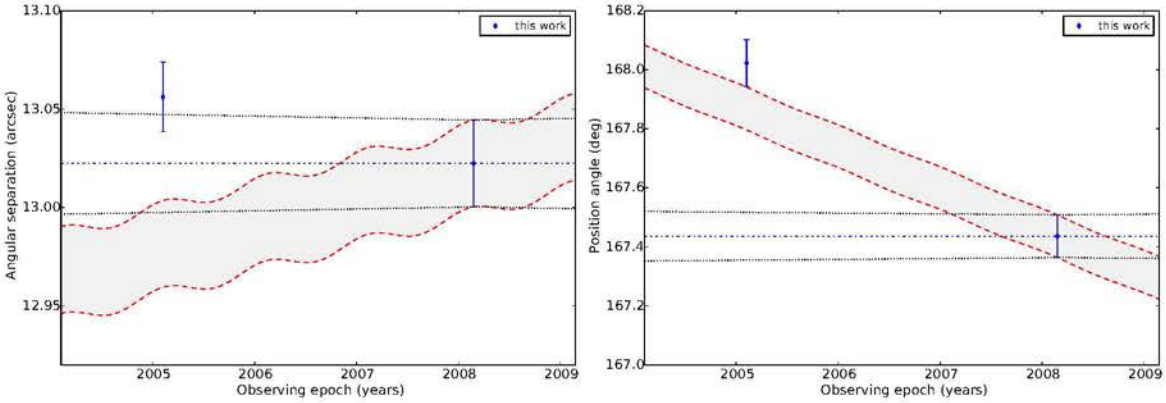


HIP56754

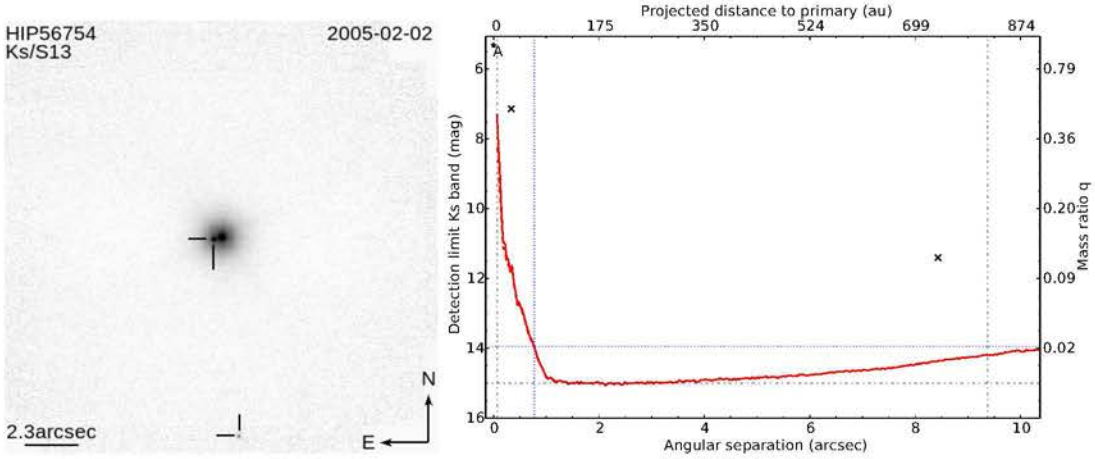


CC1: $P_{bg}$ = 0.00%, $P_{cmv}$ = 0.00%, N=3, df=4

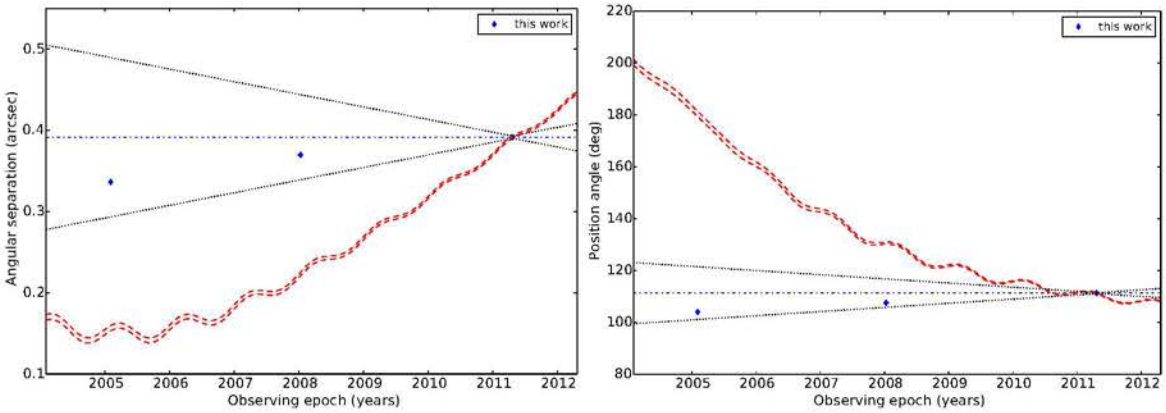


CC2: $P_{bg}$ = 0.00%, $P_{cmv}$ = 0.00%, N=3, df=4

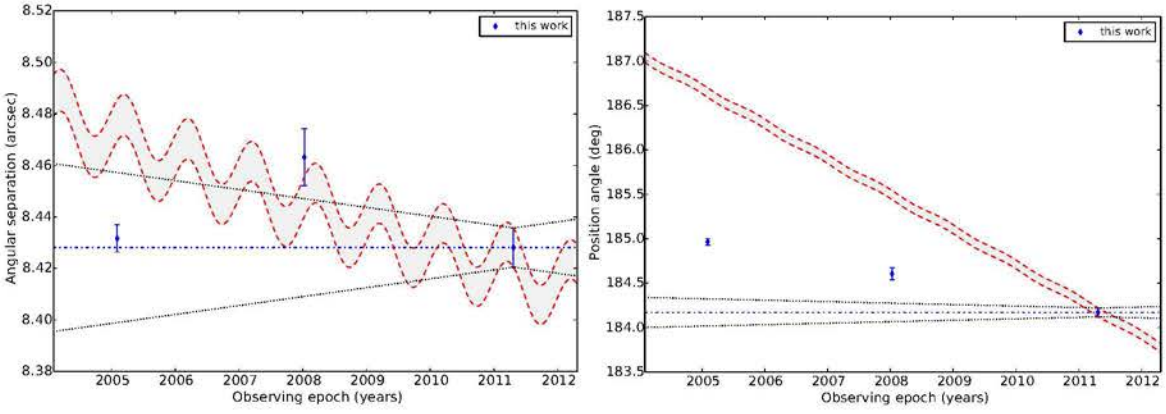

## HIP58326

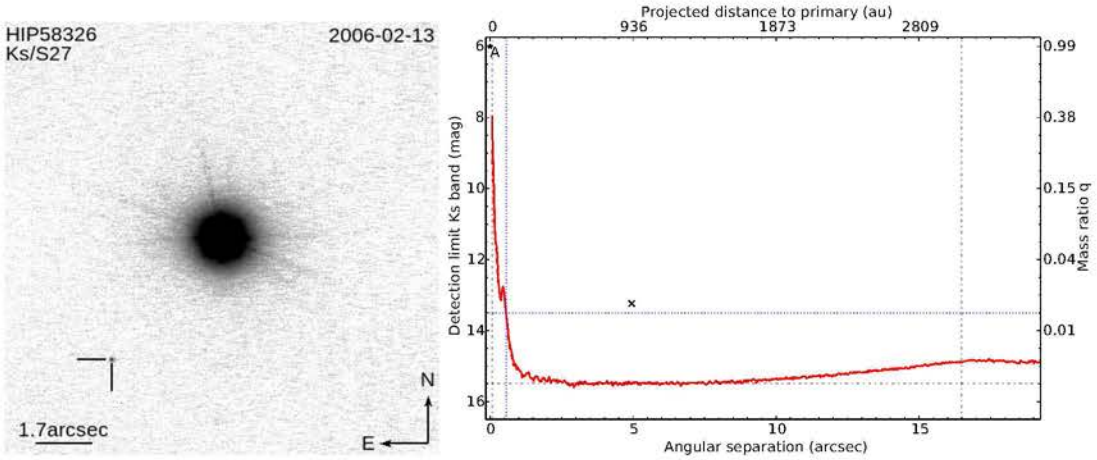


CC1: $P_{bg} = 15.62\%$, $P_{cmv} = 0.00\%$, N=3, df=4

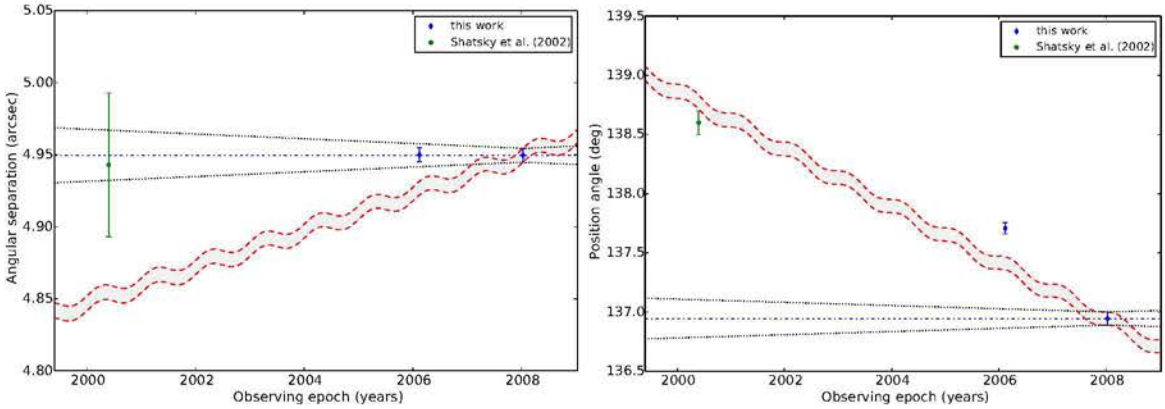


## HIP60189

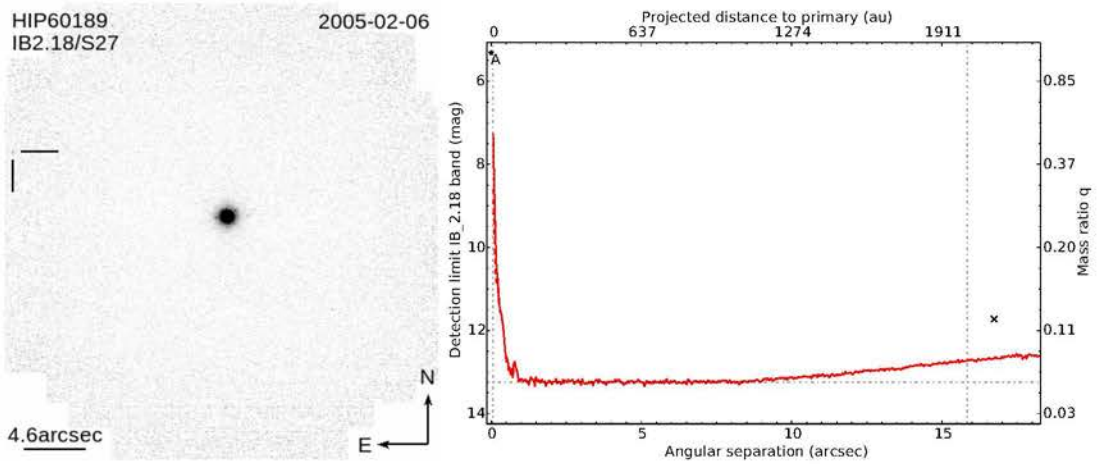


CC1: $P_{bg} = 0.00\%$, $P_{cmv} = 0.00\%$, N=4, df=6

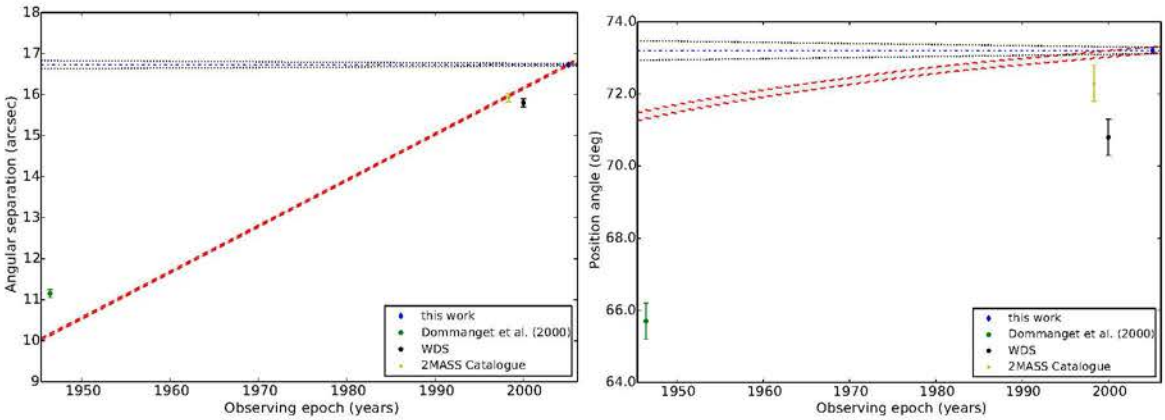

## HIP60449

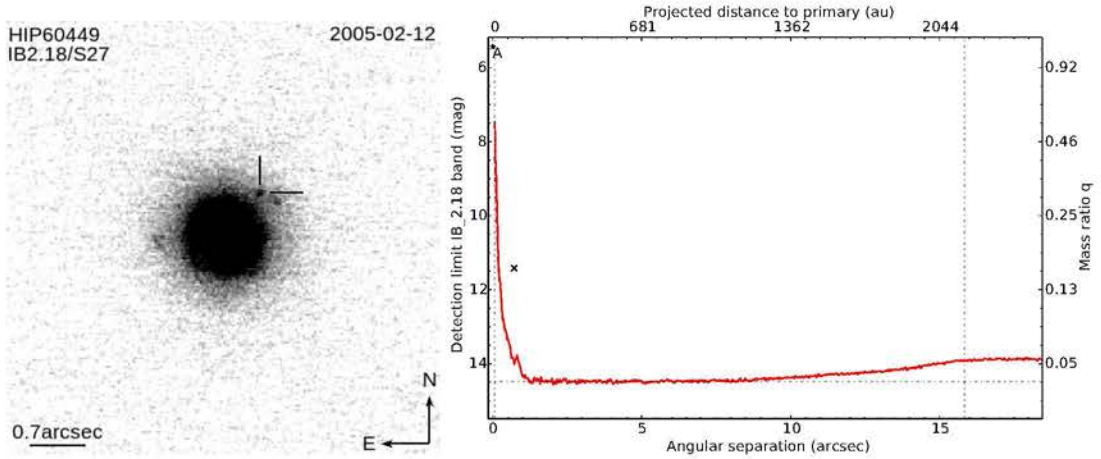


CC1: $P_{bg} = 0.00\%$, $P_{cmv} = 1.43\%$, N=2, df=2

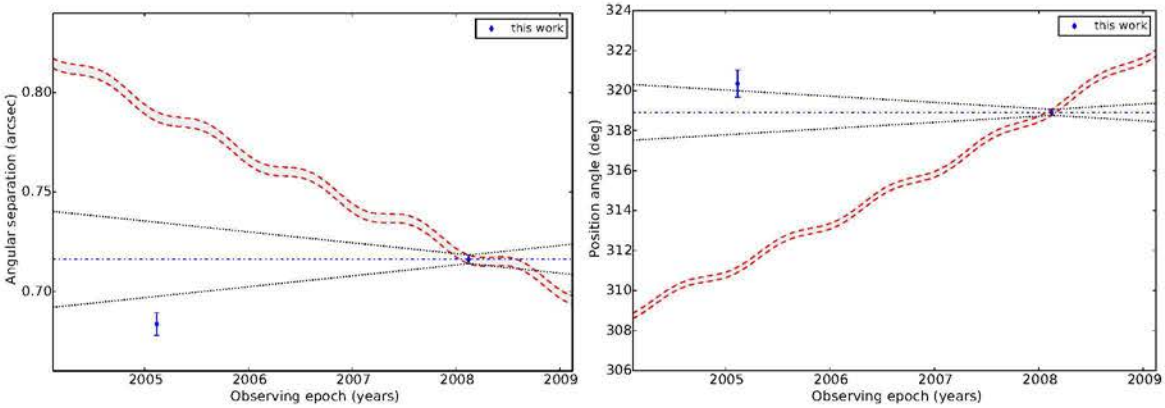


## HIP60851

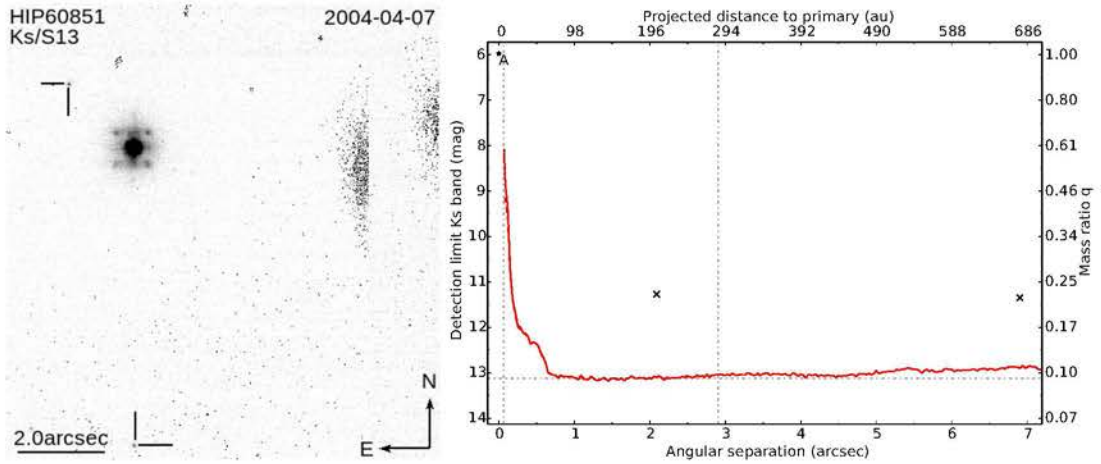


CC1: $P_{bg} = 75.89\%$, $P_{cmv} = 41.44\%$, N=2, df=2

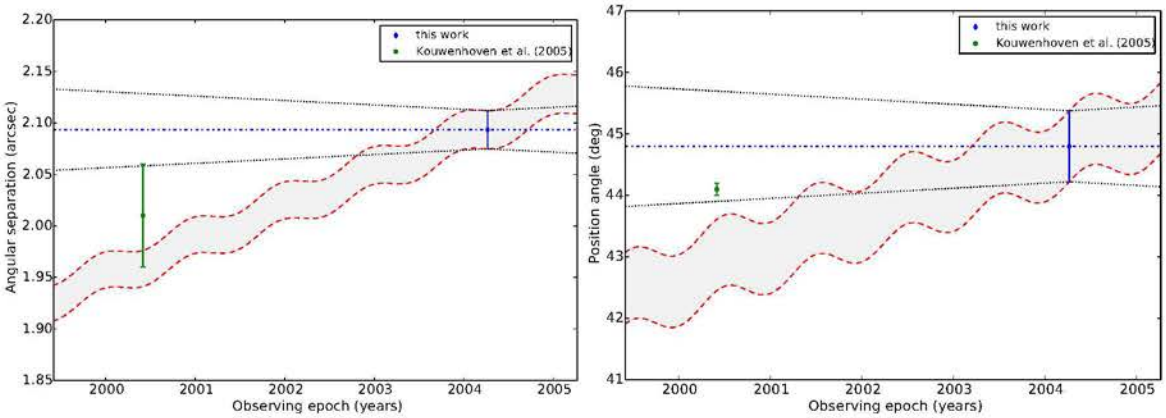

CC2: $P_{bg} = 96.24\%$, $P_{cmv} = 39.60\%$, N=2, df=2

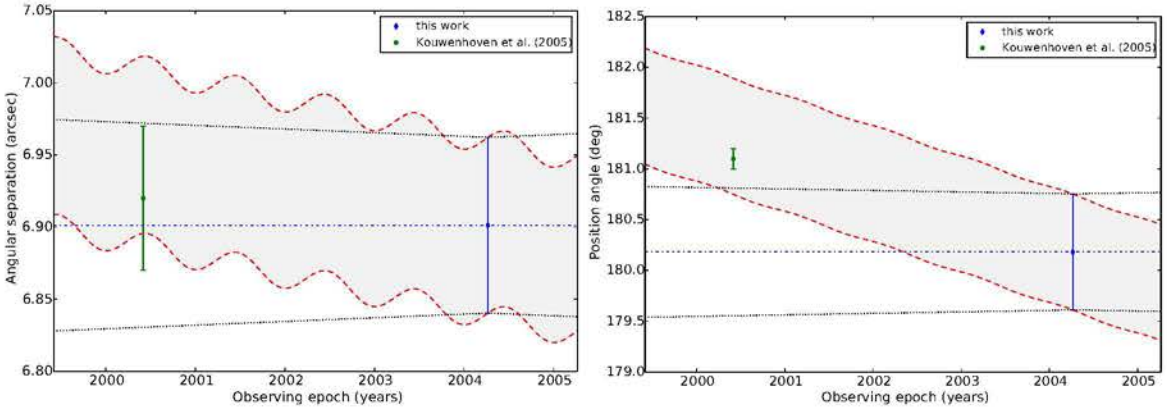


HIP61789

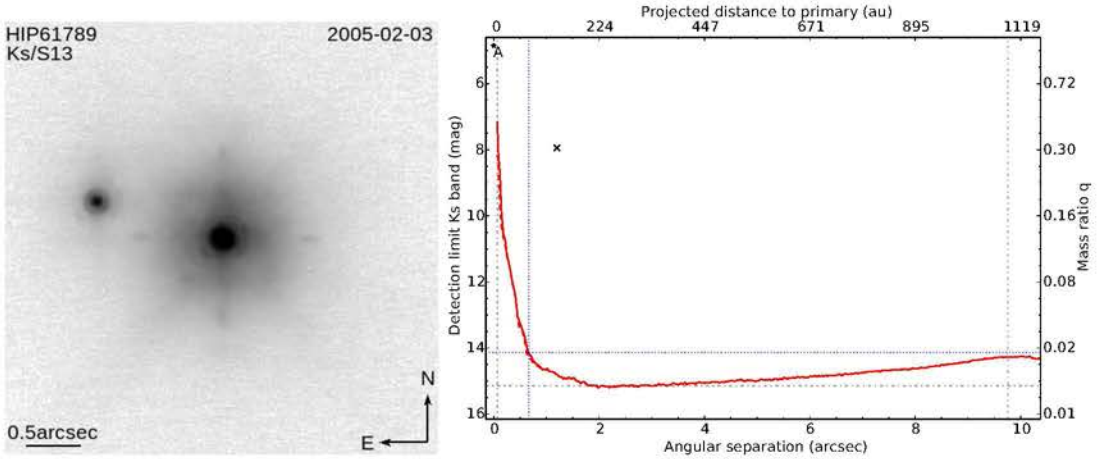


CC1: $P_{bg} = 0.00\%$, $P_{cmv} = 31.13\%$, N=2, df=2

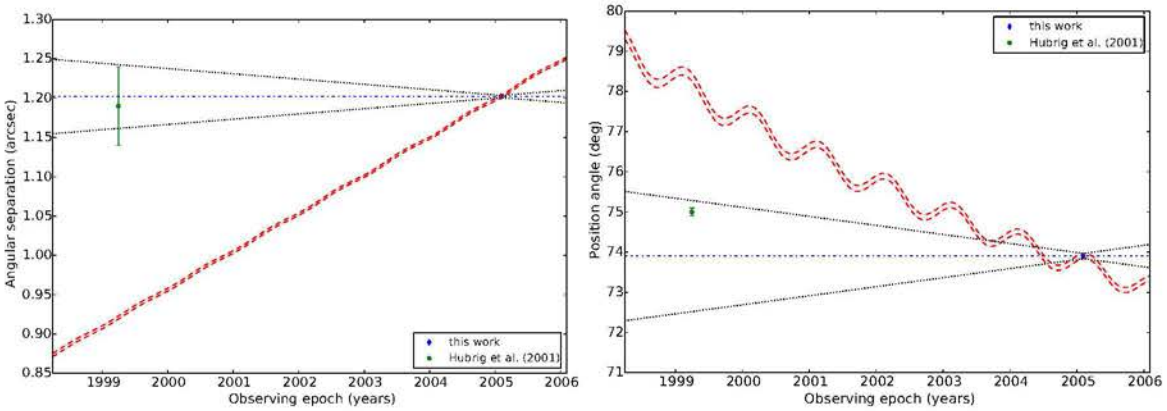


HIP62026

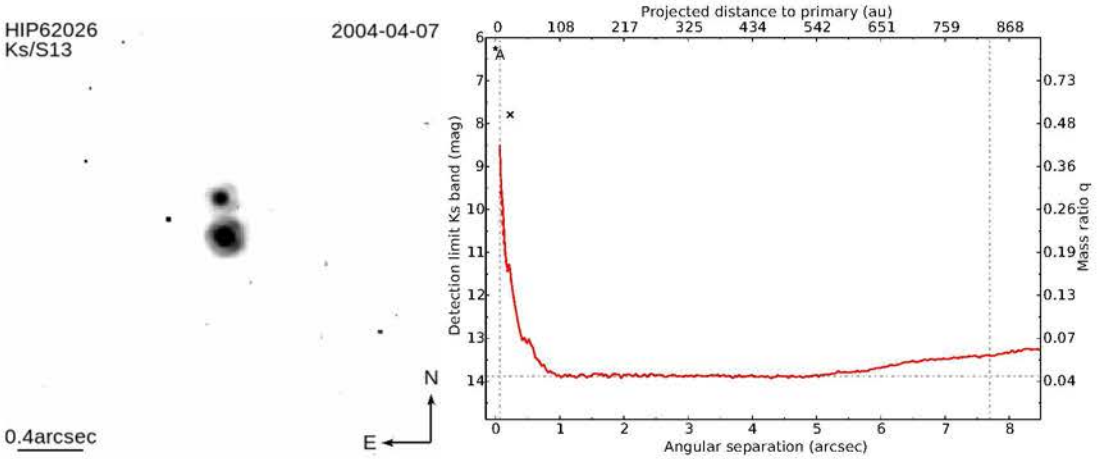

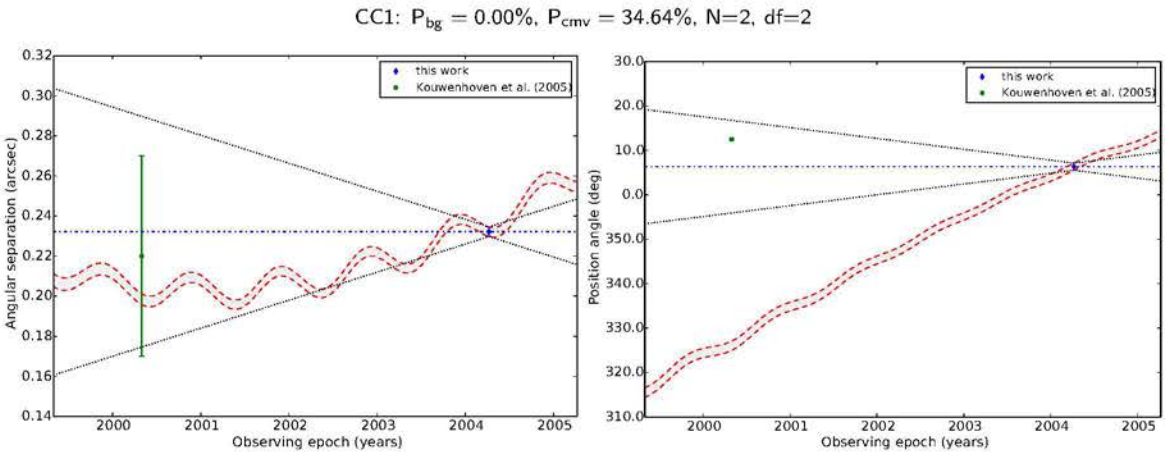
CC1: $P_{bg}$ = 0.00%, $P_{cmv}$ = 34.64%, N=2, df=2
this work
Kouwenhoven et al. (2005)
Angular separation (arcsec)
Position angle (deg)
Observing epoch (years)

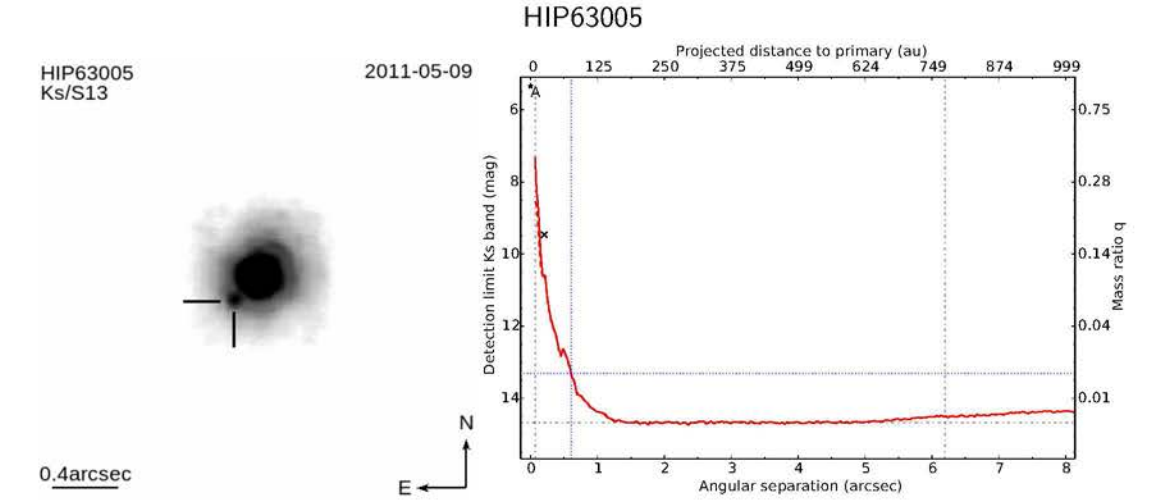
HIP63005
HIP63005
Ks/S13
2011-05-09
0.4arcsec
N
E
Projected distance to primary (au)
Detection limit Ks band (mag)
Mass ratio q
Angular separation (arcsec)

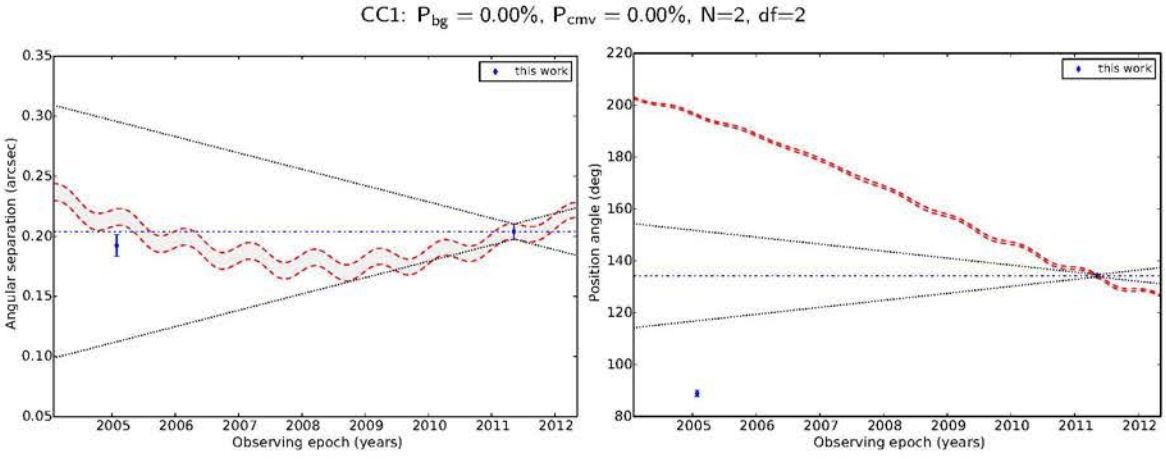
CC1: $P_{bg}$ = 0.00%, $P_{cmv}$ = 0.00%, N=2, df=2
this work
Angular separation (arcsec)
Position angle (deg)
Observing epoch (years)

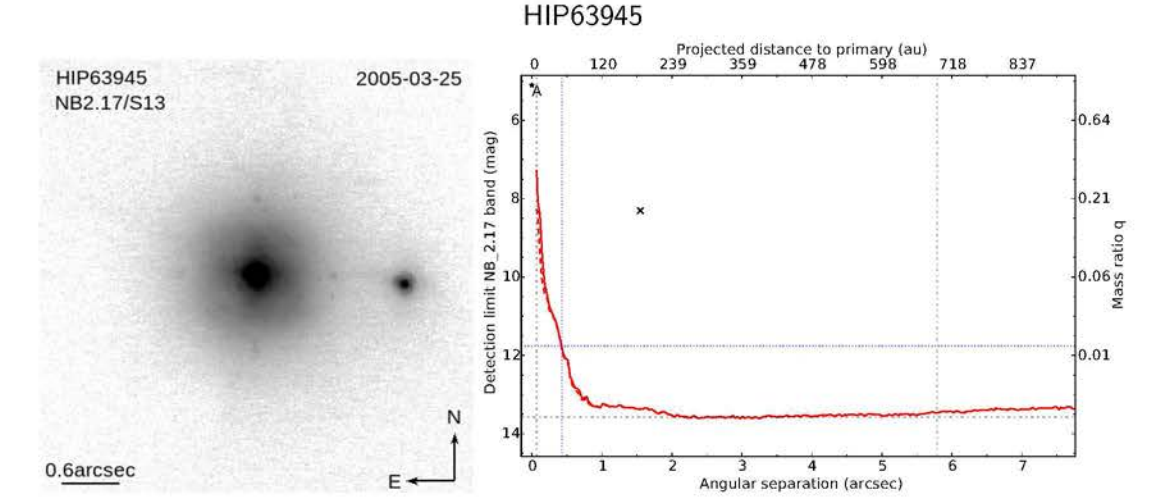
HIP63945
HIP63945
NB2.17/S13
2005-03-25
0.6arcsec
N
E
Projected distance to primary (au)
Detection limit NB_2.17 band (mag)
Mass ratio q
Angular separation (arcsec)

CC1: $P_{bg}$ = 0.00%, $P_{cmv}$ = 2.31%, N=2, df=2

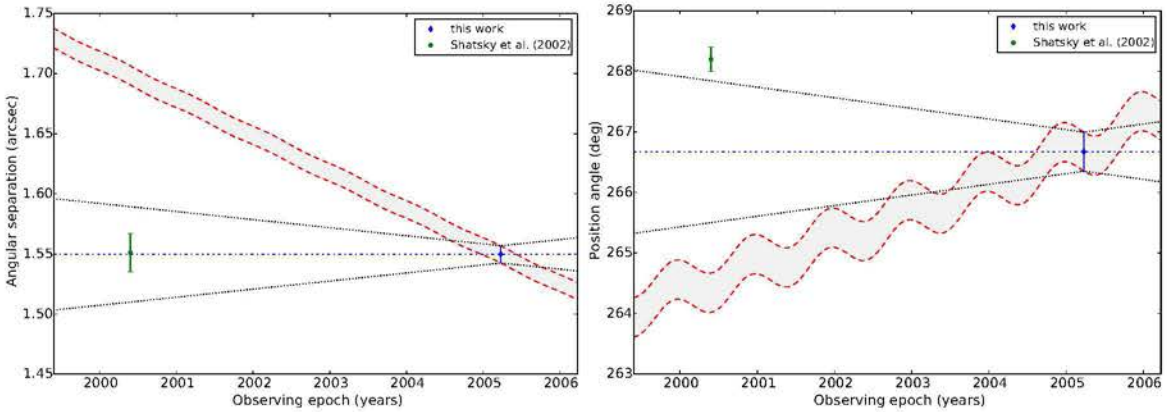


## HIP64515

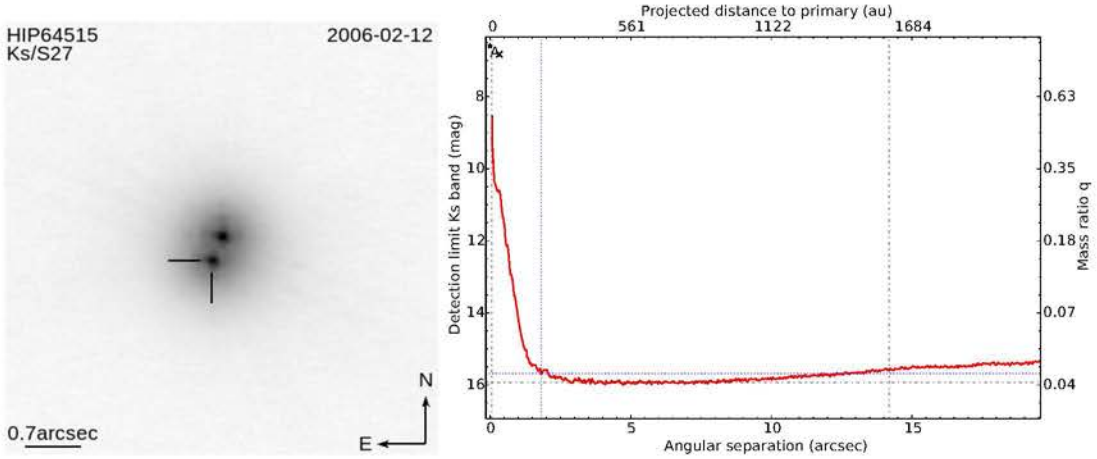


CC1: $P_{bg}$ = 0.00%, $P_{cmv}$ = 0.00%, N=3, df=4

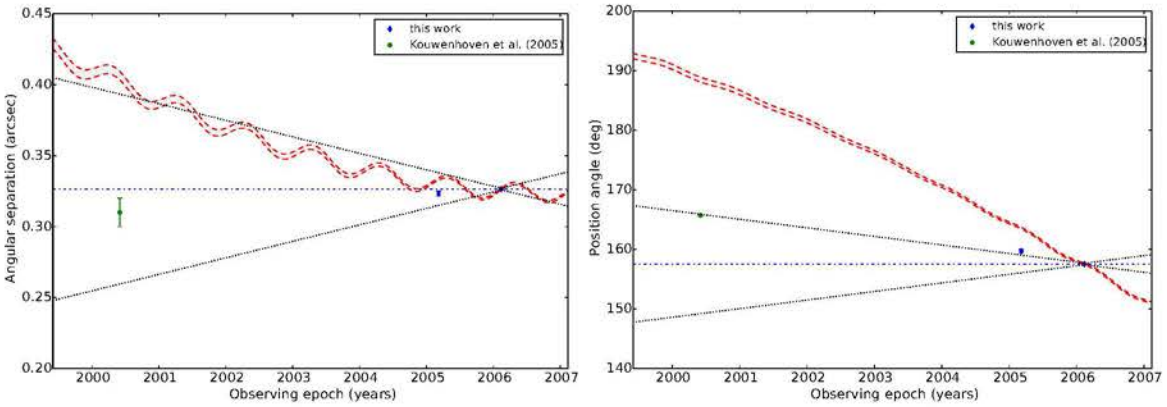


## HIP67472

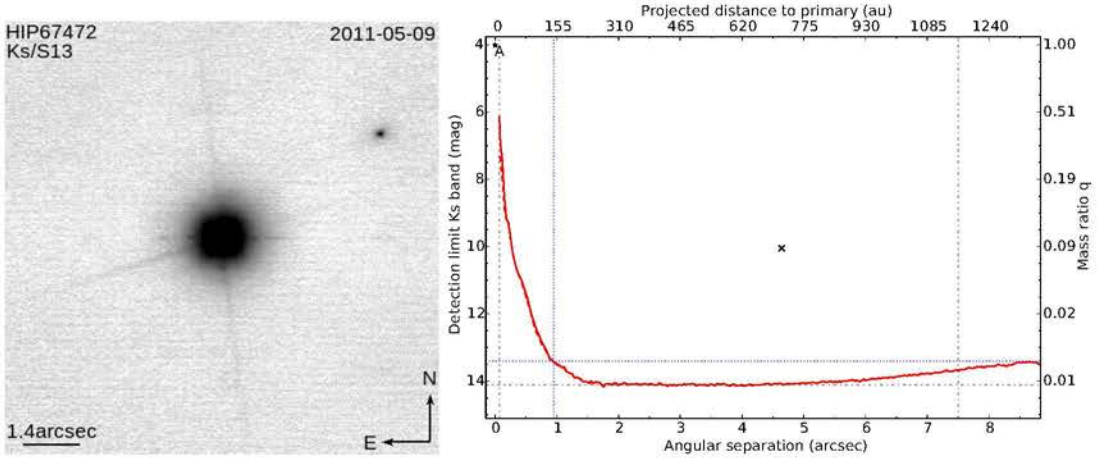

CC1: $P_{bg} = 0.00\%$, $P_{cmv} = 97.66\%$, N=3, df=4

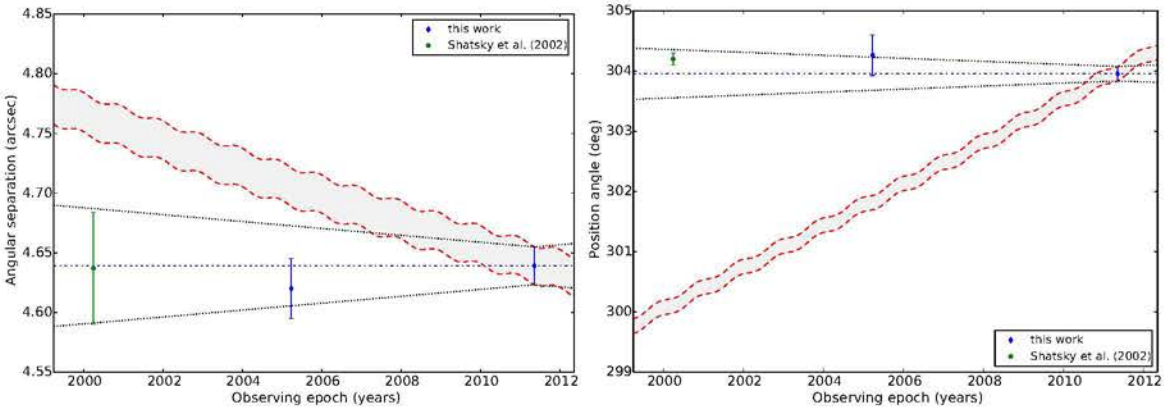


## HIP67669

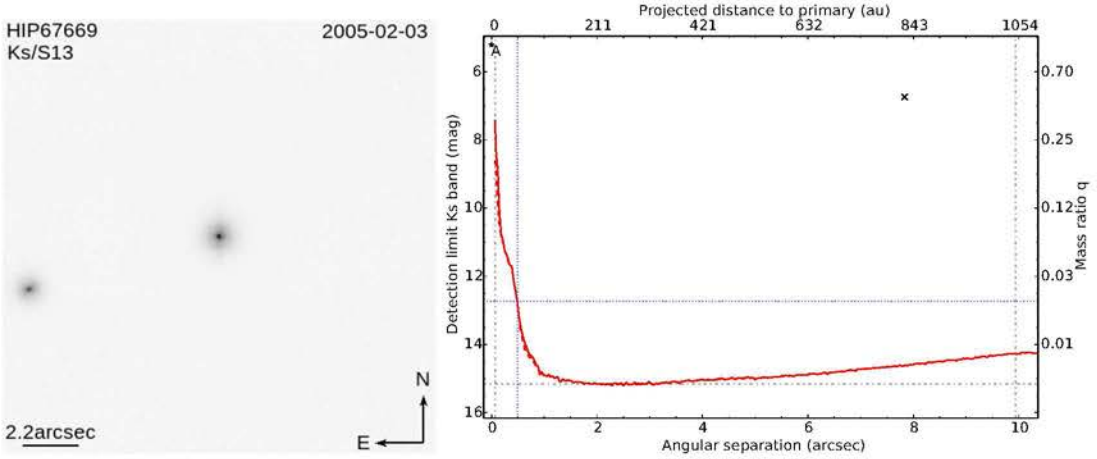


CC1: $P_{bg} = 0.00\%$, $P_{cmv} = 0.00\%$, N=3, df=4

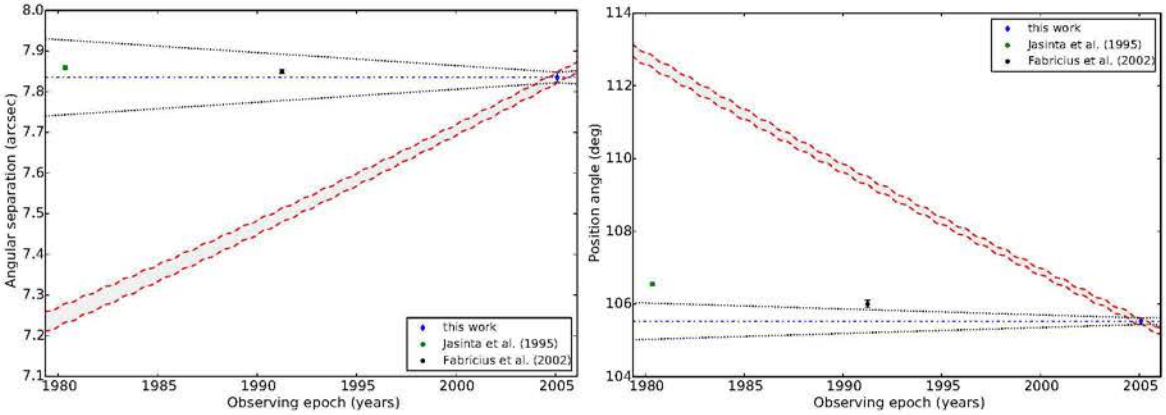


## HIP67703

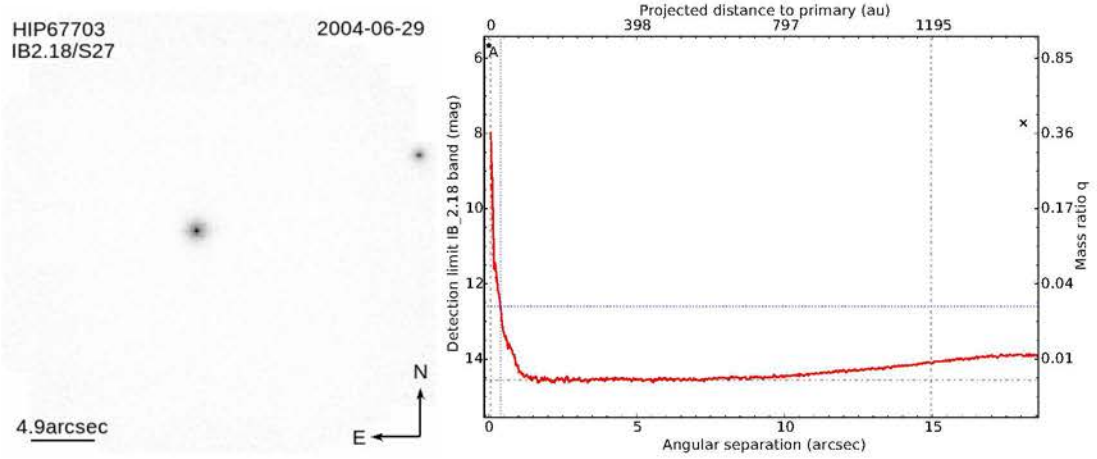

CC1: $P_{bg}$ = 0.00%, $P_{cmv}$ = 0.00%, N=4, df=6

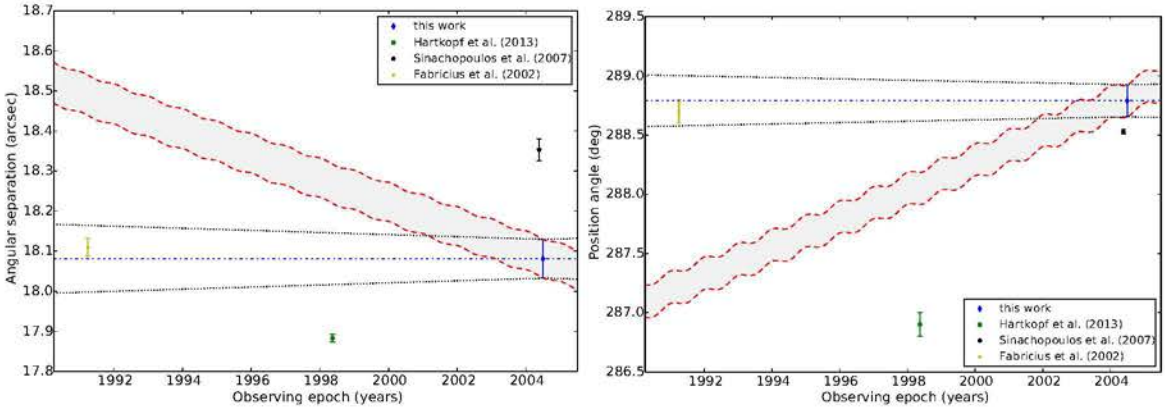


HIP69113

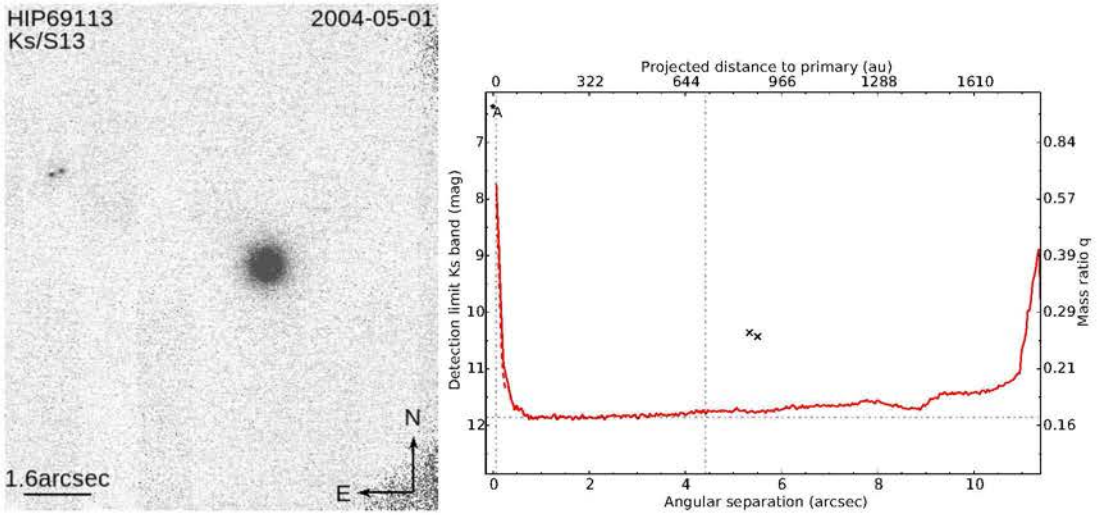


CC1: $P_{bg}$ = 47.49%, $P_{cmv}$ = 87.17%, N=2, df=2

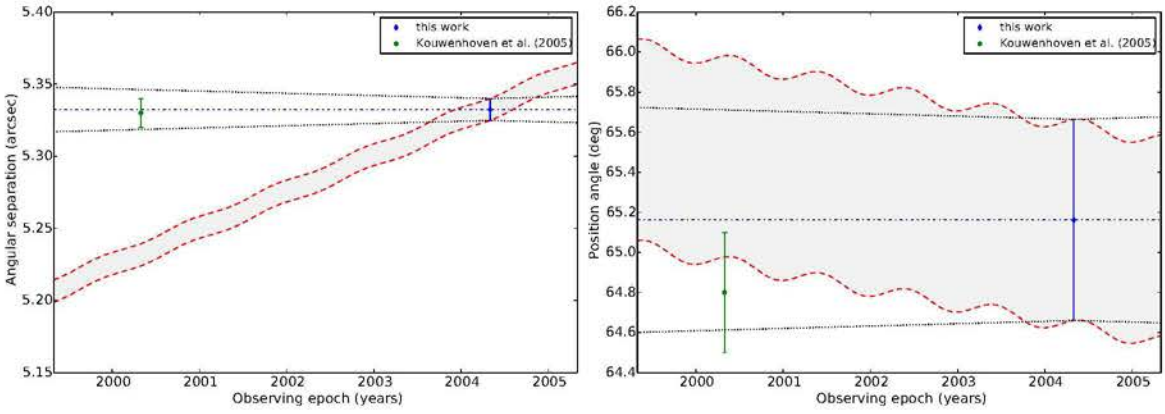


CC2: $P_{bg}$ = 32.86%, $P_{cmv}$ = 92.31%, N=2, df=2

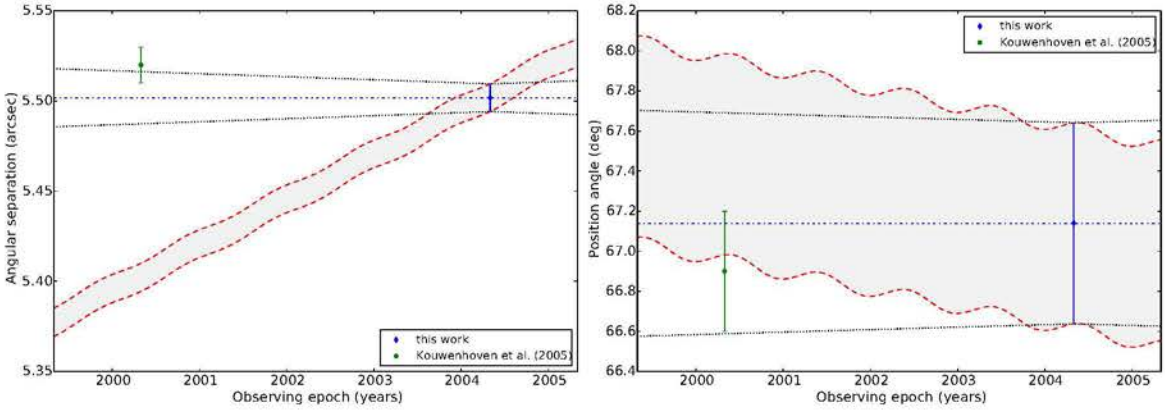

## HIP70915

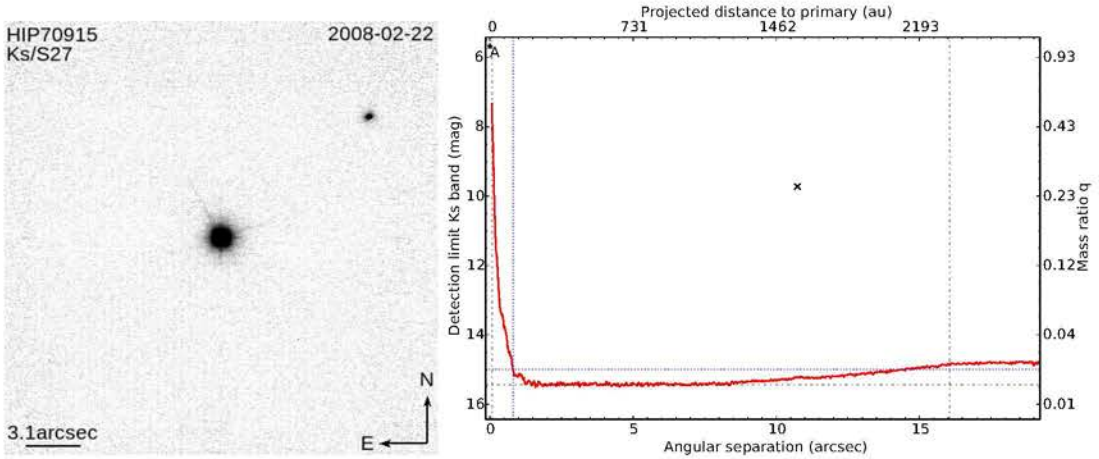


CC1: $P_{bg} = 0.00\%$, $P_{cmv} = 14.83\%$, N=3, df=4

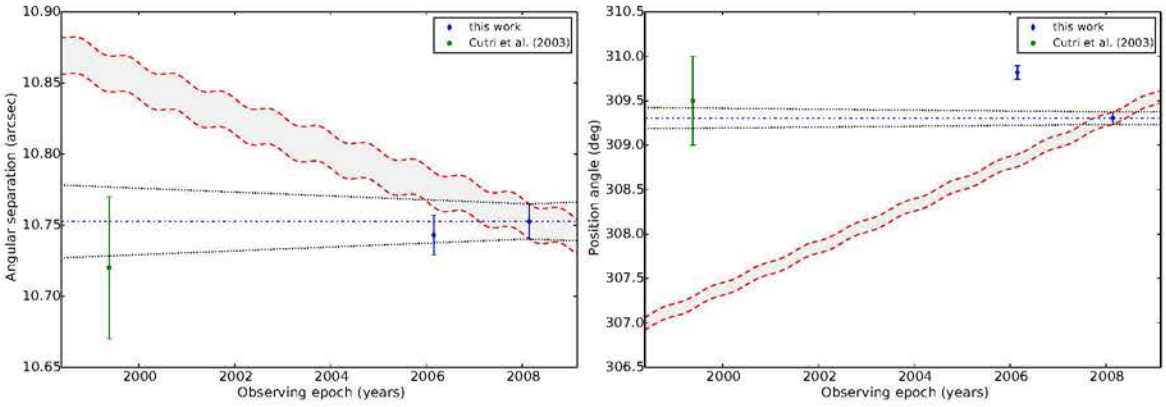


## HIP71762

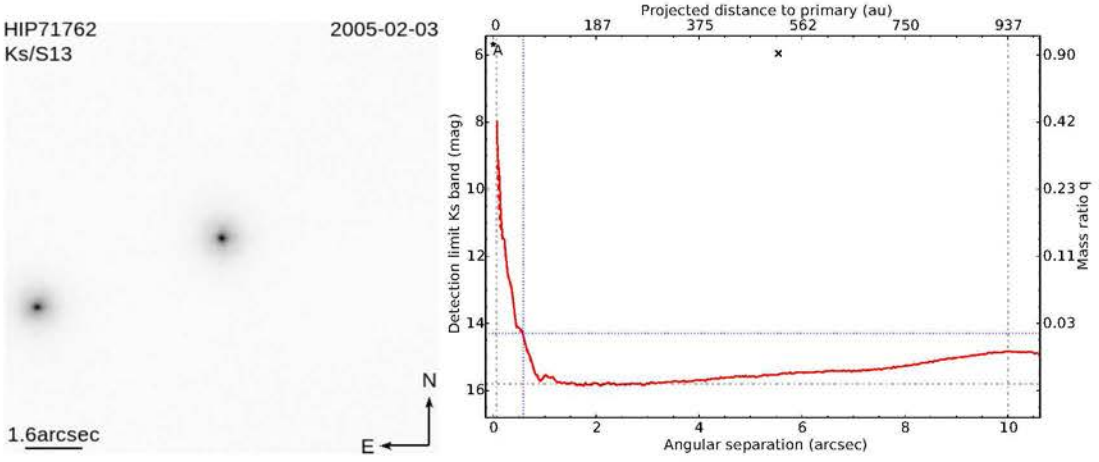


CC1: $P_{bg} = 0.00\%$, $P_{cmv} = 0.15\%$, N=4, df=6

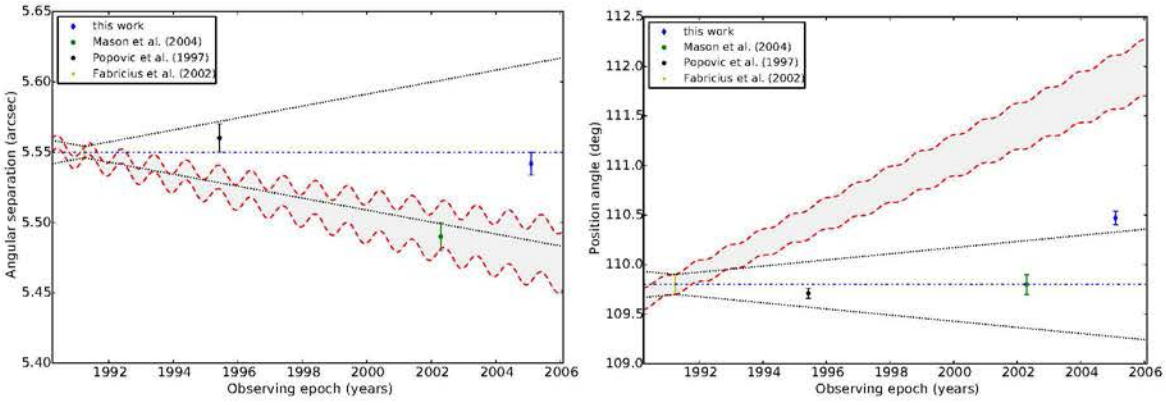

## HIP73111

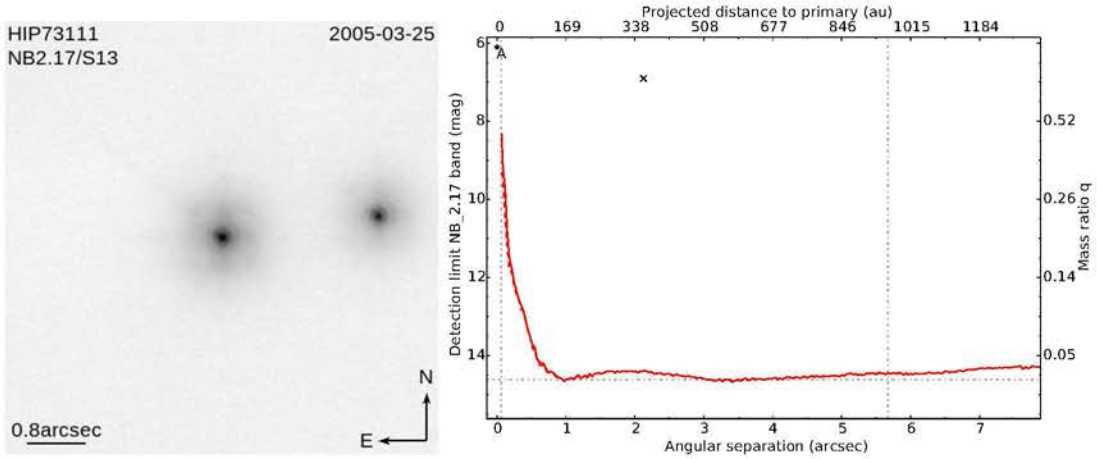


CC1: $P_{bg} = 0.00\%$, $P_{cmv} = 0.20\%$, N=2, df=2

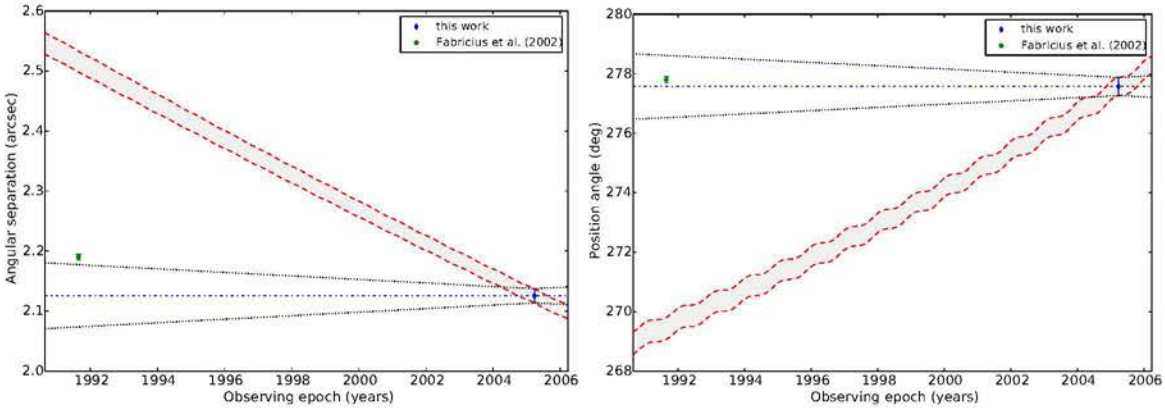


## HIP74750

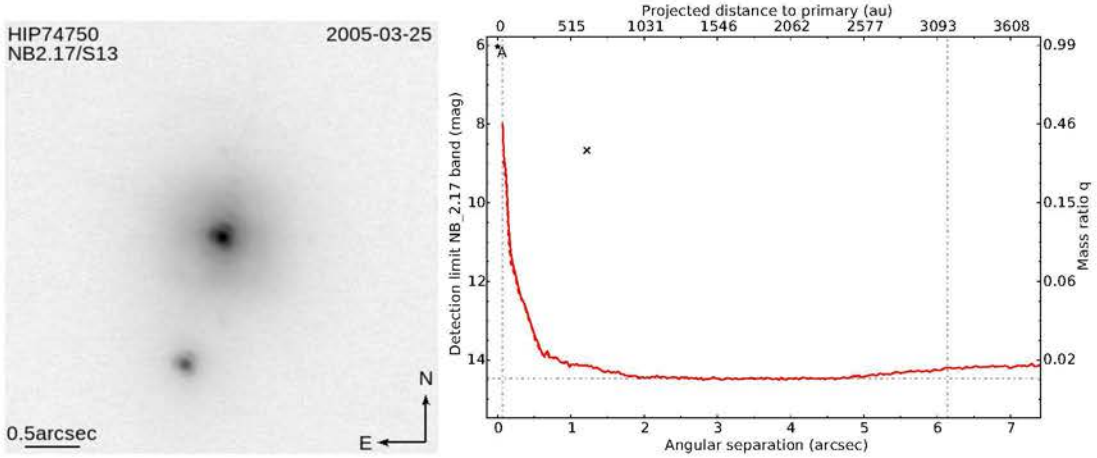


CC1: $P_{bg} = 2.05\%$, $P_{cmv} = 0.00\%$, N=2, df=2

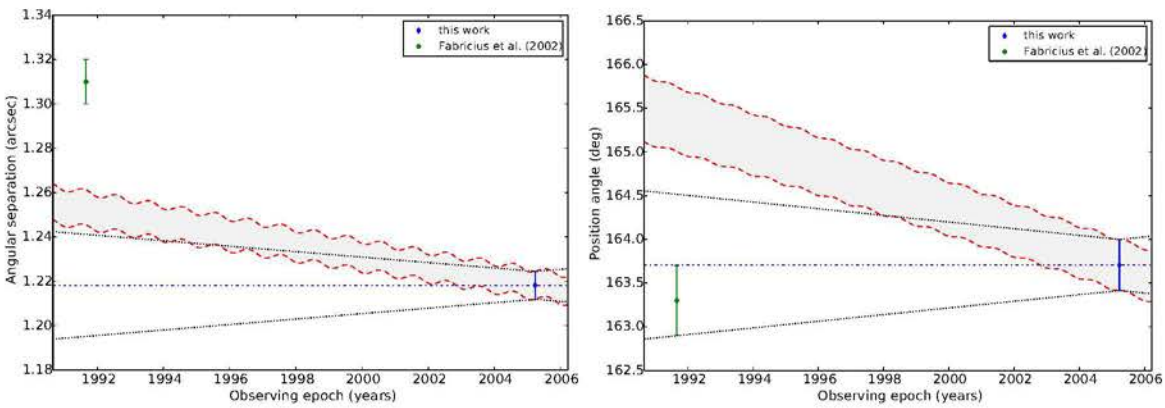

## HIP74911

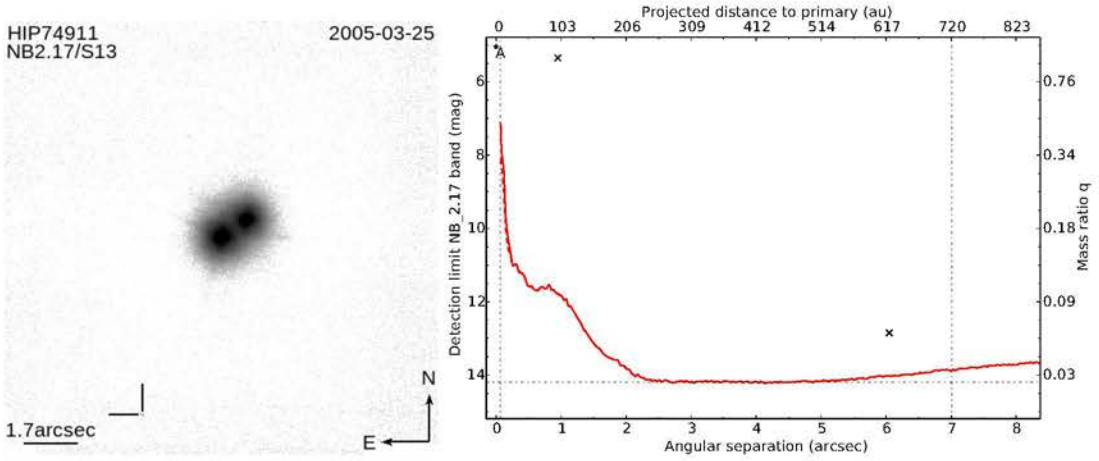


CC1: $P_{bg} = 0.00\%$, $P_{cmv} = 0.00\%$, N=3, df=4

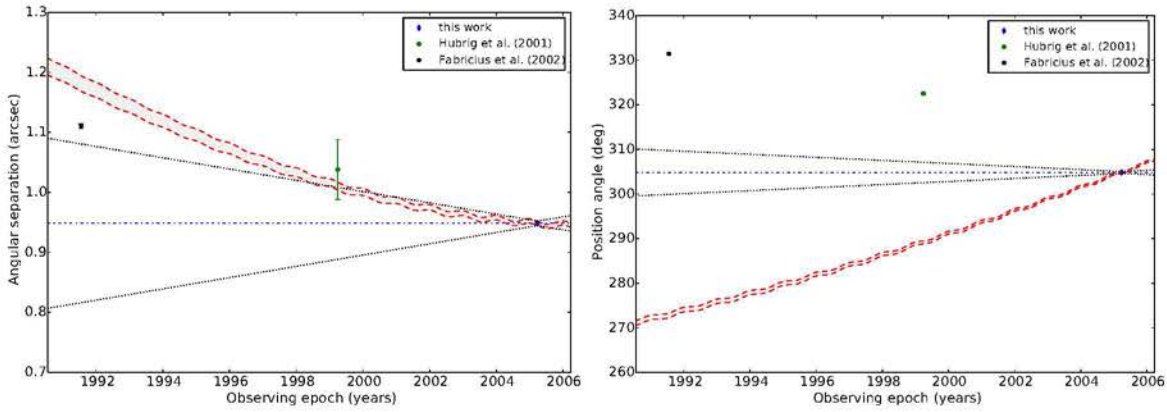


CC2: $P_{bg} = 22.41\%$, $P_{cmv} = 30.68\%$, N=2, df=2

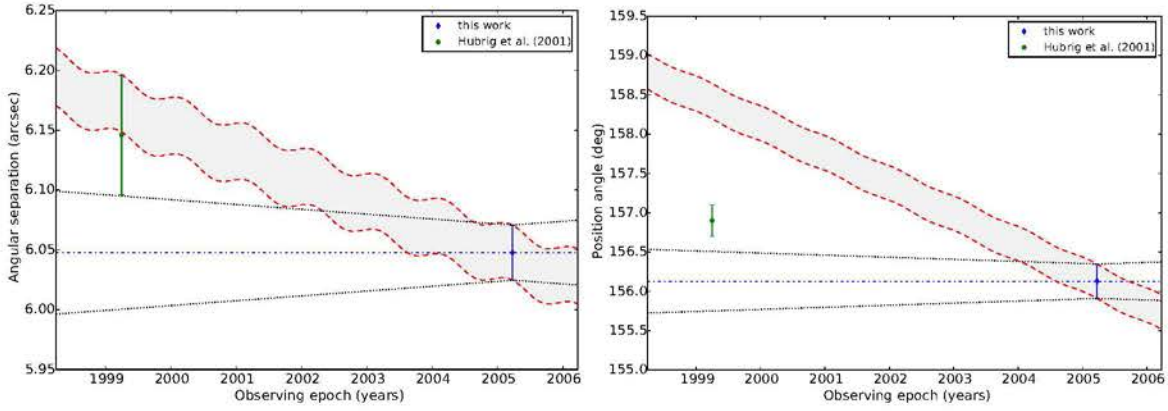


## HIP75264

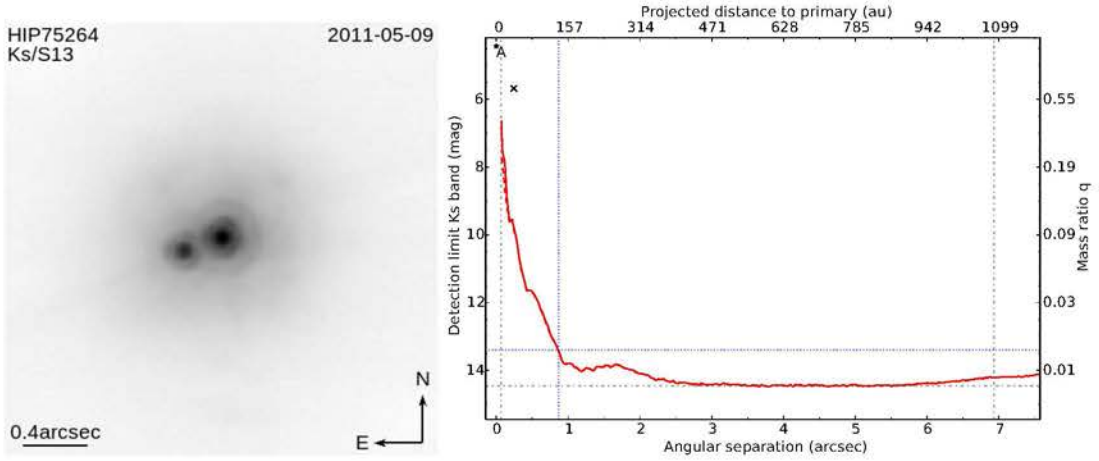

CC1: $P_{bg} = 0.00\%$, $P_{cmv} = 0.00\%$, N=4, df=6

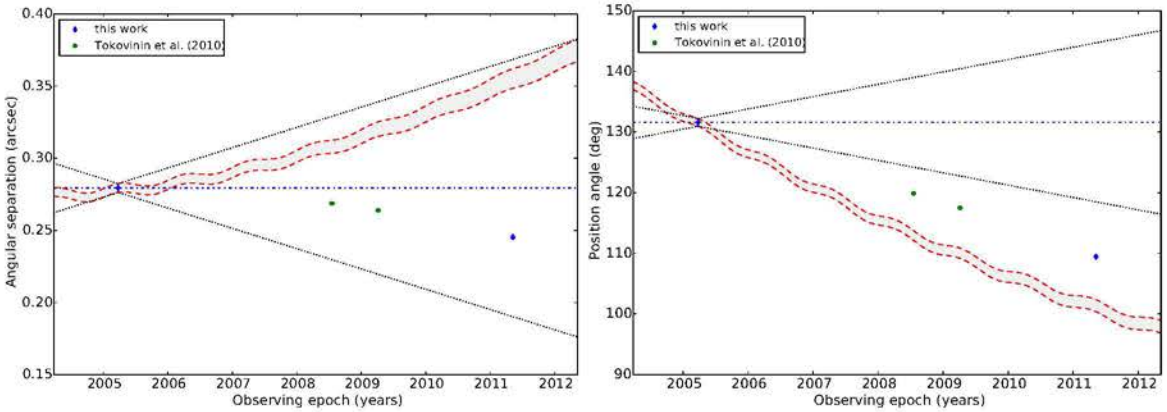


HIP77562

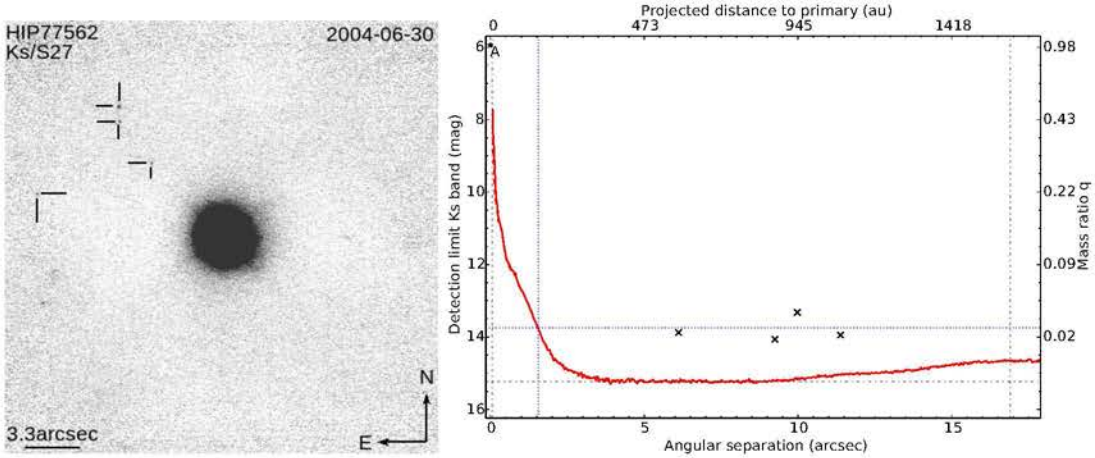


CC1: $P_{bg} = 89.15\%$, $P_{cmv} = 4.99\%$, N=2, df=2

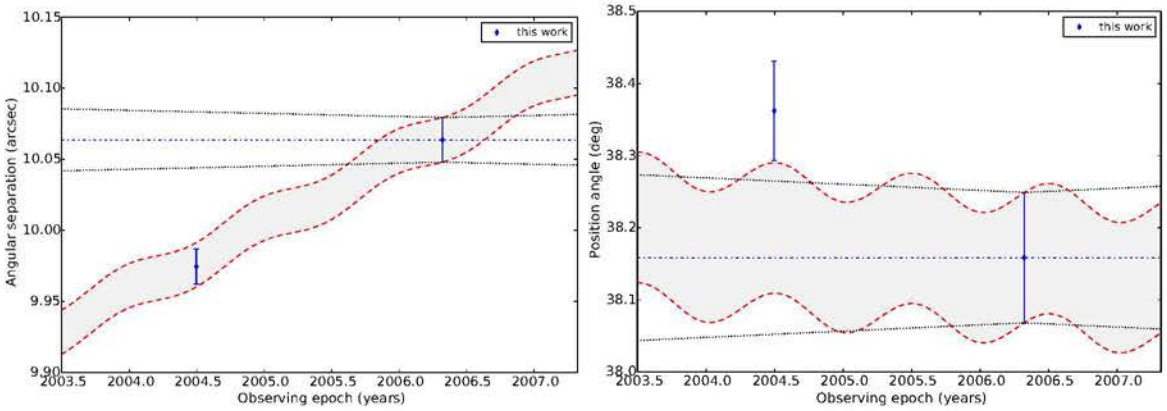


CC2: $P_{bg} = 91.08\%$, $P_{cmv} = 1.56\%$, N=2, df=2

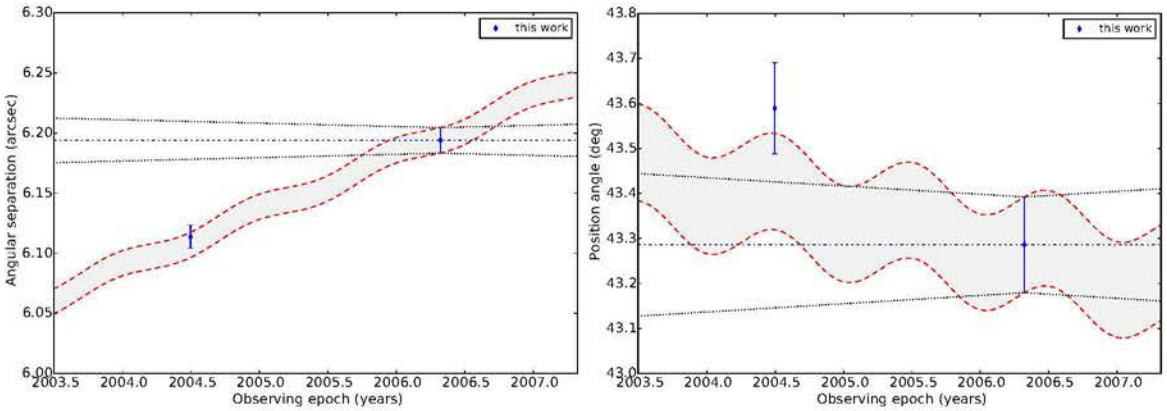

CC3: $P_{bg} = 87.93\%$, $P_{cmv} = 3.12\%$, N=2, df=2

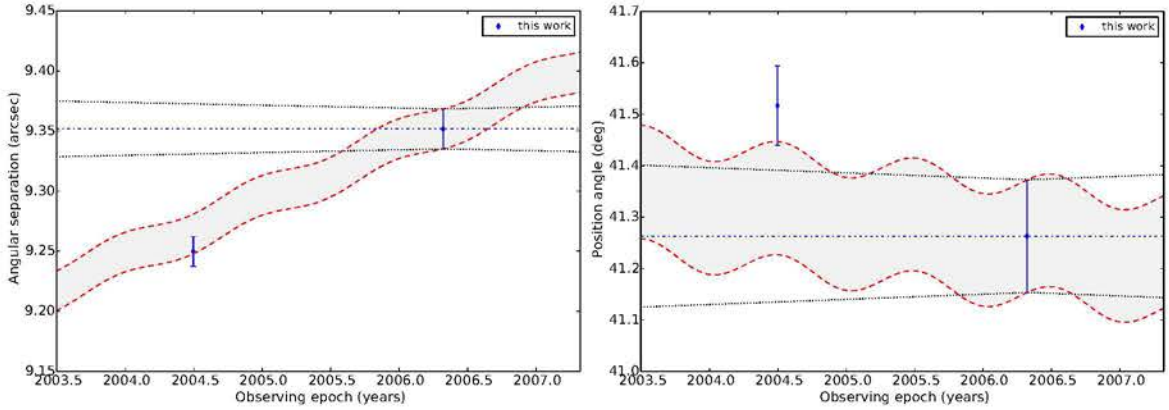


CC4: $P_{bg} = 68.75\%$, $P_{cmv} = 1.44\%$, N=2, df=2

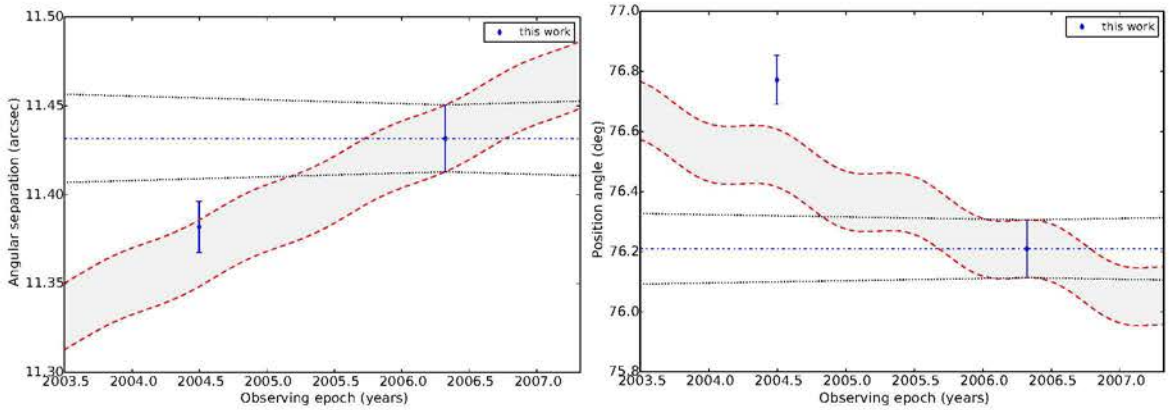


HIP77840

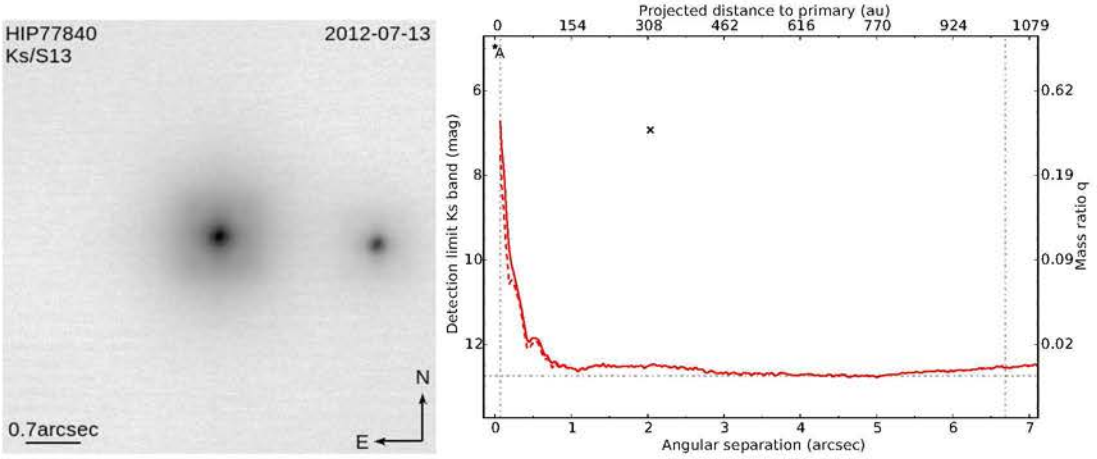


CC1: $P_{bg} = 0.00\%$, $P_{cmv} = 0.00\%$, N=3, df=4

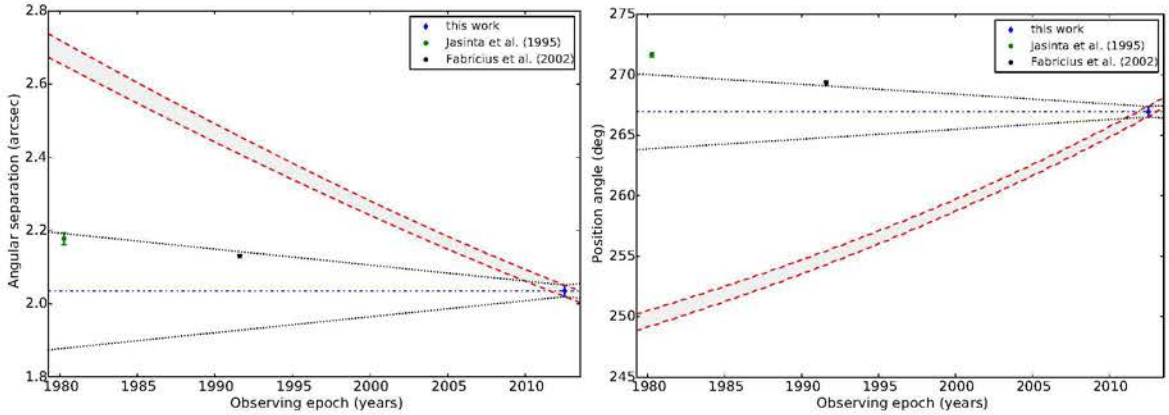

## HIP78968

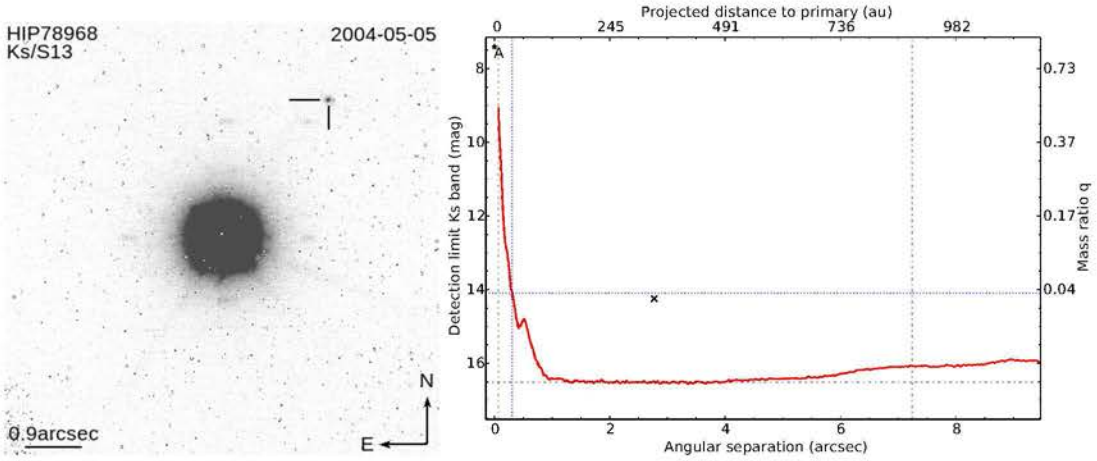


CC1: $P_{bg} = 96.41\%$, $P_{cmv} = 66.06\%$, N=2, df=2

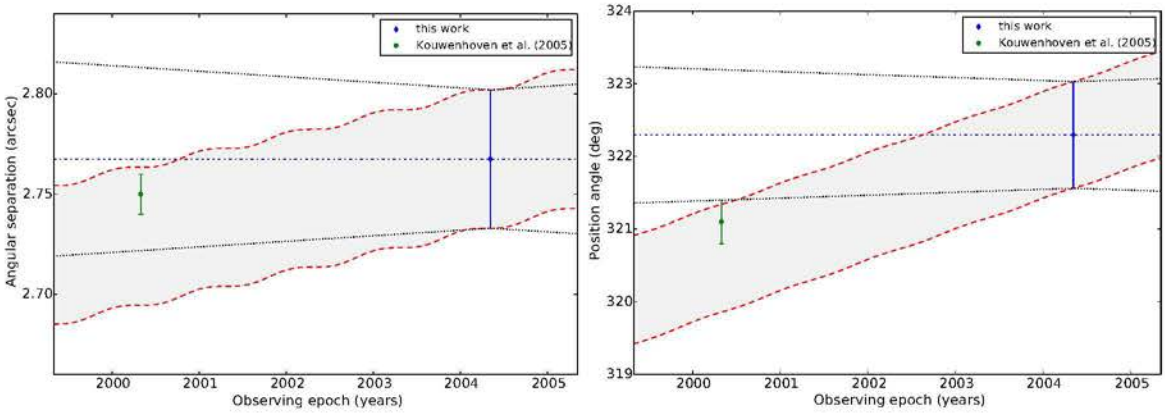


## HIP79005

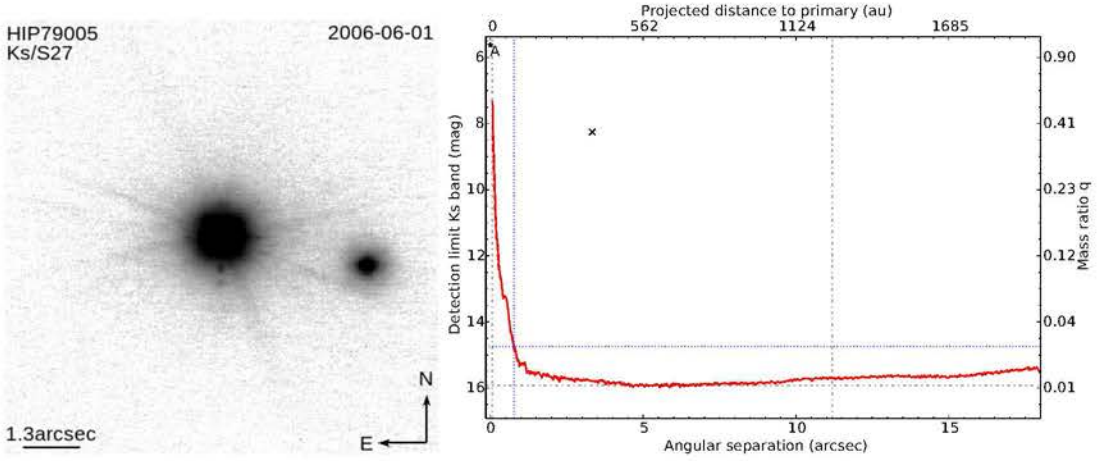


CC1: $P_{bg} = 0.00\%$, $P_{cmv} = 99.99\%$, N=4, df=6

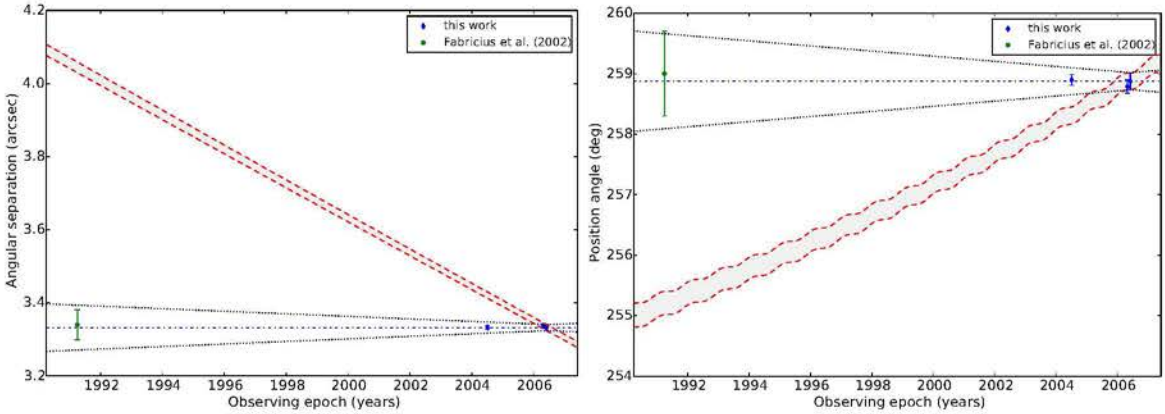

## HIP79098

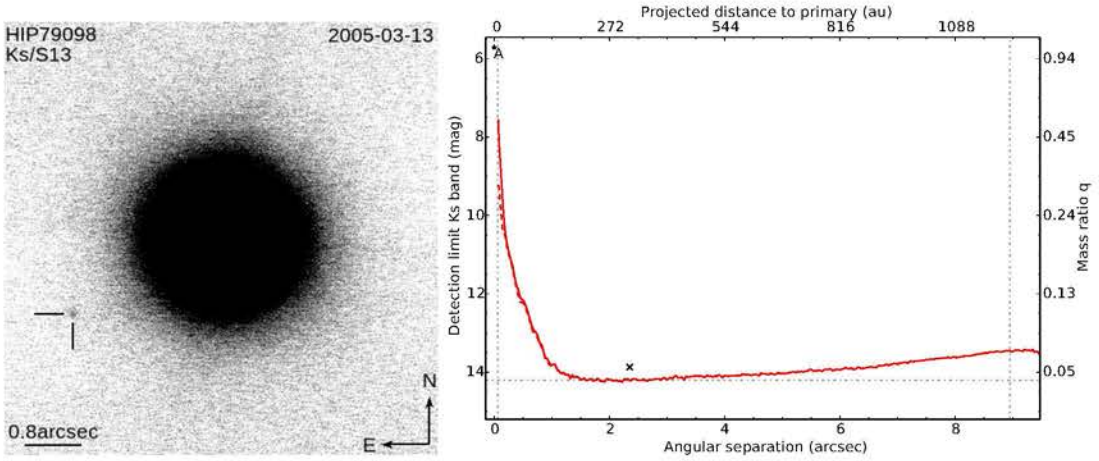


CC1: $P_{bg} = 4.09\%$, $P_{cmv} = 98.73\%$, N=2, df=2

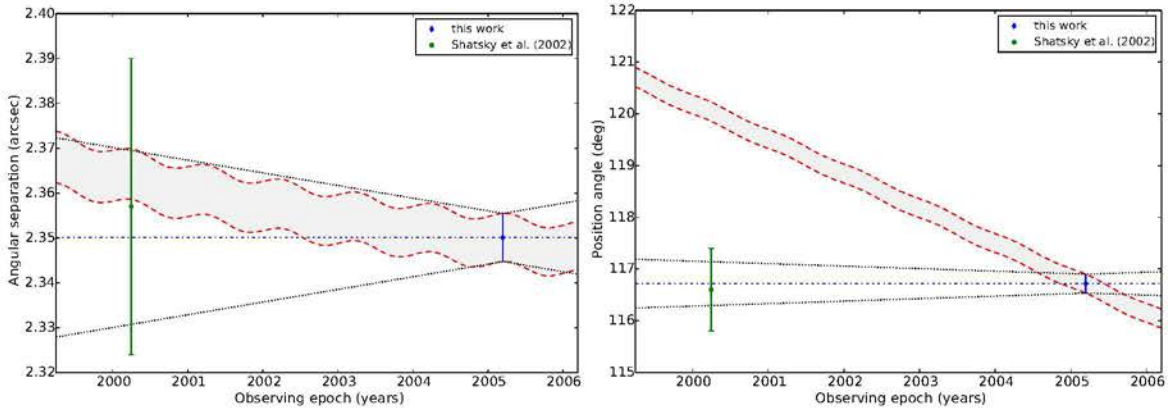


## HIP79153

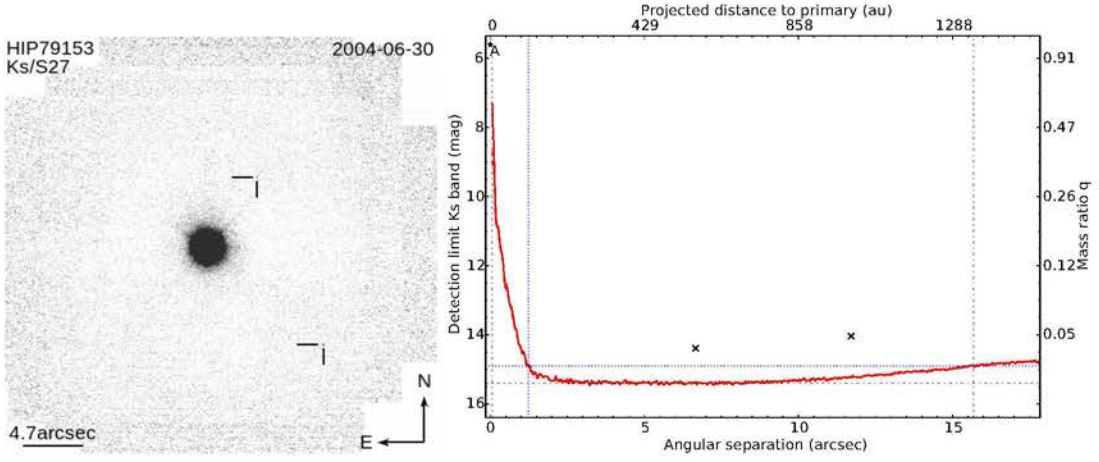


CC1: $P_{bg} = 53.06\%$, $P_{cmv} = 93.57\%$, N=2, df=2

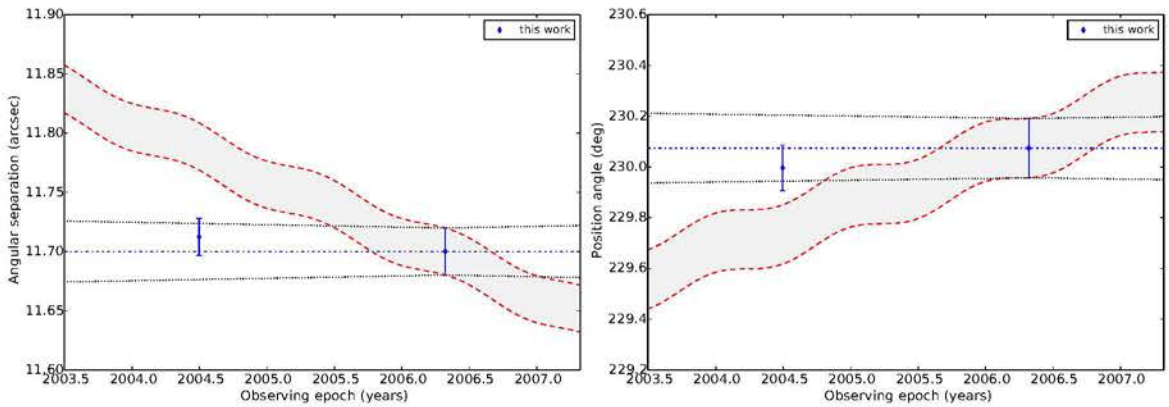

CC2: $P_{bg} = 82.93\%$, $P_{cmv} = 0.35\%$, N=2, df=2

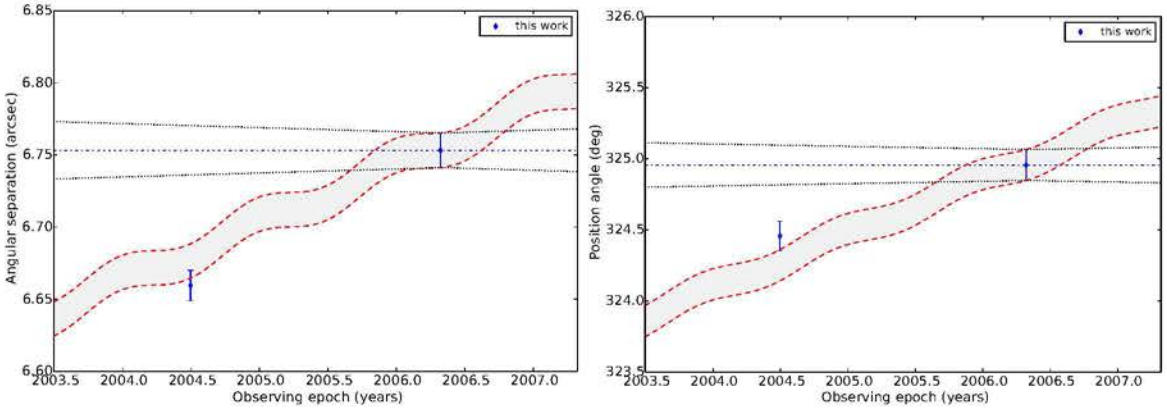


HIP79199

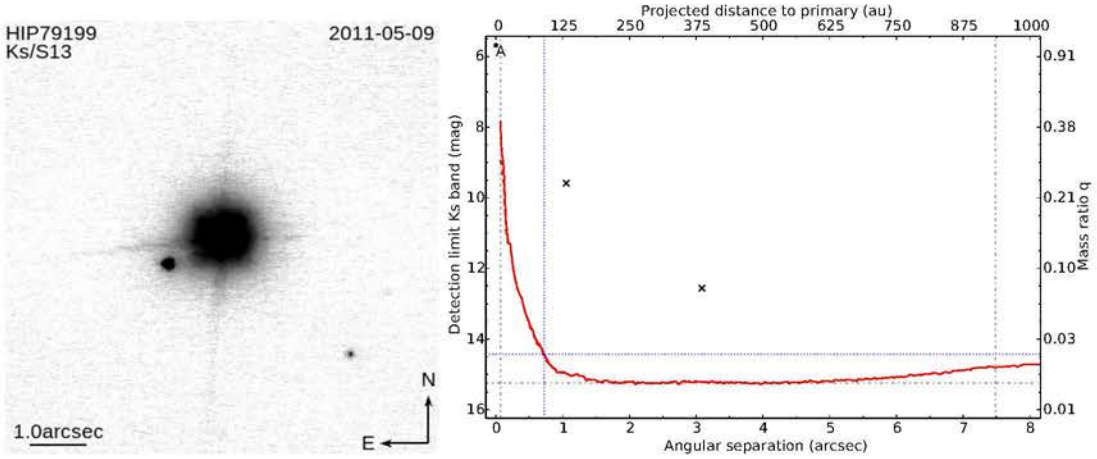


CC1: $P_{bg} = 0.00\%$, $P_{cmv} = 0.00\%$, N=3, df=4

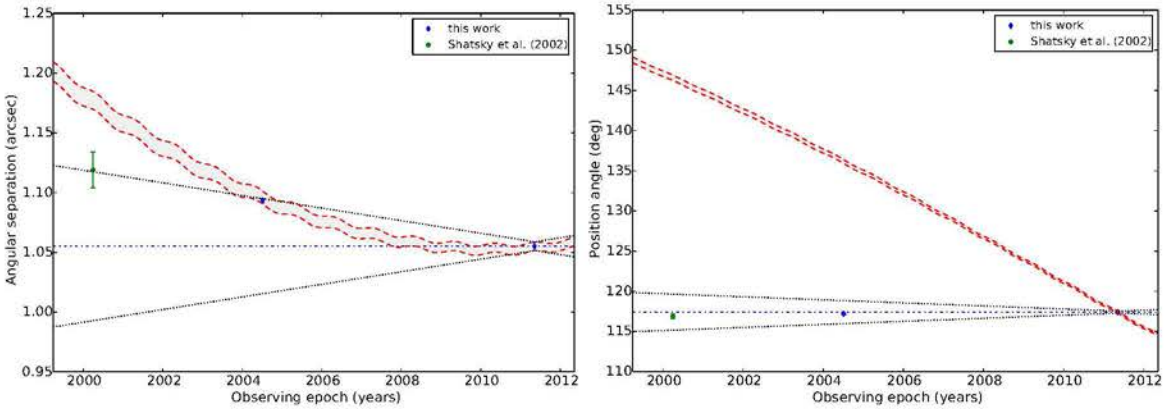


CC2: $P_{bg} = 0.00\%$, $P_{cmv} = 68.54\%$, N=3, df=4

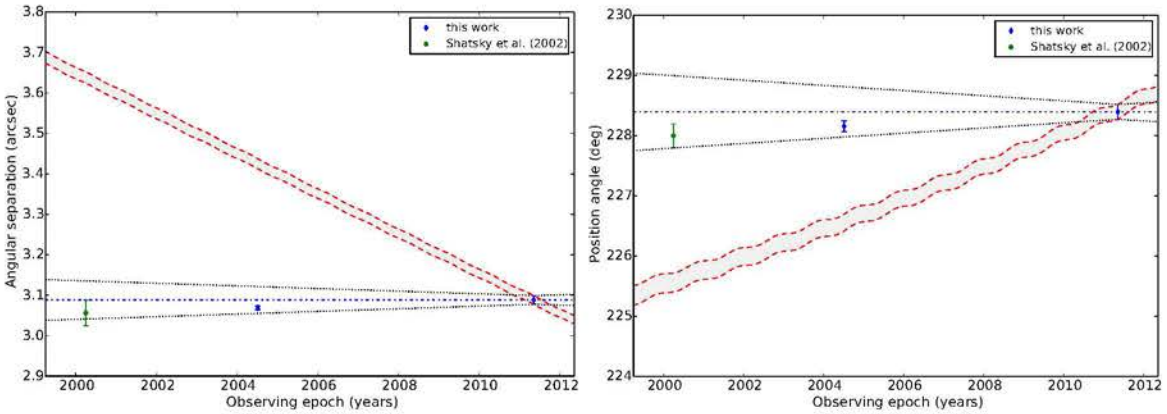

## HIP79230

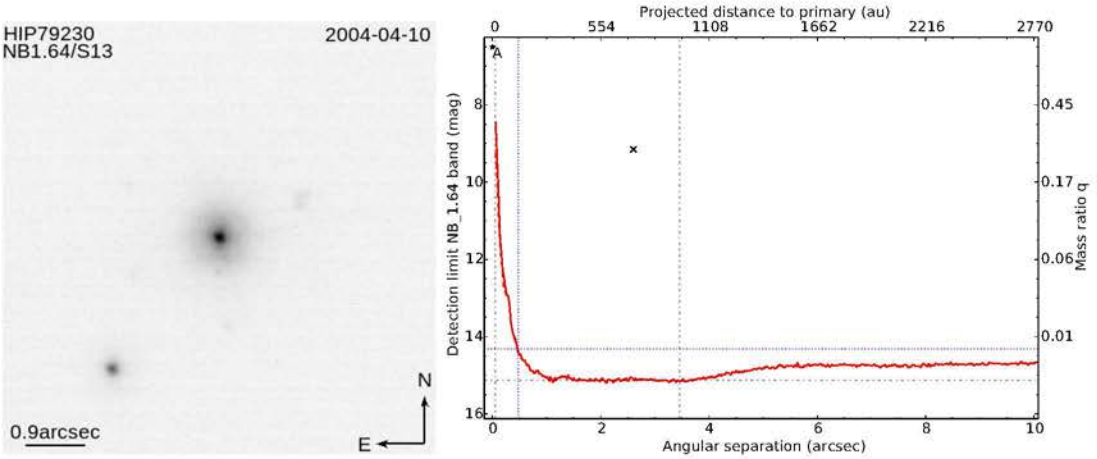


CC1: $P_{bg} = 92.39\%$, $P_{cmv} = 73.20\%$, N=2, df=2

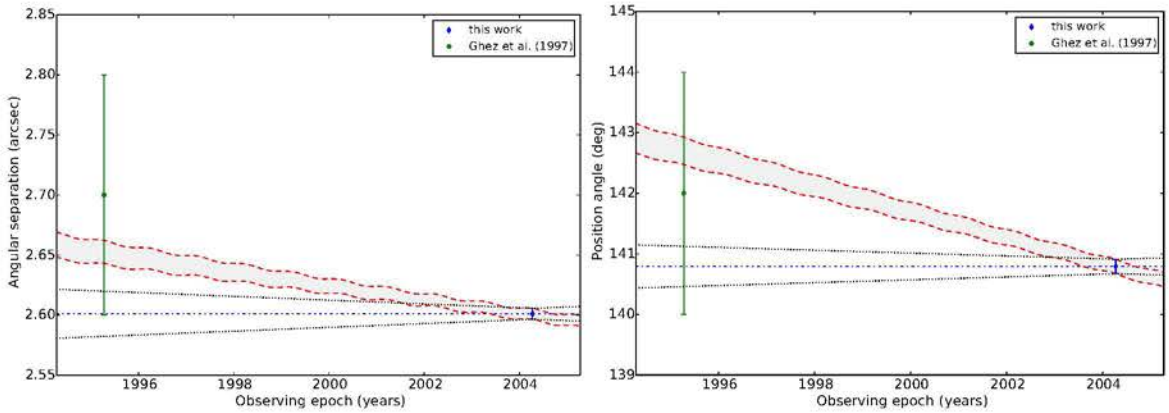


## HIP79399

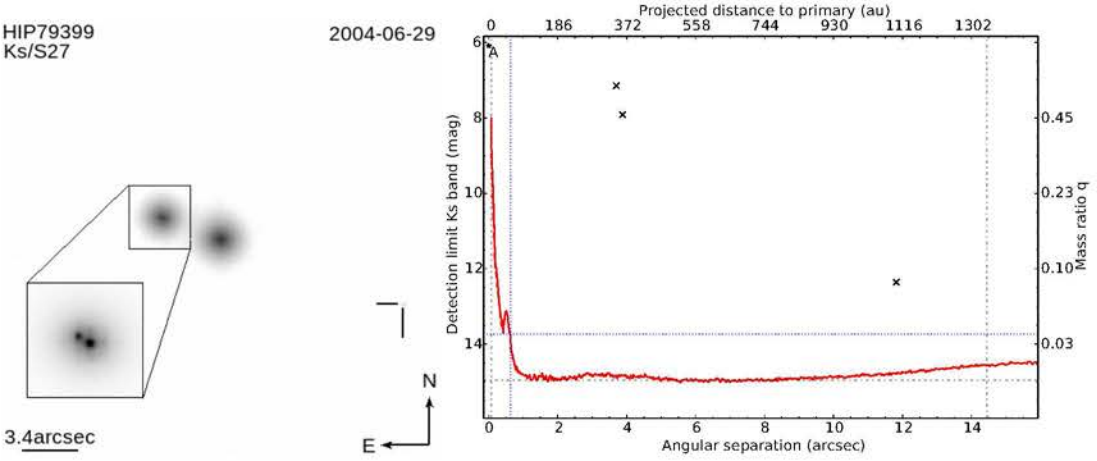


CC1: $P_{bg} = 0.53\%$, $P_{cmv} = 29.76\%$, N=2, df=2

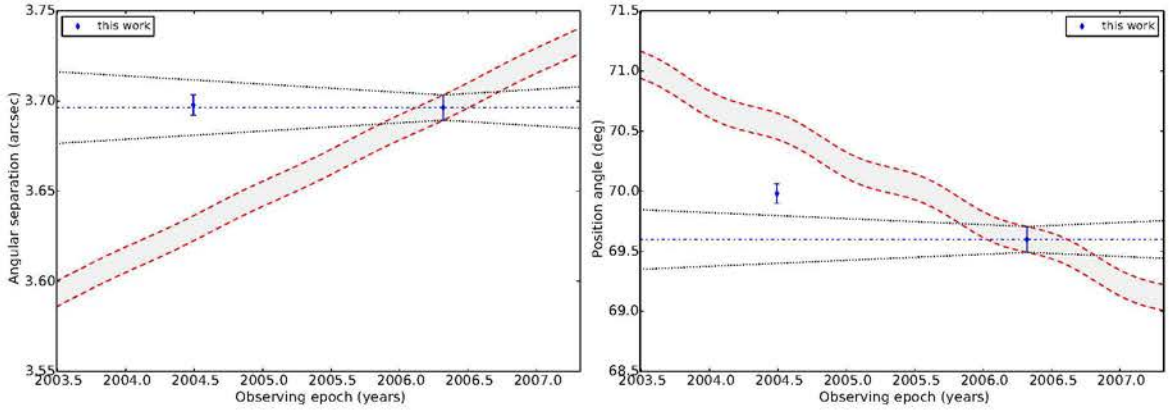

CC2: $P_{bg} = 0.02\%$, $P_{cmv} = 71.96\%$, N=2, df=2

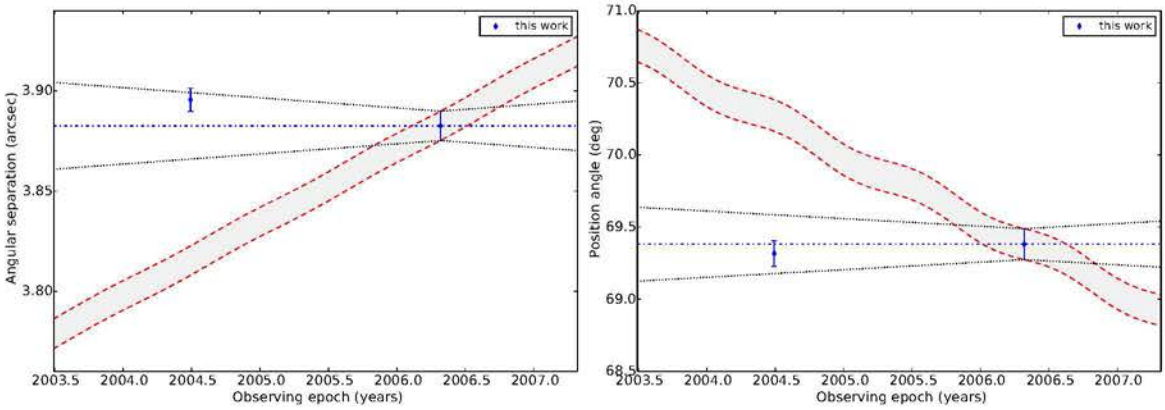


CC3: $P_{bg} = 70.53\%$, $P_{cmv} = 82.53\%$, N=2, df=2

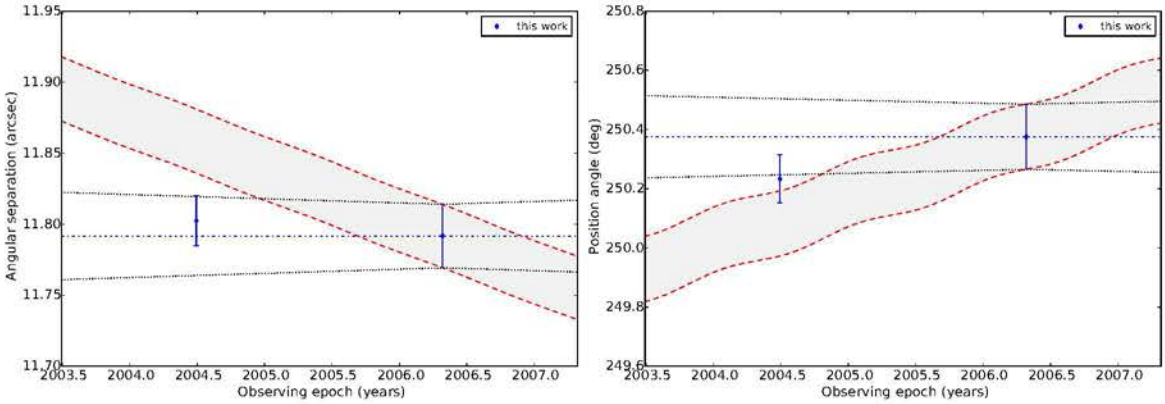


HIP79739

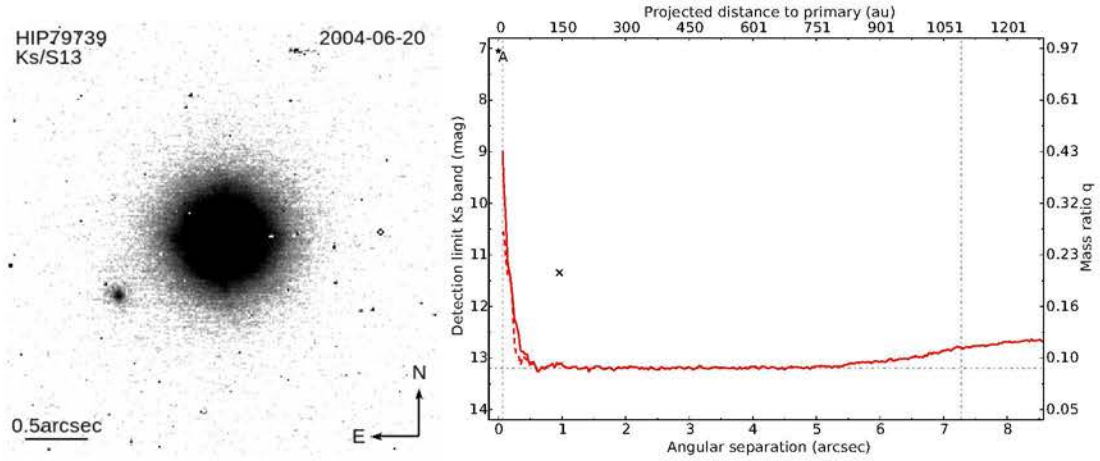


CC1: $P_{bg} = 12.95\%$, $P_{cmv} = 80.62\%$, N=2, df=2

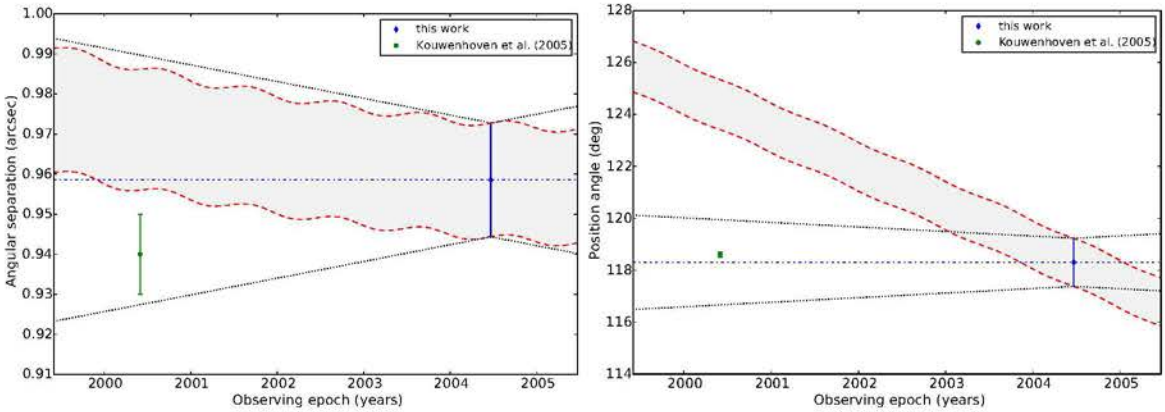

## HIP79771

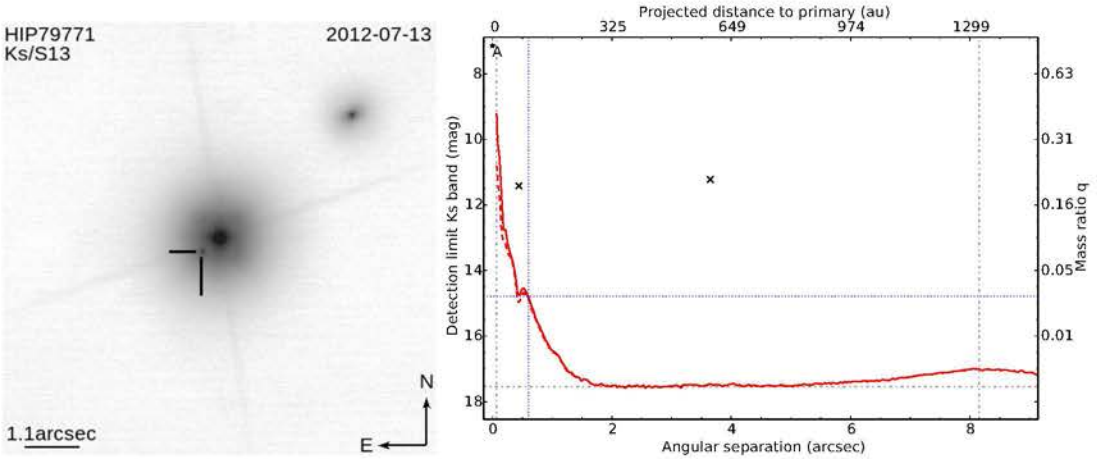


CC1: $P_{bg} = 0.00\%$, $P_{cmv} = 29.41\%$, N=3, df=4

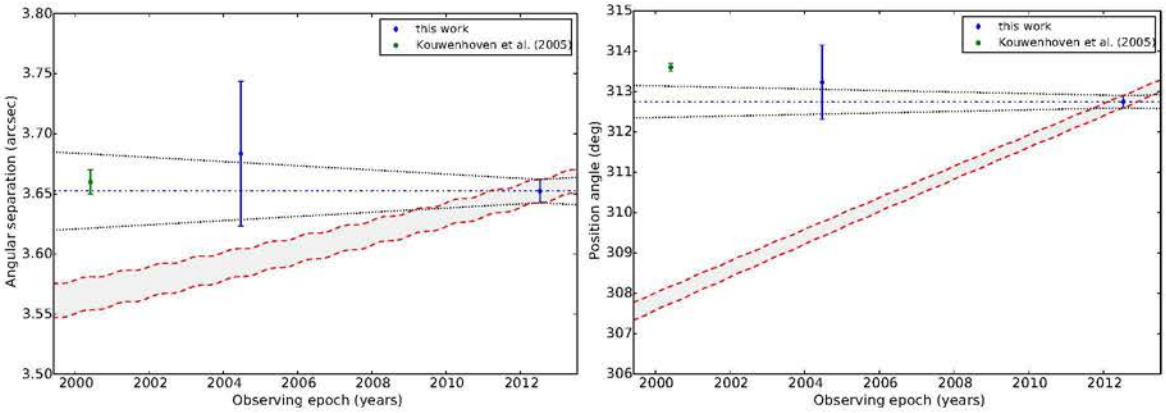


CC2: $P_{bg} = 0.00\%$, $P_{cmv} = 94.60\%$, N=2, df=2

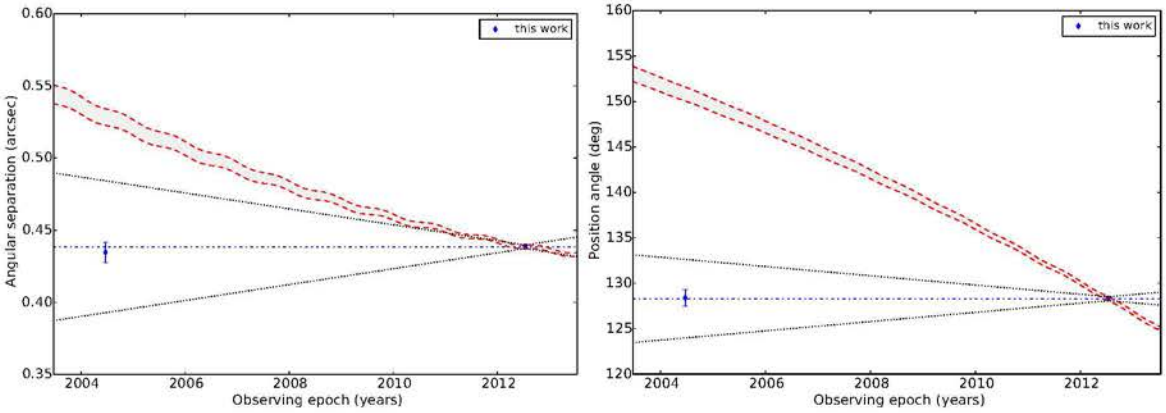


## HIP80142

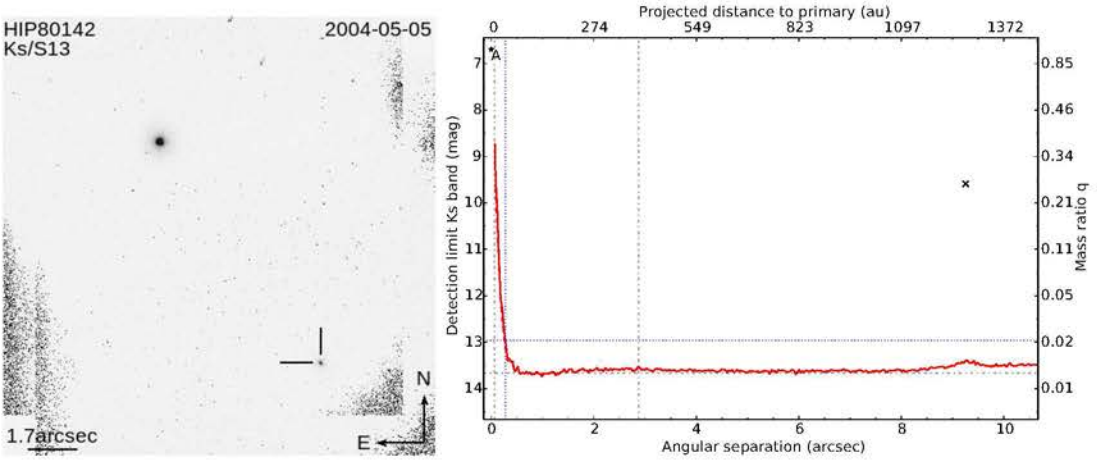

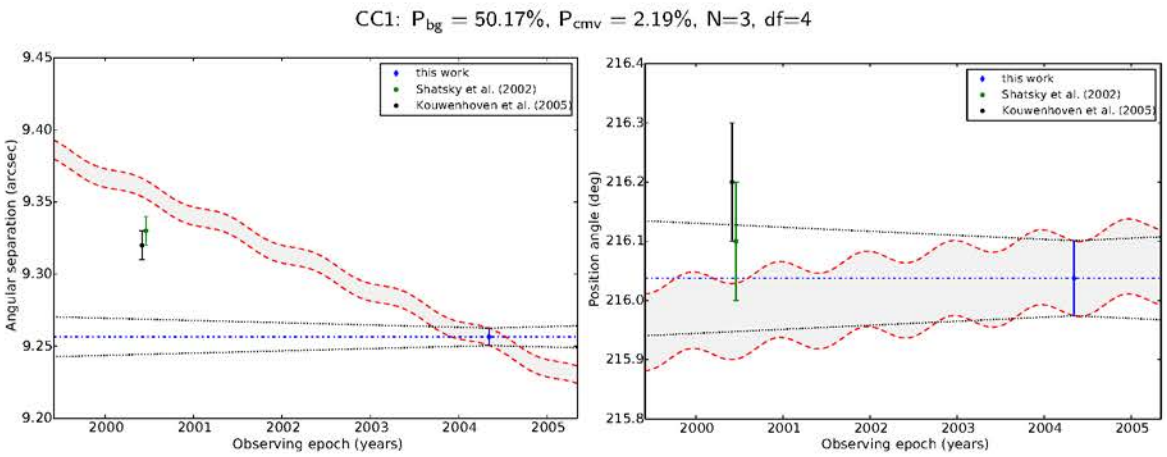


## HIP80461

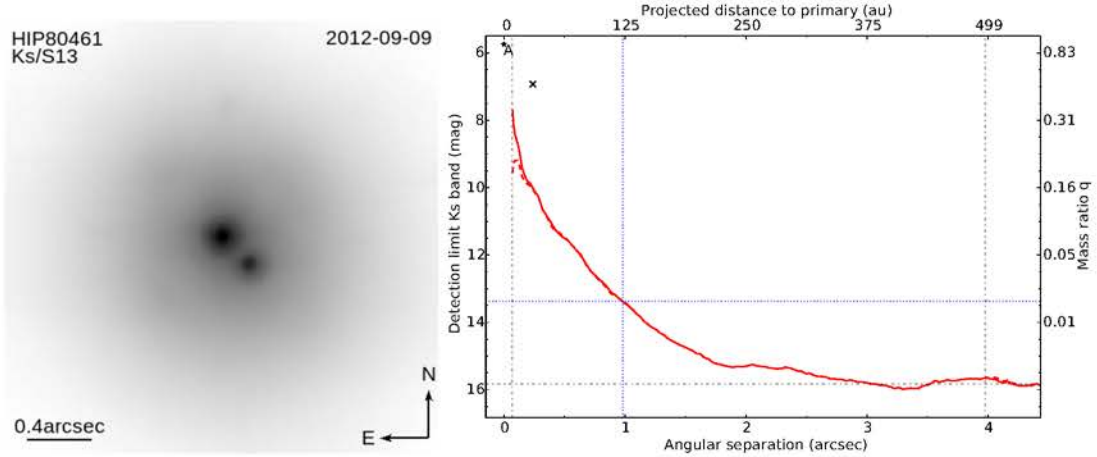


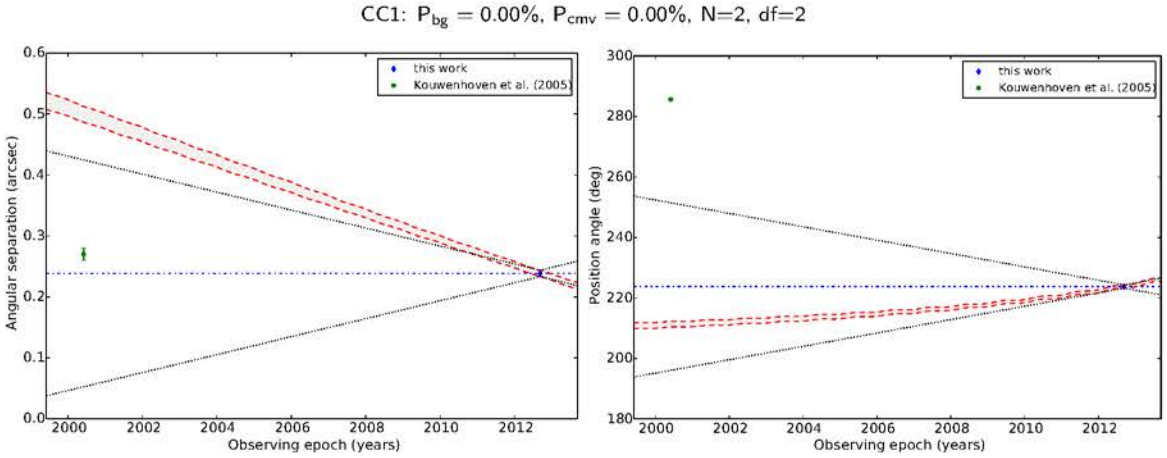


## HIP80473

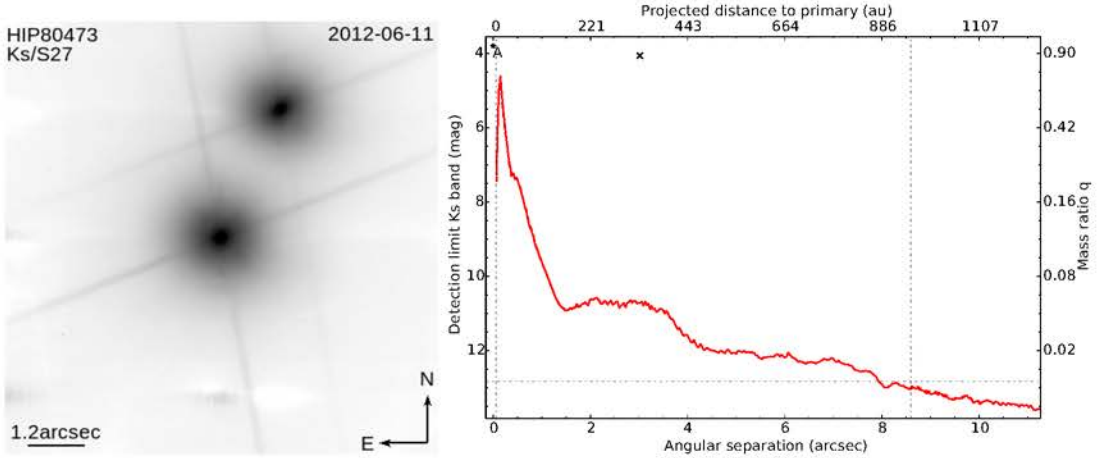

CC1: $P_{bg} = 0.00\%$, $P_{cmv} = 0.00\%$, N=5, df=8

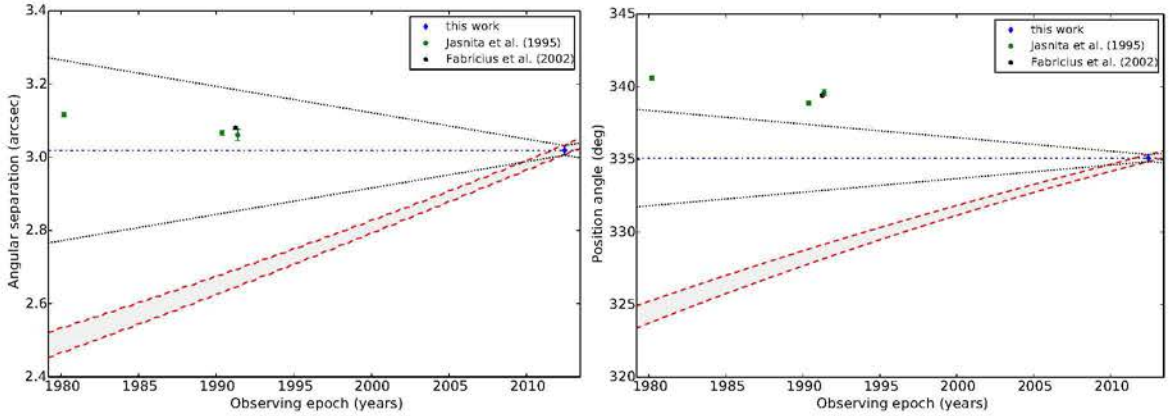


## HIP80474

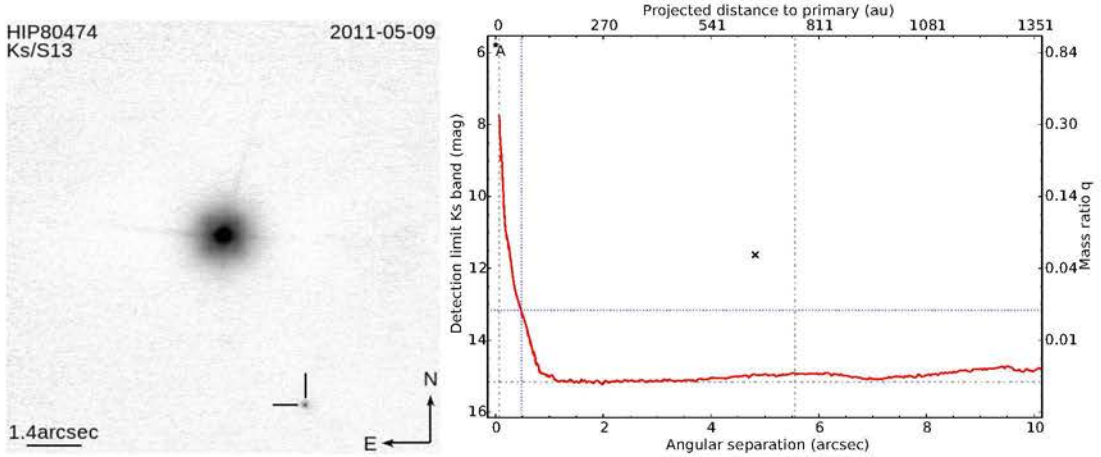


CC1: $P_{bg} = 0.00\%$, $P_{cmv} = 87.03\%$, N=3, df=4

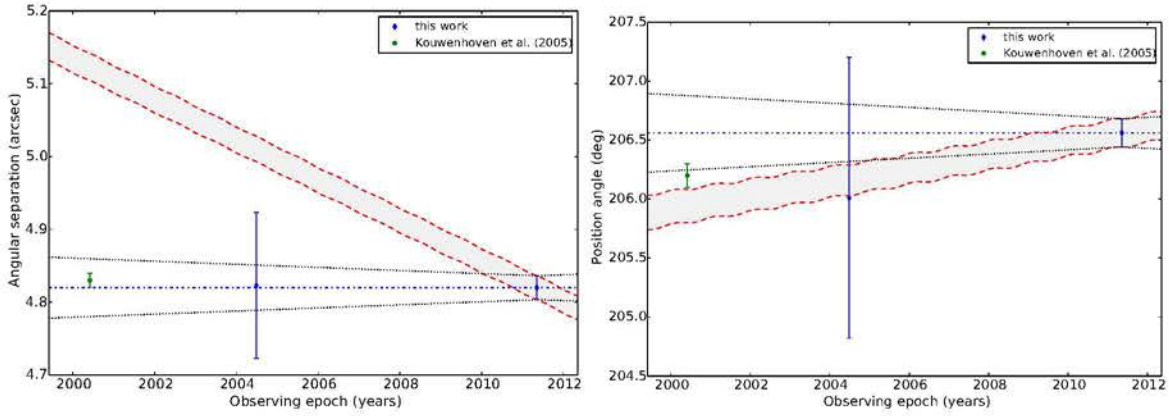


## HIP81472

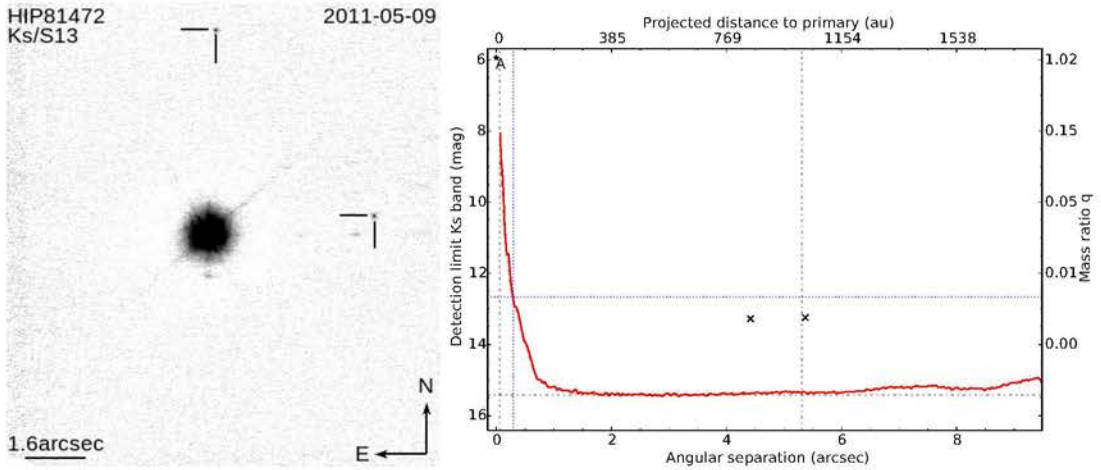

CC1: $P_{bg}$ = 97.47%, $P_{cmv}$ = 0.00%, N=4, df=6

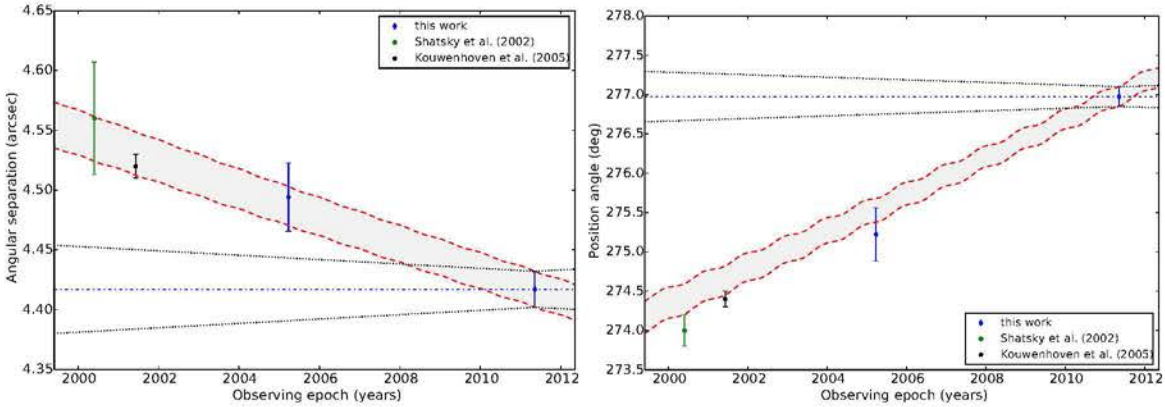


CC2: $P_{bg}$ = 23.19%, $P_{cmv}$ = 0.00%, N=4, df=6

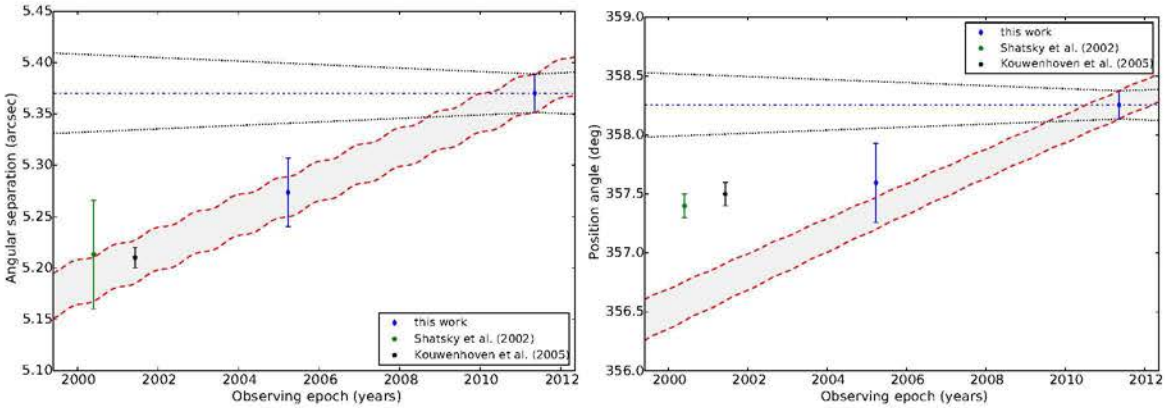


HIP81972

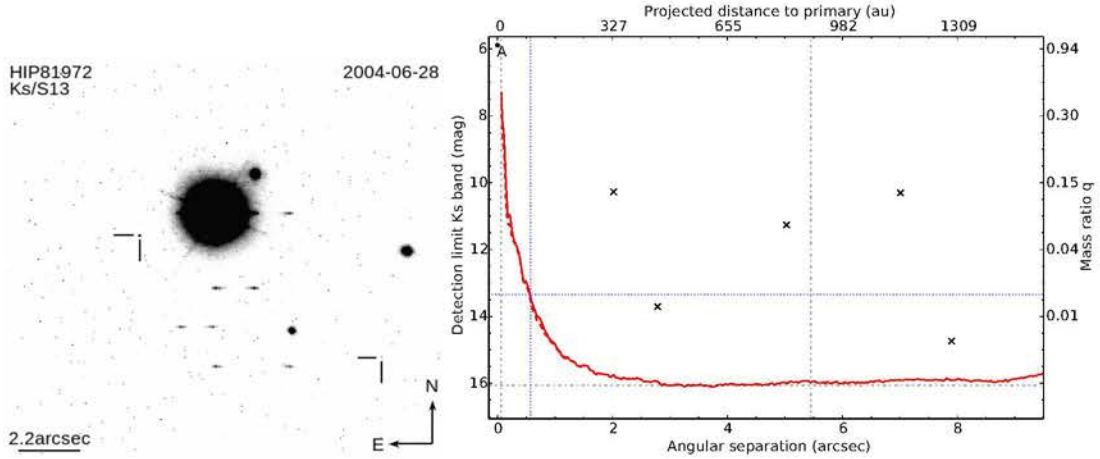


CC1: $P_{bg}$ = 91.92%, $P_{cmv}$ = 49.40%, N=2, df=2

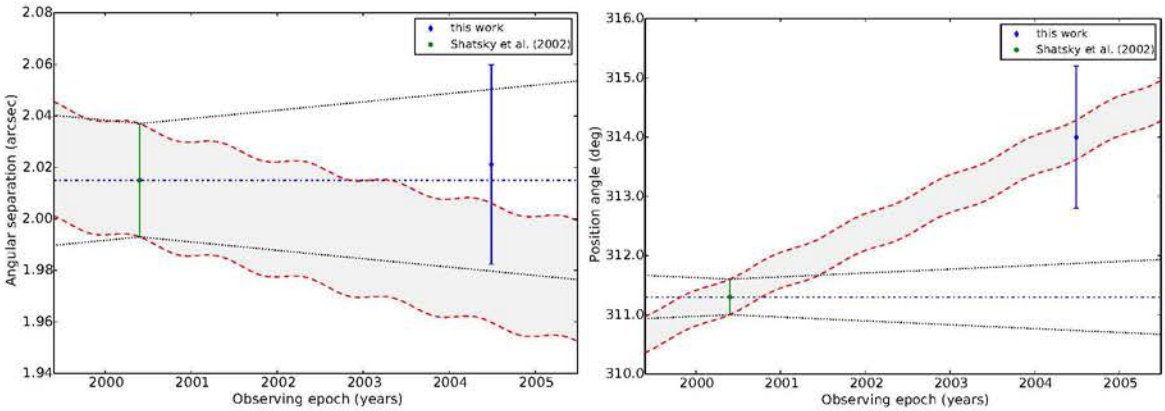

CC2: $P_{bg} = 94.97\%$, $P_{cmv} = 79.90\%$, N=2, df=2

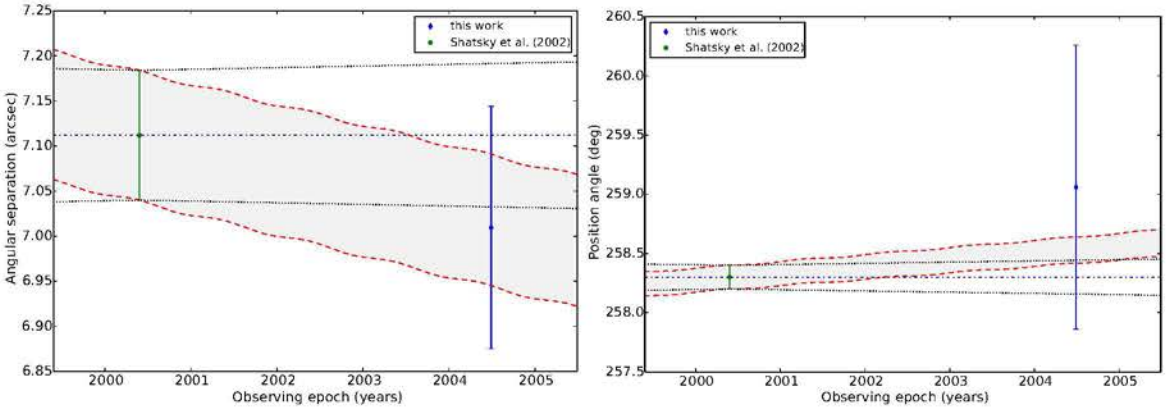


CC3: $P_{bg} = 95.17\%$, $P_{cmv} = 98.47\%$, N=2, df=2

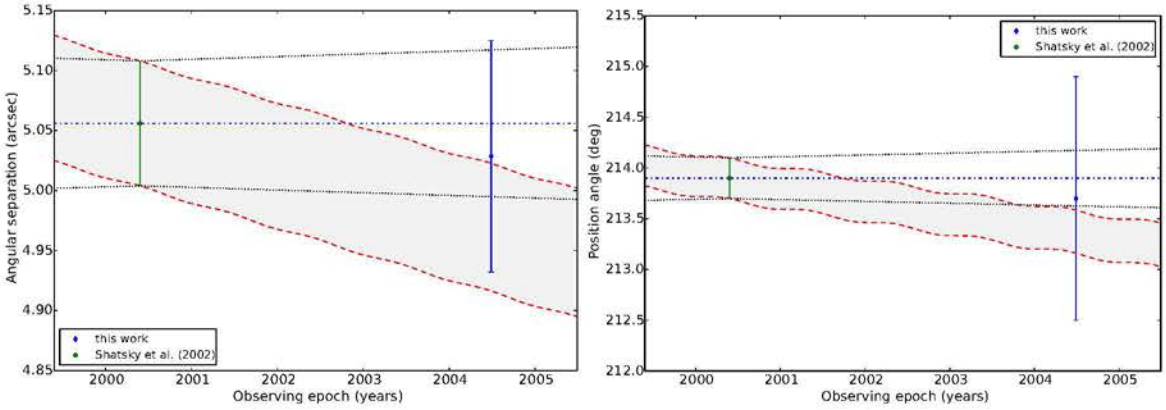


CC4: $P_{bg} = 87.42\%$, $P_{cmv} = 51.14\%$, N=2, df=2

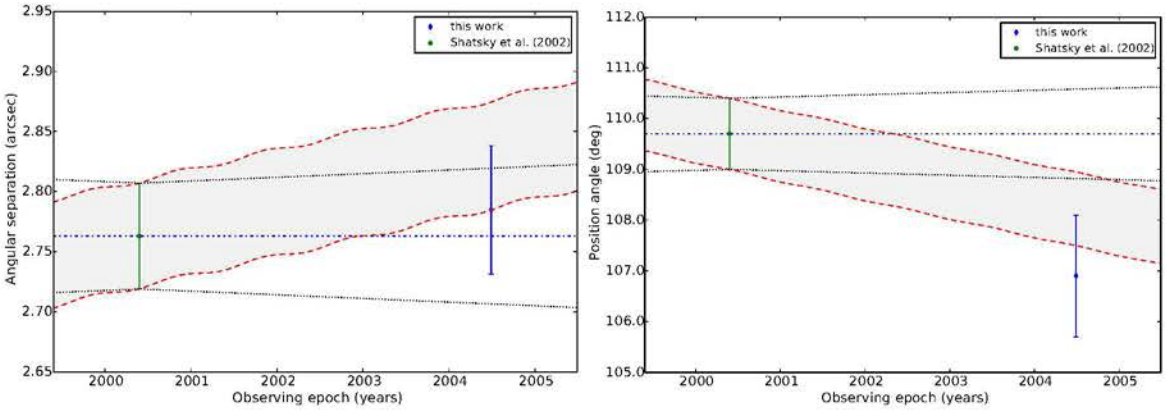


HIP82902

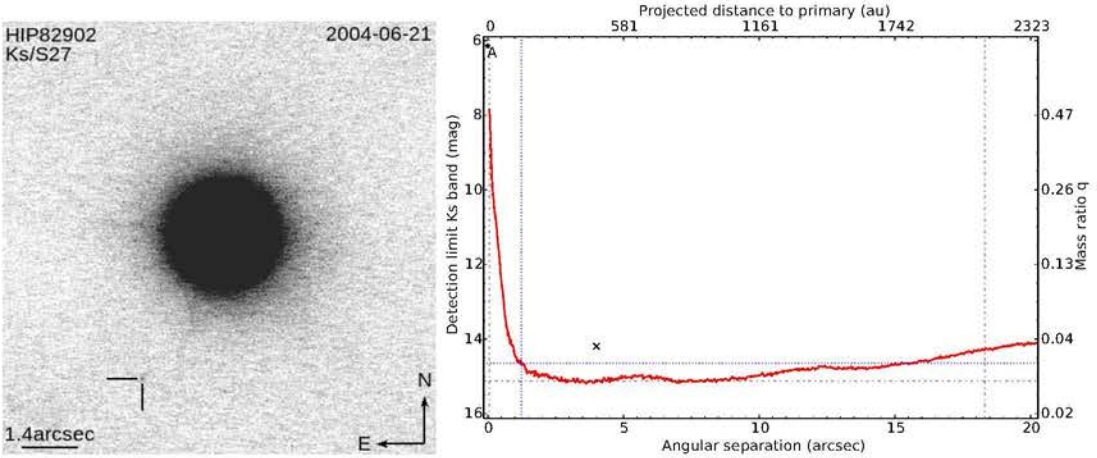

CC1: $P_{bg} = 95.98\%$, $P_{cmv} = 0.18\%$, N=2, df=2

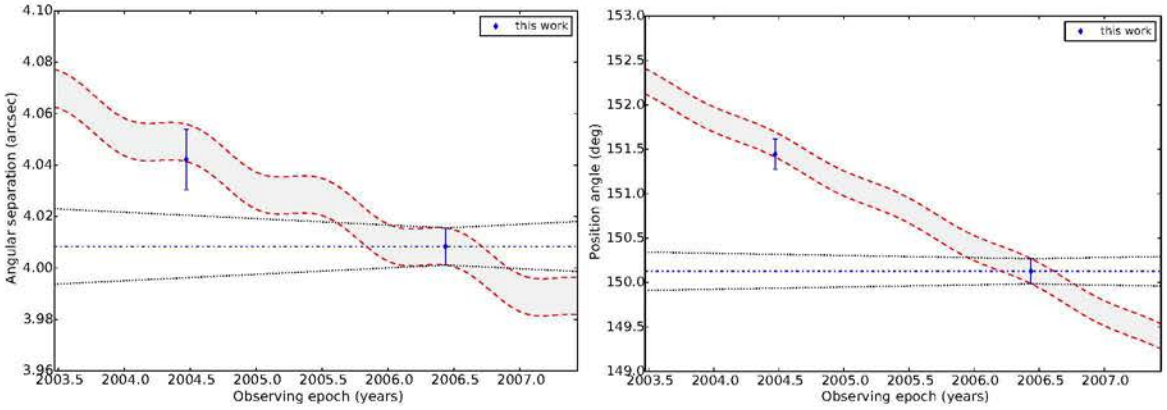


HIP83336

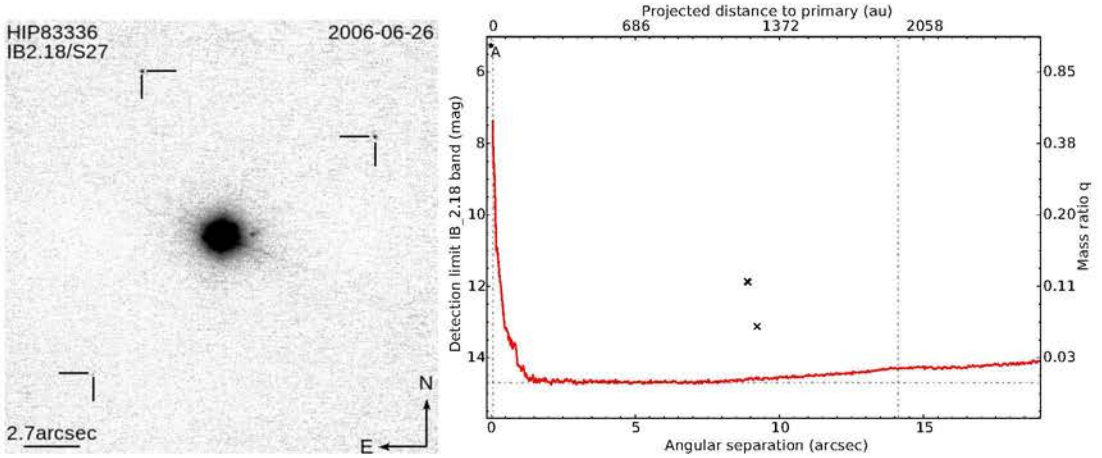


CC1: $P_{bg} = 32.39\%$, $P_{cmv} = 96.98\%$, N=2, df=2

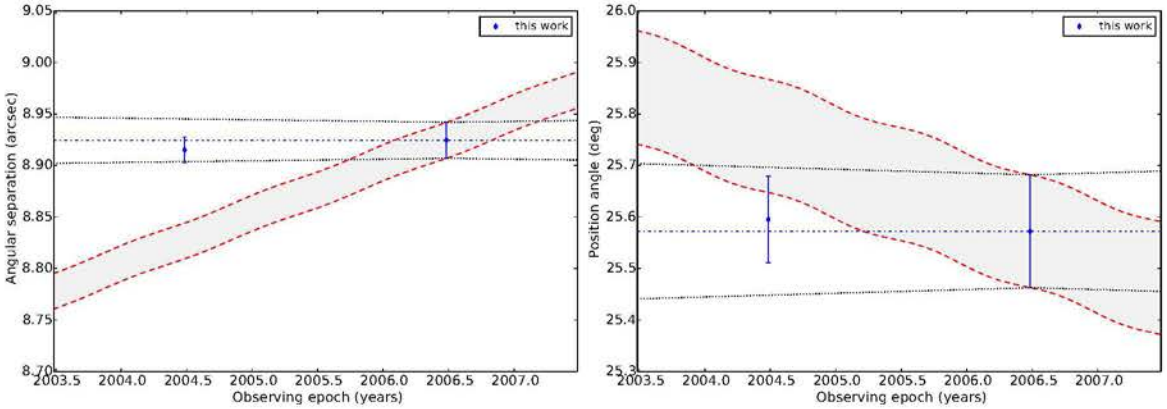


CC2: $P_{bg} = 97.35\%$, $P_{cmv} = 5.91\%$, N=2, df=2

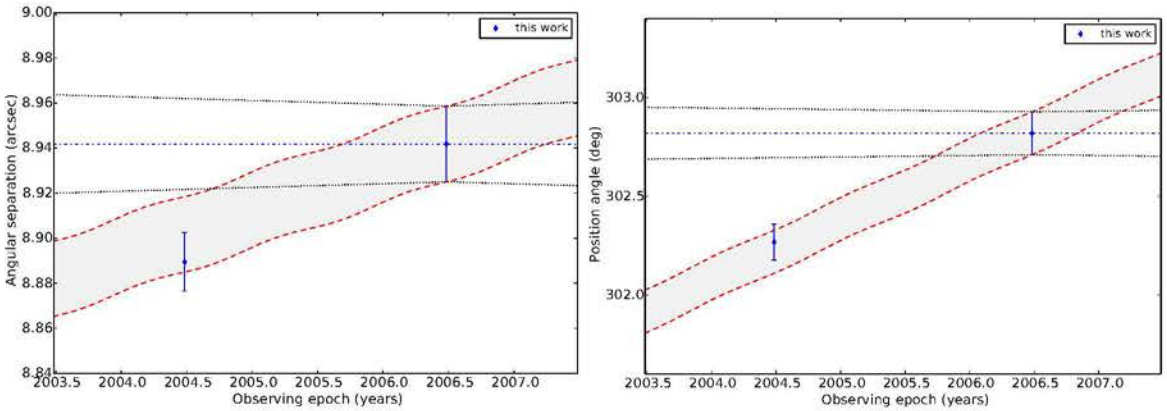

CC3: $P_{bg} = 93.53\%$, $P_{cmv} = 16.36\%$, N=2, df=2

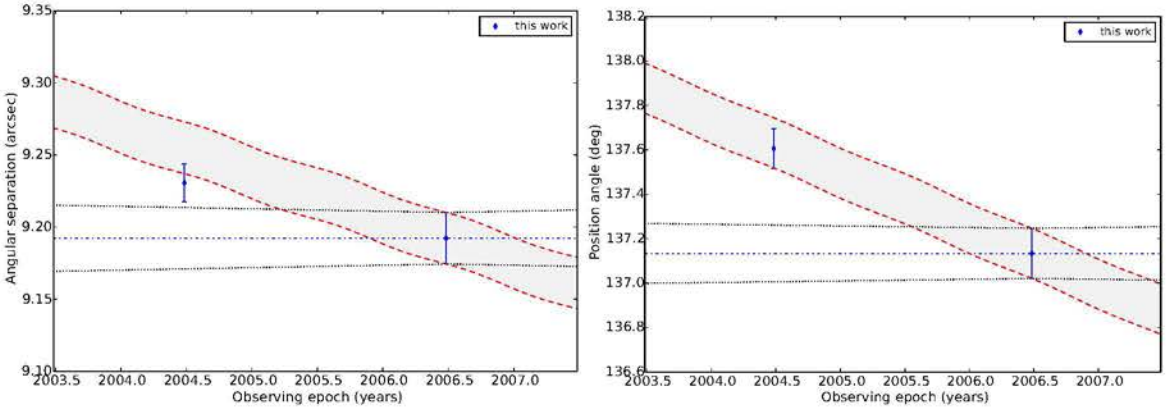


HIP85442

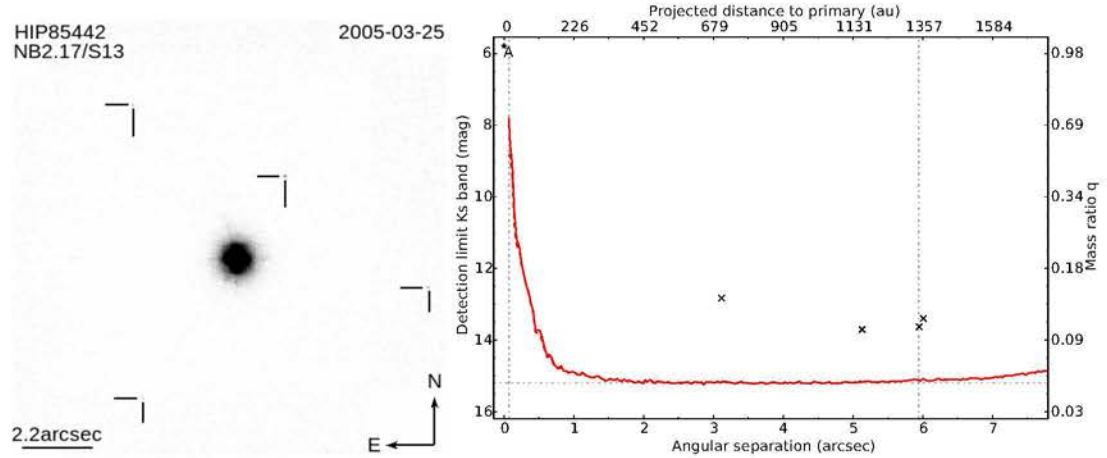


CC1: $P_{bg} = 43.59\%$, $P_{cmv} = 0.00\%$, N=2, df=2

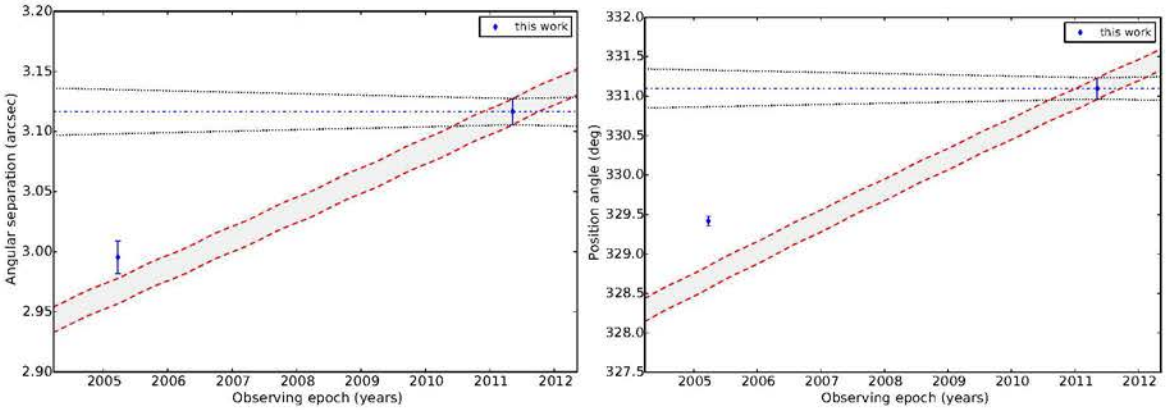


CC2: $P_{bg} = 77.14\%$, $P_{cmv} = 0.00\%$, N=2, df=2

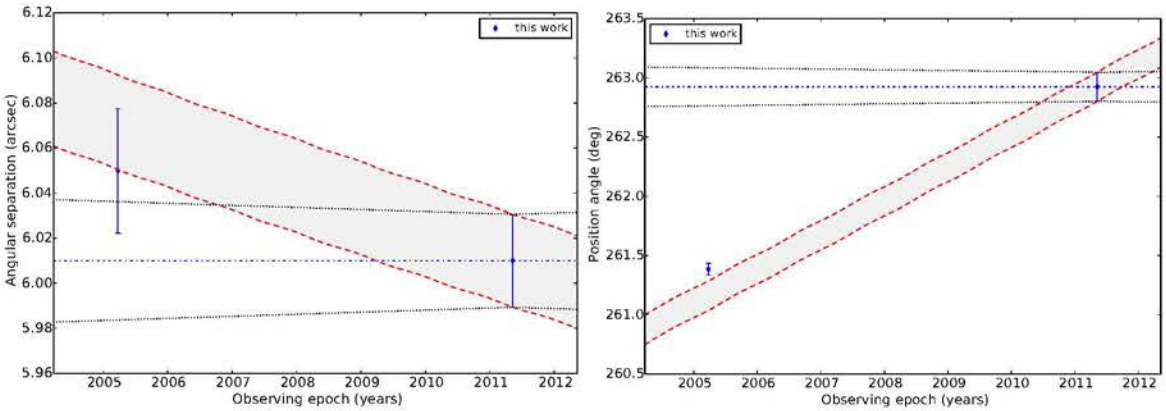

CC3: $P_{bg} = 95.25\%$, $P_{cmv} = 0.12\%$, N=2, df=2

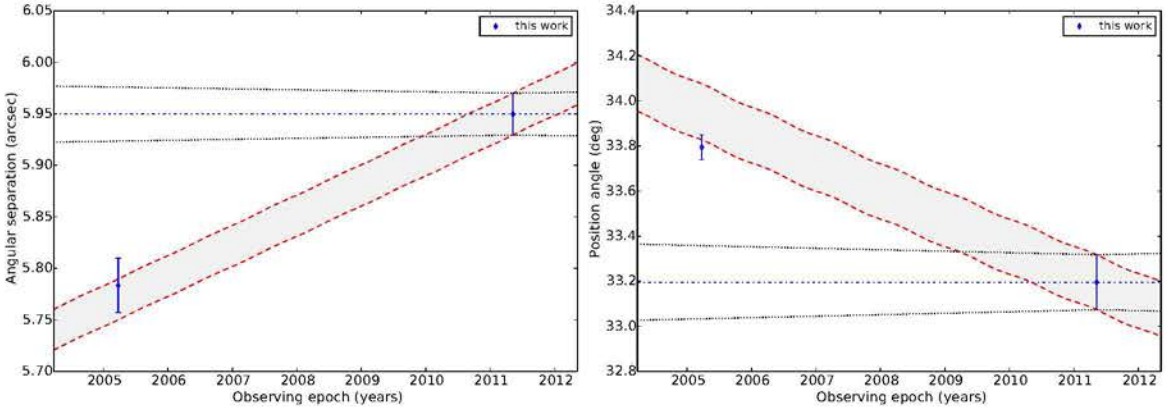


CC4: $P_{bg} = 61.20\%$, $P_{cmv} = 0.97\%$, N=2, df=2

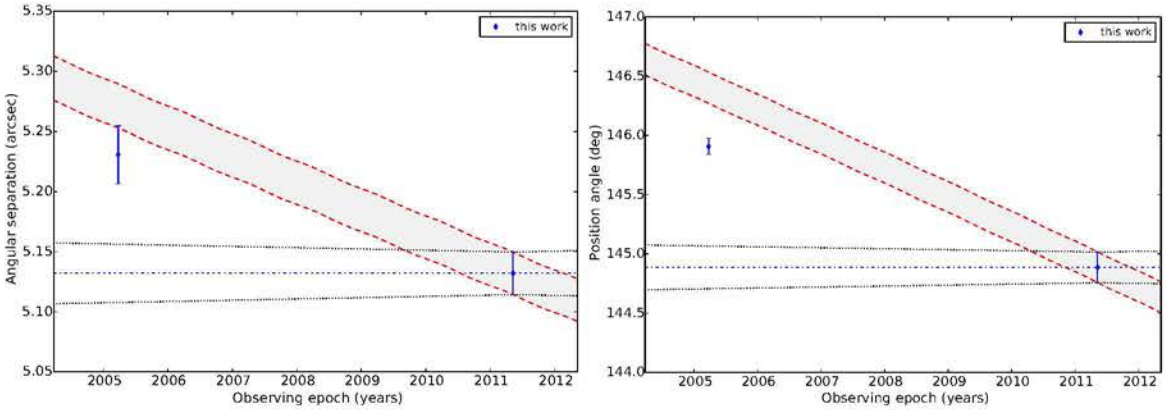


HIP85727

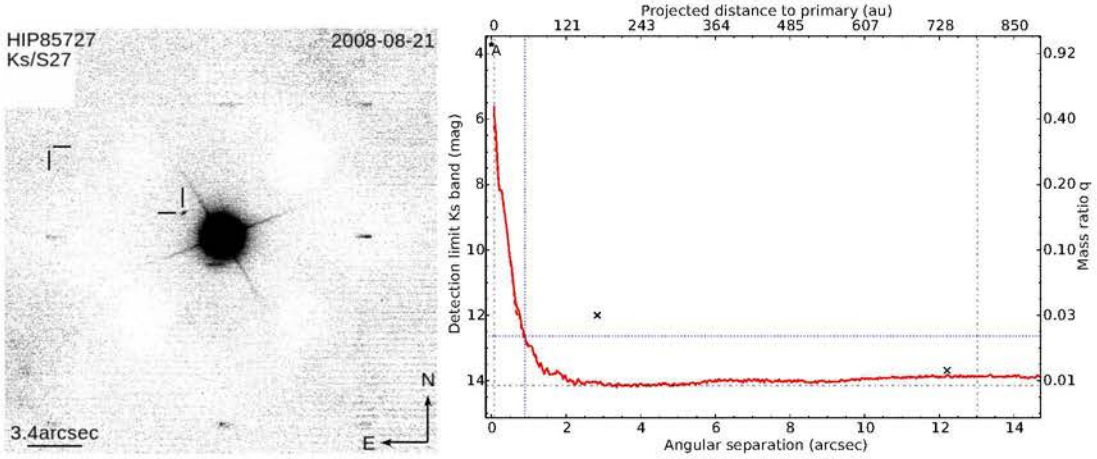


CC1: $P_{bg} = 0.00\%$, $P_{cmv} = 0.00\%$, N=2, df=2

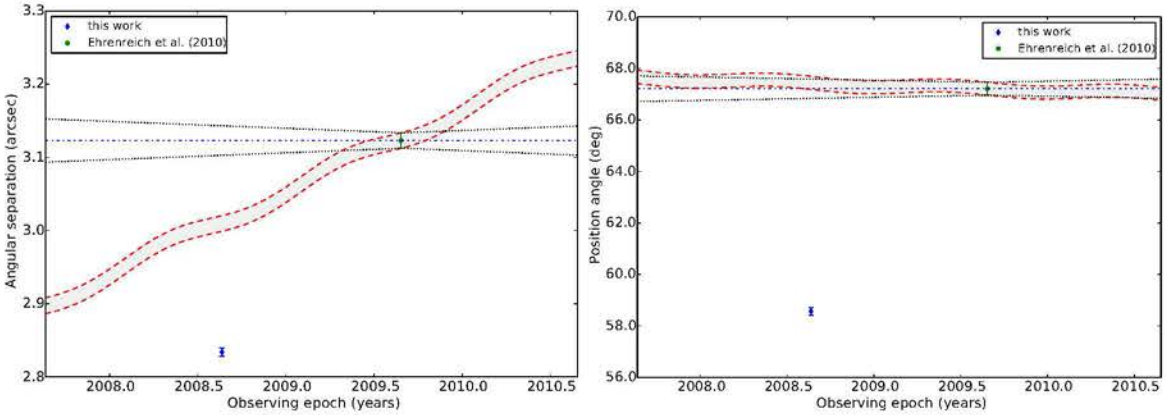

CC2: $P_{bg} = 5.26\%$, $P_{cmv} = 0.05\%$, N=2, df=2

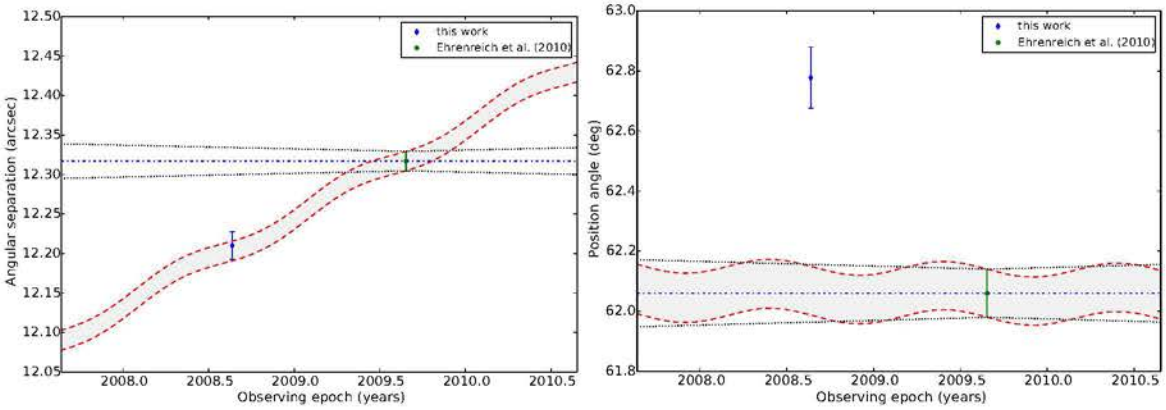


HIP85783

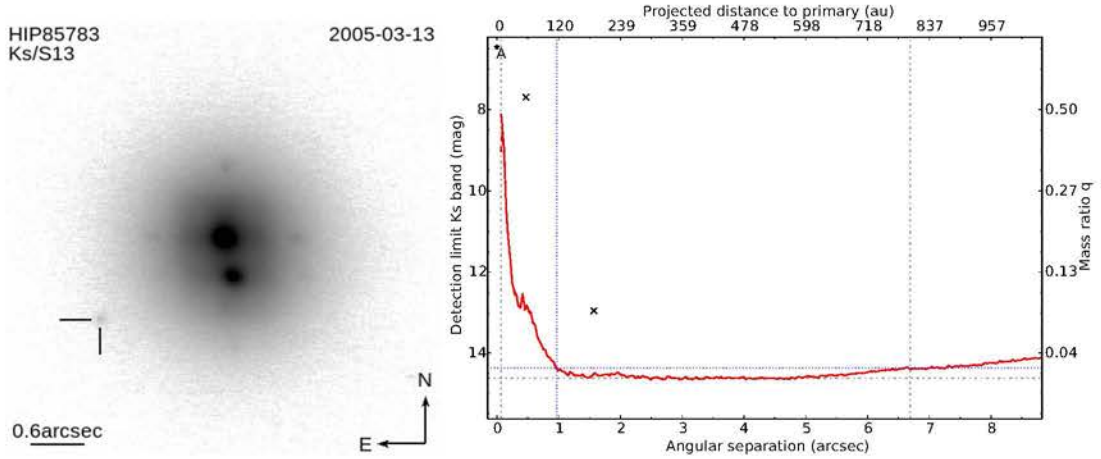


CC1: $P_{bg} = 0.00\%$, $P_{cmv} = 0.00\%$, N=3, df=4

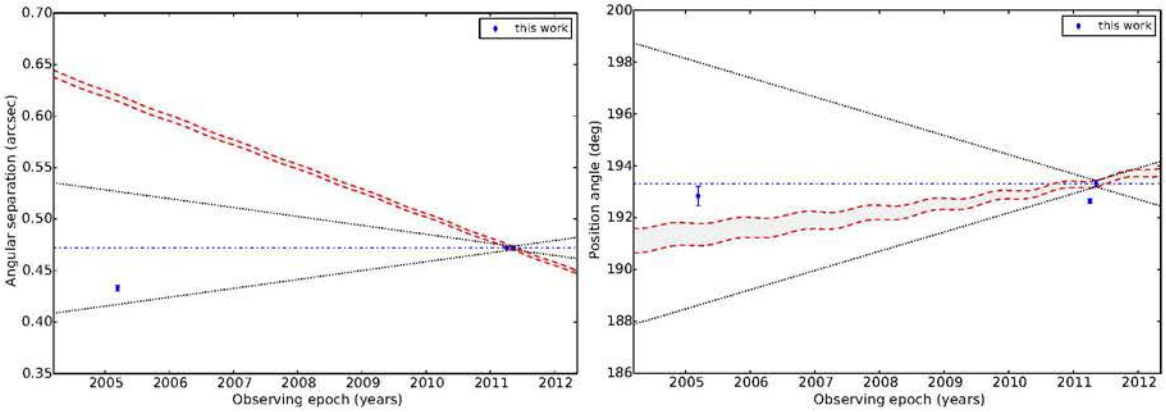


CC2: $P_{bg} = 87.20\%$, $P_{cmv} = 0.00\%$, N=3, df=4

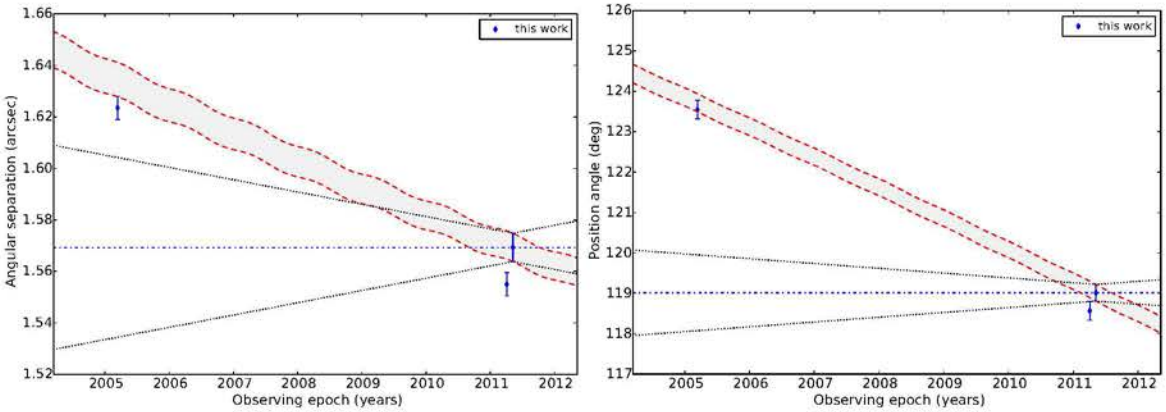

HIP87163

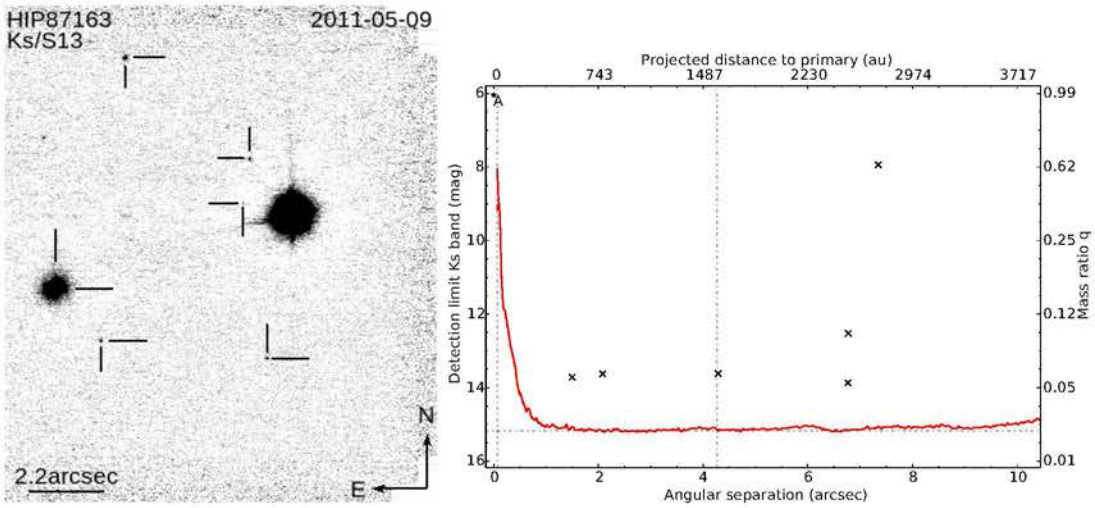


CC1: $P_{bg} = 62.86\%$, $P_{cmv} = 77.41\%$, N=2, df=2

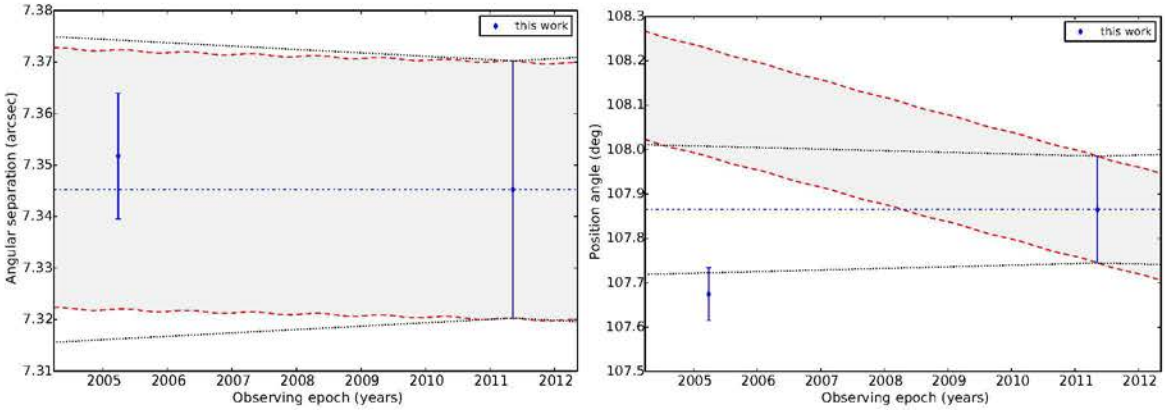


CC2: $P_{bg} = 92.87\%$, $P_{cmv} = 89.74\%$, N=2, df=2

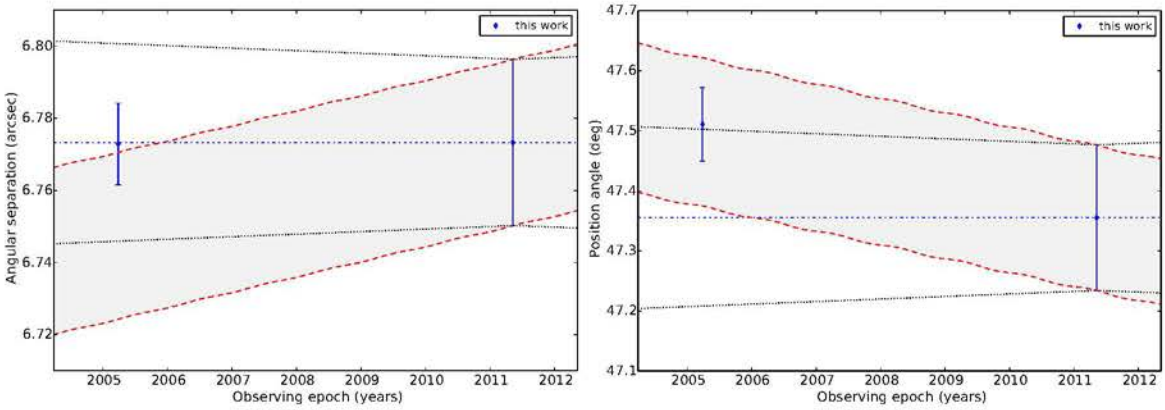


CC3: $P_{bg} = 9.51\%$, $P_{cmv} = 34.82\%$, N=2, df=2

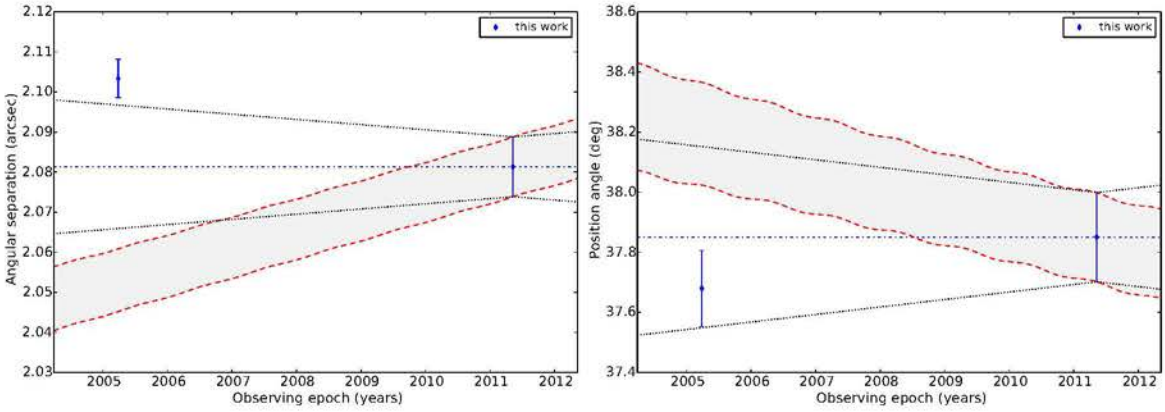

CC4: $P_{bg}$ = 66.82%, $P_{cmv}$ = 97.48%, N=2, df=2

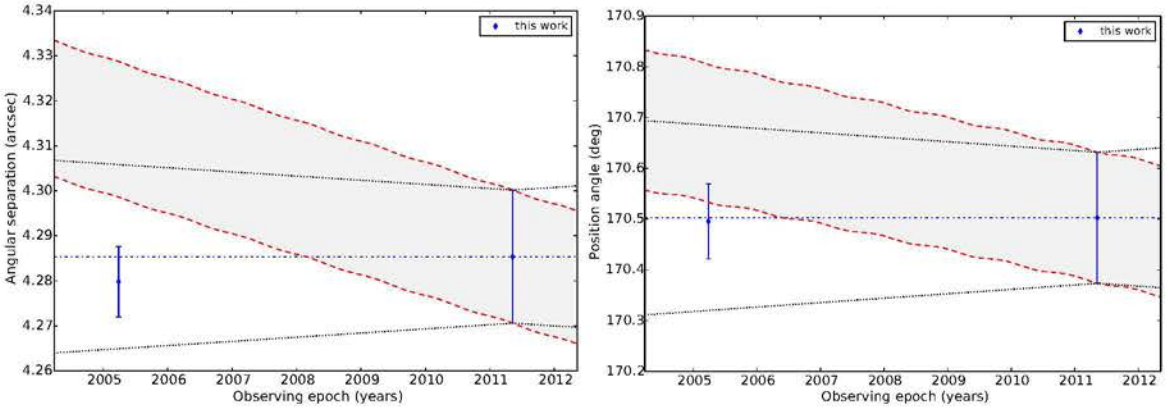


CC5: $P_{bg}$ = 55.16%, $P_{cmv}$ = 57.21%, N=2, df=2

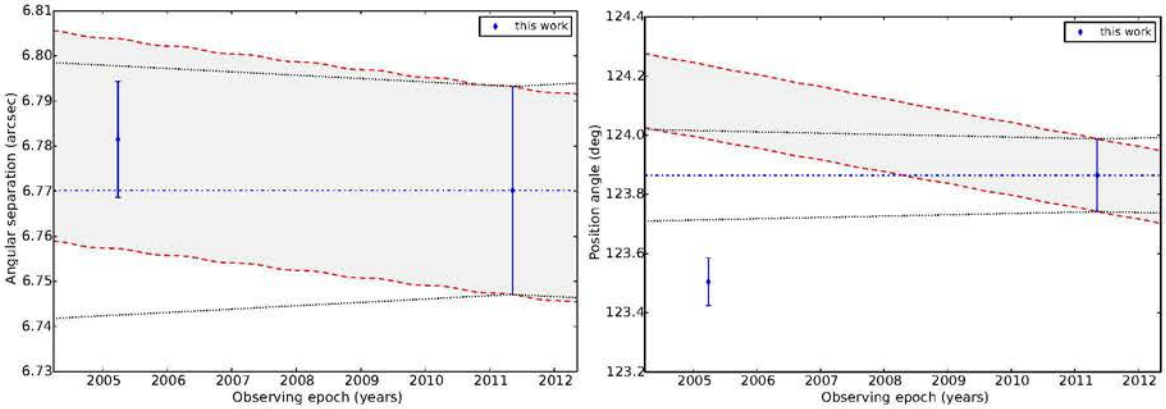


CC6: $P_{bg}$ = 9.85%, $P_{cmv}$ = 45.60%, N=2, df=2

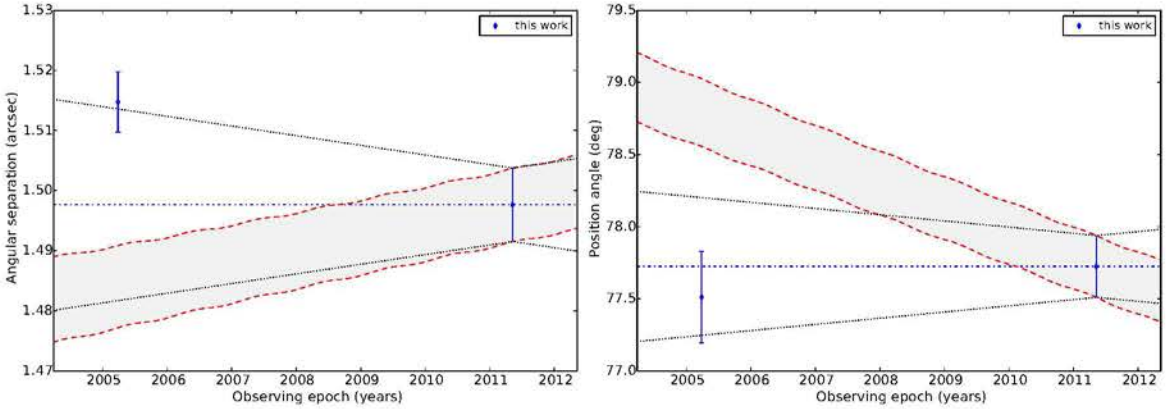


HIP87220

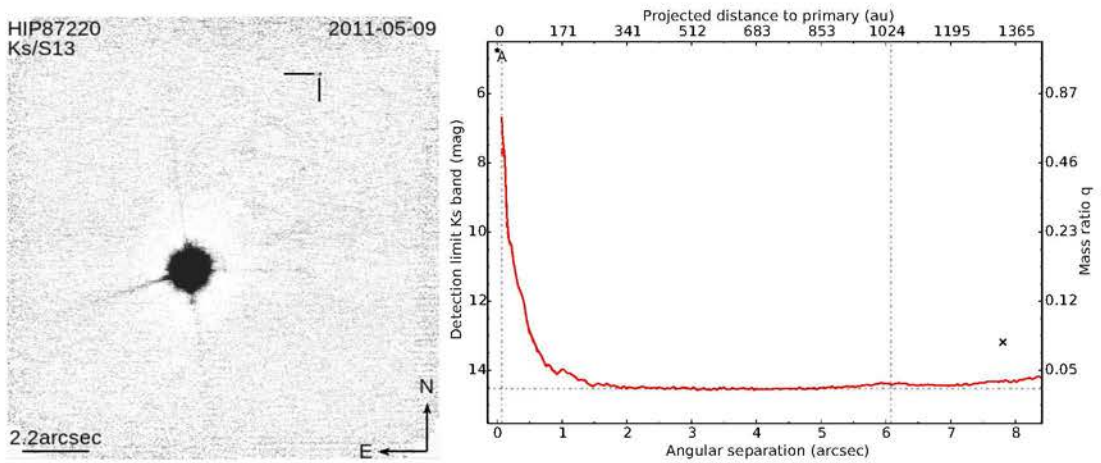

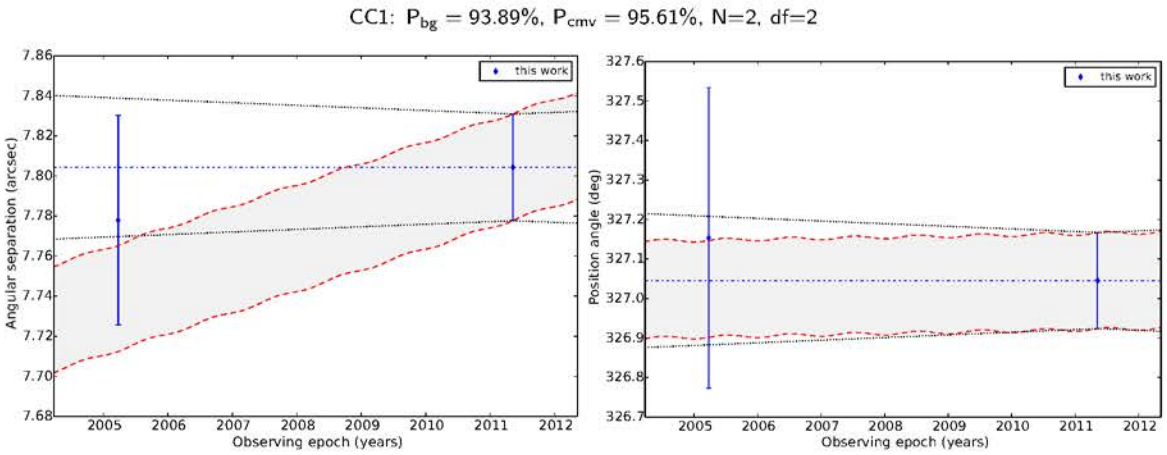


## HIP88149

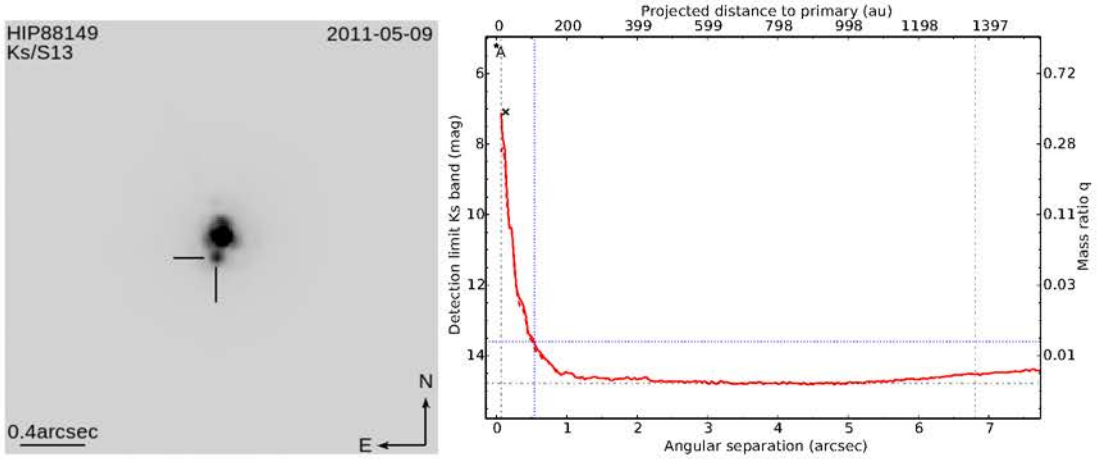


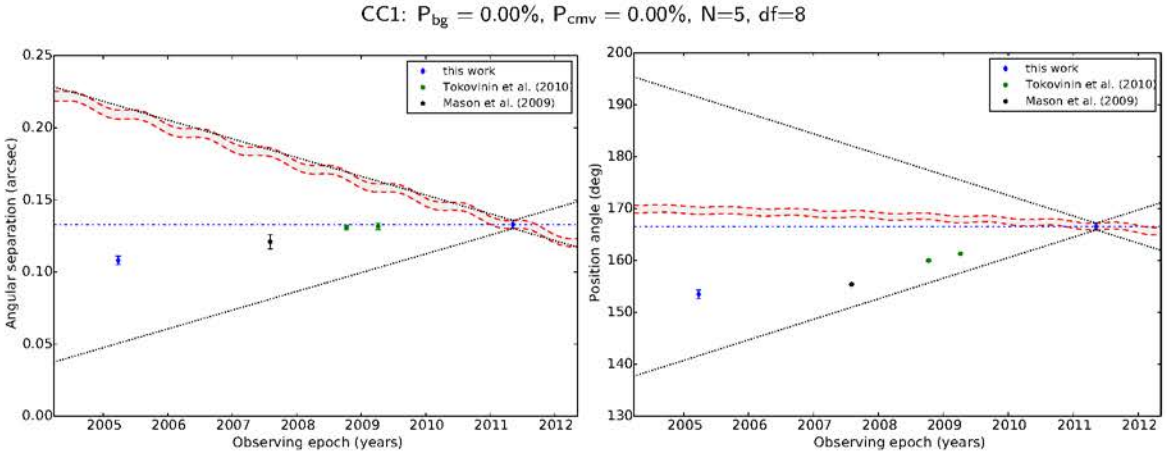


## HIP88859

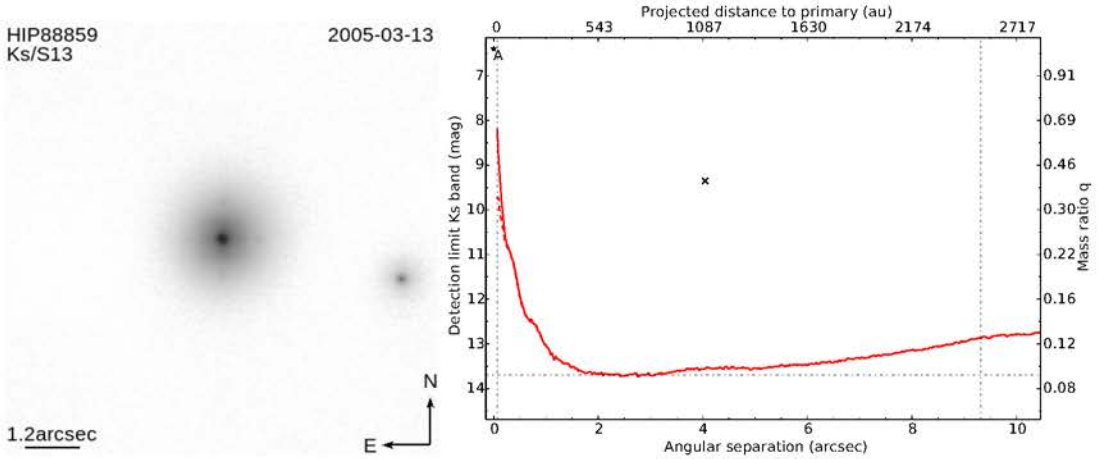

CC1: $P_{bg} = 0.00\%$, $P_{cmv} = 90.23\%$, N=2, df=2

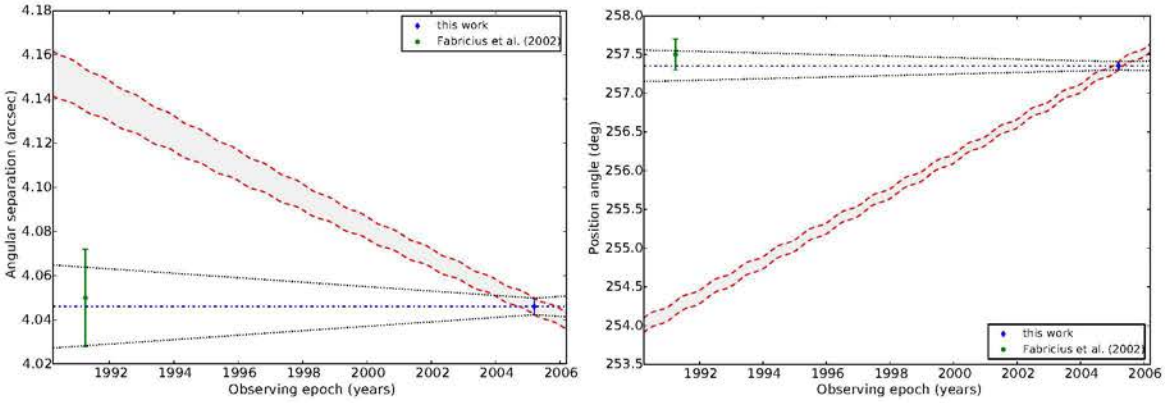


HIP89684

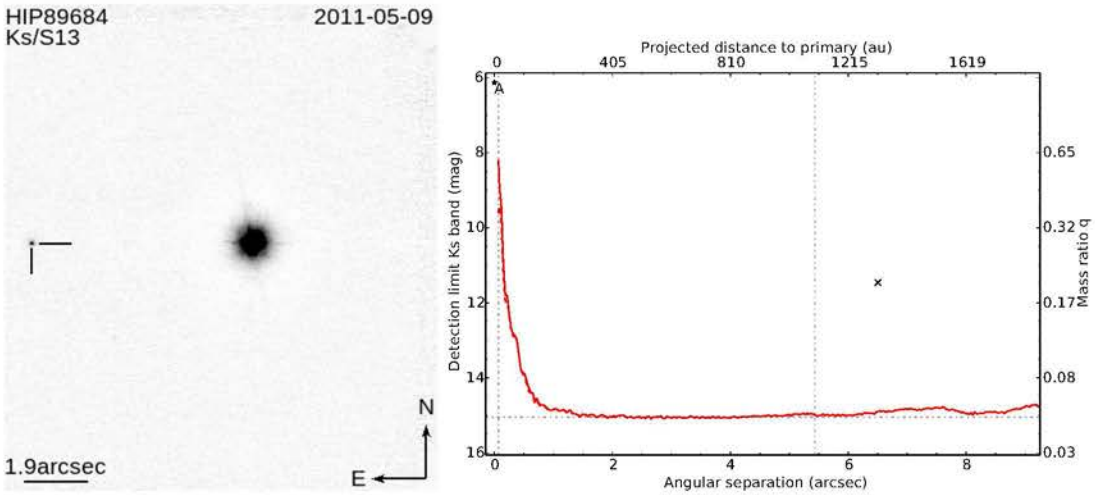


CC1: $P_{bg} = 95.69\%$, $P_{cmv} = 66.57\%$, N=2, df=2

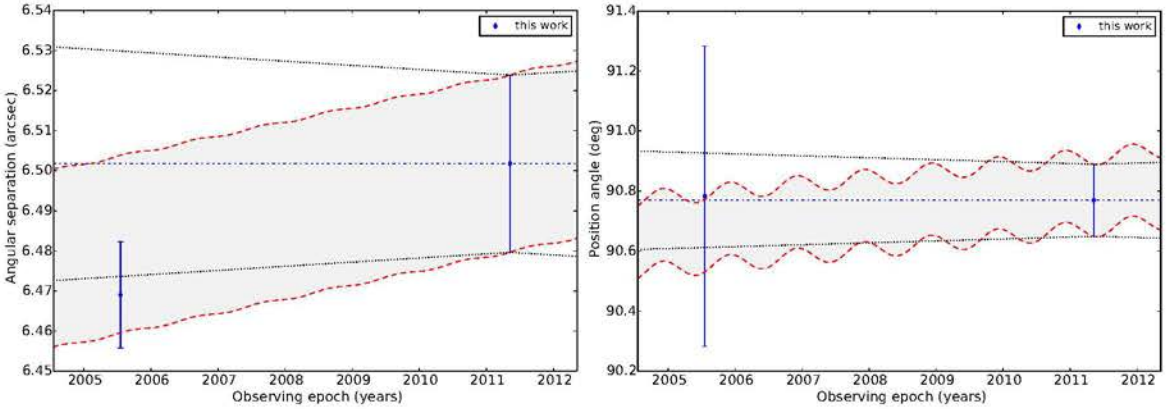


HIP89963

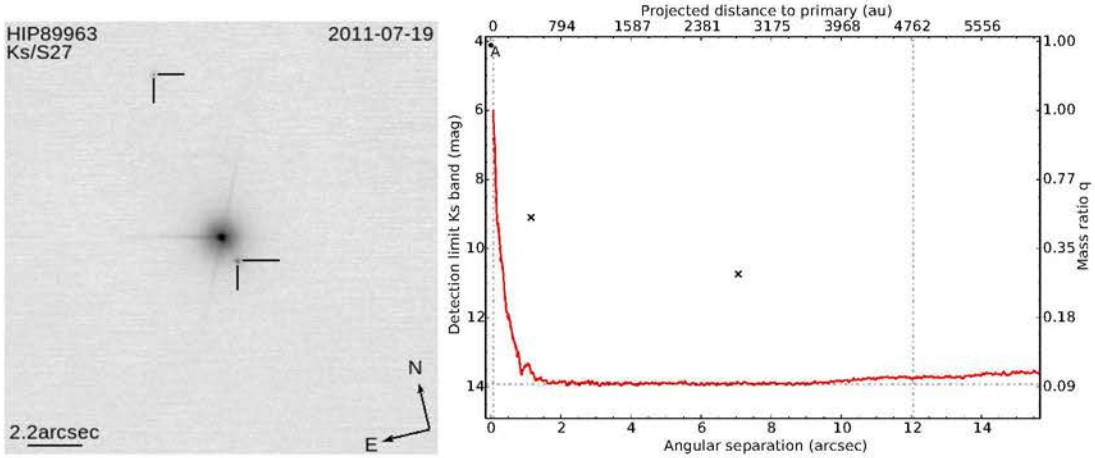

CC1: $P_{bg} = 26.53\%$, $P_{cmv} = 0.66\%$, N=2, df=2

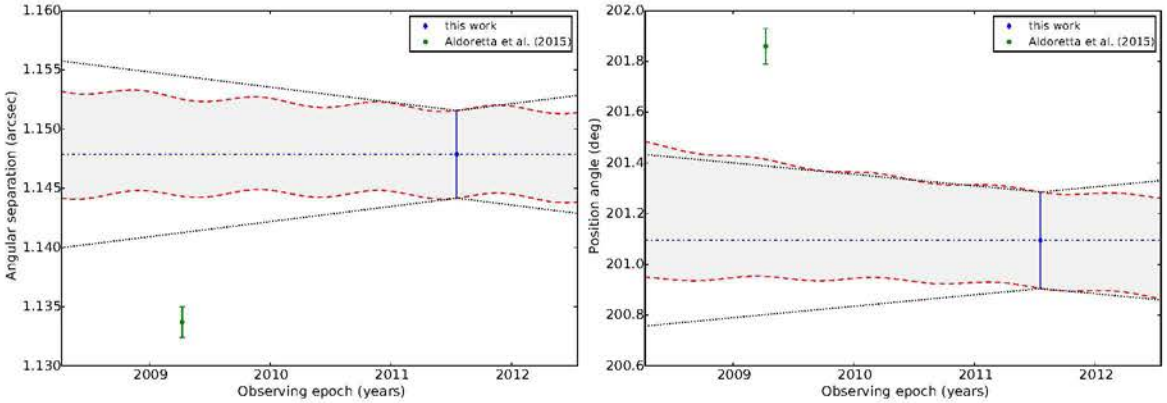


## HIP90096

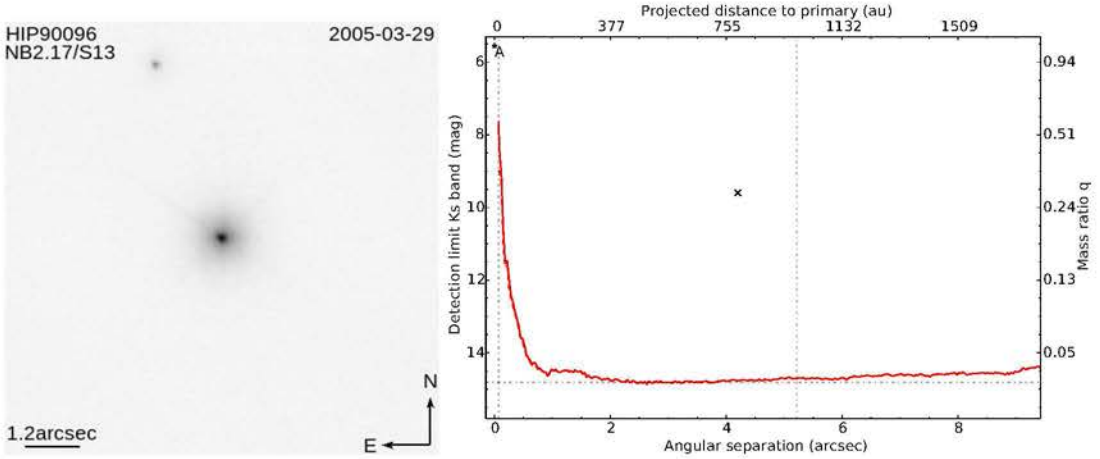


CC1: $P_{bg} = 94.20\%$, $P_{cmv} = 8.72\%$, N=2, df=2

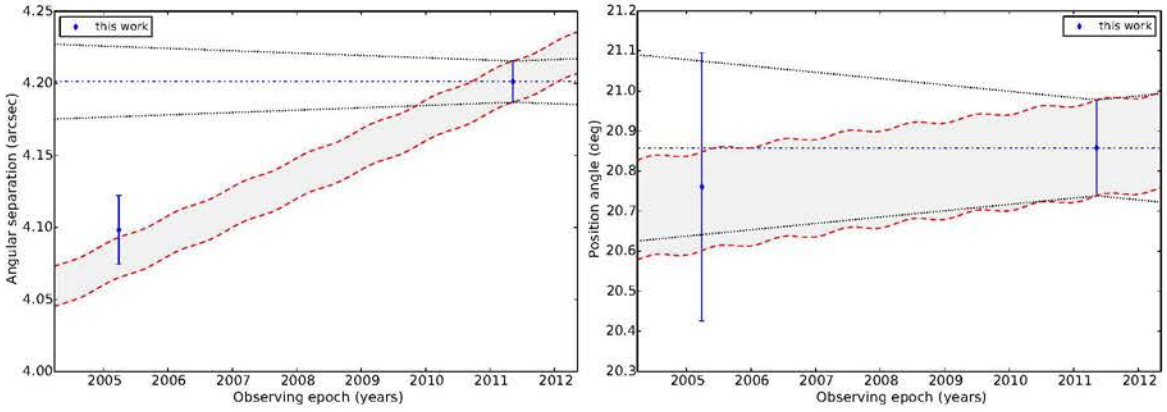


## HIP90766

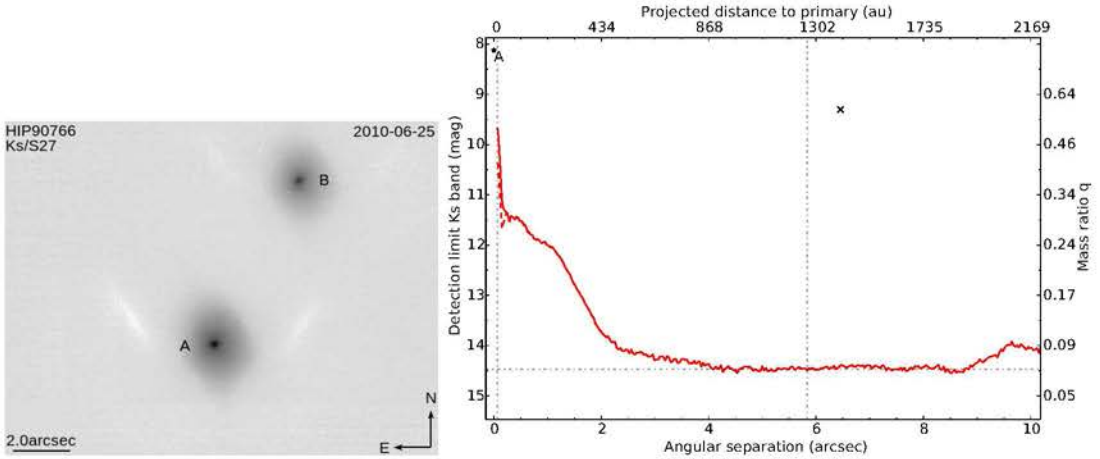

CC1: $P_{bg}$ = 9.64%, $P_{cmv}$ = 5.91%, N=3, df=4

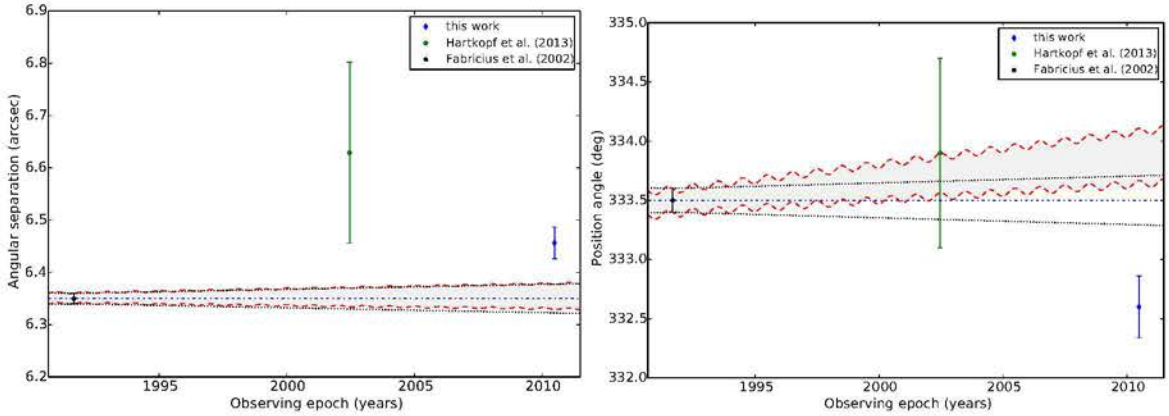


## HIP93805

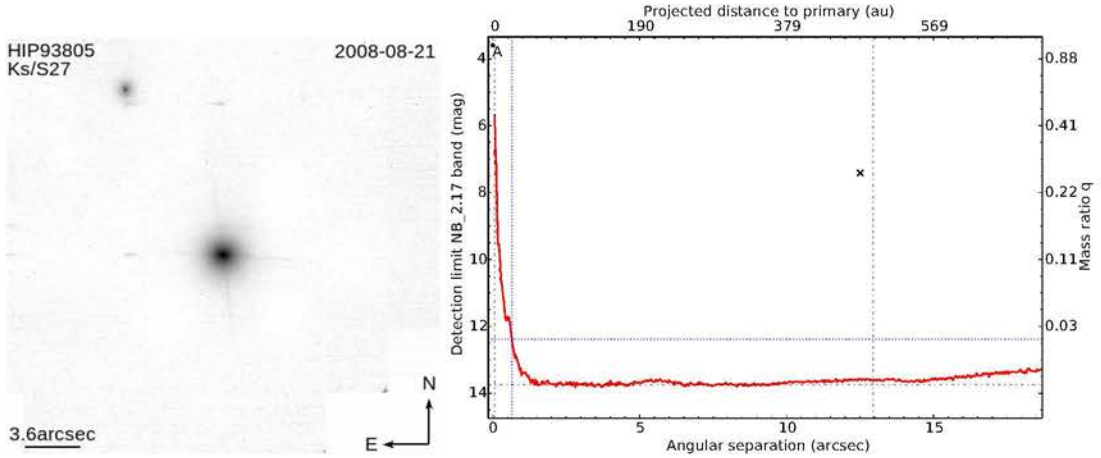


CC1: $P_{bg}$ = 37.20%, $P_{cmv}$ = 12.65%, N=2, df=2

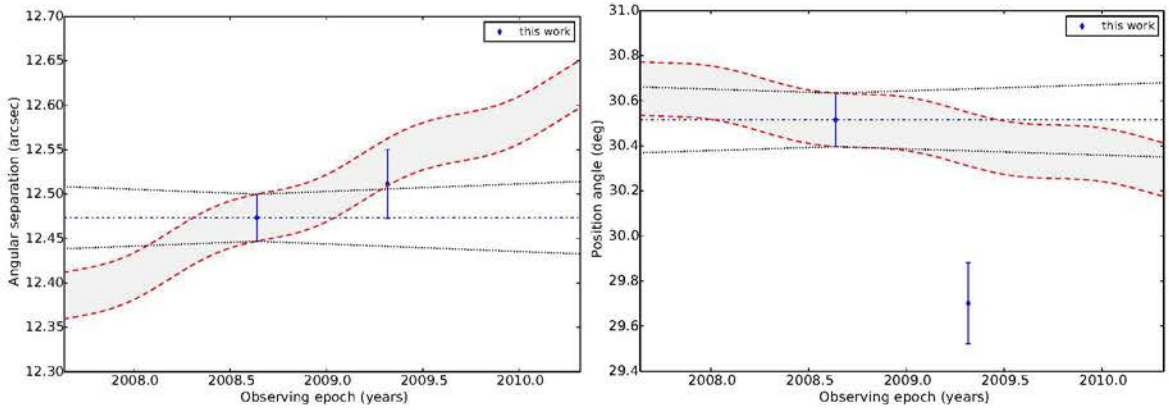


## HIP93892

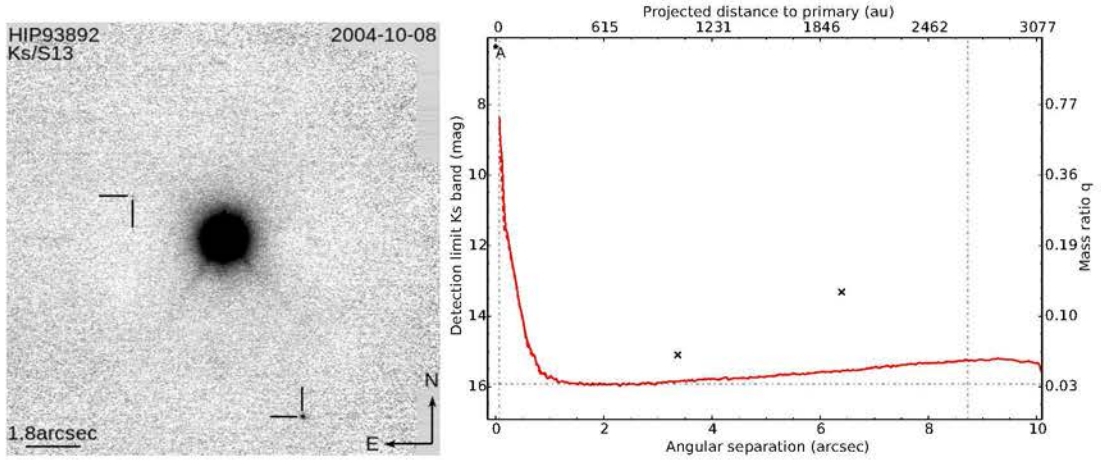

CC1: $P_{bg}$ = 8.55%, $P_{cmv}$ = 0.50%, N=2, df=2

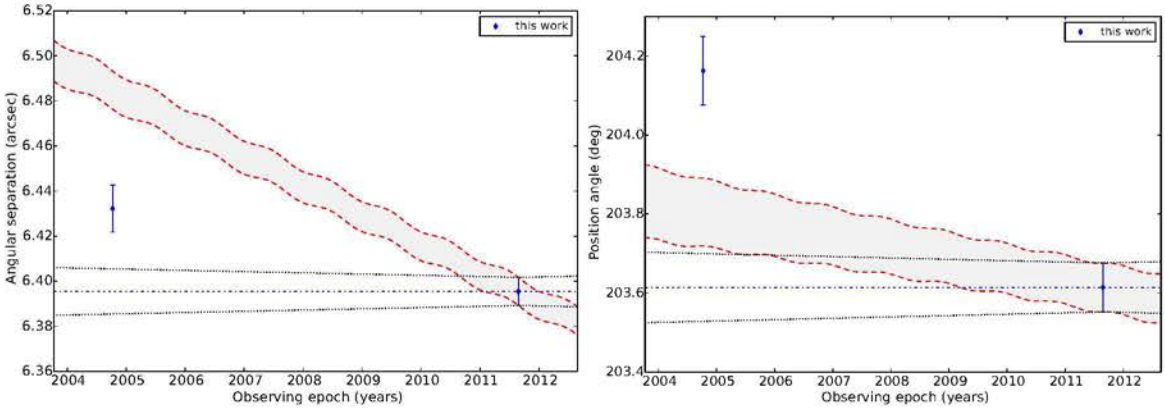


CC2: $P_{bg}$ = 13.14%, $P_{cmv}$ = 0.02%, N=2, df=2

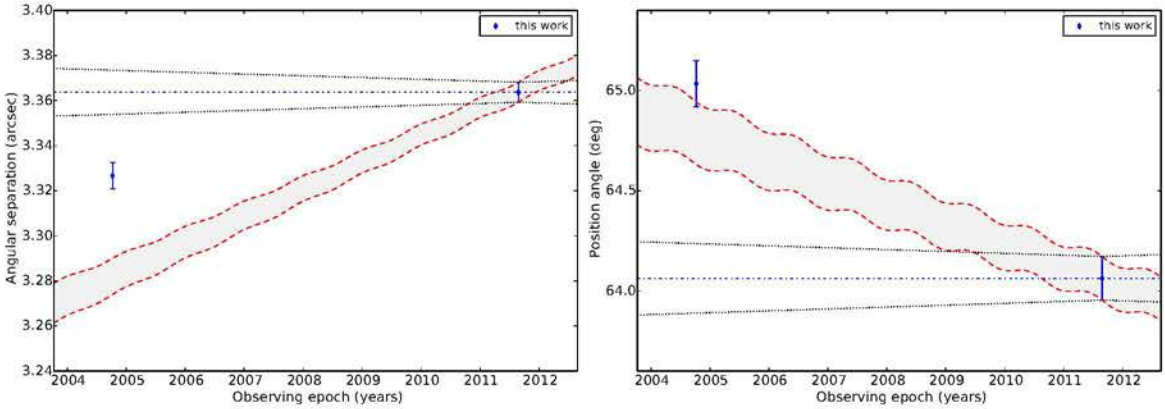


HIP100881

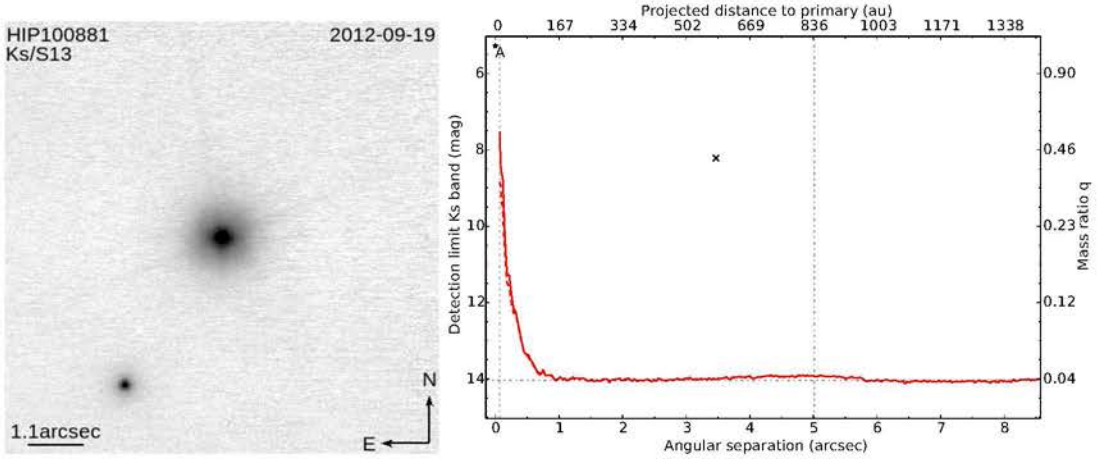


CC1: $P_{bg}$ = 0.00%, $P_{cmv}$ = 0.00%, N=3, df=4

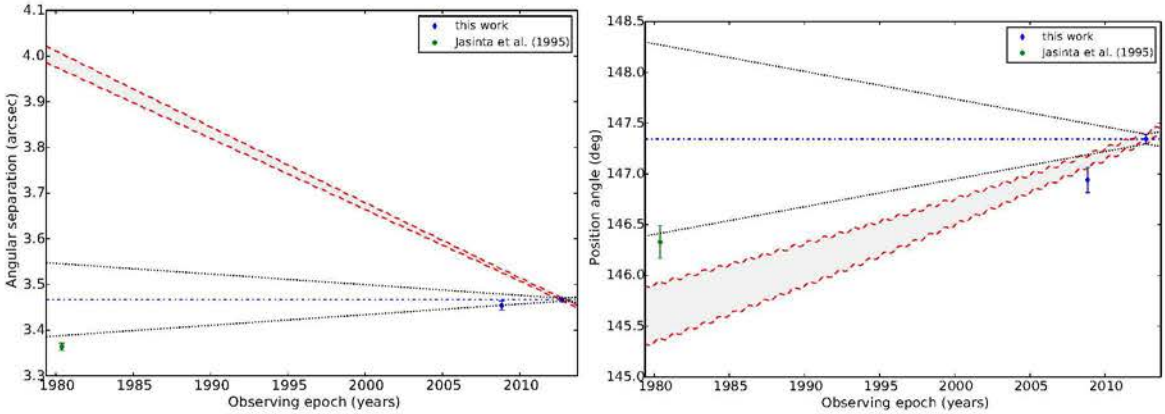

## HIP105842

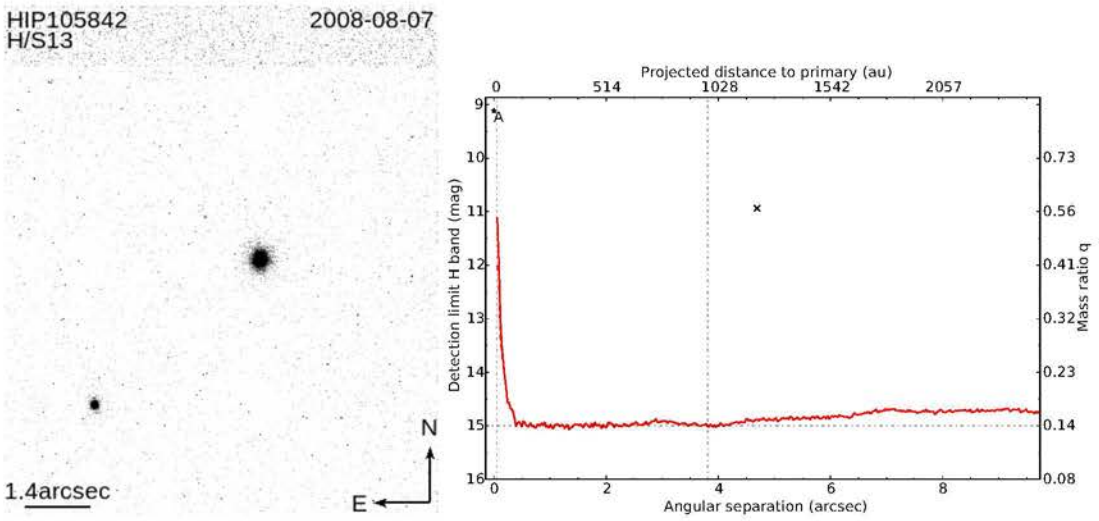


CC1: $P_{bg} = 0.00\%$, $P_{cmv} = 35.26\%$, N=2, df=2

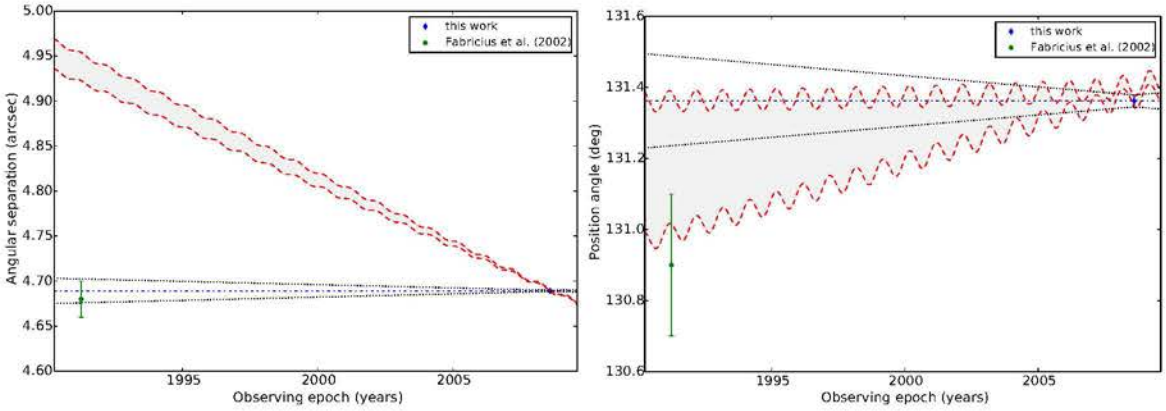


## HIP113031

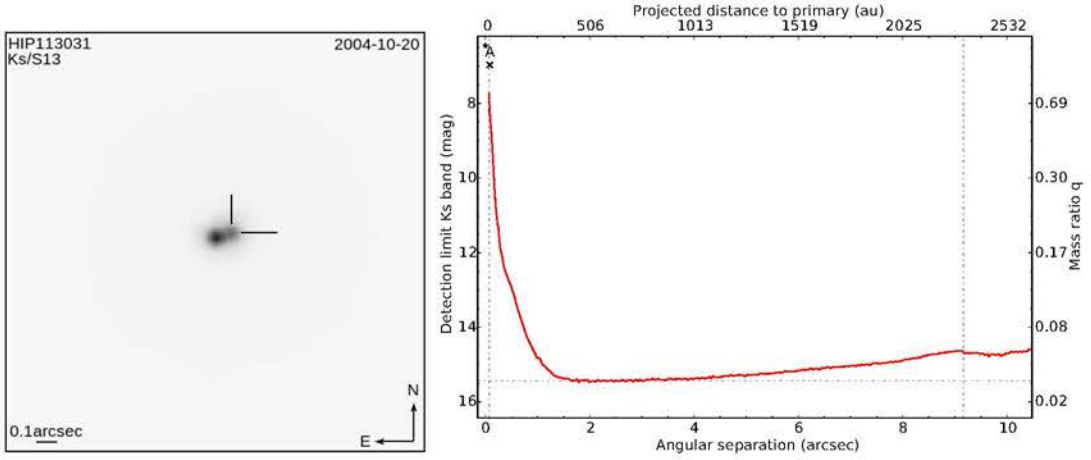


CC1: $P_{bg} = 0.00\%$, $P_{cmv} = 20.52\%$, N=2, df=2

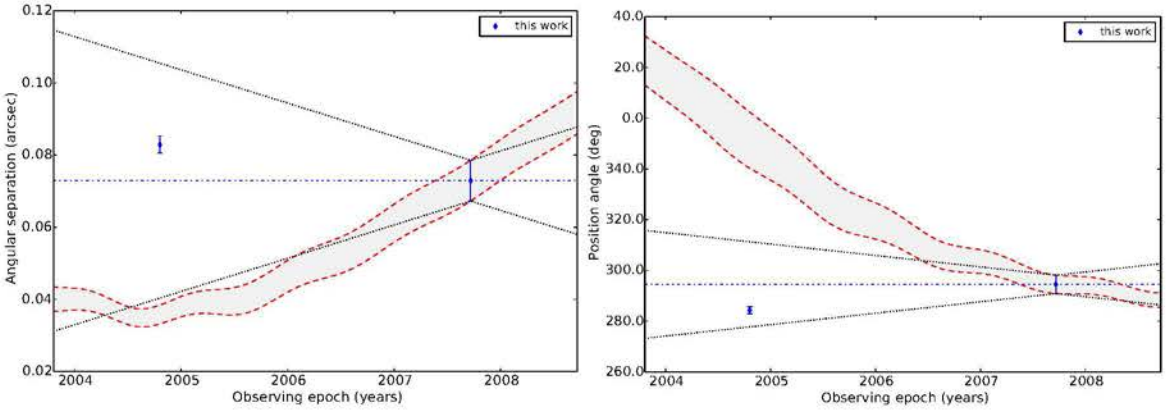

## HIP116231

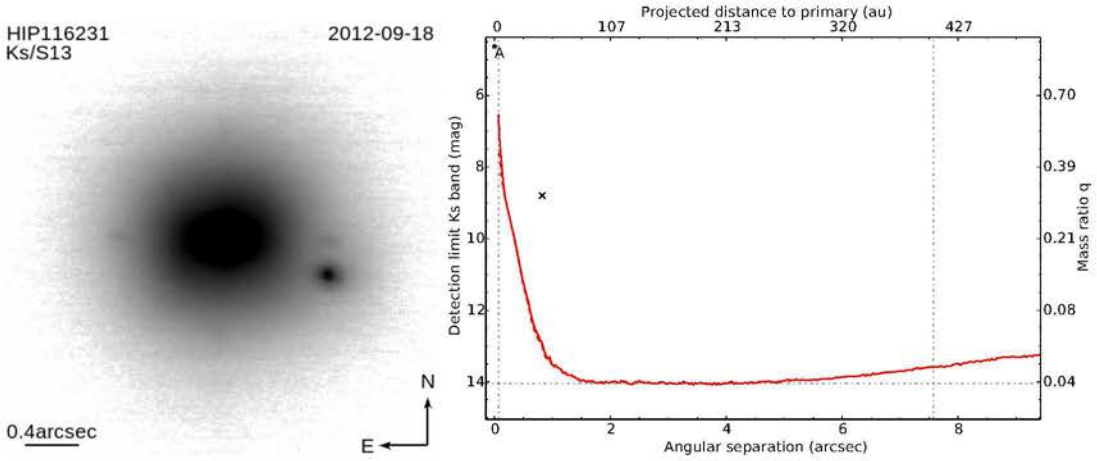


CC1: $P_{bg} = 0.00\%$, $P_{cmv} = 0.00\%$, N=3, df=4

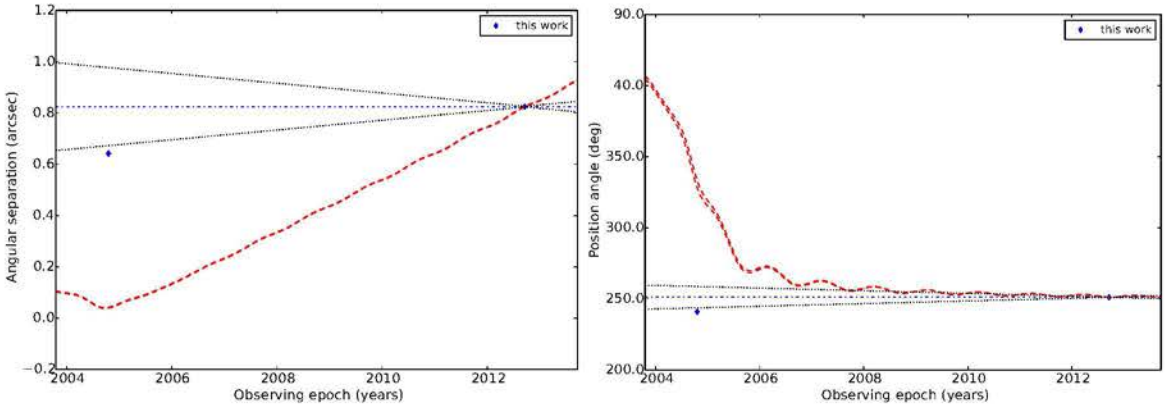


## HIP17563

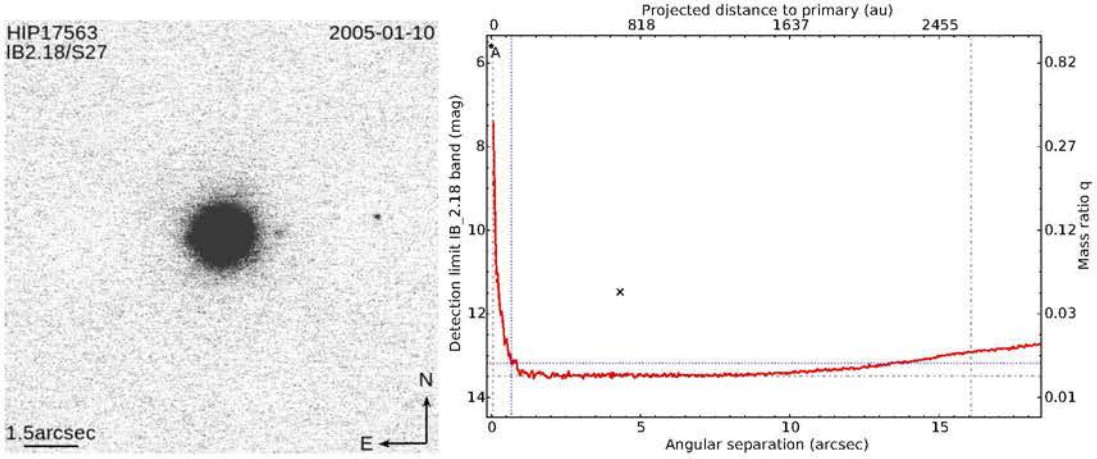


## HIP18213

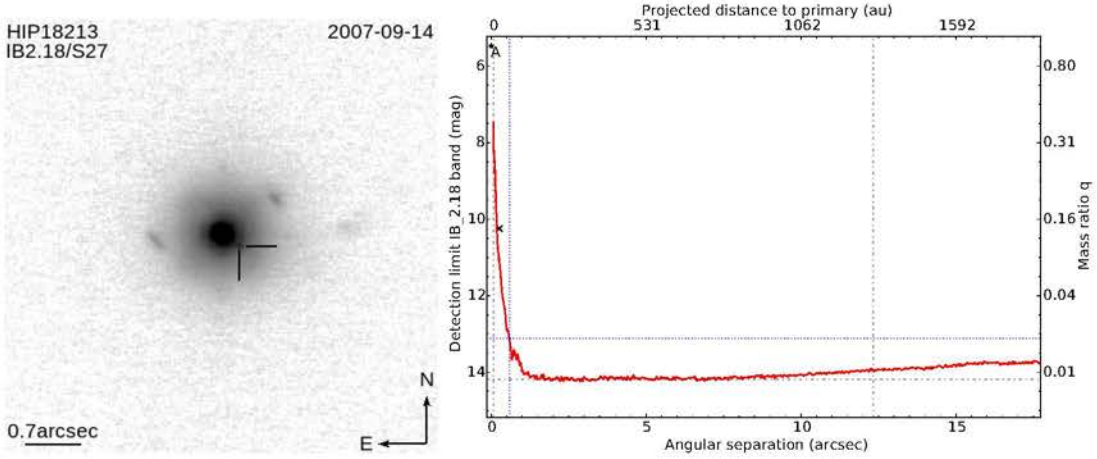

HIP25657

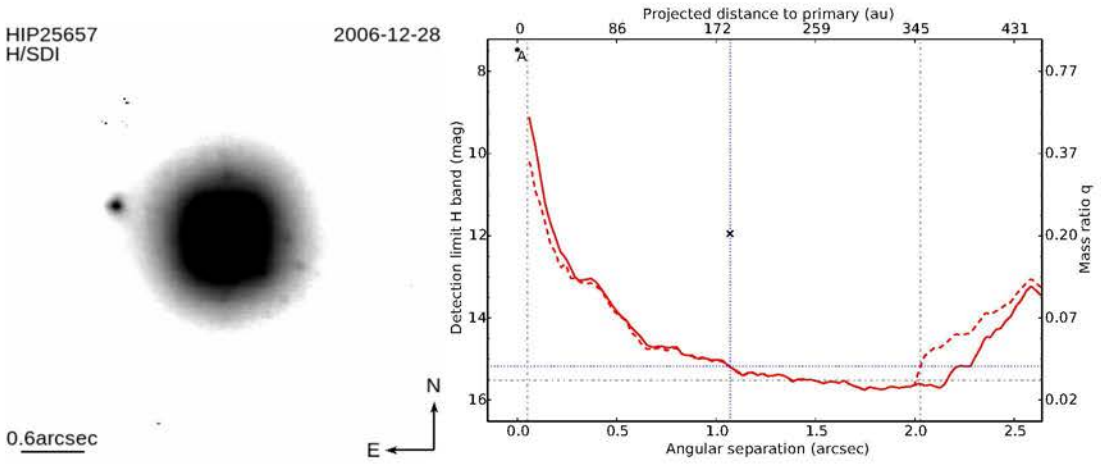


HIP27810

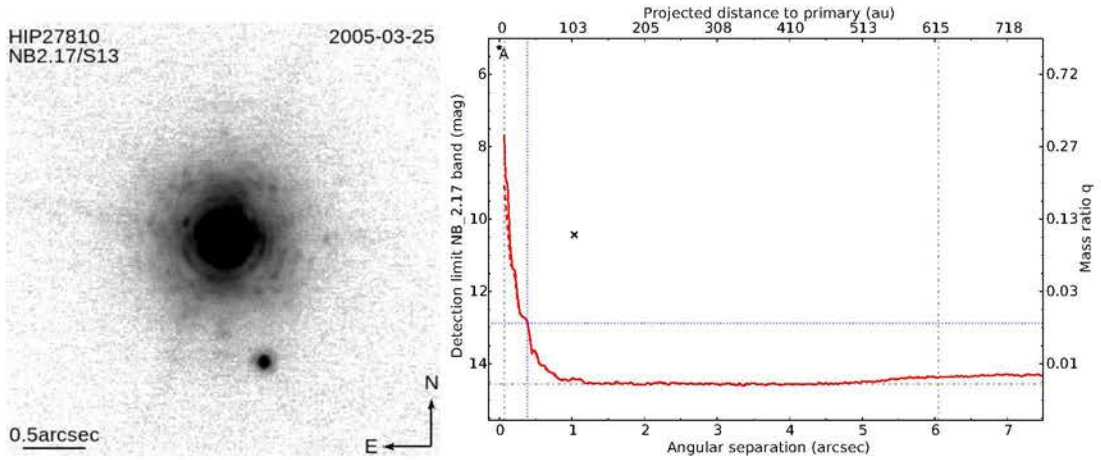


HIP32823

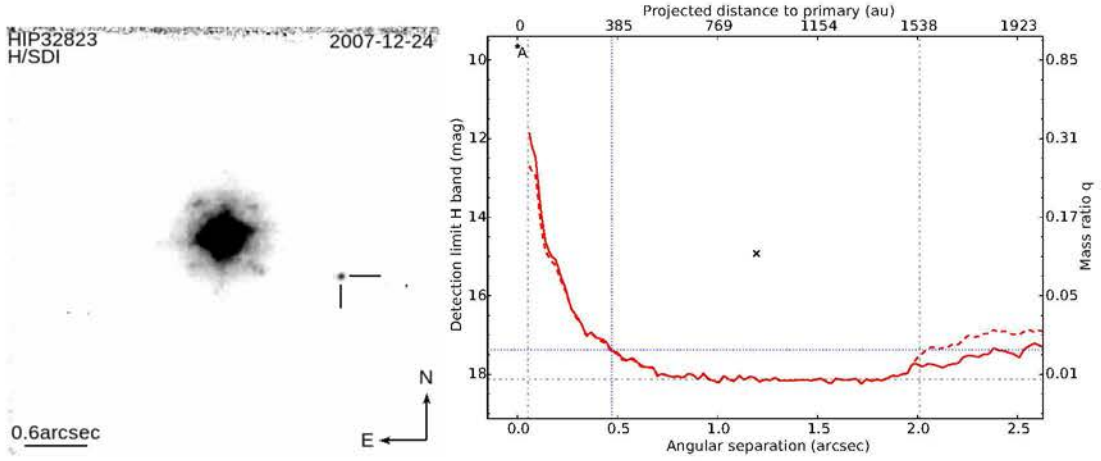


HIP34041

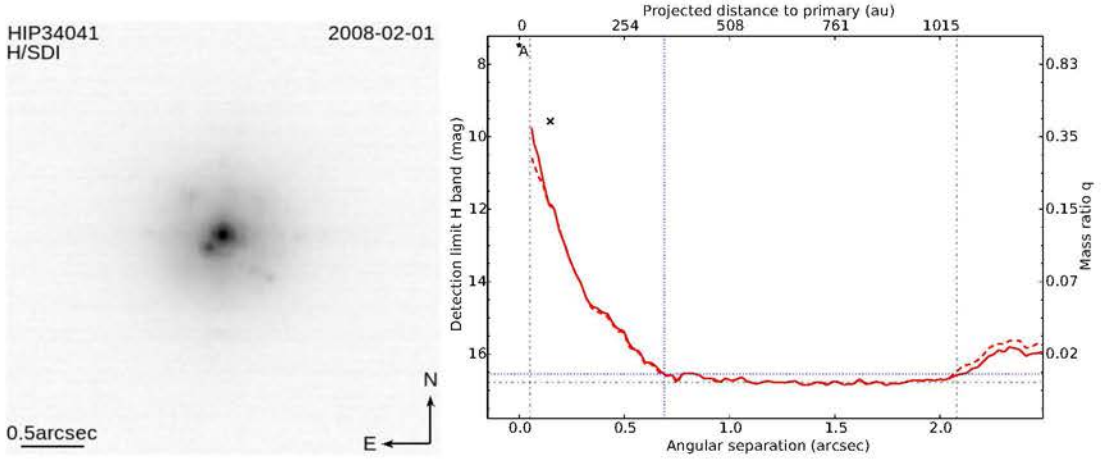

HIP34153

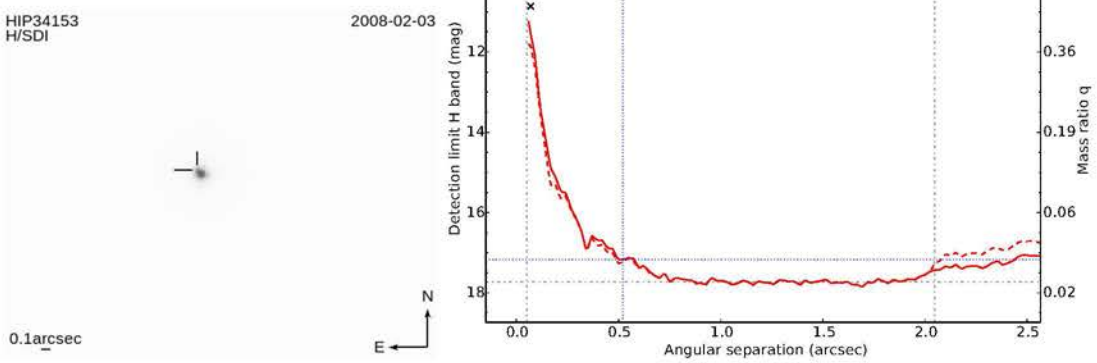


HIP35110

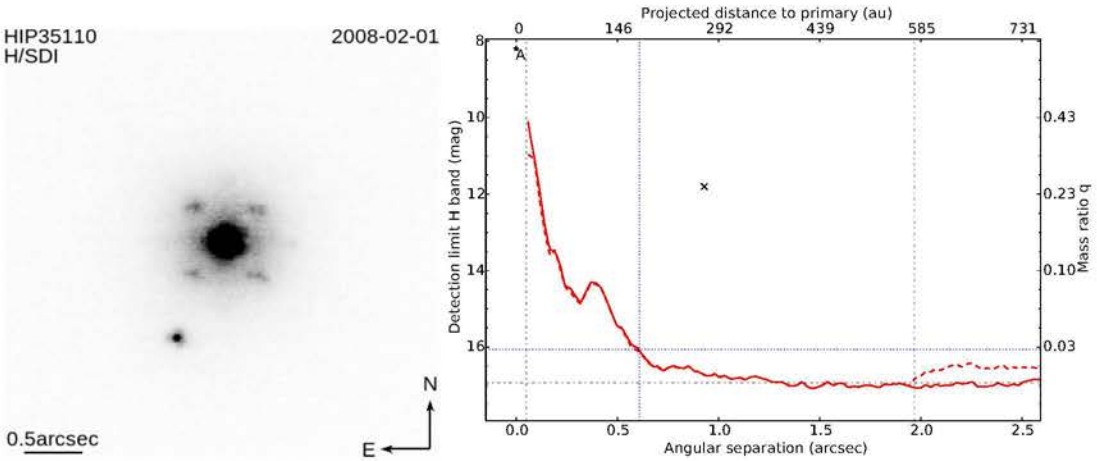


HIP35413

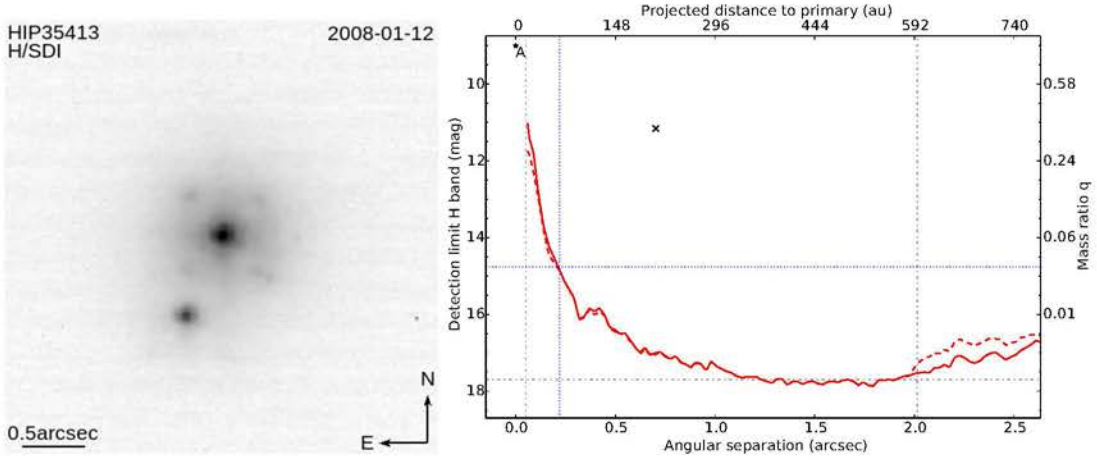


HIP39331

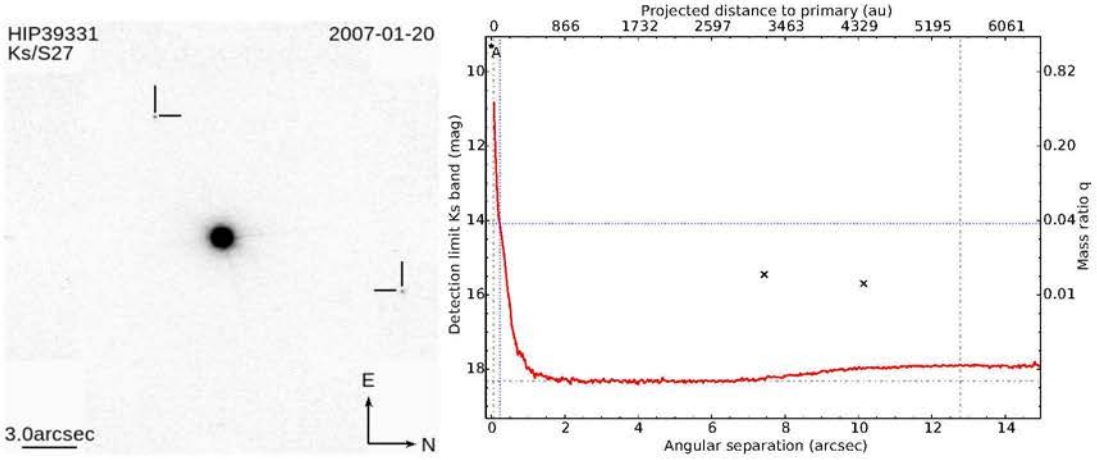

HIP39906

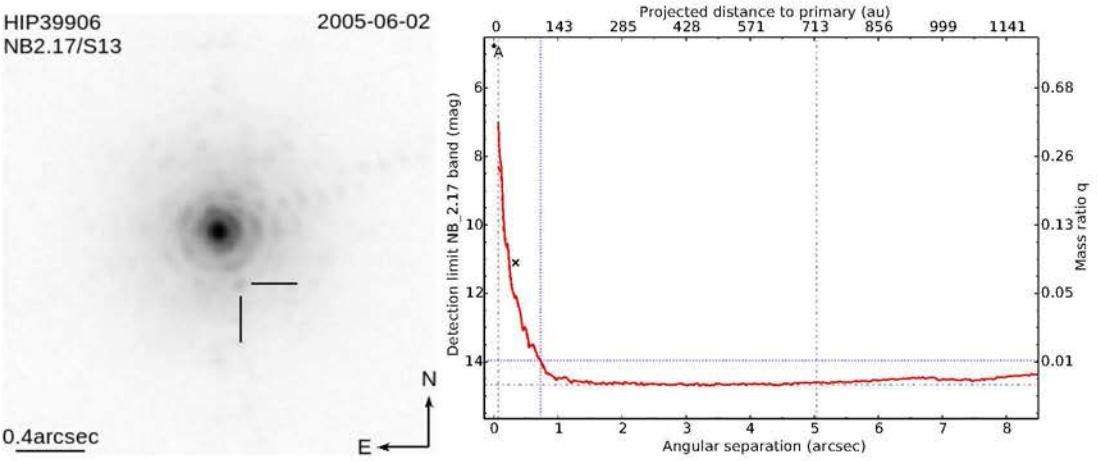


HIP42504

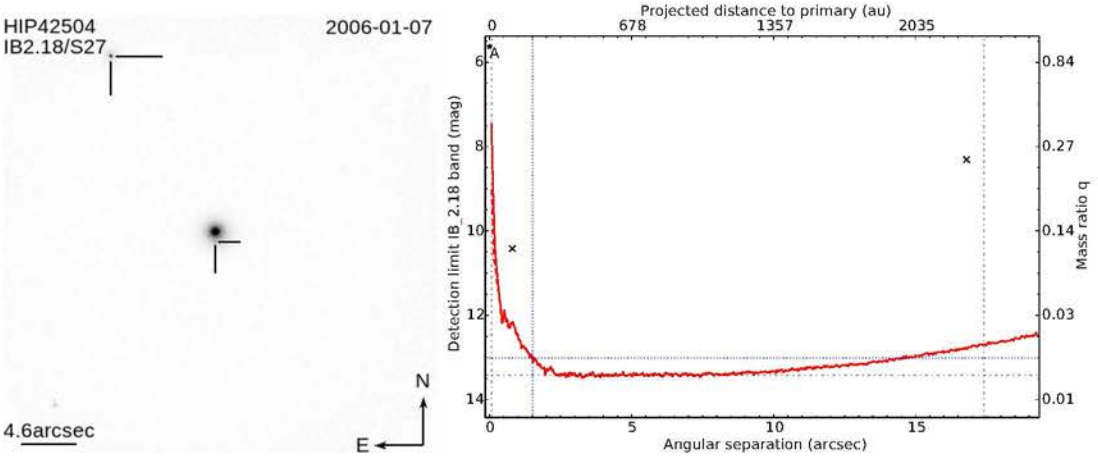


HIP49712

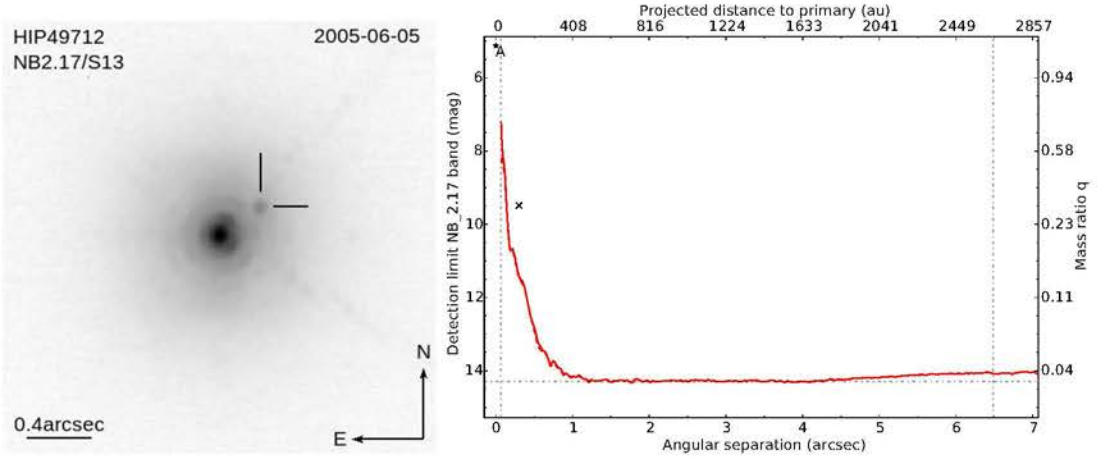


HIP50044

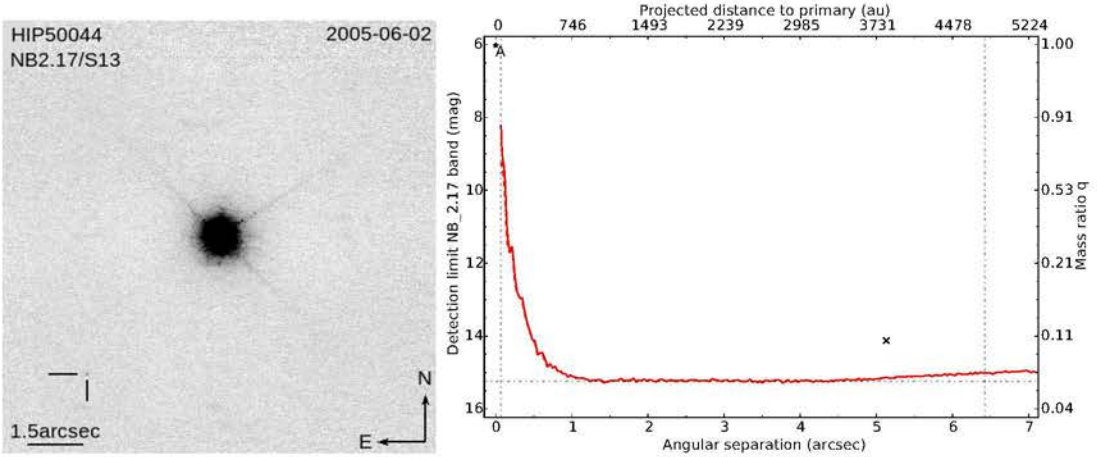

HIP54829

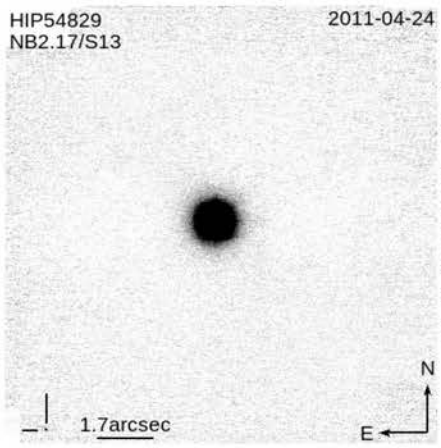


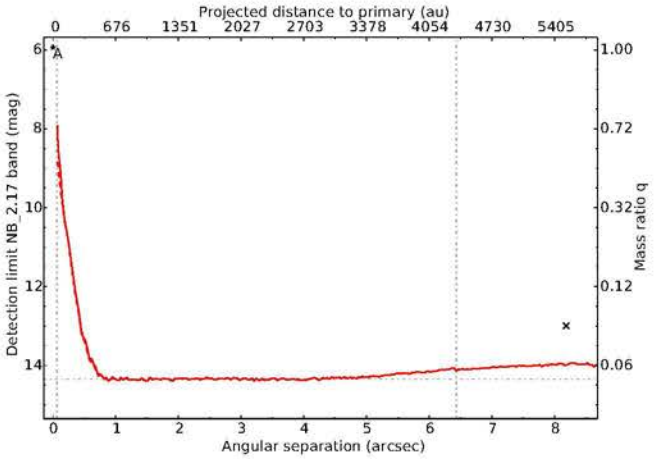


HIP62058

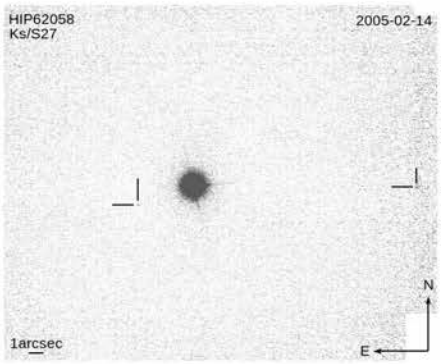


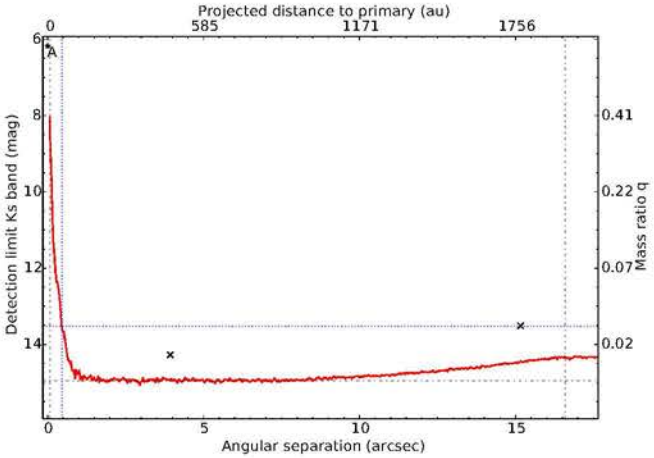


HIP64053

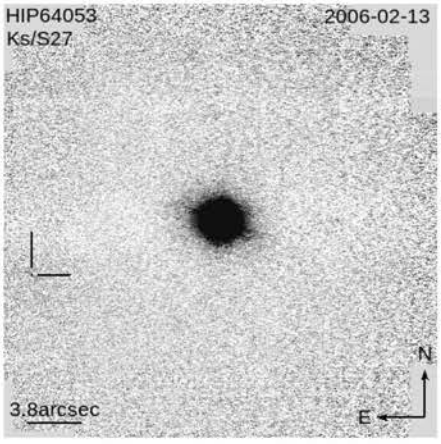


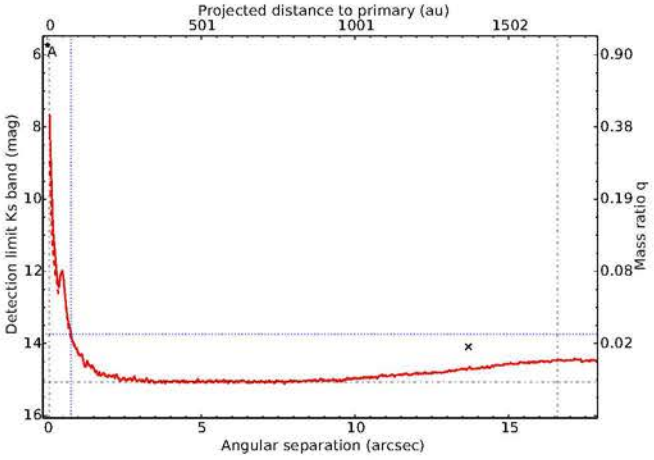


HIP76503

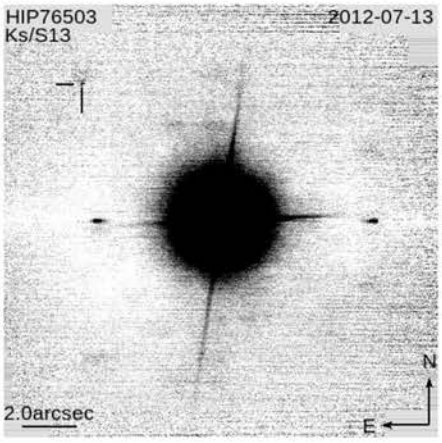


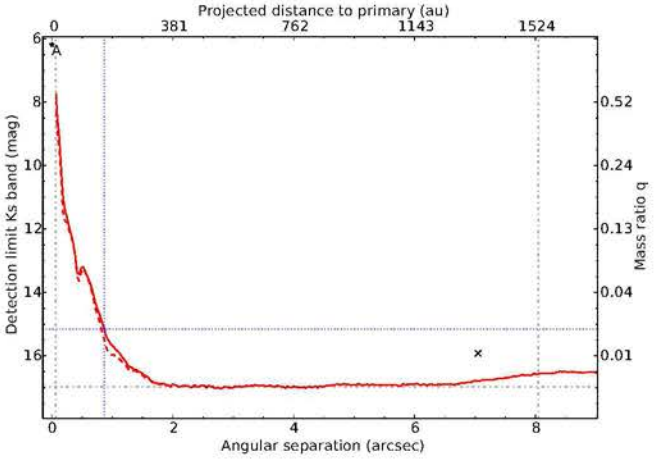

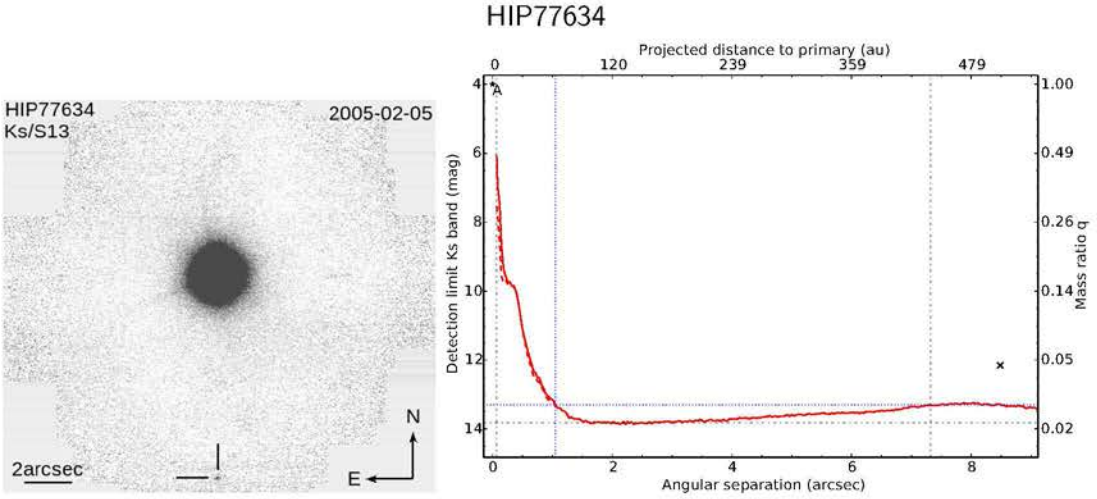
HIP77634
HIP77634
Ks/S13
2005-02-05
2arcsec
N
E
Projected distance to primary (au)
Detection limit Ks band (mag)
Mass ratio q
Angular separation (arcsec)

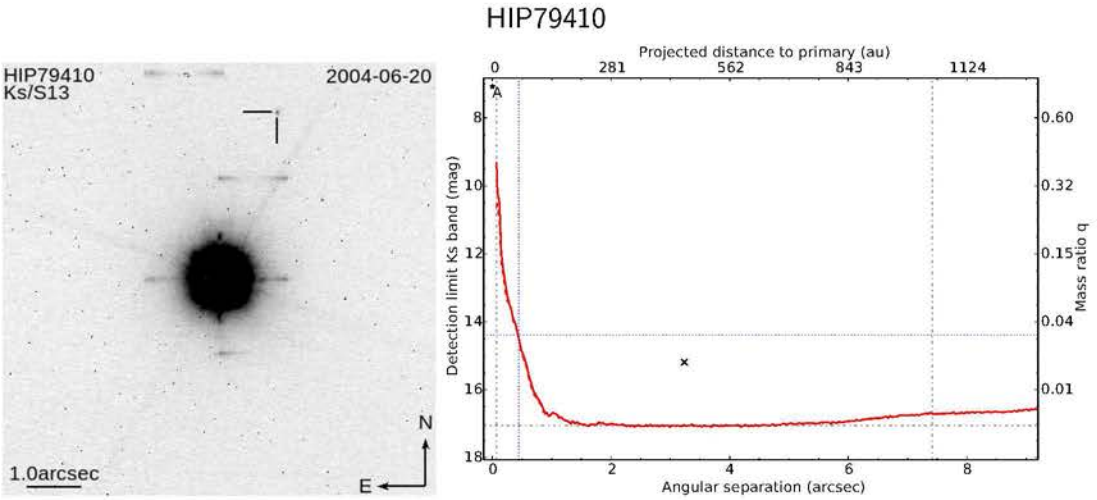
HIP79410
HIP79410
Ks/S13
2004-06-20
1.0arcsec
N
E
Projected distance to primary (au)
Detection limit Ks band (mag)
Mass ratio q
Angular separation (arcsec)

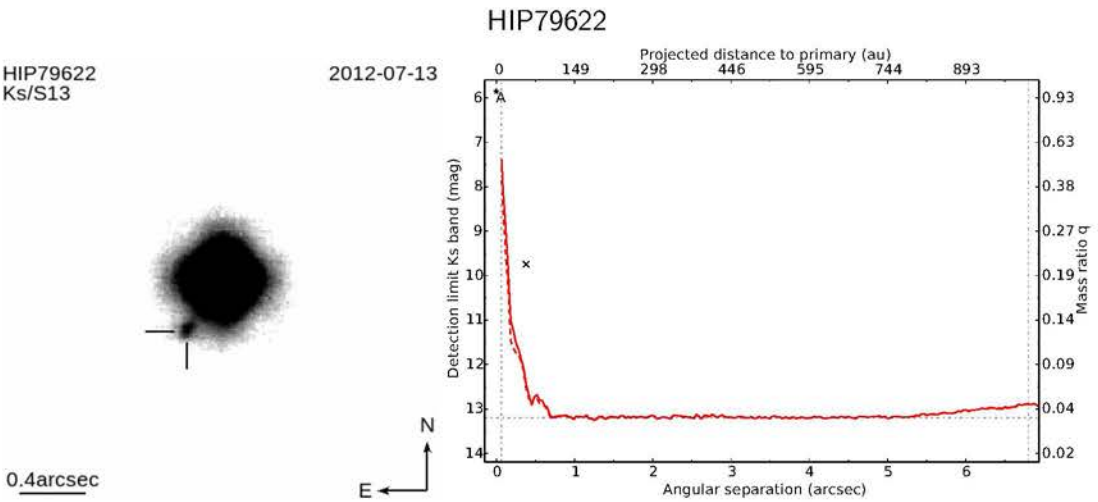
HIP79622
HIP79622
Ks/S13
2012-07-13
0.4arcsec
N
E
Projected distance to primary (au)
Detection limit Ks band (mag)
Mass ratio q
Angular separation (arcsec)

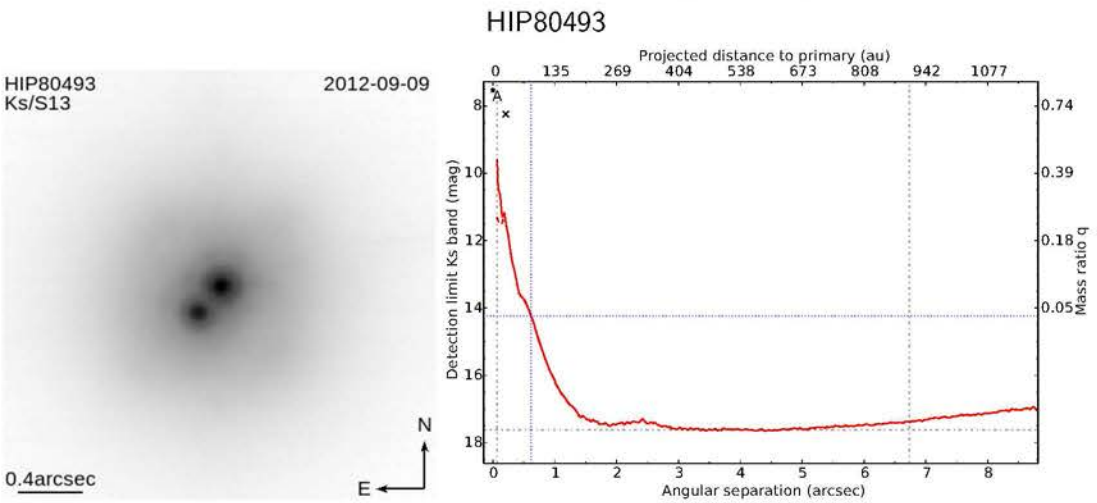
HIP80493
HIP80493
Ks/S13
2012-09-09
0.4arcsec
N
E
Projected distance to primary (au)
Detection limit Ks band (mag)
Mass ratio q
Angular separation (arcsec)

HIP88012

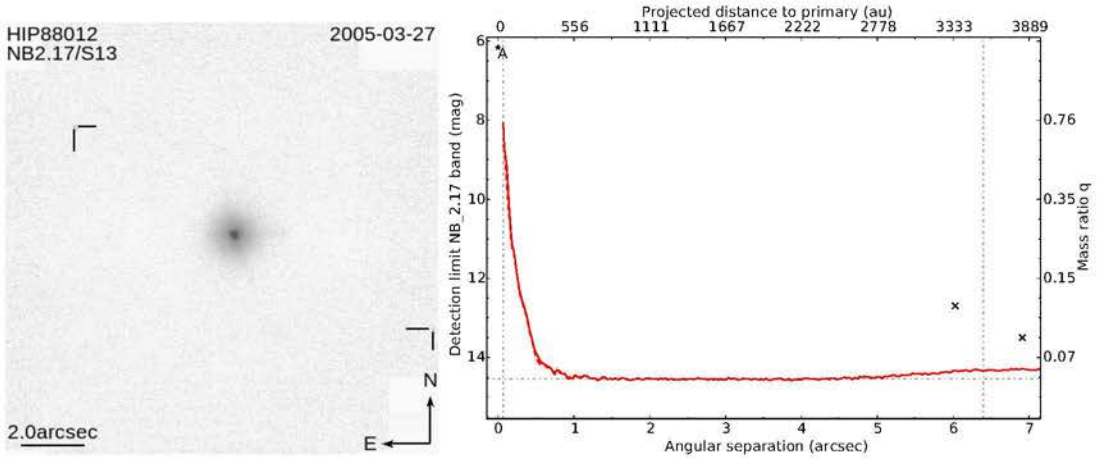


HIP91014

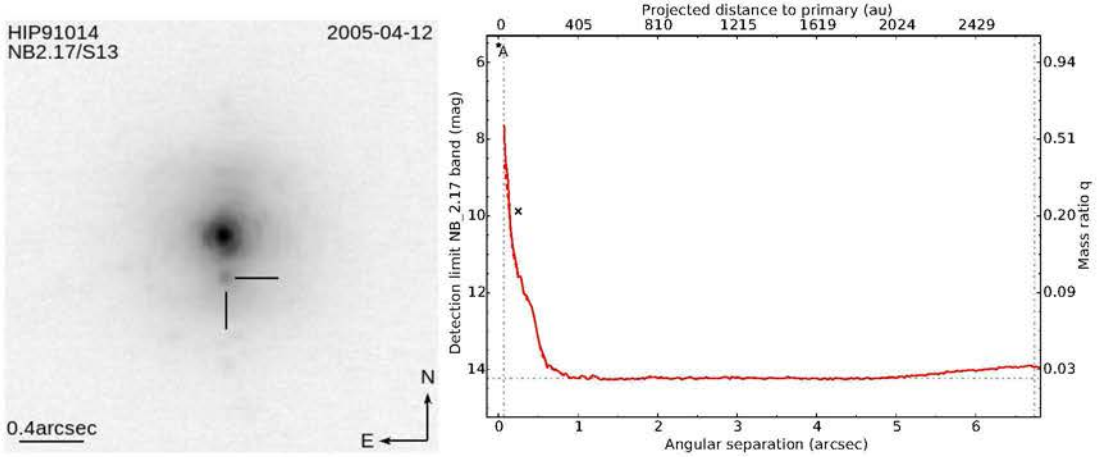


HIP99457

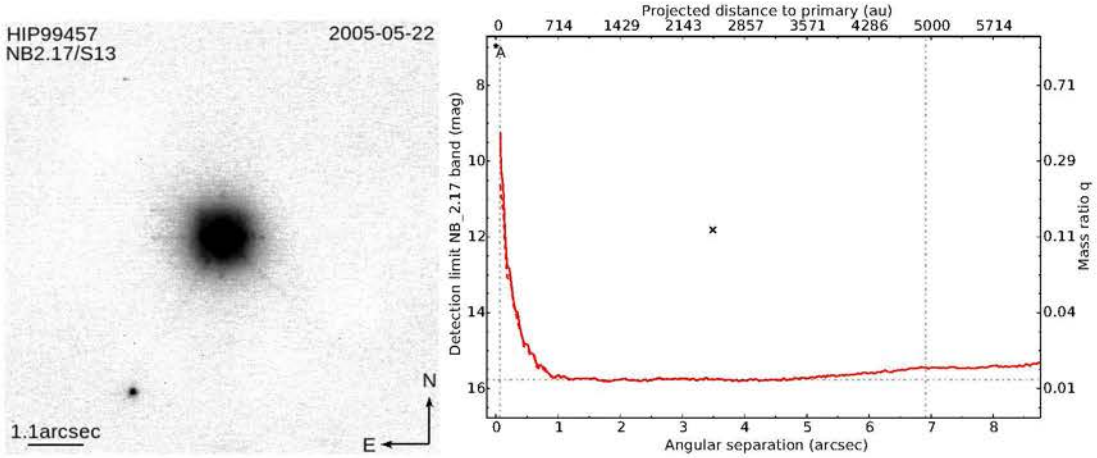


HIP100751

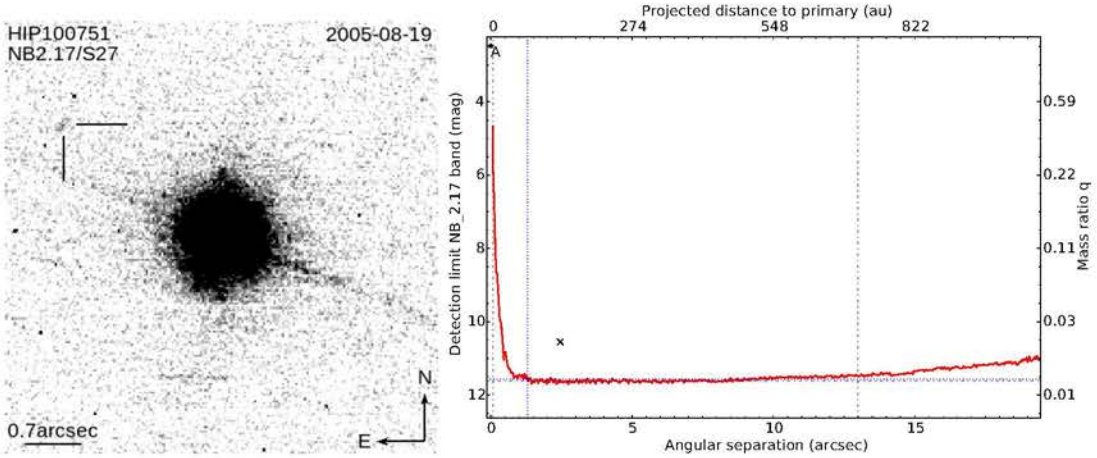

# Non-detection dynamic range plots

HIP145

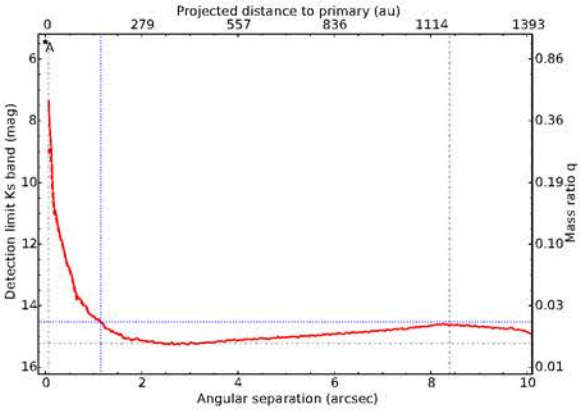


HIP377

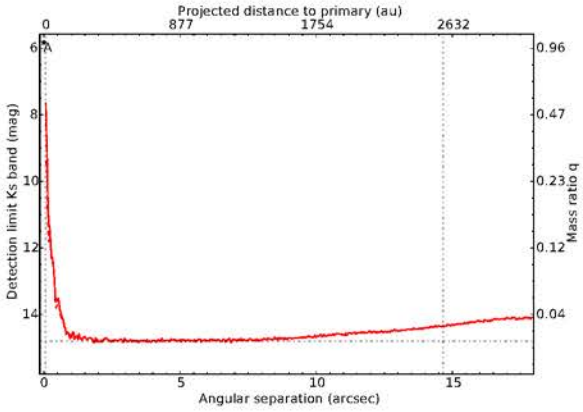


HIP1191

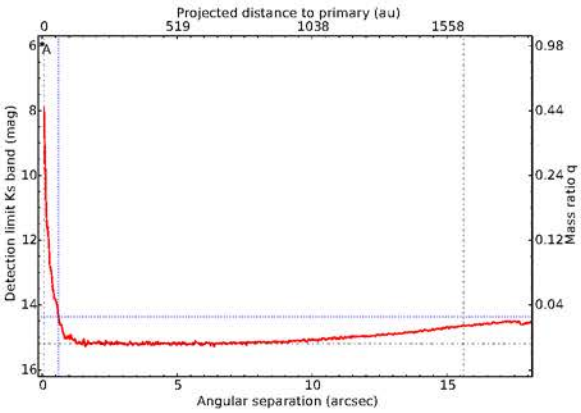


HIP1830

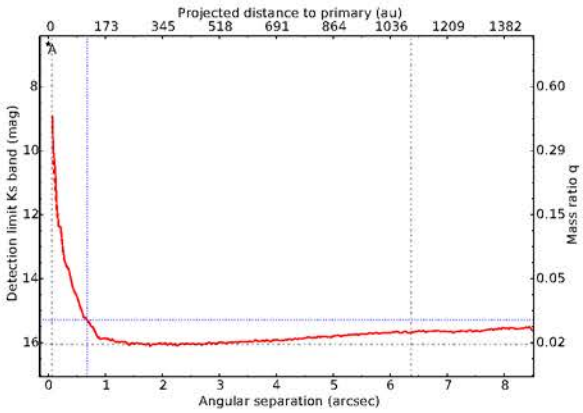


HIP3741

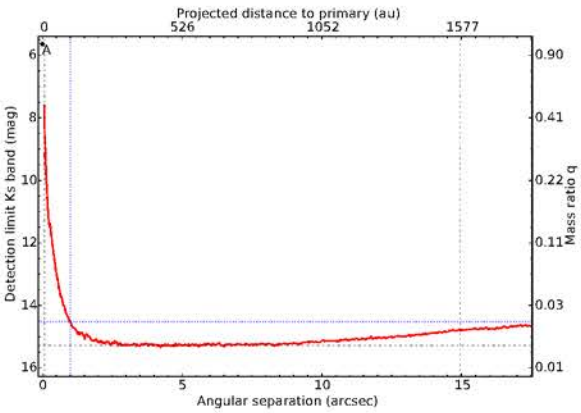


HIP5778

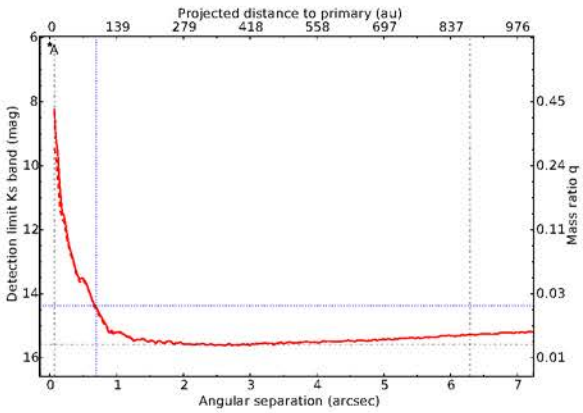


HIP10602

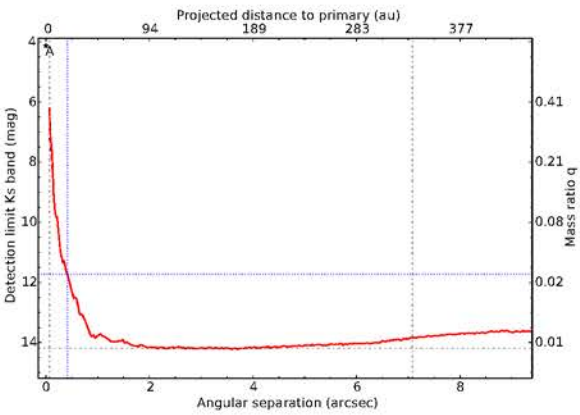


HIP13951

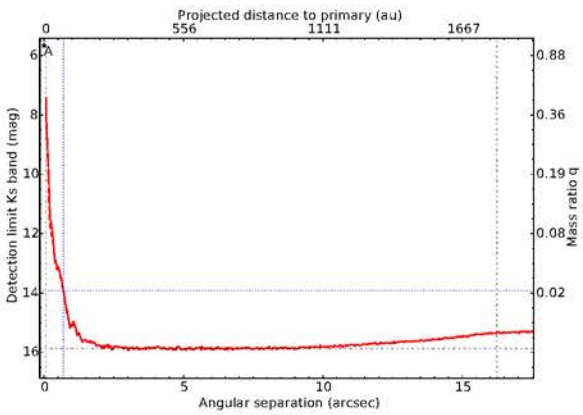

HIP14131

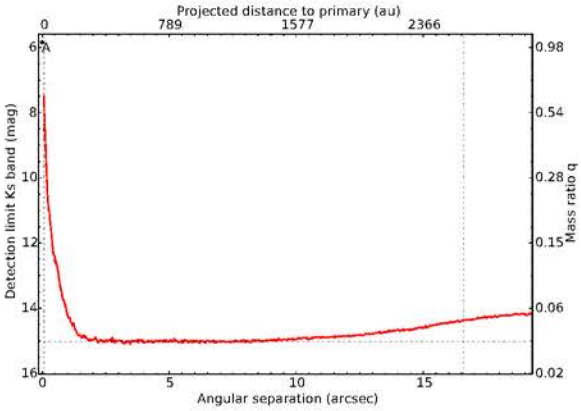


HIP17921

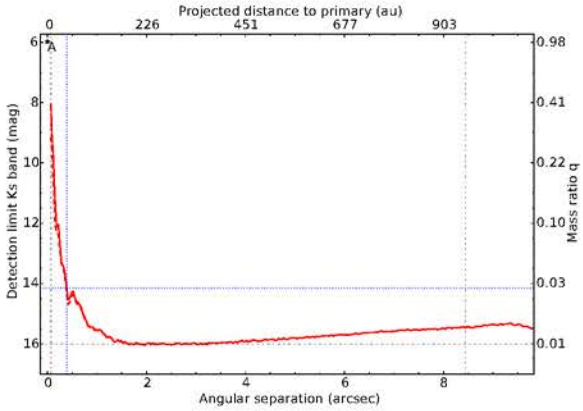


HIP18788

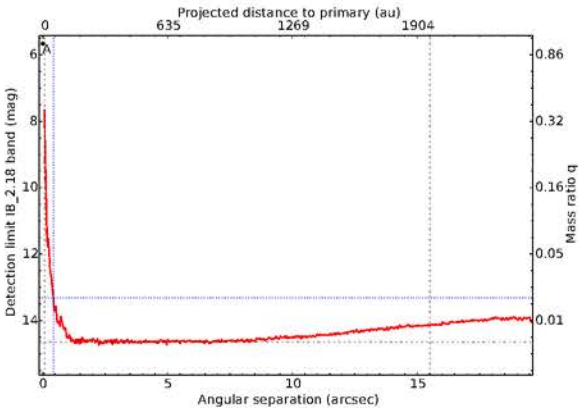


HIP19720

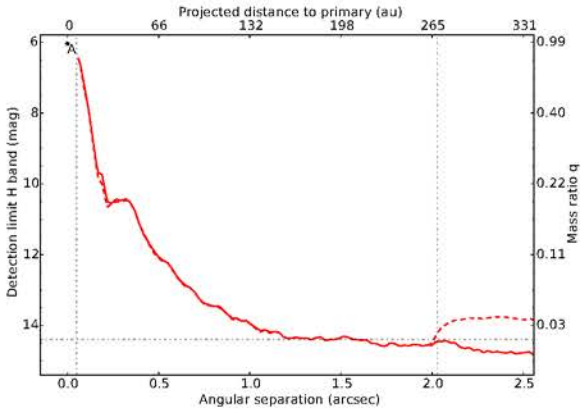


HIP19860

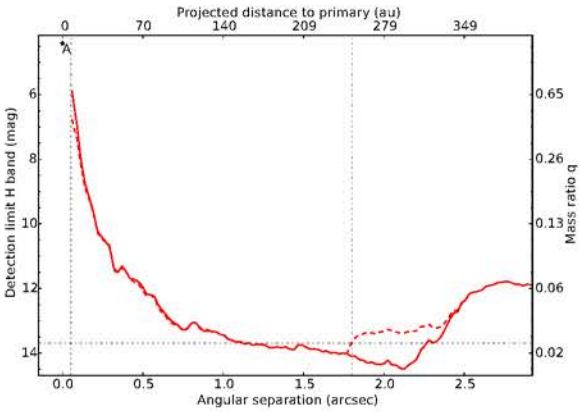


HIP20171

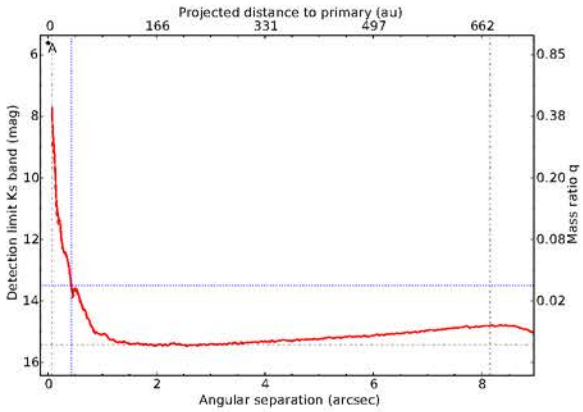


HIP21177

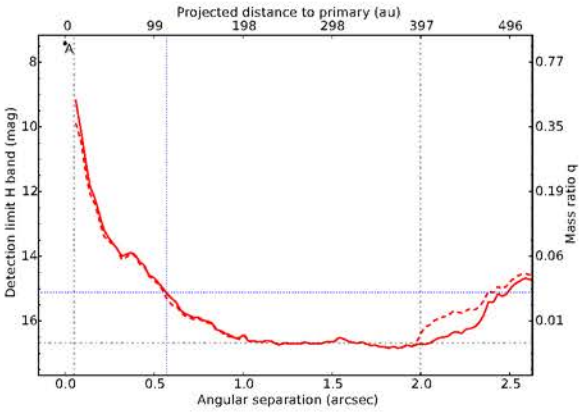


HIP21192

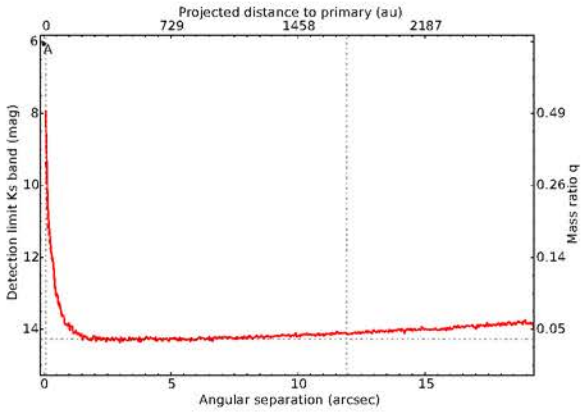

HIP21640

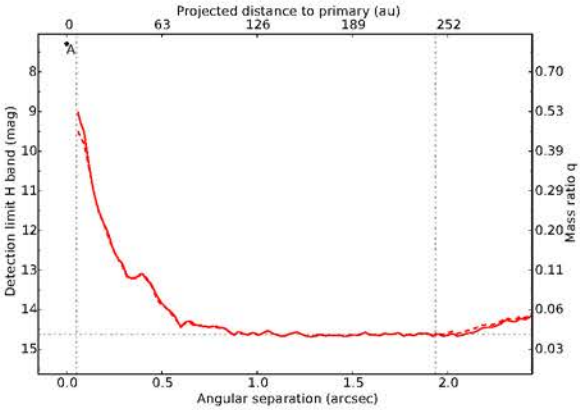


HIP21735

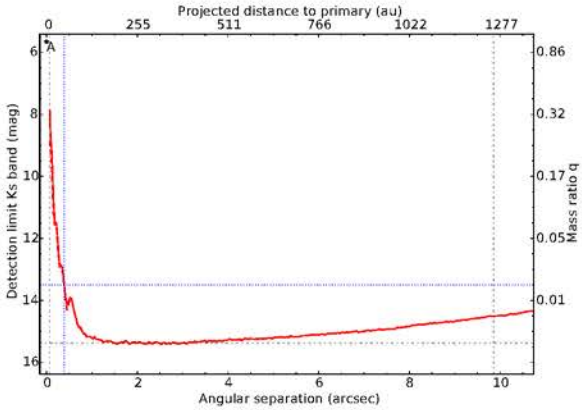


HIP21949

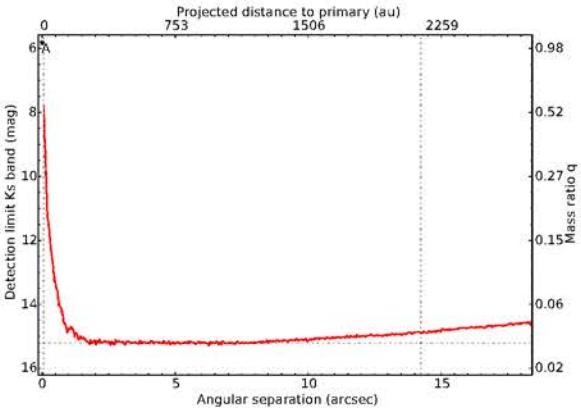


HIP22913

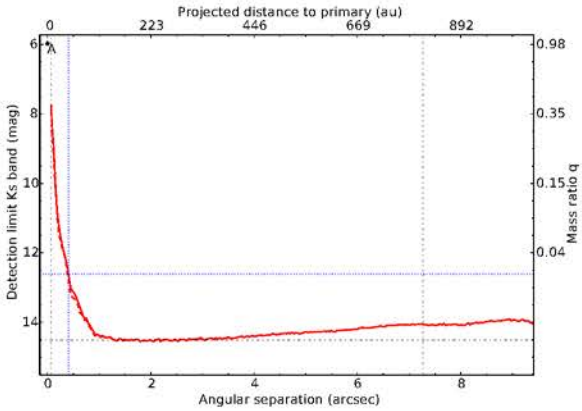


HIP23419

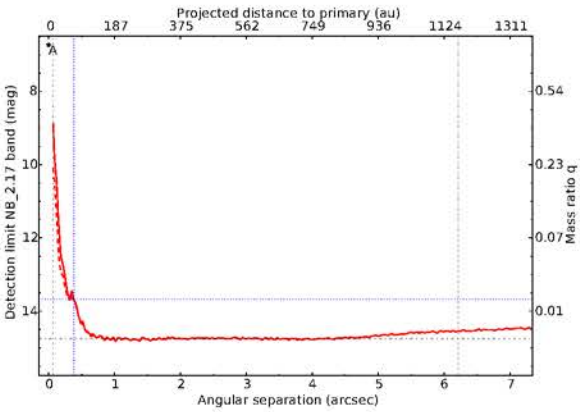


HIP23745

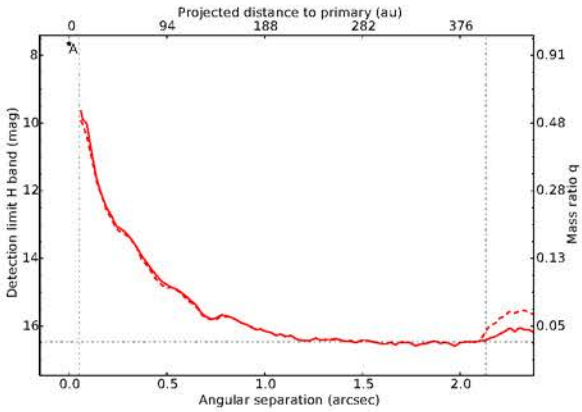


HIP24244

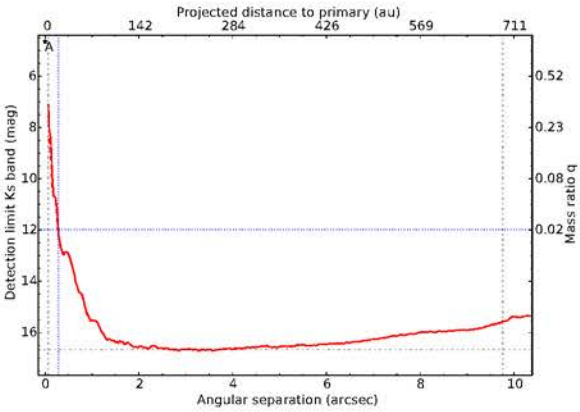


HIP24505

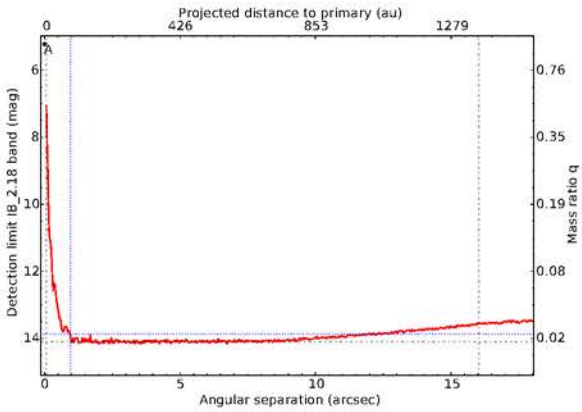

HIP24740

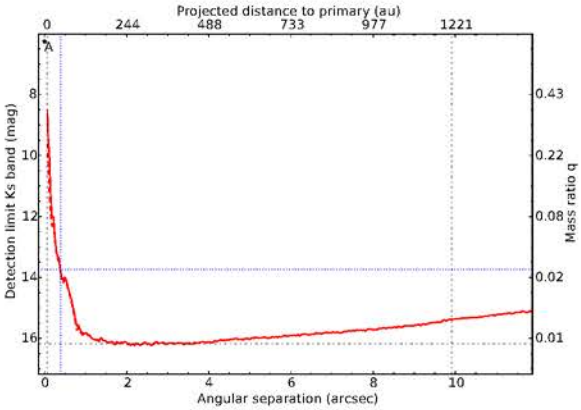


HIP26545

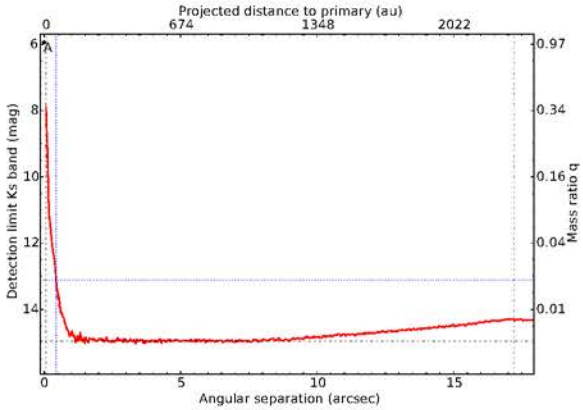


HIP26634

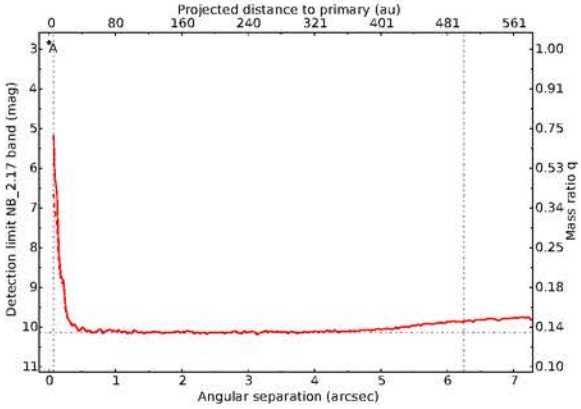


HIP26836

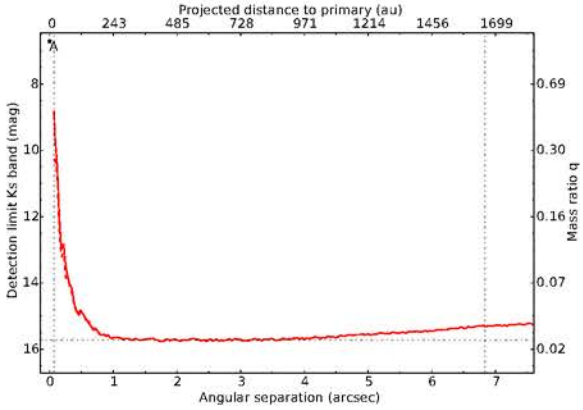


HIP26868

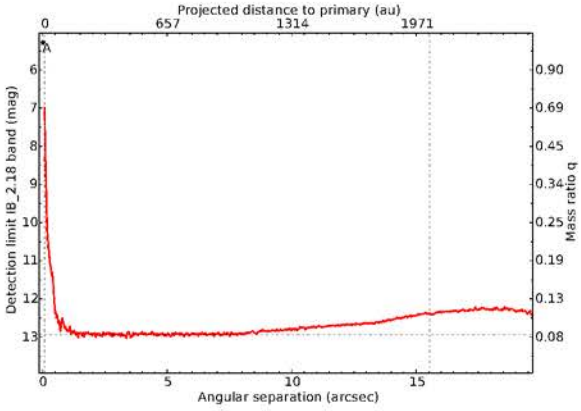


HIP27265

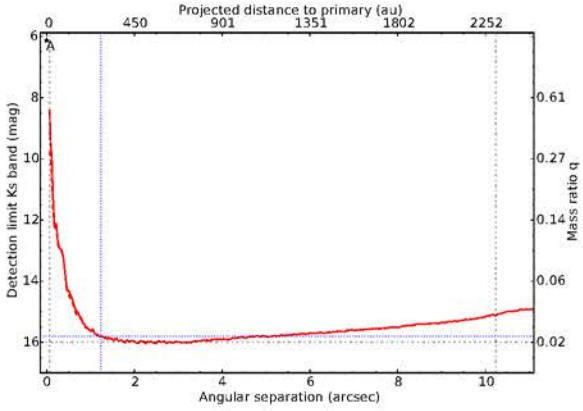


HIP27534

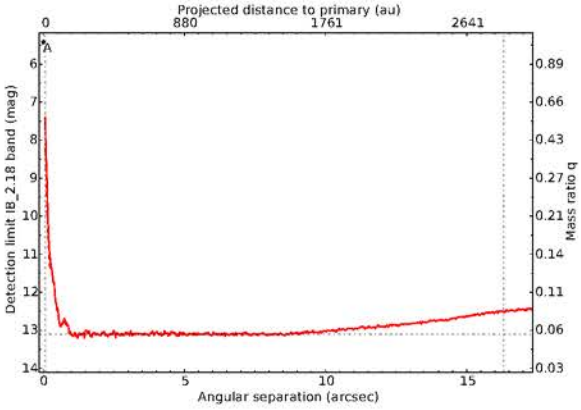


HIP27566

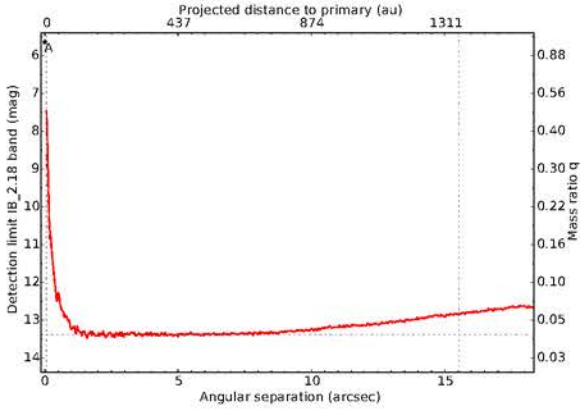

HIP28691

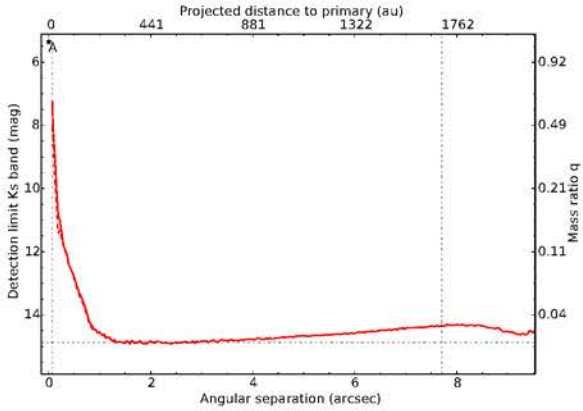


HIP28992

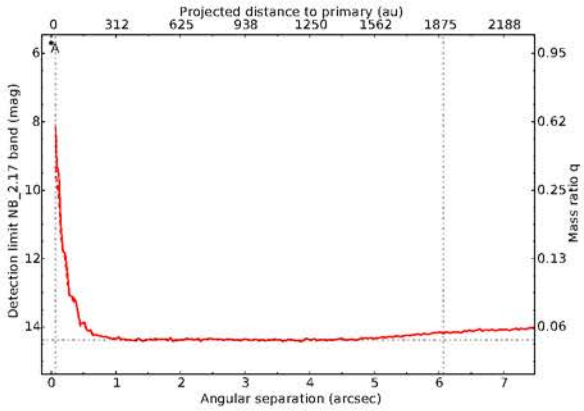


HIP29134

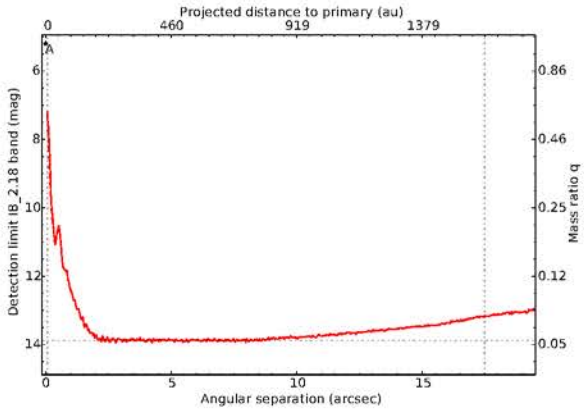


HIP29941

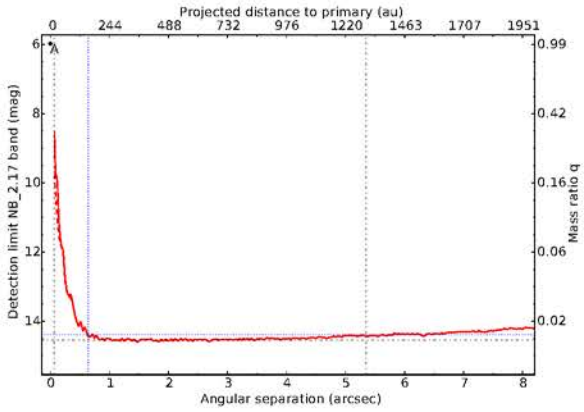


HIP30143

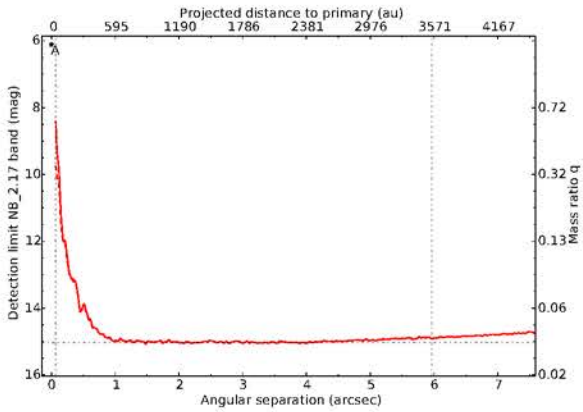


HIP30180

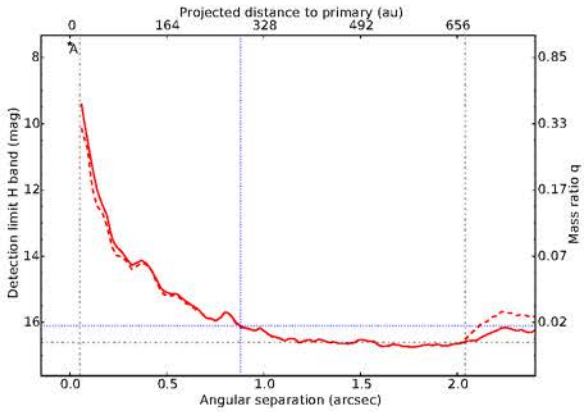


HIP30468

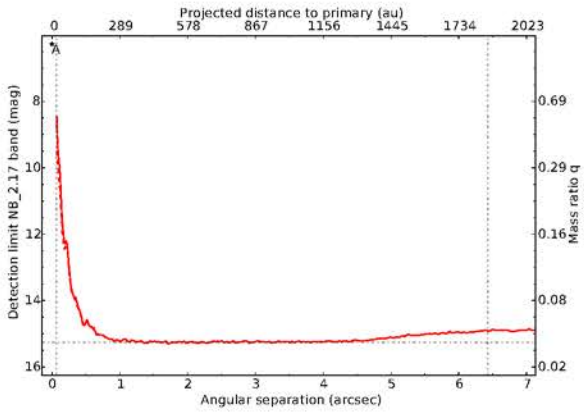


HIP30772

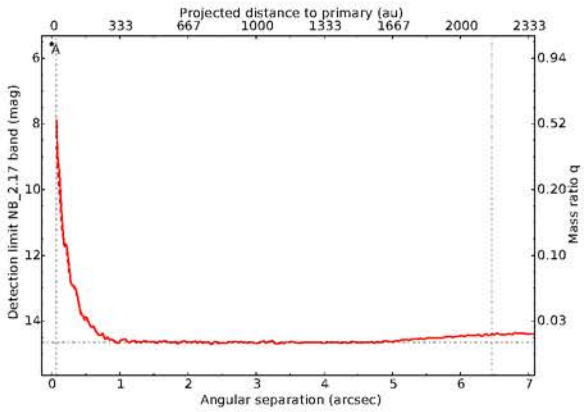

HIP31190

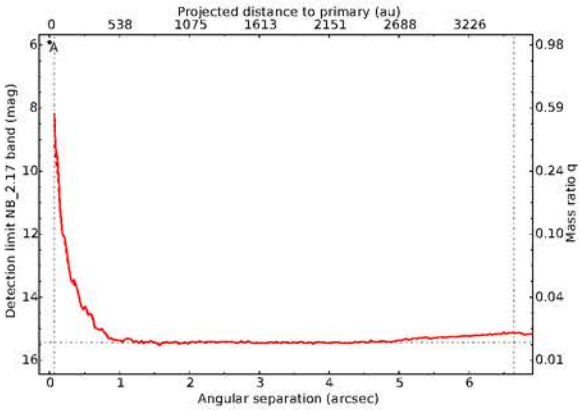


HIP31278

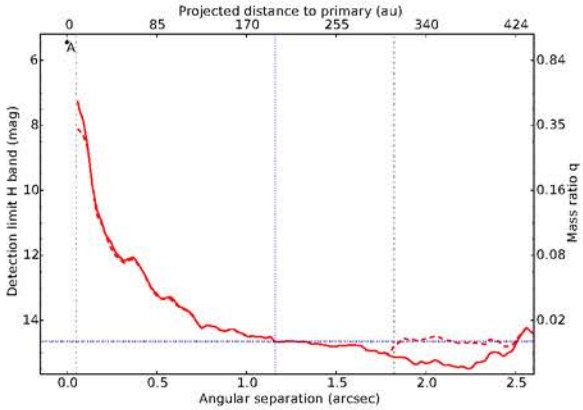


HIP32417

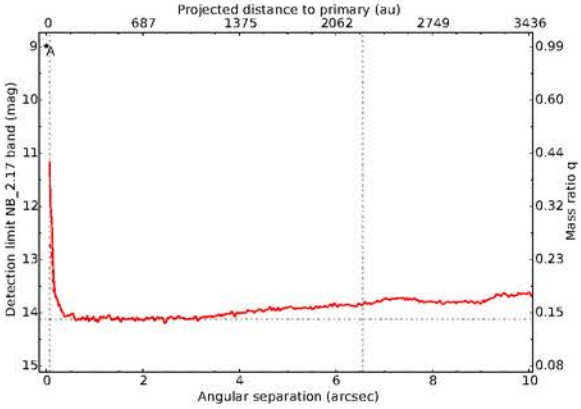


HIP32753

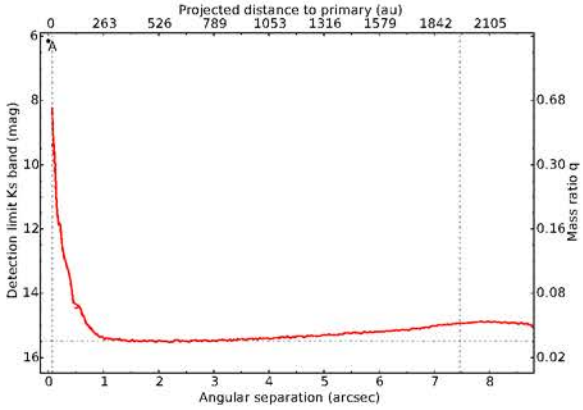


HIP32827

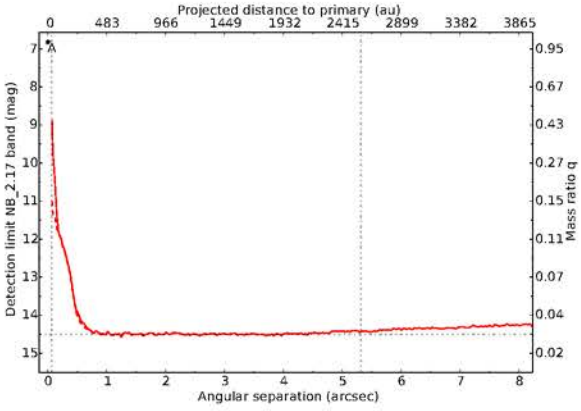


HIP32912

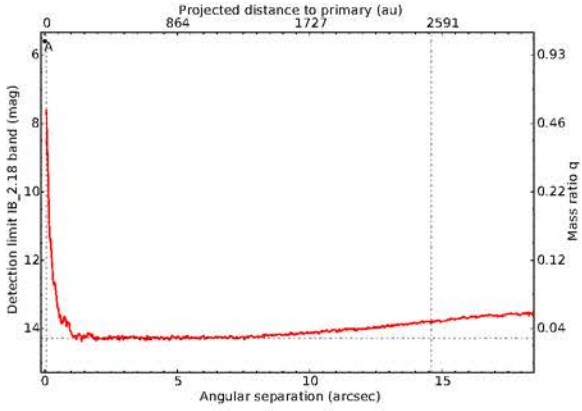


HIP33211

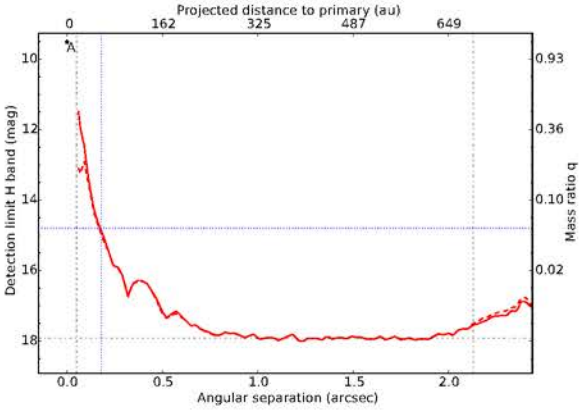


HIP33276

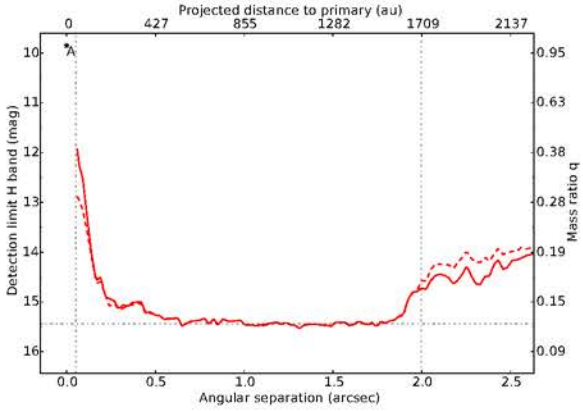

HIP33343

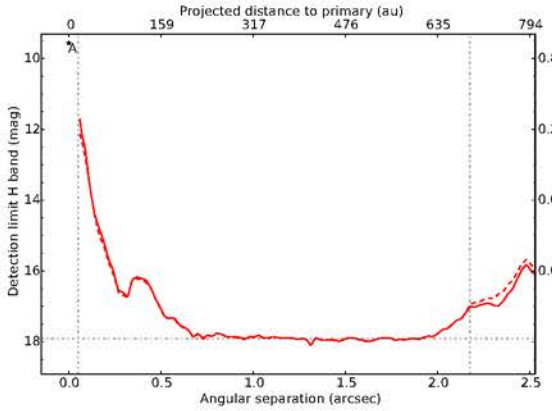


HIP33611

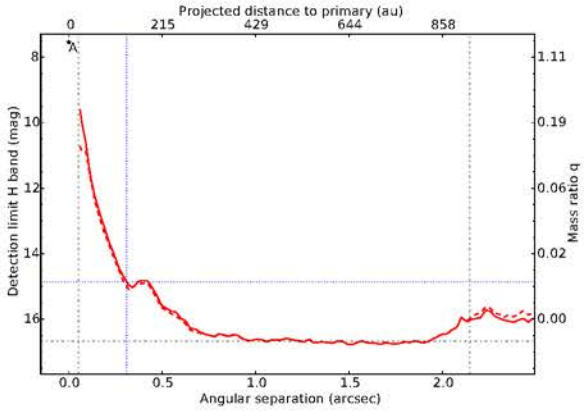


HIP33650

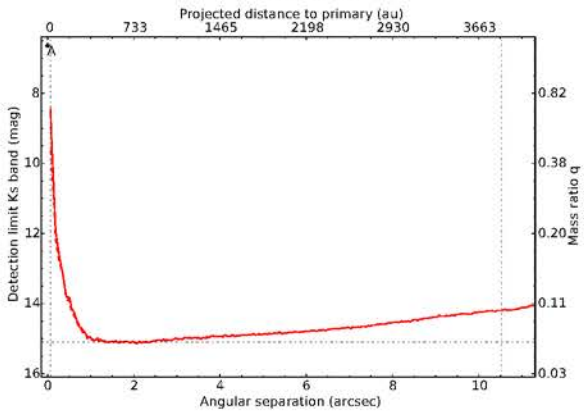


HIP33769

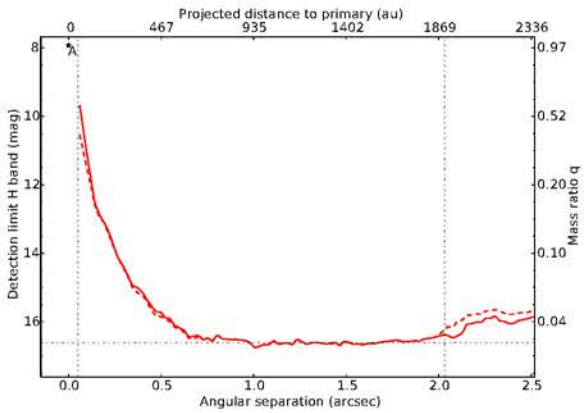


HIP33814

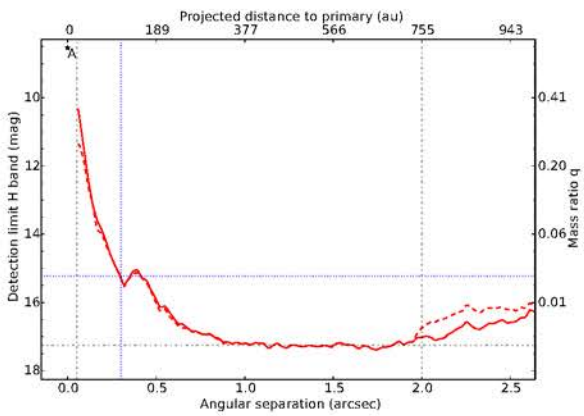


HIP33846

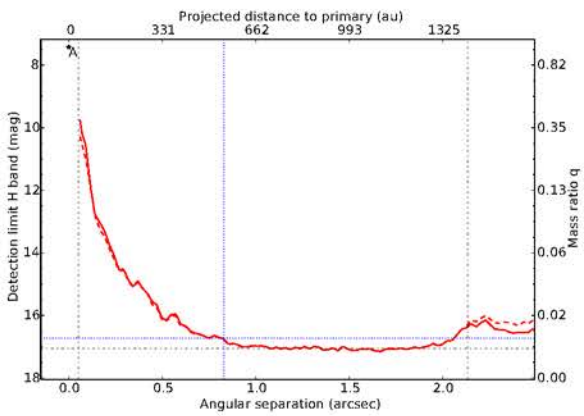


HIP34281

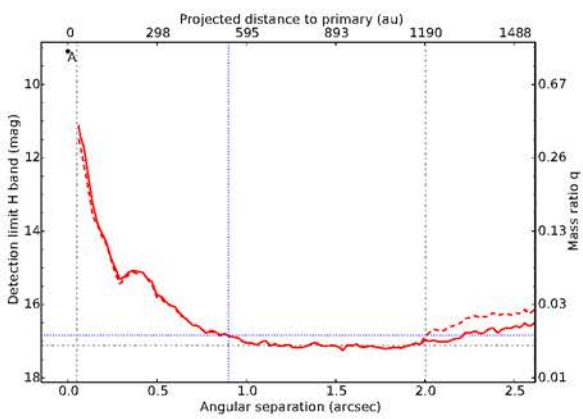


HIP34579

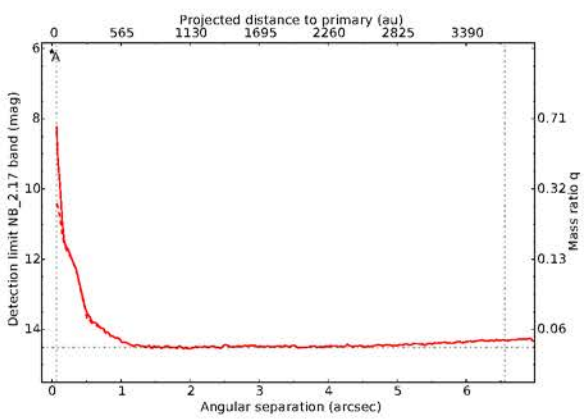

HIP34898

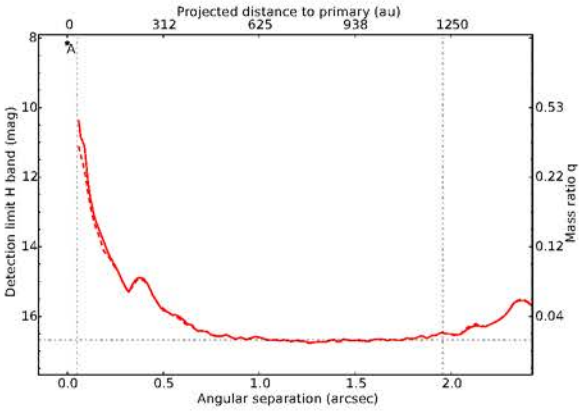


HIP34968

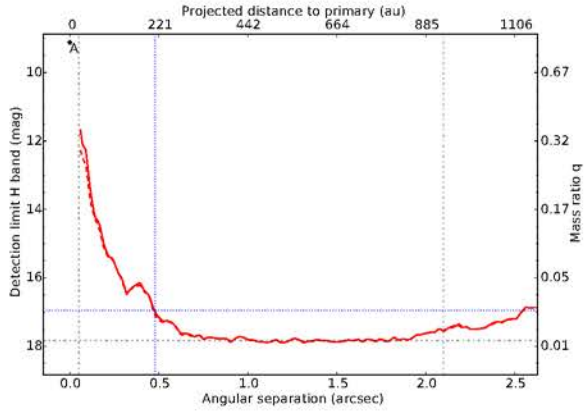


HIP35037

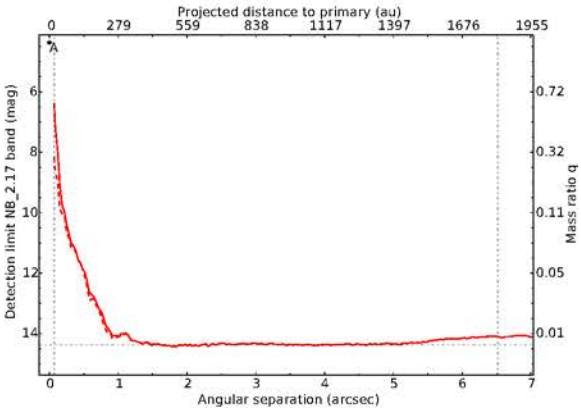


HIP35168

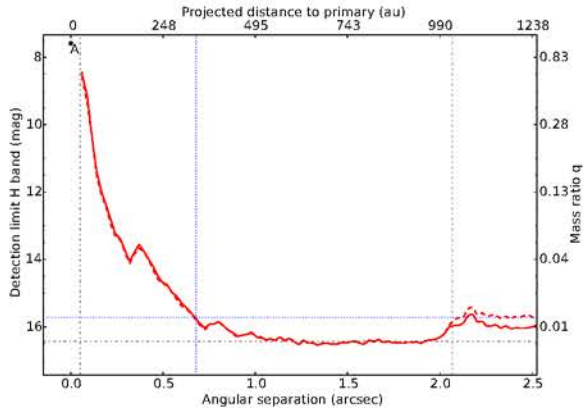


HIP35267

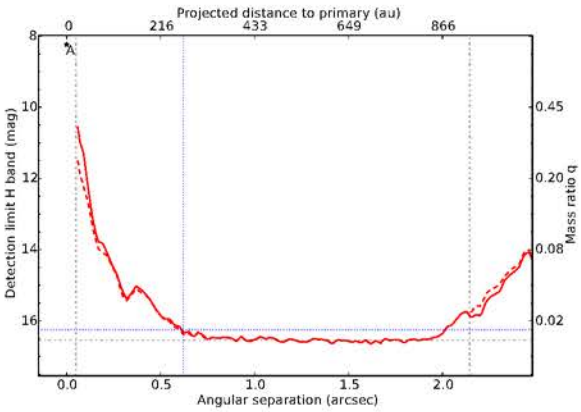


HIP35920

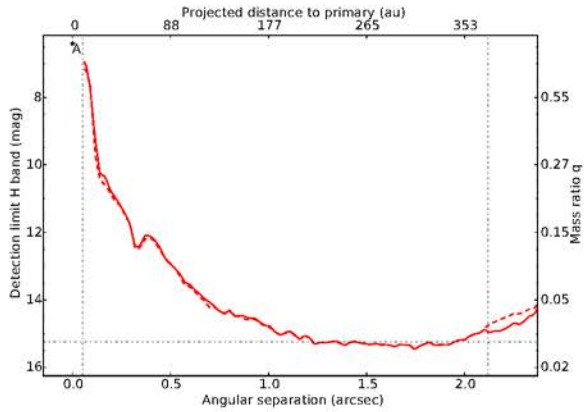


HIP35951

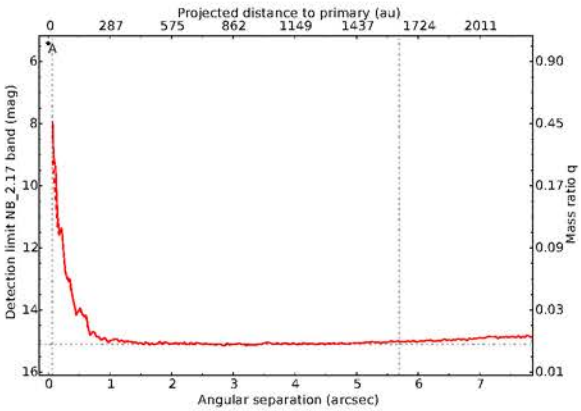


HIP36009

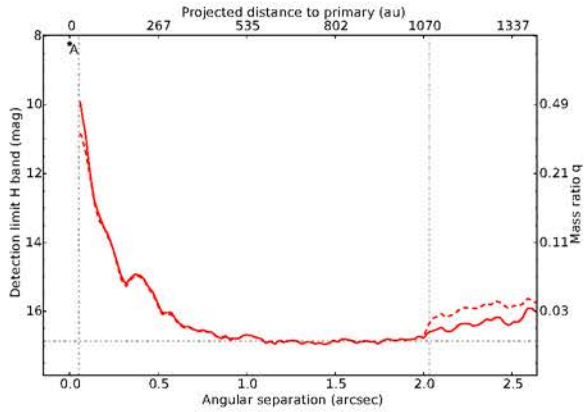

HIP36944

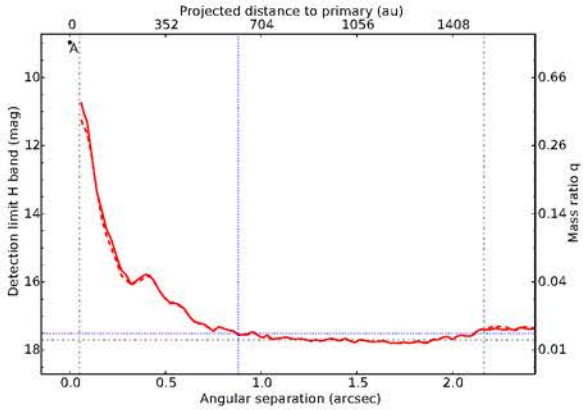


HIP37345

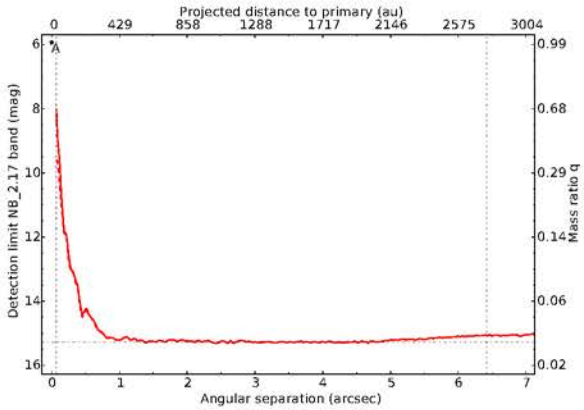


HIP37450

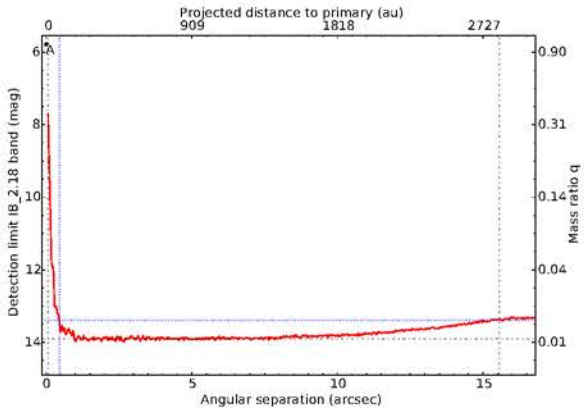


HIP37623

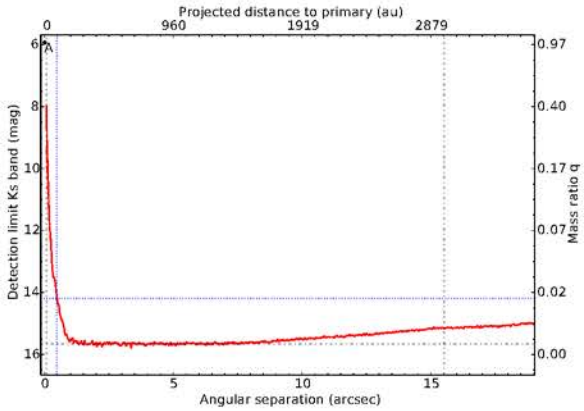


HIP37752

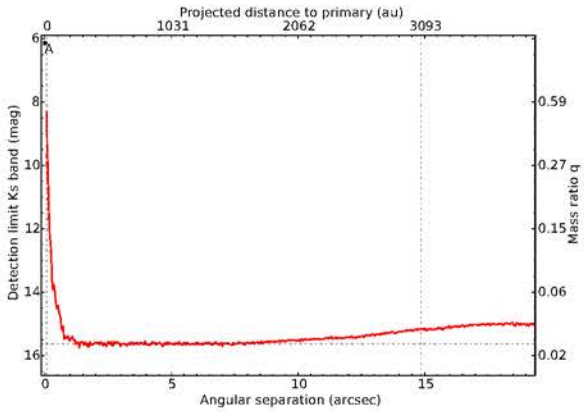


HIP38373

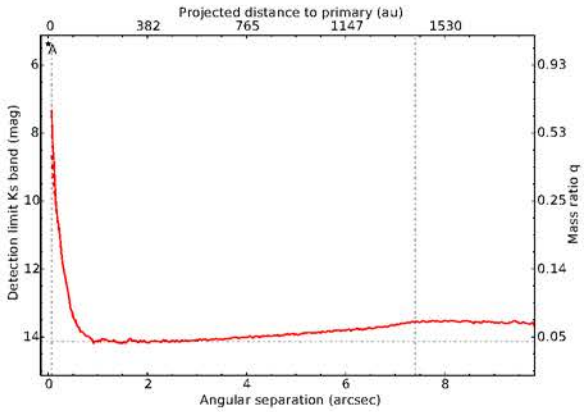


HIP38906

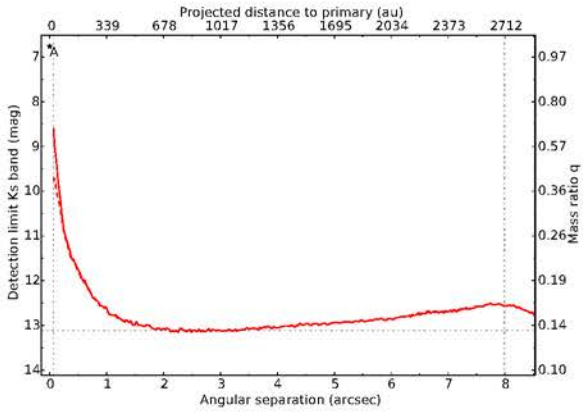


HIP39184

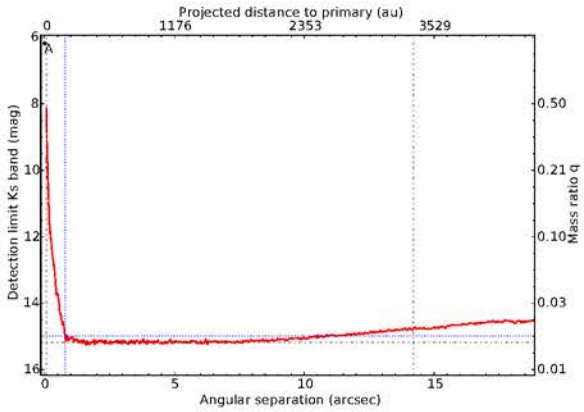

HIP39970

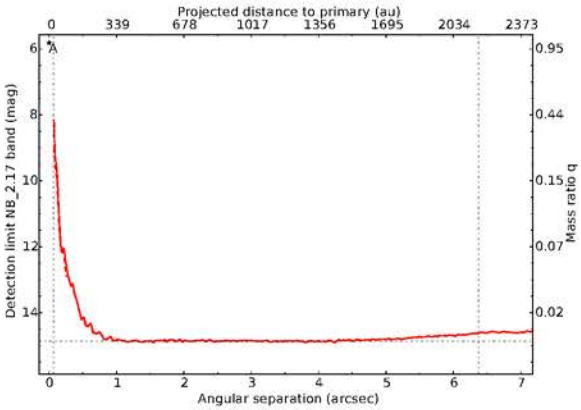


HIP40085

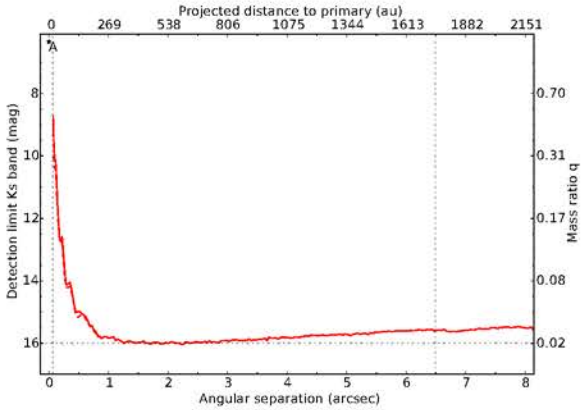


HIP40321

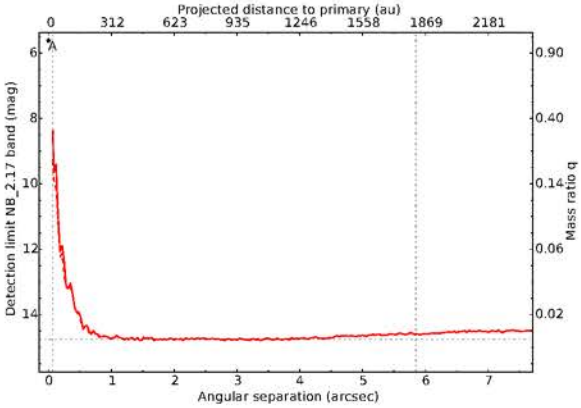


HIP40787

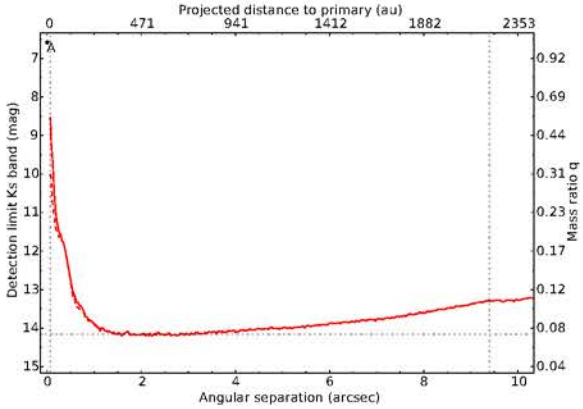


HIP40834

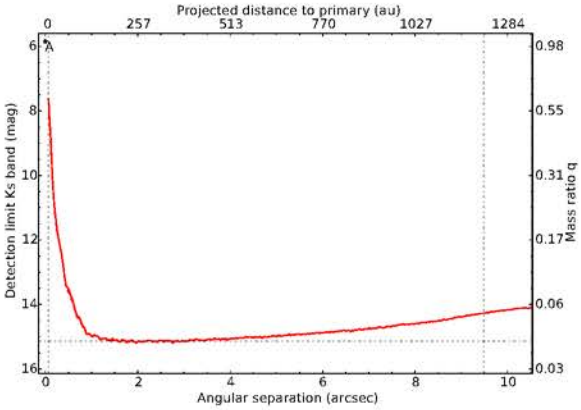


HIP41296

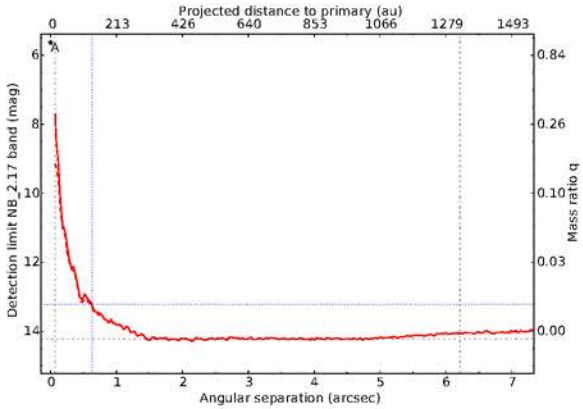


HIP41603

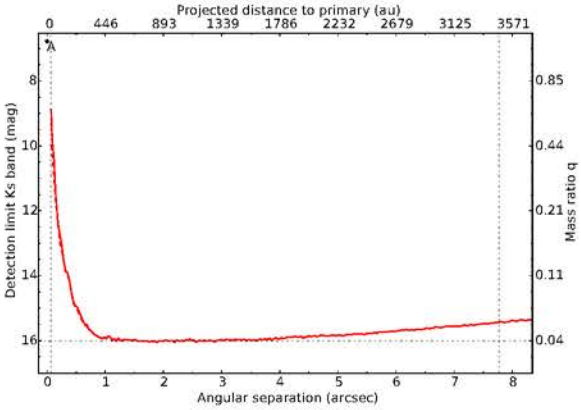


HIP41674

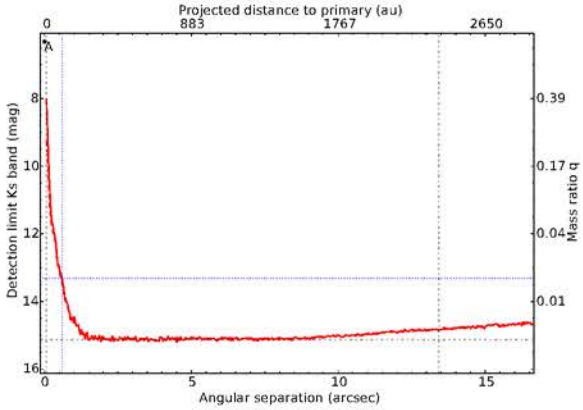

HIP42001

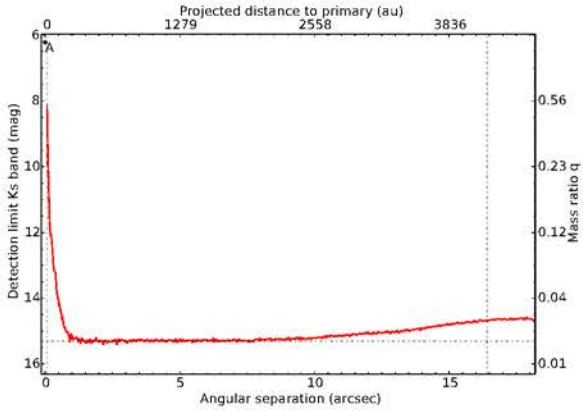


HIP42459

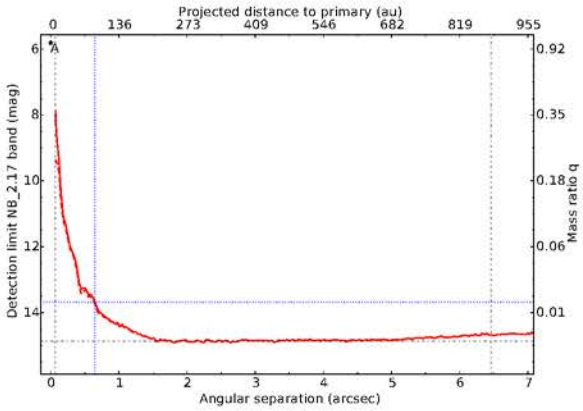


HIP42535

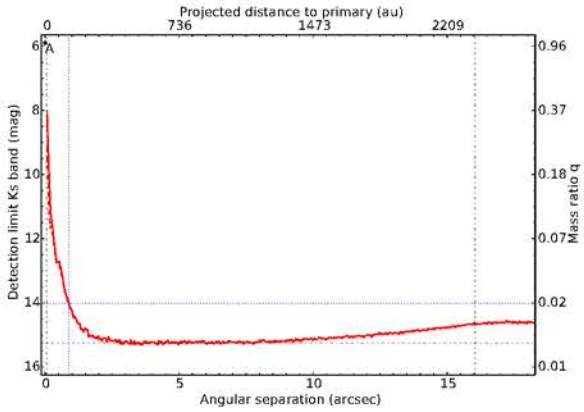


HIP42637

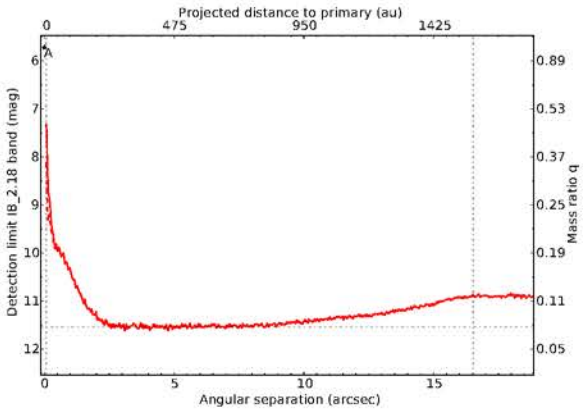


HIP43073

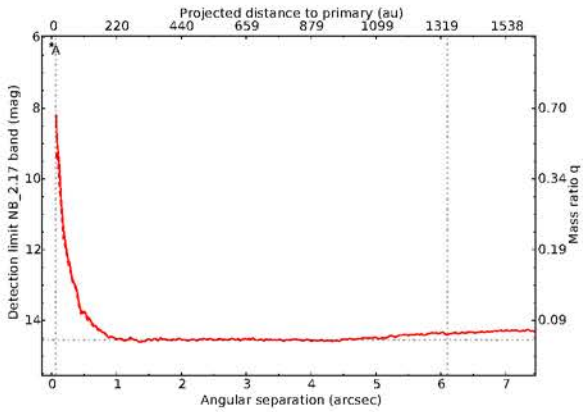


HIP43499

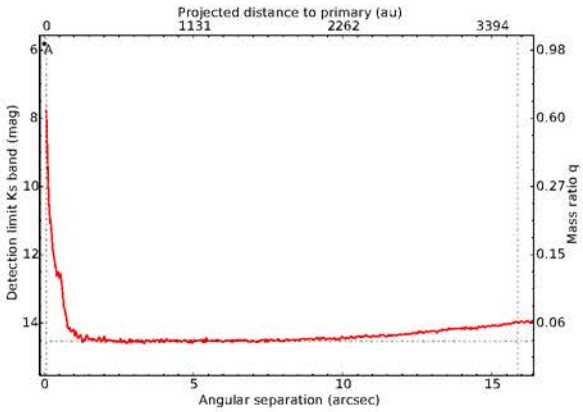


HIP45270

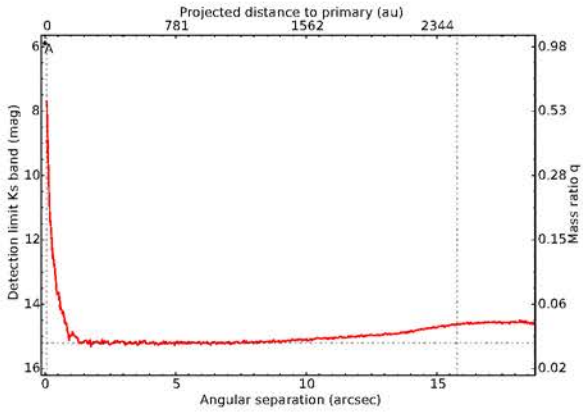


HIP45631

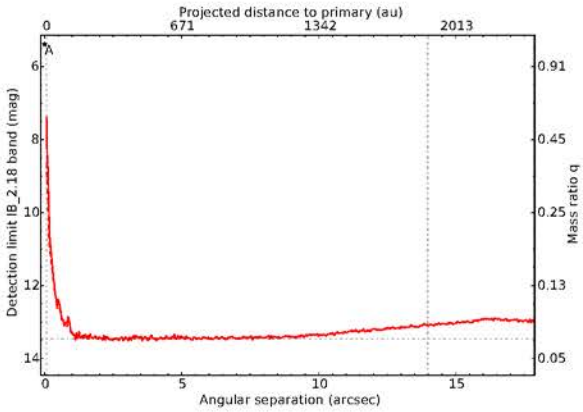

HIP45941

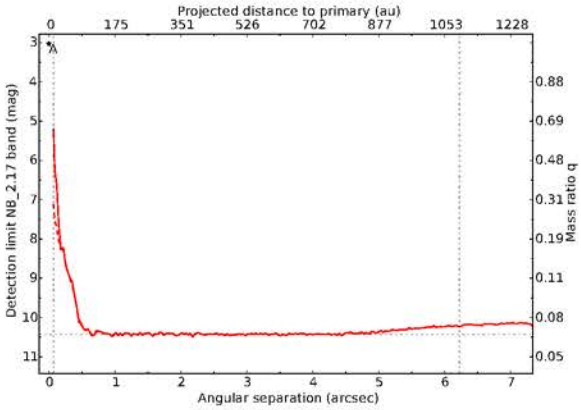


HIP47452

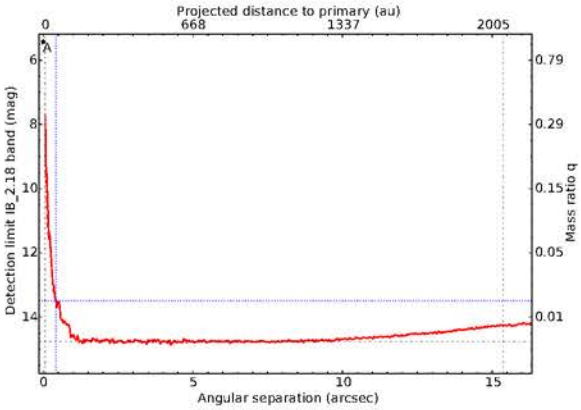


HIP47522

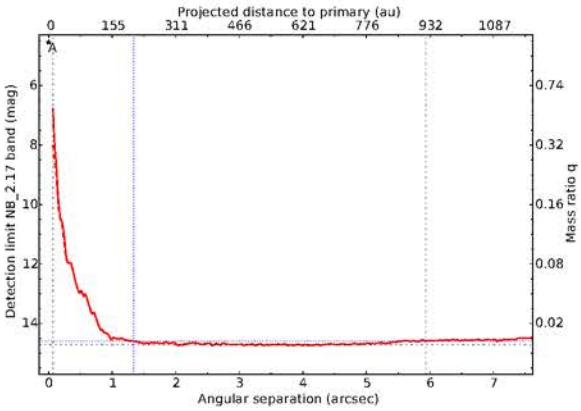


HIP48224

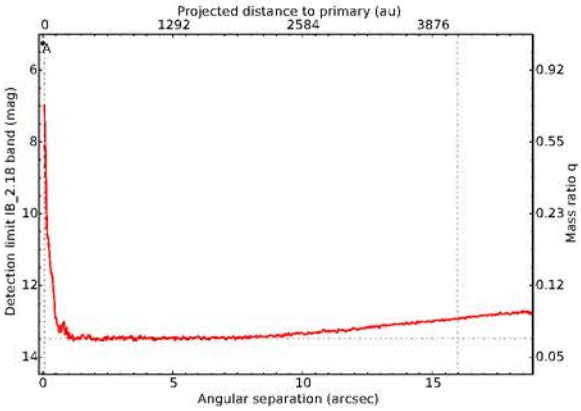


HIP50480

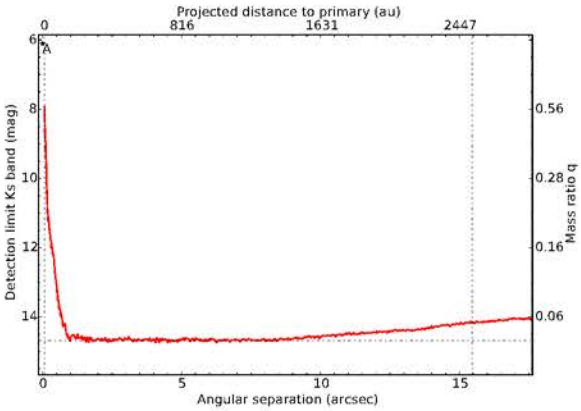


HIP51437

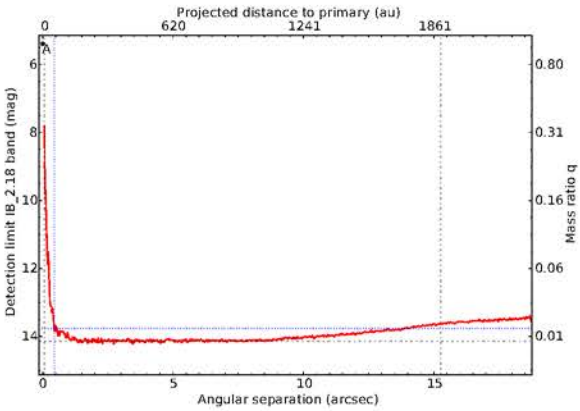


HIP51491

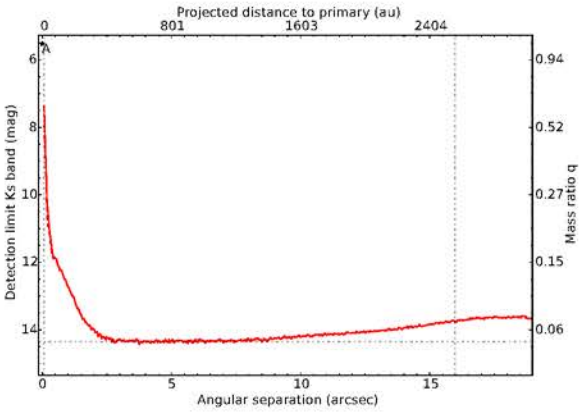


HIP52221

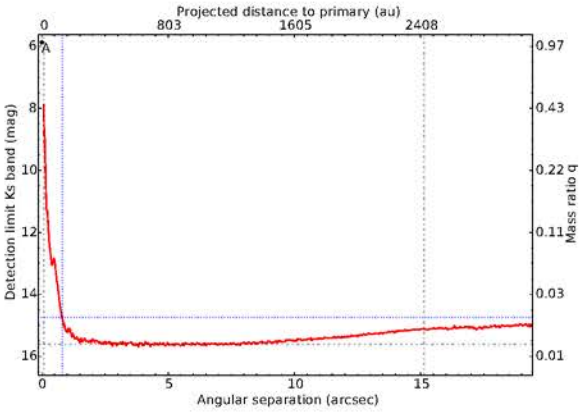

HIP53762

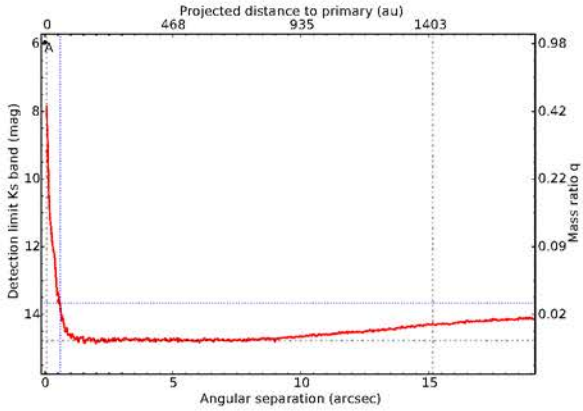


HIP54255

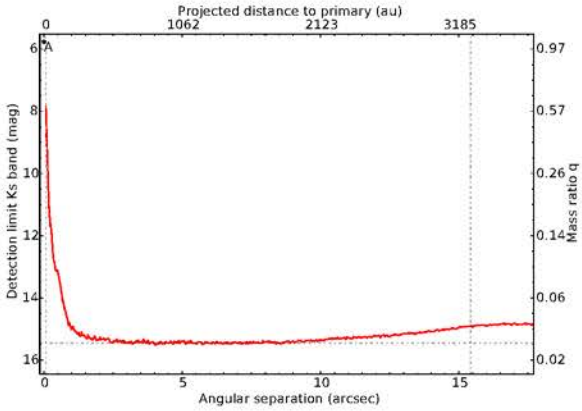


HIP54257

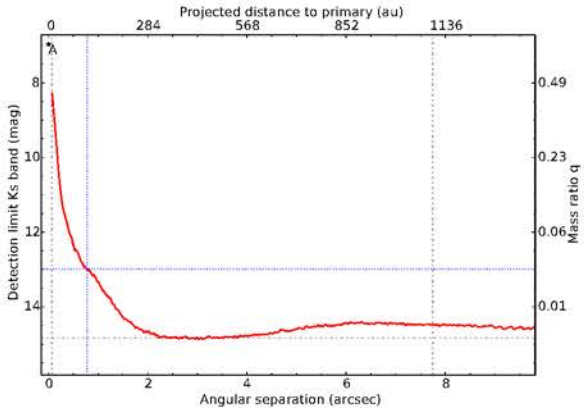


HIP54767

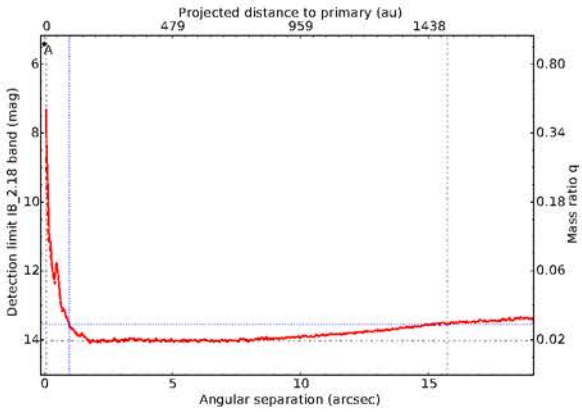


HIP55667

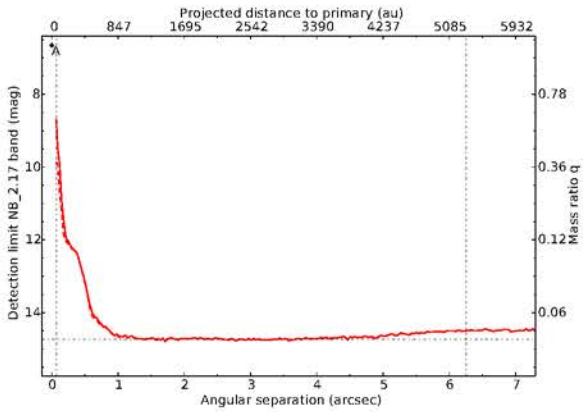


HIP56379

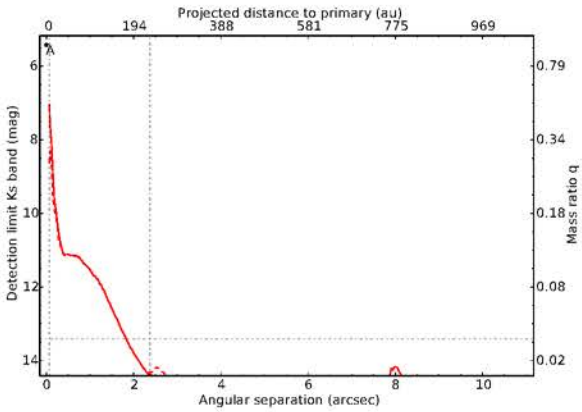


HIP56480

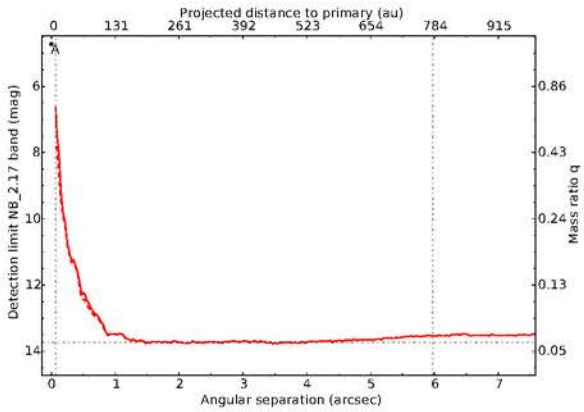


HIP57371

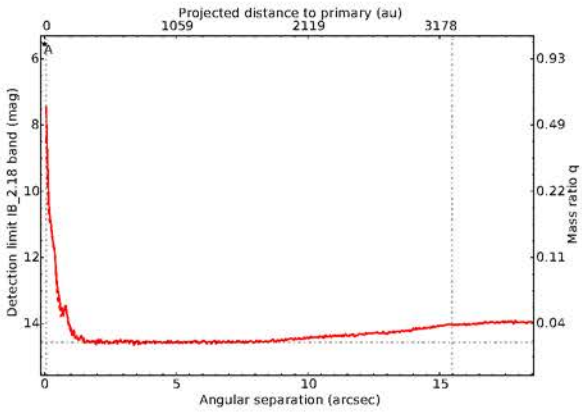

HIP58379

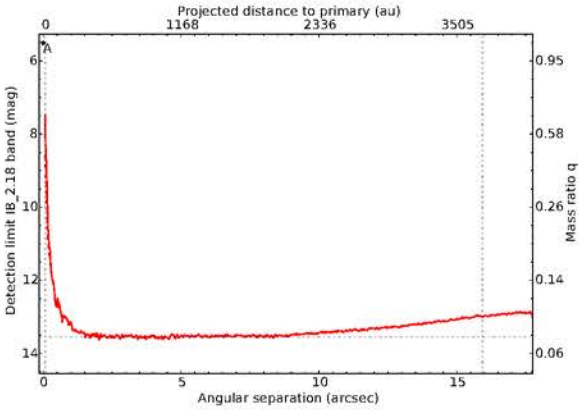


HIP58587

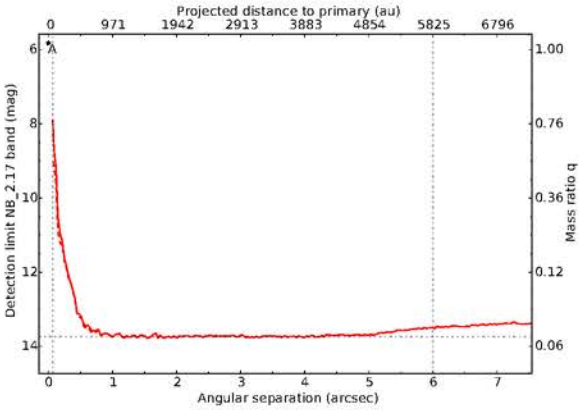


HIP58720

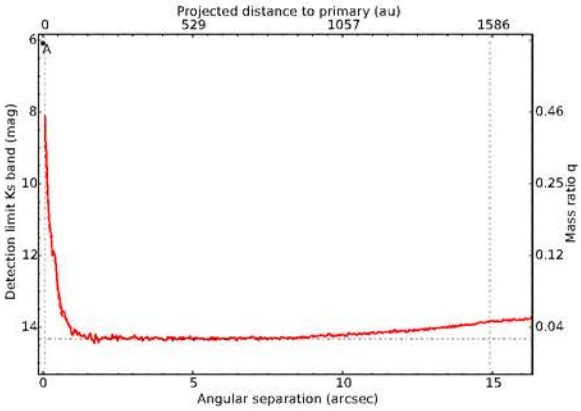


HIP59607

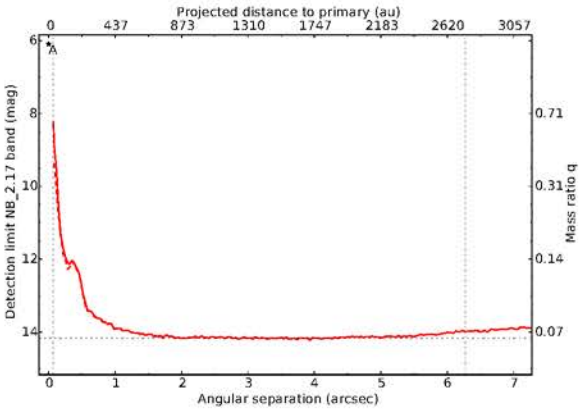


HIP60379

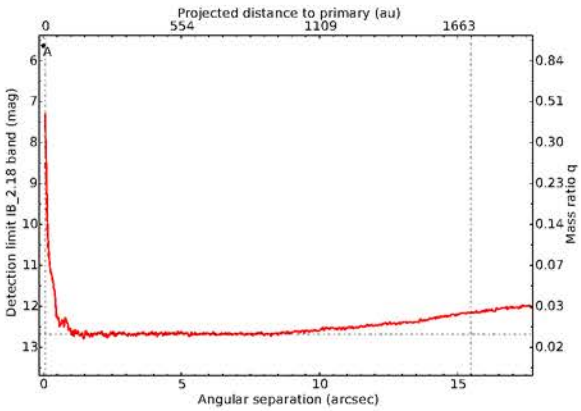


HIP60463

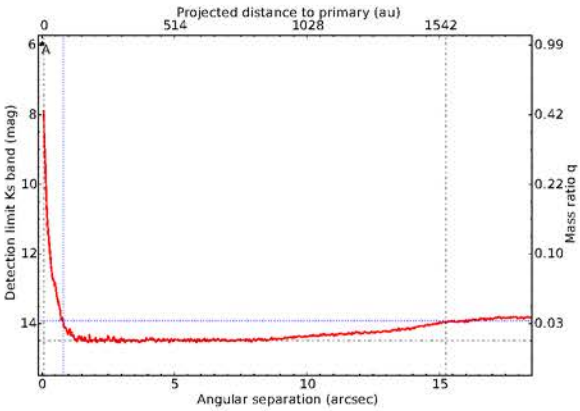


HIP60610

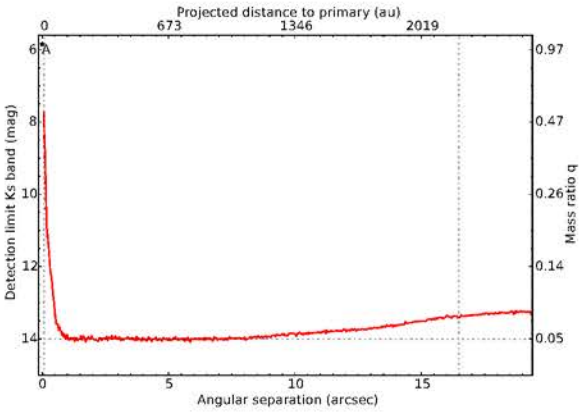


HIP60735

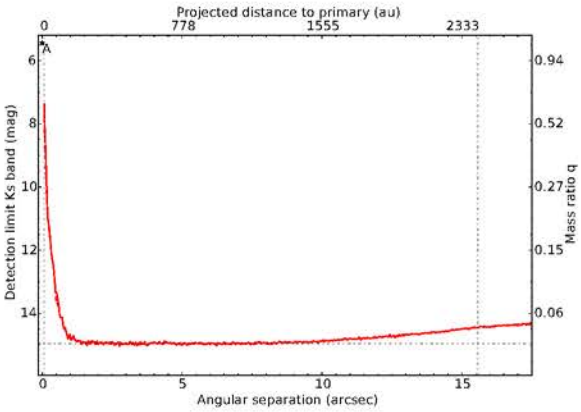

HIP60855

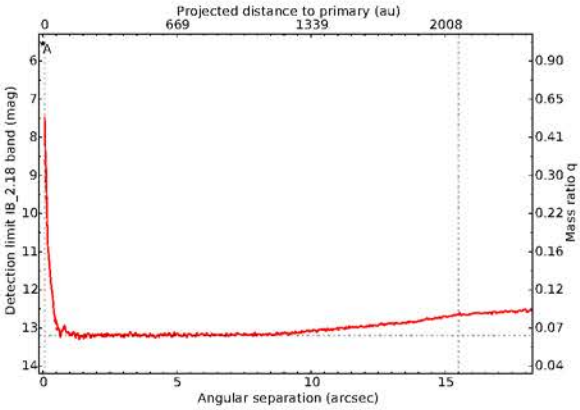


HIP61318

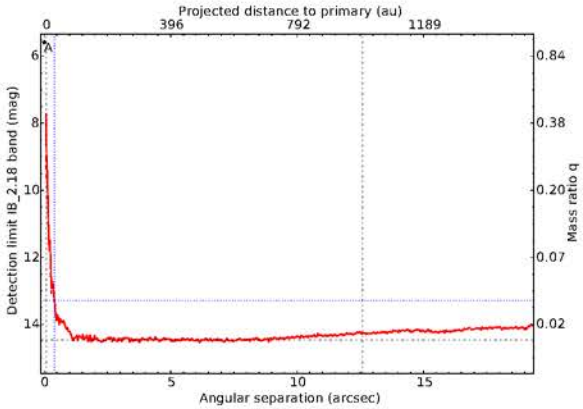


HIP61966

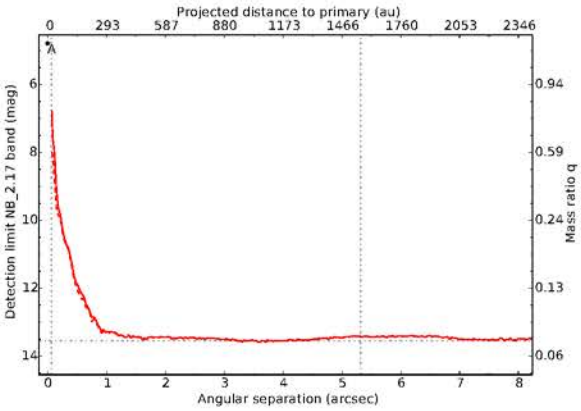


HIP62786

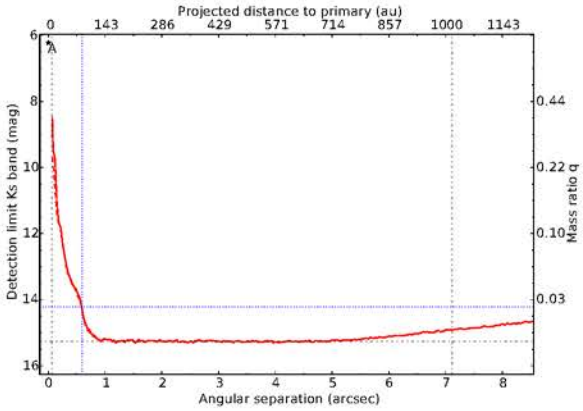


HIP63210

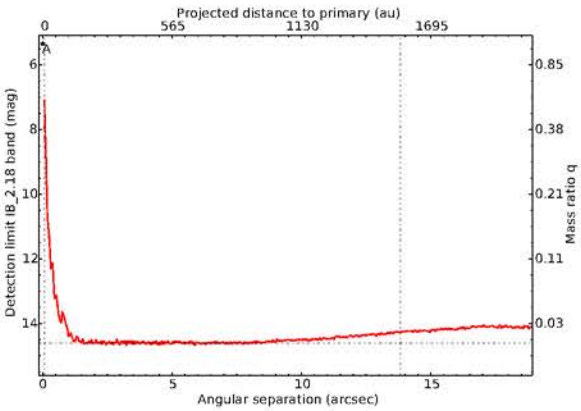


HIP65688

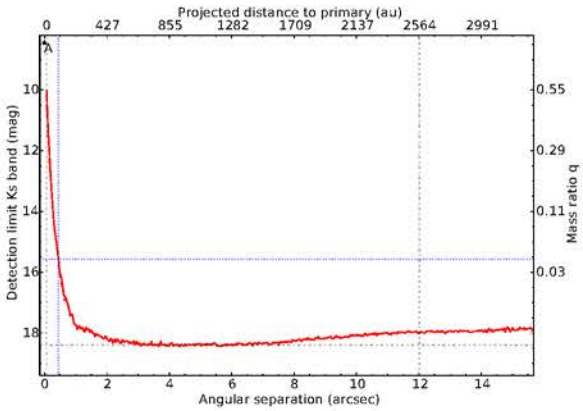


HIP66454

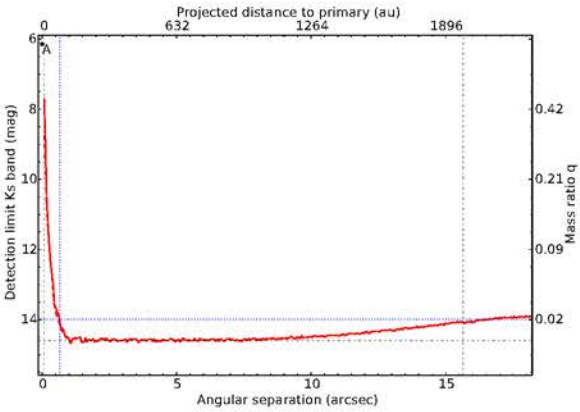


HIP66849

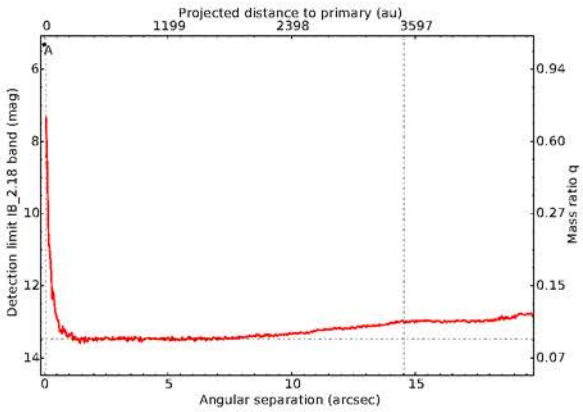

HIP68002

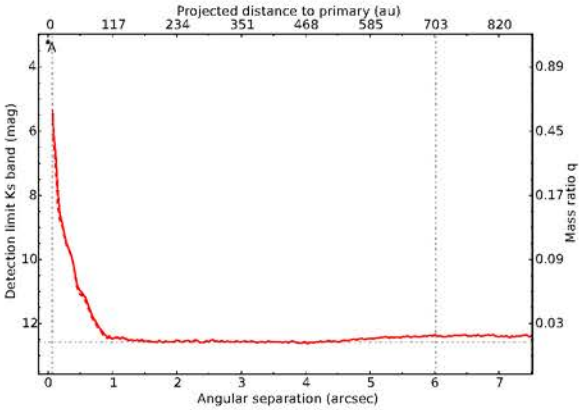


HIP68269

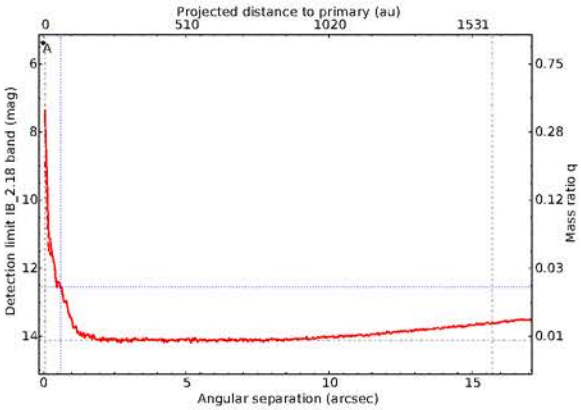


HIP69174

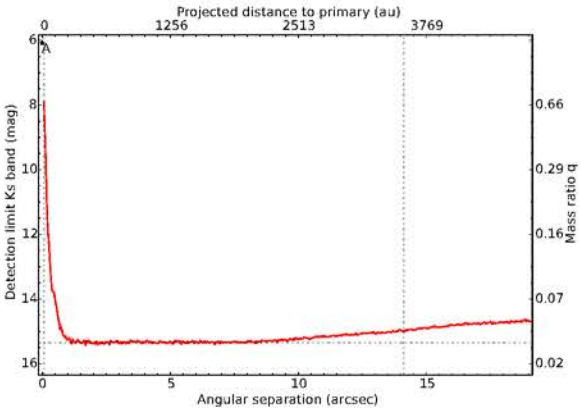


HIP69491

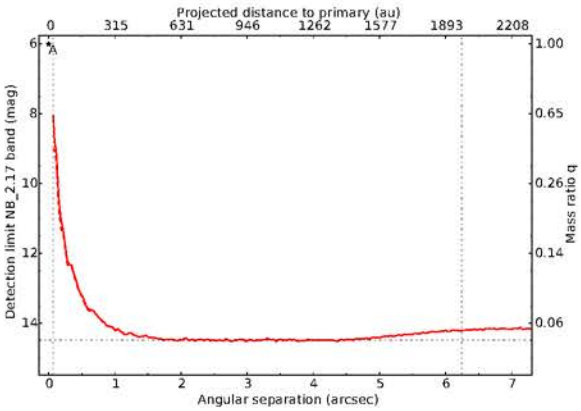


HIP69618

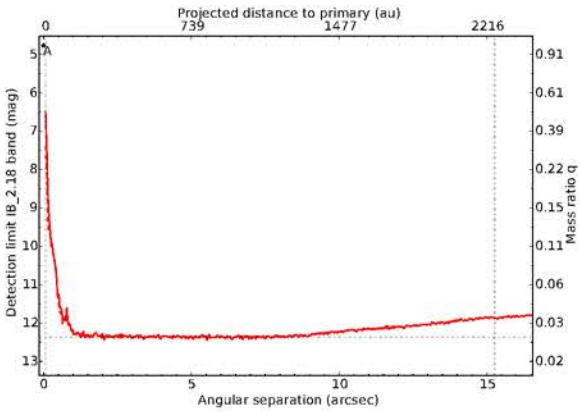


HIP69658

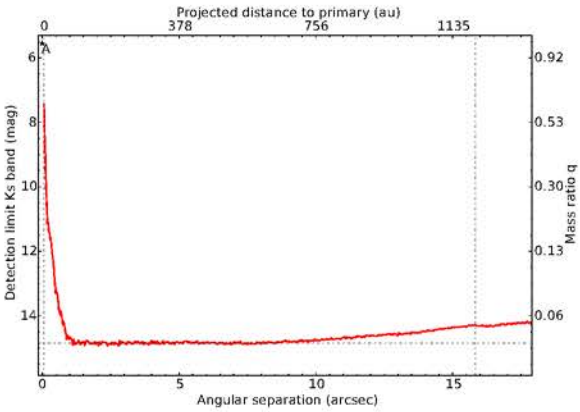


HIP70574

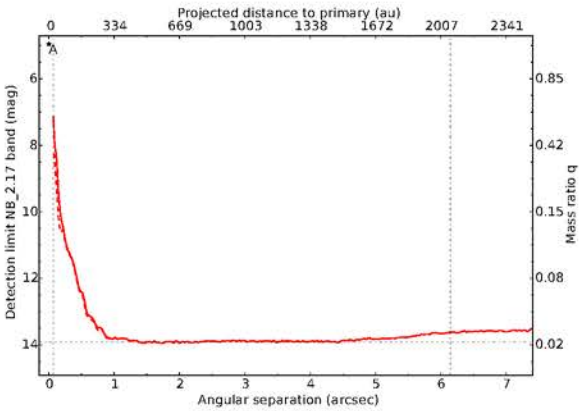


HIP71353

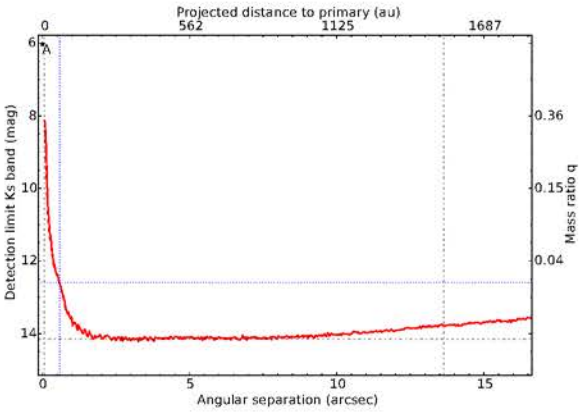

HIP71783

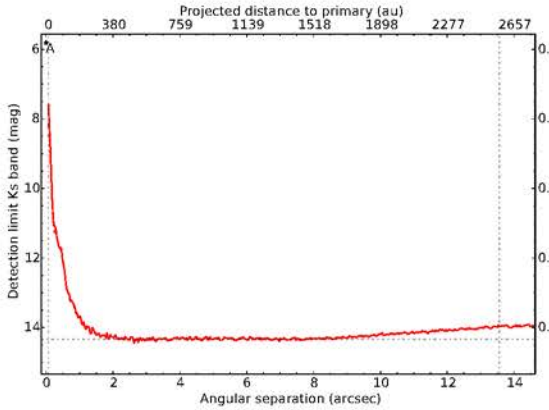


HIP71974

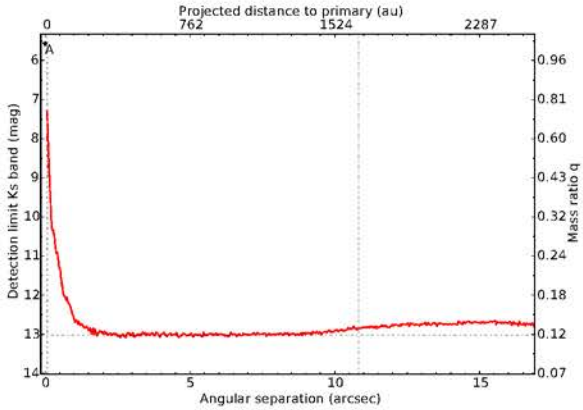


HIP72154

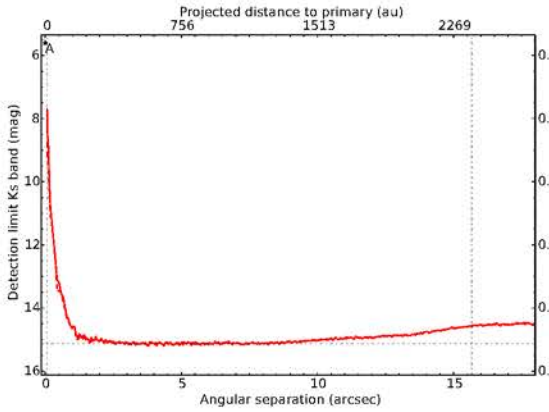


HIP73865

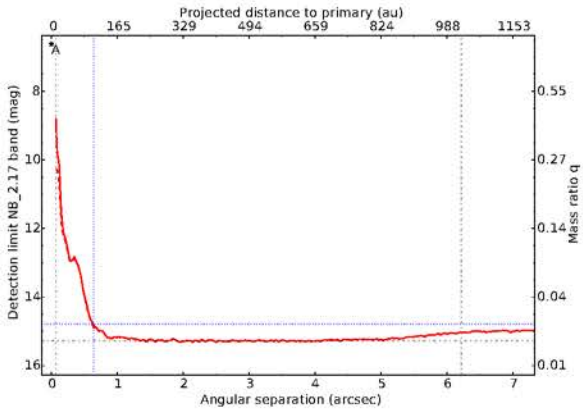


HIP76243

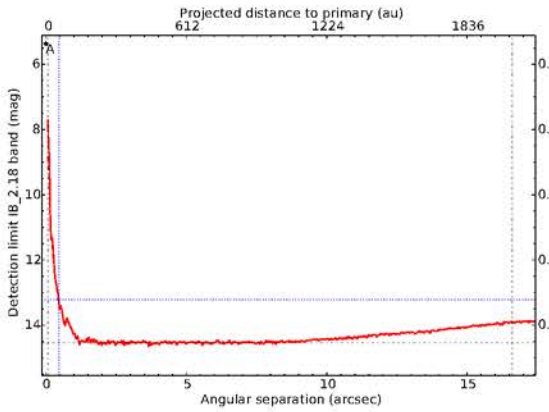


HIP76591

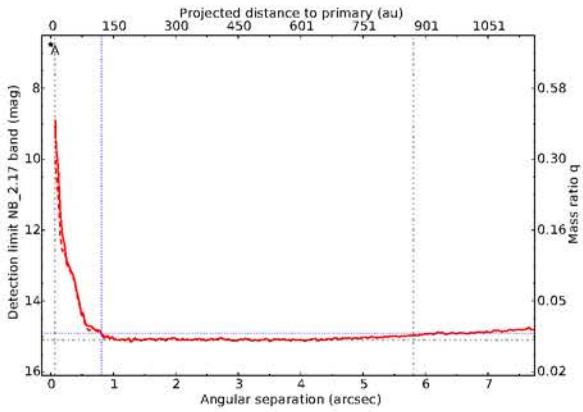


HIP77227

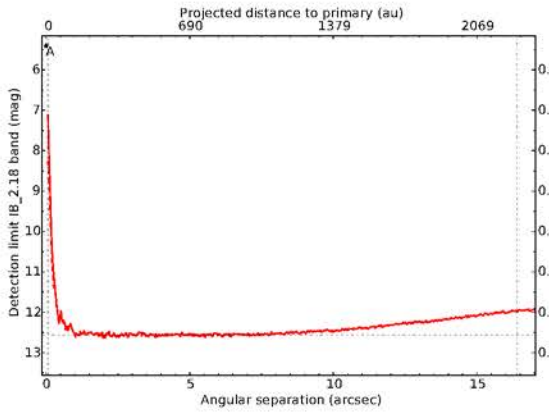


HIP77635

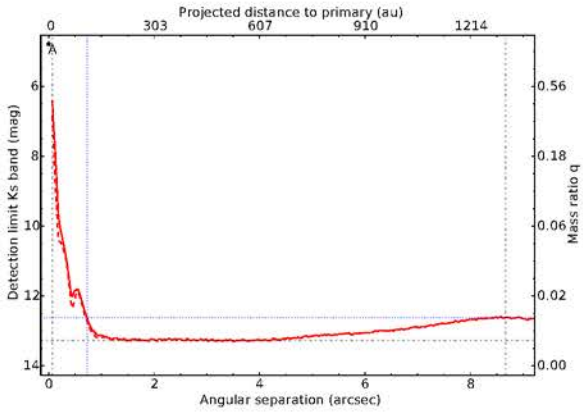

HIP77900

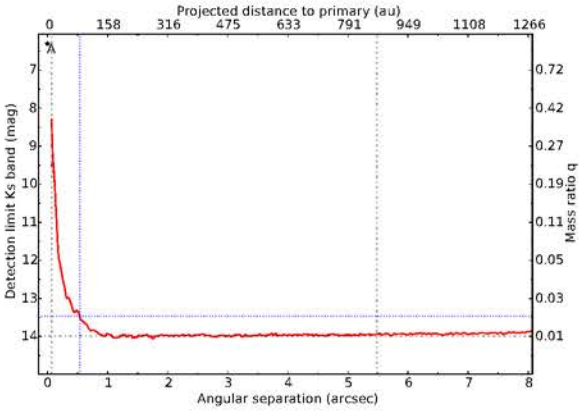


HIP78168

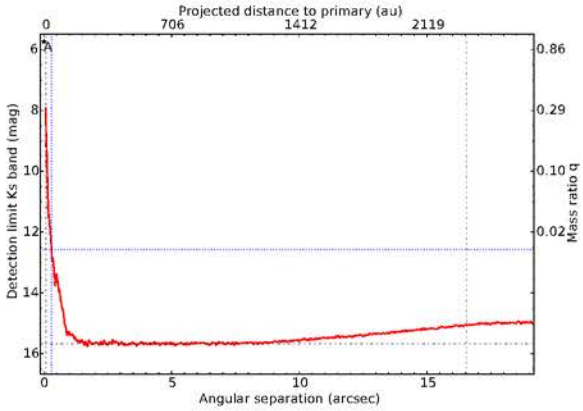


HIP78265

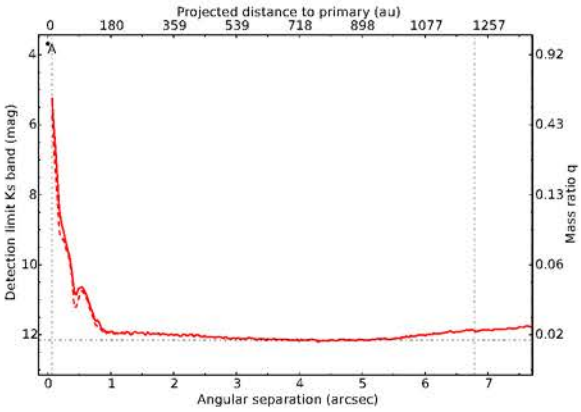


HIP78933

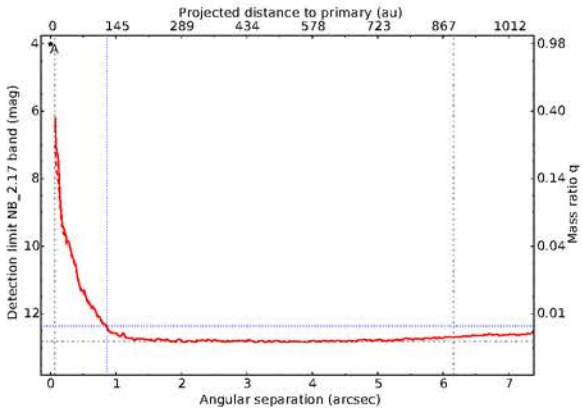


HIP79031

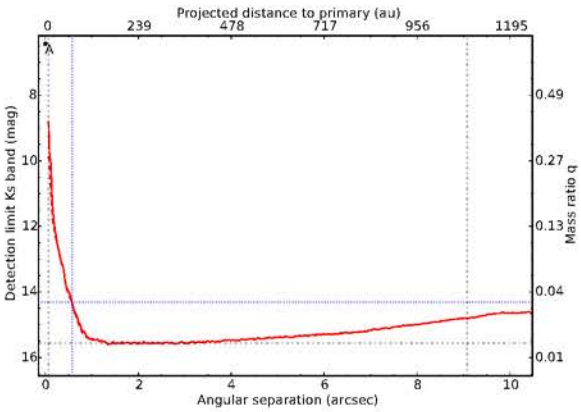


HIP79404

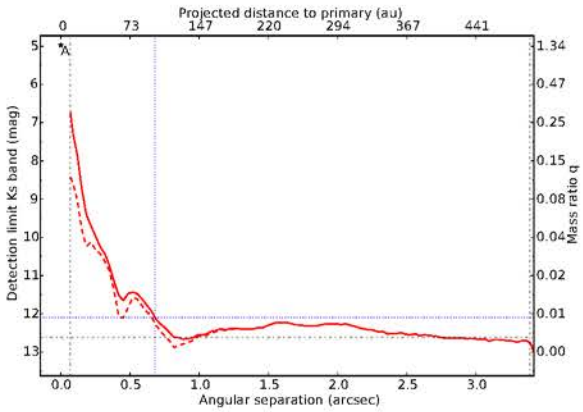


HIP79653

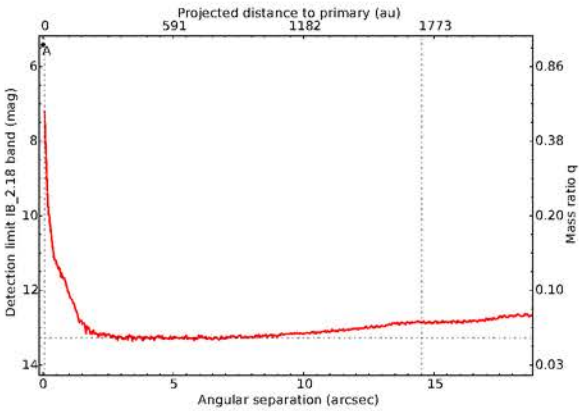


HIP80066

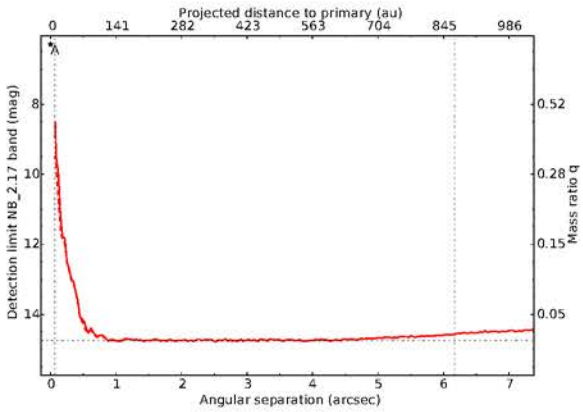

HIP81474

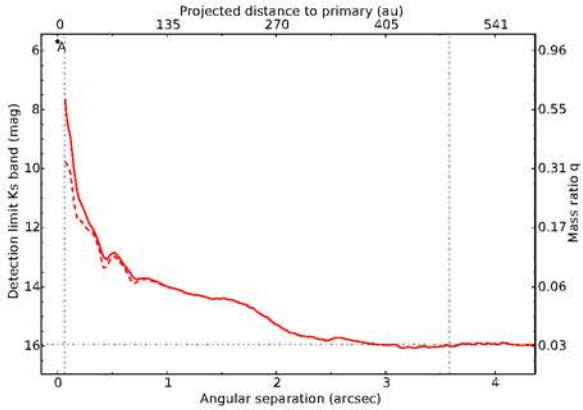


HIP85755

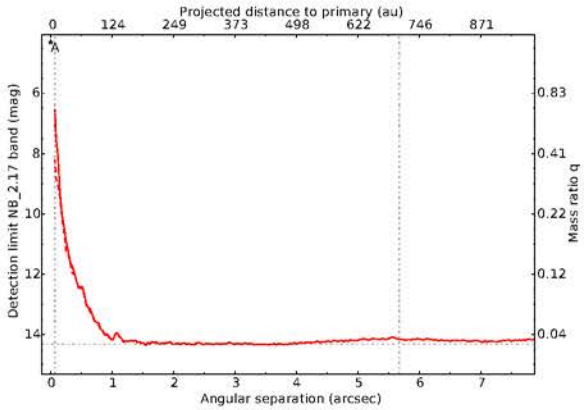


HIP89977

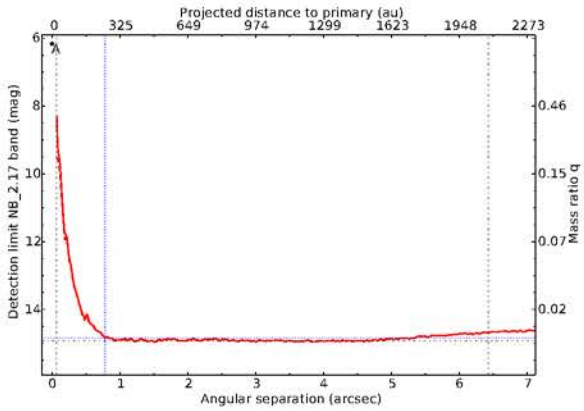


HIP90336

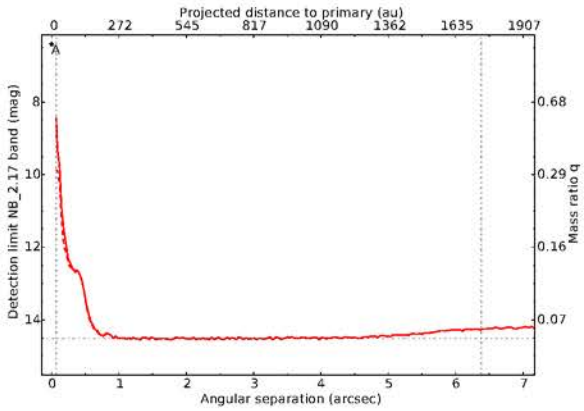


HIP93368

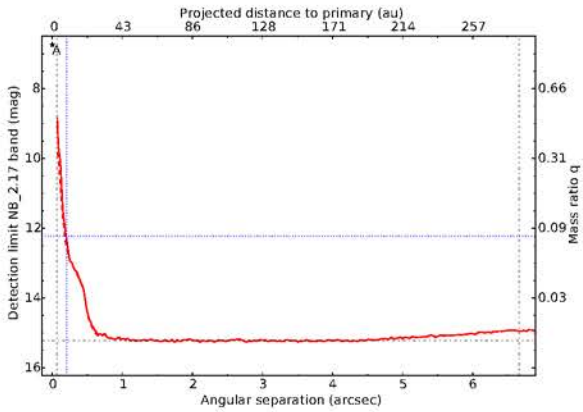


HIP93542

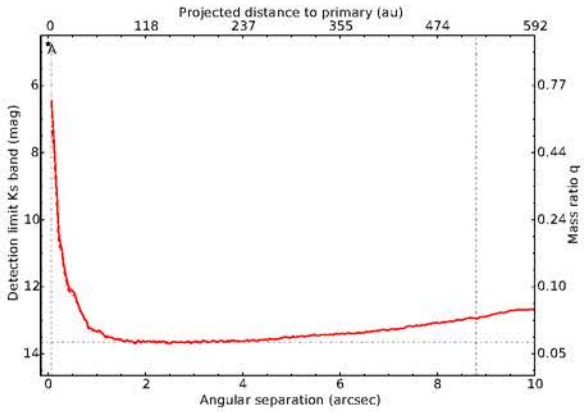


HIP93996

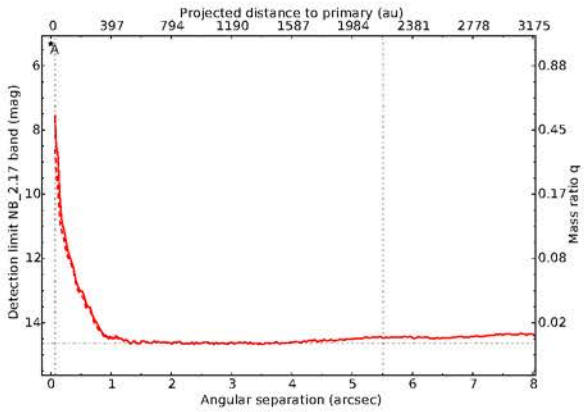


HIP95347

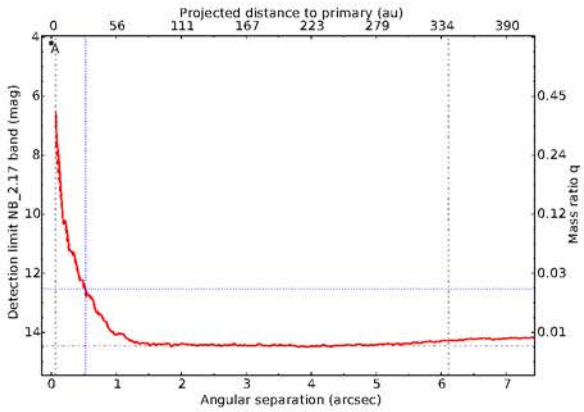

HIP97607

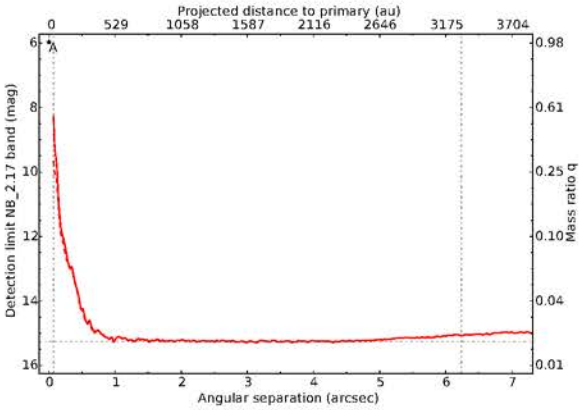


HIP102157

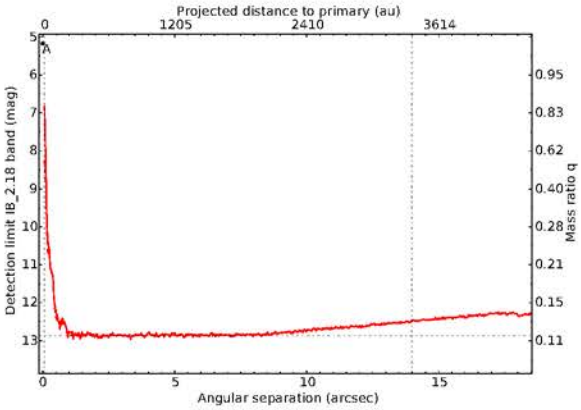


HIP105164

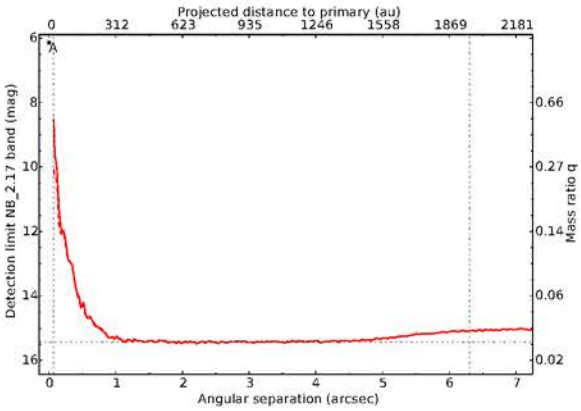


HIP108874

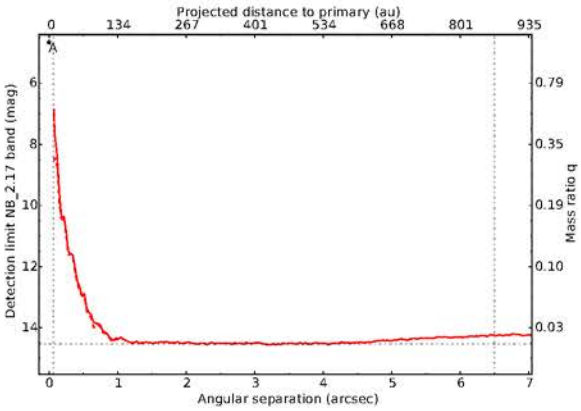


HIP109139

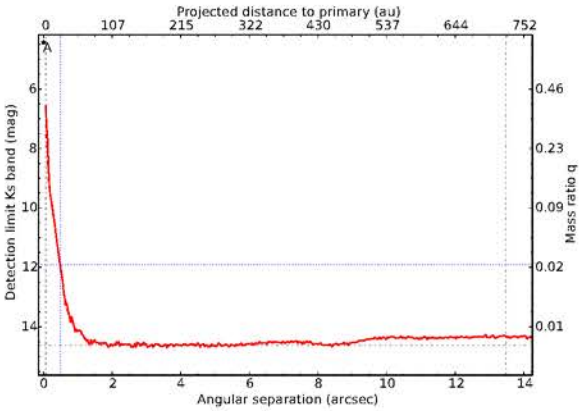


HIP110672

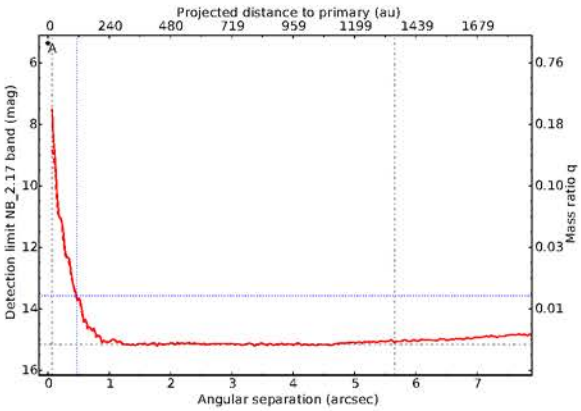


HIP112542

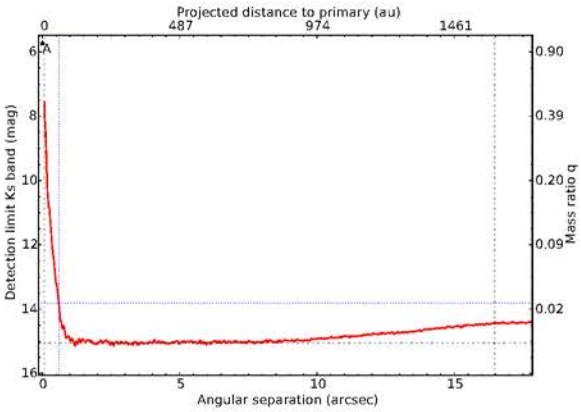


HIP112781

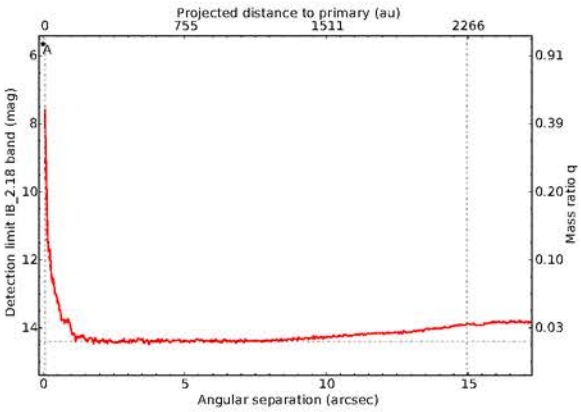

HIP113889

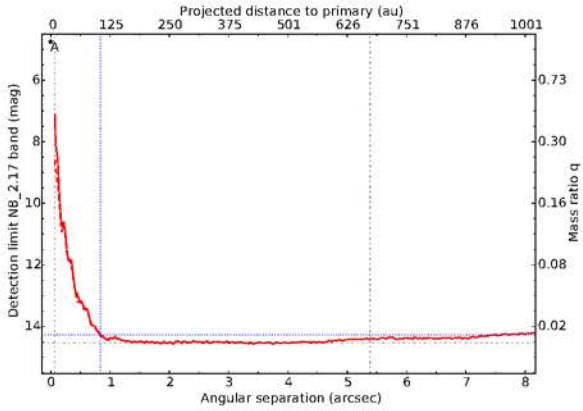


HIP117089

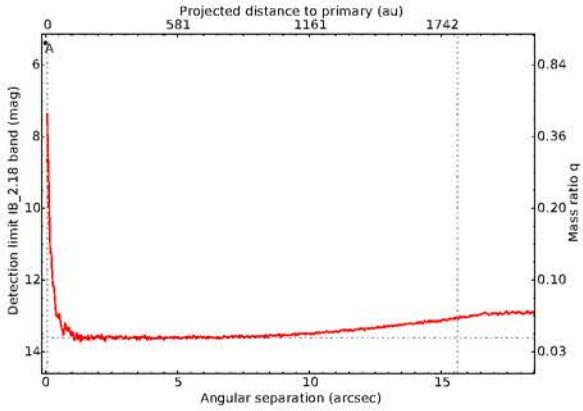


HIP117315

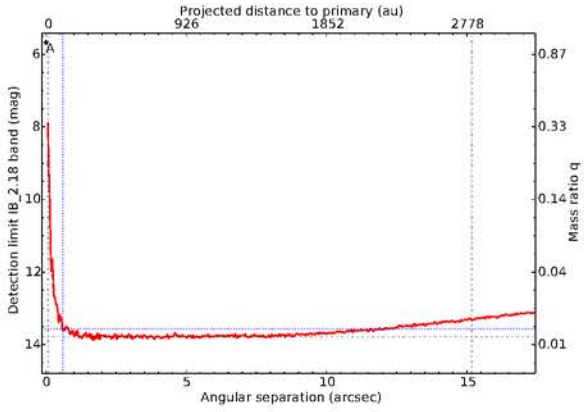


HIP117629

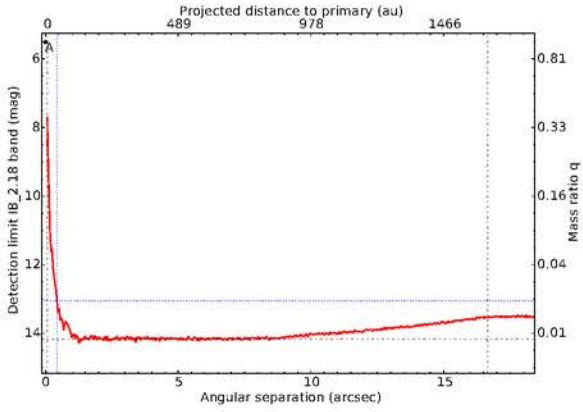


HIP120402

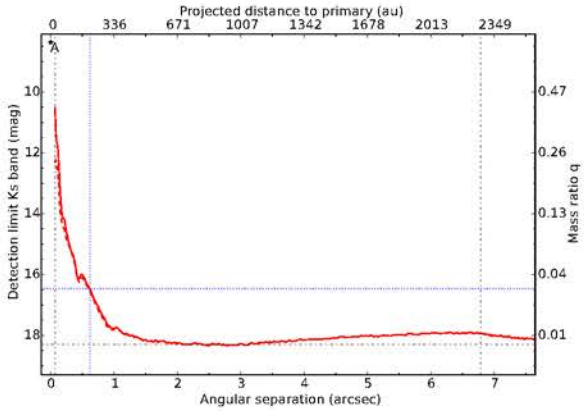


HIP120402

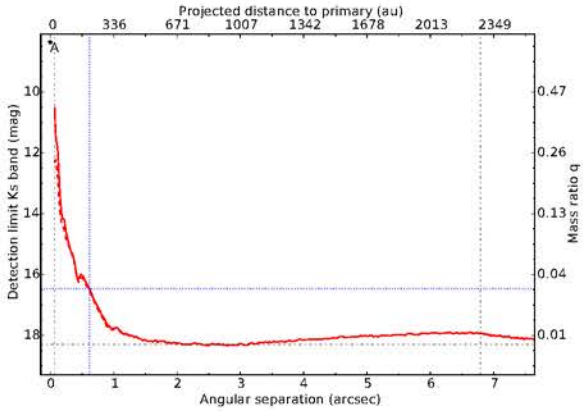

# B Publications List

## B.1 Scientific Articles

**Adam**, **C**. and Mugrauer, M. HIP 3678: a hierarchical triple stellar system in the centre of the planetary nebula NGC 246. *MNRAS*, 444:3459–3465, November 2014. doi: 10.1093/mnras/stu1677.

**Adam**, **C**., Neuhäuser, R., Mugrauer, M., Schmidt, J. G., and Schmidt, T. O. B. The low-mass companion of HIP 45314 (HR 3672). *MNRAS*, 433:402–411, July 2013. doi: 10.1093/mnras/stt733.

Chen, W. P., Hu, S. C.-L., Errmann, R., **Adam**, **C**., Baar, S., Berndt, A., Bukowiecki, L., Dimitrov, D. P., Eisenbeiß, T., Fiedler, S., Ginski, C., Gräfe, C., Guo, J. K., Hohle, M. M., Hsiao, H. Y., Janulis, R., Kitze, M., Lin, H. C., Lin, C. S., Maciejewski, G., Marka, C., Marschall, L., Moualla, M., Mugrauer, M., Neuhäuser, R., Pribulla, T., Raetz, S., Röll, T., Schmidt, E., Schmidt, J., Schmidt, T. O. B., Seeliger, M., Trepl, L., Briceño, C., Chini, R., Jensen, E. L. N., Nikogossian, E. H., Pandey, A. K., Sperauskas, J., Takahashi, H., Walter, F. M., Wu, Z.-Y., and Zhou, X. A Possible Detection of Occultation by a Proto-planetary Clump in GM Cephei. *ApJ*, 751:118, June 2012. doi: 10.1088/0004-637X/751/2/118.

Eisenbeiss, T., Ammler-von Eiff, M., Roell, T., Mugrauer, M., **Adam**, **C**., Neuhäuser, R., Schmidt, T. O. B., and Bedalov, A. The Hercules-Lyra association revisited. New age estimation and multiplicity study. *A&A*, 556:A53, August 2013. doi: 10.1051/0004-6361/201118362.

Errmann, R., Torres, G., Schmidt, T. O. B., Seeliger, M., Howard, A. W., Maciejewski, G., Neuhäuser, R., Meibom, S., Kellerer, A., Dimitrov, D. P., Dincel, B., Marka, C., Mugrauer, M., Ginski, C., **Adam**, **C**., Raetz, S., Schmidt, J. G., Hohle, M. M., Berndt, A., Kitze, M., Trepl, L., Moualla, M., Eisenbeiß, T., Fiedler, S., Dathe, A., Graefe, C., Pawellek, N., Schreyer, K., Kjurkchieva, D. P., Radeva, V. S., Yotov, V., Chen, W. P., Hu, S. C.-L., Wu, Z.-Y., Zhou, X., Pribulla, T., Budaj, J., Vaňko, M., Kundra, E., Hambálek, Ľ., Krushevska, V., Bukowiecki, Ł., Nowak, G., Marschall, L., Terada, H., Tomono, D., Fernandez, M., Sota, A., Takahashi, H., Oasa, Y., Briceño, C., Chini, R., and Broeg, C. H. Investigation of a transiting planet candidate in Trumpler 37: an astrophysical false positive eclipsing spectroscopic binary star. *ArXiv e-prints*, March 2014.

Fritzewski, D. J., Kitze, M., Mugrauer, M., Neuhäuser, R., **Adam**, **C**., Briceño, C., Buder, S., Butterley, T., Chen, W.-P., Dinçel, B., Dhillon, V. S., Errmann, R., Garai, Z., Gilbert, H. F. W., Ginski, C., Greif, J., Hardy, L. K., Hernández, J., Huang, P. C., Kellerer, A., Kundra, E., Littlefair, S. P., Mallonn, M., Marka, C., Pannicke, A., Pribulla, T., Raetz,

S., Schmidt, J. G., Schmidt, T. O. B., Seeliger, M., Wilson, R. W., and Wolf, V. Long-term photometry of IC 348 with the Young Exoplanet Transit Initiative network. *MNRAS*, 462:2396–2417, November 2016a. doi: 10.1093/mnras/stw1797.

Fritzewski, D. J., Kitze, M., Mugrauer, M., Neuhäuser, R., **Adam**, **C**., Briceño, C., Buder, S., Butterley, T., Chen, W.-P., Dinçel, B., Dhillon, V. S., Errmann, R., Garai, Z., Gilbert, H. F. W., Ginski, C., Greif, J., Hardy, L. K., Hernández, J., Huang, P. C., Kellerer, A., Kundra, E., Littlefair, S. P., Mallonn, M., Marka, C., Pannicke, A., Pribulla, T., Raetz, S., Schmidt, J. G., Schmidt, T. O. B., Seeliger, M., Wilson, R. W., and Wolf, V. Long-Term Photometry of IC 348 with the YETI Network. *ArXiv e-prints*, July 2016b.

Fritzewski, D. J., Kitze, M., Mugrauer, M., Neuhauser, R., **Adam**, **C**., Briceno, C., Buder, S., Butterley, T., Chen, W.-P., Dincel, B., Dhillon, V. S., Errmann, R., Garai, Z., Gilbert, H. F. W., Ginski, C., Greif, J., Hardy, L. K., Hernandez, J., Huang, P. C., Kellerer, A., Kundra, E., Littlefair, S. P., Mallonn, M., Marka, C., Pannicke, A., Pribulla, T., Raetz, S., Schmidt, J. G., Schmidt, T. O. B., Seeliger, M., Wilson, R. W., and Wolf, V. VizieR Online Data Catalog: Time-series photometry of IC 348 (Fritzewski+, 2016). *VizieR Online Data Catalog*, 746, August 2016c.

Garai, Z., Pribulla, T., Hambálek, Ľ., Errmann, R., **Adam**, **C**., Buder, S., Butterley, T., Dhillon, V. S., Dincel, B., Gilbert, H., Ginski, C., Hardy, L. K., Kellerer, A., Kitze, M., Kundra, E., Littlefair, S. P., Mugrauer, M., Nedoroščík, J., Neuhäuser, R., Pannicke, A., Raetz, S., Schmidt, J. G., Schmidt, T. O. B., Seeliger, M., Vaňko, M., and Wilson, R. W. Search for transiting exoplanets and variable stars in the open cluster NGC 7243. *Astronomische Nachrichten*, 337:261–285, March 2016. doi: 10.1002/asna.201512310.

Ginski, C., Neuhäuser, R., Mugrauer, M., Schmidt, T. O. B., and **Adam**, **C**. Orbital motion of the binary brown dwarf companions HD 130948 BC around their host star. *MNRAS*, 434:671–683, September 2013. doi: 10.1093/mnras/stt1059.

Maciejewski, G., Dimitrov, D., Neuhäuser, R., Niedzielski, A., Raetz, S., Ginski, C., **Adam**, **C**., Marka, C., Moualla, M., and Mugrauer, M. Transit timing variation in exoplanet WASP-3b. *MNRAS*, 407:2625–2631, October 2010. doi: 10.1111/j.1365-2966.2010.17099.x.

Maciejewski, G., Raetz, S., Nettelmann, N., Seeliger, M., **Adam**, **C**., Nowak, G., and Neuhaeuser, R. Transit light curves of WASP-10 b (Maciejewski+, 2011). *VizieR Online Data Catalog*, 353:59007, September 2011a.

Maciejewski, G., Raetz, S., Nettelmann, N., Seeliger, M., **Adam**, **C**., Nowak, G., and Neuhäuser, R. Analysis of new high-precision transit light curves of WASP-10 b: starspot occultations, small planetary radius, and high metallicity. *A&A*, 535:A7, November 2011b. doi: 10.1051/0004-6361/201117127.

Maciejewski, G., Seeliger, M., **Adam**, **C**., Raetz, S., and Neuhäuser, R. Refining Parameters of the XO-5 Planetary System with High-Precision Transit Photometry. *Acta Astron.*, 61:25–35, March 2011c.

Maciejewski, G., Niedzielski, A., Wolszczan, A., Nowak, G., Neuhäuser, R., Winn, J. N., Deka, B., Adamów, M., Górecka, M., Fernández, M., Aceituno, F. J., Ohlert, J., Errmann, R., Seeliger, M., Dimitrov, D., Latham, D. W., Esquerdo, G. A., McKnight, L., Holman, M. J., Jensen, E. L. N., Kramm, U., Pribulla, T., Raetz, S., Schmidt, T. O. B., Ginski, C., Mottola, S., Hellmich, S., **Adam**, **C**., Gilbert, H., Mugrauer, M., Saral, G., Popov, V., and Raetz, M. Constraints on a Second Planet in the WASP-3 System. *AJ*, 146:147, December 2013. doi: 10.1088/0004-6256/146/6/147.

Moualla, M., Schmidt, T. O. B., Neuhäuser, R., Hambaryan, V. V., Errmann, R., Trepl, L., Broeg, C., Eisenbeiss, T., Mugrauer, M., Marka, C., **Adam**, **C**., Ginski, C., Pribulla, T., Rätz, S., Schmidt, J., Berndt, A., Maciejewski, G., Röll, T., Hohle, M. M., Tetzlaff, N., Fiedler, S., and Baar, S. A new flare star member candidate in the Pleiades cluster. *Astronomische Nachrichten*, 332:661, August 2011. doi: 10.1002/asna.201111580.

Neuhäuser, R., Errmann, R., Berndt, A., Maciejewski, G., Takahashi, H., Chen, W. P., Dimitrov, D. P., Pribulla, T., Nikogossian, E. H., Jensen, E. L. N., Marschall, L., Wu, Z.-Y., Kellerer, A., Walter, F. M., Briceño, C., Chini, R., Fernandez, M., Raetz, S., Torres, G., Latham, D. W., Quinn, S. N., Niedzielski, A., Bukowiecki, Ł., Nowak, G., Tomov, T., Tachihara, K., Hu, S. C.-L., Hung, L. W., Kjurkchieva, D. P., Radeva, V. S., Mihov, B. M., Slavcheva-Mihova, L., Bozhinova, I. N., Budaj, J., Vaňko, M., Kundra, E., Hambálek, Ľ., Krushevska, V., Movsessian, T., Harutyunyan, H., Downes, J. J., Hernandez, J., Hoffmeister, V. H., Cohen, D. H., Abel, I., Ahmad, R., Chapman, S., Eckert, S., Goodman, J., Guerard, A., Kim, H. M., Koontharana, A., Sokol, J., Trinh, J., Wang, Y., Zhou, X., Redmer, R., Kramm, U., Nettelmann, N., Mugrauer, M., Schmidt, J., Moualla, M., Ginski, C., Marka, C., **Adam**, **C**., Seeliger, M., Baar, S., Roell, T., Schmidt, T. O. B., Trepl, L., Eisenbeiß, T., Fiedler, S., Tetzlaff, N., Schmidt, E., Hohle, M. M., Kitze, M., Chakrova, N., Gräfe, C., Schreyer, K., Hambaryan, V. V., Broeg, C. H., Koppenhoefer, J., and Pandey, A. K. The Young Exoplanet Transit Initiative (YETI). *Astronomische Nachrichten*, 332:547, July 2011. doi: 10.1002/asna.201111573.

Raetz, S., Maciejewski, G., Ginski, C., Mugrauer, M., Berndt, A., Eisenbeiss, T., **Adam**, **C**., Raetz, M., Roell, T., Seeliger, M., Marka, C., Vaňko, M., Bukowiecki, Ł., Errmann, R., Kitze, M., Ohlert, J., Pribulla, T., Schmidt, J. G., Sebastian, D., Puchalski, D., Tetzlaff, N., Hohle, M. M., Schmidt, T. O. B., and Neuhäuser, R. Transit timing of TrES-2: a combined analysis of ground- and space-based photometry. *MNRAS*, 444: 1351–1368, October 2014. doi: 10.1093/mnras/stu1505.

Raetz, S., Schmidt, T. O. B., Czesla, S., Klocová, T., Holmes, L., Errmann, R., Kitze, M., Fernández, M., Sota, A., Briceño, C., Hernández, J., Downes, J. J., Dimitrov,

D. P., Kjurkchieva, D., Radeva, V., Wu, Z.-Y., Zhou, X., Takahashi, H., Henych, T., Seeliger, M., Mugrauer, M., **Adam**, **C**., Marka, C., Schmidt, J. G., Hohle, M. M., Ginski, C., Pribulla, T., Trepl, L., Moualla, M., Pawellek, N., Gelszinnis, J., Buder, S., Masda, S., Maciejewski, G., and Neuhäuser, R. YETI observations of the young transiting planet candidate CVSO 30 b. *MNRAS*, 460:2834–2852, August 2016. doi: 10.1093/mnras/stw1159.

Schmidt, T. O. B., Neuhäuser, R., Briceño, C., Vogt, N., Raetz, S., Seifahrt, A., Ginski, C., Mugrauer, M., Buder, S., **Adam**, **C**., Hauschildt, P., Witte, S., Helling, C., and Schmitt, J. H. M. M. Direct Imaging discovery of a second planet candidate around the possibly transiting planet host CVSO 30. *A&A*, 593:A75, September 2016. doi: 10.1051/0004-6361/201526326.

Seeliger, M., Kitze, M., Errmann, R., Richter, S., Ohlert, J. M., Chen, W. P., Guo, J. K., Göğüş, E., Güver, T., Aydın, B., Mottola, S., Hellmich, S., Fernandez, M., Aceituno, F. J., Dimitrov, D., Kjurkchieva, D., Jensen, E., Cohen, D., Kundra, E., Pribulla, T., Vaňko, M., Budaj, J., Mallonn, M., Wu, Z.-Y., Zhou, X., Raetz, S., **Adam**, **C**., Schmidt, T. O. B., Ide, A., Mugrauer, M., Marschall, L., Hackstein, M., Chini, R., Haas, M., Ak, T., Güzel, E., Özdönmez, A., Ginski, C., Marka, C., Schmidt, J. G., Dincel, B., Werner, K., Dathe, A., Greif, J., Wolf, V., Buder, S., Pannicke, A., Puchalski, D., and Neuhäuser, R. Ground-based transit observations of the HAT-P-18, HAT-P-19, HAT-P-27/WASP40 and WASP-21 systems. *MNRAS*, 451:4060–4072, August 2015. doi: 10.1093/mnras/stv1187.

## B.2 Scientific Talks

- "Multiplicity-study of nearby B-type stars using near-infrared data from ESO-VLT Archive" at the Department of Planetology in Kobe, Japan. 2011 January 19
- "Multiplicity-study of nearby B-type stars using near-infrared data from ESO-VLT Archive" at the ESO-Headquarters in Santiago, Chile. 2011 May 10
- "Direct Imaging and Spectroscopy of planetary companions to young solar-analogue stars" at the 2nd annual meeting of the SPP 1385 in Mainz. 2011 October 18
- "Search for young transiting planets in the Trumpler 37 cluster" at the UK-Germany National Astronomy Meeting in Manchester, England. 2012 March 29
- "AO search for substellar companions around B-type stars" at the annual meeting of the Astronomische Gesellschaft in Hamburg. 2012 May 27

# C Declaration of authenticity

I hearby declare on oath that I created this work independently without the help of any third party and only with the aids and literature indicated. All results taken from other sources are indicated as such and the sources are listed accordingly.
The following person was directly involved in the creation of content shown in this work as described:

- The masses and ages of primary objects were calculated using software developed by Dr. rer. nat. Janos Schmidt.

There were no additional persons directly involved in the creation of the content shown in this work. In particular none received any monetarily benefits to aid or assist in this work. This work has not been submitted in any form for another degree or diploma at any university or other institute of tertiary education be it domestic or foreign. I am aware of the doctoral regulations of the faculty for physics and astronomy of the Friedrich-Schiller-University Jena.
I declare on oath that I said the truth and nothing but the truth to my best knowledge.

Ich erkläre hiermit an Eides statt, dass ich die vorliegende Arbeit selbstständing und nur unter zu Hilfe nahme der angegebenen Hilfsmittel und Literatur erstellt habe. Alle Resultate die aus anderen Quellen stammen sind als solche gekennzeichnet und die entsprechende Quelle angegeben.
Die folgende Person war in der beschriebenen Weise direkt an der Erstellung dieser Arbeit beteiligt:

- Die Massen und Alter der Primär Objekte wurden mit Hilfe eines von Dr. rer. nat. Janos Schmidt erstellten Programms bestimmt.

Weitere Personen waren an der Erstellung dieser Arbeit nicht direkt beteiligt. Insbesondere hat niemand durch mich monetäre Mittel für Leistungen erhalten, die im Zusammenhang mit dem Inhalt dieser Arbeit stehen. Diese Arbeit wurde bisher nicht, ganz oder in Teilen, einer anderen in- oder ausländischen Prüfungsbehörde vorgelegt. Die Promotionsordnung der Physikalisch-Astronomischen Fakultät der Friedrich-Schiller-Universität Jena ist mir bekannt. Ich erkläre das ich nach bestem Wissen und Gewissen die Wahrheit gesagt und nichts verschwiegen habe.

..... .....

Ort, Datum Unterschrift d. Verfassers